UNIWERSYTET MARII CURIE-SKŁODOWSKIEJ
W LUBLINIE

Szkoła Doktorska Nauk Ścisłych i Przyrodniczych

Dziedzina: **Nauki Ścisłe i Przyrodnicze**

Dyscyplina: **Nauki chemiczne**

Marlena Groszek

nr albumu: 278866

Wytwarzanie biosorbentów na drodze pirolizy i aktywacji odpadowych materiałów roślinnych oraz ich potencjalne wykorzystanie w ochronie środowiska i do celów energetycznych
(Preparation of biosorbents on the way of pyrolysis and activation of waste plant materials and their potential application in environmental protection and for energy purposes)

Rozprawa doktorska przygotowywana pod kierunkiem naukowym

Prof. dr hab. Małgorzaty Wiśniewskiej

w Instytucie Nauk Chemicznych

LUBLIN, 2025

Pragnę złożyć serdeczne podziękowania
Pani prof. dr hab. Małgorzacie Wiśniewskiej
za wprowadzenie mnie w świat nauki, całe wsparcie merytoryczną, wszelkie porady i pomoc, a także ogrom cierpliwości i wyrozumiałości.

Serdeczne podziękowania składam również
Panu dr hab. Piotrowi Nowickiemu prof. UAM
za nieocenione wsparcie merytoryczne, wiele cennych wskazówek i nieustanną gotowość do pomocy.

Dziękuję ***Pracownikom Katedry Radiochemii i Chemii Środowiskowej***
za całą otrzymaną pomoc.

Chciałabym również podziękować ***Moim Rodzicom***
za nieustanną i niezachwianą wiarę we mnie.

Szczególnie dziękuję ***Mojemu Mężowi Marcinowi***
za mnóstwo wsparcia i ogrom motywacji,
nikt nie rozumie tak jak Ty.

Spis treści

1. Lista publikacji będących podstawą rozprawy doktorskiej

D1. **M. Gęca**, M. Wiśniewska, P. Nowicki, *Biochars and activated carbons as adsorbents of inorganic and organic compounds from multicomponent systems – A review,* Advances in Colloid and Interface Science, 305, 2022, 102687, DOI:10.1016/j.cis.2022.102687 **(IF_{2022}: 15,6; $IF_{5\text{-letni}}$: 19,5; MNiSW: 200 pkt)**

D2. **M. Gęca**, M. Wiśniewska, P. Nowicki, *Modified method of lignocellulose content determination and its use for the analysis of selected herbs - precursors of biochars and activated carbons,* Measurement (Journal of the International Measurement Confederation), 212, 2023, 112672, DOI: 10.1016/j.measurement.2023.112672 **(IF_{2023}: 5,2; $IF_{5\text{-letni}}$: 5,4; MNiSW: 200 pkt)**

D3. **M. Gęca**, M. Wiśniewska, P. Nowicki, *Preparation of biochars by conventional pyrolysis of herbal waste and their potential application for adsorption and energy purposes,* ChemPhysChem, 2024, e202300507, DOI: 10.1002/cphc.202300507 **(IF_{2024}: 2,2; $IF_{5\text{-letni}}$: 2,5; MNiSW: 100 pkt)**

D4. **M. Groszek**, G. Wójcik, M. Wiśniewska, P. Nowicki, *Application of environmentally friendly activated carbons derived from herbal industry waste for water purification: A study on the removal of selected organic and inorganic pollutants,* Journal of Water Process Engineering, 2025, 75, 107952, DOI: 10.1016/j.jwpe.2025.107952 **(IF_{2024}: 6,7; $IF_{5\text{-letni}}$: 6,7; MNiSW: 100 pkt)**

D5. **M. Groszek**, M. Wiśniewska, P. Nowicki, *Simultaneous determination of ionic polymers and heavy metal ions concentrations in aqueous solution after their adsorptive removal using eco-friendly activated biocarbons*, Frontiers in Chemistry, 13, 2025, 1621297, DOI: 10.3389/fchem.2025.1621297 **(IF_{2024}: 4,2; $IF_{5\text{-letni}}$: 4,9; MNiSW: 100 pkt)**

D6. **M. Gęca**, M. Wiśniewska, P. Nowicki, *Simultaneous removal of polymers with different ionic character from their mixed solutions using herb-based biochars*

and activated carbons, Molecules, 27, 2022, 7557, DOI: 10.3390/molecules27217557 **(IF$_{2022}$: 4,6; IF$_{5\text{-letni}}$: 5,0; MNiSW: 140 pkt)**

D7. **M. Gęca**, M. Wiśniewska, T. Urban, P. Nowicki, *Temperature effect on ionic polymers removal from aqueous solutions using activated carbons obtained from biomass,* Materials, 16, 2022, 350, DOI: 10.3390/ma16010350 **(IF$_{2022}$: 3,4; IF$_{5\text{-letni}}$: 3,5; MNiSW: 140 pkt)**

D8. **M. Gęca**, M. Wiśniewska, P. Nowicki, K. Jędruchniewicz, *Cd(II) and As(V) removal from the multicomponent solutions in the presence of ionic polymers using carbonaceous adsorbents obtained from herbs,* Pure and Applied Chemistry, 2023, 95, 5, 563-578, DOI: 10.1515/pac-2023-0201 **(IF$_{2023}$: 2,0; IF$_{5\text{-letni}}$: 2,2; MNiSW: 140 pkt)**

D9. **M. Gęca**, M. Wiśniewska, P. Nowicki, *Investigation of ionic polymers stabilizing and flocculating properties in dispersed activated carbons systems,* Materials, 2024, 17, 693, DOI: 10.3390/ma17030693 **(IF$_{2024}$: 3,2; IF$_{5\text{-letni}}$: 3,5; MNiSW: 140 pkt)**

D10. **M. Gęca**, M. Wiśniewska, P. Nowicki, G. Wójcik *Arsenate and cadmium ions removal from multicomponent solutions of ionic polymers using mesoporous activated biocarbons*, Journal of Molecular Liquids, 2024, 407, 125270, DOI: 10.1016/j.molliq.2024.125270 **(IF$_{2024}$: 5,2; IF$_{5\text{-letni}}$: 5,1; MNiSW: 100 pkt)**

Sumaryczny IF: 52,3

Sumaryczny IF$_{5\text{-letni}}$: 58,3

Sumaryczna liczba punktów MNiSW: 1360

2. Uzasadnienie wyboru tematyki badawczej

Współczesne wyzwania środowiskowe, takie jak między innymi zanieczyszczenie wód i gleb toksycznymi jonami metali oraz związkami wielkocząsteczkowymi, wzrost zapotrzebowania na alternatywne źródła energii, czy też nadmierna produkcja odpadowej materii organicznej wymagają opracowania nowych, efektywnych i zrównoważonych ścieżek gospodarki obiegu zamkniętego. W tym kontekście biosorbenty wytwarzane z odpadów roślinnych stanowią obiecujące rozwiązanie, łączące zarówno korzyści ekologiczne, jak i ekonomiczne. Przekształcenie materiałów organicznych w surowce energetyczne lub w adsorbenty ogranicza bowiem ilość odpadów stałych, dzięki czemu zmniejszona zostaje emisja CO_2 i innych gazów powstających podczas procesów gnicia [1]. Ponadto składowanie takich odpadów w nieodpowiedni sposób może prowadzić do eutrofizacji wód oraz uwalniania patogenów do środowiska [2]. Dodatkowo (w aspekcie ekonomicznym), w wyniku tego typu działań redukcji ulegają wydatki związane z przechowywaniem biomasy, a ponowne wykorzystanie już zużytego materiału pozwala ograniczyć kosztowne pozyskiwanie nowych prekursorów, służących do produkcji adsorbentów.

W dobie ciągle zmniejszających się zasobów konwencjonalnych surowców energetycznych konieczne jest poszukiwanie nowych rozwiązań, które pozwolą na pozyskiwanie energii ze źródeł odnawialnych. Coraz bardziej powszechne są elektrownie wiatrowe i słoneczne, jednakże pomimo ich nieskończonego źródła zasilania, w dalszej perspektywie mogą one stanowić poważny problem przy utylizacji zużytych elementów. Wykorzystanie biomasy odpadowej do pozyskania biowęgla nie stwarza takich zagrożeń, a ponadto pozwala ograniczyć w znacznym stopniu ilość materii organicznej wymagającej składowania [3]. Otrzymane w ten sposób materiały charakteryzują się ciepłem spalania porównywalnym do konwencjonalnych surowców energetycznych, co świadczy o ich wysokim potencjale aplikacyjnym [4, 5].

Adsorbenty węglowe są szeroko stosowane do oczyszczania wody, jednakże ich wykorzystanie ogranicza się głównie do adsorpcji jonów metali oraz barwników [6, 7]. Nie są natomiast dostępne doniesienia literaturowe na temat usuwania związków polimerowych z roztworów wodnych przy użyciu biowęgli aktywnych. Sporadycznie

opisywane są układy, w których sprawdzana jest efektywność sorpcji substancji organicznych i nieorganicznych z roztworów dwuskładnikowych, jednakże nie dotyczą one charakterystyki zdolności adsorpcyjnych biowęgli aktywnych w odniesieniu do polimerów rozpuszczalnych w wodzie [D1]. W związku z powyższym, wytypowanie do badań układów zawierających polimery jonowe stanowi o nowatorskim charakterze niniejszej pracy. W dobie coraz szerszego zastosowania związków wielkocząsteczkowych konieczna jest ocena możliwości ich skutecznego usuwania z roztworów wodnych oraz ich wpływu na adsorpcję innych substancji, takich jak np. jony metali ciężkich.

W związku z powyższym do badań adsorpcyjnych wytypowano anionowy poli(kwas akrylowy) (PAA) stosowany w przemyśle kosmetycznym oraz kationową polietylenoiminę (PEI) wykorzystywaną w biotechnologii, natomiast jako modelowe zanieczyszczenia metaliczne wybrano jony Cd(II) oraz As(V) obecne w środowisku na skutek przetwórstwa skał i minerałów. Dodatkowo wykorzystanie do celów adsorpcyjnych biowęgli aktywnych otrzymanych z odpadowej materii roślinnej na drodze bezpośredniej aktywacji fizycznej i aktywacji chemicznej ma ważny aspekt ekonomiczny oraz wpisuje się w trendy gospodarki obiegu zamkniętego [8].

Powyższe aspekty środowiskowo-ekonomiczne oraz występujące luki badawcze doprowadziły do sformułowania następujących hipotez:

H1. Odpady pochodzące z przemysłu zielarskiego (takie jak łodygi pokrzywy, szałwii, melisy oraz mięty) mogą posłużyć do produkcji alternatywnych materiałów energetycznych oraz efektywnych adsorbentów węglowych.

H2. Proces pirolizy pozwoli uzyskać biowęgle charakteryzujące się wysoką wartością ciepła spalania, co umożliwi ich zastosowanie jako surowców energetycznych.

H3. Materiały otrzymane na drodze bezpośredniej aktywacji fizycznej oraz aktywacji chemicznej będą charakteryzować się korzystnymi właściwościami teksturalno-powierzchniowymi, pozwalającymi na ich zastosowanie w procesach adsorpcyjnych.

H4. Biowęgle aktywne otrzymane na drodze aktywacji chemicznej będą posiadać silniej rozwiniętą powierzchnię właściwą oraz większy średni rozmiar porów, co powinno sprzyjać adsorpcji dużych makrocząsteczek polimerowych, z kolei materiały uzyskane poprzez bezpośrednią aktywację fizyczną będą bardziej efektywnie wiązać jony metali ciężkich.

H5. Obecność w roztworze wodnym różnoimiennie naładowanych adsorbatów (tj. dwóch polimerów lub polimeru i jonu metalu) spowoduje wzrost wielkości adsorpcji obu substancji.

W celu weryfikacji powyższych założeń otrzymane materiały węglowe zostały poddane analizie struktury porowatej oraz ocenie właściwości kwasowo-zasadowych powierzchni. Ponadto, wykorzystane prekursory roślinne zbadano pod kątem składu lignocelulozowego. Produkty procesu pirolizy – biowęgle – scharakteryzowano w kierunku ich właściwości energetycznych, ze szczególnym uwzględnieniem ciepła spalania. Z kolei materiały otrzymane na drodze bezpośredniej aktywacji fizycznej i aktywacji chemicznej (biowęgle aktywne) zastosowano jako adsorbenty polimerów jonowych (PAA i PEI) oraz jonów metali ciężkich (Cd(II) i As(V)). Oceniono wpływ pH roztworu na wielkość adsorpcji oraz zbadano kinetykę tego procesu. Dodatkowo sprawdzono efektywność usuwania substancji organicznych i nieorganicznych z roztworów dwuskładnikowych. W celu określenia mechanizmu wiązania adsorbatów przeprowadzono analizę parametrów charakteryzujących podwójną warstwę elektryczną utworzoną na powierzchni cząstek materiałów węglowych, takich jak gęstość ładunku powierzchniowego, potencjał dzeta, punkt ładunku zerowego i punkt izoelektryczny. Ważnym aspektem przeprowadzonych badań było również określenie możliwości regeneracji materiałów węglowych przy zastosowaniu różnych czynników desorpcyjnych, a także ich tendencji do agregacji. Przeprowadzone badania pozwoliły wytypować najbardziej obiecujące układy, które wykazują wysoki potencjał aplikacyjny w procesach oczyszczania wody i ścieków oraz w sektorze energetycznym.

3. Część eksperymentalna

3.1. Preparatyka materiałów węglowych

W celu uzyskania biosorbentów zastosowano biomasę odpadową pochodzącą z przemysłu zielarskiego, na którą składały się cztery rodzaje prekursorów roślinnych (P) – łodygi pokrzywy (PO), szałwii (SZ), melisy (ML) oraz mięty (MT). Łodygi ziół wysuszono w temperaturze 110 °C, a następnie rozdrobniono na kawałki o rozmiarze 1,5-2,0 cm.

Procedura otrzymywania biowęgli (B) obejmowała pirolizę materiału roślinnego w atmosferze azotu (przepływ 170 cm^3/min) w temperaturze 400 °C przez 60 min [D3]. Z kolei w celu uzyskania biowęgli aktywnych zastosowano dwie procedury obróbki termochemicznej – tj. bezpośrednią aktywację fizyczną (AF) oraz aktywację chemiczną (AC). W pierwszej z nich łodygi ziół poddano równoczesnej pirolizie i aktywacji z zastosowaniem CO_2 (przepływ 250 cm^3/min) w temperaturze 800 °C przez 30 min [D4, D5]. Z kolei celem przeprowadzenia aktywacji chemicznej próbki zostały poddane 24-godzinnej impregnacji z użyciem H_3PO_4 (stosunek wagowy prekursor-aktywator: 1:2). Po tym czasie materiały wysuszono w temperaturze 110 °C, w celu odparowania wody i poddano dwuetapowemu ogrzewaniu w atmosferze azotu (przepływ 200 cm^3/min). W pierwszym etapie próbki ogrzewano przy naroście temperatury 5 °C/min, aż do osiągnięcia 200 °C, po czym termostatowano przez 30 minut. Następnie temperaturę podnoszono (przy takim samym naroście) do 500 °C i ponownie termostatowano przez 30 minut. Produkty aktywacji przemywano 10 dm^3 wrzącej wody destylowanej, a następnie suszono w temperaturze 110 °C do stałej masy [D6-D10].

3.2. Charakterystyka otrzymanych materiałów

Morfologię powierzchni otrzymanych materiałów węglowych określono przy zastosowaniu skaningowej mikroskopii elektronowej (SEM) – aparat Quanta 250 FEG (FEI, Hillsboro, OR, USA).

Parametry teksturalne wyznaczono z użyciem metody niskotemperaturowej adsorpcji/desorpcji azotu (analizator ASAP 2020, Micromeritics Instrument Corporation, Norcross, GA, USA).

Zawartość popiołu wyznaczono zgodnie z normą PN-ISO 1171:2002 poprzez spalenie 1 g materiału w temperaturze 815 °C z wykorzystaniem pieca mikrofalowego Phoenix (CEM Corporation, Matthews, NC, USA). Zwartość pierwiastków C, H, N oraz S określona została z wykorzystaniem analizatora elementarnego EuroEA3000 (EuroVector, Pavia, PV, Włochy). Dla obu oznaczeń procedurę powtórzono dwukrotnie, a za wynik przyjęto średnią, z kolei zawartość tlenu obliczono z różnicy. Wykorzystano również fluorescencyjną spektrometrię rentgenowską (XRF) w celu określenia składu pierwiastkowego uzyskanych biowęgli i biowęgli aktywnych (aparat Axios mAX, PANalytical, Almelo, Holandia).

Stężenie powierzchniowych grup funkcyjnych o charakterze kwasowym i zasadowym wyznaczono w oparciu o metodę alkacymetryczną zaproponowaną przez Boehma [9]. Typ grup funkcyjnych obecnych na powierzchni adsorbentów określono przy wykorzystaniu rentgenowskiej spektroskopii fotoelektronów (XPS) (aparat Gammadata Scienta, Uppsala, Szwecja) oraz spektroskopii w podczerwieni (FTIR) (spektrometr Nicolet 8700A, Thermo Fisher Scientific Inc., Waltham, MA, USA).

3.3. Charakterystyka adsorbatów

Jako modelowe zanieczyszczenia środowiska zastosowano substancje organiczne - poli(kwas akrylowy) i polietylenoiminę oraz nieorganiczne - jony kadmu i arsenu. Analizy prowadzono w układach zawierających jeden lub dwa składniki jednocześnie, a także w obecności elektrolitu podstawowego (NaCl), co pozwoliło w znacznym stopniu na odwzorowanie rzeczywistych układów ściekowych.

Polimery jonowe wytypowane do badań znajdują szerokie zastosowanie w przemyśle farmaceutycznym i kosmetycznym, a także w biotechnologii. Poli(kwas akrylowy) (PAA) (Rys. 1a), dzięki swojej wysokiej biokompatybilności, wykorzystywany jest w systemach dostarczania leków oraz w inżynierii genetycznej [10, 11]. Z kolei polietylenoimina (PEI), (Rys. 1b) z uwagi na swoje zdolności do migracji poprzez

eukariotyczne błony komórkowe oraz łatwość wiązania z cząsteczkami DNA, stosowana jest w procesach hodowli komórkowych i modyfikacji genetycznych [12]. Jako substancje syntetyczne i wpływające na funkcjonowanie komórek oba polimery nie powinny jednak występować w środowisku naturalnym, dlatego też należy je skutecznie usuwać ze ścieków.

Zastosowane polimery charakteryzowały się średnią wagową masą cząsteczkową wynoszącą 2000 Da. Poli(kwas akrylowy) jest polimerem anionowym, którego pK_a jest równe 4,5 [13]. Poniżej tej wartości pH, większość jego karboksylowych grup funkcyjnych występuje w postaci niezdysocjowanej, co skutkuje skłębioną konformacją makrocząsteczki. Wraz ze wzrostem pH coraz więcej grup funkcyjnych ulega dysocjacji, co prowadzi do rozwinięcia łańcucha. Z kolei polietylenoimina jest substancją kationową, zawierającą grupy aminowe. Jej wartość pK_b jest równa 9,0 [14], co sprawia, że poniżej tej wartości pH, PEI przyjmuje rozwiniętą konformację z uwagi na znaczną ilość zjonizowanych grup funkcyjnych. Powyżej pH 9, jej makrocząsteczki przyjmują strukturę skłębioną, co związane jest ze zmniejszającym się stopniem protonacji grup aminowych.

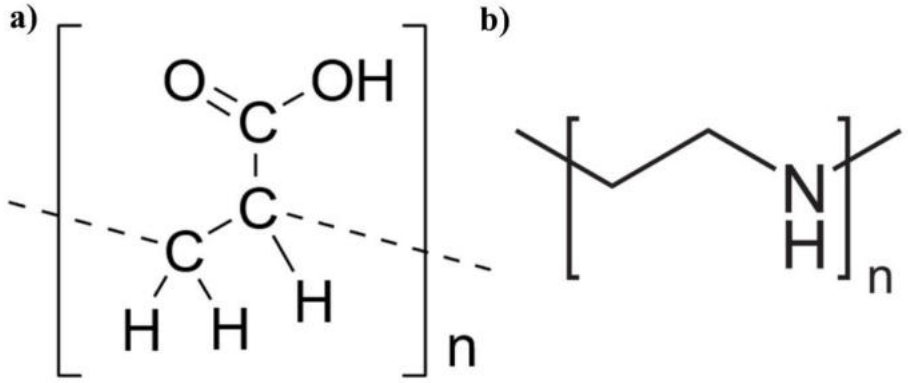

Rysunek 1. Wzory strukturalne PAA (a) oraz PEI (b)

Wykorzystane w badaniach jony metali ciężkich są wysoce toksyczne, a z powodu ich szerokiego zastosowania często występują w ściekach. Szacuje się, że rocznie do środowiska uwalniane jest 500-2600 ton kadmu, głównie ze źródeł antropogenicznych, takich jak spalanie paliw kopalnych, stosowanie nawozów o wysokiej zawartości fosforanów oraz eksploatacja złóż w przemyśle wydobywczym

[15]. Z kolei arsen obecny jest w środowisku głównie jako zanieczyszczenie minerałów. Jednakże z uwagi na swoją dobrą rozpuszczalność i wysoką mobilność łatwo przedostaje się do wód gruntowych. W krajach rozwijających się znaczna część źródeł wody pitnej jest zanieczyszczona arsenem [16]. Oba pierwiastki mogą wywoływać silne zatrucia oraz negatywnie wpływają na funkcjonowanie układów nerwowego, krążenia oraz wydalniczego [17, 18]. Z tego powodu należy poszukiwać efektywnych metod pozwalających na zminimalizowanie ich uwalniania do środowiska.

W badaniach wykorzystano jony Cd(II), których źródłem był czterowodny azotan(V) kadmu - $CdN_2O_6{\cdot}4H_2O$. Z uwagi na ograniczoną rozpuszczalność kadmu analizy prowadzone były w pH poniżej 8. Jako źródło jonów As(V) zastosowano arsenian(V) potasu - KH_2AsO_4. Związek ten ulega dysocjacji na kation potasu oraz anion arsenianowy(V), którego stopień uwodornienia zależy od pH roztworu. W układach silnie zasadowych występuje on w postaci jonu AsO_4^{3-}, wraz z obniżaniem pH jego cząsteczka ulega stopniowemu uwodornieniu do form: $HAsO_4^{2-}$, $H_2AsO_4^-$ oraz H_3AsO_4 [19].

3.4. Metodyka badań

Prekursory roślinne wykorzystane w badaniach poddano analizie umożliwiającej określenie zawartości ligniny, celulozy, hemicelulozy oraz substancji mineralnych i ekstrakcyjnych w ich strukturze. Miało to na celu określenie wpływu składu lignocelulozowego na właściwości otrzymanych materiałów węglowych [D2]. Zaproponowano nową procedurę oznaczania tych składników, eliminującą błąd wynikający z rozpuszczalności ligniny oraz hemicelulozy w roztworach zasadowych. Do procesu oznaczania hemicelulozy dodano etap wytrącania przy pomocy etanolu, co umożliwiło jej oddzielenie od ligniny. Z kolei wieloetapowy proces służący do określenia zawartości ligniny zastąpiono prostszą procedurą oznaczania celulozy.

Prekursory oraz biowęgle zostały poddane analizie ciepła spalania (*ang. higher heating value, HHV* [MJ/kg]). Badania prowadzono zgodnie z normą ISO 1928:2009, wykorzystując kalorymetr KL-12Mn (Precyzja-Bit, Bydgoszcz, Polska). Wartości badanych parametrów wyznaczono z poniższych równań:

$$HHV = \frac{C \times \Delta T - Q_{iw}}{m} \quad (1)$$

$$EDR = \frac{HHV_B}{HHV_P} \quad (2)$$

$$EY = MY \times EDR \quad (3)$$

gdzie: C – pojemność cieplna bomby kalorymetrycznej [MJ/°C], ΔT – zmiana temperatury wody w kalorymetrze bombowym [°C], Q_{iw} – ilość ciepła wygenerowana przez żelazny drucik oporowy [MJ/kg], m – masa próbki [kg], EDR – wskaźnik zagęszczenia energetycznego, HHV_B – ciepło spalania biowęgla [MJ/kg], HHV_P – ciepło spalania prekursora [MJ/kg], EY – wydajność energetyczna [%], MY – wydajność pirolizy [%].

Pomiary adsorpcyjne z wykorzystaniem biowęgli oraz biowęgli aktywnych prowadzono w temperaturze 25 °C. Jako elektrolit podstawowy zastosowano chlorek sodu o stężeniu 0,001 mol/dm^3. Naważki adsorbentów oraz stężenia adsorbatów do badań dobierane były indywidualnie dla każdego układu, z uwagi na zróżnicowaną efektywność procesu oraz ograniczenia związaniem z oznaczaniem poszczególnych substancji. Izotermy adsorpcji uzyskano w układach o pH 3, 6 oraz 9, badania prowadzono przez 24 h. Otrzymane wyniki dopasowano do teoretycznych modeli adsorpcji Langmuira, Freundlicha, Temkina oraz Dubinina-Radushkevicha [20]. Kinetykę procesu adsorpcji badano w układach o pH 3, za względu na najwyższą adsorpcję substancji organicznych i nieorganicznych w tych warunkach. Uzyskane dane eksperymentalne dopasowano modelami kinetyki pseudo-pierwszego-rzędu oraz pseudo-drugiego-rzędu [21]. Oceniono również zdolności adsorpcyjne materiałów węglowych w układach dwuskładnikowych (metal + polimer oraz polimer + polimer), w roztworach o pH 3 i stężeniu początkowym adsorbatów wynoszącym 200 ppm (adsorpcję prowadzono przez 24 h). Ponadto, określono możliwość regeneracji biowęgli aktywnych na drodze desorpcji przy użyciu H_2O oraz NaOH i HNO_3 o stężeniach 0,1 mol/dm^3. Dla wybranych układów oceniono również wpływ temperatury na efektywność procesu adsorpcji, stabilność wodnych suspensji materiałów węglowych (bez i w obecności polimerów) oraz zdolności regeneracyjne adsorbentów w następujących po sobie cyklach adsorpcyjno-desorpcyjnych. Wielkość adsorpcji wyznaczono wykorzystując metodę statyczną, z różnicy stężeń danego adsorbatu w roztworze przed i po procesie:

$$\Gamma = \frac{(C_0 - C)V}{m} \quad (4)$$

gdzie: Γ – wielkość adsorpcji [mg/g], C_0 – stężenie początkowe [mg/dm^3], C – stężenie końcowe adsorbatu [mg/dm^3], V – objętość roztworu [dm^3], m – masa adsorbentu [g]. Stężenie polimerów określono przy zastosowaniu spektrofotometru UV-VIS Carry 100 Bio (Palo Alto, Santa Clara, CA, USA). Do oznaczenia stężenia poli(kwasu akrylowego) wykorzystano reakcję kompleksowania z hyaminą 1622, pozwalającą otrzymać zabarwiony na biało roztwór pochłaniający światło przy długości fali 500 nm [22]. W przypadku politeylenoiminy jako czynnik kompleksujący wykorzystano $CuCl_2$, który powoduje powstanie niebiesko zabarwionego roztworu. Jego absorbancję mierzono przy długości fali wynoszącej 285 nm [23]. Do oznaczenia zawartości jonów Cd(II) oraz As(V) zastosowano spektrometr ICP-EOS iCAP™ 7200 (Thermo Fisher Scientific Inc., Waltham, MA, USA).

W celu uzyskania dodatkowych informacji odnośnie najbardziej prawdopodobnego mechanizmu adsorpcji przeprowadzono badania mające na celu określenie struktury podwójnej warstwy elektrycznej (*pwe*) utworzonej na powierzchni cząstek materiałów węglowych (w obecności elektrolitu podstawowego). Obejmowały one wyznaczenie znaku i gęstości ładunku zgromadzonego w warstwie powierzchniowej oraz w obszarze płaszczyzny poślizgu. Pomiary prowadzono w zakresie pH 3-11 (przy zastosowaniu pH-metru pHM 240, Radiometer, Warszawa, Polska), w roztworach o stężeniu 100 ppm. Masę materiału węglowego dobierano indywidualnie, dla każdego układu, zapewniając optymalne warunki pomiarów.

Gęstość ładunku powierzchniowego (σ_0) oraz położenie punktu ładunku zerowego (*pzc*) adsorbentów węglowych uzyskano dzięki zastosowaniu metody miareczkowania potencjometrycznego. Badania wykonano przy użyciu zestawu złożonego z naczynka teflonowego, termostatu RE204 (Lauda Scientific GmbH, Lauda-Königshofen, Niemcy), elektrody szklanej i kalomelowej (Beckman Instruments, Brea, CA, USA), pH-metru PHM240 (Radiometer, Warszawa, Polska) oraz automatycznej mikrobiurety 765 Dosimat (Metrohm, Opacz-Kolonia, Polska), sterowanej przy pomocy programu komputerowego „Titr_v3”. Obliczenia wykonano w oparciu o równanie [25]:

$$\sigma_0 = \frac{\Delta V c F}{m S} \quad (5)$$

gdzie: σ_0 – gęstość ładunku powierzchniowego [μC/cm^2], ΔV – różnica w objętości NaOH, którą należy dodać, aby doprowadzić pH suspensji i elektrolitu podstawowego do określonej wartości [dm^3], c – stężenie NaOH [mol/dm^3], F – stała Faradaya [C/mol], m – masa ciała stałego [g], S – powierzchnia właściwa ciała stałego [m^2/g].

Wartość potencjału dzeta (ζ) oraz położenie punktu izoelektrycznego (*iep*) określono z wykorzystaniem pomiaru ruchliwości elektroforetycznej (U_e). Doświadczenia prowadzono z użyciem aparatu Zetasizer Nano ZS (Malvern Instruments, Malvern, UK). Potencjał dzeta wyznaczono w oparciu o zjawisko dopplerowskiej elektroforezy laserowej i statycznego rozpraszania światła, stosując następujące równanie:

$$U_e = \frac{2\varepsilon_0 \varepsilon \zeta}{3\eta} f(\kappa a) \quad (6)$$

gdzie: U_e – ruchliwość elektroforetyczna [m^2/V·s], ε_0 – przenikalność elektryczna próżni [F/m], ε – stała dielektryczna [F/m], ζ – potencjał dzeta [mV], η – lepkość fazy ciągłej [Pa·s], $f(\kappa\alpha)$ – funkcja Henry'ego [24].

Układy o pH 3, 6 oraz 9 wykorzystano dodatkowo do sprawdzenia wpływu zastosowanych adsorbatów na wielkość agregatów utworzonych przez cząstki biowęgla aktywnego. Pomiary te prowadzono wykorzystując ten sam aparat co w przypadku testów elektrokinetycznych.

4. Wyniki badań i ich interpretacja

4.1. Wpływ rodzaju prekursora na właściwości materiałów węglowych

Rysunek 2 przedstawia obrazy SEM otrzymanych materiałów. Na większości z nich można dostrzec podłużne, wklęsłe struktury, które wynikają ze stosowania łodyg ziół jako prekursorów. Biowęgle wyróżniają się jednak brakiem małych cząstek na ich powierzchni, świadczących o fragmentacji matrycy węglowej na skutek obróbki termochemicznej oraz znacznego udziału domieszek mineralnych (tzw. popiołu), co obserwuje się w przypadku biowęgli aktywnych.

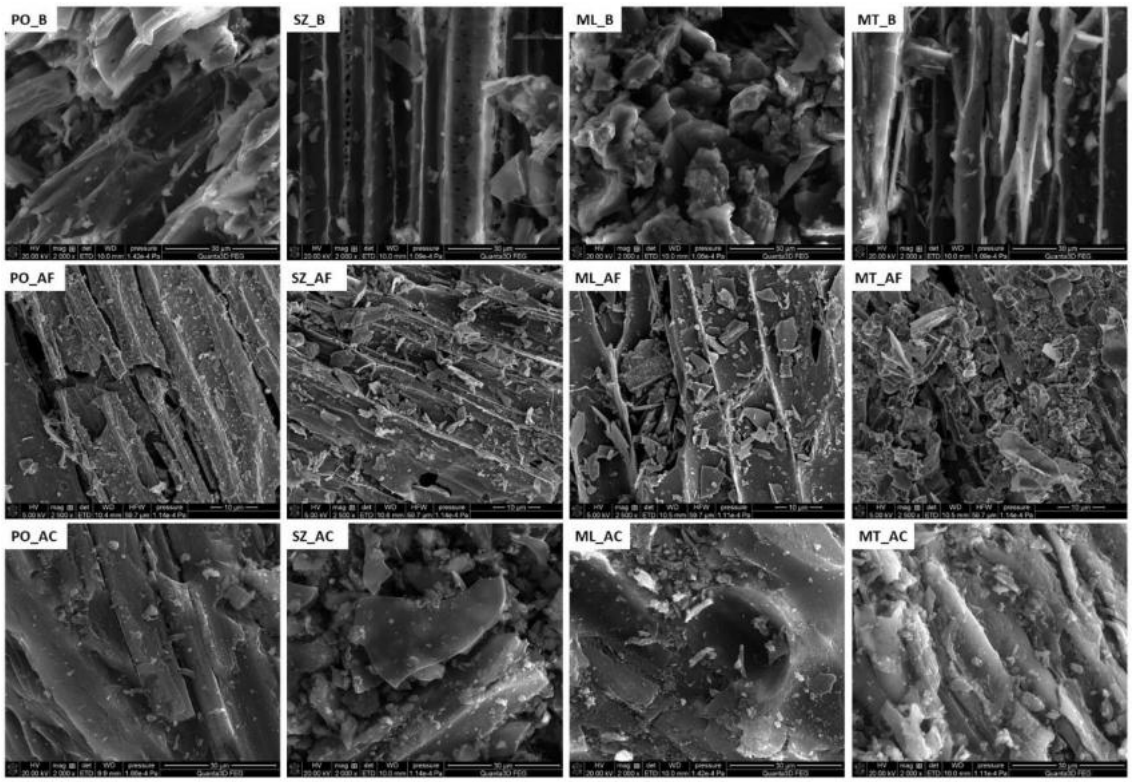

Rysunek 2. Obrazy SEM otrzymanych materiałów węglowych

Prekursory roślinne wykorzystane do produkcji materiałów węglowych składają się głównie z węgla oraz tlenu (Tabela 1). Procesy pirolizy oraz aktywacji skutkują zwiększeniem zawartości węgla w otrzymanych materiałach. Efekt ten jest bardziej widoczny w przypadku biowęgli aktywnych. Stwierdzono również, że materiały otrzymane na drodze bezpośredniej aktywacji fizycznej charakteryzują się najniższą zawartością wodoru, z kolei te uzyskane poprzez aktywację chemiczną najniższą

zawartością azotu. Wzrost zawartości węgla kosztem innych pierwiastków w badanych biowęglach i biowęglach aktywnych jest związany prawdopodobnie ze zmniejszeniem alifatycznego charakteru struktury materiałów i jednoczesnym wzrostem zawartości termicznie stabilnych fragmentów aromatycznych, co prowadzi do powstania licznych produktów ubocznych aktywacji, bogatych w wodór, azot i tlen. Spośród wszystkich badanych ciał stałych biowęgle aktywne otrzymane z wykorzystaniem H_3PO_4, wykazują najniższą zawartość popiołu (substancji mineralnych).

Tabela 1. Zawartość popiołu oraz pierwiastków C, H, N oraz O w prekursorach oraz otrzymanych materiałach węglowych [% wag.]

Materiał	Popiół	C^{daf}	H^{daf}	N^{daf}	O^{diff}
PO_P	9,4	41,9	7,7	4,6	45,7
SZ_P	11,0	49,5	8,3	1,9	40,4
ML_P	6,8	43,5	7,2	2,8	46,5
MT_P	8,0	44,6	7,4	3,4	44,6
NE_B	2,6	65,8	4,8	3,7	25,7
SA_B	6,8	65,0	4,7	1,8	28,5
ML_B	4,4	66,0	4,7	3,3	26,0
MT_B	4,8	70,7	4,7	3,1	21,5
PO_AF	17,5	77,9	1,3	3,9	17,0
SZ_AF	13,0	89,0	0,9	2,0	8,2
ML_AF	9,5	83,5	1,1	2,8	12,6
MT_AF	23,5	74,7	1,7	3,1	20,5
PO_AC	0,5	81,2	2,8	1,4	14,6
SZ_AC	0,8	79,5	2,5	1,0	17,0
ML_AC	2,6	83,9	2,8	1,3	12,1
MT_AC	2,7	82,4	2,8	1,3	13,6

^{daf} – sucha i bezpopiołowa zawartość pierwiastka; ^{diff} – zawartość obliczono z różnicy

Analiza składu lignocelulozowego wykorzystanych prekursorów wykazała, że głównym elementem budulcowym zastosowanych ziół jest lignina (Tabela 2). Jest to związane z faktem, że lignina jest składnikiem odpowiedzialnym za sztywność rośliny, a do produkcji materiałów węglowych wykorzystywano głównie łodygi, czyli najtwardszy fragment pędu ziół. Wykazano również, że wraz ze wzrostem zawartości hemicelulozy w prekursorach, wzrasta powierzchnia właściwa uzyskanych z nich biowęgli aktywnych (Tabela 3) [D2].

Tabela 2. Skład lignocelulozowy prekursorów

Materiał	Zawartość [% wag.]				
	Części ekstrakcyjne	Hemiceluloza	Celuloza	Lignina	Substancje mineralne
PO_P	10,7	10,3	18,1	60,1	0,8
SZ_P	21,0	19,1	19,4	39,2	1,3
ML_P	10,2	24,5	12,3	51,5	1,5
MT_P	12,1	27,4	16,7	43,1	0,7

Biowęgle charakteryzują się najmniejszą powierzchnią właściwą oraz największym średnim rozmiarem porów. Proces aktywacji pozwala uzyskać materiały o znacznie silniej rozwiniętej powierzchni niż ma to miejsce w przypadku procesu pirolizy. Biowęgle aktywne wytworzone z wykorzystaniem CO_2 wykazują mniej korzystne parametry teksturalne, w porównaniu do analogicznych materiałów otrzymanych z użyciem H_3PO_4. Zatem można przypuszczać, że z uwagi na mezoporowaty charakter są bardziej odpowiednie do adsorpcji dużych cząsteczek, takich jak polimery. Z kolei biowęgle uzyskane z wykorzystaniem fizycznego wariantu aktywacji jako materiały mikro-/mezoporowate prawdopodobnie będą skuteczniej wiązały jony metali ciężkich.

Tabela 3. Właściwości teksturalne otrzymanych materiałów węglowych

Materiał	Powierzchnia [m^2/g]		Objętość porów [cm^3/g]		Średni rozmiar porów [nm]	Udział mikroporów
	całkowita	mikropory	całkowita	mikropory		
PO_B	2,5	-	0,01	-	9,54	-
SZ_B	2,2	-	0,01	-	10,56	-
ML_B	2,2	-	0,01	-	9,40	-
MT_B	3,1	-	0,01	-	8,40	-
PO_AF	368	248	0,21	0,10	2,26	0,47
SZ_AF	399	327	0,20	0,13	1,96	0,65
ML_AF	547	430	0,26	0,17	1,92	0,65
MT_AF	666	535	0,32	0,21	1,91	0,66
PO_AC	801	157	0,85	0,07	4,23	0,09
SZ_AC	842	155	0,83	0,07	3,93	0,09
ML_AC	950	149	1,10	0,07	4,63	0,06
MT_AC	1145	184	1,47	0,07	5,12	0,05

Analiza właściwości kwasowo-zasadowych powierzchni materiałów węglowych wykazała, że próbki otrzymane na drodze bezpośredniej aktywacji fizycznej charakteryzują się najwyższą sumaryczną zawartością powierzchniowych grup funkcyjnych (Tabela 4). W przypadku tego wariantu aktywacji można stwierdzić, że stężenie grup funkcyjnych jest tym większe, im wyższa ich zawartość na powierzchni prekursorów. Z kolei w przypadku aktywacji chemicznej zawartość powierzchniowych grup funkcyjnych można powiązać z zawartością ligniny w wykorzystanym prekursorze [D2]. Punkt ładunku zerowego biowęgli aktywnych jest ściśle związany z rodzajem grup występujących w przewadze na ich powierzchni. Wyższa zawartość grup zasadowych skutkuje wartościami *pzc* lokującymi się w zakresie pH powyżej 7 (maksymalnie pH 9,7), z kolei wyższa zawartość kwasowych grup funkcyjnych powoduje przesunięcie *pzc* w stronę niższych wartości pH (w zakresie 3,1 – 4). Znaczna rozbieżność pomiędzy wartościami pH_{pzc} oraz pH_{iep} związana jest z dużymi rozmiarami porów badanych materiałów, co prowadzi do częściowego nakładania się dyfuzyjnej części podwójnej warstwy elektrycznej utworzonej na wewnętrznej powierzchni tych struktur [D4].

Tabela 4. Właściwości kwasowo-zasadowe prekursorów oraz otrzymanych materiałów węglowych

Materiał	Zawartość kwasowych grup funkcyjnych [mmol/g]	Zawartość zasadowych grup funkcyjnych [mmol/g]	Całkowita zawartość grup funkcyjnych [mmol/g]	pH_{pzc}	pH_{iep}
PO_P	1,30	0,77	2,07	-	-
SZ_P	0,84	1,15	1,96	-	-
ML_P	0,94	0,82	1,76	-	-
MT_P	0,57	0,93	1,50	-	-
PO_B	1,04	1,75	2,79	7,3	6,1
SZ_B	1,11	1,01	2,11	8,6	5,2
ML_B	0,82	0,80	1,62	8,0	5,1
MT_B	1,37	0,65	2,01	7,6	6,3
PO_AF	0,32	4,57	4,89	9,7	<3
SZ_AF	0,48	1,96	2,44	9,1	<3
ML_AF	0,29	2,03	2,33	8,8	3,8
MT_AF	0,63	1,56	2,19	8,5	3,3
PO_AC	0,86	0,27	1,13	3,1	4,9
SZ_AC	0,44	0,22	0,65	4,0	6,2
ML_AC	0,68	0,31	0,98	3,4	3,8
MT_AC	0,49	0,30	0,79	3,4	<3

4.2. Właściwości energetyczne biowęgli

Wartość ciepła spalania prekursorów nie przekracza 15 MJ/kg. Jak wynika z danych zawartych w Tabeli 5 proces pirolizy skutkuje wzrostem ciepła spalania do ok. 20 MJ/kg. Otrzymane biowęgle charakteryzują się ciepłem spalania porównywalnym do typowych wartości tego parametru uzyskiwanych dla brykietów z drewna, pelletu drzewnego oraz węgla brunatnego (~18-25 MJ/g) [26]. Pomimo zastosowania takich samych warunków pirolizy, wskaźnik zagęszczenia energetycznego różni się dla poszczególnych biowęgli. Najwyższą wartość tego parametru zaobserwowano w przypadku materiału uzyskanego z pokrzywy (1,6), natomiast najniższą dla próbki otrzymanej z łodyg szałwii (1,4). Pozwala to wysnuć wniosek, że wartość wskaźnika zagęszczenia energetycznego wzrasta wraz ze wzrostem zawartości ligniny w prekursorze [D3]. Wydajność energetyczna biowęgli otrzymanych z poszczególnych ziół, także jest zróżnicowana. Najwyższą wartość tego parametru (67,3 %) uzyskano dla biowęgla wytworzonego z łodyg melisy.

Tabela 5. Właściwości energetyczne prekursorów i biowęgli

Materiał	Ciepło spalania [MJ/kg]	Wskaźnik zagęszczenia energetycznego	Wydajność energetyczna [%]
PO_P	11,7	-	-
SZ_P	14,5	-	-
ML_P	13,4	-	-
MT_P	13,1	-	-
PO_B	18,2	1,6	66,5
SZ_B	19,7	1,4	62,5
ML_B	20,4	1,5	67,3
MT_B	18,2	1,4	58,5

Podsumowując powyższe dane należy stwierdzić, że biowęgle uzyskane z odpadowej biomasy ziołowej mogą stanowić alternatywę dla powszechnie stosowanych klasycznych surowców opałowych.

4.3. Właściwości adsorpcyjne biowęgli aktywnych

4.3.1. Efektywność adsorpcji i desorpcji polimerów oraz jonów metali ciężkich w układach jedno- i dwuskładnikowych

Biowęgle aktywne uzyskane na drodze aktywacji chemicznej charakteryzują się wyższymi pojemnościami adsorpcyjnymi w kierunku poli(kwasu akrylowego), polietylenoiminy oraz jonów Cd(II) i As(V), w porównaniu do materiałów otrzymanych z wykorzystaniem bezpośredniej aktywacji fizycznej (Rys. 3). Jest to związane przede wszystkim ze znacznie silniej rozwiniętą powierzchnią właściwą biowęgli aktywnych wytworzonych z użyciem H_3PO_4.

Na efektywność adsorpcji, poza wielkością powierzchni ciała stałego, wpływają również inne parametry fizykochemiczne charakteryzujące adsorbenty i adsorbaty oraz roztwór, w którym ten proces ma miejsce. Wartość pH układu, może mieć znaczący wpływ na zmianę powinowactwa adsorpcyjnego, szczególnie w przypadku substancji jonowych. Punkt ładunku zerowego definiuje wartość pH, przy której ładunki ujemne i dodatnie na powierzchni ciała stałego równoważą się, a więc sumaryczny ładunek jest równy zero. Poniżej wartości pH_{pzc} powierzchnia adsorbentów naładowana jest dodatnio, a powyżej ujemnie [D4-D6, D8, D10]. Przeprowadzone badania adsorpcyjne w pH 3, 6 oraz 9 wykazały, że odczyn roztworu znacząco wpływa na wielkość adsorpcji badanych substancji organicznych i nieorganicznych (Rys. 3). Polimery jonowe są najefektywniej wiązane na powierzchni biowęgli aktywnych w pH 3. W przypadku anionowego poli(kwasu akrylowego) ma to związek ze skłębioną konformacją łańcuchów polimerowych w tych warunkach (minimalna dysocjacja grup karboksylowych). Makrocząsteczki w formie kłębków mogą z łatwością penetrować pory adsorbentów co skutkuje zwiększoną pojemnością adsorpcyjną. Przy wyższych wartościach pH łańcuchy polimerowe ulegają stopniowemu rozwinięciu, co znacząco ogranicza możliwość ich adsorpcji w porach. Polietylenoimina, ze względu na swój kationowy charakter w pH 3, występuje w postaci rozwiniętych i całkowicie zjonizowanych łańcuchów. Z uwagi na dodatni ładunek zarówno polimeru, jak i powierzchni biowęgli aktywnych, adsorpcja makrocząsteczki zachodzi w kierunku prostopadłym do powierzchni ciała stałego, co skutkuje znacznym upakowaniem warstwy adsorpcyjnej PEI w pH 3 [D4-D6]. Jony

metali ciężkich są adsorbowane w podobnej ilości niezależnie od wartości pH roztworu. Ma to związek z niezmiennym znakiem ładunku jonów bez względu na odczyn układu [D4, D5, D8, D10].

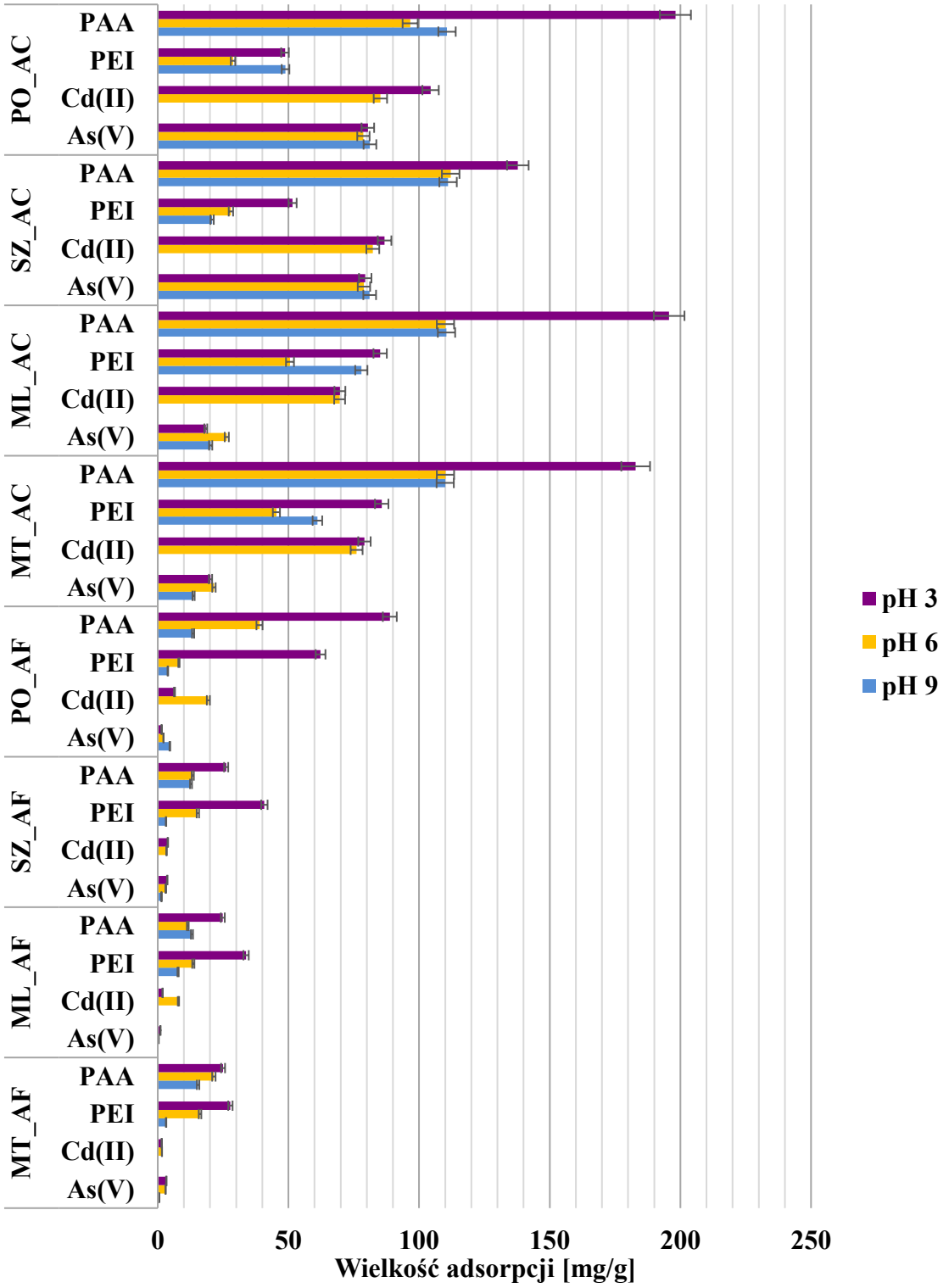

Rysunek 3. Wielkość adsorpcji PAA i PEI oraz jonów Cd(II) i As(V) na powierzchni materiałów węglowych w pH 3, 6 oraz 9 z układów jednoskładnikowych (C_0=200 ppm)

Badania przebiegu równowagowych izoterm adsorpcji pozwoliły określić maksymalną pojemność adsorpcyjną biowęgli aktywnych dla badanych adsorbatów. Przebieg krzywych uzyskanych dla jonów metali dopasowano do teoretycznych modeli izoterm i stwierdzono, że adsorpcja jonów Cd(II) oraz As(V) na powierzchni wszystkich adsorbentów najlepiej opisywana jest za pomocą modeli Freundlicha i Dubinina-Radushkevicha, co świadczy o adsorpcji zachodzącej w porach, heterogenicznym energetycznie charakterze miejsc aktywnych oraz tworzeniu wielowarstwy adsorpcyjnej. Z uwagi na założenia zastosowanych teorii niemożliwe było użycie ich do opisu adsorpcji makrocząsteczek polimerowych. Analiza kinetyki adsorpcji polimerów jonowych i jonów metali ciężkich oraz jej dopasowanie do modeli teoretycznych wykazała, że wiązanie PAA i PEI oraz jonów Cd(II) i As(V) na powierzchni biowęgli aktywnych zachodzi głównie na drodze oddziaływań chemicznych (model pseudo-drugiego-rzędu).

Poli(kwas akrylowy) jest adsorbowany w największych ilościach spośród wszystkich badanych adsorbatów (Rys. 4). W układach jednoskładnikowych jego adsorpcja jest częściowo zależna od liczby grup funkcyjnych obecnych na powierzchni adsorbentu. W przypadku zastosowania biowęgli aktywnych AC, ilość zaadsorbowanego PAA jest wyraźnie niższa na powierzchni materiału SZ_AC, który charakteryzuje się najniższą zawartością grup funkcyjnych (Tabela 4). Z kolei wśród węgli AF, najbardziej efektywny pod względem wiązania PAA okazał się biowęgiel aktywny uzyskany z pokrzywy, wykazujący najwyższą liczbę powierzchniowych grup funkcyjnych. W układach dwuskładnikowych, obecność polietylenoiminy powoduje spadek wielkości adsorpcji poli(kwasu akrylowego) na powierzchni biowęgli otrzymanych na drodze aktywacji chemicznej (w pH 3). Jest to związane z adsorpcją PEI na zewnętrznej powierzchni ciała stałego, co skutkuje blokowaniem dostępu kłębkom PAA do wnętrza porów. Z kolei na powierzchni materiałów otrzymanych z zastosowaniem bezpośredniej aktywacji fizycznej obecność kationowego polimeru zwiększa adsorpcję PAA. W tym przypadku, z uwagi na słabiej rozwiniętą powierzchnię adsorbentów decydujący wkład wnosi adsorpcja tworzących się w roztworze kompleksów PAA-PEI, umożliwiająca formowanie wielowarstwy adsorpcyjnej [D4-D7, D9]. Jony kadmu i arsenu, ze względu na swoje znacznie niższe powinowactwo do powierzchni biowęgli aktywnych, nie mają znaczącego wpływu na wielkość adsorpcji PAA.

Wielkość adsorpcji polietylenoiminy w układzie jednoskładnikowym zależy głównie od wielkości zewnętrznej powierzchni właściwej adsorbentów. Wynika to z faktu jej rozwiniętej konformacji w szerokim zakresie pH, co praktycznie uniemożliwia wnikanie łańcuchów PEI do struktur porowatych materiałów węglowych. Obecność poli(kwasu akrylowego) w roztworze, skutkuje powstaniem kompleksów PAA-PEI, które wykazują niższe powinowactwo do powierzchni adsorbentu, w porównaniu do cząsteczek PEI [D4-D7, D9]. Proces formowania kompleksów między różnoimiennie naładowanymi polimerami prowadzi do neutralizacji ich ładunku, przez co ich oddziaływanie elektrostatyczne z powierzchnią ciał stałych jest znacznie mniej efektywne. Obecność jonów Cd(II) oraz As(V) ma negatywny wpływ na wielkość adsorpcji kationowego polimeru na powierzchni materiałów uzyskanych na drodze bezpośredniej aktywacji fizycznej. Ma to związek z blokowaniem dostępnych miejsc adsorpcyjnych i modyfikacją powierzchni adsorbentów przez zaadsorbowane jony metali ciężkich. Na powierzchni biowęgli aktywnych otrzymanych przy zastosowaniu wariantu chemicznego, efekt ten nie jest widoczny z uwagi na znacznie silniej rozwiniętą powierzchnię właściwą tych ciał stałych.

Jony metali ciężkich są adsorbowane mniej efektywnie na powierzchni wszystkich badanych materiałów w porównaniu do polimerów jonowych. Biowęgle aktywne uzyskane z łodyg pokrzywy charakteryzują się najwyższą zawartością powierzchniowych grup funkcyjnych, zarówno wśród materiałów uzyskanych na drodze bezpośredniej aktywacji fizycznej, jak i aktywacji chemicznej, dzięki czemu są najlepszymi adsorbentami jonów kadmu(II) z układów jednoskładnikowych. Dodatek polimerów jonowych skutkuje obniżeniem wielkości adsorpcji jonów Cd(II) na skutek formowania kompleksów metal-polimer (typu Cd(II)-PAA), wykazujących tendencję do pozostania w roztworze. W związku z konkurencją o miejsca adsorpcyjne dodatnio naładowanych makrocząsteczek polietylenoiminy oraz jonów kadmu, spadek efektywności adsorpcji jonów Cd(II) jest bardziej zauważalny w przypadku obecności PEI niż PAA [D4, D5, D8, D10].

Jony As(V) w układach jednoskładnikowych wykazują najwyższe powinowactwo do biowęgli aktywnych PO_AC oraz SZ_AC. Obecność polimerów jonowych całkowicie blokuje adsorpcję jonów arsenu na powierzchni biowęgli aktywnych otrzymanych

poprzez bezpośrednią aktywację fizyczną oraz znacznie obniża wielkość adsorpcji na powierzchni materiałów uzyskanych z wykorzystaniem aktywacji chemicznej. Podobnie jak w przypadku jonów kadmu, w układach zawierających jednoimiennie naładowane jony oraz polimer jonowy spadek adsorpcji wynika przede wszystkim z konkurencji o powierzchniowe miejsca aktywne [D4, D5, D8, D10].

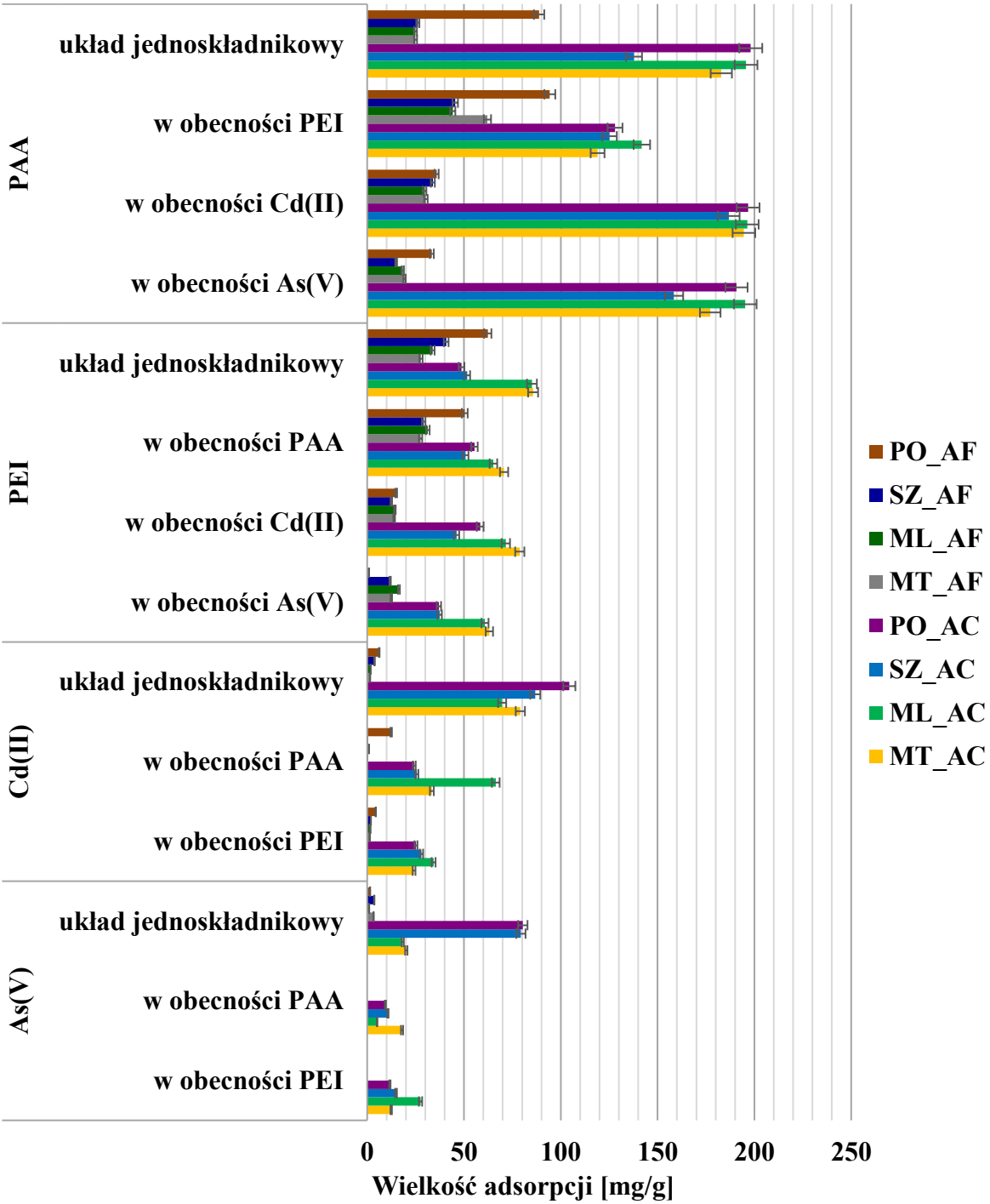

Rysunek 4. Wielkość adsorpcji PAA i PEI oraz jonów Cd(II) i As(V) na powierzchni biowęgli aktywnych w pH 3, z układów jedno- i dwuskładnikowych (C_0=200 ppm)

Maksymalne wielkości adsorpcji uzyskane dla poszczególnych materiałów węglowych zestawiono w Tabeli 6. Wskazują one jednoznacznie, że biowęgle aktywne charakteryzują się wyższymi pojemnościami adsorpcyjnymi w kierunku polimerów jonowych. Należy podkreślić, że pojemności adsorpcyjne biowęgla aktywnego ML_AC w odniesieniu do polimerów jonowych są najwyższymi wartościami dostępnymi w literaturze (PAA – 430,3 mg/g; PEI – 495,9 mg/g), co świadczy o wysokim potencjale aplikacyjnym uzyskanych materiałów.

Tabela 6. Maksymalne pojemności sorpcyjne dla poszczególnych biowęgli aktywnych

Materiał	Maksymalna wielkość adsorpcji [mg/g]			
	PAA	PEI	Cd(II)	As(V)
PO_AF	80,8	80,0	19,4	4,0
SZ_AF	23,9	51,3	3,8	3,6
ML_AF	27,4	94,2	7,9	1,0
MT_AF	59,3	47,9	5,0	3,0
PO_AC	272,8	156,0	218,3	205,5
SZ_AC	148,0	139,1	214,0	204,9
ML_AC	430,3	495,9	135,8	109,6
MT_AC	413,8	495,2	124,4	69,8

Analiza skuteczności biowęgli aktywnych otrzymanych z łodyg melisy w kolejnych cyklach adsorpcyjno-desorpcyjnych udowodniła, że adsorbenty te mogą być z powodzeniem regenerowane i stosowane wielokrotnie (Rys. 5). W przypadku biowęgla ML_AC wielkość adsorpcji poli(kwasu akrylowego) spadła w trzech początkowych cyklach adsorpcji, co jest zapewne związane ze zmniejszeniem dostępności przestrzeni w obrębie struktury porowatej i w konsekwencji spadkiem ilości miejsc aktywnych. W czwartym cyklu obserwowano jednak wzrost wielkości adsorpcji wynikający z tworzenia kompleksów polimerowych na powierzchni adsorbentu (o ok. 50 mg/g). W układzie jednoskładnikowym formowane są kompleksy PAA-PAA na drodze wiązań wodorowych, natomiast w układzie dwuskładnikowym możliwe jest powstawanie zarówno kompleksów PAA-PAA, jak i PAA-PEI. Potwierdzeniem zwiększenia udziału adsorpcji powierzchniowej w kolejnych cyklach jest wzrastająca efektywność desorpcji. W związku z mniej rozbudowaną strukturą porowatą węgla aktywnego ML_AF i powierzchniową adsorpcją polimeru w tym układzie, zaobserwowano wzrost wielkości adsorpcji PAA w kolejnych cyklach [D4].

Wielkość adsorpcji oraz efektywność desorpcji polietylenoiminy z powierzchni obu biowęgli aktywnych pozostaje na podobnym poziomie we wszystkich cyklach adsorpcyjnych. Jest wynikiem adsorpcji PEI głównie na zewnętrznej powierzchni adsorbentu, co skutkuje jej modyfikacją poprzez wytworzeniem nowych miejsc aktywnych i w konsekwencji formowaniem kompleksów polimer-polimer w warstwie adsorpcyjnej.

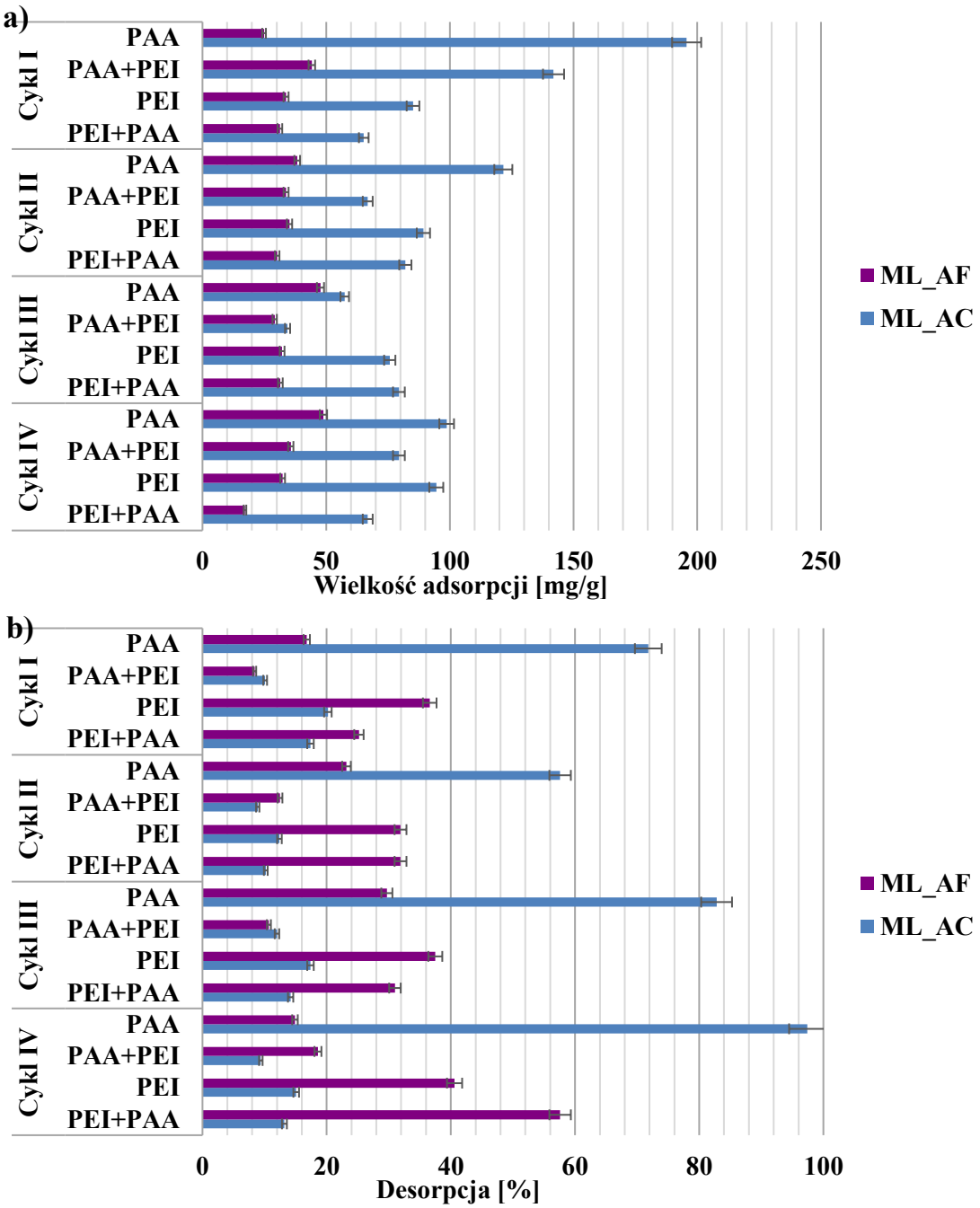

Rysunek 5. Wielkość adsorpcji (a) oraz efektywność desorpcji (b) polimerów jonowych w kolejnych cyklach adsorpcyjno-desorpcyjnych dla biowęgli aktywnych otrzymanych z łodyg melisy

4.3.2. Wpływ obecności adsorbatów na właściwości elektrokinetyczne biowęgli aktywnych

Wpływ adsorbatów na właściwości elektrokinetyczne biowęgli aktywnych omówiono na przykładzie materiału ML_AC (Rys. 6 i 7). Polimery adsorbują się na powierzchni ciał stałych poprzez oddziaływanie tylko fragmentów ich łańcuchów, a dokładnie poprzez segmenty znajdujące się w strukturach typu ciągów (bezpośrednio przyłączonych do powierzchni adsorbentu). Pozostałe części zaadsorbowanych makrocząsteczek tworzą struktury typu pętli oraz ogonów znajdujące się w warstwie przypowierzchniowej roztworu. Znak i gęstość ładunku powierzchniowego (σ_0) uzależnione są od liczby zdysocjowanych grup funkcyjnych polimeru w tych trzech rodzajach struktur. Ujemnie naładowane grupy PAA znajdujące się w segmentach typu ciągów powodują wzrost wartości σ_0 na skutek indukowania dodatkowej ilości grup powierzchniowych o ładunku dodatnim, podczas gdy zdysocjowane grupy karboksylowe polikwasu ulokowane w strukturach typu pętli i ogonów wpływają na obniżenie wartości σ_0. Sumaryczny wkład tych drugich jest większy i w efekcie obserwuje się spadek gęstości ładunku powierzchniowego biowęgla aktywnego w całym badanym zakresie pH. Z kolei obdarzone ładunkiem dodatnim aminowe ugrupowania zaadsorbowanych łańcuchów PEI powodują wzrost wartości σ_0 zgodnie z analogicznym mechanizmem jak w przypadku PAA (Rys. 6). Zjawiskom tego typu towarzyszy zmiana położenia punktów pH_{pzc} w stosunku do układów bez polimerów, odpowiednio w kierunku niższych wartości pH dla PAA oraz wyższych wartości pH w przypadku PEI. Wpływ polimerów na wartość σ_0 jest najmniej widoczny przy wartościach pH, w których łańcuchy polimerowe występują w formie niezjonizowanej i wzrasta wraz ze stopniem naładowania łańcucha. W dwuskładnikowych roztworach polimerowych obserwuje się zależności pośrednie w porównaniu do układów jednoskładnikowych, a uzyskane krzywe lokują się pomiędzy tymi otrzymanymi dla pojedynczych związków wielkocząsteczkowych [D4-D6].

Wpływ jonów metali na gęstość ładunku powierzchniowego biowęgli aktywnych jest mniej zauważalny w porównaniu do polimerów, co może mieć związek ze znacząco niższym poziomem adsorpcji substancji nieorganicznych. Jony Cd(II) oraz As(V) podczas wiązania na granicy faz ciało stałe/roztwór indukują powstawanie grup powierzchniowych o przeciwnym znaku ładunku do znaku ładunku adsorbującego się

jonu. Kationy kadmu(II) powodują wytworzenie grup o ładunku ujemnym, zmniejszając gęstość ładunku powierzchniowego, natomiast adsorpcja anionów arsenu(V) skutkuje powstaniem grup powierzchniowych o ładunku dodatnim, co podwyższa nieznacznie wartość σ_0. W przypadku układów zawierających jony metalu oraz polimery jonowe, znak ładunku makrocząsteczek ma decydujący wpływ na gęstość ładunku powierzchniowego, co jest szczególnie zauważalne w przypadku układów zwierających PEI [D4, D5, D8, D10].

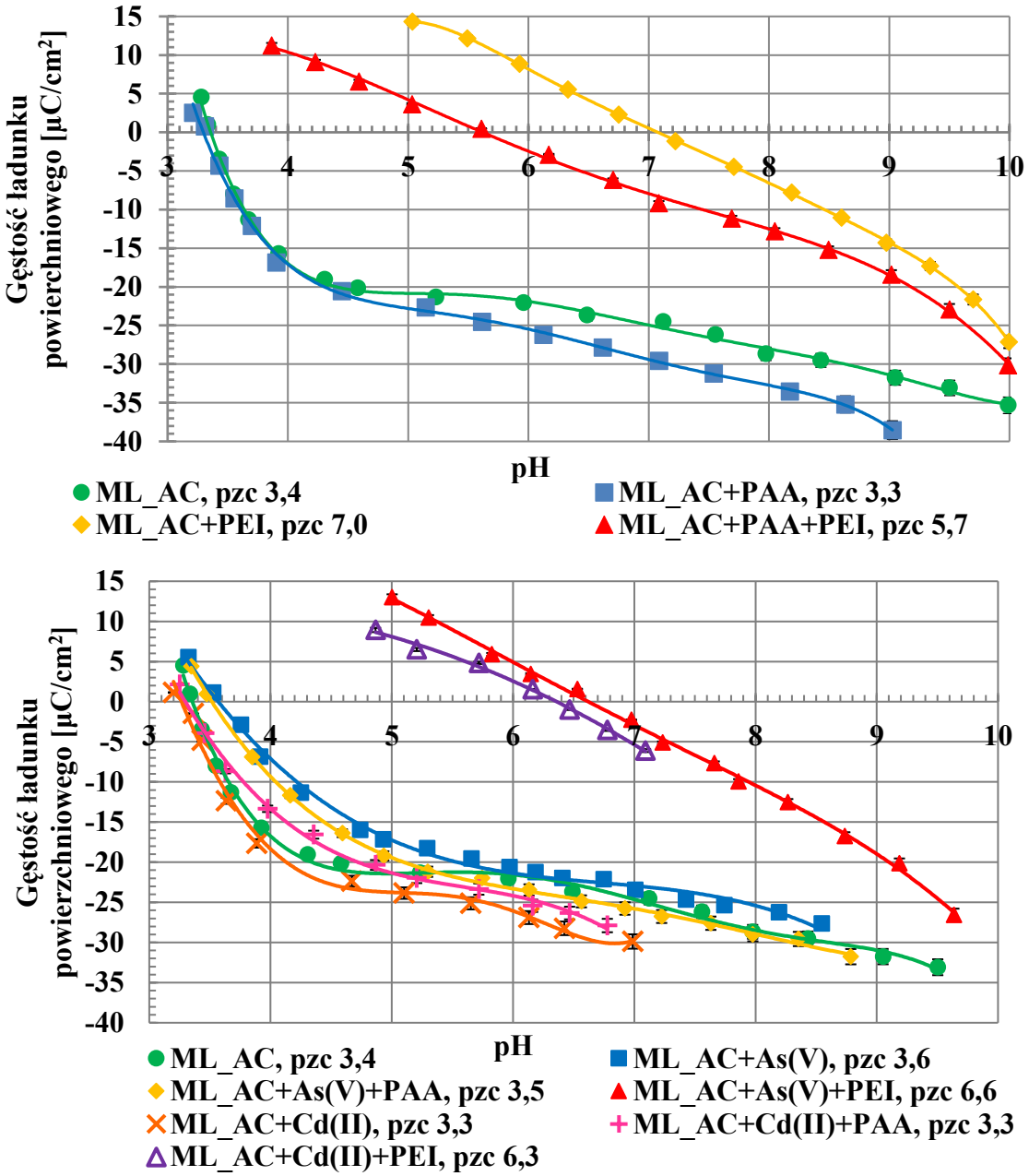

Rysunek 6. Wpływ obecności adsorbatów na gęstość ładunku powierzchniowego biowęgla aktywnego ML_AC w zależności od pH roztworu

Na rysunku 7 przedstawiono zmiany potencjału dzeta (ζ) cząstek biowęgla aktywnego ML_AC w funkcji pH roztworu będące konsekwencją dodatku adsorbatów. Wskazują one, że dodatek poli(kwasu akrylowego) powoduje obniżenie potencjału dzeta oraz przesunięcie punktu pH_{iep} w stronę niższych wartości pH. Jest to związane z dużym rozmiarem makrocząsteczek polimerowych, które jak już wspomniano wcześniej, wiążą się z powierzchnią adsorbentu tylko przez pojedyncze segmenty występujące w strukturach ciągów. Znaczne fragmenty zaadsorbowanego łańcucha ulokowane są w pewnej odległości od powierzchni materiału węglowego (tworząc struktury pętli i ogonów) oraz występują w obszarze płaszczyzny poślizgu, której ładunek jest charakteryzowany przez potencjał elektrokinetyczny. W przypadku PAA jego zdysocjowane grupy karboksylowe obecne w tym obszarze *pwe* są odpowiedzialne za obniżenie potencjału ζ, natomiast zjonizowane grupy aminowe PEI powodują wyraźny wzrost wartości tego parametru (w stosunku do układu bez polimerów). W przypadku suspensji zawierającej oba związki wielkocząsteczkowe obserwuje się efekt pośredni w porównaniu do jednoskładnikowych układów tych adsorbatów [D4-D6].

Dodatek jonów kadmu(II) skutkuje wzrostem wartości potencjału ζ, za co odpowiada przede wszystkim zmiana składu jonowego warstwy przypowierzchniowej roztworu. Proces wiązania jonów metalu z powierzchnią adsorbentu wymusza przemieszczenie się dodatnio naładowanych jonów elektrolitu podstawowego (Na^+) w kierunku płaszczyzny poślizgu, co skutkuje zwiększeniem liczby tych ładunków w obrębie płaszczyzny poślizgu, a w konsekwencji wzrostem wartości potencjału dzeta. Wpływ jonów arsenu(V) na wartość potencjału elektrokinetycznego zależy od stopnia jego hydratacji. W zakresie niskich wartości pH, w których jon As(V) jest całkowicie zhydratowany obserwuje się wzrost potencjału dzeta. Wraz ze wzrostem pH, któremu towarzyszy dehydratacja jonów As(V) i wzrost ich ładunku ujemnego, ma miejsce stopniowy spadek wartości potencjału ζ. Dla układów dwuskładnikowych zawierających polimer jonowy oraz jon metalu, decydujący wpływ na właściwości elektrokinetyczne układu wywiera związek wielkocząsteczkowy, podobnie jak w przypadku zmian gęstości ładunku powierzchniowego [D4, D5, D8, D10].

Zależności elektrokinetyczne uzyskane dla wodnych suspensji cząstek ML_AC są analogiczne do tych obserwowanych dla innych badanych układów materiał węglowy – polimer jonowy/jon metalu.

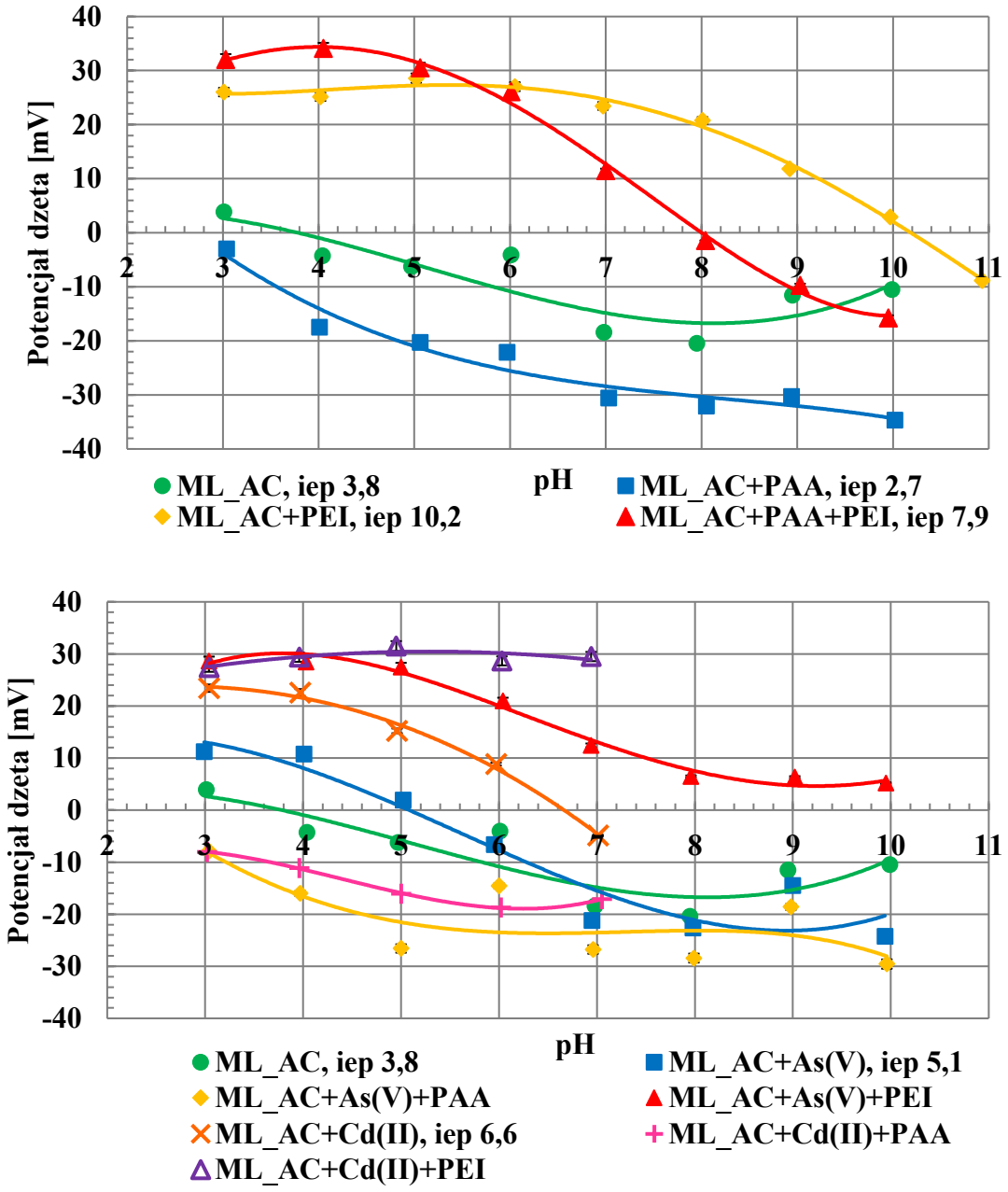

Rysunek 7. Wpływ obecności adsorbatów na potencjał dzeta cząstek biowęgla aktywnego ML_AC w zależności od pH roztworu

4.3.3. Stabilność suspensji wodnych zawierających biowęgle aktywne oraz polimery jonowe

Wpływ dodatku polimerów jonowych na wielkość agregatów tworzonych przez cząstki biowęgla aktywnego ML_AC w układach o różnym pH przestawiono na rysunku 8. W przypadku obecności poli(kwasu akrylowego) w formie skłębionej (w pH 3), obserwowany jest wzrost wielkości agregatów, co związane jest z neutralizacją dodatniego ładunku powierzchni adsorbentu. Wraz ze wzrostem pH dysocjacja grup funkcyjnych zaadsorbowanych łańcuchów PAA ulega intensyfikacji, co prowadzi do wzrostu odpychania elektrostatycznego cząstek ciała stałego pokrytego warstewkami polimerowymi. Skutkuje to zmniejszeniem się rozmiaru agregatów w układach o pH 6 i 9 w efekcie pojawiających się oddziaływań elektrosterycznych. Obecność polietylenoiminy, której makrocząsteczki adsorbowane są w kierunku prostopadłym do powierzchni adsorbentu (w pH 3), powoduje nieznaczny wzrost wielkości agregatów, co może wynikać z tworzenia się nielicznych mostków polimerowych między cząstkami ciała stałego. Wraz ze wzrostem pH jonizacja zaadsorbowanych łańcuchów PEI zmniejsza się, co skutkuje coraz bardziej równoległym ułożeniem makrocząsteczek na powierzchni i neutralizacją ujemnego ładunku cząstek biowęgla aktywnego (w pH 6 i 9). Prowadzi to do zmniejszenia odpychania elektrostatycznego między cząstkami adsorbentu i w konsekwencji wzrostu rozmiaru powstających agregatów. W układach zawierających równocześnie dwa polimery jonowe obserwowany jest wzrost wielkości agregatów tworzonych przez cząstki biowęgla aktywnego. Jest to wynikiem obecności na powierzchni adsorbentu kompleksów PAA-PEI, która sprzyja efektywnej agregacji cząstek ciała stałego.

Ocena stabilności suspensji cząstek biowęgla aktywnego ML_AC w obecności polimerów w pH 3 wykazała, że PAA ma minimalny wpływ na ten parametr (Rys. 9). Jest to związane ze skłębioną konformacją łańcucha polimerowego, który adsorbuje się w znaczącej mierze w porach materiału węglowego. Obserwowany w tym pH wzrost rozmiaru agregatów tworzonych w układzie ML_AC+PAA sugerowałby większą tendencję suspensji do sedymentacji, czego nie potwierdziły jednak pomiary absorbancji. Zatem struktura tworzonych na drodze neutralizacji ładunku flokuł jest bardziej luźna, co sprawia, że mogą one w dłuższym czasie pozostawać w roztworze nie opadając na dno

fiolki pomiarowej. Obecność PEI powoduje z kolei obniżenie stabilności suspensji, poprzez zwiększenie rozmiaru agregatów i wzrost tendencji do flokulacji mostkowej [27]. W układzie zawierającym oba polimery jonowe, stwierdzono zdecydowany wzrost stabilności suspensji, na skutek tworzenia agregatów o luźnej strukturze oraz obecności w roztworze niezaadsorbowanych łańcuchów polimerowych (spadek wielkości adsorpcji obu polimerów w ich układach dwuskładnikowych) [D10].

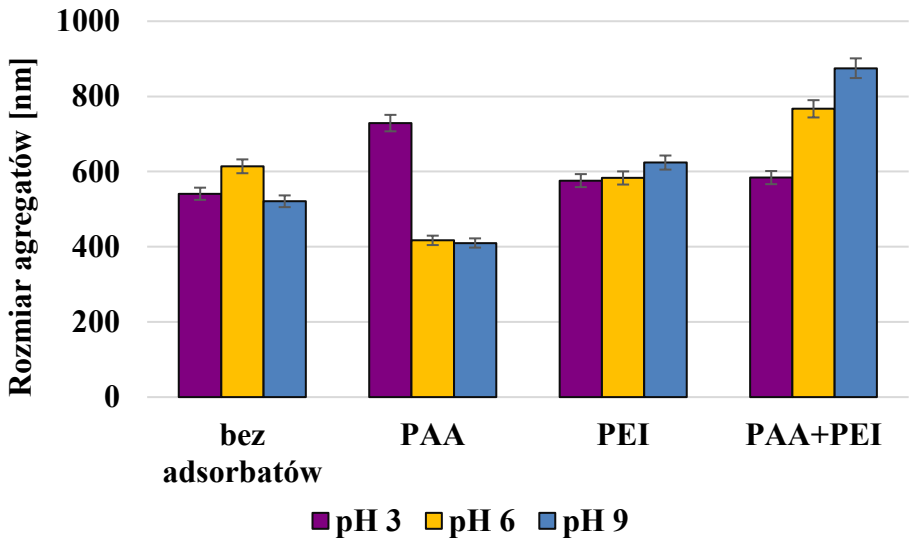

Rysunek 8. Wpływ dodatku polimerów jonowych na wielkość agregatów biowęgla aktywnego ML_AC tworzonych w suspensjach wodnych

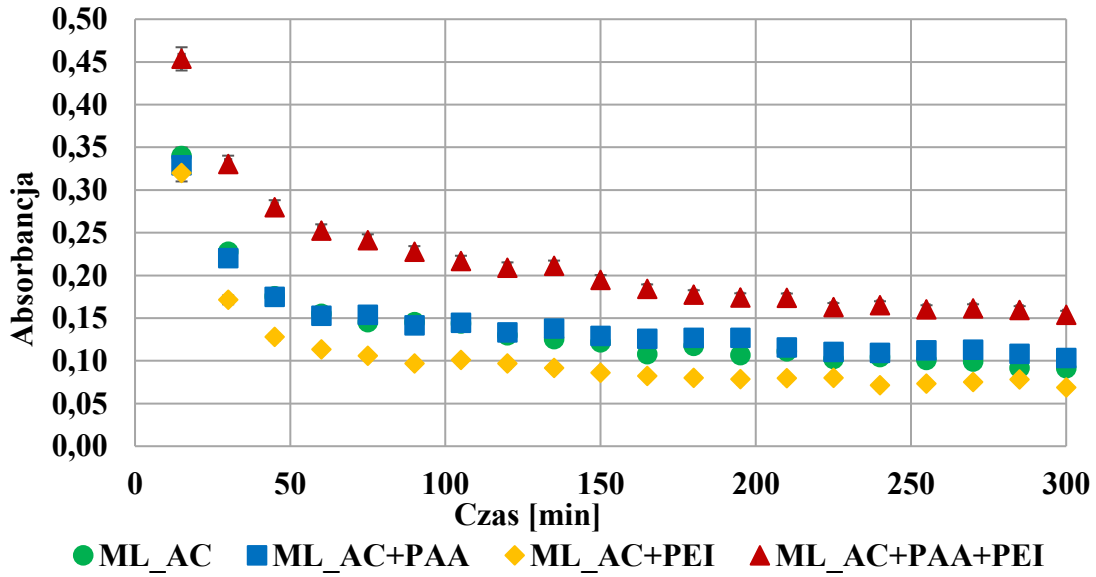

Rysunek 9. Stabilność wodnych suspensji cząstek biowęgla aktywnego ML_AC w obecności adsorbatów polimerowych w pH 3

5. Podsumowanie

Przeprowadzone w ramach realizacji rozprawy doktorskiej badania umożliwiły sformułowanie następujących wniosków:

1. Analiza zawartości związków lignocelulozowych w prekursorach roślinnych wykazała, że zastosowane materiały składają się głównie z ligniny. Stwierdzono również, że wraz z jej wzrastającą zawartością wzrasta stężenie grup funkcyjnych na powierzchni biowęgli aktywnych uzyskanych z wykorzystaniem chemicznego wariantu aktywacji. Ponadto, zawartość hemicelulozy w prekursorach ma bezpośredni wpływa na rozwinięcie powierzchni właściwej materiałów węglowych, niezależnie od zastosowanej procedury pirolizy lub aktywacji.

2. Łodygi pokrzywy, szałwii, melisy oraz mięty (stanowiące materiał odpadowy przemysłu zielarskiego) mogą zostać z powodzeniem zastosowane jako prekursory do wytwarzania biowęgli oraz biowęgli aktywnych. Materiały uzyskane na drodze pirolizy charakteryzują się słabo rozwiniętą powierzchnią właściwą. Aktywacja chemiczna pozwoliła otrzymać biowęgle aktywne o najbardziej rozbudowanej strukturze porowatej (powierzchnia właściwa: 801-1145 m^2/g; średni rozmiar porów: 3,93-5,12 nm), z kolei bezpośrednia aktywacja fizyczna doprowadziła do uzyskania materiałów o najwyższej zawartości powierzchniowych grup funkcyjnych (2,19-4,89 mmol/g).

3. Biowęgle wykazują korzystne właściwości fizykochemiczne, które predysponują je do potencjalnego zastosowania w energetyce. Najwyższą wartość ciepła spalania uzyskano dla materiału ML_B (20,4 MJ/kg), który charakteryzuje się również najlepszym wskaźnikiem wydajności energetycznej – 67,3 %.

4. Biowęgle aktywne otrzymane na drodze aktywacji chemicznej odznaczają się lepszymi właściwościami adsorpcyjnymi w odniesieniu do wszystkich badanych substancji, w porównaniu do analogicznych materiałów uzyskanych z wykorzystaniem CO_2. Najwyższą efektywność adsorpcję zaobserwowano w przypadku poli(kwasu akrylowego), osiągając niemal 100 %, przy początkowym stężeniu C_0=200 ppm.

5. Maksymalne poziomy adsorpcji polimerów jonowych uzyskano na powierzchni biowęgla aktywnego ML_AC i wynoszą one odpowiednio 430,3 mg/g dla PAA oraz 495,9 mg/g dla PEI. Są to najwyższe zaadsorbowane ilości tych polimerów opisane dotychczas w literaturze.

6. Polimery jonowe są adsorbowane w największych ilościach z roztworów o pH 3. W przypadku PAA jest to związane ze skłębioną konformacją łańcucha polimerowego, który może wnikać również do wnętrza porów, natomiast dla PEI z adsorpcją rozwiniętej makrocząsteczki w kierunku prostopadłym do powierzchni adsorbentu. Obie formy makrocząsteczek polimerowych skutkują znacznym upakowaniem warstwy adsorpcyjnej. Adsorpcja jonów metali jest w niewielkim stopniu zależna od pH roztworu.

7. Obecność w układzie dwóch polimerów o odmiennym charakterze jonowym prowadzi do powstawania kompleksów polimer-polimer, które wykazują niższe powinowactwo do powierzchni biowęgli aktywnych w porównaniu do pojedynczych związków wielkocząsteczkowych.

8. W układach dwuskładnikowych zawierających polimer i jon metalu obserwuje się spadek wielkości adsorpcji tych substancji w porównaniu do ich układów jednoskładnikowych. Jest to konsekwencją tworzenia kompleksów metal-polimer, wykazujących mniejsze powinowactwo do powierzchni biowęgli aktywnych, a także w przypadku adsorbatów naładowanych jednoimiennie - konkurencji o miejsce aktywne adsorbentu.

9. Biowęgle aktywne mogą być z powodzeniem regenerowane i wykorzystywane ponownie do adsorpcji polimerów jonowych w kolejnych cyklach. Niecałkowita desorpcja makrocząsteczek z powierzchni adsorbentów skutkuje tworzeniem dodatkowych centrów adsorpcyjnych i powstawaniem kompleksów powierzchniowych, czego rezultatem jest wzrost ilości zaadsorbowanego polimeru.

10. Polimery jonowe i jony metali ciężkich powodują wyraźne modyfikacje w strukturze podwójnej warstwy elektrycznej utworzonej na powierzchni

materiałów węglowych, czego przejawem są uzyskane zmiany w wartościach gęstości ładunku powierzchniowego i potencjału dzeta.

11. Polimery jonowe na skutek adsorpcji na powierzchni biowęgli aktywnych, wywołują wyraźne zmiany w gęstości ładunku powierzchniowego oraz potencjale dzeta, które są zgodne ze znakiem ładunku grup funkcyjnych obecnych w strukturach pętli i ogonów zaadsorbowanych łańcuchów polimerowych, znajdujących się w warstwie przypowierzchniowej roztworu oraz w obszarze płaszczyzny poślizgu. W przypadku anionowego PAA obserwuje się obniżenie wartości σ_0 i ζ, natomiast dla kationowej PEI – wzrost wartości tych parametrów.

12. Adsorpcja jonów metali ciężkich skutkuje powstawaniem grup powierzchniowych o znaku ładunku przeciwnym do znaku ładunku adsorbowanego jonu, co prowadzi do zmian gęstości ładunku powierzchniowego. Dodatkowo migracja jonów metali w kierunku powierzchni ciała stałego, wywołuje przemieszczenie jonów elektrolitu podstawowego (Na^+ lub Cl^-) do obszaru płaszczyzny poślizgu, prowadząc do zmian w wartości potencjału elektrokinetycznego.

13. Polimery jonowe wpływają na stabilność suspensji wodnych zawierających biowęgle aktywne, jednakże mechanizm stabilizacji bądź destabilizacji zależy od pH roztworu determinującego stopień jonizacji łańcuchów polimerowych oraz znak i gęstość ładunku powierzchniowego adsorbentu.

W efekcie przeprowadzonych badań oraz wnikliwej analizy uzyskanych rezultatów w pełni potwierdzono hipotezy badawcze H1-H3. Łodygi ziół stanowiących odpad z przemysłu zielarskiego, zostały z powodzeniem zastosowane do wytworzenia materiałów węglowych. Biowęgle otrzymane na drodze pirolizy charakteryzują się korzystnymi właściwościami fizykochemicznymi, umożliwiającymi ich wykorzystanie w celach energetycznych, z kolei biowęgle aktywne uzyskane na drodze bezpośredniej aktywacji fizycznej i aktywacji chemicznej wykazują satysfakcjonujące właściwości adsorpcyjne.

Hipoteza H4 została potwierdzona częściowo, gdyż aktywacja chemiczna pozwoliła na otrzymanie materiałów o większym średnim rozmiarze porów niż

bezpośrednia aktywacja fizyczna, jednakże wszystkie biowęgle aktywne wykazują wyższą pojemność adsorpcyjną w kierunku polimerów jonowych.

Z kolei hipoteza H5 nie została potwierdzona. Badania wykazały jednoznacznie, że w układach dwuskładnikowych zawierających różnoimiennie naładowane makrocząsteczki polimerowe i jony metali, wielkość ich adsorpcji maleje na skutek tworzenia kompleksów polimer-polimer i polimer-metal, które wykazują większą tendencję do pozostawania w roztworze.

6. Bibliografia

1. Mohan, D., Pittman Jr, C. U., Steele, P. H. (2006). Pyrolysis of wood/biomass for bio-oil: a critical review. Energy fuels, 20(3), 848-889, doi: 10.1021/ef0502397
2. Diaz, L. F., De Bertoldi, M., & Bidlingmaier, W. (Eds.). (2011). Compost science and technology (Vol. 8). Elsevier
3. Waqas, M., Aburiazaiza, A. S., Miandad, R., Rehan, M., Barakat, M. A., Nizami, A. S. (2018). Development of biochar as fuel and catalyst in energy recovery technologies. J. Cleaner Prod., 188, 477-488, doi: 10.1016/j.jclepro.2018.04.017
4. Ro, K. S., Cantrell, K. B., Hunt, P. G. (2010). High-temperature pyrolysis of blended animal manures for producing renewable energy and value-added biochar. Ind. Eng. Chem. Res., 49(20), 10125-10131, doi: 10.1021/ie101155m
5. Chen, W., Meng, J., Han, X., Lan, Y., Zhang, W. (2019). Past, present, and future of biochar. Biochar, 1(1), 75-87, doi: 10.1007/s42773-019-00008-3
6. Sultana, M., Rownok, M. H., Sabrin, M., Rahaman, M. H., Alam, S. N. (2022). A review on experimental chemically modified activated carbon to enhance dye and heavy metals adsorption. Cleaner Eng. Technol., 6, 100382, doi: 10.1016/j.clet.2021.100382
7. Wang, B., Lan, J., Bo, C., Gong, B., Ou, J. (2023). Adsorption of heavy metal onto biomass-derived activated carbon. RSC Adv., 13(7), 4275-4302, doi: 10.1039/D2RA07911A
8. Avila, A. M., Araoz, M. E. (2023). Merging renewable carbon-based materials and emerging separation concepts to attain relevant purification applications in a circular economy. Ind. Eng. Chem. Res., 62(12), 4793-4799, doi: 10.1021/acs.iecr.2c04517
9. Boehm H.P., Diehl, E., Heck, W., Sappok, R. (1964). Surface oxides of carbon, Angew. Chem. 3 669–677, doi: 10.1002/anie.196406691
10. Arkaban, H., Barani, M., Akbarizadeh, M. R., Pal Singh Chauhan, N., Jadoun, S., Dehghani Soltani, M., Zarrintaj, P. (2022). Polyacrylic acid nanoplatforms: antimicrobial, tissue engineering, and cancer theranostic applications. Polymers, 14(6), 1259, doi: 10.3390/polym14061259

11. Shin, W., Chung, K. (2023). Preparation and characterization of poly (acrylic acid)-based self-healing hydrogel for 3D shape fabrication via extrusion-based 3D printing. Materials, 16(5), 2085, doi: 10.3390/ma16052085

12. Vancha, A.R., Govindaraju, S., Parsa, K.V.; Jasti, M., González-García, M., Ballestero, R.P. (2004). Use of polyethyleneimine polymer in cell culture as attachment factor and lipofection enhance. BMC Biotechnol., 4, 23, doi: 10.1186/1472-6750-4-23

13. Chibowski, S. Wiśniewska, M., Marczewski, A.W., Pikus, S. (2003). Application of the SAXS method and viscometry for determination of the thickness of adsorbed polymer layers at the ZrO2 –polymer solution interface. J. Colloid Interface Sci., 267, 1–8, doi: 10.1016/S0021-9797(03)00698-2

14. Von Harpe, A., Petersen, H., Li, Y., Kissel, T. (2000). Characterization of commercially available and synthesized polyethylenimines for gene delivery. J. Control. Release, 69, 309–322, doi: 10.1016/S0168-3659(00)00317-5

15. Khan, Z., Elahi, A., Bukhari, D. A., Rehman, A. (2022). Cadmium sources, toxicity, resistance and removal by microorganisms-A potential strategy for cadmium eradication. J. Saudi Chem. Soc., 26(6), 101569, doi: 10.1016/j.jscs.2022.101569

16. Patel, K. S., Pandey, P. K., Martín-Ramos, P., Corns, W. T., Varol, S., Bhattacharya, P., Zhu, Y. (2023). A review on arsenic in the environment: contamination, mobility, sources, and exposure. RSC Adv., 13(13), 8803-8821, doi: 10.1039/D3RA00789H

17. Hamid, N. H. A., Rushdan, A. I., Nordin, A. H., Husna, S. M. N., Faiz Norrrahim, M. N., Knight, V. F., Tahir, M. I. H. M., Li, G. X., Quan, T. L., Abdullah, A. M., Azwa, N. F. T., Asyraf, M. R. M. (2024). A state-of-art review on the sustainable technologies for cadmium removal from wastewater. Water Reuse, 14(3), 312-341, doi: 10.2166/wrd.2024.143

18. Raju, N. J. (2022). Arsenic in the geo-environment: A review of sources, geochemical processes, toxicity and removal technologies. Environ. Res., 203, 111782, doi: 10.1016/j.envres.2021.111782

19. Das, T.K., Bezbaruah, A.N. (2021). Comparative study of arsenic removal by iron-based nanomaterials: potential candidates for field applications, Sci. Total Environ. 764, 142914, doi: 10.1016/j.scitotenv.2020.142914

20. Awad, A. M., Shaikh, S. M., Jalab, R., Gulied, M. H., Nasser, M. S., Benamor, A., Adham., S. (2019). Adsorption of organic pollutants by natural and modified clays: a comprehensive review. Sep. Purif. Technol. 228, 115719, doi: 10.1016/j.seppur.2019.115719

21. Wang, J., Guo, X. (2020). Adsorption kinetic models: physical meanings, applications, and solving methods, J. Hazard. Mat. 390, 122156, doi: 10.1016/j.jhazmat.2020.122156

22. Crummett, W.B., Hummel, R.A. (1963). The determination of traces of polyacrylamides in water. J. Am. Water Work. Assoc., 55, 209–219, doi: 10.1002/j.1551-8833.1963.tb01016.x

23. Patkowski, J., Myśliwiec, D., Chibowski, S. (2016). Validation of a new method for spectrophotometric determination of polyethylenimine. Int. J. Polym. Anal. Charact. 21, 486–494, doi: 10.1080/1023666X.2016.1168651

24. Ohshima,, H.A. (1994). Simple expression for Henry's function for the retardation effect in electrophoresis of spherical colloidal particles, J. Colloid Interf. Sci. 168 269–271, doi: 10.1006/jcis.1994.1419

25. Janusz, W. (1999). Electrical double layer at the metal oxide–electrolyte interface w: "Interfacial Forces and Fields: Theory and Applications". M. Dekker, New York, vol. 85, Chapter 4

26. Wiśniewska, M., Rejer, K., Pietrzak, R., Nowicki, P. (2022). Biochars and activated biocarbons prepared via conventional pyrolysis and chemical or physical activation of mugwort herb as potential adsorbents and renewable fuels. Molecules, 27(23), 8597, doi: 10.3390/molecules27238597

27. Pelssers EG, M., Stuart MA, C., Fleer, G.J. (1990). Kinetics of bridging flocculation. Role of relaxations in the polymer layer. J. Chem. Soc. Faraday Trans., 86, 1355, doi: 10.1039/ft9908601355

7. Streszczenie pracy w języku polskim

W ramach niniejszej dysertacji doktorskiej sprawdzono możliwość zastosowania łodyg ziół, stanowiących odpad przemysłu zielarskiego do wytwarzania biowęgli i biowęgli aktywnych. Uzyskane materiały poddano ocenie właściwości energetycznych oraz adsorpcyjnych. Produkcja i wykorzystywanie materiałów węglowych pochodzących z odnawialnych surowców jest szczególnie istotna w kontekście wyczerpujących się zasobów naturalnych. Ponadto stosowanie biomasy odpadowej pozwala ograniczyć ilość produkowanych śmieci, których składowanie i utylizacja stanowi istotne wyzwania ekonomiczne i środowiskowe.

Łodygi pokrzywy, szałwii, melisy oraz mięty poddano procesom pirolizy, bezpośredniej aktywacji fizycznej z użyciem CO_2 oraz aktywacji chemicznej z wykorzystaniem H_3PO_4, co pozwoliło na uzyskanie trzech grup materiałów węglowych. Poddano je charakterystyce powierzchniowej z zastosowaniem techniki niskotemperaturowej adsorpcji-desorpcji azotu, określono zawartość powierzchniowych grup funkcyjnych (miareczkowanie Boehma), sprawdzono zawartość pierwiastków C, H, N, S oraz przeprowadzono analizy SEM, XPS i XRF. W przypadku biowęgli otrzymanych na drodze pirolizy wyznaczono parametry energetyczne zgodnie z normą ISO 1928:2009. Z kolei uzyskane biowęgle aktywne zastosowano do adsorpcji poli(kwasu akrylowego), polietylenoiminy, jonów Cd(II) i As(V) z jedno- i dwuskładnikowych roztworów wodnych.

Biowęgle aktywne poddano również analizie właściwości elektrokinetycznych. Określono gęstość ładunku powierzchniowego oraz wartość potencjału dzeta w zależności od pH dla układów bez oraz w obecności adsorbatów. Wyznaczono punkt ładunku zerowego oraz punkt izoelektryczny badanych materiałów, a dla wybranych wartości pH sprawdzono także wielkość agregatów. Uzyskane wyniki miały istotne znaczenie przy określaniu mechanizmu wiązania poszczególnych substancji z powierzchnią adsorbentów. W celu określenia właściwości adsorpcyjnych biowęgli aktywnych zbadano przebieg izoterm adsorpcji w pH 3, 6 oraz 9, a także określono kinetykę procesu.

Analiza parametrów energetycznych biowęgli wykazała, że charakteryzują się one wartością ciepła spalania porównywalną do tradycyjnie stosowanych surowców, takich jak węgiel brunatny czy pellet.

Na podstawie analizy uzyskanych wyników stwierdzono, że wartość pH nie ma znaczącego wpływu na efektywność adsorpcji jonów metali. Z kolei polimery jonowe wykazywały najwyższe wielkości adsorpcji w pH 3. W tych warunkach PAA przyjmuje konformację kłębka polimerowego, co umożliwia mu penetrację porów biowęgla aktywnego, natomiast PEI adsorbuje się w kierunku prostopadłym do powierzchni ciała stałego, co skutkuje największym upakowaniem warstwy adsorpcyjnej.

Udowodniono, że PAA jest najlepiej adsorbowaną substancją ze wszystkich badanych adsorbatów, zarówno układów jedno-, jak i dwuskładnikowych. Obecność w układzie dwóch adsorbatów generalnie obniża wielkość adsorpcji polimerów oraz jonów metali, gdyż powstające wówczas kompleksy polimer-polimer oraz polimer-jon metalu wykazują tendencję do pozostawania w roztworze.

Przeprowadzone badania zdolności regeneracyjnych materiałów węglowych oraz cykli adsorpcji-desorpcji wskazały, że biowęgle aktywne mogą z powodzeniem być regenerowane oraz stosowane ponownie. Ponadto dowiedziono, że wartość adsorpcji polimerów jonowych pozostaje na podobnym poziomie w kolejnych cyklach adsorpcji-desorpcji na skutek powstawania kompleksów polimerowych na powierzchni adsorbentu i tworzenia wielowarstwy adsorpcyjnej.

W toku przeprowadzonych badań potwierdzono możliwość wykorzystania łodyg ziół stanowiących odpad przemysłu zielarskiego do wytwarzania materiałów węglowych, a także wykazano, że otrzymane biowęgle i biowęgle aktywne wykazują znaczący potencjał aplikacyjny w przemyśle energetycznym oraz w ochronie środowiska.

8. Streszczenie pracy w języku angielskim

As part of this doctoral dissertation, the possibility of using herb stalks, a by-product of the herbal industry, for the production of biochars and activated biocarbons was investigated. The obtained materials were evaluated in terms of their energy and adsorption properties. The production and utilization of carbonaceous materials derived from renewable resources is particularly important in the context of depleting natural reserves. Moreover, the use of biomass helps reduce the amount of waste produced, the storage and disposal of which pose significant economic and environmental challenges.

Stalks of the nettle, sage, lemon balm, and mint herbs were subjected to pyrolysis, direct physical activation with CO_2, and chemical activation with H_3PO_4, which allowed for obtaining three groups of carbonaceous materials. They were characterized in terms of the surface properties using the low-temperature nitrogen adsorption–desorption technique, the content of surface functional groups (Boehm titration), the elemental composition (C, H, N, S), as well as SEM, XPS, and XRF analyses. For biochars obtained via pyrolysis, energy parameters were determined in accordance with ISO 1928:2009 standard. In turn, activated biocarbons, were used for adsorption of poly(acrylic acid), polyethyleneimine, Cd(II) and As(V) ions from one- and two-component aqueous solutions.

Activated biocarbons were also analysed for their electrokinetic properties. Surface charge density and zeta potential values as a function of pH were determined for systems both without as well as in the presence of adsorbates. The point of zero charge and the isoelectric point of the studied materials were established, and for selected pH values, the size of aggregates was also determined. The obtained results have a significant impact in identifying the mechanism of examined substances binding to the adsorbent surface. To determine the adsorption properties of activated biocarbons, adsorption isotherms were studied at pH 3, 6, and 9, and the adsorption kinetics were also evaluated.

The analysis of energy parameters of the biochars proved that they are characterized by the calorific value comparable to conventionally used raw materials such as lignite or pellets.

Based on the analysis of the obtained results, it was concluded that pH does not have a significant impact on the adsorption efficiency of metal ions. In contrast, ionic polymers exhibited the highest adsorption values at pH 3. Under these conditions, PAA occurs in a polymeric coil conformation, enabling it to penetrate the pores of activated biocarbon, whereas PEI adsorbs perpendicularly to the solid surface, resulting in the most dense packing of the adsorption layer.

It was demonstrated that PAA is adsorbed in the greatest amount among all the tested adsorbates, in both one- and two-component systems. The presence of two adsorbates in the system generally reduces the adsorption capacity of both polymers and metal ions, since the resulting polymer–polymer and polymer–metal ion complexes tend to remain in solution.

Studies on the regeneration ability of carbonaceous materials and adsorption–desorption cycles indicated that activated biocarbons can be successfully regenerated and reused. Furthermore, it was shown that the adsorption capacity of ionic polymers remains at a similar level in subsequent adsorption–desorption cycles due to the formation of polymer complexes on the adsorbent surface and the formation of an adsorption multilayer.

The performed research confirmed the feasibility of utilizing herb stalks, a by-product of the herbal industry, for the production of carbonaceous materials and demonstrated that the obtained biochars and activated biocarbons exhibit significant application potential in the energy sector and in environmental protection.

9. Osiągnięcia naukowe

Prace naukowe				
Opublikowane prace naukowe		**$IF_{z\ roku\ opublikowania}$**	**$IF_{5\text{-}letni}$**	**MNiSW**
Artykuły objęte rozprawą doktorską	10	52,3	58,3	1360
Artykuły nieobjęte rozprawą doktorską	4	18,7	18,8	400
Rozdziały w monografiach i recenzowanych wydawnictwach pokonferencyjnych	5			100
Łącznie	19	71,0	77,1	1860
Prezentacja wyników na konferencjach naukowych				
Wystąpienia ustne	14			
Postery	21			
Łącznie	35			
Indeks Hirscha (baza Scopus, 27.09.2025)	6			
Liczba cytowań (baza Scopus, 27.09.2025)	242			

9.1. Artykuły naukowe objęte rozprawą doktorską

D1. **M. Gęca**, M. Wiśniewska, P. Nowicki, *Biochars and activated carbons as adsorbents of inorganic and organic compounds from multicomponent systems – A review,* Advances in Colloid and Interface Science, 305, 2022, 102687, DOI:10.1016/j.cis.2022.102687 **(IF_{2022}: 15,6; $IF_{5\text{-letni}}$: 19,5; MNiSW: 200 pkt)**

D2. **M. Gęca**, M. Wiśniewska, P. Nowicki, *Modified method of lignocellulose content determination and its use for the analysis of selected herbs - precursors of biochars and activated carbons,* Measurement (Journal of the International Measurement Confederation), 212, 2023, 112672, DOI: 10.1016/j.measurement.2023.112672 **(IF_{2023}: 5,2; $IF_{5\text{-letni}}$: 5,4; MNiSW: 200 pkt)**

D3. **M. Gęca**, M. Wiśniewska, P. Nowicki, *Preparation of biochars by conventional pyrolysis of herbal waste and their potential application for adsorption and energy purposes,* ChemPhysChem, 2024, e202300507, DOI: 10.1002/cphc.202300507 **(IF_{2024}: 2,2; $IF_{5\text{-letni}}$: 2,5; MNiSW: 100 pkt)**

D4. **M. Groszek**, G. Wójcik, M. Wiśniewska, P. Nowicki*, Application of environmentally friendly activated carbons derived from herbal industry waste for water purification: A study on the removal of selected organic and inorganic pollutants,* Journal of Water Process Engineering, 2025, 75, 107952, DOI: 10.1016/j.jwpe.2025.107952 **(IF_{2024}: 6,7; $IF_{5\text{-letni}}$: 6,7; MNiSW: 100 pkt)**

D5. **M. Groszek**, M. Wiśniewska, P. Nowicki, *Simultaneous determination of ionic polymers and heavy metal ions concentrations in aqueous solution after their adsorptive removal using eco-friendly activated biocarbons*, Frontiers in Chemistry, 13, 2025, 1621297, DOI: 10.3389/fchem.2025.1621297 **(IF_{2024}: 4,2; $IF_{5\text{-letni}}$: 4,9; MNiSW: 100 pkt)**

D6. **M. Gęca**, M. Wiśniewska, P. Nowicki, *Simultaneous removal of polymers with different ionic character from their mixed solutions using herb-based biochars*

and activated carbons, Molecules, 27, 2022, 7557, DOI: 10.3390/molecules27217557 **(IF$_{2022}$: 4,6; IF$_{5\text{-letni}}$: 5,0; MNiSW: 140 pkt)**

D7. **M. Gęca**, M. Wiśniewska, T. Urban, P. Nowicki, *Temperature effect on ionic polymers removal from aqueous solutions using activated carbons obtained from biomass,* Materials, 16, 2022, 350, DOI: 10.3390/ma16010350 **(IF$_{2022}$: 3,4; IF$_{5\text{-letni}}$: 3,5; MNiSW: 140 pkt)**

D8. **M. Gęca**, M. Wiśniewska, P. Nowicki, K. Jędruchniewicz, *Cd(II) and As(V) removal from the multicomponent solutions in the presence of ionic polymers using carbonaceous adsorbents obtained from herbs,* Pure and Applied Chemistry, 2023, 95, 5, 563-578, DOI: 10.1515/pac-2023-0201 **(IF$_{2023}$: 2,0; IF$_{5\text{-letni}}$: 2,2; MNiSW: 140 pkt)**

D9. **M. Gęca**, M. Wiśniewska, P. Nowicki, *Investigation of ionic polymers stabilizing and flocculating properties in dispersed activated carbons systems,* Materials, 2024, 17, 693, DOI: 10.3390/ma17030693 **(IF$_{2024}$: 3,2; IF$_{5\text{-letni}}$: 3,5; MNiSW: 140 pkt)**

D10. **M. Gęca**, M. Wiśniewska, P. Nowicki, G. Wójcik *Arsenate and cadmium ions removal from multicomponent solutions of ionic polymers using mesoporous activated biocarbons*, Journal of Molecular Liquids, 2024, 407, 125270, DOI: 10.1016/j.molliq.2024.125270 **(IF$_{2024}$: 5,2; IF$_{5\text{-letni}}$: 5,1; MNiSW: 100 pkt)**

9.2. Artykuły naukowe nieobjęte rozprawą doktorską

1. M. Wiśniewska, P. Nowicki, K. Szewczuk-Karpisz, **M. Gęca**, K. Jędruchniewicz, P. Oleszczuk, *Simultaneous removal of toxic Pb(II) ions, poly(acrylic acid) and Triton X-100 from their mixed solution using engineered biochars obtained from horsetail herb precursor – Impact of post-activation treatment*, Separation and Purification Technology, 276, 2021, 1192697, DOI:10.1016/j.seppur.2021.119297 **(IF$_{2021}$: 9,1; IF$_{5\text{-letni}}$: 8,3; MNiSW: 140 pkt)**

2. M. Wiśniewska, D. Sternik, P. Nowicki, S. Chibowski, M. Medykowska, **M. Gęca**, K. Szewczuk-Karpisz, *Adsorption, viscosity and thermal behaviour of nanosized proteins with different internal stability immobilised on the surface of mesoporous activated biocarbon obtained from the horsetail herb precursor,* Applied Nanoscience, 12, 2022, 1323–1336, DOI:10.1007/s13204-021-01759-x **(IF_{2022}: 3,9; $IF_{5\text{-letni}}$: 4,3; MNiSW: 100 pkt)**

3. M. Wiśniewska, M. Marciniak, **M. Gęca**, K. Herda, R. Pietrzak, P. Nowicki, *Activated biocarbons obtained from plant biomass as adsorbents of heavy metal ions,* Materials, 15, 2022, 5856, DOI:10.3390/ma15175856 **(IF_{2022}: 3,4; $IF_{5\text{-letni}}$: 3,5; MNiSW: 140 pkt)**

4. **M. Gęca,** AM. Khalil, M. Tang, A.K. Bhakta, Y. Snoussi, P. Nowicki, M. Wiśniewska, M.M. Chehim, *Surface treatment of biochar—methods, surface analysis and potential applications: A comprehensive review*. Surfaces, 2023, 6, 179–213. DOI: 10.3390/surfaces6020013 **(IF_{2023}: 2,3; $IF_{5\text{-letni}}$: 2,7; MNiSW: 20 pkt)**

9.3. Rozdziały w monografiach i recenzowanych wydawnictwach pokonferencyjnych

1. **M. Gęca**, M. Wiśniewska, P. Nowicki, *Badanie właściwości adsorpcyjnych biowęgli aktywnych w układzie mieszanych adsorbatów: Pb(II), PAA, Triton X-100*, Nauka i przemysł - lubelskie spotkania studenckie, Wydawnictwo UMCS, Lublin, 2021 **(MNiSW: 20 pkt)**

2. **M. Gęca**, M. Wiśniewska, P. Nowicki, *Badanie możliwości usuwanie polimerów o różnych charakterze jonowym przy użyciu biowęgli i węgli aktywnych pochodzenia roślinnego*, Nauka i przemysł – metody spektroskopowe, nowe wyzwania i możliwości, Wydawnictwo UMCS, Lublin, 2022 **(MNiSW: 20 pkt)**

3. **M. Gęca**, M. Wiśniewska, P. Nowicki, *Biowęgle otrzymane z odpadów pochodzących z zakładów zielarskich jako potencjalne adsorbenty i materiały*

energetyczne, Nauka i przemysł – metody spektroskopowe, nowe wyzwania i możliwości, Wydawnictwo UMCS, Lublin, 2023 **(MNiSW: 20 pkt)**

4. **M. Gęca**, M. Wiśniewska, P. Nowicki, *Zastosowanie węgli aktywnych uzyskanych z prekursorów roślinnych do adsorpcji poli(kwasu akrylowego) oraz polietylenoiminy*, Nauka i przemysł - lubelskie spotkania studenckie, Wydawnictwo UMCS, Lublin, 2024 **(MNiSW: 20 pkt)**

5. **M. Gęca**, M. Wiśniewska, P. Nowicki **,** *Effect of the activation procedure on the adsorption properties of carbonaceous materials obtained from herbs towards ionic polymers***,** Science and industry challenges and opportunities, Wydawnictwo UMCS, Lublin, 2024 **(MNiSW: 20 pkt)**

9.4. Prezentacja wyników na konferencjach – wystąpienia ustne

1. **M. Gęca**, M. Wiśniewska, P. Nowicki, *Badanie możliwości usuwanie polimerów o różnych charakterze jonowym przy użyciu biowęgli i węgli aktywnych pochodzenia roślinnego*, Nauka i przemysł – metody spektroskopowe, nowe wyzwania i możliwości, 28-29 czerwca 2022, Lublin

2. **M. Gęca**, M. Wiśniewska, P. Nowicki, *Węgle aktywne pochodzenia roślinnego jako efektywne adsorbenty substancji organicznych i nieorganicznych,* 64 Zjazd Naukowy PTChem, 11-16 września 2022, Lublin

3. **M. Gęca**, M. Wiśniewska, P. Nowicki, *Zmodyfikowana metoda oznaczania związków ligninocelulozowych w prekursorach roślinnych wykorzystanych do otrzymania węgli aktywnych,* Innowacje w praktyce, 20-21 października 2022, Lublin

4. **M. Gęca**, M. Wiśniewska, P. Nowicki – *Węgle aktywne otrzymane z łodyg melisy i mięty jako adsorbenty polimerów jonowych,* Fizykochemia granic faz – metody instrumentalne, 16-20 kwietnia 2023, Lublin

5. **M. Gęca**, M. Wiśniewska, P. Nowicki, *Badania właściwości elektrokinetycznych węgli aktywnych pochodzenie roślinnego – wpływ polimerów jonowych,* Zjazd Wiosenny Sekcji Młodych PTChem, 3-7 maja 2023, Chęciny

6. **M. Gęca**, M. Wiśniewska, P. Nowicki, *Wpływ jonów metali ciężkich oraz polimerów jonowych na właściwości elektrokinetyczne węgli aktywnych otrzymanych z łodyg melisy i mięty*, Innowacje w praktyce, 15-16 czerwca 2023, Lublin

7. **M. Gęca**, M. Wiśniewska, P. Nowicki, *Biowęgle otrzymane z odpadów pochodzących z zakładów zielarskich jako potencjalne adsorbenty i materiały energetyczne*, Nauka i przemysł – metody spektroskopowe, nowe wyzwania i możliwości, 27-29 czerwca 2023, Lublin

8. **M. Gęca**, M. Wiśniewska, P. Nowicki, *Badania możliwości usuwania polimerów jonowych z roztworów wodnych z wykorzystaniem węgli aktywnych uzyskanych z łodyg melisy i mięty,* Zjazd Wiosenny Sekcji Młodych PTChem 2024, 1-5 maja 2024, Poronin

9. **M. Gęca,** M. Wiśniewska, P. Nowicki, *Zastosowanie węgli aktywnych uzyskanych z prekursorów roślinnych do adsorpcji poli(kwasu akrylowego) oraz polietylenoiminy,* Nauka i przemysł – lubelskie spotkania studenckie, 3 czerwca 2024, Lublin

10. **M. Groszek,** M. Wiśniewska, P. Nowicki, *Węgle aktywne uzyskane z prekursorów roślinnych na drodze aktywacji fizycznej jako adsorbenty jonów kadmu(ii) oraz polimerów jonowych,* 66 Zjazd Naukowy PTChem, 15-20 września 2024, Poznań

11. **M. Groszek,** M. Wiśniewska, G. Wójcik, P. Nowicki, *Biowęgle aktywne jako adsorbenty jonów metali ciężkich z roztworów wodnych – wpływ metody aktywacji na efektywność sorpcji*, Zjazd Wiosenny Sekcji Młodych PTChem 2025, 26-30 kwietnia 2025, Bąkowo

12. **M. Groszek**, M. Wiśniewska, P. Nowicki, *Ocena efektywności usuwania jonów metali ciężkich i polimerów jonowych z roztworów wodnych przy użyciu biowęgli*

aktywnych otrzymanych z łodyg mięty, Fizykochemia granic faz – metody instrumentalne, 11-15 maja 2025, Lublin

13. **M. Groszek**, M. Wiśniewska, P. Nowicki, *Materiały węglowe otrzymane z łodyg pokrzywy jako przyjazne środowisku adsorbenty polimerów jonowych*, Innowacje w praktyce 2025, 5-6 czerwca 2025, Lublin

14. **M. Groszek**, M. Wiśniewska, P. Nowicki, *Wytwarzanie biowęgli aktywnych na drodze aktywacji fizycznej i chemicznej odpadowych materiałów roślinnych oraz ich zastosowanie do adsorpcji substancji organicznych i nieorganicznych,* 67. Zjazd Naukowy PTChem, 22-26 września 2025, Wrocław

9.5. Prezentacja wyników na konferencjach – postery

1. **M. Gęca,** M. Wiśniewska, P. Nowicki, *Biochar as soil additive*, 13th International Conference on Agrophysics: Agriculture in changing climate, 15-16 November 2021, Lublin, Poland

2. M. Wiśniewska, K. Szewczuk-Karpisz, P. Nowicki, M. Medykowska, **M. Gęca**, *Zeolite and carbon materials as soil additives improving the substrate structure and stimulating plant growth,* XLV Międzynarodowe Seminarium Naukowo Techniczne „Chemistry for Agriculture", 21-24 November 2021, Karpacz, Poland

3. **M. Gęca**, M. Wiśniewska, P. Nowicki, *Biowęgle jako adsorbenty substancji organicznych i nieorganicznych z roztworów złożonych,* Zjazd Zimowy SMPTChem 2021, 29 stycznia 2022, Poznań

4. **M. Gęca**, M. Wiśniewska, P. Nowicki, *Activated carbons obtained from herbs as polymers adsorbents*, 1st International PhD Student's Conference at the University of Life Sciences in Lublin, Poland: ENVIRONMENT- PLANT-ANIMAL-PRODUCT (ICDSUPL)**,** 26 April 2022, Lublin, Poland

5. M. Wiśniewska, **M. Gęca**, P. Nowicki, *Biowęgle oraz węgle aktywne otrzymane z surowców roślinnych jako potencjalne adsorbenty związków*

wielkocząsteczkowych z fazy wodnej, X Kongres Technologii Chemicznej, 11-14 maja 2022, Karpacz

6. **M. Gęca**, M. Wiśniewska, P. Nowicki, *Węgle aktywne otrzymane z ziela pokrzywy oraz szałwii jako adsorbenty polietlenoiminy oraz jonów metali z roztworów dwuskładnikowych*, Zjazd Letni SMPTChem 2022, 29 czerwca – 3 lipca 2022, Szczecinek

7. **M. Gęca**, M. Wiśniewska, P. Nowicki, *Polymers and metal ions adsorption on the surface of biochars obtained from the nettle and sage herbs*, "Nanotechnology and nanomaterials" (NANO-2022), 25-27 August 2022, Lviv, Ukraine

8. **M. Gęca**, M. Wiśniewska, P. Nowicki, *Biochars and activated carbons obtained from herbs as low-cost and regenerable adsorbents of polymers,* 9th IUPAC International Conference series on Green Chemistry, 5-9 September 2022, Athens, Greece

9. Małgorzata Wiśniewska, Stanisław Chibowski, Teresa Urban, Konrad Terpiłowski, **Marlena Gęca***, Badanie wpływu struktury mieszanej warstwy adsorpcyjnej poli(kwasu akrylowego) i poli(glikolu etylenowego) na właściwości elektrokinetyczne i stabilnościowe wodnej suspensji tlenku itru(III),* 64 Zjazd Naukowy PTChem, 11-16 września 2022, Lublin

10. M. Wiśniewska, P. Nowicki, K. Herda, **M. Gęca**, *Adsortpion of poly(acrylic acid) in the biocarbon-aqueous solution system in the presence of surfactants,* 23rd International Symposium on Surfactants in Solutions, 11-16 September 2022, Lublin, Poland

11. M. Wiśniewska, S. Chibowski, T. Urban, **M. Gęca**, K. Herda, *Ionic polyacrylamides as modifers of stability properties of solid particles dispersed in the liquid medium*, 23rd International Symposium on Surfactants in Solutions, 11-16 September 2022, Lublin, Poland

12. **M. Gęca**, M. Wiśniewska, P. Nowicki, *Polymers adsorption onto activated carbons obtained from nettle herb and sage herb – influence of temperature*, Eleventh International Symposium Effects of Surface Heterogeneity

in Adsorption, Catalysis and related Phenomena, 18-22 September 2022, Zegrze, Poland

13. **M. Gęca**, M. Wiśniewska, P. Nowicki, *Zastosowanie węgli aktywnych otrzymanych z melisy oraz mięty do usuwania poli(kwasu akrylowego) i polietylenoiminy z pojedynczych i mieszanych roztworów wodnych,* Zjazd Zimowy Sekcji Młodych PTChem, 10 grudnia 2022, Opole

14. **M. Gęca**, M. Wiśniewska, P. Nowicki, *Wpływ zawartości związków ligninocelulozowych w prekursorach roślinnych na właściwości biowęgli i węgli aktywnych*, III Interdyscyplinarna Konferencja Doktorantów Nauk Biologicznych BIO-IDEA, 4 lutego 2023, Lublin

15. **M. Gęca**, M. Wiśniewska, P. Nowicki, *Comparison of adsorption affinity of the plant derived activated carbons toward ionic polymers and heavy metal ions*, "Nanotechnology and nanomaterials" (NANO-2023), 16-19 August 2023, Bukovel , Ukraine

16. **M. Gęca**, M. Wiśniewska, P. Nowicki, *Zastosowanie węgli aktywnych uzyskanych z biomasy do równoczesnego usuwania jonów metali ciężkich oraz polimerów jonowych z roztworów wodnych,* 65. Zjazd Naukowy PTChem, 18-22 września 2023, Toruń

17. **M. Gęca**, M. Wiśniewska, P. Nowicki, *Węgle aktywne uzyskane z biomasy roślinnej na drodze aktywacji fizycznej jako adsorbenty polimerów jonowych*, Zjazd Zimowy Sekcji Młodych PTChem 2023, 9 grudnia 2023, Łódź

18. . Wiśniewska, **M. Gęca**, P. Nowicki, *Effect of the activation procedure on the adsorption properties of carbonaceous materials obtained from herbs towards ionic polymers*, Science and Industry – challenges and opportunities, 4-6 June 2024, Lublin

19. **M. Gęca**, M. Wiśniewska, P. Nowicki, *Badania adsorpcji jonów kadmu oraz polietylenoiminy na powierzchni materiałów węglowych otrzymanych z prekursorów roślinnych na drodze aktywacji fizycznej*, Innowacje w praktyce 2024, 6-7 czerwca 2024, Lublin

20. **M. Groszek,** M. Wiśniewska, P. Nowicki, *Application of activated carbons obtained from herbal industry waste for ionic polymers removal from multicomponent systems,* XLVIII Międzynarodowe Seminarium Naukowo-Techniczne „Chemistry for Agriculture and Human Health", 24-27 listopada 2024, Karpacz

21. **M. Groszek,** M. Wiśniewska, P. Nowicki, *Węgle aktywne uzyskane z łodyg szałwii i melisy jako adsorbenty substancji organicznych i nieorganicznych z jedno- i wieloskładnikowych roztworów wodnych,* Zjazd Zimowy Sekcji Młodych PTChem 2024, 14 grudnia 2024, Lublin

9.6. Wyróżnienia

1. Laureat stypendium dla najlepszych doktorantów z „Własnego Funduszu Stypendialnego UMCS na rok akademicki 2022/2023"
2. Laureat stypendium dla najlepszych doktorantów z „Własnego Funduszu Stypendialnego UMCS na rok akademicki 2023/2024"
3. Wyróżnienie w konkursie na najlepszy poster - *Zastosowanie węgli aktywnych uzyskanych z biomasy do równoczesnego usuwania jonów metali ciężkich oraz polimerów jonowych z roztworów wodnych,* prezentowany podczas 65. Zjazdu Naukowego PTChem w Toruniu

9.7. Pozostała aktywność

1. Udział w organizacji 64. Zjazdu Naukowego PTChem, który odbył się w dniach 11-16.09.2022 w Lublinie
2. Udział w grancie badawczym w ramach programu Interprojekt przyznawanego przez Związek Uczelni Lubelskich, grant pt.: *Opracowanie nowatorskiego antybakteryjnego opatrunku na rany wzbogaconego w zeolity impregnowane srebrem*, Lublin, 01.12.2022-01.12.2023

3. Staż w Katedrze Inżynierii Materiałów Budowlanych i Geoinżynierii na Wydziale Budownictwa i Architektury Politechniki Lubelskiej, w dniach 14.11.2022-13.12.2022, pod opieką Prof. dr hab. inż. Wojciecha Franusa, w ramach projektu STAŻ ZA MIEDZĄ
4. Staż w Zakładzie Chemii Stosowanej na Wydziale Chemii Uniwersytetu im. Adama Mickiewicza w Poznaniu, w dniach 8-12.05.2023, pod opieką dr hab. Piotra Nowickiego, prof. UAM
5. Tajemnica handlowa (No 340/2-РІД-Ук-2023) - komercjalizacja wyników badań naukowych z tytułu tajemnicy handlowej „Miodowe Mydło Kleopatry", N. Kurinna, M. Wiśniewska, P. Nowicki, **M. Gęca**, 10.05.2023
6. Know-how (No 341/2-РІД-Ук-2023) – komercjalizacja wyników badań naukowych z tytułu know-how „Kompozycja woskowo-olejowo-żywicowa o właściwościach antybakteryjnych i przedłużonej trwałości", N. Kurinna, M. Wiśniewska, T. Urban, **M. Gęca**, 22.05.2023
7. Tajemnice handlowa (No 433-РІДУк2024) - komercjalizacja wyników badań naukowych z tytułu tajemnicy handlowej: body cream „Dziewanna's black treasure", M. Wiśniewska, V. Vedmedenko, P. Nowicki, **M. Gęca**, 01.05.2024

ANEKS – TEKSTY PUBLIKACJI BĘDĄCYCH PRZEDMIOTEM ROZPRAWY DOKTORSKIEJ WRAZ Z OŚWIADCZENIAMI WSPÓŁAUTORÓW

D1. M. Gęca, M. Wiśniewska, P. Nowicki, *Biochars and activated carbons as adsorbents of inorganic and organic compounds from multicomponent systems – A review,* Advances in Colloid and Interface Science, 305, 2022, 102687, DOI:10.1016/j.cis.2022.102687

Advances in Colloid and Interface Science 305 (2022) 102687

Contents lists available at ScienceDirect

Advances in Colloid and Interface Science

journal homepage: www.elsevier.com/locate/cis

Historical Perspective

Biochars and activated carbons as adsorbents of inorganic and organic compounds from multicomponent systems – A review

Marlena Gęca [a], Małgorzata Wiśniewska [a,*], Piotr Nowicki [b]

[a] Department of Radiochemistry and Environmental Chemistry, Institute of Chemical Sciences, Faculty of Chemistry, Maria Curie-Sklodowska University in Lublin, M. Curie-Sklodowska Sq. 3, 20-031 Lublin, Poland
[b] Laboratory of Applied Chemistry, Faculty of Chemistry, Adam Mickiewicz University in Poznań, Uniwersytetu Poznańskiego 8, 61-614 Poznań, Poland

ARTICLE INFO

Keywords:
Biochar
Activated carbon
Competitive adsorption
Simultaneous removal
Multicomponent solutions
Mixed adsorbate systems

ABSTRACT

Biochars are obtained by biomass pyrolysis, whereas activated carbon is a biochar that has undergone chemical or physical activation. Owing to the large surface area and easy surface modification both solids are widely applied as adsorbents. They are low-costs materials, they could be regenerated and their disposal is not troublesome. Adsorption of heavy metals, dyes, pharmaceuticals on the surface of biochars and activated carbons, from simple systems of adsorbate containing only one compound, are described extensively in the literature.

The present paper provides an overview of reports on adsorption of inorganic and organic compounds onto these two types of adsorbents from the mixed adsorbate systems. The described adsorbate systems have been divided into those consisting of: two or more inorganic ions, two or more organic compounds and both of them (inorganic and organic ones). The research of this type is carried out much less frequently due to the more complicated description of interactions in the mixed adsorbate systems.

1. Introduction

One of the most important current issues is constantly growing environment degradation and pollution. Development of industry and modern technologies improve the quality of life but also create problems that never took place before. Modern science faces global warming, ozone holes and regularly expanded amounts of wastes. One of the specific types of sludge is biomass.

Storage of biomass in landfills has a negative impact on the natural environment. Dumping grounds occupy the area of ecosystems, which results in reduction of biodiversity. Biomass could be a source of toxic substances for the environment and is the habitat of pathogens. Moreover, it contributes to the increase of greenhouse gas emission as a result decaying processes. For the above mentioned reasons, some attempts should be made to reduce amounts of the biomass in the ecosystem. One way of solving this problem is biomass pyrolysis. During this procedure liquid hydrocarbons, synthetic gas and biochar are formed [1]. According to Lehman and Joseph is "*biochar a carbon (C)-rich product when biomass such as wood, manure or leaves is heated in a closed container with little or unavailable air*" [2]. Biochar can be activated physically or chemically depending on the desired surface properties. When biochar is activated, it is called activated carbon. Activation is most commonly performed with steam or carbon dioxide – physical activation, else with zinc chloride, phosphoric acid, potassium or sodium hydroxide and potassium or sodium carbonate – chemical activation [3].

The practical application of both materials is based mostly on their sorption properties. The largely developed surface area allows inorganic and organic compounds including polymers to be adsorbed [4,5]. Adsorption of sulphide onto the carbonaceous adsorbents was investigated [6]. The biochar obtained from the wheat straw and wood pin chips was applied for adsorption of nickel(II) and zinc(II) from single aqueous solutions [7]. Many other biochars were also used for metals adsorption from the single adsorbate systems [8–11]. Tran et al. [12] studied the adsorption capacity of paracetamol onto the spherical biochar derived from pure glucose and non-spherical biochar obtained from pomelo peels. Adsorption of Methylene Blue onto the sewage sludge derived biochar was also investigated [13]. The biochar usage for single substance adsorption is very common and widely applied, but one-component solutions are rarely found in real environmental and wastewater systems.

Heavy metals, dyes, pharmaceuticals and other organic compounds are the most common environment pollutants. They are dangerous for human and animal life and health, as well as they have negative influence on the plant growth. For that reason these substances should not be

* Corresponding author.
E-mail address: malgorzata.wisniewska@mail.umcs.pl (M. Wiśniewska).

https://doi.org/10.1016/j.cis.2022.102687
Received in revised form 25 April 2022;
Available online 1 May 2022

released into the environment. The role of sewage treatment plants is to prevent that. One of the processes used for this purpose is adsorption onto biochars or activated carbons surfaces. Due to the complex composition of the sewage simultaneous removal of different structures from the mixed solutions should be carefully examined. Nevertheless, the studies in the mixed adsorbate systems (double) are still rarely carried out, and triple and more multiple systems are even less often tested. This paper is a review of the reports on the possibility of simultaneous removal of inorganic and organic substances from aqueous solutions with the use of biochar and activated carbons.

2. Simultaneous adsorption of inorganic ions on biochars and activated carbons surface

Biochars and activated carbons are both effective adsorbents of different metal ions, but the presence of other species affects that process considerably. The mutual effect can be synergistic, antagonistic or no net interaction, depending on ion and adsorbent surface properties. De Lima et al. [14] claim that metal ions adsorption could be strongly related to ionic substance properties such as ionic radius, ionic potential and electronegativity. It has been proved that small ions with high electronegativity were adsorbed the best.

Qian et al. [15] studied adsorption of Cd(II) in the presence of aluminium onto rice straw-derived biochars before and after oxidation by HNO_3/H_2SO_4. They proved that Al(III) ions have a negative effect on cadmium adsorption and this effect is greater the smaller is the solution pH, and the drop was nearly 50%. This can be caused by the fact that Al species changes from Al^{3+} to $Al(OH)^{2+}$ and $Al(OH)_2^+$ forms. With the increasing concentration of Al(III), adsorption of Cd(II) also decreases. The maximum adsorption of Cd(II) in the single solution reached 6.66 mg/g.

Lead and copper adsorb well on the surface of activated carbon obtained from the *Eucalyptus camaldulensis Dehn* bark from their mixed solution. The adsorbed amounts of these two elements from their binary system are similar for low concentration, but for the higher concentration system the sorption capacity decreases [16]. Adsorption onto the granular activated carbon derived from the coconut shell proved that the pH value influences these metals sorption too - adsorption is minimal at low pHs, and increases with the increasing pH [17].

Adsorption from the mixed solution of lead and cadmium was investigated on the surface of two different adsorbents – commercial activated carbon cloths and biochar produced from water hyacinths. The main adsorption mechanism is an electrostatic attraction between positively charged ions and the negative surface of the adsorbents. Carboxylic groups dissociation could have the main role in the adsorption process. The adsorption amount of Cd(II) is smaller in the binary solution than in the single one, but the presence of cadmium in the system has no significant influence on the lead adsorption. The maximum adsorption on the surface of activated carbon cloths reached 20.68 mg/g for Cd(II), 33.15 mg/g for Pb(II), and 74.99 mg/g for Cd(II), 128.95 mg/g for Pb(II) onto the biochar produced from water hyacinths [18,19].

Competitive adsorption between cadmium and zinc onto the granular activated carbons is difficult to explain. In the tested systems adsorption from the binary solutions decreased for both metals. This effect is more noticeable for zinc than for cadmium [20,21]. However according to some studies zinc adsorption capacity does not depend on the cadmium cations presence, but Cd(II) ions adsorb in the smaller amount from the binary solution [22]. The above allows to conclude that simultaneous adsorption of zinc and cadmium depends significantly on the adsorbent surface properties.

The studies on competitive adsorption of Zn(II) and Pb(II) on the surface of activated carbon prepared from Van apple pulp showed that individual amount of adsorption decreased in a binary solution, but the total ion adsorption amount is greater than in the single solutions. Adsorption of these two metals is strongly dependent on their mobility which increases with increasing temperature and metal concentration. In binary solution the total concentration of ions is higher than in single one, which have positive influence on the metals mobility leading to the adsorption increase. The maximum sorption capacity was 9.28 mg/g for zinc and 10.48 mg/g for lead, respectively [23].

The studies on adsorption of Ni(II) and Cr(VI) using activated carbon obtained from the coconut shells from their binary solution showed that the presence of nickel has negative influence on the chromium adsorption. The presence of Cr(VI) has also an unfavourable effect on the Ni(II) adsorbed amount. However the increasing concentration of Cr(VI) causes the increasing adsorption of Ni(II) cations. Adsorption capacity is greater in the single solutions for both metals. Independent of the presence of each, Cr(VI) is adsorbed in the greater amounts at low pHs whereas Ni(II) - at higher pH values [24].

The competitive adsorption between Zn(II) and Cu(II) ions on the surface of biochars was also investigated. The obtained results showed that the presence of both metals in the system have no influence on metal ion individual adsorption at their low concentrations. However, at high heavy metal ions concentration, the presence of Cu(II) in the solution causes 70–85% decrease of Zn(II) adsorption capacity. Zn(II) ions at higher concentrations also have a negative effect on the Cu(II) adsorption, but to a smaller extent, only 20% decrease was observed. Both metals are better adsorbed at pH lower than 5. It can be caused by competitive adsorption between metal ions and protons under such pH conditions [25].

The competition between Cu(II) and Cd(II) ions was also investigated onto the fresh and aged corn stalk biochars. The obtained data showed that both metals are better adsorbed at higher pH values. The adsorption capacity on the biochar surface decreased in the binary solution for both metals in case of the examined adsorbents. This effect is more noticeable for the adsorption of Cd(II), and the maximum adsorption values are 8.15 mg/g for Cu(II) and 12.67 mg/g for Cd(II) [26].

The studies on the competitive adsorption between Cd(II) and Co(II) on the surface of straw derived biochar showed that both metals are worse adsorbed from their binary systems compared to the single ones. What is more, Cd(II) has a stronger inhibitory effect on the Co(II) ions adsorption than Co(II) on the Cd(II) adsorption. This effect could be explained by different affinity of Cd(II) and Co(II) toward binding sites on the biochar surface. The maximum adsorption capacity was 5.3 mg/g for Co(II) and 21.69 mg/g for Cd(II) cations, respectively [27].

The competitive adsorption in the binary solutions of $Hg^{2+}/Pb^{2+}/Cd^{2+}/Ca^{2+}$ was investigated using the steam activated coconut shell derived activated carbon. In the solution containing cadmium and calcium, cadmium was better adsorbed metal, but its adsorption amount was smaller than that in the single-component solution. A similar effect was observed in both Pb^{2+}/Ca^{2+} and Pb^{2+}/Cd^{2+} systems, where lead was a better adsorbed substance. In all binary solutions mercury was the best adsorbed ion. The adsorption of all above metals occurs mainly by an ion exchange mechanism, which causes strong competition between individual inorganic ions [28]. The adsorption from the Hg^{2+}, Pb^{2+} and Cd^{2+} ternary solution on the groundnut shell biochar confirms the above observations. The metal adsorbed amounts were the largest for mercury and lead [29].

The competitive adsorption on the EDTA modified biochar obtained from the peanut shells among Cu(II), Cd(II) and Ni(II) was investigated. The obtained results showed that the adsorption capacity of Cd(II) and Ni(II) cations is smaller for their binary solution for both metals. However, a larger decrease was found for Cd(II). In the binary system of Cu (II) and Ni(II) the amount of adsorbed nickel ions dropped significantly, Cu(II) adsorption capacity also decreased but to a smaller extent. Cd(II) present in the solution had no significant effect on the Cu(II) adsorption. However, the Cu(II) presence in the solution causes the Cd(II) adsorption reduction to the zero level. The order of adsorption is compatible with binding constants of metal cations with EDTA [30].

The investigations on the simultaneous adsorption of Cd(II) and As (III)/As(V) on two different adsorbents obtained from the rice husk –

biochar and the birnessite-loaded biochar showed that these two metals are better adsorbed from their binary solutions. On the surface of unmodified biochar both metals adsorbed well, but better from their mixed solution. On the other hand, on the surface of birnessite-loaded biochar, adsorption of As did not take place from the single solution but in the presence of Cd(II) it occurred [31]. The adsorption of As(V) and Cd(II) ions from their binary solution on the Fe-modified rice straw biochars was also investigated. The adsorption capacity of As(V) was smaller from the binary solution, however, the amount of adsorbed Cd(II) increased in the presence of arsenate, compared to the single solution. Due to the difference in charge sign of these ions, the adsorption of As(V) and Cd(II) can occur on oppositely charged adsorption sites [32]. The studies on the simultaneous adsorption of Cd(II) and As(III) on the surface of α-FeOOH modified wheat straw biochar proved that the adsorption capacities of both metals are smaller from the binary solution compared to the single one [33].

The studies on the competitive adsorption between Ni(II) and As(V) using the Fe-biochar composite derived from the orange peel and red mud showed that the presence of Ni(II) in the solution has a positive effect on the As(V) adsorption. At a small concentration of As(V) ions, no significant effect on Ni(II) was observed, but at the larger As(V) concentration the inhibition effect on the Ni(II) adsorption capacity was observed. The competition between these metal ions is caused by the presence of different adsorption sites on the solid surface. The determined maximum adsorption capacity of Ni(II) was 20.71 mg/g, and that of As(V) was 13.71 mg/g [34].

The Cr(VI) adsorption in the presence of Ni(II) and Cu(II) on the activated carbons prepared from the ricinus communis leaves was investigated. The results showed that Ni(II) and Cu(II) have slightly inhibitory influence on the Cr(VI) ions adsorption and this effect is similar in both the binary and ternary solutions. The amount of adsorbed Cr(VI) ions dropped by about 10–20 percentage points in all systems [35].

Adsorption of Cr(VI), Ni(II) and As(III) was also investigated in the binary and ternary solutions on the surface of coconut charcoal. The results revealed that Ni(II) and As(III) exhibit a small inhibitory effect on the Cr(VI) adsorption in the binary systems, however, As(III) influence is greater. Cr(VI) affects positively the As(III) adsorption, its capacity is larger in the presence of chromium in the system, however it decreases with the increasing Cr(VI) concentration. In turn, Ni(II) has negative influence on the As(III) adsorption. On the other hand, the amount of adsorbed Ni(II) improves with the growing concentration of Cr(VI) ions. The presence of As(III) reduced the Ni(II) adsorption capacity slightly. In the ternary solutions, the presence of Ni(II) and As(III) has no significant effect on the Cr(VI) adsorption. The adsorption capacity of As(III) was larger in the ternary system than in the single one, but still smaller compared to in the binary solution with Cr(VI). The amount of adsorbed Ni(II) was the largest in the ternary system. These three metals compete for the same adsorption sites, and the metal ion with lower normal reduction potential could replace that with higher one – so Ni(II) could displace As(III) and As(III) could displace Cr(VI) [36].

As follows from the studies on competitive adsorption of lead, copper and cadmium on the peanut shell and sawdust, the adsorption of heavy metals from the mixed solution is smaller compared to that from the one-component solution. Metal ions concentration has great influence on the adsorption reduction [37]. The pH value affects largely these metals adsorption on the chitosan-pyromellitic dianhydride modified rice straw biochar, the influence was more noticeable for the adsorption of lead and cadmium than that of copper [38]. The adsorption of these three metals on the peat surface proved that lead is the best adsorbed in the binary and ternary solutions and copper is always better adsorbed than cadmium [39].

The studies on adsorption from the mixed solution of lead, cadmium and nickel on the surface of commercial granular activated carbon showed that nickel is the least adsorbed metal in the presence of other ions. The adsorption of lead and cadmium does not differ so much and the presence of other metals does not affect their adsorbed amounts. The factors having the greatest influence on the metals adsorption are adsorbent dosage, Pb(II) and Cd(II) concentrations, whereas pH value has the smallest effect [40].

The studies on the adsorption of lead, zinc and copper from their ternary solutions on the surface of hydroxyapatite-biochar nanocomposite derived from the rice straw and biochar obtained from the pomelo peel demonstrated that the order of adsorption affinity was different for the examined adsorbents. However, the adsorption capacities from the ternary solutions are consistent with the ordering for a single metal adsorption. The adsorbed metals amounts are smaller from the mixed solution, independent of the adsorbent type. The metals are better adsorbed at higher pH values, which can be attributed to the decrease in adsorption competition with protons. [41]. In the binary solution of copper and zinc/lead, the Cu(II) adsorption capacity on the biochar obtained from the pomelo peel is reduced with both metals, but this effect is more noticeable in the lead presence. The adsorption of lead from the binary solutions including zinc/copper, is extended at small metal concentrations and reduced at large metal concentrations. The lead/copper presence in the solution of zinc ions has negative influence on the Zn(II) adsorption. However, in case of zinc the decrease is the smallest of all tested systems [42].

The studies on the competitive adsorption of lead, zinc and cadmium on the surface of rice husk biochar and wood chips biochar showed that the competition among these three metals depend largely on the biochar modification. However, in general in the mixed solution the adsorption capacity of zinc and cadmium drops and that's of lead remains the same or even increases depending on the adsorbent properties [43].

The studies on the competitive adsorption from the ternary solution of Hg(II), Zn(II) and Cu(II) on the magnetic biochar derived from the banana peel showed that the adsorption capacity for all metals drops in the ternary solution compared to that in the single systems. Hg(II) was the best adsorbed ion and its adsorption decrease from the ternary solution was the smallest. The investigated metal ions are endowed with the same charge, hence, the observed selectivity was probably governed by their ionic radii and electronegativity. 83.4 mg/g was the maximum adsorption capacity obtained for Hg(II), 72.8 mg/g - for Zn(II) and 75.9 mg/g - for Cu(II) [44].

The studies on the competitive adsorption of Zn(II), Mn(II) and Cu(II) using the banana stalk biochar showed that the adsorption capacity decreases in the multi-component system of all three metals. However, the smallest decrease was observed for the Cu(II) adsorption and the largest reduction was found for Mn(II). The adsorbed amount increases with the pH increase in both single and mixed solutions. The maximum adsorption of particular metals was 108.10 mg/g for Zn(II), 109.10 mg/g for Mn(II) and 134.88 mg/g for Cu(II) [45].

The studies on the adsorption of Pb(II), Cu(II) and Ni(II) onto the date seed biochar from the binary and ternary solutions proved that Pb(II) and Cu(II) have negative influence on the mutual adsorption. A similar effect was observed in the binary system of Cu(II) and Ni(II). The adsorption capacity from the solution of Pb(II) and Ni(II) also decreases compared to that of the single systems. The adsorbed metals amounts were even smaller in the ternary solution compared to that on the binary solutions. A reasonable explanation of the metals inhibitory effect on each other adsorption could be the difference in the metals covalent binding indices. Metals with a higher covalent index showed more chelating affinity to ligands relative to ionic interactions [46].

The studies on the competitive adsorption between Cu(II), Zn(II) and Ni(II) on the surface of activated carbon prepared from the datestones, prove that Cu(II) is the best adsorbed metal and Zn(II) is the worst adsorbed one. The total adsorption capacity of heavy metals in the multi-component systems increased, but the individual metal ion adsorption decreased. The amount of adsorbed metal was dependent on the pH value. All metals were adsorbed in small amounts at low pHs due to the high concentration of hydrogen ions competing with metal ones. Their largest adsorption was found at pH about 5 [47].

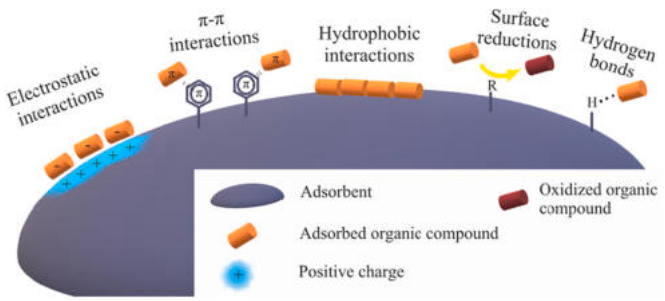

Fig. 1. Possible mechanisms of metal adsorption on the biochar and activated carbon surface.

The adsorption from the multi-component solution of Pb(II), Cr(III), Cd(II), Cu(II) and Zn(II) was investigated using the pepper stem biochar. The obtained data showed that lead is the best adsorbed metal, but the smallest decrease in adsorption compared to that in the single solution was observed for copper. The greatest decrease in the adsorption capacity took place for cadmium, which was the worst adsorbed metal. The main factor influencing the adsorbed amount was the mobility potential of metals. The metal with low mobility can be easily exchanged by another ion. The determined maximum adsorption capacity was as follows: Pb(II) ~120 mg/g, Cr(III) ~77 mg/g, Cd(II) ~66 mg/g, Cu(II) ~45 mg/g, Zn(II) ~32 mg/g [48].

The studies on the simultaneous adsorption of Pb(II), As(III), Cr(VI) and Cd(II) on the surface of cassava root husk derived biochar loaded with the ZnO nanoparticles showed also that lead is the best adsorbed metal. The adsorption capacities of As(III) and Cd(II) are insignificantly smaller and chromium adsorption is much worse compared to the other three metals. The most probable adsorption mechanisms are surface precipitation and ion exchange. The maximum adsorbed amounts were: 42.05 mg/g for Pb(II), 40.89 mg/g for As(III), 28.37 mg/g for Cr(VI) and 39.52 mg/g for Cd(II), respectively [49].

The simultaneous adsorption of Pb^{2+} and CrO_4^{2-} was studied using the biochar obtained from the pinewood sawdust. It was proved that both ions have positive influence on the mutual adsorption capacity and temperature has no significant effect on both ions adsorption. The amounts of adsorbed ions were greater from the binary solution than from the single one for both substances and being: 1420.38 mg/g for Pb^{2+} and 487.62 mg/g for CrO_4^{2-}. The greater adsorption of Pb^{2+} cations can be attributed to its higher mobility [50].

The studies on the competitive adsorption of Cd^{2+} and Ni^{2+}/NH_4^+ onto the straw rice biochar showed that with the increasing cadmium concentration, the adsorption capacity of ammonium decreases. The higher adsorption level of Cd^{2+} can be explained by its smaller ionic radius. When both nickel and cadmium are present in the solution, they have negative influence on the mutual adsorption [51].

As following from the studies on the adsorption of NO_3^- and PO_4^{3-} on the pinewood biochar at smaller metal concentrations there is no competition between the examined anions. At the greater anions concentrations the adsorption of both substances decreases in their binary solution, compared to the single one. The obtained results proved that PO_4^{3-} ions have stronger inhibitory influence on the NO_3^- adsorption, than the other way round. The sorption capacity decrease was 10.6% for PO_4^{3-} and 54.8% for NO_3^- [52].

The simultaneous adsorption of NH_4^+, NO_3^- and PO_4^{3-} was also investigated on the rice straw biochar surface modified with Mg, Al or these both. In the binary solution of NH_4^+ and NO_3^- the adsorption capacity of NH_4^+ increases, but that of NO_3^- decreases. The NH_4^+ adsorption in the presence of PO_4^{3-} has not changed significantly onto the non-modified biochar, the Mg modified biochar and the Al modified biochar. On the Mg—Al modified biochar the NH_4^+ adsorption increase in the presence of PO_4^{3-}. PO_4^{3-} capacity of adsorption in the binary solution of NH_4^+ and PO_4^{3-} decreased, remained the same or increased depending on the biochar modifications. The PO_4^{3-} adsorption capacity does not change in the presence of NO_3^-, however the NO_3^- adsorption capacity in the binary system dropped. In the ternary solution the NO_3^- adsorption decreases on the surfaces of all tested adsorbents. NH_4^+ and PO_4^{3-} adsorption capacities remained on the same level on three different adsorbents, but onto the Mg—Al modified biochar the increase in the adsorption for both ions was observed [53].

Physical adsorption, cation exchange, surface precipitation, surface oxidation, complexation and cation-π interactions are the most common cation adsorption mechanisms. In the solution containing more than one inorganic cation, there is often competition for the active sites between ions. Fig. 1 presents the possible mechanisms of metals adsorption on the biochar and activated carbon surfaces, whereas Table 1 shows the recapitulation of the above described studies.

3. Simultaneous adsorption of inorganic ions and organic compounds on the biochar and activated carbons surface

In nature metals occur not only with other ions but also with organic substances. The presence of these compounds can influence metals adsorption and the other way out.

Tetracycline present in the aqueous solutions has positive influence on the copper adsorption on the granular activated carbon derived from the coconut shell. The amount of adsorbed Cu(II) is larger in the binary solution than in the single one [54]. Cu(II) present in solution at a small concentration has positive influence on the tetracycline adsorption on the sawdust derived biochar, but with the increasing Cu(II) concentrations, tetracycline adsorption decreases [55].

The studies on the simultaneous adsorption of copper and bisphenol A on the kenaf bar biochar-supported zero valent iron showed that small concentration of Cu(II) in solution have positive influence on adsorption of the organic compound, however, with the increasing concentration of metal, bisphenol A adsorption decreases. The larger adsorbed amounts of these substances were obtained from their binary solution [56].

The studies of the competitive adsorption of Methylene Blue and Pb (II) ions on the surface of nano-magnetic activated carbon derived from the peach stone and wood proved that lead ions have a negative effect on the organic dye adsorption. The maximal adsorption value was 61.82 mg/g for Pb(II) and 437.78 mg/g for Methylene Blue [57]. However, the competition between Pb(II) and dye molecules depends largely on the adsorbent properties.

The cadmium and sulfamethoxazole adsorption from their binary solution showed that both substances undergo better adsorption onto the rice straw biochar in their mutual presence. The effect is more noticeable for the organic compound adsorption. The maximum sorption capacity toward sulfamethoxazole is 8 times higher in the binary solution compared to the single one [58].

The simultaneous adsorption of humic substances and chromium using the commercial activated carbon was studied by Ferro-Garcìa et al. [59]. The presence of Cr(III) has positive influence on the acids adsorption. The amount of adsorbed chromium ions drops at their small concentrations. However, the increasing concentration of acids causes enhanced Cr(III) adsorption. The humic acids adsorption on the activated carbon prepared from the rice husk was also studied in the presence of Na^+, Ca^{2+}, Mg^{2+} and Al^{3+} cations. Aluminium ions have a negative effect on the humic substances adsorption, the presence of Na^+ has no significant effect, whereas calcium and magnesium ions result in the adsorption increase. The studies on the influence of nitrate ions on the humic acids adsorption indicates, that the presence of negatively charged ions causes dropping adsorption on the acidic surface of activated carbon prepared from the rice husk [60].

Bautista-Toledo et al. [61] proved that the presence of electrolyte (NaCl) increases the bisphenol A adsorption onto the positively charged surface of charcoal-based activated carbon. The adsorption from the binary solution including bisphenol A and lead on the β-cyclodextrin modified rice husk biochar was investigated. The adsorption capacities

Table 1
Summary of adsorption of inorganic ions on the surface of biochars and activated carbons from the multi-component solutions.

Adsorbent	Adsorbates	Adsorption influencing factors	Maximal adsorption	References
Fresh and oxidized rice straw-derived biochars	Cd(II)	Fresh/oxidized adsorbent, pH, Presence of Al(III)	Cd(II) 6.66 mg/g	[15]
Activated carbon obtained form *Eucalyptus camaldulensis Dehn* bark	Cu(II) Pb(II)	Single/binary solution.	Cu(II) 28.89 mg/g Pb(II) 110.64 mg/g	[16]
Granular activated carbon derived from coconut shell	Cu(II) Pb(II)	pH, Contact time.	Cu(II) 3.56 mg/g Pb(II) 10.77 mg/g	[17]
Commercial activated carbon cloths	Cd(II) Pb(II) Phenol	Surface properties of adsorbents.	Cd(II) 20.68 mg/g Pb(II) 33.15 mg/g	[18]
Biochars produced from water hyacinths	Cd(II) Pb(II)	pH, Biochars pyrolysis temperature, Background ionic strength, Single/binary solutions.	Cd(II) 74.99 mg/g Pb(II) 128.95 mg/g	[19]
Granular activated carbon	Cd(II) Zn(II)	pH, Molar metal/carbon ratio.	100%	[20]
Granular activated carbon	Cd(II) Zn(II)	pH, Molar metal/carbon ratio.	Cd(II) ~5.06 mg/g Zn(II) ~4.19 mg/g	[22]
Activated carbon prepared from Van apple pulp	Zn(II) Pb(II)	pH, Temperature, Metals concentrations, Adsorbent dosage, Contact time.	Zn(II) 9.28 mg/g Pb(II) 10.48 mg/g	[23]
Activated carbon obtained from coconut shell	Cr(VI) Ni(II)	pH, Initial concentration.	Cr(VI) 1.99 mg/g Ni(II) 1.99 mg/g	[24]
Biochars produced from hardwood and corn straw	Cu(II) Zn(II)	Different adsorbents, pH, Adsorbent concentration, Single/binary solution.	Cu(II) 14.34 mg/g Zn(II) 12.20 mg/g	[25]
Corn stalk biochar	Cu(II) Cd(II)	pH, Adsorbent ageing, Single/binary solutions.	Cu(II) 8.15 mg/g Cd(II) 12.67 mg/g	[26]
Straw derived biochar	Co(II) Cd(II)	pH, Single/binary solutions.	Co(II) 5.3 mg/g Cd(II) 21.69 mg/g	[27]
Steam activated coconut shell derived activated carbon	Ca(II) Cd(II) Pb(II) Hg(II)	Competitive adsorption with the displaced proton, Single/binary solutions.	Ca(II) 10.8 mg/g Cd(II) 38.22 mg/g Pb(II) 118.1 mg/g Hg(II) 260.78 mg/g	[28]
Groundnut shell biochar	Cd(II) Pb(II) Hg(II)	Single/binary/ternary solutions.	100%	[29]
Biochar obtained from peanut shell	Cu(II) Cd(II) Ni(II)	pH, Single/binary solutions.	Cu(II) 48.73 mg/g Cd(II) 61.95 mg/g Ni(II) 40.38 mg/g	[30]
Rice husk biochar Rice husk birnessite-loaded biochar	Cd(II) As(III) As(V)	Different adsorbents, Single/binary solutions.	Cd(II) 3.89 mg/g As(III) 1.96 mg/g As(V) 1.74 mg/g	[31]
Fe-modified rice straw biochars	Cd(II) As(V)	Different adsorbents, Single/binary solutions, Initial metal concentrations, Dosage of biochars.	Cd(II) 9.80 mg/g As(V) 9.70 mg/g	[32]
α-FeOOH modified wheat straw biochar	Cd(II) As(III)	Different adsorbents, Single/binary solution, Initial concentration.	Cd(II) 62.9 mg/L As(III) 86.1 mg/L	[33]
Fe-biochar composite obtained from orange peel and red mud	Ni(II) As(V)	pH, Single/binary solutions, Different ways of pyrolysis.	Ni(II) 20.71 mg/g As(V) 13.70 mg/g	[34]
Activated carbons prepared from ricinus communis leaves	Cr(VI) Ni(II) Cu(II)	pH, Adsorbent dosage, Contact time, Initial concentration, Different adsorbents, Single/binary/ternary solutions.	Cr(VI) ~70%	[35]
Coconut charcoal	Ni(II) Cr(VI) As(III)	pH, Single/binary/ternary solutions.	Ni(II) 0.411 mg/g Cr(VI) 2.25 mg/g As(III) 0.043 mg/g	[36]
Peanut shell, Sawdust	Pb(II) Cd(II) Cu(II)	Different adsorbents, Single/mix solutions, Initial concentration, Adsorption time.	Pb(II) ~13.9 mg/g Cd(II) ~5.3 mg/g Cu(II) ~12.8 mg/g	[37]
Chitosan-pyromellitic dianhydride modified rice straw biochar	Pb(II) Cd(II) Cu(II)	pH, Single/ternary solutions.	Pb(II) 13.93 mg/g Cd(II) 38.24 mg/g Cu(II) 96.11 mg/g	[38]

(*continued on next page*)

Table 1 (*continued*)

Adsorbent	Adsorbates	Adsorption influencing factors	Maximal adsorption	References
Peat	Pb(II) Cd(II) Cu(II)	pH, Single/binary/ternary solutions.	Pb(II) 118.73 mg/g Cd(II) 50.24 mg/g Cu(II) 34.04 mg/g	[39]
Granular activated carbon	Pb(II) Cd(II) Ni(II)	Initial concentration of metals, pH, Adsorbent dosage, Contact time.	100%	[40]
Hydroxyapatite-biochar nanocomposite derived from rice straw	Zn(II) Pb(II) Cu(II)	pH, Single/ternary solutions, Ionic strength, Coexisting cations, Different adsorbents.	Zn(II) 935.93 mg/g Pb(II) 1000 mg/g Cu(II) 833.33 mg/g	[41]
Rice husk biochar Wood chips biochar	Zn(II) Pb(II) Cd(II)	Biochar properties, Single/ternary solutions.	Zn(II) ~10 mg/g Pb(II) ~10 mg/g Cd(II) ~10 mg/g	[43]
Magnetic biochar derived from banana peel	Hg(II) Zn(II) Cu(II)	pH, Adsorbent dosage, Initial concentration, Single/ternary solutions,	Hg(II) 83.4 mg/g Zn(II) 72.8 mg/g Cu(II) 75.9 mg/g	[44]
Banana stalk biochar	Zn(II) Mn(II) Cu(II)	pH, Single/ternary solutions.	Zn(II) 108.10 mg/g Mn(II) 109.10 mg/g Cu(II) 134.88 mg/g	[45]
Date seed biochar	Pb(II) Cu(II) Ni(II)	pH, Single/binary/ternary solutions.	Pb(II) 148.77 mg/g Cu(II) 26.73 mg/g Ni(II) 19.54 mg/g	[46]
Activated carbon prepared from datestones	Cu(II) Ni(II) Zn(II)	pH, Initial concentration, Temperature.	Cu(II) ~11 mg/g Ni(II) ~9 mg/g Zn(II) ~6 mg/g	[47]
Pepper stem biochar	Pb(II) Cr(III) Cd(II) Cu(II) Zn(II)	Single/multi component solutions.	Pb(II) ~120 mg/g Cr(III) ~77 mg/g Cd(II) ~66 mg/g Cu(II) ~45 mg/g Zn(II) ~32 mg/g	[48]
Cassava root husk derived biochar loaded with ZnO nanoparticles	Pb(II) As(III) Cr(VI) Cd(II)	Impregnation ratio, pH, Initial concentration.	Pb(II) 42.05 mg/g As(III) 40.89 mg/g Cr(VI) 28.37 mg/g Cd(II) 39.52 mg/g	[49]
Biochar obtained from pinewood sawdust	Pb^{2+} CrO_4^{2-}	Single/binary solutions, Temperature.	Pb^{2+} 1420.38 mg/g CrO_4^{2-} 487.62 mg/g	[50]
Rice straw biochar	Cd^{2+} Ni^{2+} NH_4^+	Single/binary solutions, Fresh/ageing biochar.	Cd^{2+} ~ 60 mg/g Ni^{2+} ~ 56 mg/g NH_4^+ ~ 9 mg/g	[51]
Pinewood waste derived biochar	NO_3^- PO_4^{3-}	pH, Initial concentration, Different pyrolysis temperature, Single/binary solutions.	NO_3^-~ 4 mg/g PO_4^{3-} ~ 18 mg/g	[52]
Mg-Al-modified rice straw biochar	NH_4^+ NO_3^- PO_4^{3-}	Single/binary/ternary solutions, Different biochar modifications.	NH_4^+ ~ 9 mg/g NO_3^- ~ 42 mg/g PO_4^{3-} ~ 77 mg/g	[53]

are similar to those of the single solutions for both substances [62].

The competitive adsorption of lead and atrazine was investigated using the corn straw biochar-supported reduced graphene oxide composite. The adsorption capacity of atrazine decreased in the presence of lead, however, atrazine present in the solution has no influence on the lead adsorption. The maximal adsorption capacity was 26.1 mg/g for Pb (II) and 67.6 mg/g for atrazine [63].

The studies on the simultaneous adsorption of copper and 17β-estradiol on the activated magnetic rice straw biochar proved that at small concentrations of copper the positive effect on the organic compound adsorption was observed, however, with the increasing concentration of metal, the 17β-estradiol adsorption decreased. The copper adsorption capacity was also improved in the solution of small concentration of 17β-estradiol, but decreased at its higher concentrations [64].

The adsorption from the binary solution of Zn(II) and tetracycline on the NH_4Cl-induced magnetic ultra-fine buckwheat peel powder biochar was investigated by Ai et al. [65]. As follows from the results both substances have a positive effect on mutual adsorption. Tetracycline in a single solution is better adsorbed at low pH values, whereas in a binary system pH 6 is the best condition. Zn(II) is adsorbed in a larger amount at pH higher than 6 for both single and binary solutions.

As follows from the studies on the simultaneous adsorption of Cr(VI) and phenol onto the biochar-based iron oxide composites, the amount of adsorbed Cr(VI) slightly decreases in the presence of phenol. However, the presence of Cr(VI) has no influence on the phenol adsorption capacity. The maximum adsorption for Cr(VI) was 18.63 mg/g and for phenol - 16.37 mg/g [66].

The studies on the effect of Cr(VI) on the methyl orange adsorption on the surface of iron-loaded biochar obtained from the sludge and liriodendron leaves proved that the presence of Cr(VI) causes a decrease of the adsorbed dye amount. With the increasing concentration of methyl orange the dye removal effectiveness decreases, and after reaching the level of 0.6 mmol/L - it increases again [67].

The competitive adsorption between Cu(II) and cyromazine was also investigated using the rice straw derived biochar. The studies proved that the adsorption capacity decreases for both substances in the binary solution compared to the single systems. The Cu(II) and cyromazine

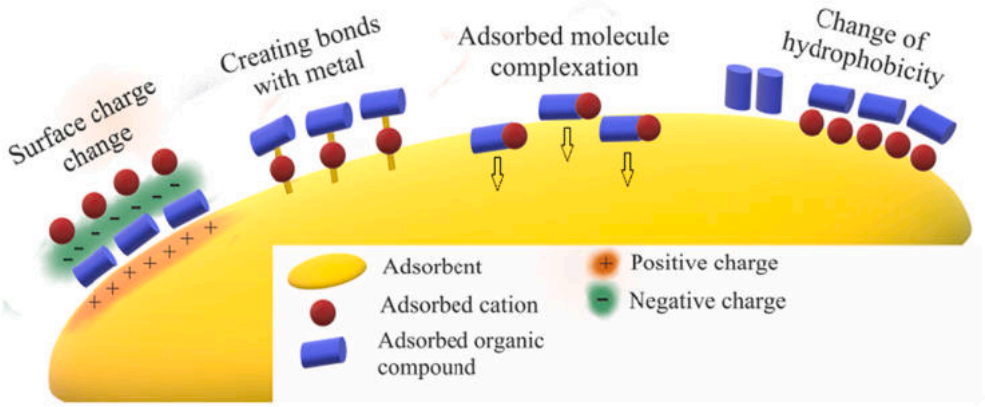

Fig. 2. Possible adsorption mechanisms of inorganic cation and organic compound on the biochar and activated carbon surface.

adsorption capacity decreases by 25% and 33% respectively and the determined maximal adsorption in the single solutions for Cu(II) was 35.92 mg/g and for cyromazine – 9.18 mg/g [68].

In the Co(II) and methylene blue containing solution, the dye adsorption capacity on the banana peels derived hierarchically porous activated carbon decreases in comparison to that observed in the single-component solution, however, the adsorbed metal amount is larger than in the single system. Positive influence of methylene blue on the Co(II) adsorption is particularly visible at higher organic dye concentrations [69].

The studies on the adsorption on the surface of biochars obtained from the corn straw from a binary solution of Hg(II) and atrazine showed the decreasing adsorption capacity for both substances in the binary solutions compared to that in the single systems. The level of decline depend on the adsorbent specific surface, being the smallest for adsorbent with the largest surface area [70].

The lead adsorption on the engineered biochar obtained from the horsetail herb in the presence of poly(acrylic acid) is more effective than without the polymer and the other way out. Triton X-100 added to the solution of lead has the same effect on the metal adsorption, however, the Triton X-100 capacity diminishes in the presence of Pb(II) ions. The adsorption from the ternary solution for lead and poly(acrylic acid) is as large as that for the binary solution. However the Triton X-100 adsorption capacity is the lowest in the ternary solution [71].

The studies on the Cr(VI) adsorption on the biochar obtained from the corn straws in the presence of bisphenol A or naphthalene proved that organic substances have a negative effect on the chromium adsorption. Cr(VI) does not affect the naphthalene adsorption, however, it has a positive effect on the bisphenol A removal. The maximum adsorption capacity for Cr(VI) was 116.28 mg/g, for bisphenol A - 476.19 mg/g and for naphthalene - about 600 mg/g [72].

The adsorption of Cu(II), Ni(II) and malachite green dye onto the biochar and activated carbon derived from the opuntia ficus-indica was investigated by Choudhary et al. [73]. The adsorption capacity of Cu(II) from the binary or ternary solution depended on the activation method. The adsorption capacity is the lowest on the biochar, and the greatest - on the carbon activated with NaOH in a ratio 1:2 – biochar/NaOH. The Ni(II) adsorption decreased in both binary and ternary solutions, independently of the adsorbent used. The presence of Cu(II) and Ni(II) in the solution has negative influence on the malachite green dye adsorption capacity.

The competitive adsorption between Acid Blue 25, Zn(II), Ni(II) and Cd(II) was investigated using the commercial activated carbon. The results showed that the presence of metals does not significantly affect the Acid Blue 25 adsorption. Moreover, it was found that the dye present in the solution has positive influence on the Zn(II), Ni(II), and Cd(II) adsorption, because it reduces competition between metals [74].

The studies on the competitive adsorption of Cu(II), sulfamethoxazole and tylosin onto the nano-hydroxyapatite modified biochar obtained from the watermelon rinds proved that tylosin adsorption capacity decreases in the presence of other substances. The sulfamethoxazole adsorption is promoted by Cu(II), but inhibited by tylosin. The Cu(II) adsorption capacity increases in the binary and ternary solutions in comparison to that observed in the single system [75].

The studies on the simultaneous adsorption of humic acid, ammonium and phosphate ions on the rice husk biochar supported $Mg(OH)_2$ showed that humic acid has negative influence on the ions adsorption at smaller pH values. With the increasing pH, the inhibitory effect of humic acid decreases. With further rise in the pH values, the adsorption capacities of ammonium and phosphate ions diminish again. The maximal sorption capacity is 50.27 mg/g for NH_4^+, 98.66 mg/g for PO_4^{3-} and 25.47 mg/g for humic acid [76].

The adsorption from a ternary solution of As(V), NO_3^- and tetracycline was investigated using the magnetic biochar derived from the corn straw. As follows from the results tetracycline has negative influence on the As(V) and NO_3^- adsorption, but this effect is more noticeable for nitrates. The tetracycline adsorption decreases in the presence of As(V) and NO_3^-, and the As(V) inhibitory effect is stronger. Comparing As(V) and NO_3^-, it can be stated that As(V) has greater influence on the NO_3^- adsorption capacity, than the other way out [77].

The studies on the competitive adsorption among metronidazole, NO_3^- and PO_4^{3-} on the activated carbon derived from the *Prosopis juliflora* branches proved that the amount of adsorbed substances decreases in the ternary system compared to that in the single-component solutions. However, with the decreasing anions concentrations, the percentage of removed substances increases, but never achieves 100% [78].

The phenol and cyanide adsorption was studied on the surface of the Cu-modified activated carbon obtained from the coconut shell. The results proved that the adsorption capacity decreases in the binary solution for both substances. Cyanide has a stronger inhibition effect on the phenol adsorption than vice versa [79].

The competitive adsorption between tetracycline and nano-TiO_2 was investigated using the coconut shell porous biochar. The results proved that nano-TiO_2 shows an inhibitory effect on the tetracycline adsorption. However, the presence of tetracycline in the solution has positive influence on the nano-TiO_2 adsorption capacity [80].

In solution containing inorganic ions and organic compound different adsorption mechanisms can take place – surface charge changes, creating bonds with metal, complexation and change of hydrophobicity. Fig. 2 presents the possible adsorption mechanisms of inorganic ions and organic compounds form the multi-component systems on the surface of biochar and activated carbon. Table 2 includes summary of the above described studies.

Table 2
Summary of inorganic ions and organic compounds adsorption on the surface of biochars or activated carbons from the multi-component solution.

Adsorbent	Adsorbates	Adsorption influencing factors	Maximal adsorption	References
Granular activated carbon derived from coconut shell	Cu(II) Tetracycline	Adsorbent oxidation, Contact time, pH.	Cu(II) 126.8 mg/g Tetracycline 714.8 mg/g	[54]
Biochar derived from sawdust	Cu(II) Tetracycline	pH, Single/binary solutions, Different biochar modifications.	Cu(II) 94.1% Tetracycline 95.7%	[55]
Kenaf bar biochar-supported zero valent iron	Cu(II) Bisphenol A	pH, Different adsorbent surface properties.	Cu(II) ~98% Bisphenol A 98.2%	[56]
Nano-magnetic activated carbon derived from peach stone and wood	Pb(II) Methylene Blue	pH, Temperature, Initial concentration, Contact time.	Pb(II) 61.82 mg/g Methylene Blue 437.78 mg/g	[57]
Rice straw biochar	Cu(II) Sulfamethoxazole	Biochar diameter, pH, Single/binary solutions.	Cu(II) 35.92 mg/g Sulfamethoxazole 9.18 mg/g	[58]
Activated carbon	Cr(III) Humic acid Gallic acid Tannic acid	Single/binary solutions.	Humic acid ~320 mg/g Gallic acid ~6 mg/g Tannic acid ~20 mg/g	[59]
Activated carbon prepared from rice husk	Humic substances	Different carbon activation procedures, Initial concentrations, Carbon dosage, Particle size, pH, Temperature, Presence of Na^{+}, Ca^{2+}, Mg^{2+}, Al^{3+}.	Humic acid 47.59 mg/g	[60]
β-cyclodextrin modified rice husk biochar	Pb(II) Bisphenol A	pH, Single/binary solutions.	Pb(II) 240.13 mg/g Bisphenol A 209.20 mg/g	[62]
Corn straw biochar-supported reduced graphene oxide composite	Pb(II) Atrazine	Single/binary solutions, Different biochar modifications.	Pb(II) 26.1 Atrazine 67.6 mg/g	[63]
Activated magnetic biochar obtained from rice straw	Cu(II) 17β-estradiol	Single/binary solutions, pH, Different adsorbents.	Cu(II) 85.93 mg/g 17β-estradiol 153.20 mg/g	[64]
NH_4Cl-induced magnetic ultra-fine buckwheat peel powder biochar	Zn(II) Tetracycline	pH, Single/binary solutions.	Zn(II) 357.14 mg/g Tetracycline 126.58 mg/g	[65]
Pomelo peel biochar-based iron oxide composites	Cr(VI) Phenol	pH, Adsorbent dosage, Single/binary solutions.	Cr(VI) 18.63 mg/g Phenol 16.37 mg/g	[66]
Iron-loaded biochar obtained from sludge and liriodendron leaves	Methyl Orange	Cr(VI) concentration.	Methyl Orange 9.50 mg/g	[67]
Rice straw derived biochar	Cu(II) Cyromazine	Pyrolysis temperature, Single/binary solutions.	Cu(II) 22.86 mg/g Cyromazine 144.43 mg/g	[68]
Banana peels derived hierarchically porous carbon	Co(II) Methylene Blue	Single/binary solutions.	Co(II) ~120 mg/g Methylene Blue ~1400 mg/g	[69]
Biochars obtained from corn straw	Hg(II) Atrazine	pH, Different adsorbents, Single/binary solutions.	Hg(II) 1.24 mg/g Atrazine 74.23 mg/g	[70]
Engineered biochar obtained from horsetail herb	Pb(II) Poly(acrylic acid) Triton X-100	Single/binary/ternary solutions, Different biochar activation procedure.	Pb(II) 183.29 mg/g Poly(acrylic acid) 195.79 mg/g Triton X-100 20.32 mg/g	[71]
Biochar obtained from corn straws	Cr(VI) Bisphenol A Naphthalene	Single/binary solutions, Different biochar activation procedure.	Cr(VI) 116.28 mg/g Bisphenol A 476.19 mg/g Naphthalene ~600 mg/g	[72]
Biochar derived from opuntia ficus-indica	Cu(II) Ni(II) Malachite Green	pH, Different adsorbents, Adsorbent dosage, Contact time, Single/binary/ternary solutions.	Cu(II) 16.38 mg/g Ni(II) 14.92 mg/g Malachite Green 165.56 mg/g	[73]
Commercial activated carbon	Acid Blue 25 Zn(II) Ni(II) Cd(II)	Ternary solutions.	Acid Blue 25,111.83 mg/g Zn(II) 8.8 mg/g Ni(II) 10.0 mg/g Cd(II) 10.0 g/g	[74]
Nano-hydroxyapatitemodified biochar obtained from watermelon rinds	Cu(II) Tylosin Sulfamethoxazole	Single/binary/ternary solutions.	Cu(II) ~60 mg/g Tylosin ~150 mg/g Sulfamethoxazole ~155 mg/g	[75]
Rice husk biochar supported $Mg(OH)_2$	NH_4^+ PO_4^{3-} Humic acid	Adsorbent dosage, pH.	NH_4^+ 50.27 mg/g PO_4^{3-} 98.66 mg/g Humic acid 25.47 mg/g	[76]
Magnetic biochar obtained from corn straw	As(V) NO_3^- Tetracycline	pH, Single/ternary solutions.	As(V) 6.77 mg/g NO_3^- 6.31 mg/g Tetracycline 612.38 mg/g	[77]

(*continued on next page*)

Table 2 (*continued*)

Adsorbent	Adsorbates	Adsorption influencing factors	Maximal adsorption	References
Activated carbon derived from *Prosopis juliflora* branches	Metronidazole NO_3^- PO_4^{3-}	Contact time, Initial concentration, Temperature, Single/ternary solutions.	Metronidazole 3.38 mg/g NO_3^-12.27 mg/g PO_4^{3-}12.15 mg/g	[78]
Cu modified activated carbon derived from coconut shell	CN^- Phenol	Adsorbent dosage, pH, Contact time, Temperature, Initial concentration.	CN^-~ 1.2 mg/g Phenol ~9 mg/g	[79]
Coconut shell porous biochar	Nano-TiO_2 Tetracycline	pH, Temperature, Single/binary solutions.	Nano-TiO_2 ~ 1.35 mg/g Tetracycline ~3.75 mg/g	[80]

4. Adsorption from the multicomponent systems of organic compounds on the surface of biochars and activated carbons

Organic substances getting into the environment in an uncontrolled manner could be very dangerous pollutants. One of the most effective ways of their removal from wastewater or exhausted gases is adsorption on the biochars or activated carbons surface. Adsorption from the solutions containing two or more organic compounds is complicated, as proved by the studies described below.

The adsorption of dibenzothiophene on the coconut-based activated carbon was investigated in the presence of benzene and olefin. In the benzene containing system the amount of adsorbed dibenzothiophene decreases with the increasing concentration of hydrocarbon and the olefin presence in the mixture stops the dibenzothiophene adsorption. The maximal removal of dibenzothiophene was 93.7% [81].

In the binary solution of p-nitrophenol and benzoic acid, the influence of p-nitrophenol on the benzoic acid adsorption on the granular activated carbon is more remarkable, than the benzoic acid effect on the p-nitrophenol removal, which indicates greater adsorption of p-nitrophenol on the carbon surface. The increasing concentration of p-nitrophenol causes a four-fold decrease in the benzoic acid sorption. On the other hand, with the increasing benzoic acid concentration the p-nitrophenol adsorption drops only to a small extent [82].

Comparison of the naphthalene and phenanthrene adsorption on the walnut shell based activated carbon from the single and binary solutions showed that naphthalene has no significant effect on the phenanthrene adsorption, but the presence of phenanthrene causes reduction of naphthalene adsorbed amount. The determined maximal adsorption capacity for naphthalene was 49.58 mg/g and for phenanthrene - 63.77 mg/g [83].

Iovino et al. [84] studied the naphthalene and toluene adsorption on the commercial activated carbon. They proved that toluene is always better adsorbed substance. The adsorption capacity in the binary solutions is smaller than in the single solution for both substances. However, the change of the initial concentration ratio causes a more pronounced effect on the naphthalene adsorption, than that of toluene.

The studies on the toluene and ethylbenzene adsorption from their binary solution on the biochar derived from the organic waste biomass showed that these substances have positive influence on mutual adsorption. The adsorption capacities are better from the binary solutions than from the single-component ones. Furthermore, the adsorbed amounts of ethylbenzene and toluene are dependent on the solution pH and in the acidic medium adsorption was smaller [85].

Dibutyl phthalate and di(2-ethylhexyl) phthalate present in one solution have negative influence on the mutual adsorption on the biochar obtained from the corncobs. The di(2-ethylhexyl) phthalate adsorbed amount decreases only to a small extent, but that of dibutyl phthalate diminishes noticeably. Thus a greater inhibition effect on di(2-ethylhexyl) phthalate dibutyl phthalate adsorption than the other way out is observed. The maximal adsorption was 13.2 mg/g for dibutyl phthalate and 16.2 mg/g for di(2-ethylhexyl) phthalate [86].

The studies on the ibuprofen and amoxicillin adsorption from their binary solution on the surface of activated carbon prepared from the olive stones showed smaller adsorption capacity for both substances compared to that in their single-component solutions. The decrease is more noticeable for amoxicillin than for ibuprofen and it takes place even when ibuprofen concentration in the solution is below 50% [87].

The studies on the competitive adsorption of carbaryl and oxytetracycline on the original and demineralized cow manure biochar showed that carbaryl is better adsorbed on the unmodified biochars, whereas oxytetracycline on the demineralized ones. The presence of oxytetracycline has negative influence on the carbaryl adsorption. However, the carbaryl presence has no effect on the oxytetracycline adsorption or causes a decrease in the adsorption capacity, depending on

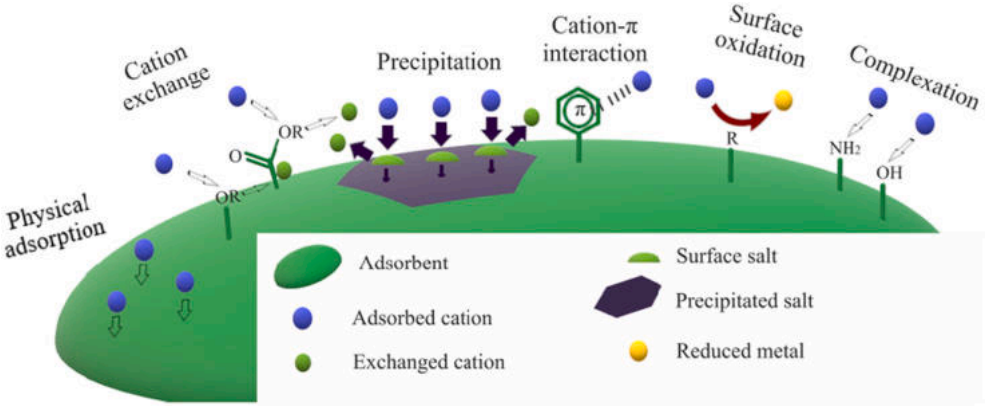

Fig. 3. Possible mechanisms of metal adsorption on the biochar and activated carbon surface.

Table 3
Recapitulation of organic compounds adsorption on the surface of biochars and activated carbons from the multi-component solution.

Adsorbent	Adsorbates	Adsorption influencing factors	Maximum adsorption	References
Coconut-based activated carbon	Tiophene Dibenzotiophene	Presence of olefin/hydrocarbon.	Tiophene 66.7% Dibenzotiophene 93.7%	[81]
Granular activated carbon	p-nitrophenol Benzoic acid	Different concentrations.	p-nitrophenol ~584.22 mg/g Benzoic acid ~537.24 mg/g	[82]
Walnut shell based activated carbon	Naphthalene Phenanthrene	Single/binary solutions.	Naphthalene 49.58 mg/g Phenanthrene 63.77 mg/g	[83]
Activated carbon Filtrasorb 400	Naphthalene Toluene	Different initial concentration ratios, Single/binary solutions.	Naphthalene ~173.03 mg/g Toluene ~165.78 mg/g	[84]
Biochar derived from biomass of organic waste	Toluene Ethylbenzene	pH, Single/binary solutions.	Toluene 0.047 mg/g Ethylobenzene 0.046 mg/g	[85]
Biochar obtained from corncob	Dibutyl phthalate Di(2-ethylhexyl) phthalate	Different adsorbent preparation, Single/binary solutions.	Dibutyl phthalate 13.2 mg/g Di(2-ethylhexyl) phthalate 16.2 mg/g	[86]
Activated carbon prepared from olive stones	Ibuprofen Amoxicillin	Different adsorbents, Single/binary solutions.	Ibuprofen ~68.08 mg/g Amoxicillin ~197.32 mg/g	[87]
Cow manure biochars	Carbaryl Oxytetracycline	Different pyrolysis factors, Single/binary solutions.	Carbaryl ~55 mg/g Oxytetracycline ~37.5 mg/kg	[88]
Biochar obtained from bamboo	Bisphenol A Sulfamethoxazole	pH, Single/binary solutions, Biochar modification.	Bisphenol A 101.5 mg/g Sulfamethoxazole 99.99 mg/g	[89]
Magnetic biochar obtained from pine sawdust	Sulfamethoxazole 17α-ethinylestradiol	pH, Ionic strength, Natural organic matter.	Sulfamethoxazole ~15 mg/g 17α-ethinylestradiol ~14 mg/g	[90]
Activated carbon obtained from peanut shells	Caffeine Diclofenac	pH, Single/binary solutions, Adsorbent dosage, Ionic strength.	Caffeine ~116.52 mg/g Diclofenac ~296.15 mg/g	[91]
Cobalt-gadolinium modified biochar derived from camellia oleifera shells	Ciprofloxacin Tetracycline	pH, Adsorbent dosage, Ionic strength, Single/binary solutions.	Ciprofloxacin 44.44 mg/g Tetracycline 119.05 mg/g	[92]
Activated carbon fiber based on phenolic resin	Atrazine Congo Red	Different microporous size distributions.	Atrazine ~100 mg/g Congo Red 545.49 mg/g	[93]
Magnetic chicken bone-based biochar	Rhodamine-B Tetracycline	pH, Ionic strength, Adsorbent dosage, Temperature, Single/binary solutions.	Rhodamine-B 96.5 mg/g Tetracycline 63.3 mg/g	[94]
Activated carbon derived from orange peels	Rhodamine-B Methylene Blue	Single/binary solutions, Batch/dynamics adsorption.	Rhodamine-B 522.11 mg/g Methylene Blue 319.85 mg/g	[95]
Biochar derived from *Auricularia auricula*	Rhodamine-B Methylene Blue Gentian Violet	pH, Single/binary solutions.	Rhodamine-B 32.33 mg/g Methylene Blue 53.62 mg/g Gentian Violet 735.73 mg/g	[96]
Biochar obtained from cornstalk	Methylene Blue Gentian Violet	Single/binary solutions.	Methylene Blue 325.15 mg/g Gentian Violet 266.57 mg/g	[97]
Activated carbon prepared from residual fuel oil	Rhodamine-6G Methylene Blue	Single/binary solutions.	Rhodamine-6G ~70 mg/g Methylene Blue ~90 mg/g	[98]
Biochar obtained from sawdust	Methyl Red Methylene Blue	Single/binary solutions, Presence of glucose/NaCl.	Methyl Red 147.32 mg/g Methylene Blue 243.04 mg/g	[99]
Maple leaf-derived biochar	Methylene Blue Congo Red	pH, Pyrolysis temperature, Adsorption time.	Methylene Blue 134 mg/g Congo Red 195 mg/g	[100]
Cadmium hydroxide nanowires loaded on activated carbon	Malachite Green Sunset Yellow	pH, Initial concentrations, Single/binary solutions.	Malachite Green ~25 mg/g Sunset Yellow ~80 mg/g	[101]
Activated carbons derived from *Persea americana* and *Ziziphus mauritiana* nuts	Basic Blue 41 Basic Yellow 28	Different adsorbents, Single/binary solutions.	Basic Blue 41–300 mg/g Basic Yellow 28–300 mg/g	[102]
Red seaweed derived biochar	Reactive Blue 4 Reactive Orange 16	pH, Single/binary solutions.	Reactive Blue 4150.43 mg/g Reactive Orange 16 58.67 mg/g	[103]
Activated carbon Filtrasorb 400	Remazol Reactive Yellow Remazol Reactive Red Remazol Reactive Black	Single/binary/ternary solutions.	Yellow 714 mg/g Red 213 mg/g Black 278 mg/g	[104]
Mesoporous activated carbons derived from kiwi, cucumber and potato peels	Methylene Blue Malachite Green Rhodamine B	pH, Temperature, Adsorbent dosage, Different adsorbents, Single/binary/ternary solutions,	Methylene Blue ~200 mg/g Malachite Green ~200 mg/g Rhodamine B ~ 175 mg/g	[105]
Sludge-based activated carbon	Phenol p-chlorophenol p-nitrophenol p-hydroxybenzoic acid	Different adsorbents, Adsorbates nature, Single/mix solutions.	Phenol 348.18 mg/g p-chlorophenol 1079.9 mg/g p-nitrophenol 570.35 mg/g p-hydroxybenzoic acid 538.67 mg/g	[108]

(*continued on next page*)

Table 3 (*continued*)

Adsorbent	Adsorbates	Adsorption influencing factors	Maximum adsorption	References
Activated carbon	Phenol p-hydroxybenzoic acid	Single/binary solutions.	Phenol ~2.35 mg/g p-hydroxybenzoic acid ~2.55 mg/g	[109]
Granular activated carbon based on coconut shell	Naproxen Diclofenac Carbamazepine Clofibric acid	Different solutions, Single/mix solutions, Presence of NaCl.	Naproxen 2.74 mg/g Diclofenac 2.52 mg/g Carbamazepine 3.00 mg/g Clofibric acid 2.48 mg/g	[110]
Ammonium-modified cassava waste-derived biochar	Norfloxacin Sulfamerazine Oxytetracycline	Temperature, Single/ternary solutions.	Norfloxacin ~1.75 mg/g Sulfamerazine ~1.65 mg/g Oxytetracycline ~2.75 mg/g	[111]
KOH modified cassava waste-derived biochar	Norfloxacin Sulfamerazine Oxytetracycline	pH, Single/ternary solutions.	Norfloxacin ~4.40 mg/g Sulfamerazine ~0.6 mg/g Oxytetracycline ~4.25 mg/g	[112]
Prosopis juliflora activated carbon	Sulphonamide Nitroimidazole Tetracycline	pH, Contact time, Adsorbent dosage, Initial concentration, Single/binary/ternary solutions.	Sulphonamide 82.6% Nitroimidazole 89.9% Tetracycline 95.3%	[113]
Paper mill sludge based carbon	Carbamazepine Oxazepam Paroxetine	Different adsorbents, Single/binary/ternary solutions.	Carbamazepine ~14.18 mg/g Oxazepam ~23.2 mg/g Paroxetine ~24.7 mg/g	[114]
Biochars produced from digestate, tomato waste and durian shell	α-hexachlorocyclohexane β-hexachlorocyclohexane γ-hexachlorocyclohexane δ-hexachlorocyclohexane	Different adsorbents, Single/mix solutions.	α-hexachlorocyclohexane ~0.9 mg/g β-hexachlorocyclohexane ~0.9 mg/g γ-hexachlorocyclohexane ~0.9 mg/g δ-hexachlorocyclohexane ~0.9 mg/g	[115]

the adsorbent type. Oxytetracycline adsorbed amount remains on the same level in case original biochars and the adsorption capacity decrease on demineralized biochars [88].

The competitive adsorption between bisphenol A and sulfamethoxazole was investigated using the biochar obtained from the bamboo. The sulfamethoxazole presence has no significant effect on the bisphenol A adsorption. However, the amount of adsorbed sulfamethoxazole decreases in the presence of bisphenol A. The maximal adsorption capacity was 101.5 mg/g for bisphenol A and 99.99 mg/g for sulfamethoxazole [89].

The sulfamethoxazole adsorption on the magnetic biochar obtained from the pine sawdust was investigated in the presence of 17α-ethinylestradiol. 17α-ethinylestradiol causes a decrease of adsorbed sulfamethoxazole amount. With the increasing concentration of 17α-ethinylestradiol to the value 1.8 mg/L, the sulfamethoxazole adsorption capacity decreases, but a further increase in the concentration of 17α-ethinylestradiol, does not reduce the sulfathoxazole adsorption. In turn, the sulfamethoxazole presence has no significant effect on the 17α-ethinylestradiol adsorption capacity [90].

The competitive adsorption between caffeine and diclofenac on the activated carbon obtained from the peanut shells was investigated at two different pH values. At pH 5 the adsorption capacity for both substances decreases, but the observed drop was more noticeable for caffeine. However, at pH 7, the diclofenac adsorption still decreases, but the amount of adsorbed caffeine remained almost the same compared to that in the single caffeine solution [91].

The studies on the competitive adsorption of antibiotics – tetracycline and ciprofloxacin on the Co—Gd modified biochar derived from the camellia oleifera shells proved that both substances have inhibitory effect on the mutual adsorption. The amounts of adsorbed antibiotics are smaller in the binary solution than in the single system for both substances. The maximum adsorption capacity was 44.44 mg/g for ciprofloxacin and 119.05 mg/g for tetracycline [92].

The adsorption from the binary solution containing organic compound and dye on the microporous phenolic resin-based activated carbon fiber was investigated. In the binary system including atrazine and Congo red the competitive adsorption takes place. Congo red blocks the active adsorbent sites, preventing the atrazine adsorption. The competition is stronger with the increasing mean pore size of the solid [93]. The studies on the adsorption of rhodamine B dye and tetracycline from their binary solution on the magnetic chicken bone-based biochar showed that adsorption capacity decreases in the binary system for both substances. This effect is more noticeable for rhodamine B. Tetracycline has the greatest inhibitory effect on the rhodamine B adsorption at its small concentration [94].

Methylene blue is a dye whose adsorption in the presence of other dyes has been studied most extensively. The competitive adsorption between Rhodamine B and Methylene Blue was investigated using the activated carbon derived from the orange peels. Based on the obtained results it was found that both dyes have negative influence on the mutual adsorption. None of the dyes exhibited a stronger inhibitory effect [95]. Their adsorption was also studied on the surface of biochar derived from *Auricularia auricula* in the presence of Gentian Violet. This dye has the strongest inhibitory effect on the Rhodamine B adsorption. Rhodamine B also caused a decrease of Gentian Violet adsorption but to a smaller extent [96]. The Methylene Blue and Gentian Violet adsorption on the biochar obtained from the cornstalk showed that at a small concentration of Gentian Violet a positive effect the Methylene Blue adsorption was observed. However, when Gentian Violet concentration increased, the Methylene Blue adsorption capacity decreased. High concentration of Methylene Blue causes an initial increase in the adsorption of Gentian Violet and then a decrease with time [97].The Methylene Blue adsorption on the activated carbon prepared from the residual fuel oil was studied in the presence of Rhodamine 6G. The results showed that both dyes have an inhibitory effect on the mutual adsorption, but the influence of Methylene Blue on the Rhodamine 6G adsorption is more noticeable [98]. The studies on the simultaneous adsorption of Methyl Red and Methylene Blue on the biochar obtained from the sawdust showed that adsorption capacity from the binary solution is reduced compared to that from the single one for both substances. The presence of glucose or NaCl reduce the amount of adsorbed Methyl Red additionally, it does not affect the Methylene Blue

adsorption significantly [99]. Methylene Blue and Congo Red were adsorbed simultaneously on the surface of maple leaf-derived biochar. The adsorption capacity of Congo Red is smaller in the binary solution, however, its presence has a positive effect on the Methylene Blue adsorption. The amount of adsorbed Methylene Blue is larger in the binary solution [100].

The adsorption from the binary solution was also investigated from the systems containing other dyes. The adsorption capacities of Malachite Green and Sunset Yellow on the cadmium hydroxide nanowires loaded on the activated carbon based on the sewage sludge decrease in the binary system, compared to those in the single solutions. The adsorption decrease is more noticeable for Malachite Green than for Sunset Yellow [101] The competitive adsorption between Basic Blue 41 and Basic Yellow 28 was investigated on two different activated carbons – one derived from the *Persea americana* nuts and the other one obtained from the *Ziziphus mauritiana* nuts. The results showed that Basic Blue 41 is better adsorbed on both adsorbents in the binary solutions than Basic Yellow 28. The Basic Blue 41 adsorbed amount is similar to that in the single system. The Basic Yellow 28 adsorption capacity decreases in the presence of Basic Blue 41 [102]. Reactive Blue 4 and Reactive Orange 16 were adsorbed from their binary solutions on the surface of red seaweed derived biochar. The obtained results showed that both dyes were worse adsorbed in the presence of each other and the better adsorbed dye was Reactive Blue 4. The maximal adsorption reached 4150.43 mg/g for Reactive Blue 4 and 1658.67 mg/g for Reactive Orange 16 [103].

The ternary systems of different dyes were also investigated. The studies on the competitive adsorption of reactive dyes on the commercial activated carbon showed the decreasing adsorption of these substances in the multi-component systems compared to those in the single ones. A greater decrease of Remazol Reactive Black adsorbed amount was observed in the Remazol Reactive Yellow and Remazol Reactive Black solution. In the system with Reactive Yellow and Reactive Red no significant difference was found. The most competitive effect was observed in the solution containing Reactive Red and Reactive Black, the largest reduction of adsorption was found for Reactive Red. The studies on the ternary solution confirm the above. The maximum adsorption was 714 mg/g for Remazol Reactive Yellow, 213 mg/g for Remazol Reactive Red and 278 mg/g for Remazol Reactive Black [104]. The studies on the adsorption of methylene blue, malachite green and rhodamine B on the mesoporous activated carbons derived from kiwi, cucumber and potato pells showed that methylene blue and malachite green are adsorbed in the greatest amounts in their simultaneous presence. Rhodamine B is worse adsorbed in the presence of methylene blue, but it does not have an inhibitory effect on the methylene blue adsorption capacity. In the ternary solution the amount of adsorbed dyes remained on the similar level to that in the binary solutions for all of them [105].

Doxorubicin adsorption on carbon nanotubes was investigated in the presence of Bromothymol Blue, Methyl Red, Neutral Red and *p*-phenylenediamine. In the solution containing doxorubicin and Bromothymol Blue adsorption amount of both substances was increased with increasing pH. Methyl Red adsorption in the presence of doxorubicin reaches the highest level in the systems characterized by the low pH values. In acidic pH doxorubicin undergoes desorption in the presence of Methyl Red. Doxorubicin and neutral red are both weakly adsorbed [106]. Presence of neutral red and *p*-phenylenediamine prevent doxorubicin adsorption onto nanotubes at neutral pH. At acidic pH above effect was not observed due to the change of dyes charge from neutral to positive [107].

The studies on the competitive adsorption of phenol, p-nitrophenol, p-chlorophenol and p-hydroxybenzoic acid on the sludge-based activated carbon showed that chemical and physical molecule properties and different functional groups located on the aromatic ring have a great effect on their adsorption capacities. The phenol sorption is the slowest of all the tested substances [108]. In the binary solution of p-hydroxybenzoic acid and phenol the adsorption capacity toward p-hydroxybenzoic acid decreases with the increasing phenol concentration. Nevertheless, the adsorbed phenol amount decreases more, independent of p-hydroxybenzoic acid concentration [109].

The adsorption on the granular activated carbon based on the coconut shell from the mixed solution of naproxen, diclofenac, carbamazepine and clofibric acid in the ultrapure water and secondary effluent was investigated. The results showed that carbamazepine was the best adsorbed substance and the clofibric acid adsorption capacity was the smallest. The adsorption capacities from the mixed solution in the ultrapure water decrease compared to those in the single systems. Removal of pharmaceuticals from the secondary effluent was close to zero but it increased in the presence of NaCl. The maximal adsorption capacity for naproxen was 2.74 mg/g, for diclofenac 2.52 mg/g, for carbamazepine 3.00 mg/g and for clofibric 2.48 mg/g [110].

The studies on the simultaneous adsorption of norfloxacin, sulfamerazine and oxytetracycline on the ammonium modified biochar derived from the cassava waste proved that the adsorption capacity of sulfamerazine decreases in the ternary solution. However, the amount of adsorbed norfloxacin and oxytetracycline is larger from the ternary solution compared to that from the single systems [111]. These three antibiotics were also adsorbed on the surface of KOH modified biochar derived from the cassava waste. The results indicate that the adsorbed amounts of all investigated substances decrease in the ternary solution on this adsorbent surface. As follows the adsorption of antibiotics depend on the adsorbent surface (acid-base) properties [112].

The adsorption of sulphonamide, nitroimidazole and tetracycline was investigated using the *P. juliflora* based activated carbon. It was shown that the adsorption of antibiotics from the binary solutions decreases. The decline was the greatest in the binary solution of nitroimidazole and tetracycline and the smallest in the sulphonamide and tetracycline system. The adsorption capacity from the ternary solution was even smaller than that in the binary solutions [113].

The three pharmaceuticals – carbamazepine, oxazepam and paroxetine were adsorbed on the paper mill sludge based activated carbon. The adsorbed paroxetine amount remained the same in the single, binary and ternary solutions. The carbamazepine presence has no significant effect on the oxazepam adsorption, but the paroxetine influence is inhibitory in case of oxazepam adsorption. The adsorbed carbamazepine amounts decrease in the binary and ternary systems. However, the total amount of adsorbed substances was the largest from the ternary solution [114].

Four isomers of hexachlorocyclohexane – α, β, γ and δ were adsorbed on the surface of biochars produced from the digestate, tomato waste and durian shell, from the single and mixed solutions. The obtained data showed that there is no competition between the isomers and the amounts of adsorbed substances are similar from the single and mixed solutions [115].

The adsorption of organic compound on the surface of biochars and activated carbons may proceed through various mechanisms: electrostatic interaction, π-π interaction, hydrophobic interaction, hydrogen bond formation and surface reduction. In the solution containing more than one organic compound, there is often competition for the active sites between compounds. Fig. 3 shows the possible mechanisms of organic compounds adsorption for the mixed solution onto the biochar and activated carbon surfaces. Table 3 presents the recapitulation of the above described investigations.

5. Conclusions

Biochars and activated carbons are widely applied as adsorbents of hazardous and undesirable substances from the liquid phase. Great interest of their usage as adsorbents of metal ions, dyes and pharmaceuticals from the aqueous solutions is still being observed. Their ability to adsorb other inorganic ions and other organic compounds is less frequently tested. Adsorption from mixed solution of the substances with similar chemicals properties often decrease, whereas the presence of two

adsorbates with different properties usually causes the adsorbed amounts increase. The competitive adsorption between different metals on the surface of biochars and activated carbons is extensively described. The results often prove antagonistic interactions between metals, however, this depends largely on metals concentrations and solution pH value. In the solutions containing ions with the same sign but different charge (valence), the competition is considerably limited, because of the different active sites which can be occupied by them on the solid surface. The adsorption of dyes from the multi-component solutions is also extensively investigated. These studies showed that two dyes present in one solution most often exert an inhibitory effect on the mutual adsorption. The studies on adsorption of other organic compounds proved that antagonistic interactions between these substances are most common. This effect is more and more significant as the concentration of both adsorbates increases. However, the systems in which there was no effect of the substances on the mutual adsorption were also found. In the system containing toluene and ethylbenzene the adsorption capacity was greater in binary solution. The adsorption from the solutions containing inorganic ions and organic compound is very complicated. In the examined systems adsorption capacities from the mixed solutions decrease, increase or remain on the same level, depending on the adsorbent properties and type of substances present in the mixed adsorbate system. Nevertheless, the presence of metals ions in the solution usually have positive influence on the organic compound adsorption.

Declaration of Competing Interest

No potential competing interest was reported by the authors.

References

[1] Zhang C, Zeng G, Huang D, Lai C, Chen M, Cheng M, et al. Biochar for environmental management: mitigating greenhouse gas emissions, contaminant treatment, and potential negative impacts. Chem Eng J 2019;373:902–22.
[2] Lehmann J, Joseph S. Biochar for environmental management: Science and technology. London, Sterling, VA: Earthscan; 2009.
[3] Angin D, Altintig E, Köse TE. Influence of process parameters on the surface and chemical properties of activated carbon obtained from biochar by chemical activation. Bioresour Technol 2013;148:542–9.
[4] Lee SM, Choi SS, Tiwari D. Simultaneous removal of Hg(II) and phenol using functionalized activated carbon derived from areca nut waste Lalhmunsiama. Metals 2017;7:248.
[5] Wiśniewska M, Nowicki P. Simultaneous removal of lead(II) ions and poly(acrylic acid) macromolecules from liquid phase using of biocarbons obtained from corncob and peanut shell precursors. J Mol Liq 2019;296:111806.
[6] Nowicki P, Skibiszewska P, Pietrzak R. Hydrogen sulphide removal on carbonaceous adsorbents prepared from coffee industry waste materials. Chem Eng J 2014;248:208–15.
[7] Alam MS, Gorman-Lewis D, Chen N, Flynn SL, Ok YS, Konhauser KO, et al. Thermodynamic analysis of nickel(II) and zinc(II) adsorption to biochar. Environ Sci Tech 2018;52:6246–55.
[8] Khan ZH, Gao M, Qiu W, Islam MS, Song Z. Mechanisms for cadmium adsorption by magnetic biochar composites in an aqueous solution. Chemosphere 2020;246:125701.
[9] Guo Y, Tang W, Wu J, Huang Z, Dai J. Mechanism of Cu(II) adsorption inhibition on biochar by its aging process. J Environ Sci 2014;26(10):2123–30.
[10] Li H, Xiong J, Zhang G, Liang A, Long J, Xiao T, et al. Enhanced thallium(I) removal from wastewater using hypochlorite oxidation coupled with magnetite-based biochar adsorption. Sci Total Environ 2020;698:134166.
[11] Jiang TY, Jiang J, Xu RK, Li Z. Adsorption of Pb(II) on variable charge soils amended with rice-straw derived biochar. Chemosphere 2012;89(3):249–56.
[12] Tran HN, Tomul F, Ha NTH, Nguyen DT, Lima EC, Le GT, et al. Innovative spherical biochar for pharmaceutical removal from water: insight into adsorption mechanism. J Hazard Mater 2020;394:122255.
[13] Fan S, Wang Y, Wang Z, Tang J, Tang J, Li X. Removal of methylene blue from aqueous solution by sewage sludge-derived biochar: adsorption kinetics, equilibrium, thermodynamics and mechanism. J Environ Chem Eng 2017;5(1):601–11.
[14] De Lima LS, Quináia SP, Melquiades FL, De Biasi GEV, Garcia JR. Characterization of activated carbons from different sources and the simultaneous adsorption of Cu, Cr, and Zn from metallurgic effluent. Sep Purif Technol 2014;122:421–30.
[15] Qian L, Chen M, Chen B. Competitive adsorption of cadmium and aluminum onto fresh and oxidized biochars during aging processes. J Soil Sediment 2015;15:1130–8.
[16] Kongsuwan A, Patnukao P, Pavasant P. Binary component sorption of Cu(II) and Pb(II) with activated carbon from Eucalyptus camaldulensis Dehn bark. J Ind Eng Chem 2009;15:465–70.
[17] Machida M, Aikawa M, Tatsumoto H. Prediction of simultaneous adsorption of Cu (II) and Pb(II) onto activated carbon by conventional Langmuir type equations. J Hazard Mater 2005;B120:271–5.
[18] Arcibar-Orozco JA, Rangel-Mendez JR, Diaz-Flores PE. Simultaneous adsorption of Pb(II)-Cd(II), Pb(II)-phenol, and Cd(II)-phenol by activated carbon cloth in aqueous solution. Water Air Soil Pollut 2014;226:2197.
[19] Ding Y, Liu Y, Liu S, Li Z, Tan X, Huang X, et al. Competitive removal of Cd(II) and Pb(II) by biochars produced from water hyacinths: performance and mechanism. RSC Adv 2016;6:5223–32.
[20] Gabaldón C, Marzal P, Ferrer J, Seco A. Single and competitive adsorption of cadmium and zinc onto granular activated carbon. Water Res 1996;30(12):3050–60.
[21] Leyva-Ramos R, Bernal-Jacome LA, Guerrero-Coronado RM, Fuentes-Rubio L. Competitive adsorption of Cd(II) and Zn(II) from aqueous solution onto activated carbon. Sep Sci Technol 2001;36:3673–87.
[22] Erto A, Di Natale F, Musmarra D, Lancia A. Modeling of single and competitive adsorption of cadmium and zinc onto activated carbon. Adsorption 2015;21:611–21.
[23] Depci T, Kul AR, Önal Y. Competitive adsorption of lead and zinc from aqueous solution on activated carbon prepared from Van apple pulp: study in single- and multi-solute systems. Chem Eng J 2012;200-202:224–36.
[24] Wu Y, Yilihan P, Cao J, Jin Y. Competitive adsorption of Cr (VI) and Ni (II) onto coconut shell activated carbon in single and binary systems. Water Air Soil Pollut 2013;224:1662.
[25] Chen X, Chen G, Chen L, Chen Y, Lehmann J, McBride MB, et al. Adsorption of copper and zinc by biochars produced from pyrolysis of hardwood and corn straw in aqueous solution. Bioresour Technol 2011;102(19):8877–84.
[26] Liu Y, Wang L, Wang X, Jing F, Chang R, Chen J. Oxidative ageing of biochar and hydrochar alleviating competitive sorption of Cd(II) and Cu(II). Sci Total Environ 2020;725:138419.
[27] Pipíška M, Richveisová BM, Frišták V, Horník M, Remenárová L, Stiller R, et al. Sorption separation of cobalt and cadmium by straw-derived biochar: a radiometric study. J Radioanal Nucl Chem 2019;311:85–97.
[28] Xiao B, Thomas KM. Competitive adsorption of aqueous metal ions on an oxidized nanoporous activated carbon. Langmuir 2004;20:4566–78.
[29] Cobbina SJ, Duwiejuah AB, Quainoo AK. Single and simultaneous adsorption of heavy metals onto groundnut shell biochar produced under fast and slow pyrolysis. Int J Environ Sci Technol 2019;16:3081–90.
[30] Zheng L, Gao Y, Du J, Zhang W, Huang Y, Zhao Q, et al. Single and binary adsorption behaviour and mechanisms of Cd^{2+}, Cu^{2+} and Ni^{2+} onto modified biochar in aqueous solutions. Processes 2021;9:1829.
[31] Wang HY, Chen P, Zhu YG, Cen K, Sun GX. Simultaneous adsorption and immobilization of As and Cd by birnessite-loaded biochar in water and soil. Environ Sci Pollut Res 2019;26:8575–84.
[32] Zhang Y, Fan J, Fu M, Ok YS, Hou Y, Cai C. Adsorption antagonism and synergy of arsenate(V) and cadmium(II) onto Fe-modified rice straw biochars. Environ Geochem Health 2017;41:1755–66.
[33] Zhu S, Qu T, Irshad MK, Shang J. Simultaneous removal of Cd(II) and As(III) from co-contaminated aqueous solution by α-FeOOH modified biochar. Biochar 2020;2:81–92.
[34] Yoon K, Cho DW, Bhatnagar A, Song H. Adsorption of As(V) and Ni(II) by Fe-Biochar composite fabricated by co-pyrolysis of orange peel and red mud. Environ Res 2020;188:109809.
[35] Makeswari M, Santhi T. Adsorption of Cr(VI) from aqueous solutions by using activated carbons prepared from Ricinus communis leaves: binary and ternary systems. Arab J Chem 2014. https://doi.org/10.1016/j.arabjc.2013.10.005. In press.
[36] Wu Y, Wen Y, Zhou J, Cao J, Jin Y, Wu Y. Comparative and competitive adsorption of Cr(VI), As(III), and Ni(II) onto coconut charcoal. Environ Sci Pollut Res 2012;20:2210–9.
[37] Xiaofeng L, Xin X, Xiaoqiang D, Jounboun P. Competitive adsorption of heavy metal ions from aqueous solutions onto activated carbon and agricultural waste materials. Polish J Environ Stud 2020;29(1):741–61.
[38] Deng J, Liu Y, Liu S, Zeng G, Tan X, Huang B, et al. Competitive adsorption of Pb (II), Cd(II) and Cu(II) onto chitosan-pyromellitic dianhydride modified biochar. J Colloid Interface Sci 2017;506:355–64.
[39] Qin F, Wen B, Shan XQ, Xie YN, Liu T, Zhang SZ, et al. Mechanisms of competitive adsorption of Pb, Cu, and Cd on peat. Environ Pollut 2006;144(2):669–80.
[40] Kavand M, Kaghazchi T, Soleimani M. Optimization of parameters for competitive adsorption of heavy metal ions (Pb^{+2}, Ni^{+2}, Cd^{+2}) onto activated carbon. Korean J Chem Eng 2014;31(4):692–700.
[41] Wang YY, Liu YX, Lu HH, Yang RQ, Yang SM. Competitive adsorption of Pb(II), Cu(II), and Zn(II) ions onto hydroxyapatite-biochar nanocomposite in aqueous solutions. J Solid State Chem 2018;261:53–61.
[42] Wu Q, Dong S, Wang L, Li X. Single and competitive adsorption behaviors of Cu^{2+}, Pb^{2+} and Zn^{2+} on the biochar and magnetic biochar of pomelo peel in aqueous solution. Water 2021;13:868.
[43] Lee HS, Shin HS. Competitive adsorption of heavy metals onto modified biochars: comparison of biochar properties and modification methods. J Environ Manage 2021;299:113651.
[44] Oladipo AA, Ahaka EO, Gazi M. High adsorptive potential of calcined magnetic biochar derived from banana peels for Cu^{2+}, Hg^{2+}, and Zn^{2+} ions removal in single and ternary systems. Environ Sci Pollut Res 2019;26:31887–99.

[45] Deng H, Li Q, Huang M, Li A, Zhang J, Li Y, et al. Removal of Zn(II), Mn(II) and Cu(II) by adsorption onto banana stalk biochar: adsorption process and mechanisms. Water Sci Technol 2020;82(12):2962–74.
[46] Mahdi Z, Yu QJ, El Hanandeh A. Competitive adsorption of heavy metal ions (Pb2+, Cu2+, and Ni2+) onto date seed biochar: batch and fixed bed experiments. Sep Sci Technol 2018:1–14.
[47] Bouhamed F, Elouear Z, Bouzid J, Ouddane B. Multi-component adsorption of copper, nickel and zinc from aqueous solutions onto activated carbon prepared from date stones. Environ Sci Pollut Res 2014;23:15801–6.
[48] Park JH, Cho JS, Ok JS, Kim SH, Heo JS, Delaune RD, et al. Comparison of single and competitive metal adsorption by pepper stem biochar. Arch Agron Soil Sci 2016;62:617–32.
[49] Tho PT, Van HT, Nguyen NH, Hoang TK, Tran TNH, Nguyen TT, et al. Enhanced simultaneous adsorption of As(III), Cd(II), Pb(II) and Cr(VI) ions from aqueous solution using cassava root husk-derived biochar loaded with ZnO nanoparticles. RSC Adv 2021;11:18881–97.
[50] Sellaoui L, Wang H, Badawi M, Bonilla-Petriciolet A, Chen Z. Synergistic adsorption of Pb^{2+} and CrO_4^{2-} on an engineered biochar highlighted by statistical physical modeling. J Mol Liq 2020;312:113483.
[51] Deng Y, Huang S, Dong C, Meng Z, Wang X. Competitive adsorption behaviour and mechanisms of cadmium, nickel and ammonium from aqueous solution by fresh and ageing rice straw biochars. Bioresour Technol 2020;303:122853.
[52] Vijayaraghavan K, Balasubramanian R. Application of pinewood waste-derived biochar for the removal of nitrate and phosphate from single and binary solutions. Chemosphere 2021;278:130361.
[53] Yin Q, Wang R, Zhao Z. Application of MgeAl-modified biochar for simultaneous removal of ammonium, nitrate, and phosphate from eutrophic water. J Clean Prod 2018;176:230–40.
[54] Qin Q, Wu X, Chen L, Jiang Z, Xu Y. Simultaneous removal of tetracycline and cu (II) by adsorption and coadsorption using oxidized activated carbon. RSC Adv 2018;8:1744.
[55] Zhou Y, Liu X, Xiang Y, Wang P, Zhang J, Zhang F, et al. Modification of biochar derived from sawdust and its application in removal of tetracycline and copper from aqueous solution: adsorption mechanism and modelling. Bioresour Technol 2017;245(A):266–73.
[56] Liu CM, Diao ZH, Huo WY, Kong LJ, Du JJ. Simultaneous removal of Cu^{2+} and bisphenol A by a novel biochar-supported zero valent iron from aqueous solution: synthesis, reactivity and mechanism. Environ Pollut 2018;239:698–705.
[57] Ebadollahzadeh H, Zabihi M. Competitive adsorption of methylene blue and Pb (II) ions on the nano-magnetic activated carbon and alumina. Mater Chem Phys 2020;248:122893.
[58] Han X, Liang Cf, Li Tq, Wang K, Huang Hg, Yang Xe. Simultaneous removal of cadmium and sulfamethoxazole from aqueous solution by rice straw biochar. J Zhejiang Univ Sci B 2013;14:640–9.
[59] Ferro-Garcìa MA, Rivera-Utrilla J, Bautista-Toledo I, Moreno-Castilla C. Adsorption of humic substances on activated carbon from aqueous solutions and their effect on the removal of Cr(III) ions. Langmuir 1998;14:1880–6.
[60] Daifullah AAM, Girgis BS, Gad HMH. A study of the factors affecting the removal of humic acid by activated carbon prepared from biomass material. Colloids Surf A Physicochem Eng Asp 2004;235(1–3):1–10.
[61] Bautista-Toledo I, Ferro-Garcìa MA, Rivera-Utrilla J, Moreno-Castilla C, Vegas Fernández FJ. Bisphenol A removal from water by activated carbon. Effects of carbon characteristics and solution chemistry. Environ Sci Technol 2005;39, 16: 6246–50.
[62] Qu J, Dong M, Wei S, Meng Q, Hu L, Hu Q, et al. Microwave-assisted one pot synthesis of β-cyclodextrin modified biochar for concurrent removal of Pb(II) and bisphenol a in water. Carbohydr Polym 2020;250:117003.
[63] Zhang Y, Cao B, Zhao L, Sun L, Gao Y, Li J, et al. Biochar-supported reduced graphene oxide composite for adsorption and coadsorption of atrazine and lead ions. Appl Surf Sci 2018;427:147–55.
[64] Yin Z, Liu Y, Liu S, Jiang L, Tan X, Zeng G, et al. Activated magnetic biochar by one-step synthesis: enhanced adsorption and coadsorption for 17β-estradiol and copper. Sci Total Environ 2018;639:1530–42.
[65] Ai T, Jiang X, Liu Q, Lv L, Dai S. Single-component and competitive adsorption of tetracycline and Zn(II) on an NH_4Cl-induced magnetic ultra-fine buckwheat peel powder biochar from water: studies on the kinetics, isotherms, and mechanism. RSC Adv 2020;10:20427–37.
[66] Dong FX, Yan L, Zhou XH, Huang ST, Liang JY, Zhang WX, et al. Simultaneous adsorption of Cr(VI) and phenol by biochar-based iron oxide composites in water: performance, kinetics and mechanism. J Hazard Mater 2021;416:125930.
[67] Cheng H, Liu Y, Li X. Adsorption performance and mechanism of iron-loaded biochar to methyl orange in the presence of Cr^{6+} from dye wastewater. J Hazard Mater 2021;415:125749.
[68] Jiang J, Peng Y, Huan M, Hong Z, Wang D, Xu R. Rice straw-derived biochar properties and functions as cu(II) and cyromazine sorbents as influenced by pyrolysis temperature. Pedosphere 2015;25(5):781–9.
[69] Yu D, Wang L, Wu M. Simultaneous removal of dye and heavy metal by banana peels derived hierarchically porous carbons. J Taiwan Inst Chem Eng 2018;000: 1–11.
[70] Tan G, Sun W, Xu Y, Wang H, Xu N. Sorption of mercury (II) and atrazine by biochar, modified biochars and biochar based activated carbon in aqueous solution. Bioresour Technol 2016;211:727–35.
[71] Wiśniewska M, Nowicki P, Szewczuk-Karpisz K, Gęca M, Jędruchniewicz K, Oleszczuk P. Simultaneous removal of toxic Pb(II) ions, poly(acrylic acid) and triton X-100 from their mixed solution using engineered biochars obtained from horsetail herb precursor – impact of post-activation treatment. Sep Purif Technol 2021;276:119297.
[72] Zhao N, Zhao C, Lv Y, Zhang W, Du Y, Hao Z, et al. Adsorption and coadsorption mechanisms of Cr(VI) and organic contaminants on H3PO4 treated biochar. Chemosphere 2017;186:422–9.
[73] Choudhary M, Kumar R, Neogi S. Activated biochar derived from Opuntia ficus-indica for the efficient adsorption of malachite green dye, Cu^{+2} and Ni^{+2} from water. J Hazard Mater 2020;392:122411.
[74] Tovar-Gómez R, del Moreno-Virgen MR, Moreno-Pérez J, Bonilla-Petriciolet A, Hernández-Montoya V, Durán-Valle CJ. Analysis of synergistic and antagonistic adsorption of heavy metals and acid blue 25 on activated carbon from ternary systems. Chem Eng Res Des 2015;93:755–72.
[75] Li Z, Wang Z, Wu X, Li M, Liu X. Competitive adsorption of tylosin, sulfamethoxazole and Cu(II) on nano-hydroxyapatite-modified biochar in water. Chemosphere 2020;240:124884.
[76] Jing HP, Li Y, Wangm X, Zhao J, Xia S. Simultaneous recovery of phosphate, ammonium and humic acid from wastewater using a biochar supported Mg $(OH)_2$/bentonite composite. Environ Sci 2019;5:931–43.
[77] Tan G, Mao Y, Wang H, Xu N. A comparative study of arsenic(V), tetracycline and nitrate ions adsorption onto magnetic biochars and activated carbon. Chem Eng Res Des 2020;159:582–91.
[78] Manjunath SV, Kumar M. Evaluation of single-component and multi-component adsorption of metronidazole, phosphate and nitrate on activated carbon from Prosopıs julıflora. Chem Eng J 2018;346:525–34.
[79] Singh N, Balomajumder C. Simultaneous removal of phenol and cyanide from aqueous solution by adsorption onto surface modified activated carbon prepared from coconut shell. J Water Process Eng 2016;9:233–45.
[80] Wang T, Meng Z, Sheng L, Liu Z, Cao X, Wang X, et al. Insights into the mechanism of co-adsorption between tetracycline and nano-TiO_2 on coconut shell porous biochar in binary system. Adv Powd Technol 2021;32(11):4120–9.
[81] Yu C, Qiu JS, Sun YF, Li XH, Chen G, Zhao ZB. Adsorption removal of thiophene and dibenzothiophene from oils with activated carbon as adsorbent: effect of surface chemistry. J Porous Mater 2008;15:151–7.
[82] Chern JM, Chien YW. Competitive adsorption of benzoic acid and p-nitrophenol onto activated carbon: isotherm and breakthrough curves. Water Res 2003;37: 2347–56.
[83] Zhansheng W, Zhonghai S, Pengyun L, Qing L, Renpeng Y, Xia Y. Competitive adsorption of naphthalene and phenanthrene on walnut shell based activated carbon and the verification via theoretical calculation. RSC Adv 2020;10: 10703–14.
[84] Iovino P, Canzano S, Capasso S, Di Natale M, Erto A, Lama A, et al. Single and competitive adsorption of toluene and naphthalene onto activated carbon. Chem Eng Trans 2013;32:67–72.
[85] Jayawardhana Y, Keerthanan S, Lam SS, Vithanage M. Ethylbenzene and toluene interactions with biochar from municipal solid waste in single and dual systems. Environ Res 2021;197:111102.
[86] Abdoul Magid ASI, Islam MS, Chen Y, Weng L, Sun Y, Chang X, et al. Competitive adsorption of Dibutyl phthalate (DBP) and Di(2-ethylhexyl) phthalate (DEHP) onto fresh and oxidized corncob biochar. Chemosphere 2021;280:130639.
[87] Mansouri H, Carmona RJ, Gomis-Berenguer A, Soussi-Najar S, Ouederni A, Ania CO. Competitive adsorption of ibuprofen and amoxicillin mixtures from aqueous solution on activated carbons. J Colloid Interface Sci 2015;449:252–60.
[88] Li M, Zhao Z, Wu X, Zhou W, Zhu L. Impact of mineral components in cow manure biochars on the adsorption and competitive adsorption of oxytetracycline and carbaryl. RSC Adv 2017;7:2127–36.
[89] Heo J, Yoon Y, Lee G, Kim Y, Han J, Park CM. Enhanced adsorption of bisphenol A and sulfamethoxazole by a novel magnetic $CuZnFe_2O_4$–biochar composite. Bioresour Technol 2019;281:179–87.
[90] Reguyal F, Sarmah AK. Adsorption of sulfamethoxazole by magnetic biochar: effects of pH, ionic strength, natural organic matter and 17α-ethinylestradiol. Sci Total Environ 2018;628-629:722–30.
[91] Medina FMO, Aguiar MB, Parolo ME, Avena MJ. Insights of competitive adsorption on activated carbon of binary caffeine and diclofenac solutions. J Environ Manage 2021;278(2):111523.
[92] Hu B, Tang Y, Wang X, Wu L, Nong J, Yang X, et al. Cobalt-gadolinium modified biochar as an adsorbent for antibiotics in single and binary systems. Microchem J 2021;166:106235.
[93] Pelekani C, Snoeyink VL. A kinetic and equilibrium study of competitive adsorption between atrazine and Congo red dye on activated carbon: the importance of pore size distribution. Carbon 2001;39(1):25–37.
[94] Oladipo AA, Ifebajo AO, Nisar N, Ajayi OA. High-performance magnetic chicken bone-based biochar for efficient removal of rhodamine-B dye and tetracycline: competitive sorption analysis. Water Sci Technol 2017;76(2):373–85.
[95] Fernandez ME, Nunell GV, Bonelli PR, Cukierman AL. Activated carbon developed from orange peels: batch and dynamic competitive adsorption of basic dyes. Ind Crop Prod 2014;62:437–45.
[96] Su L, Zhang H, Oh K, Liu N, Luo Y, Cheng H, et al. Activated biochar derived from spent *Auricularia auricula* substrate for the efficient adsorption of cationic azo dyes from single and binary adsorptive systems. Water Sci Technol 2021;84(1): 101–21.
[97] Chen Q, Zhang Q, Yang Y, Wang Q, He Y, Dong N. Synergetic effect on methylene blue adsorption to biochar with gentian violet in dyeing and printing wastewater under competitive adsorption mechanism. Case Stud Therm Eng 2021;26: 101099.

[98] Jarrah N. Competitive adsorption isotherms of rhodium 6G and methylene blue on activated carbon prepared from residual fuel oil. J Environ Chem Eng 2017;5(5):4319–26.
[99] Ding G, Wang B, Chen L, Zhao S. Simultaneous adsorption of methyl red and methylene blue onto biochar and an equilibrium modeling at high concentration. Chemosphere 2016;163:283–9.
[100] Choi YK, Gurav R, Kim HJ, Yang YH, Bhatia SK. Evaluation for simultaneous removal of anionic and cationic dyes onto maple leaf-derived biochar using response surface methodology. Appl Sci 2020;10(9):2982.
[101] Ghaedi M, Mosallanejad N. Study of competitive adsorption of malachite green and sunset yellow dyes on cadmium hydroxide nanowires loaded on activated carbon. J Ind Eng Chem 2014;20(3):1085–96.
[102] Regti A, El Kassimi A, Laamari MR, El Haddad M. Competitive adsorption and optimization of binary mixture of textile dyes: a factorial design analysis. J Assoc Arab Univ Basic Appl Sci 2017;24:1–9.
[103] Thivya J, Vijayaraghavan J. Single and binary sorption of reactive dyes onto red seaweed-derived biochar: multi-component isotherm and modelling. Desal Water Treat 2019;156:87–98.
[104] Al-Degs Y, Khraisheh MAM, Allen SJ, Ahmad MN, Walker GM. Competitive adsorption of reactive dyes from solution: equilibrium isotherm studies in single and multisolute systems. Chem Eng J 2007;128:163–7.
[105] Mahmoodi NM, Taghizadeh M, Taghizadeh A. Mesoporous activated carbons of low-cost agricultural bio-wastes with high adsorption capacity: preparation and artificial neural network modeling of dye removal from single and multicomponent (binary and ternary) systems. J Mol Liq 2018;269:217–28.
[106] Panczyk T, Wolski P, Lajtar L. Coadsorption of doxorubicin and selected dyes on carbon nanotubes. Theoretical investigation of potential application as a pH-controlled drug delivery system. Langmuir 2016;32(19):4719–28.
[107] Wolski P, Nieszporek K, Panczyk T. Pegylated and folic acid functionalized carbon nanotubes as pH controlled carriers of doxorubicin. Molecular dynamics analysis of the stability and drug release mechanism. Phys Chem Chem Phys 2017;19(13):9300–12.
[108] Mohamed EF, Andriantsiferana C, Wilhelm AM, Delmas H. Competitive adsorption of phenolic compounds from aqueous solution using sludge-based activated carbon. Environ Technol 2011;32(12):1325–36.
[109] Andriantsiferana C, Julcour-Lebigue C, Creanga-Manole C, Delmas H, Wilhelm AM. Competitive adsorption of p-hydroxybenzoic acid and phenol on activated carbon: experimental study and modeling. J Environ Eng 2013;139(3):402–9.
[110] Bo L, Gao N, Liu J, Gao B. The competitive adsorption of pharmaceuticals on granular activated carbon in secondary effluent. Desal Water Treat 2015;57(36):17023–9.
[111] Luo J, Li X, Ge C, Müller K, Yu H, Deng H, et al. Preparation of ammonium-modified cassava waste-derived biochar and its evaluation for synergistic adsorption of ternary antibiotics from aqueous solution. J Environ Manage 2021;298:113530.
[112] Luo J, Li X, Ge C, Müller K, Yu H, Huang P, et al. Sorption of norfloxacin, sulfamerazine and oxytetracycline by KOH-modified biochar under single and ternary systems. Bioresour Technol 2018;263:285–392.
[113] Manjunath SV, Singh Baghel R, Kumar M. Antagonistic and synergistic analysis of antibiotic adsorption on Prosopis Juliflora activated carbon in multicomponent systems. Chem Eng J 2019;381:122713.
[114] Calisto V, Jaria G, Silva CP, Ferreira CIA, Otero M, Estaves VI. Single and multi-component adsorption of psychiatric pharmaceuticals onto alternative and commercial carbons. J Environ Manage 2017;192:15–24.
[115] Silvani L, Cornelissen G, Hale SE. Sorption of α-, β-, γ- and δ-hexachlorocyclohexane isomers to three widely different biochars: sorption mechanisms and application. Chemosphere 2019;219:1044–51.

Lublin, 10.09.2025

mgr Marlena Groszek
Uniwersytet Marii Curie-Skłodowskiej w Lublinie,
Wydział Chemii, Instytut Nauk Chemicznych,
Katedra Radiochemii i Chemii Środowiskowej,
Pl. Marii Curie-Skłodowskiej 3, 20-031 Lublin
marlena.groszek@mail.umcs.pl

Rada Naukowa Instytutu Nauk Chemicznych
Uniwersytetu Marii Cure-Skłodowskiej
w Lublinie

Oświadczenie o współautorstwie

Niniejszym oświadczam, że mój udział w pracy: **M. Gęca**, M. Wiśniewska, P. Nowicki, *Biochars and activated carbons as adsorbents of inorganic and organic compounds from multicomponent systems – A review,* Advances in Colloid and Interface Science, 305, 2022, 102687, DOI:10.1016/j.cis.2022.102687 [D1], obejmował stworzenie koncepcji artykułu, przegląd literatury, analizę wybranych publikacji, przygotowanie manuskryptu, jego korektę po procesie oceny w redakcji oraz udzielenie odpowiedzi na uwagi recenzentów.

Marlena Groszek

Lublin, 10.09.2025

prof. dr hab. Małgorzata Wiśniewska
Uniwersytet Marii Curie-Skłodowskiej w Lublinie,
Wydział Chemii, Instytut Nauk Chemicznych,
Katedra Radiochemii i Chemii Środowiskowej,
Pl. Marii Curie-Skłodowskiej 3, 20-031 Lublin
malgorzata.wisniewska@mail.umcs.pl

Rada Naukowa Instytutu Nauk Chemicznych
Uniwersytetu Marii Cure-Skłodowskiej
w Lublinie

Oświadczenie o współautorstwie

Niniejszym oświadczam, że mój udział w pracy: M. Gęca, **M. Wiśniewska**, P. Nowicki, *Biochars and activated carbons as adsorbents of inorganic and organic compounds from multicomponent systems – A review,* Advances in Colloid and Interface Science, 305, 2022, 102687, DOI:10.1016/j.cis.2022.102687 [D1], obejmował nadzór merytoryczny pracy i korektę pierwszej wersji manuskryptu.

Małgorzata Wiśniewska

Poznań, 10.09.2025

dr hab. Piotr Nowicki, prof. UAM
Uniwersytet im. Adama Mickiewicza w Poznaniu,
Wydział Chemii, Zakład Chemii Stosowanej,
Ul. Uniwersytetu Poznańskiego 8, 61-614 Poznań
piotr.nowicki@amu.edu.pl

Rada Naukowa Instytutu Nauk Chemicznych
Uniwersytetu Marii Cure-Skłodowskiej
w Lublinie

Oświadczenie o współautorstwie

Niniejszym oświadczam, że mój udział w pracy: M. Gęca, M. Wiśniewska, **P. Nowicki**, *Biochars and activated carbons as adsorbents of inorganic and organic compounds from multicomponent systems – A review,* Advances in Colloid and Interface Science, 305, 2022, 102687, DOI:10.1016/j.cis.2022.102687 [D1], obejmował korektę pierwszej wersji manuskryptu oraz udział w przygotowaniu odpowiedzi na uwagi recenzentów.

Piotr Nowicki

D2. M. Gęca, M. Wiśniewska, P. Nowicki, *Modified method of lignocellulose content determination and its use for the analysis of selected herbs - precursors of biochars and activated carbons,* Measurement (Journal of the International Measurement Confederation), 212, 2023, 112672, DOI: 10.1016/j.measurement.2023.112672

Measurement 212 (2023) 112672

Contents lists available at ScienceDirect

Measurement

journal homepage: www.elsevier.com/locate/measurement

Modified method of lignocellulose content determination and its use for the analysis of selected herbs - precursors of biochars and activated carbons

Marlena Gęca [a], Małgorzata Wiśniewska [a,*], Piotr Nowicki [b]

[a] Department of Radiochemistry and Environmental Chemistry, Institute of Chemical Sciences, Faculty of Chemistry, Maria Curie-Skłodowska University in Lublin, M. Curie-Skłodowska Sq. 3, 20-031 Lublin, Poland
[b] Department of Applied Chemistry, Faculty of Chemistry, Adam Mickiewicz University in Poznań, Uniwersytetu Poznańskiego 8, 61-614 Poznań, Poland

ARTICLE INFO

Keywords:
Lignocellulose content
Herbs analysis
Activated carbon
Mineral substance
Extractives

ABSTRACT

Determination of extractives, lignin, hemicellulose, cellulose and mineral substance is a complex procedure. Lignin and hemicellulose are both alkali soluble and their mutual determination is disturbed. Moreover, the lignin occurs in two fractions - soluble and insoluble in acids, which make its determination difficult. In this paper a new, modified method of all the above components determination was described. The inaccuracies in methods reported in the literature so far were solved. There was applied not sophisticated equipment aimed at the costs reduction. The complicated, multistep lignin content determination was replaced by easier procedure of cellulose evaluation. Moreover the hemicellulose determination was improved (the error related with lignin dissolution in alkaline solution was eliminated).

The presented method was used for the nettle, sage, lemon balm and mint herbs analyses. The herbs contain a small percentage of mineral substance and are very suitable for the activated carbons preparation. It has been shown that the content of hemicellulose affects the activated carbons surface area development, whereas the lignin content has influence on the concentration of total surface functional groups. Activated carbons with the best surface properties were obtained from the herbs containing high concentrations of hemicellulose and lignin.

1. Introduction

Plants and biomass are found to be environmental friendly and useful materials. They are applied for activated carbons preparation, biofuels production as well as chemicals synthesis [1,2]. However, their industrial application is strictly related to their composition. Plant materials include the extraction parts (lipids, chlorophyll and moisture), cellulose, hemicellulose, lignin and mineral substance. Contents of the above components varies in genre, harvesting sites and shoot fragments. Cellulose, hemicellulose and lignin form together lignocellulose, which is the fibrous material making the cell walls of the plants [3]. The content of all plant material components has direct influence on their chemical and physical properties.

Various methods of cellulose, hemicellulose, lignin, extractives and mineral substance contents determination are widely described in the literature. However, most of these methods require the use of expensive and complex equipment [4,5]. On the other hand, the gravimetric methods are often multi-stage and focus on the labelling substances, ignoring the interfering ingredients. The basic extraction commonly used for hemicellulose quantification caused also partial lignin dissolution. Moreover, the lignin content determination is difficult due to its occurrence in two fractions - soluble and insoluble in acids [6].

In this paper the modified method of lignocellulose content determination, based on the [7] procedure (Fig. 1), was described. The inaccuracies related to the methods reported in the literature so far were solved. Difficult lignin quantification that requires the use of a calibration curve was eliminated and a new cellulose determination method was proposed. The developed procedure was used for the extraction parts, cellulose, hemicellulose, lignin and mineral substance contents determination in the nettle (NE), sage (SA), lemon balm (LB) and mint (MT) herbs stems (mostly stalks). The examined herbs were used as precursors (P) for biochars (B) and activated carbons (AC) preparation. The lignocellulose content in the precursors was related to the obtained solids textural parameters and their acidic-basic properties.

* Corresponding author.
E-mail address: malgorzata.wisniewska@mail.umcs.pl (M. Wiśniewska).

https://doi.org/10.1016/j.measurement.2023.112672
Received 4 November 2022; Received in revised form 31 January 2023; Accepted 1 March 2023
Available online 8 March 2023

2. Material and methods

2.1. Modified procedure of the lignocellulosic components determination

2.1.1. Extractives content determination

150 cm^3 of acetone (Sigma Aldrich) was used for extraction. The process was conducted for 4 h with the usage of ROTAX 6.8 Overhead Mixer, provided by VELP Scientifica Srl, Italy. After the extraction the suspensions were filtered and the solids were dried at 105 °C (Fig. 2b, c). The % (w/w) of the extractives content was evaluated as the difference in weight between the raw initial biomass and the extractives-free biomass. The Soxhlet extraction (used in the previously described procedures) was replaced by the simpler equipment – the stirrer and filters, without deterioration of quality.

2.1.2. Hemicellulose content determination

For the hemicellulose quantification 1 ± 0.001 g of the extracted dried biomass was transferred into a 500 cm^3 round bottom flask and 150 cm^3 of 0.5 mol/dm^3 NaOH (Stanlab) was added. The mixture was boiled under a reflux condenser for 3 h. After that time the suspension was cooled and filtrated (Fig. 2d). During the basic extraction both hemicellulose and lignin are extracted [8]. To specify the hemicellulose content in the herbs it should be precipitated. For this purpose the concentrated HCl solution (Chempur) was added to the filtrate until a solution pH reached the value 5.5. Next 500 cm^3 of 95 % ethanol was added, the solution was mixed up until hemicellulose was precipitated [9]. The suspension was filtered under the vacuum using a filtering crucible. The precipitate was dried at 105 °C, cooled down and weighed. The hemicellulose mass was obtained in such a way. Compared to the original method the precipitation step was added because the filtrate contained both hemicellulose and lignin.

2.1.3. Cellulose content determination

To determine the cellulose content 1 ± 0.001 g of the extracted dried biomass was transferred into the 100 cm^3 round bottom flask and 20 cm^3 of 3 % HNO_3 (Chempur) was added. The mixture was boiled under the reflux condenser for 30 min (Fig. 2e). After that time the suspension was cooled down and filtrated (Fig. 2f). The solid was again introduced into the 100 cm^3 round bottom flask and 20 cm^3 of 3 % NaOH (Stanlab) was added. The mixture was again boiled under the reflux condenser for 30 min, cooled and filtrated. The obtained cellulose was dried at 95 °C, cooled and weighed [10]. The cellulose content was calculated by the difference between the raw biomass and the other components as in the original method. In this paper the lignin determination stage was

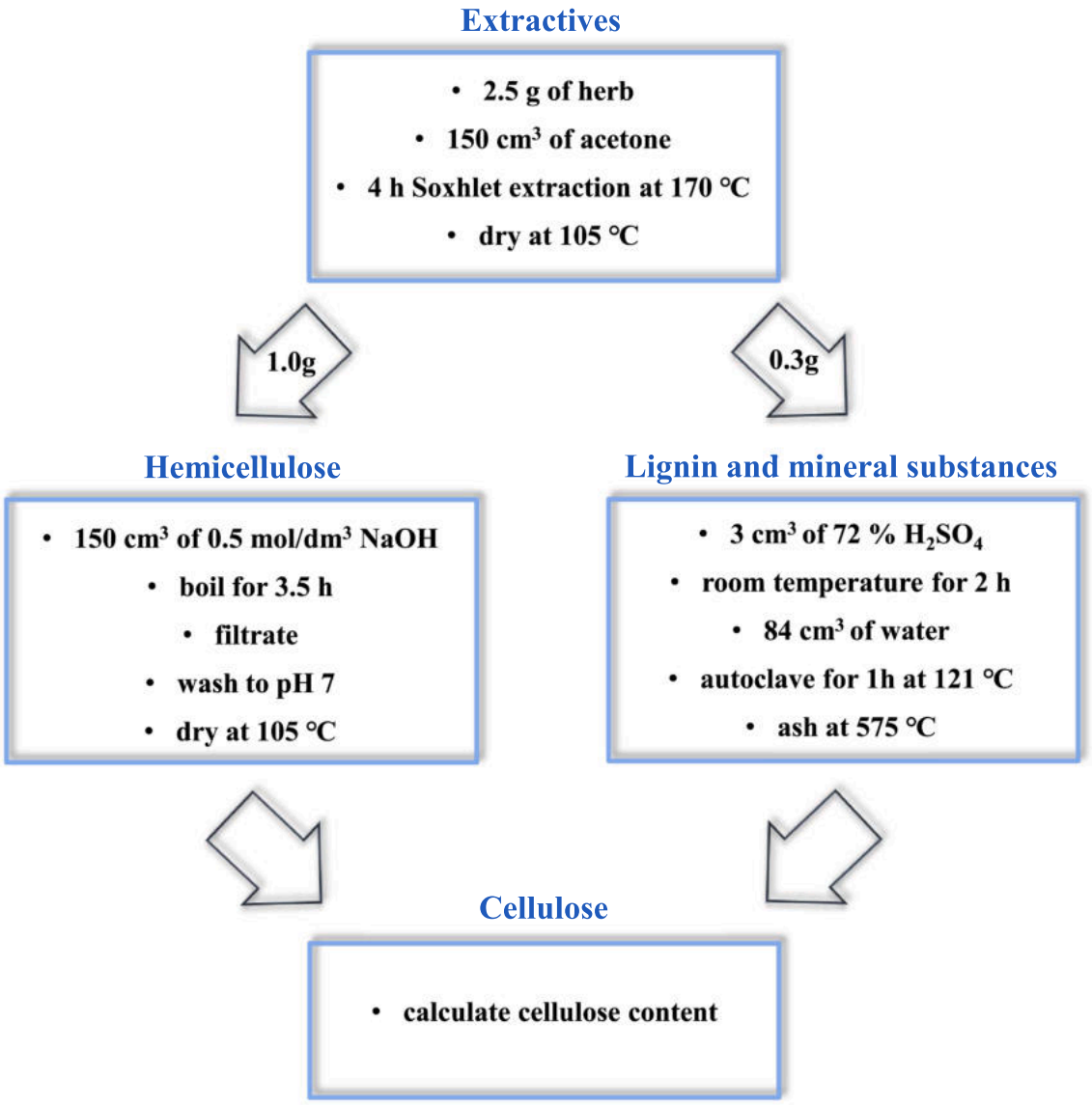

Fig. 1. Schematic representation of the analysis of the lignocellulosic components content determination proposed by [7].

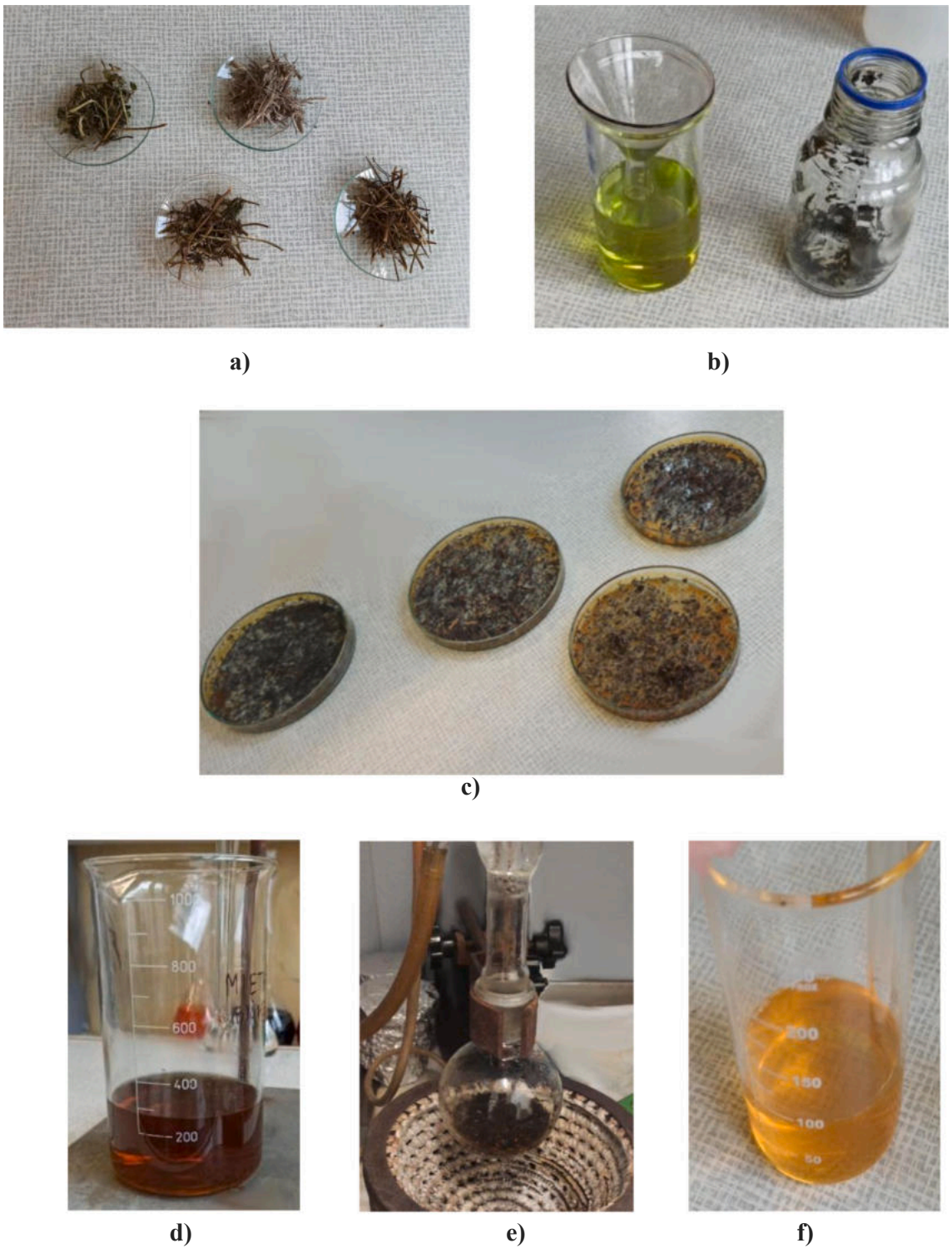

Fig. 2. Lignocellulose determination: a – herbs before the procedure, b - filtrate and extraction residue, c - dry residues after the extraction, d - filtrate containing hemicellulose and some amounts of lignin, e - boiling during the cellulose content determination, f - filtrate after boiling with HNO_3.

replaced by the cellulose determination procedure.

2.1.4. Mineral substance content determination

The mineral substance content was determined without any modifications in the previously described procedure. For this purpose 0.3 ± 0.001 g of extracted dried biomass was incinerated at 575 °C for 90 min, using the chamber furnace (MT-1100–5-B2, provided by MagmaTherm, Turkey). The mineral residue was cooled down and weighed.

2.1.5. Lignin content calculation

The lignin content was calculated by the difference between the raw biomass and already determined components (extractives,

Table 1
Composition of the nettle, sage, lemon balm and mint herbs (including the standard deviations (SD)).

Plant	Content [%]				
	Extractives	Hemicellulose	Cellulose	Lignin	Mineral substance
NE_P	10.73 ± 0.44	10.25 ± 0.49	18.10 ± 0.49	60.15 ± 0.73	0.77 ± 0.03
SA_P	21.04 ± 0.91	19.06 ± 0.65	19.35 ± 0.94	39.22 ± 1.21	1.33 ± 0.04
LB_P	10.25 ± 0.28	24.49 ± 0.64	12.25 ± 0.54	51.51 ± 1.12	1.50 ± 0.06
MT_P	12.05 ± 0.48	27.42 ± 1.10	16.28 ± 0.51	43.13 ± 1.15	0.67 ± 0.03

$$SD = \sqrt{\frac{x_1^2 + x_2^2 + x_3^2 + x_4^2}{4} - \left(\frac{x_1 + x_2 + x_3 + x_4}{4}\right)^2}$$

hemicellulose, cellulose, mineral substance). The lignin direct determination is difficult due to its two fractions - soluble and insoluble in acids. Calculating its content seems to be a more accurate and convenient method. The original lignin content determination was eliminated due to its complexity and requirements of the use of a calibration curve and lignin standard.

Each experiment was repeated four times. The standard deviations were also calculated (Table 1). The obtained values proved that they not exceed 5 % which means that the proposed modified method is right and gives reliable results. The scheme of the new modified procedure of the lignocellulose content determination is presented in Fig. 3.

Table 2
Elemental composition of the nettle, sage, lemon balm and mint herbs.

Plant	Content [wt. %]		
	Carbon	Hydrogen	Nitrogen
NE_P	38.02	7.01	4.17
SA_P	43.96	7.35	1.62
LB_P	40.60	6.77	2.61
MT_P	41.06	6.80	3.09

Table 3
Textural parameters of the biochars and activated carbons.

Material	Specific surface area [m^2/g]	Pore volume [cm^3/g]	Mean pore size [nm]
NE_B	2.5	0.006	9.594
SA_B	2.2	0.006	10.555
LB_B	2.2	0.005	9.397
MT_B	3.1	0.007	8.403
NE_AC	801	0.847	4.423
SA_AC	842	0.826	3.926
LB_AC	950	1.100	4.630
MT_AC	1145	1.465	5.115

2.2. Precursors and activated carbons characterization

The nettle, sage, lemon balm and mint herbs used in this paper were harvested in Wielkopolska region (Poland). The precursors were cut into 1.5–2.0 cm pieces, dried at 110 °C (Fig. 2a) and subjected to the procedure described below. For the biochars preparation purpose, the

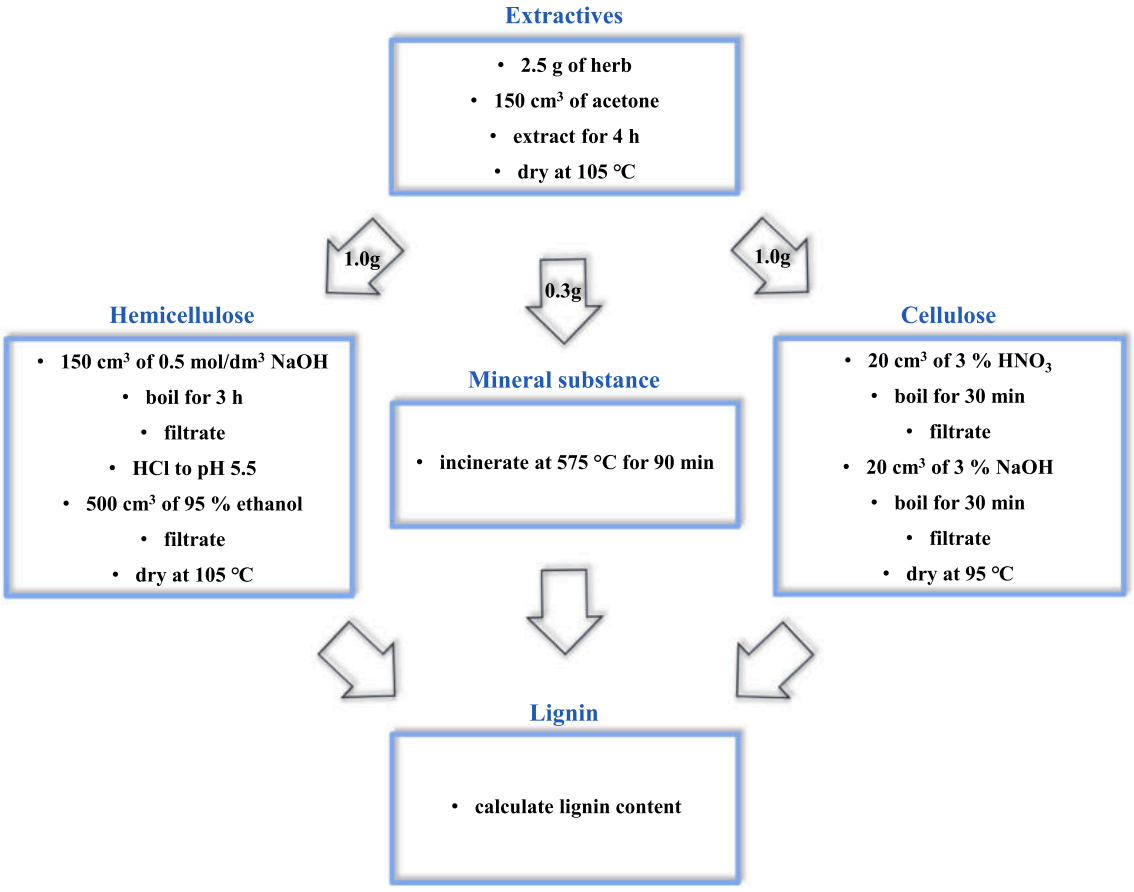

Fig. 3. Schematic representation of the modified procedure of the lignocellulosic components determination.

Table 4
Acidic-basic properties of the precursors, biochars and activated carbons.

Material	Acidic functional groups content [mmol/g]	Basic functional groups content [mmol/g]	Total functional groups content [mmol/g]
NE_P	1.302	0.766	2.068
SA_P	0.838	1.148	1.986
LB_P	0.936	0.818	1.754
MT_P	0.572	0.930	1.502
NE_B	1.041	1.753	2.794
SA_B	1.109	1.008	2.197
LB_B	0.822	0.804	1.624
MT_B	1.365	0.650	2.015
NE_AC	0.858	0.272	1.130
SA_AC	0.436	0.215	0.651
LB_AC	0.682	0.305	0.987
MT_AC	0.494	0.300	0.764

precursors were pyrolyzed for 60 min at 400 °C. In order to obtain the activated carbons, the precursors were impregnated with 50 % phosphoric(V) acid solution for 24 h, dried at 110 °C and next subjected to the two-step heat treatment (for 30 min at 200 °C and 30 min at 500 °C).

The C,H,N,S content in all examined herbs were determined with the use of EuroVector EA 3000 Elemental Analyzer (Perkin-Elmer, Waltham, Massachusetts, USA). The total surface area, total pore volume and average pore diameter of the obtained biochars and activated carbons were determined by the low-temperature nitrogen adsorption – desorption isotherms measured at − 196 °C using ASAP 2420 (Accelerated Surface Area and Porosimetry System) provided by Micromeritics (Norcross, GA, USA). The surface functional groups content (of basic and acidic character) was determined according to the Boehm method [11].

3. Results and discussion

The basic compositions of the nettle, sage, lemon balm and mint herbs are presented in Table 1. The main component of all the examined herbs is lignin, which is the component responsible for the plant stiffness. The examined plant materials consisted mainly of stalks, which justify the high content of lignin. It should be noted that there were not experimental data concerning determination of contents of extractives, hemicellulose, cellulose, lignin and mineral substance in the studied herbs in available literature reports. Table 2 presents the elemental composition of the examined herbs. Hemicellulose, cellulose and lignin contains only carbon, hydrogen and oxygen atoms. High content of C and H confirm that these three substances are most probably the main components of the used herbs. The precursors used for the study contain also some amounts of nitrogen, ranging from 1.62 to 4.17 wt%. In turn, sulfur has not been found in the structure of any material.

Textural parameters of the biochars and activated carbons obtained by pyrolysis or activation of the above-mentioned precursors are presented in Table 3. Additionally, the acidic-basic properties of the precursors and carbonaceous materials are presented in Table 4. The MT_AC sample obtained by means of chemical activation of the mint herb has the most developed specific surface area (1145 m^2/g), whereas the smallest value of this textural parameter (only 801 m^2/g) is observed for the activated carbon obtained from the nettle herb. The biochars prepared from these herbs show the analogous properties. This dependence can be related to the hemicellulose content in the used precursors, nettle contains the smallest amount of hemicellulose and mint the largest one.(See Table 1).

All obtained activated carbons are characterized by higher content of the acidic functional groups than the basic ones, most probably due to the impregnation with H_3PO_4 before activation step. However, the total amount of the surface functional groups can be related to the lignin content in the precursors structure. As can be seen, NE_AC sample obtained by chemical activation of nettle herb (containing the largest amount of lignin) shows the greatest total functional groups content among all materials under investigation. For the same reason the usage of the sage herb as the precursor with the smallest lignin content, results in preparation of the activated carbon containing the smallest total concentration of surface groups.

4. Conclusions

The presented method is a very simple procedure for extractive parts, hemicellulose, cellulose, lignin and mineral substance content determination. The proposed experimental steps are economically justified, there is no need to use complex equipment and all chemicals used are commonly available. The extractives content determination methods were simplified. The precipitation step was added to the hemicellulose content determination, in order to eliminate the error related to the alkaline lignin extraction. The difficult lignin content determination method was omitted and replaced by the simpler cellulose content determination one. The lignin content was calculated by the difference of raw initial biomass weight and the weights of the other determined components. The proposed modified method could be used for both wood and raw plant materials.

The examined herbs contain a small content of mineral substance and can be successfully used for biochars and activated carbons preparation. The activated carbons obtained from the nettle, sage, lemon balm and mint stalks have well developed specific surface areas. With the increasing content of hemicellulose in the precursors, the activated carbon surface area increases. In turn, the total functional group content for the activated carbons can be related to the lignin content in the herb precursors - their concentration increases significantly with the increasing lignin content.

CRediT authorship contribution statement

Marlena Gęca: Writing – original draft, Investigation, Methodology, Visualization. **Małgorzata Wiśniewska:** Writing – review & editing, Resources, Supervision. **Piotr Nowicki:** Conceptualization, Investigation, Writing – review & editing, Resources.

Declaration of Competing Interest

The authors declare that they have no known competing financial interests or personal relationships that could have appeared to influence the work reported in this paper: [Marlena Geca reports financial support was provided by Maria Curie-Sklodowska University. Malgorzata Wisniewska reports financial support was provided by Maria Curie-Sklodowska University. Piotr Nowicki reports financial support was provided by Adam Mickiewicz University.].

Data availability

Data will be made available on request.

References

[1] M. Gęca, M. Wiśniewska, P. Nowicki, Biochars and activated carbons as adsorbents of inorganic and organic compounds from multicomponent systems – a review, Adv. Colloid Interface Sci. 305 (2022), 102687, https://doi.org/10.1016/j.cis.2022.102687.
[2] E. Scott, F. Peter, J. Sanders, Biomass in the manufacture of industrial products – the use of proteins and amino acids, Appl. Microbiol. Biotechnol. 75 (4) (2007) 751–762, https://doi.org/10.1007/s00253-007-0932-x.
[3] J.P. Lange, Lignocellulose conversion: an introduction to chemistry, process and economic, Biofuels, Bioproducts and Biorefining: Innovation for a sustainable economy 1 (1) (2007) 39–48, https://doi.org/10.1002/bbb.7.
[4] N. Terinte, R. Ibbett, K.C. Schuster, Overview on native cellulose and microcrystalline cellulose I structure studied by X-ray diffraction (WAXD): comparison between measurement techniques, Lenzinger Berichte 89 (1) (2011) 118–131.
[5] A. B. Bjerre, A. Plöger, T. Simonsen, A. Woidemann, A. S. Schmidt, Quantification of solubilized hemicellulose from pretreated lignocellulose by acid hydrolysis and

high-performance liquid chromatography. Denmark. Forskningscenter Risoe. Risoe-R No. 855(EN) 1996.
[6] R. Hatfield, R.S. Fukushima, Can lignin be accurately measured? Crop Sci. 45 (3) (2005) 832–839, https://doi.org/10.2135/cropsci2004.0238.
[7] A.O. Ayeni, O.A. Adeeyo, O.M. Oresegun, T.E. Oladimeji, Compositional analysis of lignocellulosic materials: evaluation of an economically viable method suitable for woody and non-woody biomass, Am. J. Eng. Res. 4 (4) (2015) 14–19.
[8] H.N. Rabetafika, B. Bchir, C. Blecker, M. Paquot, B. Wathelet, Comparative study of alkaline extraction process of hemicelluloses from pear pomace, Biomass Bioenergy 61 (2014) 254–264, https://doi.org/10.1016/j.biombioe.2013.12.022.
[9] W. Geng, R. Narron, X. Jiang, J.J. Pawlak, H.M. Chang, S. Park, H. Jameel, R. A. Venditti, The influence of lignin content and structure on hemicellulose alkaline extraction for non-wood and hardwood lignocellulosic biomass, Cellul. 26 (5) (2019) 3219–3230, https://doi.org/10.1007/s10570-019-02261-y.
[10] S. Prosiński, R. Babicki, O nowej metodzie oznaczania celulozy przy użyciu rozcieńczonych roztworów kwasu azotowego i wodorotlenku sodu [On a new method of cellulose determination using dilute solutions of nitric acid and sodium hydroxide], Sylwan 104 (1) (1960) 95–99 [in Polish].
[11] A. Bazan-Wozniak, P. Nowicki, R. Pietrzak, The effect of demineralization on the physicochemical and sorption properties of activated bio-carbons, Adsorption 25 (2019) 337–343, https://doi.org/10.1007/s10450-019-00009-5.

Lublin, 10.09.2025

mgr Marlena Groszek
Uniwersytet Marii Curie-Skłodowskiej w Lublinie,
Wydział Chemii, Instytut Nauk Chemicznych,
Katedra Radiochemii i Chemii Środowiskowej,
Pl. Marii Curie-Skłodowskiej 3, 20-031 Lublin
marlena.groszek@mail.umcs.pl

Rada Naukowa Instytutu Nauk Chemicznych
Uniwersytetu Marii Cure-Skłodowskiej
w Lublinie

Oświadczenie o współautorstwie

Niniejszym oświadczam, że mój udział w pracy: **M. Gęca**, M. Wiśniewska, P. Nowicki, *Modified method of lignocellulose content determination and its use for the analysis of selected herbs - precursors of biochars and activated carbons,* Measurement (Journal of the International Measurement Confederation), 212, 2023, 112672. DOI: 10.1016/j.measurement.2023.112672 [D2], obejmował stworzenie koncepcji manuskryptu, opracowanie nowej metodyki oznaczania związków lignocelulozowych w biomasie, przeprowadzenie badań, przygotowanie artykułu i jego korektę zgodnie z uwagami recenzentów.

Marlena Groszek

Lublin, 10.09.2025

prof. dr hab. Małgorzata Wiśniewska
Uniwersytet Marii Curie-Skłodowskiej w Lublinie,
Wydział Chemii, Instytut Nauk Chemicznych,
Katedra Radiochemii i Chemii Środowiskowej,
Pl. Marii Curie-Skłodowskiej 3, 20-031 Lublin
malgorzata.wisniewska@mail.umcs.pl

Rada Naukowa Instytutu Nauk Chemicznych
Uniwersytetu Marii Cure-Skłodowskiej
w Lublinie

Oświadczenie o współautorstwie

Niniejszym oświadczam, że mój udział w pracy: M. Gęca, **M. Wiśniewska**, P. Nowicki, *Modified method of lignocellulose content determination and its use for the analysis of selected herbs - precursors of biochars and activated carbons,* Measurement (Journal of the International Measurement Confederation), 212, 2023, 112672. DOI: 10.1016/j.measurement.2023.112672 [D2], obejmował korektę manuskryptu – przed i po procesie recenzji oraz nadzór merytoryczny w czasie całego cyklu wydawniczego.

Małgorzata Wiśniewska

Poznań, 10.09.2025

dr hab. Piotr Nowicki prof. UAM
Uniwersytet im. Adama Mickiewicza w Poznaniu,
Wydział Chemii, Zakład Chemii Stosowanej
Ul. Uniwersytetu Poznańskiego 8, 61-614 Poznań
piotr.nowicki@amu.edu.pl

Rada Naukowa Instytutu Nauk Chemicznych
Uniwersytetu Marii Cure-Skłodowskiej
w Lublinie

Oświadczenie o współautorstwie

Niniejszym oświadczam, że mój udział w pracy: M. Gęca, M. Wiśniewska, **P. Nowicki**, *Modified method of lignocellulose content determination and its use for the analysis of selected herbs - precursors of biochars and activated carbons,* Measurement (Journal of the International Measurement Confederation), 212, 2023, 112672. DOI: 10.1016/j.measurement.2023.112672 [D2], obejmował stworzenie koncepcji artykułu, przeprowadzenie eksperymentów, korektę pierwszej wersji manuskryptu i przygotowanie odpowiedzi na uwagi recenzentów.

Piotr Nowicki

D3. M. Gęca, M. Wiśniewska, P. Nowicki, *Preparation of biochars by conventional pyrolysis of herbal waste and their potential application for adsorption and energy purposes,* ChemPhysChem, 2024, e202300507, DOI: 10.1002/cphc.202300507

ChemPhysChem

Research Article
doi.org/10.1002/cphc.202300507

Chemistry Europe
European Chemical Societies Publishing

www.chemphyschem.org

Preparation of biochars by conventional pyrolysis of herbal waste and their potential application for adsorption and energy purposes

Marlena Gęca,*[a] Małgorzata Wiśniewska,[a] and Piotr Nowicki[b]

The nettle, sage, mint and lemon balm herbs were used for biochars preparation. The physicochemical parameters of obtained materials were related to the lignocellulose composition of the precursors. It has been proved that the content of mineral substance has a significant influence on development of surface area, whereas the amount of hemicellulose affects the content of surface functional groups. It has been also shown that the obtained biochars are characterized by great energy parameters. The higher heating values (HHV) of the carbonaceous materials are comparable to the typical energy sources. The greatest HHV value (20.36 MJ/kg) was characteristic for the biochar obtained by pyrolysis of the lemon balm. In addition, the biochars were used for ionic polymers adsorption from one- and two-components solutions. Despite the adsorbed amounts of macromolecules are not great is has been proved that polyethylenimine and polyacrylic acid have positive influence on their mutual adsorption.

Introduction

According to the Lehman and Joseph's definition biochar is a carbon (C)-rich and porous product of the thermal treatment of biomass such as wood, manure or leaves conducted in a closed container with a partial or total absence of oxygen access.[1] Most often, biochar is obtained in the process of pyrolysis, torrefaction, gasification, hydrothermal carbonization (HTC) and hydrothermal liquefaction.[2,3] The physical properties of the material produced depend significantly on structure of the used biomass and the process conditions (e.g. temperature, heating rate, residence time, feedstock pre-treatment).[4,5] In recent time biochar usage has increased because it reduces the negative impacts of biomass on the natural environment. It is used on a large scale as an adsorbent for water and air purification, as a precursor for the activated carbons production, as an energy source, as a catalyst carrier as well as a soil additive, conditioner or remediation assistant.[6–8]

The application of biochar obtained from biomass and organic waste for energy purposes is respond for many global problems as the constantly growing world energy demand, declining of fossil fuel sources, climate changes and rising concentration of dicey waste.[9,10] The ecofriendly nature of biochars reduces the emission of greenhouses gases, and the renewable precursors allow to manage waste and solve the problem of running out of energy resources.[11,12] The energy usefulness of materials is defined by the higher heating value (HHV), also known as gross calorific value (GCV). The biochars derived from different types of biomass are characterized by great HHV, comparable to the conventional energy sources and they can be potentially used for energy production.[13–16]

The specific surface area of biochars are commonly low developed, but they are characterized by large pore sizes.[17] The use of these materials for sorption purposes are widely described in the literature.[18–20] The most common application of biochars is inorganic metal ions and organic dyes adsorption.[21–23] However due to their specific porous structure, biochars could be potential effective polymers adsorbents.

Taking the above into account, in the present paper the nettle, sage, mint and lemon balm herbs were used for biochars production via conventional pyrolysis. These herbs were chosen because that they are easy and cheap to grow and harvest, and due to their annual character they are renewable resources. Moreover, they can quickly get large sizes and have a relatively high bulk density, which is very important for the biochars production on an industrial scale. The obtained materials were characterized in terms of textural parameters and acidic-basic character of the surface as well as used for adsorption and energy purposes. The higher heating value was determined for biochars and precursors and the relation between the plant composition and the energy parameters of obtained materials was checked. Ionic polymers – polyethylenimine and polyacrylic acid – were applied for adsorption studies. These tests were taken in one- and two-component solutions and the influence of the macromolecules witch different ionic character on their mutual adsorption was investigated. Studies on the adsorption of polymers on the surface of biochars are not conducted by

[a] M. Gęca, Prof. M. Wiśniewska
Department of Radiochemistry and Environmental Chemistry
Faculty of Chemistry
Institute of Chemical Sciences
Maria Curie- Sklodowska University in Lublin
M. Curie-Sklodowska Sq. 3, 20-031 Lublin, Poland
E-mail: marlena.geca@wp.pl

[b] Prof. P. Nowicki
Department of Applied Chemistry
Faculty of Chemistry
Adam Mickiewicz University in Poznań
Uniwersytetu Poznańskiego 8, 61-614 Poznań, Poland

other research teams, which proved the innovative character of the performed research.

Methods and materials

Biochars preparation

The stalks of nettle (NE), sage (SA), mint (MT) and lemon balm (LB) herbs were cut into 1.5–2.0 cm pieces and dried at 110 °C. Next, the fragmented starting materials were subjected to conventional pyrolysis using a horizontal resistance furnace equipped with a quartz tube reactor (one-zone model PRW75/LM, Czylok, Jastrzębie-Zdrój, Poland). About 15 g of the precursors were placed in the nickel boats, heated to 400 °C (with a rate 5 °C/min) and annealed at the final pyrolysis temperature for 1 h. After pyrolysis, the samples were cooled down in a nitrogen atmosphere (Linde Gaz, Kościan, Poland) with a flow rate of 10 dm^3/h. The obtained materials were denoted as NE_B, SA_B, MT_B and LB_B, respectively.

Biochars and precursors characterization

The SEM technique (Quanta 250 FEG by FEI, Waltham, MA, USA) was used for determination of surface morphology of the examined solids. The total surface area, total pore volume and average pore diameter were determined based on the nitrogen adsorption-desorption isotherms measured at −196 °C, applying ASAP 2420 (Accelerated Surface Area and Porosimetry System) provided by Micromeritics (Norcross, GA, USA).

The lignin, hemicellulose, cellulose and extractives content in the precursors (P) were also determined. The gravimetric methods described in our previous paper were used for this purpose.[24]

The surface charge density (σ_0) of the obtained biochars was determined applying the potentiometric titration method. For this purpose the 0.5 g of material was added to the 0.05 dm^3 of NaCl solution with concentration of 0.001 mol/dm^3 (supporting electrolyte). The examined suspension was placed in a thermostated Teflon vessel (RE 204 thermostat, Lauda Scientific, Lauda-Königshofen, Germany), in which glass and calomel electrodes (Beckman Instruments, Brea, CA, USA) were introduced to monitor pH changes (pHM 240 pH meter, Radiometer, Warsaw, Poland), after each portion of base added to the system (NaOH with a concentration of 0.1 mol/dm^3) by automatic Dosimat 765 microburette (Metrohm, Opacz-Kolonia, Poland). The measurements were made at 25 °C. The changes in the surface charge density value as a function of solution pH, were calculated with the computer program "Titr_v3", which also controlled the course of the titration process. These calculations were based on the difference in the base volume added to the suspension and the supporting electrolyte solution providing the specified pH value (Eq. 1).[25]

$$\sigma_0 = \frac{\Delta V c F}{m_b S} \quad (1)$$

where: σ_0 – surface charge density [μC/cm^2], ΔV – difference in the volume of base which must be added to bring the pH of suspension and reference solution to the specified value [dm^3], c – base concentration [mol/dm^3], F – Faraday constant [C/mol], m_b – mass of biochar [g], S – adsorbent surface area [m^2/g].

Determination of the zeta potential (ζ) of the biochars prepared was performed by Doppler laser electrophoresis method using Zetasizer Nano ZS (Malvern Instruments, Malvern, UK). The calculations were made based on the Henry's Equation (2):

$$U_e = \frac{2\varepsilon_0 \varepsilon \zeta}{3\eta} f(\kappa a) \quad (2)$$

where: U_e – electrophoretic mobility [m^2/V*s], ε_0 – vacuum permittivity [F/m], ε – absolute permittivity [F/m], η – viscosity [Pa*s], f(κa) – Henry's function.

For the measurements 0.2 dm^3 of the suspensions containing the NaCl as the supporting electrolyte with a concentration of 0.001 mol/dm^3 and 0.03 g of the solids, were prepared. These systems were subjected to the action of ultrasounds (XL 2020 ultrasonic head, Misonix, Farmingdale, NY, USA) for 3 min and divided into several parts. In each of the obtained samples a different pH value (changing in the range from 3 to 10) was adjusted, using HCl and NaOH solutions, with concentrations of 0.1 mol/dm^3, as well as a Φ360 pH-meter (Beckman, Brea, CA, USA). These measurements were performed at 25 °C.

The concentration of surface functional groups was determined applying the Boehm back titration method.[26] The volumetric standards of NaOH and HCl with concentration of 0.1 mol/dm^3 (Avantor Performance Materials, Gliwice, Poland) were used as the titrants.

Energy parameters of the biochars prepared

In order to determine the higher heating value (HHV) of precursors and biochars, all of the samples were dried for 12 h at 110 °C to complete water evaporation. The HHV studies were performed according to the procedure presented in the ISO 1928:2009 Standard, using the KL-12Mn calorimeter, provided by PRECYZJA-BIT (Bydgoszcz, Poland). The samples in the form of compressed tablets weighing 0.5–1.0 g (with a piece of iron resistance wire pressed in) were connected to the electrodes and then placed in a calorimetric bomb (Figure 1). The measuring vessel was filled with pure oxygen to a pressure of 2.5 MPa, to supply sufficient gas for combustion. Next, the bomb was placed in a calorimetric vessel and filled with distilled water, then the electrical wires were connected and the sample was ignited by means of an electric impulse.

The heat released during the combustion of the sample was transferred to the water surrounding the bomb calorimeter. By recording the difference in the water temperature during the

Figure 1. Compressed tablet connected to the electrodes (on the left) and the bomb calorimeter filled with oxygen (on the right).

whole process, the system calculated the *HHV* (MJ/kg) using the following Equation (3):

$$HHV = \frac{C_{bomb} \times \Delta T - Q_{iw}}{m_{sample}} \quad (3)$$

where: C_{bomb} – the heat capacity of the bomb calorimeter [MJ/°C], ΔT – the change of water temperature [°C], Q_{iw} – the amount of heat generated by iron wire [MJ/kg], m_{sample} – the mass of biochar used [kg].

Based on the precursors and biochars masses as well as their higher heating values, the mass yield of pyrolysis process (*MY*), energy densification ratio (*EDR*) as well as energy yield (*EY*) were calculated, using the following Equations (4)–(6):

$$MY = \frac{m_{biochar}}{m_{precursor}} \times 100\% \quad (4)$$

$$EDR = \frac{HHV_{biochar}}{HHV_{precursor}} \quad (5)$$

$$EY = MY \times EDR \quad (6)$$

Adsorption/Desorption studies

Two polymers with different ionic character were used for adsorption/desorption studies. Polyacrylic acid (PAA) (Fluka, Saint Louis, MO, USA) with an average molecular weight equal to 2000 Da is a weak, anionic polymer with a carboxyl groups present in its chains. The PAA pK_a value is about 4.5, which means that below this pH value PAA functional groups are poorly dissociated and occurs in more coiled conformation. With the increasing pH value the PAA conformation becomes more and more developed.[27] In turn, polyethylenimine (PEI) (Sigma Aldrich, Saint Louis, MO, USA) with an average molecular weight equal to 2000 Da is a cationic polymer, containing an amine functional group in the molecule. The PEI pK_b is about 9. Below this pH value great amount of amine groups present in the chains is dissociated which result in their considerably developed conformation. At pH above 9 the PEI chain occurs in more coiled conformation, which is the result of significant reduction in the ionization of its functional groups.[28] Figure 2 presents the structural formulas of both adsorbates.

The adsorption tests were performed for 24 h, at pH 3, at 25 °C. The 0.1 g of biochar was added to the 0.01 dm^3 solution containing 200 ppm of appropriate polymer and 0.001 mol/$dm^3$of NaCl solution (supporting electrolyte). The adsorption was tested in single and binary systems of polymeric adsorbates. After the process was completed, the solids were separated from the solutions using a microcentrifuge (Centrifuge MPW 233e MPW Med. Instruments, Warsaw, Poland) and the concentrations of adsorbates in the supernatants were determined. The separated solids with the adsorbed polymers were, next, subjected to the desorption process (for 24 h, at 25 °C) using the H_2O and HNO_3 solution (with concentrations of 0.1 mol/dm^3). The adsorbed/desorbed amounts of PAA and PEI were determined using the static method based on the change of the adsorbate concentration in the solution before and after the process (Eq. 7).

$$A_p = \frac{(C_0 - C)V}{m_b} \quad (7)$$

where: A_p – polymer adsorbed amount [mg/g], C_0 – initial polymer concentration [mg/dm^3], C – polymer concentration after adsorption/ desorption step [mg/dm^3], V – volume of the solution [dm^3], m_b – mass of biochar [g].

The polymer concentrations were measured using the UV-VIS spectrophotometer Carry 100 (Varian, Palo Alto, Santa Clara, CA, USA). The PAA concentration was determined based on its reaction with hyamine 1622 resulting in formation of a white-colored complex, absorbing light at the wavelength of 500 nm.[29] In turn, the PEI concentration was determined based on its reaction with $CuCl_2$, which gives a blue-colored complex, absorbing light at the wavelength of 285 nm.[30]

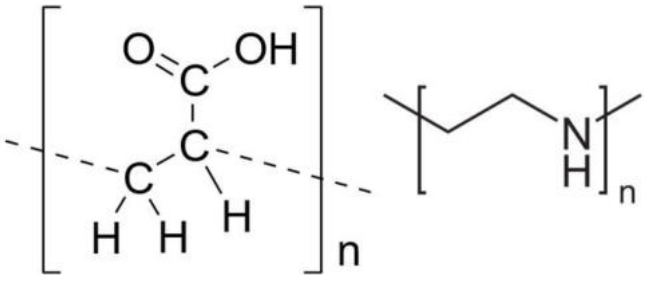

Figure 2. The structural formulas of polyacrylic acid (on the left) and polyethylenimine (on the right).

Results and discussion

Precursors and biochars characterization

The SEM images of the obtained biochars are presented in Figure 3. All of these materials are characterized by a porous, parallel structure with several bright and small clumps on their surface, which are most likely particles of a mineral substance (ash).

According to the data collected in Figure 4, all precursors are characterized by a very high content of lignin. It is a substance responsible of the plant stiffness. Due to the fact, that only herbs stalks were used for biochars preparation, the high content of lignin is justified. The amount of extractives, hemicellulose and cellulose present in the raw materials varies depending on the precursor type. It is also worth emphasizing that all the plants are characterized by the low content of mineral substance.

The textural parameters of the obtained biochars were discussed in detail in our previous work.[24] Briefly: the biochars are characterized by a poorly developed specific surface area ranging from 2.2 to 3.1 m^2/g and total pore volume varying between 0.005–0.007 cm^3/g, which can limit their adsorption capacity. However, it should be noted that all of the obtained adsorbents are classified as mesoporous (mean pore size in the range of 8.4–10.6 nm), which is a desirable property for the adsorption of large polymer macromolecules.

Changes in the surface charge density of biochars as a function of the solution pH are presented in Figure 5. The occurrence of point of zero charge (pzc) at above 7 proves that all materials show weak basic character of the surface. The biochar obtained from the nettle herb (NE_B) is characterized by the lowest value of pH_{pzc} (7.4), whereas the one obtained from sage herb (SA_B) by the highest pH_{pzc} (8.5).

Figure 6 presents the zeta potential of examined materials. The isoelectric point (iep) of all biochars occur at pH about 5–6. The difference in the pzc and iep values can be a result of the partial overlapping of the electrical double layers (edl) that are formed on the pore walls. This effect in the case of mesoporous materials have been previously described in the literature.[31] The greatest difference between point of zero charge and isoelectric point is observed in the case of the biochar (SA_B) obtained by pyrolysis of the sage herb.

According to the data presented in Figure 7 all obtained biochars are characterized by great content of surface functional (1.62–2.79 mmol/g), which can bind to the functional groups of adsorbates and thus increase the amount of adsorbed polymer molecules. Due to the fact that there is no

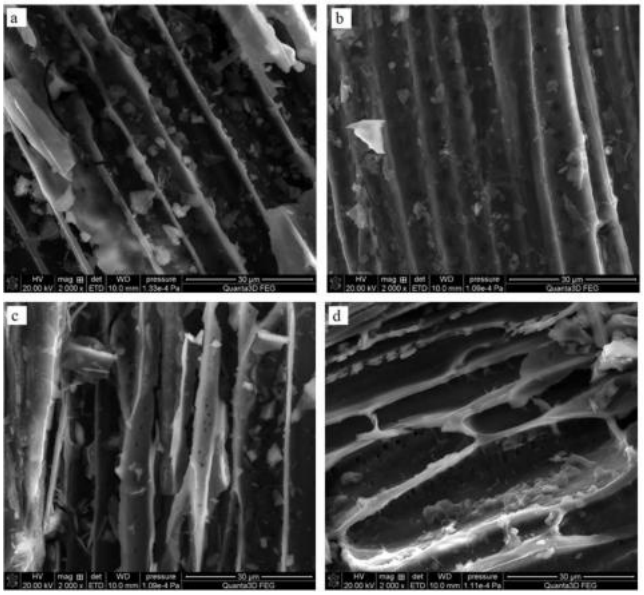

Figure 3. SEM images of the NE_B (a), SA_B (b), MT_B (c) and LB_B (d) biochars.

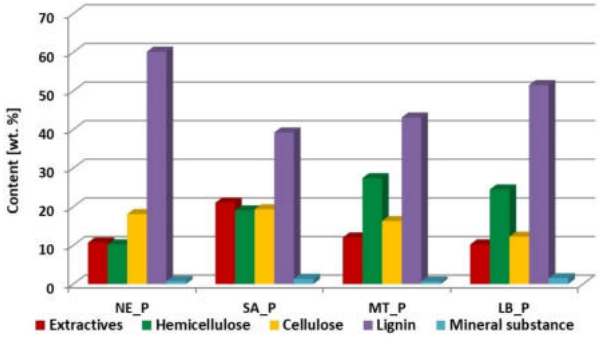

Figure 4. Composition of the nettle, sage, mint and lemon balm herbs.

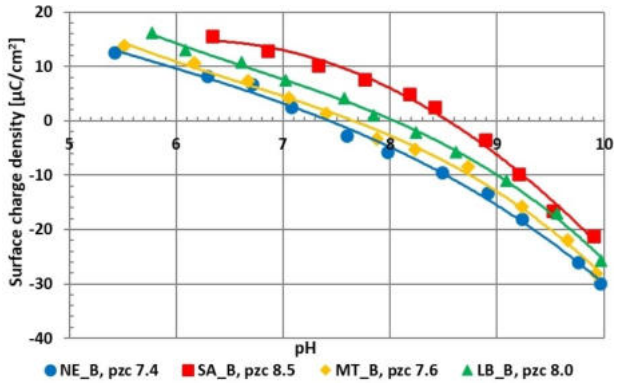

Figure 5. Surface charge density of the obtained biochars.

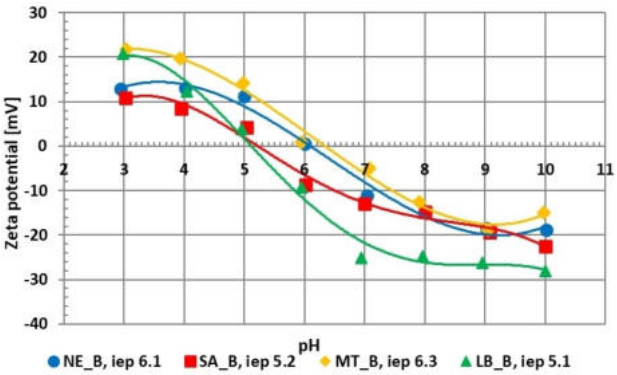

Figure 6. Zeta potential of the obtained biochars.

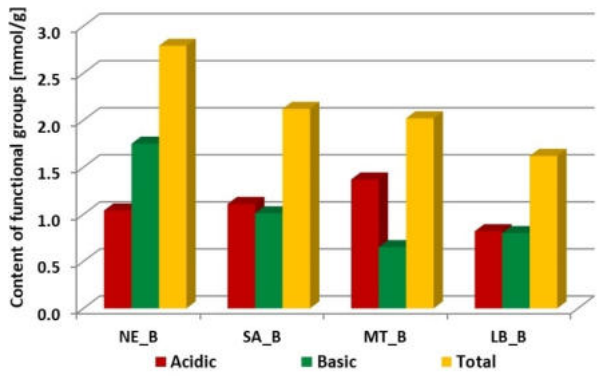

Figure 7. Acidic-basic properties of the obtained biochars.

basic groups present in the hemicellulose structure, with the increasing content of this substance in the precursors, the amount of the basic groups present on the surface of appropriate biochar decreases.

Energy characteristics of the obtained biochars

Analysis of the energy parameters presented in Figure 8 allows to determine whether carbonaceous materials obtained as a result of conventional pyrolysis of plant precursors can be applied as renewable fuels. According to these data the mass yield of pyrolysis process for all precursors exceeds 40 wt.% (Figure 8a). However, as the value of MY increases, the surface area of pyrolysis products decreases. The MT_B biochar with the best developed surface area (3.1 m^2/g) is characterized by the lowest pyrolysis mass yield (41.9%). The highest value of MY (45.8 wt.%) is observed in case of the SA_B sample.

The highest value of HHV parameter (20.36 MJ/kg) is shown by LB_B sample, obtained via lemon balm pyrolysis. In the case of the precursors, the highest HHV (14.45 MJ/kg) presents the sage herb. In general, the biochars are characterized by the significantly higher heating value than the corresponding precursors (Figure 8b). The greatest difference in this respect (6.95 MJ/kg) is observed for LB_P and LB_B samples. The higher heating value, energy densification ratio and energy yield of obtained biochars were compared to other available in literature materials (Table 1). The obtained results do not differ from the others reports. Moreover, the HHV of all the biochars prepared is comparable to the typical lignite briquettes, wood or wood pellets (~18–25 MJ/kg).[32]

As follows from the data presented in Figure 8c the biochars obtained via conventional pyrolysis of herbs are characterized by the similar values of energy densification ratio (~1.3–1.6). The value of this parameter can be related to the lignin content in the precursors structure, as the EDR increases with the increasing lignin concentration. In the case of the energy yield (Figure 8d), the greatest value of 67.3% is found for the LB_B sample, prepared by lemon balm pyrolysis. However, the differences in this energy parameter for individual biochars do not exceed 10%. Based on the results discussed above, it can

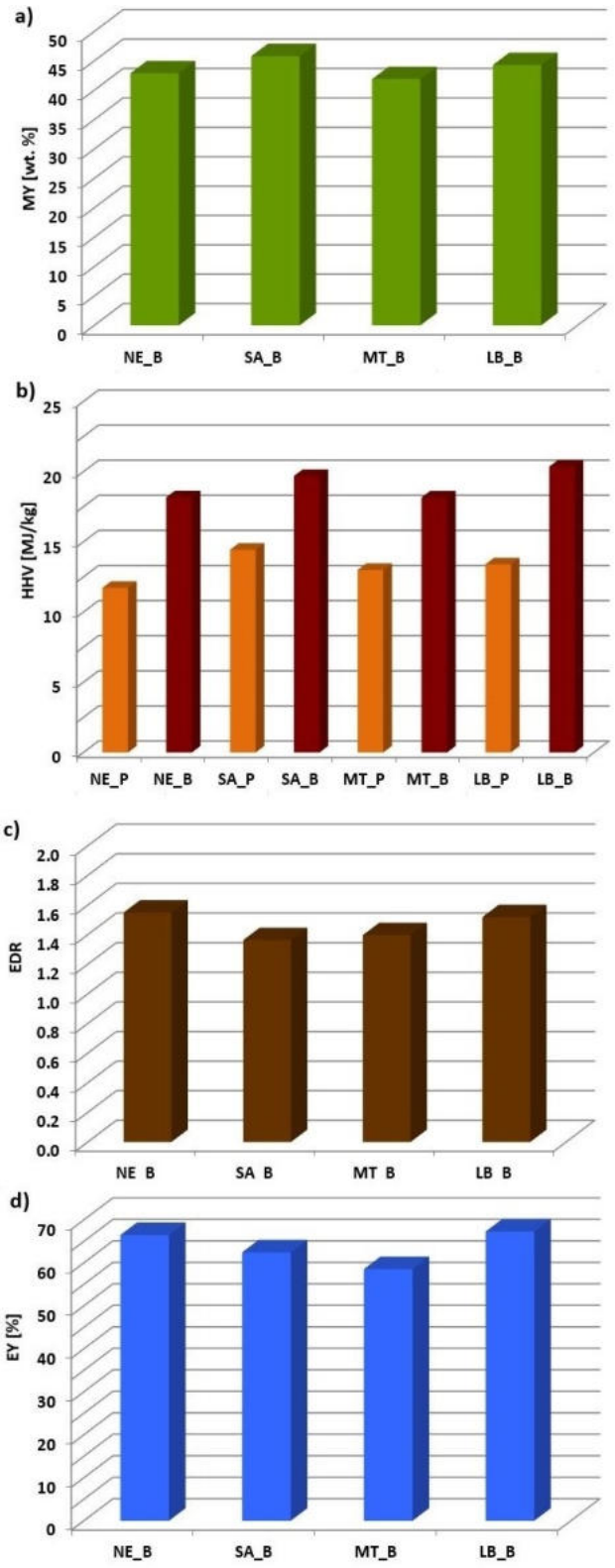

Figure 8. Energy parameters of the obtained biochars: the mass yield of pyrolysis process (a), higher heating value (b), energy densification ratio (c), energy yield (d).

Table 1. The HHV of different biochars.

Precursor	Preparation conditions	HHV [MJ/kg]	EDR	EY [%]	Reference
Nettle herb	Pyrolysis at 400 °C for 60 min	18.18	1.55	66.5	Present study
Sage herb	Pyrolysis at 400 °C for 60 min	19.70	1.36	62.5	Present study
Mint herb	Pyrolysis at 400 °C for 60 min	18.17	1.40	58.5	Present study
Lemon balm herb	Pyrolysis at 400 °C for 60 min	20.36	1.52	67.3	Present study
Wheat straw	Fast pyrolysis at 450 °C for 30 min	22.00	–	–	[11]
Pinewood	Fast pyrolysis at 450 °C for 30 min	27.80	–	–	[11]
Poultry litter	Pyrolysis at 300 °C for 15 min	15.00	1.25	–	[15]
Mugwort leaves/stems	Pyrolysis at 400 °C for 30 min	25.29 and 30.27	1.45 and 1.75	55.0 and 72.0	[32]
Sewage sludge	Torrefaction at 240 °C for 60 min	13.40	0.99	88.4	[33]
Manure pellet biomass	Microwave pyrolysis at 500 °C for 20 min	4.65	0.90	56.5	[34]
Canola straw	Microwave pyrolysis at 500 °C for 20 min	24.55	1.30	39.7	[34]
Bamboo	Carbonization at 200 °C for 60 min	18.52	-	-	[35]
Dried sewage sludge	Slow solar pyrolysis at 800 °C for 190 min	13.00	0.81	-	[36]
Coconut fiber	Pyrolysis at 200 °C for 20 min	19.93	1.04	87.5	[37]
Coconut fiber	Pyrolysis at 330 °C for 20 min	25.36	1.32	53.5	[37]

be concluded that biochars obtained as a result of herb stalks pyrolysis at 400 °C, can potentially be used as valuable renewable fuels.

Adsorption/desorption studies

According to the data collected in Figure 9 polyacrylic acid is more effective adsorbed on the surface of the examined biochars than polyethylenimine. It can be related to the polymers conformation at pH 3. Under this condition PAA occurs in the coiled form due to the small extent of dissociated carboxyl groups, whereas in the PEI chain most of the amine groups are dissociated, which results in developed conformation of the macromolecules. In addition, at pH 3 the biochar's surface is charged positively, which cause an attraction of the anionic substance to the adsorbent surface. Both polymers in the one-component systems were shown the greatest affinity to the surface of lemon balm derived biochar. Polyethylenimine adsorbed amount increases with the decreasing content of functional groups present on the adsorbent surface. The interaction between PEI molecules and surface functional groups may results in flatter adsorption of macromolecules, while the decrease in the content of functional species leads to a perpendicular polymer binding to the solid surface, which increases the packing of the adsorption layer. Polyacrylic acid and polyethylenimine have positive influence on their mutual adsorption. In binary systems, an increase in the amount of adsorbed both polymers is noticed on the surface of all tested materials. The polymer-polymer complexes formation could be explanation of this fact. Both hydrogen bond formation and chemical reactions can be main mechanism responsible for these complexes creation. They can have an inter- and intramolecular structure, thus they can be formed within one polymeric chain and between two macromolecules.[38] The

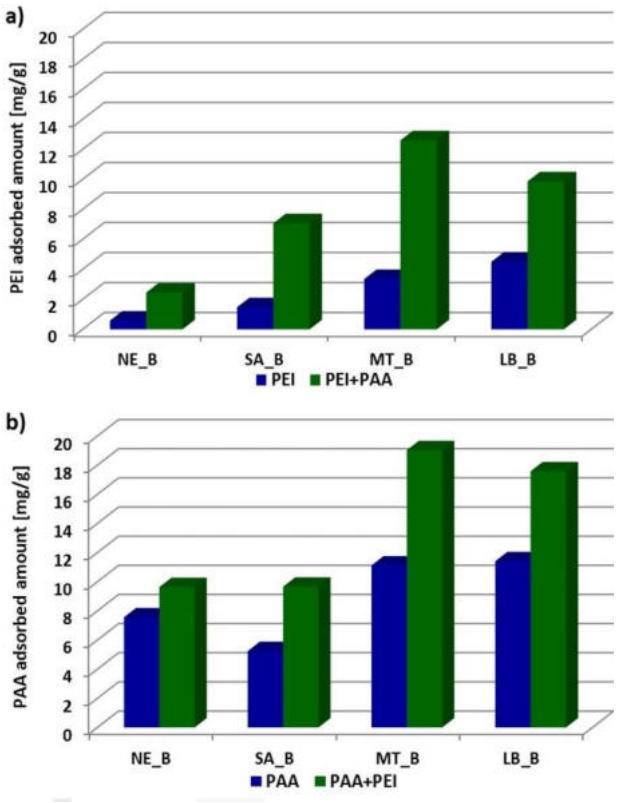

Figure 9. The adsorbed amounts of polyethylenimine (a) and polyacrylic acid (b) on the surface of obtained biochars.

greatest amounts of polymers from the binary solution are adsorbed on the surface of biochar obtained from the mint herb as a result of the greatest development of MT_B biochar surface area.

Conclusions

The performed studies have proved that the nettle, sage, mint and lemon balm herb can be successfully used for carbonaceous materials preparation. The biochars obtained from these plant precursors have poorly developed surface area (below 4 m^2/g) and can be classified as mesoporous adsorbents. The content of surface functional groups with basic character is dominant for all biochars. The higher heating value of the obtained biochars is about 19 MJ/kg, which is comparable with results observed for the typical energy sources. It has been proved that with the increasing lignin content in the structure of the precursor, the energy densification ratio of carbonaceous materials increases. The adsorption tests have shown that the obtained biochars are characterized by a relatively low sorption capacity towards ionic polymers. However, it has also been proved that polyethylenimine and polyacrylic acid have positive influence on their mutual adsorption on the biochars surface.

Conflict of Interests

The authors declare no conflict of interest.

Data Availability Statement

The data that support the findings of this study are available from the corresponding author upon reasonable request.

Keywords: plant precursors · pyrolysis · biochar · renewable fuels · ionic polymers adsorption

[1] J. Lehmann, S. Joseph, *Biochar for environmental management: Science and technology*. Earthscan, London, Sterling, VA, **2009**.
[2] S. Meyer, B. Glaser, P. Quicker, *Environ. Sci. Technol.* **2011**, *45(22)*, 9473–9483.
[3] N. T. L. Chi, S. Anto, T. S. Ahamed, S. S. Kumar, S. Shanmugam, M. S. Samuel, T. Mathimani, K. Brindhadevi, A. Pugazhendhi, *Fuel* **2021**, *287*, 119411.
[4] H. K. S. Panahi, M. Dehhaghi, Y. S. Ok, A. S. Nizami, B. Khoshnevisan, S. I. Mussatto, M. Aghbashlo, M. Tabatabaei, S. S. Lam, *J. Cleaner Prod.* **2020**, *270*, 122462.
[5] D. Wang, P. Jiang, H. Zhang, W. Yuan, *Sci. Total Environ.* **2020**, *723*, 137775.
[6] K. Qian, A. Kumar, H. Zhang, D. Bellmer, R. Huhnke, *Renewable Sustainable Energy Rev.* **2015**, *42*, 1055–1064.
[7] M. Gęca, A. M. Khalil, M. Tang, A. K. Bhakta, Y. Snoussi, P. Nowicki, M. Wiśniewska, M. M. Chehimi, *Surfaces* **2023**, *6(2)*, 179–213.
[8] M. Bartoli, M. Giorcelli, P. Jagdale, M. Rovere, A. Tagliaferro, *Materials* **2020**, *13(2)*, 261.
[9] M. P. Suh, H. J. Park, T. K. Prasad, D. W. Lim, *Chem. Rev.* **2012**, *112(2)*, 782–835.
[10] M. K. Awasthi, *Environ. Pollut.* **2022**, *298*, 118831.
[11] S. Nanda, A. K. Dalai, F. Berruti, J. A. Kozinski, *Waste Biomass Valorization* **2016**, *7*, 201–235.
[12] H. Abdullah, H. Wu, *Energy Fuels* **2009**, *23(8)*, 4174–4181.
[13] M. Waqas, A. S. Aburiazaiza, R. Miandad, M. Rehan, M. A. Barakat, A. S. Nizami, *J. Cleaner Prod.* **2018**, *188*, 477–488.
[14] K. S. Ro, K. B. Cantrell, P. G. Hunt, *Ind. Eng. Chem. Res.* **2010**, *49(20)*, 10125–10131.
[15] M. Mierzwa-Hersztek, K. Gondek, M. Jewiarz, K. Dziedzic, *J. Mater. Cycles Waste Manage.* **2019**, *21*, 786–800.
[16] W. Chen, J. Meng, X. Han, Y. Lan, W. Zhang, *Biochar.* **2019**, *1*, 75–87.
[17] H. Li, X. Dong, E. B. da Silva, L. M. de Oliveira, Y. Chen, L. Q. Ma, *Chemosphere* **2017**, *178*, 466–478.
[18] M. Gęca, M. Wiśniewska, P. Nowicki, *Adv. Colloid Interface Sci.* **2022**, *305*, 102687.
[19] N. Cheng, B. Wang, P. Wu, X. Lee, Y. Xing, M. Chen, B. Gao, *Environ. Pollut.* **2021**, *273*, 116448.
[20] Y. Dai, N. Zhang, C. Xing, Q. Cui, Q. Sun, *Chemosphere* **2019**, *223*, 12–27.
[21] M. Sadeghi Afjeh, G. Bagheri Marandi, M. J. Zohuriaan-Mehr, *Water Environ. Res.* **2020**, *92(6)*, 934–947.
[22] S. Fan, Y. Wang, Z. Wang, J. Tang, J. Tang, X. Li, *J. Environ. Chem. Eng.* **2017**, *5(1)*, 601–611.
[23] N. Zhu, T. Yan, J. Qiao, H. Cao, *Chemosphere* **2016**, *164*, 32–40.
[24] M. Gęca, M. Wiśniewska, P. Nowicki, *Measurement* **2023**, *212*, 112672.
[25] W. Janusz, *Pol. J. Chem.* **1994**, *68*, 1871–1880.
[26] H. P. Boehm, E. Diehl, W. Heck, R. Sappok, *Angew. Chem.* **1964**, *3*, 669–677.
[27] S. Chibowski, M. Wiśniewska, A. W. Marczewski, S. Pikus, *J. Colloid Interface Sci.* **2003**, *267*, 1–8.
[28] A. Von Harpe, H. Petersen, Y. Li, T. Kissel, *J. Controlled Release* **2000**, *69*, 309–322.
[29] W. B. Crummett, R. A. Hummel, *J. Am. Water Works Assoc.* **1963**, *55*, 209–219.
[30] J. Patkowski, D. Myśliwiec, S. Chibowski, *Int. J. Polym. Anal. Charact.* **2016**, *21*, 486–494.
[31] M. Wiśniewska, P. Nowicki, K. Szewczuk-Karpisz, M. Gęca, K. Jędruchniewicz, P. Oleszczuk, *Sep. Purif. Technol.* **2021**, *276*, 119297.
[32] M. Wiśniewska, K. Rejer, R. Pietrzak, P. Nowicki, *Molecules* **2022**, *27(23)*, 8597.
[33] J. Pulka, P. Manczarski, J. A. Koziel, A. Białowiec, *Energies* **2019**, *12(3)*, 565.
[34] C. Nzediegwu, M. Arshad, A. Ulah, M. A. Naeth, S. X. Chang, *Bioresour. Technol.* **2021**, *320*, 124282.
[35] Z, Liu, B. Fei, Z. Jiang, *Bioresour. Technol.* **2014**, *167*, 94–99.
[36] M. Dudziak, S. Werle, A. Marszałek, S. Sobek, A. Magdziarz, *Energy* **2022**, *261*, 125360.
[37] Z. Liu, G. Han, *Fuel* **2015**, *158*, 159–165.
[38] M. Gęca, M. Wiśniewska, P. Nowicki, K. Jędruchniewicz, *Pure Appl. Chem.* **2023**, *95*, 563–578.

Manuscript received: July 20, 2023
Revised manuscript received: November 30, 2023
Version of record online: ■■, ■■

RESEARCH ARTICLE

Herbs stems were used for biochars preparation. The obtained materials were applied for adsorption of ionic polymers and energy purposes. The results showed that the higher heating values of the biochars are comparable to the typical energy sources. The adsorbed amounts of polymers were not significant, however it was shown that the adsorption from the binary systems is more effective than from the single ones.

M. Gęca, Prof. M. Wiśniewska, Prof. P. Nowicki*

1 – 8

Preparation of biochars by conventional pyrolysis of herbal waste and their potential application for adsorption and energy purposes

Lublin, 10.09.2025

mgr Marlena Groszek
Uniwersytet Marii Curie-Skłodowskiej w Lublinie,
Wydział Chemii, Instytut Nauk Chemicznych,
Katedra Radiochemii i Chemii Środowiskowej,
Pl. Marii Curie-Skłodowskiej 3, 20-031 Lublin
marlena.groszek@mail.umcs.pl

Rada Naukowa Instytutu Nauk Chemicznych
Uniwersytetu Marii Cure-Skłodowskiej
w Lublinie

Oświadczenie o współautorstwie

Niniejszym oświadczam, że mój udział w pracy: **M. Gęca**, M. Wiśniewska, P. Nowicki, *Preparation of biochars by conventional pyrolysis of herbal waste and their potential application for adsorption and energy purposes,* ChemPhysChem, 2024, e202300507, DOI: 10.1002/cphc.202300507 [D3], obejmował opracowanie koncepcji badań, przeprowadzenie eksperymentów, analizę uzyskanych wyników, przygotowanie manuskryptu i jego korektę po procesie oceny w redakcji oraz sformułowanie odpowiedzi na uwagi recenzentów.

Marlena Groszek

Lublin, 10.09.2025

prof. dr hab. Małgorzata Wiśniewska
Uniwersytet Marii Curie-Skłodowskiej w Lublinie,
Wydział Chemii, Instytut Nauk Chemicznych,
Katedra Radiochemii i Chemii Środowiskowej,
Pl. Marii Curie-Skłodowskiej 3, 20-031 Lublin
malgorzata.wisniewska@mail.umcs.pl

Rada Naukowa Instytutu Nauk Chemicznych
Uniwersytetu Marii Cure-Skłodowskiej
w Lublinie

Oświadczenie o współautorstwie

Niniejszym oświadczam, że mój udział w pracy: M. Gęca**, M. Wiśniewska**, P. Nowicki, *Preparation of biochars by conventional pyrolysis of herbal waste and their potential application for adsorption and energy purposes,* ChemPhysChem, 2024, e202300507, DOI: 10.1002/cphc.202300507 [D3], obejmował stworzenie koncepcji badań, korektę manuskryptu – przed i po procesie recenzji oraz nadzór merytoryczny w czasie całego cyklu wydawniczego.

Małgorzata Wiśniewska

Poznań, 10.09.2025

dr hab. Piotr Nowicki, prof. UAM
Uniwersytet im. Adama Mickiewicza w Poznaniu,
Wydział Chemii, Zakład Chemii Stosowanej,
Ul. Uniwersytetu Poznańskiego 8, 61-614 Poznań
piotr.nowicki@amu.edu.pl

Rada Naukowa Instytutu Nauk Chemicznych
Uniwersytetu Marii Cure-Skłodowskiej
w Lublinie

Oświadczenie o współautorstwie

Niniejszym oświadczam, że mój udział w pracy: M. Gęca, M. Wiśniewska, **P. Nowicki**, *Preparation of biochars by conventional pyrolysis of herbal waste and their potential application for adsorption and energy purposes,* ChemPhysChem, 2024, e202300507, DOI: 10.1002/cphc.202300507 [D3], obejmował stworzenie koncepcji pracy, przeprowadzenie eksperymentów, analizę uzyskanych wyników, korektę pierwszej wersji manuskryptu oraz przygotowanie odpowiedzi na uwagi recenzentów.

Piotr Nowicki

D4. M. Groszek, G. Wójcik, M. Wiśniewska, P. Nowicki*, Application of environmentally friendly activated carbons derived from herbal industry waste for water purification: A study on the removal of selected organic and inorganic pollutants,* Journal of Water Process Engineering, 2025, 75, 107952, DOI: 10.1016/j.jwpe.2025.107952

Journal of Water Process Engineering 75 (2025) 107952

Contents lists available at ScienceDirect

Journal of Water Process Engineering

journal homepage: www.elsevier.com/locate/jwpe

Application of environmentally friendly activated carbons derived from herbal industry waste for water purification: A study on the removal of selected organic and inorganic pollutants

Marlena Groszek [a], Grzegorz Wójcik [b], Małgorzata Wiśniewska [a], Piotr Nowicki [c,*]

[a] Department of Radiochemistry and Environmental Chemistry, Institute of Chemical Sciences, Faculty of Chemistry, Maria Curie-Sklodowska University in Lublin, M. Curie-Sklodowska Sq. 3, 20-031 Lublin, Poland
[b] Department of Inorganic Chemistry, Institute of Chemical Sciences, Faculty of Chemistry, Maria Curie-Sklodowska University in Lublin, M. Curie-Sklodowska Sq. 3, 20-031 Lublin, Poland
[c] Department of Applied Chemistry, Faculty of Chemistry, Adam Mickiewicz University in Poznań, Uniwersytetu Poznańskiego 8, 61-614 Poznań, Poland

ARTICLE INFO

Editor: Ludovic F. Dumée

Keywords:
Activated carbons development
Physical activation
Purification of multicomponent solutions
Ionic polymers
Metal ions
Competitive adsorption
Electrical double layer structure

ABSTRACT

Waste from the herbal industry was subjected to simultaneous pyrolysis and physical activation with CO_2 to obtain environmentally friendly adsorbents. The resulting activated carbons are characterized by a well-developed specific surface area and a high concentration of surface functional groups, with a distinct predomination of basic ones. The prepared adsorbents were used to remove ionic polymers (poly(acrylic acid)/polyethyleneimine) and heavy metal ions (Cd(II)/As(V)) from both single/binary solutions. The structure of the electrical double layer in the presence of adsorbates was studied to determine the adsorption mechanisms. The results showed that polymers are adsorbed in greater amounts on the surface of the carbonaceous materials than metal ions. In single-adsorbate systems, the maximum adsorption capacities were 94 mg/g for polyethyleneimine, 27 mg/g for poly(acrylic acid), 8 mg/g for Cd(II), and 4 mg/g for As(V), respectively. Studies on the simultaneous removal of selected pollutants have shown that metal ions and ionic polymers have negatively affected their mutual adsorption. Furthermore, the removal of As(V) ions from solutions containing poly(acrylic acid) or polyethyleneimine was completely inhibited. At pH 3, the adsorption of an anionic polymer was enhanced by the presence of a cationic one, whereas poly(acrylic acid) had no significant effect on polyethyleneimine adsorption.

1. Introduction

Environmental pollution remains a critical global issue, and its severity and complexity continue to increase with rapid urbanization, industrialization, and human population growth. Pollutants, including chemical contaminants and greenhouse gases to microplastics and agricultural runoff, contribute to the network of environmental degradation that affects air, water, and soil quality. In turn, this degradation has a huge impact on human health, biodiversity, and climate stability, deepening challenges faced by communities and ecosystems worldwide [1,2]. The problem is most noticeable in developing countries, where the limited capacity to regulate pollution, coupled with growing industrial activities and weak enforcement of environmental standards, exacerbates the impact of pollution-related diseases [3–5].

The excessive use of chemicals in industry and agriculture has raised significant environmental and health concerns, since conventional chemical processes often rely on hazardous substances, generate significant amounts of waste, and contribute to pollution [6–9]. Recognizing these risks, scientists and policymakers have advocated for "green chemistry," a sustainable approach aimed at designing chemical products and processes that reduce or eliminate the use and generation of hazardous substances [10,11]. Green chemistry operates on several foundational principles, such as waste prevention, atom economy, and the use of safer solvents and reaction conditions [12]. By focusing on inherently safer and more efficient chemical processes, green chemistry seeks to minimize environmental impact and improve sustainability across chemical industries. Incorporating green chemistry into industrial practices is increasingly seen as essential for addressing global challenges such as climate change, resource depletion, and pollution [13]. By limiting harmful chemical usage and employing safer, more

* Corresponding author.
E-mail address: piotr.nowicki@amu.edu.pl (P. Nowicki).

https://doi.org/10.1016/j.jwpe.2025.107952
Received 21 March 2025; Received in revised form 14 May 2025; Accepted 14 May 2025

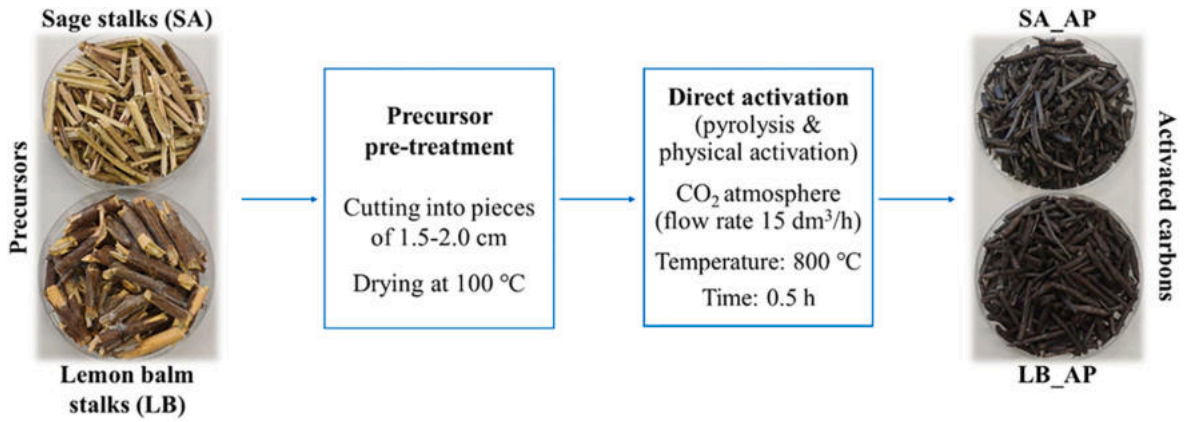

Fig. 1. Procedure for the preparation of activated carbons.

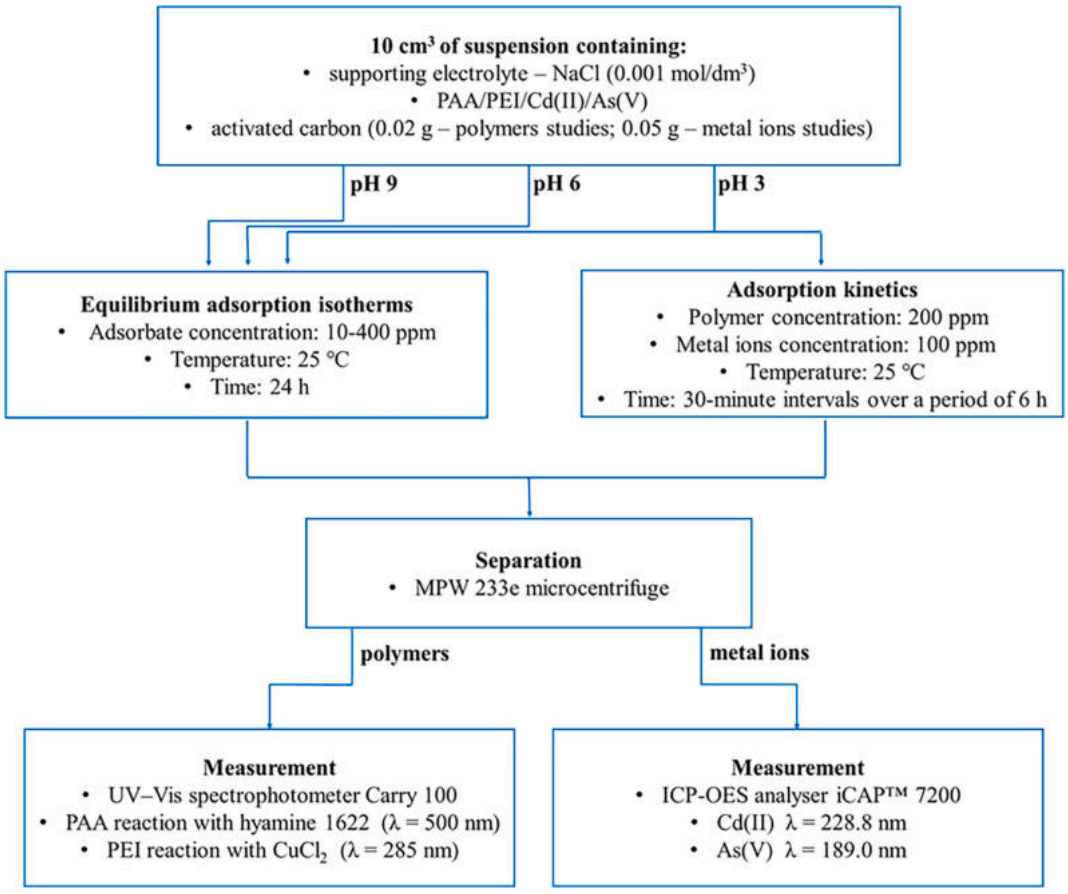

Fig. 2. Procedure for adsorption tests: equilibrium and kinetics studies.

sustainable alternatives, green chemistry can contribute to a circular economy that minimizes waste and encourages resource recovery [14,15]. However, while the benefits of green chemistry are well recognized, its broader implementation faces challenges, including high initial costs, limited access to greener alternatives, and the need for regulatory support [16,17].

Carbon dioxide used as an activation agent offers an environmentally friendly alternative by utilizing this greenhouse gas to produce valuable carbon materials that help protect the environment from various pollutants. Activation process involves a series of complex chemical reactions that lead to the thermal decomposition (partial gasification) of carbon precursor and the formation of activated carbon with a highly developed surface area and porous structure [18]. There are examples in the literature of increasing biochar surface area from 8 to over 1100 m^2/g, after the activation with carbon dioxide [19]. However, despite its many advantages, this process also faces challenges, including the need for high temperatures to initiate the reaction and the optimization of process conditions for different precursor materials [20].

In the present paper, waste from the herbal industry was used for the preparation of environmentally friendly activated carbons. The stalks of sage and lemon balm were dried, fragmented and submitted to simultaneous pyrolysis and physical activation (so-called direct activation). Due to the low reagent consumption, the use of environmentally friendly precursors, and the reduction of energy usage, the synthesis method

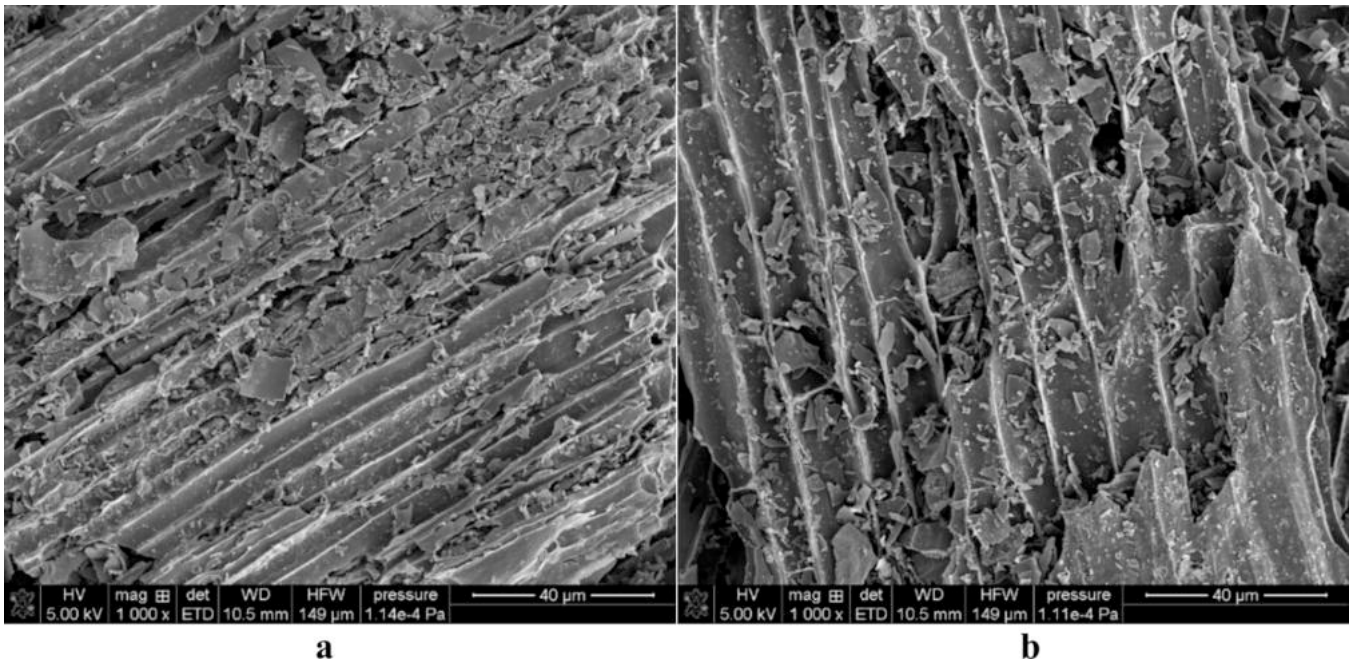

Fig. 3. SEM images of SA_AP (a) and LB_AP (b) activated carbons.

Table 1
XRF analysis results – elemental composition of the activated carbons.

Element	Content [mg/g]	
	SA_AP	LB_AP
Mg	0.008	–
Al	–	0.019
Si	0.048	0.032
P	0.091	0.146
S	0.009	0.010
Cl	0.008	0.007
K	0.026	0.020
Ca	0.407	0.505
Ti	0.003	0.002
Cr	0.002	0.002
Mn	0.001	–
Fe	0.010	0.009
Ni	0.002	0.002
Cu	0.001	0.002
Zn	0.001	0.002

Table 2
Chemical composition of the surface layer of activated carbons based on XPS analysis.

Adsorbent	Content of element [at. %]						
	C	N	O	Si	P	Ca	Mg
SA_AP	87.1	0.9	8.4	0.6	0.4	1.7	0.8
LB_AP	85.5	1.7	9.9	1.0	0.7	1.2	–

complies with the principles of green chemistry [21]. The obtained materials were characterized and used for the adsorption of PAA and PEI ionic polymers, as well as Cd(II) and As(V) heavy metal ions. The influence of the adsorbates on the solids' zeta potential, surface charge density, and the size of aggregates was tested. In addition, adsorption studies were performed at different adsorbate concentrations, contact times, and solution pH values. The effect of polymers and metal ions on their mutual adsorption was also examined. The possibility of reusing the adsorbents through polymer desorption was tested using H_2O, HNO_3 and NaOH.

The use of environmentally friendly activated carbons for the simultaneous removal of ionic polymers and heavy metal ions offers a novel and promising strategy for water purification. While carbonaceous materials have been extensively studied for metal ions adsorption, the role of macromolecules in this process has not been systematically investigated [22,23]. Notably, the adsorption of polymers on activated carbons, as well as their impact on the behavior and stability of activated carbon suspensions, remains an unexplored area. Therefore, this study addresses a significant gap in the current knowledge and introduces a new perspective on the multifunctional use of activated biocarbons in complex water treatment scenarios.

2. Experimental

2.1. Preparation and characterization of adsorbents

The activated carbons preparation procedure is presented in Fig. 1. The surface morphology of the activated carbons was analysed using scanning electron microscopy (SEM) (Quanta 250 FEG by FEI). The elemental composition of the materials was determined by X-ray fluorescence (XRF) (Axios mAX, PANanalytical). X-ray photoelectron spectroscopy (XPS) (Gammadata Scienta) was used to analyze the surface chemistry and identify C-, N-, and O-containing functional groups present on the tested materials. Nitrogen adsorption-desorption at −196 °C was employed to determine the textural parameters of the adsorbents (ASAP 2420, Micromeritics). The content of acidic and basic surface functional groups was determined using the procedure proposed by Boehm [24] based on back titration. Volumetric standards of 0.1 mol/dm^3 NaOH and 0.1 mol/dm^3 HCl (Avantor Performance Materials) were used as titrants.

2.2. Adsorbates

Two weak polyelectrolytes with an average molecular weight of 2000 Da were used for the studies – anionic poly(acrylic acid) (PAA) (Fluka) and cationic polyethyleneimine (PEI) (Sigma Aldrich). The pK_a of the first one occurs at pH 4.5, below this value, the degree of dissociation is lower than 50 %, which leads to a coiled conformation of the polymer chain. Conversely, at pH values above 4.5, the number of

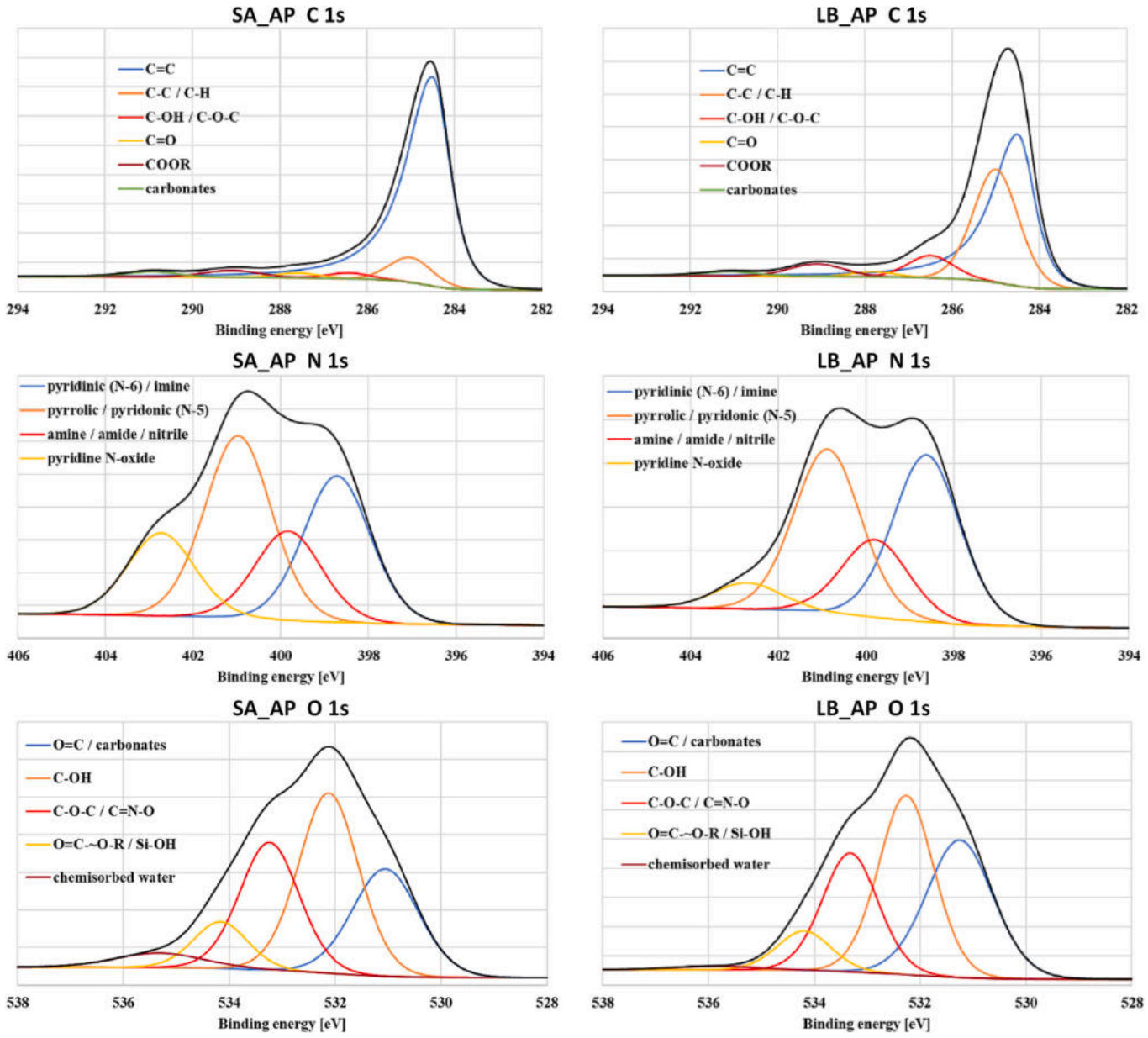

Fig. 4. XPS spectra of the C 1 s, N 1 s, and O 1 s regions for SA_AP and LB_AP activated carbons.

Table 3
Textural parameters of the synthesized activated carbons.

Adsorbent	Surface area [m^2/g]		Pores volume [cm^3/g]		Micropore contribution	Average pore size [nm]
	Total	Micropore	Total	Micropore		
SA_AP	399	327	0.20	0.13	0.65	1.96
LB_AP	547	430	0.26	0.17	0.65	1.92

Table 4
Acid-base properties of the examined activated carbons.

Adsorbent	Acidic groups concentration [mmol/g]	Basic groups concentration [mmol/g]	Total concentration of surface functional groups [mmol/g]
SA_AP	0.48	1.96	2.44
LB_AP	0.29	2.03	2.32

dissociated carboxyl groups increases, resulting in a more expanded polymer structure [25]. On the other hand, PEI is characterized by the pK_b value of 9. At this value, 50 % of the functional groups are dissociated. As the pH value decreases, the degree of amine groups protonation increases. This results in the existence of more and more numerous positive charges along polymeric chains, causing their expansion [26].

The Cd(II) and As(V) were chosen as heavy metals representation. Cadmium ions were introduced into the solution in the form of $CdN_2O_6{\cdot}4H_2O$ (Sigma Aldrich) and the arsenic ones as KH_2AsO_4 (Sigma Aldrich). Due to the Cd(II) ions precipitation at pH above 7, studies with

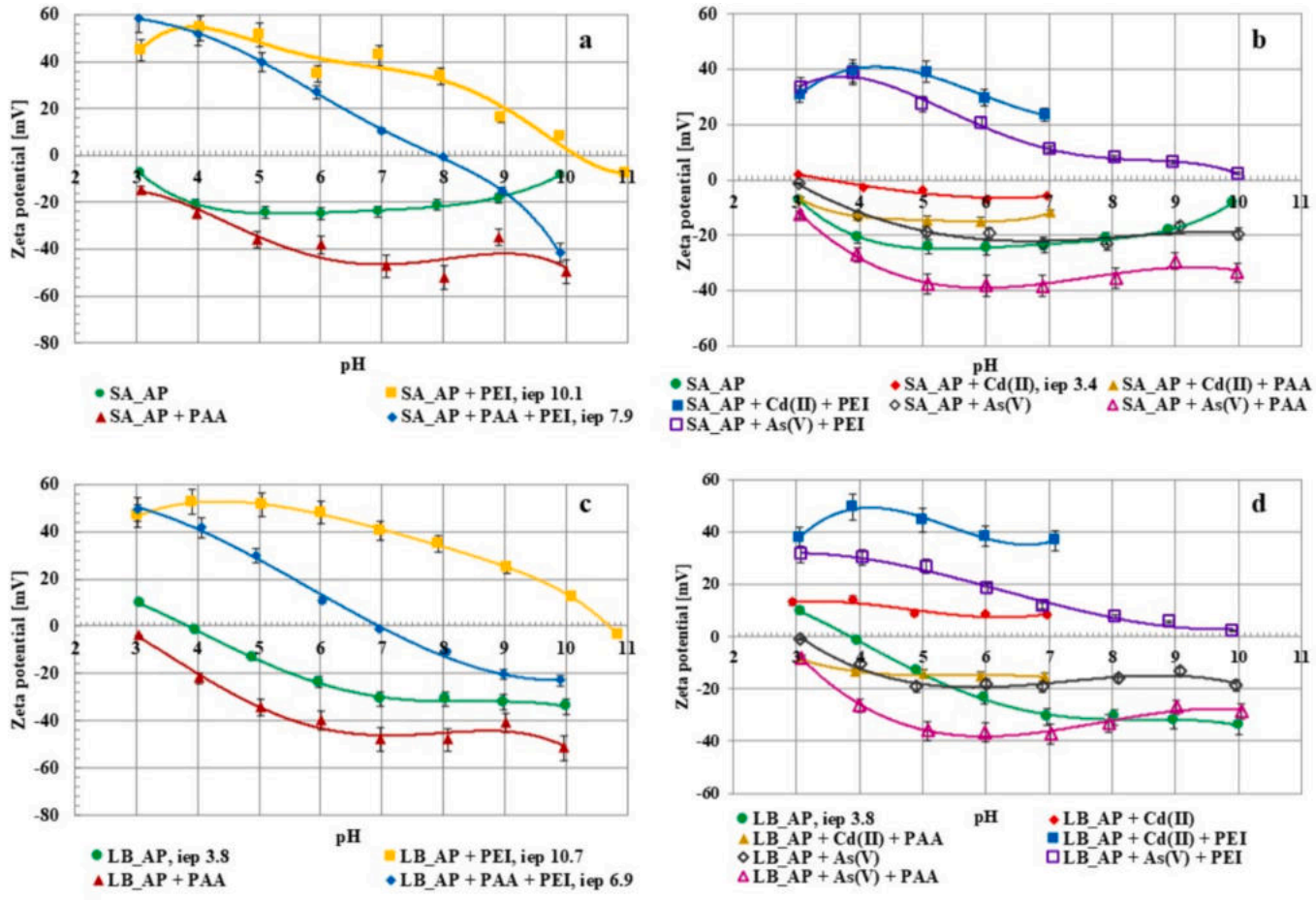

Fig. 5. Zeta potential as a function of pH for SA_AP (a, b) and LB_AP (c, d) activated carbons dispersed in a solution without adsorbates as well as with single and binary adsorbates.

this metal were limited to the pH range of 3–7. In turn As(V) is well soluble in the entire pH range. However, the hydration state of arsenate ions varies with pH. At high pH values, the As(V) ion is completely dehydrated and occurs in the AsO_4^{3-} form. As the pH value decreases, the level of hydration increases leading to formation of $HAsO_4^{2-}$, $H_2AsO_4^{-}$, and H_3AsO_4 [27].

2.3. Zeta potential, surface charge density and aggregates size studies

The zeta potential (ζ) and aggregate sizes of the activated carbon particles, both with and without the adsorbates, were determined using the following procedure. Suspensions (200 cm^3) were prepared, containing the examined polymers and/or metal ions at the concentration of 200 ppm, NaCl (0.001 mol/dm^3) as a supporting electrolyte in all of the studies, and 0.03 g of the solid. The zeta potential was measured at pH the range of 3–10, using the Doppler laser electrophoresis with a Zetasizer Nano ZS (Malvern Instruments). Based on the obtained results, the zeta potential (ζ) was calculated using the Henry's equation [28]. The average aggregate sizes of the examined solids were determined at pH 3, 6 and 9 using the static light scattering phenomenon. All measurements were performed at 25 °C for the following systems: SA_AP, SA_AP + PAA, SA_AP + PEI, SA_AP + PAA + PEI, SA_AP + Cd(II), SA_AP + Cd(II) + PAA, SA_AP + Cd(II) + PEI, SA_AP + As(V), SA_AP + As(V) + PAA, SA_AP + As(V) + PEI, LB_AP, LB_AP + PAA, LB_AP + PEI, LB_AP + PAA + PEI, LB_AP + Cd(II), LB_AP + Cd(II) + PAA, LB_AP + Cd(II) + PEI, LB_AP + As(V), LB_AP + As(V) + PAA, LB_AP + As(V) + PEI.

The surface charge density (σ_0) determination was performed in analogues systems. For this purpose, 50 cm^3 of suspensions were prepared, containing the examined adsorbates (with the initial concentration C_0 = 100 ppm), the supporting electrolyte and 0.05 g of SA_AP or 0.037 g of LB_AP. The prepared suspension was placed in a thermostated Teflon vessel (RE 204 thermostat, Lauda Scientific), in which the changes in the pH value was monitored after each addition of titrant (NaOH - 0.1 mol/dm^3) with application of glass and calomel electrodes (Beckman Instruments). All measurements were performed at 25 °C. The "Titr_v3" software was applied to monitor changes in the σ_0 value as a function of solution pH, perform calculations and control the titration procedure. These calculations were based on the difference in the titrant volume added to the suspension and the supporting electrolyte solution, which provided the specified pH value [29].

2.4. Adsorption-desorption studies

The adsorption isotherms and kinetics studies are schematically presented in Fig. 2. The obtained data were fitted to theoretical models. In the case of metal ions, the Langmuir (Eq. (1)), Freundlich (Eq. (2)), Dubinin-Radushkevich (Eq. (3)), and Temkin (Eq. (4)) models were applied [30]. The kinetics data for polymers were fitted to pseudo-first-order (Eq. (5)) and pseudo-second-order (Eq. (6)) models [31].

$$q_e = \frac{q_m K_L C_e}{1 + K_L C_e} \tag{1}$$

$$q_e = K_F C_e^{1/n} \tag{2}$$

$$q_e = q_m \exp\left(-\beta\varepsilon^2\right) \tag{3}$$

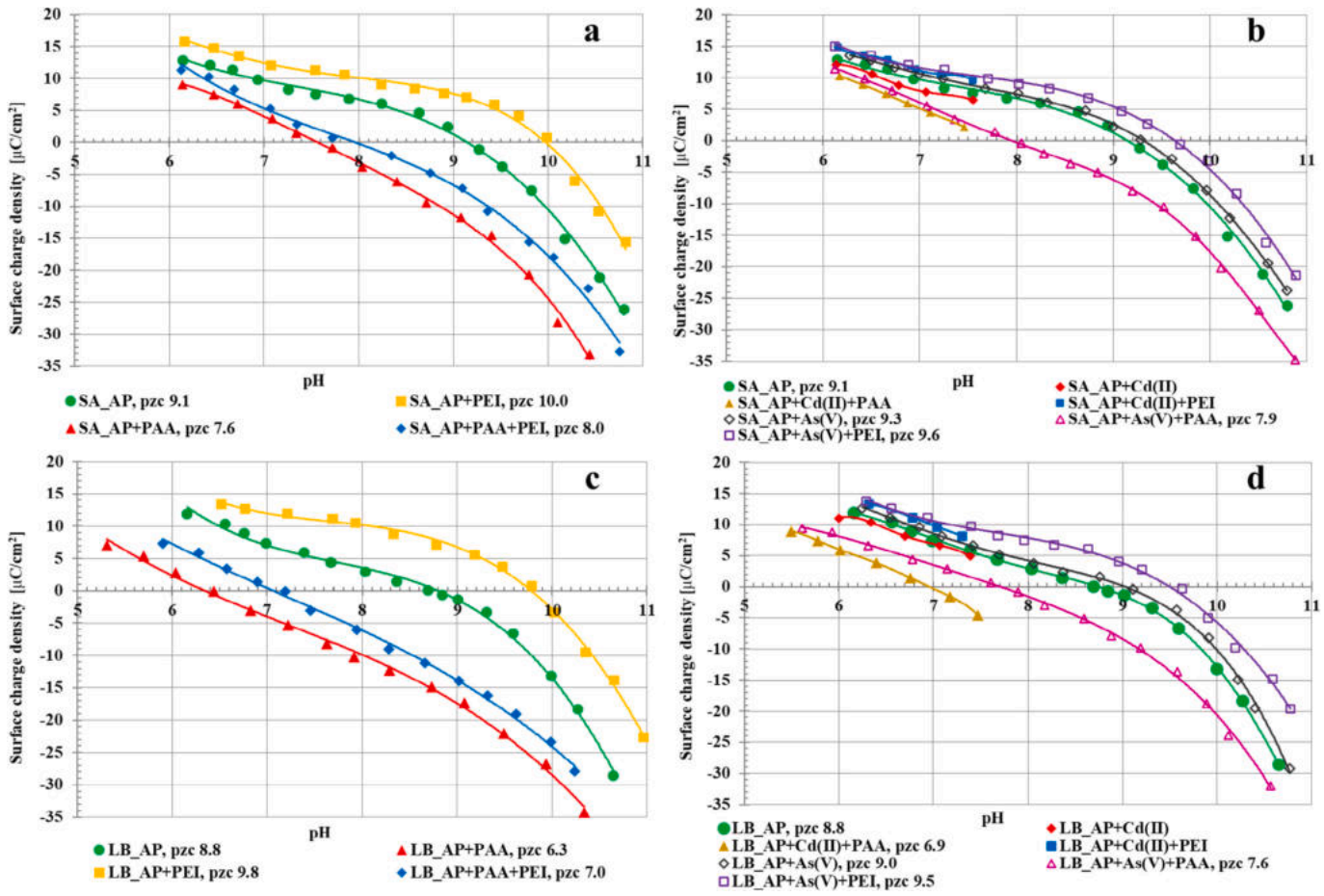

Fig. 6. Surface charge density as a function of pH for SA_AP (a, b) and LB_AP (c, d) activated carbons dispersed in the solution without, as well as with single and binary adsorbates.

Table 5
Size of activated carbon aggregates at pH 3, 6, and 9 in the system without adsorbates, as well as with single and binary adsorbates.

System	Aggregates size [nm]		
	pH 3	pH 6	pH 9
SA_AP	2358	4762	1988
SA_AP + PAA	2048	3463	1939
SA_AP + PEI	2568	2376	1870
SA_AP + Cd(II)	2854	3087	–
SA_AP + As(V)	3860	7547	6455
SA_AP + PAA + PEI	1079	7114	475
SA_AP + PAA + Cd(II)	4491	1659	–
SA_AP + PAA + As(V)	6238	3678	2206
SA_AP + PEI + Cd(II)	1541	2407	–
SA_AP + PEI + As(V)	3505	5591	3750
LB_AP	1831	1916	1573
LB_AP + PAA	2005	3252	3188
LB_AP + PEI	3853	4583	5291
LB_AP + Cd(II)	4662	8147	–
LB_AP + As(V)	9456	13,468	6670
LB_AP + PAA + PEI	2698	773	868
LB_AP + PAA + Cd(II)	4845	4585	–
LB_AP + PAA + As(V)	3856	3515	2856
LB_AP + PEI + Cd(II)	1382	2120	–
LB_AP + PEI + As(V)	3663	5706	8962

$$q_e = \frac{RT}{b_T}\ln A_T + \frac{RT}{b_T}\ln C_e \tag{4}$$

$$\frac{dq_t}{dt} = k_1(q_e - q_t) \tag{5}$$

$$\frac{dq_t}{dt} = k_2(q_e - q_t)^2 \tag{6}$$

where: q_e – the adsorbed amount at equilibrium [mg/g], q_m – the maximum adsorption capacity in the Langmuir model [mg/g], K_L – the Langmuir parameter [dm^3/mg], C_e – the equilibrium aqueous phase concentration [mg/dm^3], K_F – the Freundlich parameter [mg/g (mg/dm^3)$^{1/n}$], n_F – the Freundlich constant, R – gas constant (8.314 J/(mol K), T – temperature [K], b_T – Temkin constant [J/mol], A_T – Temkin constant [dm^3/g], β – Dubinin-Radushkievich constant, ε – adsorption potential [kJ/mol].

For the single and binary adsorption studies, suspensions similar to those used in the previous part of the studies were prepared, with polymer and/or metal ions concentration of 200 ppm. The process was carried out at 25 ℃ for 24 h at pH 3. After the adsorption stage was completed, activated carbon particles were centrifuged from the suspensions (MPW 233e microcentrifuge, MPW MED. INSTRUMENTS). The solids containing the adsorbed substances were subjected to the desorption procedure (at 25 ℃ for 24 h) using H_2O, HNO_3, or NaOH solutions (with an acid and base concentrations of 0.1 mol/dm^3). The concentration of polymers in the supernatants obtained after the adsorption and desorption processes was determined spectrophotometrically (Cary 100, Varian), following the procedure described in detail in

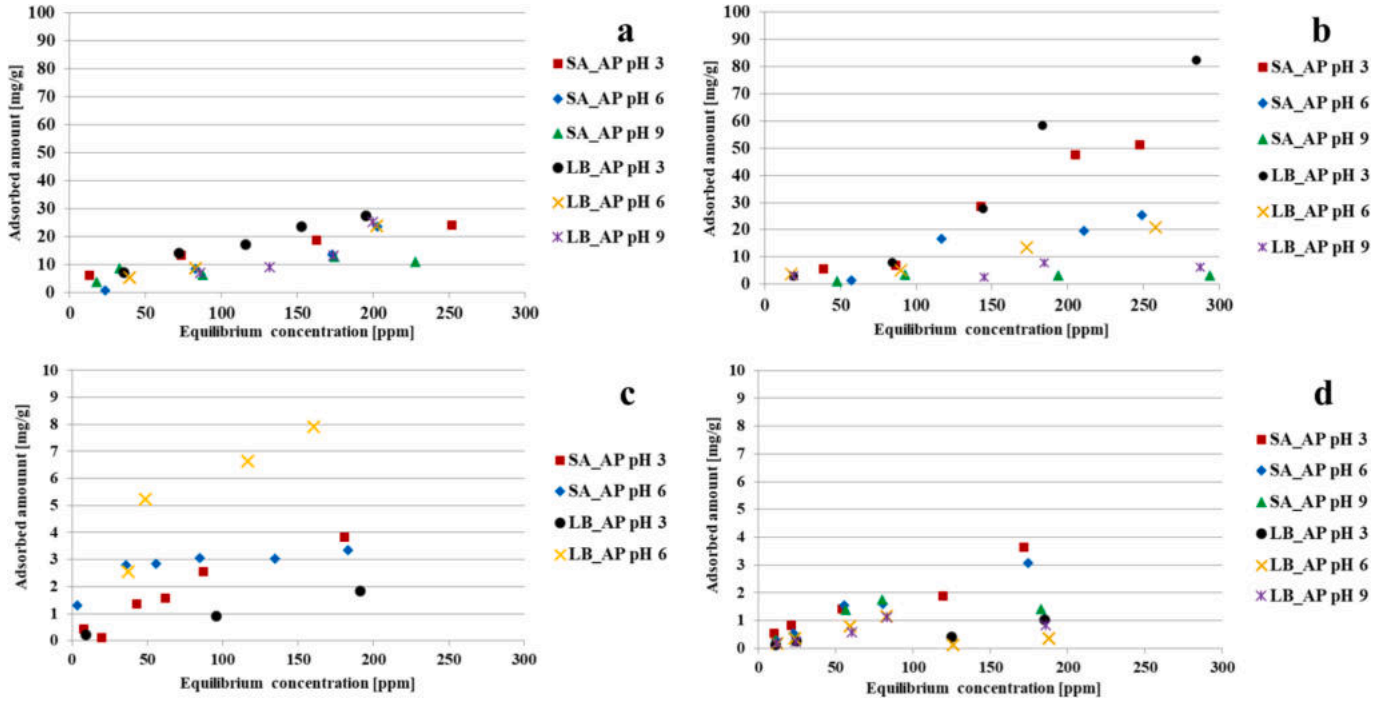

Fig. 7. Adsorption isotherms of poly(acrylic acid) (a), polyethyleneimine (b), cadmium (c) and arsenic (d) on the surface of SA_AP and LB_AP activated carbons at different pH values.

Table 6
Calculated isotherm parameters for Cd(II) and As(V) ions adsorption on the surface of activated carbons.

Isotherm parameters		Cd(II)		As(V)	
		SA_AP	LB_AP	SA_AP	LB_AP
Experimental	q_{exp} [mg/g]	3.84	1.84	3.63	1.03
Langmuir	q_m [mg/g]	7.07	2.82	3.74	1.22
	K_L [dm^3/mg]	0.0060	0.0075	0.0129	0.0089
	R^2	0.7822	0.7253	0.4862	0.4794
Freundlich	n_F	1.5913	1.4769	1.7556	1.4916
	K_F [mg/g(mg/dm^3)$^{1/n}$]	0.3970	0.9275	0.4875	0.6422
	R^2	0.9477	0.9881	0.8342	0.9209
Dubinin-Radushkevich	β	$-6.2{\cdot}10^{-9}$	$-6.6{\cdot}10^{-9}$	$-6.3{\cdot}10^{-9}$	$-6.9{\cdot}10^{-9}$
	ε [kJ/mol]	9.0062	8.7184	8.9034	8.5132
	q_m [mg/g]	11.59	8.26	12.18	3.77
	R^2	0.8386	0.9766	0.8329	0.8861
Temkin	b_T [J/mol]	1476	6583	2911	9867
	A_T [dm^3/g]	0.0508	0.0857	0.1487	0.1268
	R^2	0.9803	0.4641	0.6808	0.7194

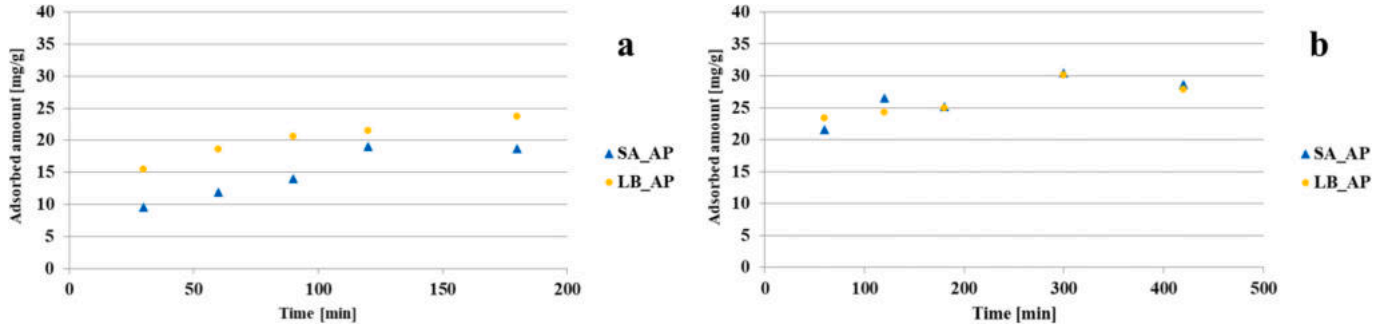

Fig. 8. Adsorption kinetics of poly(acrylic acid) (a) and polyethyleneimine (b) on the surface of activated carbons (pH 3, C_0 200 ppm).

our previous paper [32]. The concentration of heavy metal ions was measured using inductively coupled plasma optical emission spectrometry (ICP-OES) with an iCAP™ 7200 analyzer (THERMO FISHER Scientific), according to the procedure described in [33]. Due to the significantly smaller amounts of adsorbed Cd and As ions, the desorption studies were burdened with a large margin of error and were therefore

Table 7
Calculated kinetic parameters of polymers adsorption on the activated carbons surface.

Kinetics parameters		PAA		PEI	
		SA_AP	LB_AP	SA_AP	LB_AP
Experimental	q_{exp} [mg/g]	18.6900	23.7597	28.6286	27.8800
Pseudo first-order model	q_e [mg/g]	1.0338	1.0311	1.0071	1.0067
	k_1 [1/min]	10.8831	9.1855	5.1988	5.0889
	R^2	0.8222	0.8853	0.3373	0.2875
Pseudo second-order model	q_e [mg/g]	44.2478	29.4985	30.9598	30.1205
	k_2 [g/(mg*min)]	0.0002	0.0006	0.0013	0.0014
	R^2	0.9481	0.9971	0.9908	0.9893

omitted. The exhausted activated carbons from the systems containing single and binary polymers, were dried at 110 °C for 90 min and subjected to the another cycle of adsorption and desorption studies. Four cycles of adsorbent regeneration were carried out.

The adsorption tests were also performed using commercially available activated carbons – lewatite (LWT) (Lanxess), characterized by a specific surface area of 550–650 m^2/g and purolite (PRT) (Lenntech), with a specific surface area of 900–1000 m^2/g.

3. Results and discussion

3.1. Activated carbons characterization

The SEM images of the obtained activated carbons are presented in Fig. 3. Both samples exhibit a distinct layered structure with numerous cracks and crevices, indicating their porosity. Small fragments of irregular shapes are visible on the surface of both carbonaceous materials, suggesting fragmentation of the carbon matrix due to the action of elevated temperature and carbon dioxide. A noticeably higher number of these fragments is visible in the case of the sample derived from sage stems, which makes its structure appear less ordered.

Table 1 presents the results of the XRF analysis. According to these data, activated carbons derived from sage and lemon balm stems are characterized by a low content of mineral matter in their structure, ranging from 0.62 to 0.76 mg/g. Both samples contain mainly calcium, phosphorus, silicon, and potassium, which may indicate a high content of carbonates, phosphates, and silicates in the soil where the herbs grew. The contribution of other elements, such as Fe, Al, Mg, S, Cl, and especially transition metals, is much lower.

According to the XPS data presented in Table 2 and Fig. 4, carbon is the dominant element in the structure of the studied solids. Its content exceeds 85 at.%, but the contribution of its individual species varies significantly. In both materials, the presence of C═C, C—H, C–O–C, C–OH, C═O, COOH, and carbonates groups was identified. In the case of the SA_AP sample, the former clearly predominates, as its share in the C1s spectrum exceeds 83 %. The LB_AP sample is characterized by a significantly lower contribution of C═C groups (52 %) and, at the same time, a much higher content of C—C and C—H bonds (~34 %). Furthermore, activated carbon derived from lemon balm stems contains more hydroxyl, ether, and carboxyl groups than analogous material obtained from sage stems. Oxygen is the second most abundant element on the surface of the obtained carbon adsorbents (8.4–9.9 at.%), and its main forms are hydroxyl, carbonyl, and ether groups. The content of carboxyl groups in both activated carbons is about 3 to 5 times lower than that of the other species. The tested carbon materials also contain nitrogen functional groups, among which pyridinic and pyrrolic/pyridonic structures predominate. XPS tests also confirmed the presence of mineral admixtures in the structure of the obtained adsorbents, including calcium, phosphorus, silicon, and magnesium.

Textural parameters of the SA_AP and LB_AP samples are presented in Table 3. Both activated carbons are characterized by a moderately developed surface area (399–547 m^2/g), but the material derived from

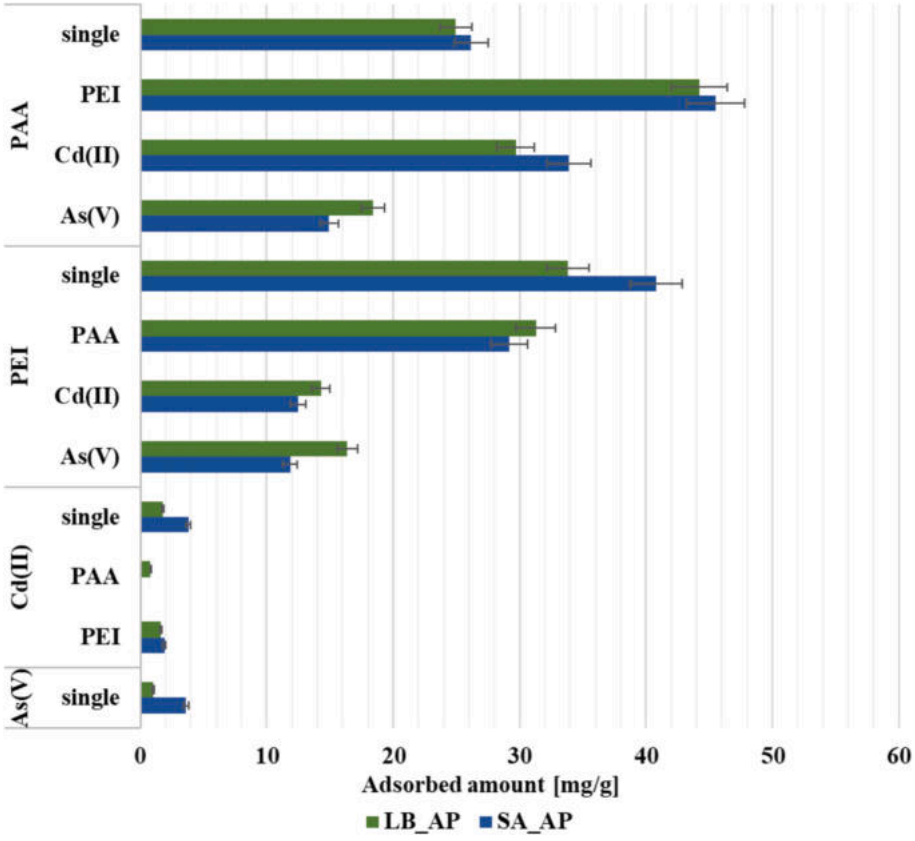

Fig. 9. Adsorbed amounts of PAA, PEI, Cd(II), and As(V) on the surface of activated carbons from single and binary systems (pH 3, C_0 200 ppm).

Table 8
Comparison of the adsorbed amounts of PAA, PEI, Cd(II), and As(V) on different adsorbents.

Adsorbent	Maximum adsorption	Reference
Poly(acrylic acid)		
Activated carbon obtained from the lemon balm	27 mg/g	This study
Alumina	14 mg/g	[45]
Titanium dioxide	24 mg/g	[46]
H_3PO_4 activated carbon derived from the nettle herb	273 mg/g	[32]
H_3PO_4 activated carbon derived from the sage herb	150 mg/g	[32]
Polyethyleneimine		
Activated carbon obtained from the lemon balm	94 mg/g	This study
Hematite	19 mg/g	[47]
Silicon carbide	16 mg/g	[48]
H_3PO_4 activated carbon derived from the nettle herb	156 mg/g	[32]
H_3PO_4 activated carbon derived from the sage herb	145 mg/g	[32]
Cadmium(II)		
Activated carbon obtained from the lemon balm	8 mg/g	This study
Rice straw biochar	7 mg/g	[49]
Granular activated carbon oxidized with nitric acid	6 mg/g	[50]
α-FeOOH modified wheat straw biochar	63 mg/g	[51]
Untreated *Pinus halepensis* sawdust	5 mg/g	[52]
H_3PO_4 activated carbon derived from *Typha angustifolia*	48 mg/g	[53]
Arsenic(V)		
Activated carbon obtained from the sage	4 mg/g	This study
Modified peanut shell biochar	2 mg/g	[54]
Iron modified activated carbon	5 mg/g	[55]
Iron impregnated activated carbon	3 mg/g	[56]
Ce(IV)-doped iron oxide adsorbent	16 mg/g	[57]
Calcium alginate/activated carbon composite beads	58 mg/g	[58]

lemon balm stems is slightly more advantageous in this regard. Its S_{BET} surface area is approximately 37 % larger than that of the analogous material prepared from sage stalks. Both carbonaceous adsorbents are also characterized by a comparable average pore diameter (not exceeding 2 nm) and an identical share of micropores in the total pore volume, which is 65 %.

The content of surface functional groups in the activated carbons derived from herbal industry waste is presented in Table 4. As seen, the total amount of functional groups present on the surface of both adsorbents is very similar, however, it should be emphasized that basic species clearly predominate. The only significant difference between samples SA_AP and LB_AP was observed in the content of surface groups with an acidic nature.

3.2. Zeta potential, surface charge density and aggregates size studies

The results of zeta potential determination are summarized in Fig. 5. The isoelectric point (iep) of LB_AP activated carbon occurs at pH 3.8, whereas the zeta potential values of SA_AP activated carbon remain negative over the entire pH range, making it impossible to determine its isoelectric point [34].

In the presence of poly(acrylic acid) the zeta potential decreases for both activated carbons. Negatively charged polymeric chains (adsorbed on the solid surface) are present in the slipping plane area due to formation of the loops and tail structures [35]. Conversely, positively charged polyethyleneimine increases the zeta potential value in a similar manner. In the binary solution of PAA and PEI, an intermediate effect is observed compared to the single-component systems, however the zeta potential values are higher than in the suspension without adsorbates. The presence of oppositely charged molecules as well as the shift of the slipping plane are the mechanisms which can cause such behavior [32]. Cadmium ions cause an increase in ζ parameter value. The adsorption of cations results in migration of positively charged species (Na^+ cations of the supporting electrolyte) from the by-surface layer of the solution to the slipping plane area [36]. The influence of arsenic ions on the zeta potential value depends on their hydration levels. At lower pH values, As(V) occurs in the hydrated forms of H_3AsO_4 and $H_2AsO_4^-$, which increases the zeta potential values. In contrast, at higher pH values the dehydrated forms $HAsO_4^{2-}$ and AsO_4^{3-} predominate, resulting in a decrease in the value of tested parameter [37]. In a binary solution of polymer and metal ions, macromolecules of considerable size have a decisive influence on the zeta potential. However, it should be noted that the ζ parameter has a greater value in the system containing Cd(II) and PAA/PEI compared to the single polymeric solution, whereas the presence of As(V) in the binary solution limits the influence of macromolecules on the characteristics of the electrical double layer and causes the zeta potential values to be closer to the system without adsorbates. These effects can be explained by the adsorption of metal-polymer complexes, which can assume different intramolecular or intermolecular structures depending on the charge sign of the molecules/ions involved in their formation [38].

The surface charge density of the tested activated carbons as a function of pH is presented in Fig. 6. The point of zero charge (pzc) of the SA_AP sample occurs at pH 9.1, while for the LB_AP sample at pH 8.8. The presence of poly(acrylic acid), which contain carboxyl groups in its chain, decreases the solid surface charge density. This phenomenon is related to the incomplete adsorption of macromolecules (not all of the segments constituting them) on the activated carbon surface. Some of the formed loop and tail structures remain in the by-surface area, which influences the σ_0 parameter value. In the case of PEI, the amino groups present in its structure cause the opposite effect and an increase in surface charge density is observed [39]. In the binary system of poly (acrylic acid) and polyethyleneimine, the pzc value shifts to a the lower pH value in comparison to the suspension without adsorbates. The adsorption of considerably smaller molecules or ions affects the surface charge density through a different mechanism. The adsorption of cadmium cations on the activated carbon surface causes the generation of additional negatively charged groups, which leads to the decrease in the σ_0 value. On the other hand, the adsorption of arsenic anions induces additional surface-active sites with positive charges, and as a consequence of this phenomenon, an increase in surface charge density takes place [40]. In the binary solution of a polymer and metal ions, the macromolecule has crucial effect on the examined parameter due to the greater number of charges delivered by polymeric chains compared to metals ions.

Table 5 contains a summary of results regarding the sizes of activated carbon aggregates formed in the suspensions without and with adsorbates at different pH values. In the system without polymers or metal ions, both activated carbons form the largest aggregates at pH 6. The presence of poly(acrylic acid) causes small differences in aggregate size at pH 3, which is related to the polymer coiled conformation. In systems with more developed PAA chains the effect is more noticeable. Polyethyleneimine in most examined systems demonstrates a stabilizing effect, similarly to PAA and PEI when present in solution simultaneously. The impact of Cd(II) ions on the size of adsorbent aggregates depends on the pH value and the type of activated carbon. In turn, the presence of As (V) ions causes an increase in the size of aggregates both in single and binary solutions. This can lead to the destabilization of the system and effective sedimentation of activated carbon particles.

3.3. Adsorption-desorption studies

According to the adsorption data presented in Fig. 7 poly(acrylic

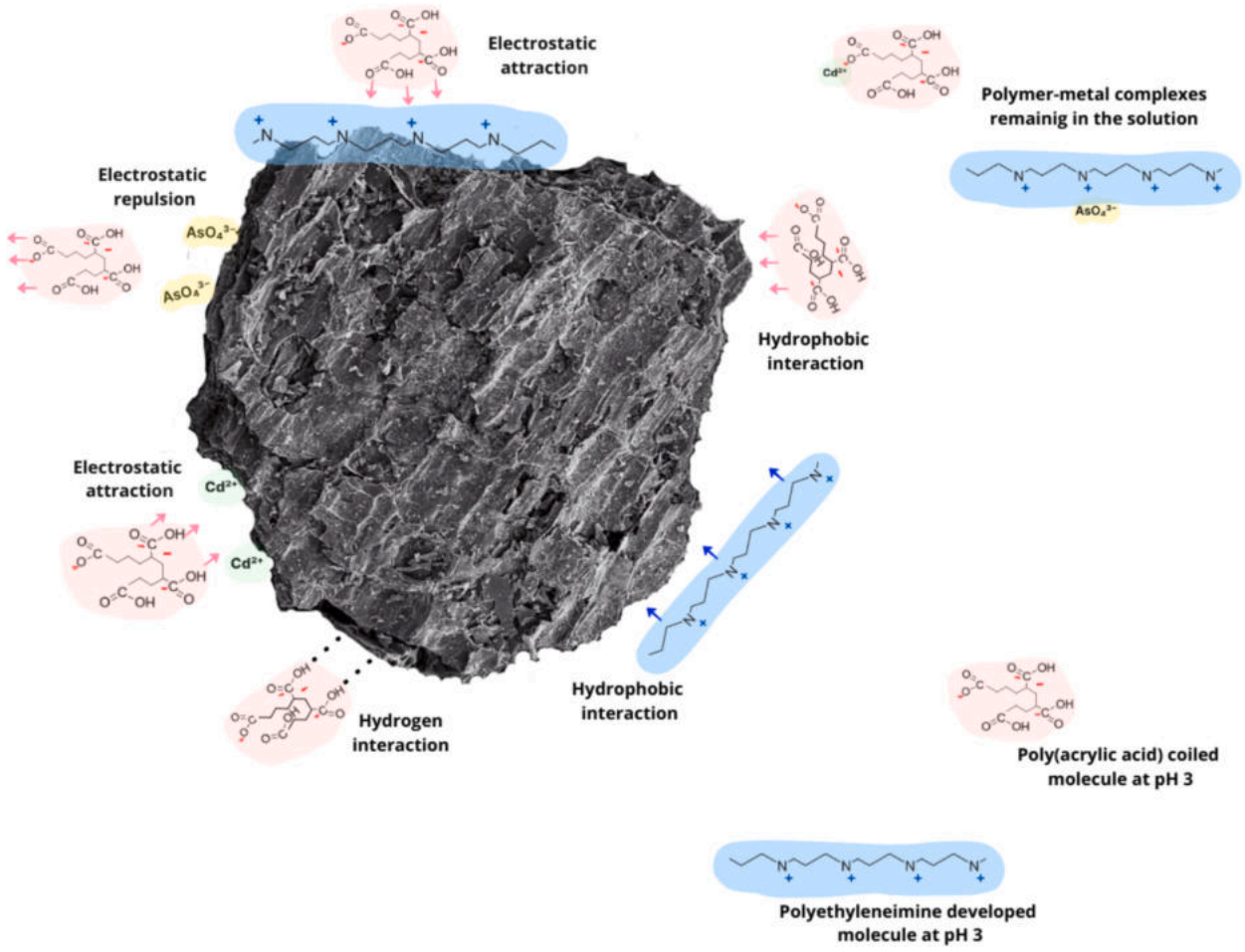

Fig. 10. The schematic representation of adsorption mechanism taking place in the binary systems.

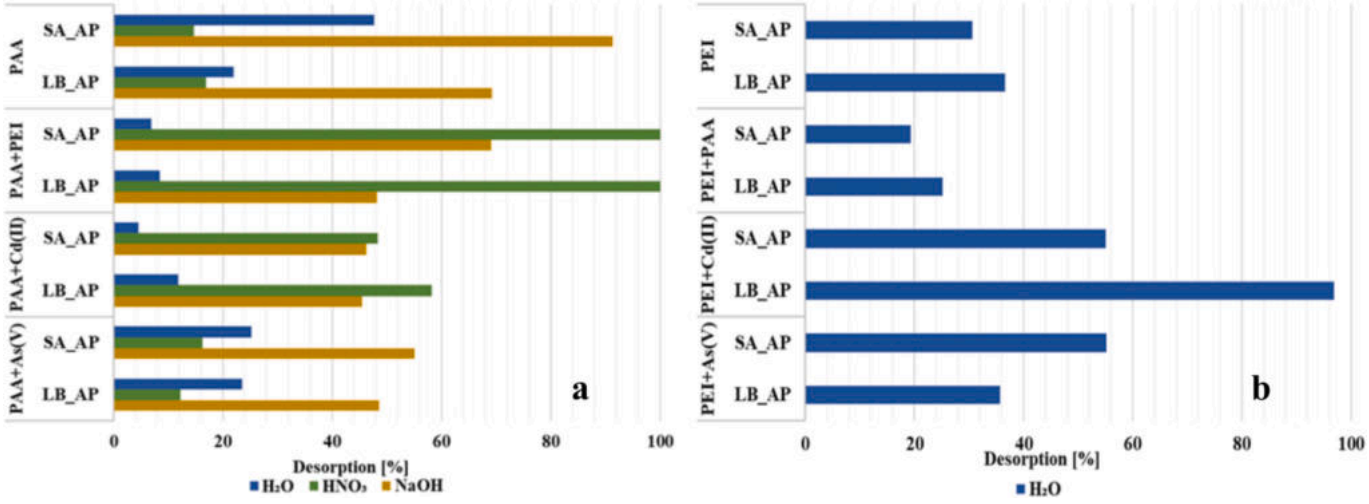

Fig. 11. Desorption efficiency of poly(acrylic acid) (a) and polyethyleneimine (b) for single and binary systems with the application of H_2O, HNO_3, and NaOH solutions.

acid) is efficiently adsorbed at pH 3, on both activated carbons. Under this condition the polymeric carboxyl groups are fully protonated and PAA occurs in coiled conformation. At pH 6 and 9, carboxyl groups present in the PAA macromolecules are dissociated and their chains undergo expansion, which results in a lower adsorbed amount. Polyethyleneimine is also adsorbed in the greatest amounts at lower pHs, and with the increase in pH of the solution, its adsorption level decreases. It can be explained by the PEI layer structure formed at the solid-liquid interface. At pH 3 the polymer is fully dissociated and the activated carbon surface is charged positively, which results in a perpendicular arrangement of polymer chains. With the increasing pH value, the dissociation level of PEI decreases, with a simultaneous decrease in the

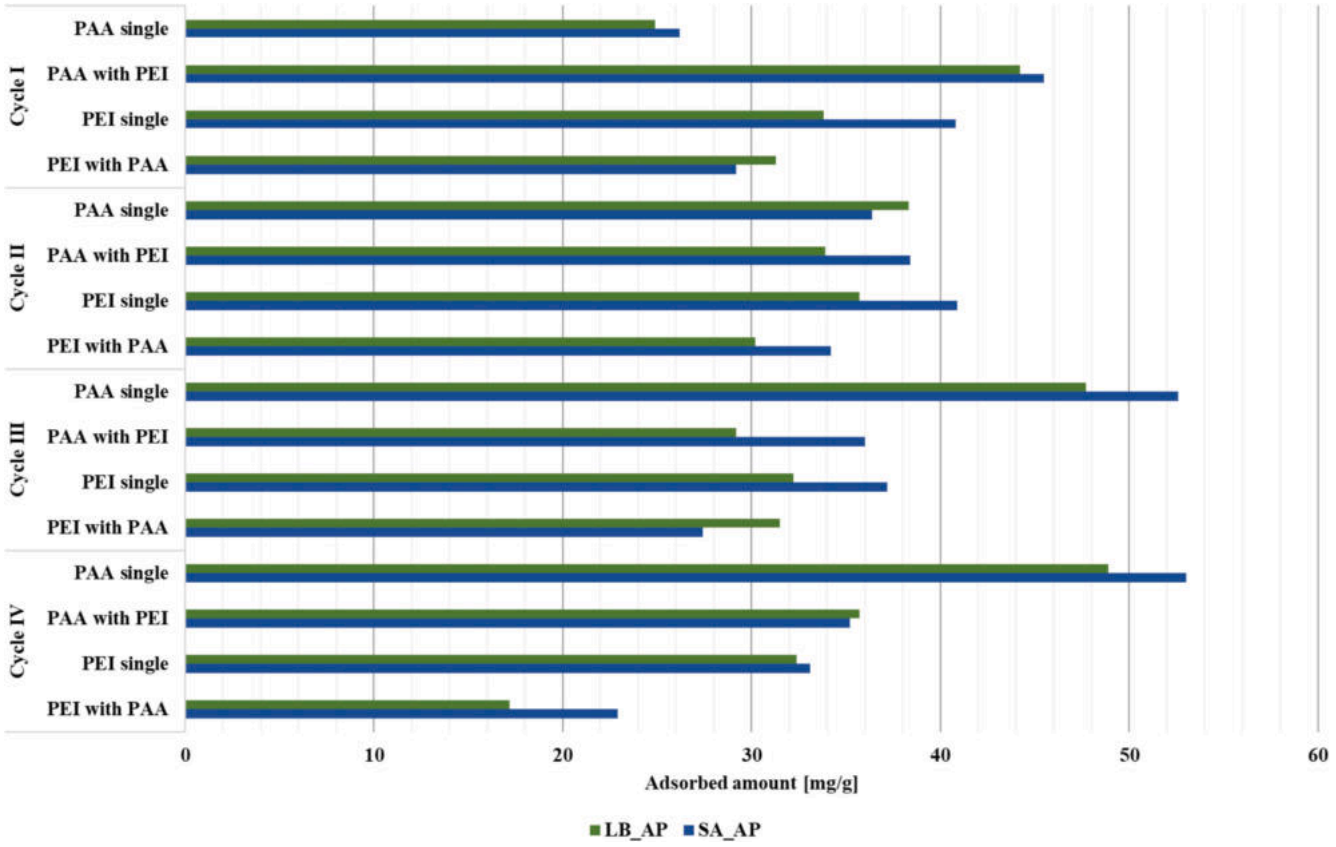

Fig. 12. Amounts of the PAA and PEI adsorbed on the surface of activated carbons from single and binary systems in the subsequent adsorption-desorption cycles (pH 3, C0 200 ppm).

positive charge on the surface, which leads to more and more parallel adsorption of polymeric chains and smaller packing of the adsorption layer.

Metal ions are adsorbed in significantly smaller quantities than polymers macromolecules. Cadmium is better adsorbed at pH 6. With increasing pH, the surface charge density of activated carbons decreases, which results in lower repulsion between solid surface and Cd(II) cations. As(V) is adsorbed at a very small level, so the influence of the pH value is practically unnoticeable. Due to the better-developed specific surface area (Table 3), LB_AP activated carbon is able to adsorb greater amounts of individual adsorbates compared to the SA_AP material.

Table 6 contains the calculated model data. The adsorption of both metal ions is best described by the Freundlich and Dubinin-Radushkevich models, which confirm the heterogenous adsorbent surface with active sites of different binding energy and the formation of an adsorbate multilayer [41]. Moreover, this process takes place primarily inside the porous structure of carbonaceous materials. Very low R^2 values for the Langmuir model in the case of As(V) adsorption is related to small adsorbed amount of the ions. This model is optimal for describing systems close to the maximum surface saturation [42].

Fig. 8 presents the obtained adsorption kinetics results. In the systems containing PAA, the equilibrium is reached after 2 h, whereas in those with PEI after 5 h. At pH 3, poly(acrylic acid) occurs in the coiled conformation, facilitating faster migration from the bulk solution to the surface layer compared to more extended polyethyleneimine chains, which encounter greater resistance. The obtained results fit better with the pseudo-second order kinetic model, which is typical for ionic polymers and mainly indicates the chemical adsorption mechanism (Table 7) [43]. Due to the very small amounts of adsorbed substances, the kinetic studies for metal ions were highly error-prone, and thus, the results were rejected.

The amount of poly(acrylic acid) adsorbed from the mixed adsorbate solutions increases in the system containing positively charged species (Fig. 9). The presence of negatively charged As(V) ions leads to a decrease in PAA adsorption. These effects are primarily driven by the electrostatic interactions: PEI and Cd(II) ions increase the attraction between PAA and adsorbent surface, whereas the presence of arsenic ions results in repulsive interactions [44].

The amount of polyethyleneimine adsorbed decreases in all binary solutions compared to the single-component systems. The occupation of adsorbent's active sites by other species results in their effective blockade and a significant reduction in accessibility for spatially expanded PEI chains. The presence of polymers in the solution has a negative influence on the amount of metal ions adsorbed. In such a case, poly(acrylic acid) and polyethyleneimine show greater affinity to the surface of activated carbon and are preferentially adsorbed, blocking access to the active sites for heavy metal ions. In addition, polymer-metal complexes with a tendency to remain in solution are formed [33]. The obtained maximum adsorbed amounts of all substances are comparable to most of the data found in the literature (Table 8). Greater adsorption is achieved only in the case of less environmentally friendly adsorbents, which are often produced using large amounts of energy and aggressive chemical reagents. The schematic representation of adsorption mechanism taking place in the binary system is shown in Fig. 10.

The efficiency of desorption of individual polymers is presented in Fig. 11. In the single-component systems NaOH is the most effective desorption agent, whereas in those containing polyethyleneimine, HNO_3 causes complete desorption of PAA. In the presence of metal ions, the desorption efficiency using an acidic agent increases. This may indicate the reaction of nitric(V) acid with metal-polymer complexes, which causes their removal from the surface layer. The 0.1 M NaOH solution proved to be a much less effective desorbing agent in a mixture of both

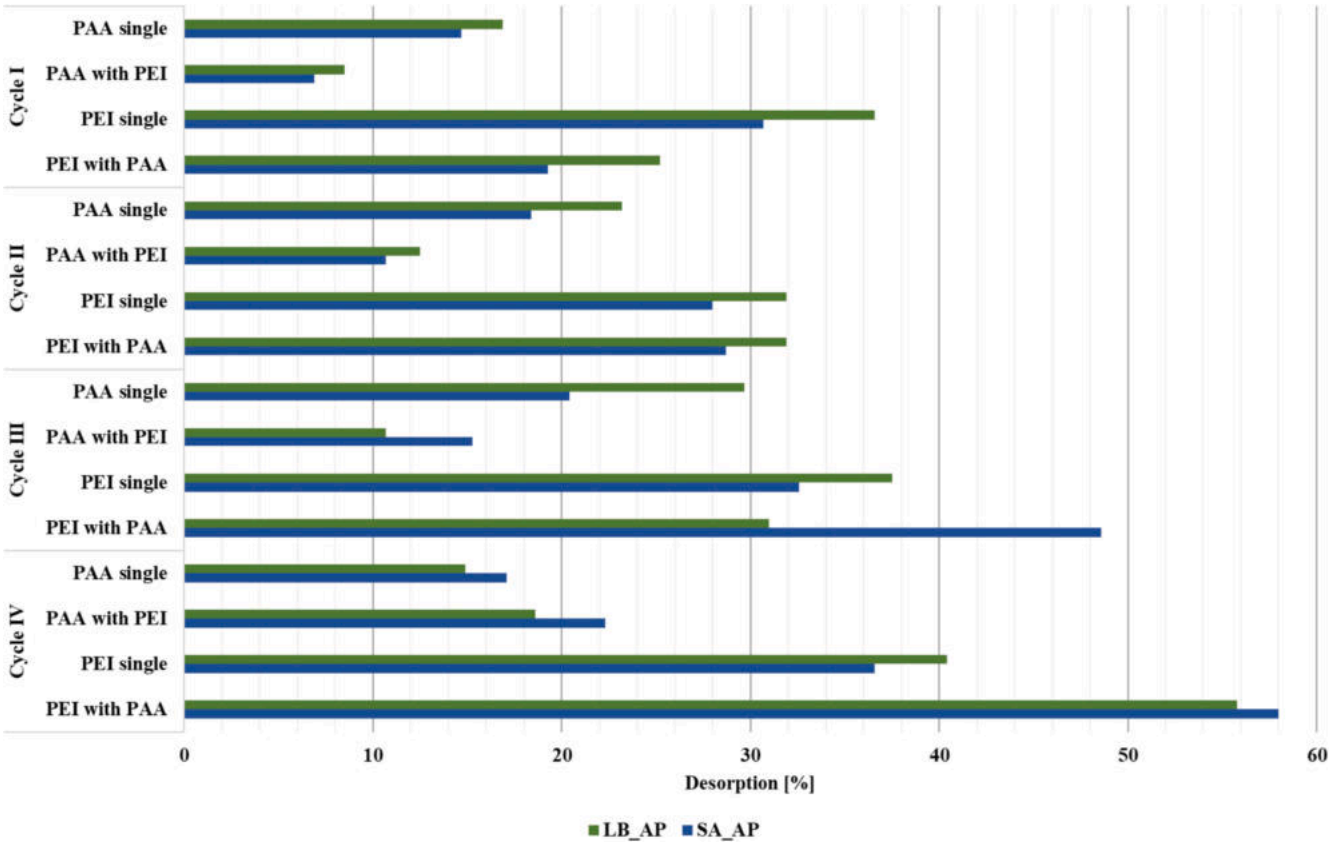

Fig. 13. Desorption efficiency of the PAA and PEI in subsequent adsorption-desorption cycles.

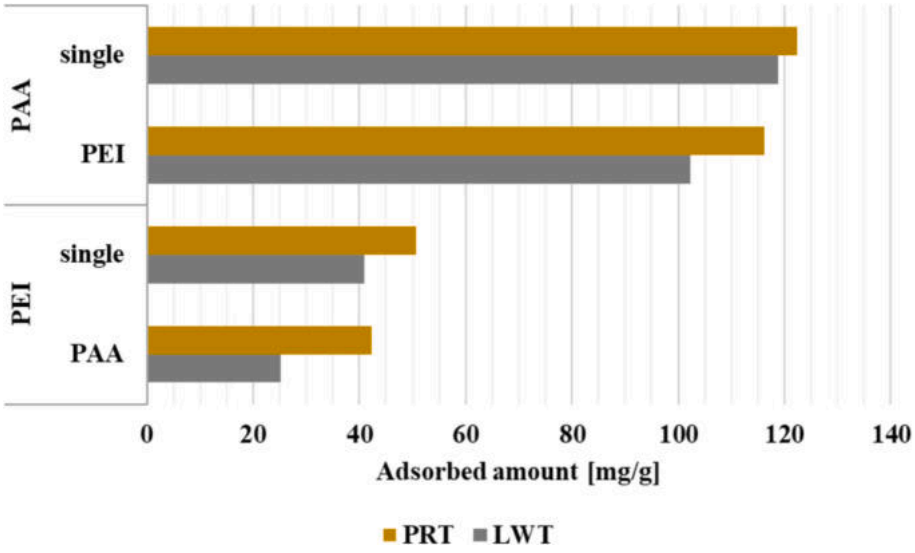

Fig. 14. Amounts of PAA and PEI adsorbed on the surface of commercially available activated carbons (single and binary systems, pH = 3, C_0 = 200 ppm).

polymers. A completely different trend was observed in the presence of metal ions, especially in activated carbon/PAA/As(V) systems, where its efficiency was clearly higher than that of nitric acid. Water was unfortunately the least effective desorption agent for poly(acrylic acid), in systems containing PAA and PEI or PAA and Cd(II) ions simultaneously. Moreover, for this agent, depending on the adsorbent type, significant differences in desorption efficiency were observed. Due to difficulties in determining the PEI concentration in suspensions with high ionic strength, only H_2O was used for its desorption. The best result in this respect (97 %) was achieved in the LB_AP + PEI + Cd(II) system. Polyethyleneimine is better desorbed by water than PAA, which proves that the basic functional groups that predominate on the adsorbent surface interact more strongly with the acidic polymer.

The results obtained in the subsequent adsorption-desorption cycles are presented in Figs. 12 and 13. Desorption tests in the systems containing PEI were performed using H_2O (due to the problems with correct determination of its concentration in acidic or alkaline medium), whereas in the single PAA solutions, HNO_3 was applied to check the

possibility of regeneration using the least effective desorption agent. The adsorbed amount of polymers in the most systems, remains on the same level from cycle I to IV. This may be the result of permanent binding of PEI and PAA macromolecules to the activated carbons, which modifies their surface. It is especially noticeable in single PAA systems where adsorbed amount increases with the number of cycle. The coiled macromolecule penetrate the pores and it is not desorbed from that places, resulting in creation the greater amount of adsorbents active sites.

The amount of polymers adsorbed on the surface of commercially available activated carbons depend on the surface area (Fig. 14). Polyethyleneimine and poly(acrylic acid) show higher affinity to the surface of PRT material. Moreover, PAA is adsorbed in greater amounts on the surface of commercial adsorbents, compared to the LB_AP and SA_AP materials. It is probably related to coiled conformation of anionic polymer, which can penetrate the pores and find more active sites on the surface of LWT and PRT adsorbents. The adsorption capacity of LWT, PRT, LB_AP and SA_AP towards PEI are comparable, which proves that activated carbons described in this paper can be successfully used in the adsorption of spatially expanded polymeric macromolecules.

4. Conclusions

The obtained environmentally friendly activated carbons are characterized by good adsorption properties. Their specific surface area ranges from 399 to 547 m^2/g, while the total content of functional surface groups is almost 2.5 mmol/g. The presence of poly(acrylic acid), polyethyleneimine, Cd(II) and As(V) ions has a strong impact on the adsorbents' electric double-layer structure. However, it should be noted that the influence of ionic polymers on the surface charge density, zeta potential and aggregate size values is more noticeable both in single and binary systems than that of metal ions.

Polyethyleneimine is adsorbed in the greatest amount from a single-component solution. In general, polymers showed a stronger affinity to the activated carbons surface than metal ions The maximum obtained adsorbed amounts are 94 mg/g for PEI, 27 mg/g for PAA, 8 mg/g for Cd (II), and 4 mg/g for As(V). The calculated parameters of the kinetics models indicate that PAA and PEI are adsorbed from single-component systems mainly via chemical interactions. In the case of Cd(II) and As(V) ions the Freundlich and Dubinin-Radushkevich models best described the experimental adsorption isotherms data. Adsorption studies from binary solutions have shown that competition between individual adsorbates occurs in most examined systems. Only in the case of poly (acrylic acid) adsorption in the presence of PEI or Cd(II) ions an increase in PAA adsorbed amount was observed. Furthermore, it has been proven that polymers can be successfully desorbed from the surface of activated carbons. The highest desorption efficiency achieved was 100 % for PAA (HNO_3, binary solutions with PEI) and 97 % for PEI (LB_AP + PEI + Cd (II) system).

Activated carbons obtained by environmentally friendly one-step physical activation (direct activation) can be successfully used to remove ionic polymers and heavy metal ions from aqueous solutions. Moreover, these adsorbents can be effectively regenerated and reused for water treatment purposes.

CRediT authorship contribution statement

Marlena Groszek: Writing – original draft, Methodology, Investigation, Data curation, Conceptualization. **Grzegorz Wójcik:** Software, Methodology, Investigation, Formal analysis. **Małgorzata Wiśniewska:** Writing – review & editing, Writing – original draft, Resources, Conceptualization. **Piotr Nowicki:** Writing – review & editing, Writing – original draft, Visualization, Supervision, Methodology, Investigation.

Declaration of competing interest

The authors declare that they have no known competing financial interests or personal relationships that could have appeared to influence the work reported in this paper.

Data availability

Data will be made available on request.

References

[1] S. Tyagi, N. Garg, R. Paudel, Environmental degradation: Causes and consequences, Eur. Res. 81 (2014) 1491–1498, https://doi.org/10.13187/er.2014.81.1491.
[2] M. Kampa, E. Castanas, Human health effects of air pollution, Environ. Pollut. 151 (2008) 362–367, https://doi.org/10.1016/j.envpol.2007.06.012.
[3] K. Warner, M. Hamza, A. Oliver-Smith, F. Renaud, A. Julca, Climate change, environmental degradation and migration, Nat. Hazards 55 (2010) 689–715, https://doi.org/10.1007/s11069-009-9419-7.
[4] X. Xu, S. Nie, H. Ding, F.F. Hou, Environmental pollution and kidney diseases, Nat. Rev. Nephrol. 14 (2018) 313–324, https://doi.org/10.1038/nrneph.2018.11.
[5] J. Caravanos, B. Ericson, J. Ponce-Canchihuamán, D. Hanrahan, M. Block, B. Susilorini, R. Fuller, Rapid assessment of environmental health risks posed by mining operations in low-and middle-income countries: selected case studies, Environ. Sci. Pollut. Res. 20 (2013) 7711–7718, https://doi.org/10.1007/s11356-012-1424-9.
[6] S.H. Chien, L.I. Prochnow, A.H. Cantarella, Recent developments of fertilizer production and use to improve nutrient efficiency and minimize environmental impacts, Adv. Agron. 102 (2009) 267–322, https://doi.org/10.1016/S0065-2113(09)01008-6.
[7] I. Ostolska, M. Wiśniewska, Investigation of the colloidal Cr_2O_3 removal possibilities from aqueous solution using the ionic polyamino acid block copolymers, J. Hazard. Mat. 290 (2015) 69–77, https://doi.org/10.1016/j.jhazmat.2015.02.068.
[8] R.A. Sheldon, The E factor 25 years on: the rise of green chemistry and sustainability, Green Chem. 19 (2017) 18–43, https://doi.org/10.1039/C6GC02157C.
[9] K. Szewczuk-Karpisz, M. Wiśniewska, M. Medykowska, M.V. Galaburda, V. M. Bogatyrov, O.I. Oranska, M. Błachnio, P. Oleszczuk, Simultaneous adsorption of Cu(II) ions and poly(acrylic acid) on the hybrid carbon-mineral nanocomposites with metallic elements, J. Hazard. Mat. 412 (2021) 125138, https://doi.org/10.1016/j.jhazmat.2021.125138.
[10] W. Abdussalam-Mohammed, A.Q. Ali, A.O. Errayes, Green chemistry: principles, applications, and disadvantages, Chem. Methodol. 4 (2020) 408–423, https://doi.org/10.33945/SAMI/CHEMM.2020.4.4.
[11] P. Anastas, N. Eghbali, Green chemistry: principles and practice, Chem. Soc. Rev. 39 (2010) 301–312, https://doi.org/10.1039/B918763B.
[12] I.T. Horvath, P.T. Anastas, Innovations and green chemistry, Chem. Rev. 107 (2007) 2169–2173, https://doi.org/10.1021/cr078380v.
[13] A. Raj, A. Chowdhury, S.W. Ali, Green chemistry: its opportunities and challenges in colouration and chemical finishing of textiles, Sustain. Chem. Pharm. 27 (2022) 100689, https://doi.org/10.1016/j.scp.2022.100689.
[14] T. Keijer, V. Bakker, J.C. Slootweg, Circular chemistry to enable a circular economy, Nat. Chem. 11 (2019) 190–195, https://doi.org/10.1038/s41557-019-0226-9.
[15] K. Kümmerer, J.H. Clark, V.G. Zuin, Rethinking chemistry for a circular economy, Science 367 (2020) 369–370, https://doi.org/10.1126/science.aba4979.
[16] A.K. Roy Choudhury, Green chemistry and the textile industry, Text. Prog. 45 (2013) 3–143, https://doi.org/10.1080/00405167.2013.807601.
[17] R. Ratti, Industrial applications of green chemistry: status, challenges and prospects, SN Appl. Sci. 2 (2020) 263, https://doi.org/10.1007/s42452-020-2019-6.
[18] J. Pallarés, A. González-Cencerrado, I. Arauzo, Production and characterization of activated carbon from barley straw by physical activation with carbon dioxide and steam, Biomass Bioenergy 115 (2018) 64–73, https://doi.org/10.1016/j.biombioe.2018.04.015.
[19] X. Zhang, W. Xiang, B. Wang, J. Fang, W. Zou, F. He, Y. Li, D.C.W. Tsang, Y.S. Ok, B. Gao, Adsorption of acetone and cyclohexane onto CO2 activated hydrochars, Chemosphere 245 (2020) 125664, https://doi.org/10.1016/j.chemosphere.2019.125664.
[20] Y. Li, X. Yan, Z. Cui, J. Yuan, B. Xu, G. Yang, Design and preparation of activated carbon with high specific surface area and porosity through an organic activator coupled with CO2 activation, Adv. Mater. Interfaces 12 (3) (2025) 2400450, https://doi.org/10.1002/admi.202400450.
[21] K.J. Ardila-Fierro, J.G. Hernández, Sustainability assessment of mechanochemistry by using the twelve principles of green chemistry, ChemSusChem 14 (2021) 2145–2162, https://doi.org/10.1002/cssc.202100478.
[22] Y. Wu, P. Yilihan, J. Cao, Y. Jin, Competitive adsorption of Cr (VI) and Ni (II) onto coconut shell activated carbon in single and binary systems, Water Air Soil Pollut. 224 (2013) 1662, https://doi.org/10.1007/s11270-013-1662-6.

[23] M. Mariana, H.P.S. Abdul Khalil, E.M. Mistar, E.B. Yahya, T. Alfatah, M. Danish, M. Amayreh, Recent advances in activated carbon modification techniques for enhanced heavy metal adsorption, J. Water Process Eng. 43 (2021) 102221, https://doi.org/10.1016/j.jwpe.2021.102221.
[24] H.P. Boehm, E. Diehl, W. Heck, R. Sappok, Surface oxides of carbon, Angew. Chem. 3 (1964) 669–677, https://doi.org/10.1002/anie.196406691.
[25] S. Chibowski, M. Wiśniewska, A.W. Marczewski, S. Pikus, Application of the SAXS method and viscometry for determination of the thickness of adsorbed polymer layers at the ZrO_2 - polymer solution interface, J. Colloid Interf. Sci. 267 (2003) 1–8, https://doi.org/10.1016/S0021-9797(03)00698-2.
[26] A. Von Harpe, H. Petersen, Y. Li, T. Kissel, Characterization of commercially available and synthesized polyethylenimines for gene delivery, J. Control. Release 69 (2000) 309–322, https://doi.org/10.1016/S0168-3659(00)00317-5.
[27] T.K. Das, A.N. Bezbaruah, Comparative study of arsenic removal by iron-based nanomaterials: potential candidates for field applications, Sci. Total Environ. 764 (2021) 142914, https://doi.org/10.1016/j.scitotenv.2020.142914.
[28] H.A. Ohshima, Simple expression for Henry's function for the retardation effect in electrophoresis of spherical colloidal particles, J. Colloid Interf. Sci. 168 (1994) 269–271, https://doi.org/10.1006/jcis.1994.1419.
[29] W. Janusz, Electrical double layer in the system TiO_2 (anathase)/aqueous solution of NaCl, Pol. J. Chem. 68 (1994) 1871–1880.
[30] K.Y. Foo, B.H. Hameed, Insights into the modeling of adsorption isotherm systems, Chem. Eng. J. 156 (2010) 2–10, https://doi.org/10.1016/j.cej.2009.09.013.
[31] J. Wang, X. Guo, Adsorption kinetic models: physical meanings, applications, and solving methods, J. Hazard. Mat. 390 (2020) 122156, https://doi.org/10.1016/j.jhazmat.2020.122156.
[32] M. Gęca, M. Wiśniewska, P. Nowicki, Simultaneous removal of polymers with different ionic character from their mixed solutions using herb-based biochars and activated carbons, Molecules 27 (2022) 7557, https://doi.org/10.3390/molecules27217557.
[33] M. Gęca, M. Wiśniewska, P. Nowicki, G. Wójcik, Arsenate and cadmium ions removal from multicomponent solutions of ionic polymers using mesoporous activated biocarbons, J. Mol. Liq. 407 (2024) 125270, https://doi.org/10.1016/j.molliq.2024.125270.
[34] R. Maršálek, M. Švidrnoch, The adsorption of amitriptyline and nortriptyline on activated carbon, diosmectite and titanium dioxide, Environ. Chall. 1 (2020) 100005, https://doi.org/10.1016/j.envc.2020.100005.
[35] M. Wiśniewska, P. Nowicki, Peat-based activated carbons as adsorbents for simultaneous separation of organic molecules from mixed solution of poly (acrylic acid) polymer and sodium dodecyl sulfate surfactant, Colloids Surf. A Physicochem. Eng. Asp. 585 (2020) 124179, https://doi.org/10.1016/j.colsurfa.2019.124179.
[36] M. Wiśniewska, P. Nowicki, K. Szewczuk-Karpisz, M. Gęca, K. Jędruchniewicz, P. Oleszczuk, Simultaneous removal of toxic Pb(II) ions, poly(acrylic acid) and Triton X-100 from their mixed solution using engineered biochars obtained from horsetail herb precursor – impact of post-activation treatment, Sep. Purif. Technol. 276 (2021) 1192697, https://doi.org/10.1016/j.seppur.2021.119297.
[37] V.K. Sharma, M. Sohn, Aquatic arsenic: toxicity, speciation, transformations, and remediation, Environ. Int. 35 (2009) 743759, https://doi.org/10.1016/j.envint.2009.01.005.
[38] M. Medykowska, M. Wiśniewska, K. Szewczuk-Karpisz, R. Panek, M. Franus, Simultaneous removal of inorganic and organic pollutants from multicomponent solutions by the use of zeolitic materials obtained from fly ash waste, Clean Techn. Environ. Policy 25 (2023) 11331148, https://doi.org/10.1007/s10098-022-02429-4.
[39] K. Szewczuk-Karpisz, P. Krasucka, P. Boguta, K. Skic, Z. Sokołowska, G. Fijałkowska, M. Wiśniewska, Electrical double layer at the gibbsite/anionic polyacrylamide/supporting electrolyte interface–adsorption, spectroscopy and electrokinetic studies, J. Mol. Liq. 261 (2018) 439445, https://doi.org/10.1016/j.molliq.2018.04.030.
[40] M. Gęca, M. Wiśniewska, T. Urban, P. Nowicki, Temperature effect on ionic polymers removal from aqueous solutions using activated carbons obtained from biomass, Materials 16 (2023) 350, https://doi.org/10.3390/ma16010350.
[41] S.J. Allen, G. Mckay, J.F. Porter, Adsorption isotherm models for basic dye adsorption by peat in single and binary component systems, J. Colloid Interface Sci. 280(2) (2004) 322–333, https://doi.org/10.1016/j.jcis.2004.08.078.
[42] M.A. Al-Ghouti, D.A. Da'ana, Guidelines for the use and interpretation of adsorption isotherm models: a review, J. Hazard. Mater. 393 (2020) 122383, https://doi.org/10.1016/j.jhazmat.2020.122383.
[43] M. Gęca, M. Wiśniewska, P. Nowicki, K. Jędruchniewicz, Cd(II) and As(V) removal from the multicomponent solutions in the presence of ionic polymers using carbonaceous adsorbents obtained from herbs, Pure Appl. Chem. 955 (2023) 563578, https://doi.org/10.1515/pac-2023-0201.
[44] S. Yang, J. Hu, C. Chen, D. Shao, X. Wang, Mutual effects of Pb (II) and humic acid adsorption on multiwalled carbon nanotubes/polyacrylamide composites from aqueous solutions, Environ. Sci. Technol. 45 (2011) 3621–3627, https://doi.org/10.1021/es104047d.
[45] D. Santhiya, S. Subramanian, K.A. Natarajan, S.G. Malghan, Surface chemical studies on the competitive adsorption of poly (acrylic acid) and poly (vinyl alcohol) onto alumina, J. Colloid Interf. Sci. 216 (1) (1999) 143–153, https://doi.org/10.1006/jcis.1999.6289.
[46] S. Liufu, H. Xiao, Y. Li, Adsorption of poly (acrylic acid) onto the surface of titanium dioxide and the colloidal stability of aqueous suspension, J. Colloid Interf. Sci. 281 (2005) 155–163, https://doi.org/10.1016/j.jcis.2004.08.075.
[47] S. Chibowski, J. Patkowski, E. Grządka, Adsorption of polyethyleneimine and polymethacrylic acid onto synthesized hematite, J. Colloid Interf. Sci. 329 (1) (2009) 1–10, https://doi.org/10.1016/j.jcis.2008.09.075.
[48] A. Alemdar, N. Öztekin, N. Güngör, Ö.I. Ece, F.B. Erim, Effects of polyethyleneimine adsorption on the rheological properties of purified bentonite suspensions, Colloids Surf. A Physicochem. Eng. Asp. 252 (2005) 9598, https://doi.org/10.1016/j.colsurfa.2004.10.009.
[49] L. Qian, M. Chen, B. Chen, Competitive adsorption of cadmium and aluminum onto fresh and oxidized biochars during aging processes, J. Soil. Sediment. 15 (2015) 1130–1138, https://doi.org/10.1007/s11368-015-1073-y.
[50] X. Huang, N.Y. Gao, Q.L. Zhang, Thermodynamics and kinetics of cadmium adsorption onto oxidized granular activated carbon, J. Environ. Sci. 19 (2007) 1287–1292, https://doi.org/10.1016/S1001-0742(07)60210-1.
[51] S. Zhu, T. Qu, M.K. Irshad, J. Shang, Simultaneous removal of Cd(II) and As(III) from co-contaminated aqueous solution by α-FeOOH modified biochar, Biochar 2 (2020) 81–92, https://doi.org/10.1007/s42773-020-00040-8.
[52] L. Semerjian, Equilibrium and kinetics of cadmium adsorption from aqueous solutions using untreated Pinus halepensis sawdust, J. Hazard. Mat. 173 (2010) 236–242, https://doi.org/10.1016/j.jhazmat.2009.08.074.
[53] C. Tang, Y. Shu, R. Zhang, X. Li, J. Song, B. Li, Y. Zhang, D. Ou, Comparison of the removal and adsorption mechanisms of cadmium and lead from aqueous solution by activated carbons prepared from *Typha angustifolia* and *Salix matsudana*, RSC Adv. 7 (2017) 16092–16103, https://doi.org/10.1039/C6RA28035H.
[54] R. Kushwaha, R.S. Singh, D. Mohan, Comparative study for sorption of arsenic on peanut shell biochar and modified peanut shell biochar, Bioresour. Technol., 375 (2023)128831, doi: 10.1016/j.biortech.2023.128831.
[55] C. Nieto-Delgado, J. Gutiérrez-Martínez, J.R. Rangel-Méndez, Modified activated carbon with interconnected fibrils of iron-oxyhydroxides using Mn^{2+} as morphology regulator, for a superior arsenic removal from water, Environ. Sci. 76 (2019) 403–414, https://doi.org/10.1016/j.jes.2018.06.002.
[56] X.J. Gong, Y.S. Li, Y.Q. Dong, W.G. Li, Arsenic adsorption by innovative iron/calcium in-situ-impregnated mesoporous activated carbons from low-temperature water and effects of the presence of humic acids, Chemosphere 250 (2020) 126275, https://doi.org/10.1016/j.chemosphere.2020.126275.
[57] Y. Zhang, M. Yang, X. Huang, Arsenic (V) removal with a Ce (IV)-doped iron oxide adsorbent, Chemosphere 51 (2003) 945–952, https://doi.org/10.1016/S0045-6535(02)00850-0.
[58] A.F. Hassan, A.M. Abdel-Mohsen, H. Elhadidy, Adsorption of arsenic by activated carbon, calcium alginate and their composite beads, Int. J. Biol. Macromol. 68 (2014) 125–130, https://doi.org/10.1016/j.ijbiomac.2014.04.006.

Lublin, 10.09.2025

mgr Marlena Groszek
Uniwersytet Marii Curie-Skłodowskiej w Lublinie,
Wydział Chemii, Instytut Nauk Chemicznych,
Katedra Radiochemii i Chemii Środowiskowej,
Pl. Marii Curie-Skłodowskiej 3, 20-031 Lublin
marlena.groszek@mail.umcs.pl

Rada Naukowa Instytutu Nauk Chemicznych
Uniwersytetu Marii Cure-Skłodowskiej
w Lublinie

Oświadczenie o współautorstwie

Niniejszym oświadczam, że mój udział w pracy: **M. Groszek**, G. Wójcik, M. Wiśniewska, P. Nowicki, *Application of environmentally friendly activated carbons derived from herbal industry waste for water purification: A study on the removal of selected organic and inorganic pollutants,* Journal of Water Process Engineering, 2025, 75, 107952, DOI: 10.1016/j.jwpe.2025.107952 [D4], obejmował stworzenie koncepcji pracy, opracowanie metodyki pomiarów i ich przeprowadzenie, zestawienie i analizę uzyskanych wyników, przygotowanie manuskryptu oraz sformułowanie odpowiedzi na uwagi recenzentów.

Lublin, 10.09.2025

dr hab. Grzegorz Wójcik, prof. UMCS
Uniwersytet Marii Curei-Skłodowskiej w Lublinie,
Wydział Chemii, Instytut Nauk Chemicznych,
Katedra Chemii Nieorganicznej,
Pl. Marii Curie-Skłodowskiej 2, 20-031 Lublin
grzegorz.wojcik2@mail.umcs.pl

Rada Naukowa Instytutu Nauk Chemicznych
Uniwersytetu Marii Cure-Skłodowskiej
w Lublinie

Oświadczenie o współautorstwie

Niniejszym oświadczam, że mój udział w pracy: M. Groszek, **G. Wójcik**, M. Wiśniewska, P. Nowicki, *Application of environmentally friendly activated carbons derived from herbal industry waste for water purification: A study on the removal of selected organic and inorganic pollutants,* Journal of Water Process Engineering, 2025, 75, 107952, DOI: 10.1016/j.jwpe.2025.107952 [D4], obejmował opracowanie metodyki i przeprowadzenie oznaczania jonów metali w roztworach wodnych.

Grzegorz Wójcik

Lublin, 10.09.2025

prof. dr hab. Małgorzata Wiśniewska
Uniwersytet Marii Curie-Skłodowskiej w Lublinie,
Wydział Chemii, Instytut Nauk Chemicznych,
Katedra Radiochemii i Chemii Środowiskowej,
Pl. Marii Curie-Skłodowskiej 3, 20-031 Lublin
malgorzata.wisniewska@mail.umcs.pl

Rada Naukowa Instytutu Nauk Chemicznych
Uniwersytetu Marii Cure-Skłodowskiej
w Lublinie

Oświadczenie o współautorstwie

Niniejszym oświadczam, że mój udział w pracy: M. Groszek, G. Wójcik, **M. Wiśniewska**, P. Nowicki, *Application of environmentally friendly activated carbons derived from herbal industry waste for water purification: A study on the removal of selected organic and inorganic pollutants*, Journal of Water Process Engineering, 2025, 75, 107952, DOI: 10.1016/j.jwpe.2025.107952 [D4], obejmował stworzenie koncepcji pracy, przygotowanie i korektę manuskryptu - przed i po procesie recenzji oraz sformułowanie odpowiedzi na uwagi recenzentów.

Małgorzata Wiśniewska

Poznań, 10.09.2025

dr hab. Piotr Nowicki, prof. UAM
Uniwersytet im. Adama Mickiewicza w Poznaniu,
Wydział Chemii, Zakład Chemii Stosowanej,
Ul. Uniwersytetu Poznańskiego 8, 61-614 Poznań
piotr.nowicki@amu.edu.pl

Rada Naukowa Instytutu Nauk Chemicznych
Uniwersytetu Marii Cure-Skłodowskiej
w Lublinie

Oświadczenie o współautorstwie

Niniejszym oświadczam, że mój udział w pracy: M. Groszek, G. Wójcik, M. Wiśniewska, **P. Nowicki**, *Application of environmentally friendly activated carbons derived from herbal industry waste for water purification: A study on the removal of selected organic and inorganic pollutants,* Journal of Water Process Engineering, 2025, 75, 107952, DOI: 10.1016/j.jwpe.2025.107952 [D4], obejmował opracowanie metodyki badań, przeprowadzenie eksperymentów, analizę uzyskanych wyników, korektę manuskryptu - przed i po procesie recenzji oraz nadzór merytoryczny w czasie całego cyklu wydawniczego.

Piotr Nowicki

D5. M. Groszek, M. Wiśniewska, P. Nowicki, *Simultaneous determination of ionic polymers and heavy metal ions concentrations in aqueous solution after their adsorptive removal using eco-friendly activated biocarbons*, Frontiers in Chemistry, 13, 2025, 1621297, DOI: 10.3389/fchem.2025.1621297

frontiers | Frontiers in Chemistry

TYPE Original Research
PUBLISHED 02 July 2025
DOI 10.3389/fchem.2025.1621297

OPEN ACCESS

EDITED BY
Olena Goncharuk,
National Academy of Sciences of Ukraine, Ukraine

REVIEWED BY
Manish Pratap Singh,
Veer Bahadur Singh Purvanchal University, India
Łukasz Klapiszewski,
Poznań University of Technology, Poland

*CORRESPONDENCE
Małgorzata Wiśniewska,
malgorzata.wisniewska@mail.umcs.pl

RECEIVED 30 April 2025
ACCEPTED 20 June 2025
PUBLISHED 02 July 2025

CITATION
Groszek M, Wiśniewska M and Nowicki P (2025) Simultaneous determination of ionic polymers and heavy metal ions concentrations in aqueous solution after their adsorptive removal using eco-friendly activated biocarbons. *Front. Chem.* 13:1621297.
doi: 10.3389/fchem.2025.1621297

Simultaneous determination of ionic polymers and heavy metal ions concentrations in aqueous solution after their adsorptive removal using eco-friendly activated biocarbons

Marlena Groszek[1], Małgorzata Wiśniewska[1]* and Piotr Nowicki[2]

[1]Department of Radiochemistry and Environmental Chemistry, Institute of Chemical Sciences, Faculty of Chemistry, Maria Curie-Sklodowska University in Lublin, Lublin, Poland, [2]Department of Applied Chemistry, Faculty of Chemistry, Adam Mickiewicz University in Poznań, Poznań, Poland

Growing contamination of aquatic systems by industrial and domestic pollutants necessitates the development of efficient and sustainable wastewater treatment technologies. Activated biocarbons derived from renewable biomass sources have proven to be promising materials for this purpose thanks to their large specific surface area, well-developed porosity, high content of surface groups and cost-effectiveness. This paper describes the preparation, physicochemical characterization and practical application of carbonaceous adsorbents derived from the nettle and mint herbs residues using an environmentally friendly method–single-stage (direct) physical activation with carbon dioxide. The obtained activated biocarbons were fully characterized in terms of their texture, surface properties, and chemical composition, and then used to remove ionic polymers (poly(acrylic acid) and polyethyleneimine) as well as Cd(II) and As(V) ions from aqueous solutions. The influence of the above-mentioned substances on their mutual adsorption was investigated. The obtained eco-friendly carbonaceous materials are characterized by moderately developed surface area (368–666 m^2/g) and high content of the surface functional groups (2.19–4.89 mmol/g). The maximum adsorbed amounts of ionic polymers reached the level of about 80 mg/g, while those of heavy metal ions varied in the range of 4–19 mg/g. Competitive adsorption between the polymer chains and heavy metal ions was confirmed. In the binary system containing both types of macromolecules, an increase in the adsorbed amounts of poly(acrylic acid) and polyethyleneimine was observed. In turn, the simultaneous presence of ionic polymers and heavy metal ions leads to a reduction in the adsorbed quantities of all adsorbates. The analysis of adsorption-desorption, surface, and electrokinetic data allowed the identification of the most probable mechanisms of separation of ionic polymers and heavy metal ions from the aqueous phase using eco-friendly carbonaceous adsorbents.

KEYWORDS

activated biocarbons, eco-friendly synthesis, ionic polymers, heavy metal ions, multicomponent solutions, simultaneous adsorption

GRAPHICAL ABSTRACT

Introduction

Water is an essential resource for life, but its availability and quality are increasingly threatened by unsustainable consumption and waste management practices (Ali, 2012; Ali and Gupta, 2006). Water purification is the process of removing contaminants, pathogens, and undesirable substances to make it suitable for human consumption, industrial use, or ecological sustainability. Traditional purification methods, such as sedimentation, chemical precipitation, ion exchange, evaporation, filtration, and chlorination have proven effective in providing clean water to millions of people (Ruthiraan et al., 2015). However, the complexity of contemporary water contamination–ranging from microplastics and emerging pollutants to heavy metal ions and pharmaceutical residues–has necessitated the development of advanced purification techniques (Ganesamoorthy et al., 2021; Schwarzenbach et al., 2006; Singh et al., 2018).

In recent years, adsorption has become a highly effective and versatile technique for removing various types of pollutants from aqueous systems (Bhatnagar et al., 2015; Zhou et al., 2015). Among the many adsorption materials available, activated carbons and synthetic resins, have been widely used primarily due to their high adsorption capacities. Activated carbon is a highly porous material with a large surface area, which makes it an excellent adsorbent for removing a broad spectrum of contaminants present in natural water reservoirs (including groundwater runoff from fertilized agricultural fields) as well as municipal and industrial wastewater (Crini and Lichtfouse, 2019; Dias et al., 2007). Its excellent adsorption properties are attributed to hierarchical pore structure, consisting of micropores, mesopores and macropores, as well as the presence of surface functional groups that enable physical and chemical interactions with pollutants (Soonmin and Kabbashi, 2021; Ioannidou, and Zabaniotou, 2007). However, the production of chemically activated carbonaceous materials or synthetic resins often involves high energy consumption, significant carbon footprint, and the generation of potential secondary pollution, raising concerns about their long-term environmental sustainability.

In response to these challenges, there has been growing interest in the development of environmentally friendly adsorbents derived from renewable, biodegradable, and low-cost sources (Shannon et al., 2008). These criteria are fully met by activated biocarbon–green adsorbent obtained from plant precursors via physical activation (Kyzas and Kostoglou, 2014). Compared to chemical variant of activation, which requires the usage of aggressive chemical reagents like orthophosphoric acid or potassium hydroxide, physical activation is environmentally friendly option in this regard. Moreover, post-processing steps related to removal of residual chemicals are eliminated (Yahya et al., 2015; Yang et al., 2010).

In this paper activated biocarbons obtained from the nettle and mint herbs residues (waste from the herbal industry) through simultaneous pyrolysis and physical activation were applied for organic and inorganic pollutants removal from aqueous solutions. Four adsorbates of different ionic character and molecular weight were used in the study, including high-molecular weight anionic poly(acrylic acid) and cationic polyethyleneimine, as well as low-molecular weight cadmium(II) cations and arsenate(V) anions. The selected adsorbates were chosen due to their common presence in wastewater. Poly(acrylic acid) is widely used as a thickening agent, while polyethyleneimine increases the permeability of cell membranes and is extensively used in biotechnology. Heavy metals ions have a negative impact on human health and are released into the environment from many industries processes. The adsorption studies were performed in the solution with three different pH values (i.e. 3, 6 and 9). Due to the greatest adsorbed amounts observed at pH 3, these conditions were chosen for the multicomponent adsorption tests. In order to define the adsorption mechanism, the surface charge density, zeta potential, and aggregate sizes of the solid particles dispersed in aqueous suspensions (containing single and binary adsorbates) were determined.

It should be emphasized that the adsorption of ionic polymers on the surface of activated biocarbons remains a largely underexplored area, and very few studies have addressed their removal from complex, multicomponent systems. This research gap highlights the originality and significance of the presented results. As polymeric contaminants are increasingly detected in various aquatic systems, our findings provide a new and

important contribution to the development of more effective remediation strategies for polluted aquatic environments (drinking water, wastewater and natural water reservoirs).

Experimental

Materials

Nettle (NE) and mint (MT) herb residues were dried at 110 °C and then their stalks were cut into 1.5–2.0 cm long pieces. Fifteen-gram samples of the precursors were placed in nickel boats and subjected to simultaneous pyrolysis and physical activation in a horizontal resistance furnace equipped with a quartz tube reactor (one-zone model PRW75/LM, Czylok, Jastrzębie-Zdrój, Poland). The process involved annealing the sample at 800 °C for 30 min in a CO_2 atmosphere with a flow rate of 250 cm^3/min. After the completion of the one-step activation process, the materials were cooled to room temperature under a nitrogen flow (flow rate of 170 cm^3/min). The resulting activated products were designated as NE_AP and MT_AP.

Polyethyleneimine (PEI) (Sigma Aldrich, Saint Louis, MO, United States) is a cationic polymer with an average molecular weight of 2000 Da, containing amine groups along its chains. This weak polyelectrolyte has a pK_b value at pH 9, at which 50% of its functional groups are dissociated. As the pH decreases, the number of dissociated amine groups increases, leading to the spatial expansion of the polymer chain (Von Harpe et al., 2000).

Poly(acrylic acid) (PAA) (Fluka, Saint Louis, MO, United States) represents the group of anionic polymers and it is characterized by an average molecular weight of 2000 Da. It is also a weak polyelectrolyte and its macromolecules contain carboxyl functional groups, 50% of which dissociate at pH 4.5, to the pK_a value of PAA. Below this pH value, the degree of dissociation decreases, leading to the formation of a coiled conformation of the polymer chains. In turn, at pH values above 4.5, the number of dissociated carboxyl groups increases, resulting in a more extended chain conformation (Chibowski et al., 2003).

Cadmium nitrate tetrahydrate ($CdN_2O_6{\cdot}4H_2O$, Sigma Aldrich, Saint Louis, United States) was used as a source of Cd(II) cations. This compound dissolves well in water at pH below 8, while above this value, cadmium ions precipitate. As a result, experiments involving Cd(II) were limited to the pH range from 3 to 7.

The As(V) anions used in the study were introduced by potassium dihydrogen arsenate (KH_2AsO_4, Sigma Aldrich, Saint Louis, United States). This salt is highly water-soluble over a wide pH range. However, the form of arsenate ions varies with pH changes. At higher pH values, the As(V) ion is fully dehydrated and exists as AsO_4^{3-} anion. As the pH decreases, the degree of hydration increases, resulting in the occurrence of the following forms: $HAsO_4^{2-}$, $H_2AsO_4^-$ and H_3AsO_4 (Das and Bezbaruah, 2020).

Adsorbents characterization

The surface morphology of the activated biocarbons was examined using scanning electron microscopy (SEM) (Quanta 250 FEG, FEI, Waltham, MA, United States). The porosity characteristics, including the total/micropore surface area, total pore/micropore volume, and average pore diameter, were assessed by low-temperature (−196 °C) nitrogen adsorption-desorption measurements performed using an ASAP 2420 apparatus (Micromeritics, Norcross, GA, United States). The functional groups present on the surface of the biocarbons were quantified using the Boehm back titration method (Boehm et al., 1964). In this analytical procedure, NaOH and HCl solutions (both at a concentration of 0.1 mol/dm^3, Avantor Performance Materials, Gliwice, Poland) were used as titrants. To analyze the surface chemistry and identify C-, N-, and O-containing functional groups present on the tested materials, X-ray photoelectron spectroscopy (XPS) (Gammadata Scienta, Uppsala, Sweden) was applied. The ash content was determined according to the ISO 1171: 2002 standard, using a muffle furnace FCF-V70C (Czylok, Jastrzębie Zdrój, Poland). The total content of C, N, H, and S was determined using an elemental analyzer Vario EL III (Elementar Analysen Systeme GmbH, Germany). The chemical composition of the materials was also studied by means of X-ray fluorescence (XRF) spectrometry (Axios mAX, PANanalytical, Almelo, Netherlands).

Adsorption and desorption studies

The adsorbed amounts of PAA and PEI polymers, as well as Cd(II) and As(V) ions, were determined using the static method. This approach involved measuring the change in adsorbate concentration in the solution before and after the adsorption process.

The concentrations of the polymers were determined using a Carry 100 UV–Vis spectrophotometer (Varian, Palo Alto, Santa Clara, CA, United States). For poly(acrylic acid), its reaction with hyamine 1622 was carried out. As a result, a white-coloured complex, absorbing light at a wavelength of 500 nm, was formed (Crummett and Hummel, 1963). In turn, the concentration of polyethyleneimine was determined based on its reaction with copper(II) chloride, which results in a blue-coloured complex absorbing light at 285 nm (Patkowski et al., 2016). The calibration curves used to determine the polymer concentration determination are presented in Figure 1. The presence of heavy metal ions causes a shift of calibration curves (especially in the case of PAA). These effects were described in details in the previous paper (Gęca et al., 2024c).

The concentrations of Cd(II) and As(V) ions were determined using Inductively Coupled Plasma-Optical Emission Spectrometry (ICP-OES) with the iCAP™ 7200 analyser (Thermo Fisher Scientific, Waltham, United States). The measurement wavelengths were 228.8 nm for cadmium and 189 nm for arsenic ions, respectively. The operational parameters for the ICP-OES included the plasma with the following settings: flow rate of 15 dm^3/min, a nebulizer flow rate of 0.75 dm^3/min and a power setting of 1 kW. The presence of the polymers reduced the analytical signal by 5% and this interference was taken into account in the calculations.

Adsorption isotherms were studied over a 24-h period of time. For these tests, 10 cm^3 of solutions containing the adsorbate (with initial concentrations ranging from 10 to 300 ppm) and a 0.001 mol/dm^3 NaCl supporting electrolyte were prepared. The weights of activated

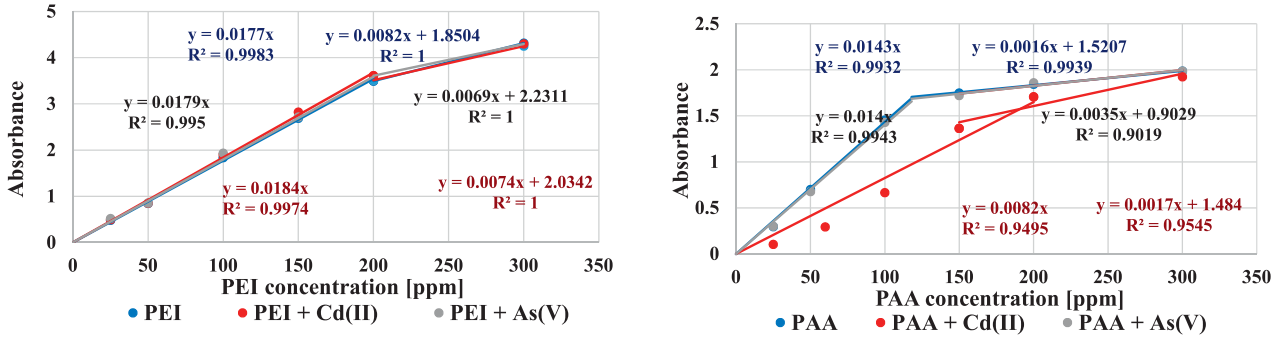

FIGURE 1
Calibration curves for PEI and PAA in the absence and presence of heavy metal ions (with concentration of 200 ppm).

TABLE 1 Textural parameters of the activated biocarbons.

Adsorbent	Surface area [m^2/g]		Pore volume [cm^3/g]		Average pore size [nm]	Micropore contribution
	Total	Micropore	Total	Micropore		
NE_AP	368	248	0.21	0.10	2.26	0.47
MT_AP	666	535	0.32	0.21	1.91	0.66

TABLE 2 Acid-base properties of the activated biocarbons.

Adsorbent	Acidic groups concentration [mmol/g]	Basic groups concentration [mmol/g]	Total concentration [mmol/g]	pH_{pzc}	pH_{iep}
NE_AP	0.32	4.57	4.89	8.5	<3
MT_AP	0.63	1.56	2.19	9.7	3.5

biocarbons used were 0.02 g for polymers and 0.05 g for metal ions. Experiments were conducted at pH 3, 6 and 9, but studies involving Cd(II) ions were limited to pH 3 and 6. At pH above 7, cadmium(II) ions precipitate in the solution. Therefore, their loss from solution at alkaline pH values is the result not only of Cd(II) ions adsorption but also of precipitation. Before the adsorption test, the pH value of all tested samples was adjusted using 0.1 mol/dm^3 NaOH or HCl solutions and measured using a Φ360 pH meter (Beckman, Brea, United States). A constant pH level was maintained throughout the adsorption process by continuous monitoring and correction as necessary. The adsorption isotherms data obtained for heavy metal ions were fitted to theoretical models. The Langmuir (Equation 1), Freundlich (Equation 2), Temkin (Equation 3) and Dubinin-Radushkevich (Equation 4) equations were applied (Awad et al., 2019):

$$q_e = \frac{q_m K_L C_e}{1 + K_L C_e} \quad (1)$$

$$q_e = K_F C_e^{1/n} \quad (2)$$

$$q_e = \frac{RT}{b_T} \ln A_T + \frac{RT}{b_T} \ln C_e \quad (3)$$

$$q_e = q_m \exp\left(-\beta \varepsilon^2\right) \quad (4)$$

where: q_e–the adsorbed amount at the equilibrium state [mg/g], q_m–the maximum adsorption capacity in the Langmuir model [mg/g], K_L–the Langmuir parameter [m^3/mg], C_e–the equilibrium aqueous phase concentration [mg/dm^3], K_F–the Freundlich parameter [mg/g (mg/dm^3)$^{1/n}$], n–the Freundlich constant, R–gas constant (8.314 J/(mol K), T–temperature [K], A_T–Temkin constant [J/mol], b_T–Temkin constant [dm^3/g], β–Dubinin-Radushkevich constant, ε–adsorption potential [kJ/mol].

Based on the obtained results, pH 3 at which the adsorbed amounts of polymers were the greatest, was chosen for the kinetics studies. In these tests, an appropriate mass of activated biocarbon was added to 10 cm^3 of a solution containing 0.001 mol/dm^3 NaCl as the supporting electrolyte. The initial concentration of both polymers was 200 ppm. Adsorption progress was monitored over time intervals ranging from 0.5 to 7 h. Kinetics data for polymers were fitted to the pseudo-first-order (Equation 5) and pseudo-second-order (Equation 6) models (Wang and Guo, 2020), according to the equations:

$$\frac{dq_t}{dt} = k_1 \left(q_e - q_t\right) \quad (5)$$

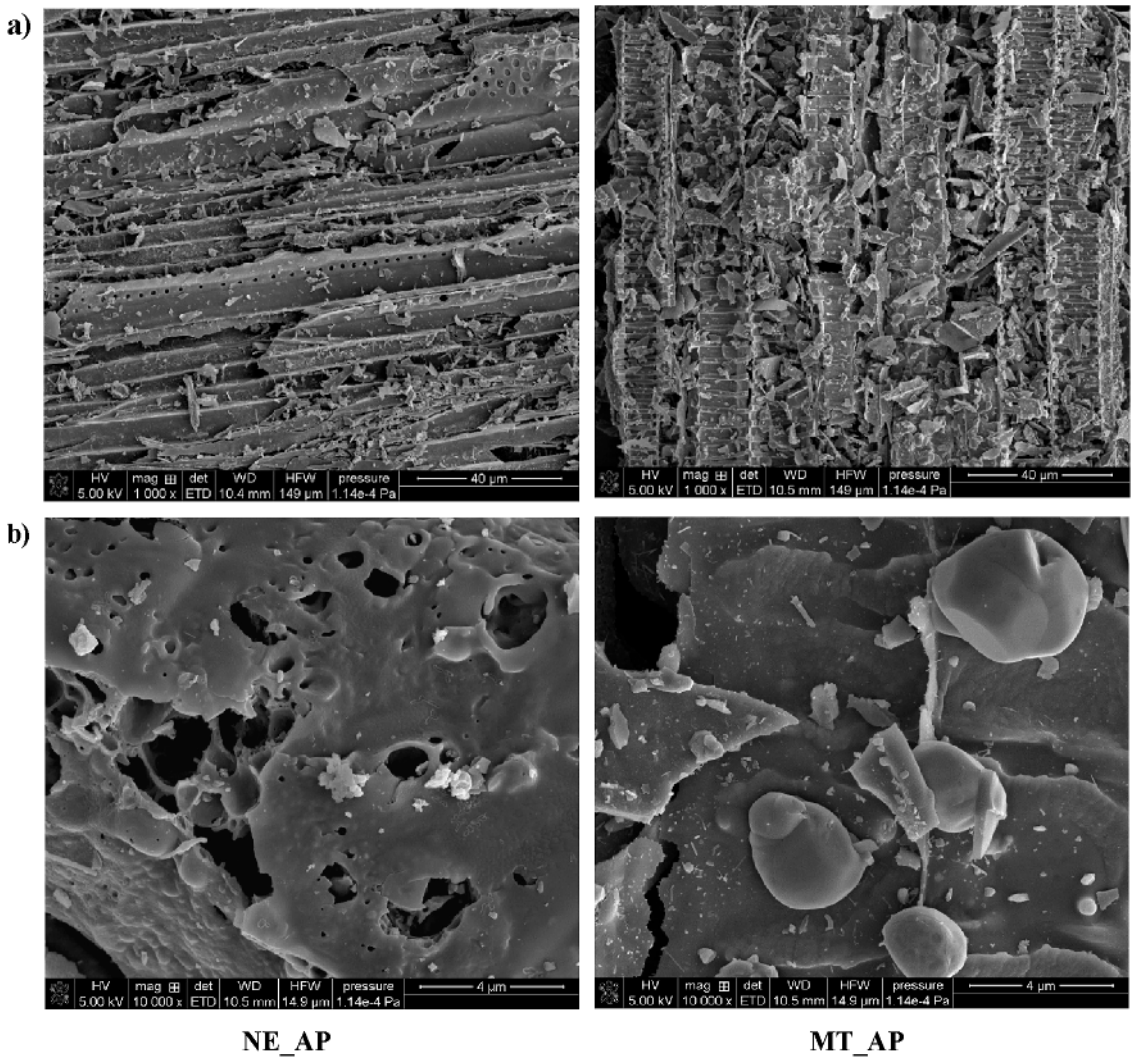

FIGURE 2
The SEM images of the activated biocarbons [**(a)**–zoom 1000x; **(b)**–zoom 10 000x].

TABLE 3 Chemical composition of the surface layer of activated biocarbons based on XPS analysis.

Element	Content of element [at%]	
	NE_AP	MT_AP
C	75.9	78.1
N	1.9	1.9
O	13.9	13.3
P	1.3	0.7
Cl	-	0.6
K	-	3.8
Ca	3.2	1.5
Mg	1.9	-
Si	1.8	-

$$\frac{dq_t}{dt} = k_2 (q_e - q_t)^2 \quad (6)$$

where: q_e–the adsorbed amount in the equilibrium state [mg/g], q_t–the adsorbed amount after time "t" [mg/g], k_1 – the equilibrium rate constant [1/min], k_2 – the equilibrium rate constant [g/(mg·min)].

Adsorption studies in single and binary adsorbate systems were conducted for 24 h at pH 3. The 10 cm^3 of the suspensions consisted of: 200 ppm adsorbate (polymers and/or metal ions), 0.001 mol/dm^3 NaCl and appropriate mass of activated biocarbon, were prepared. After the adsorption process, activated biocarbon was separated using a microcentrifuge (Centrifuge MPW 233e, MPW Med. Instruments, Warsaw, Poland). The concentrations of adsorbates in the supernatants were measured. For polymers, desorption from the surface of biocarbon materials was also investigated, while for metal ions, desorption studies were not conducted due to the small amounts adsorbed and the high associated errors. The H_2O, HNO_3 or NaOH solutions (acidic and basic solutions with a concentration

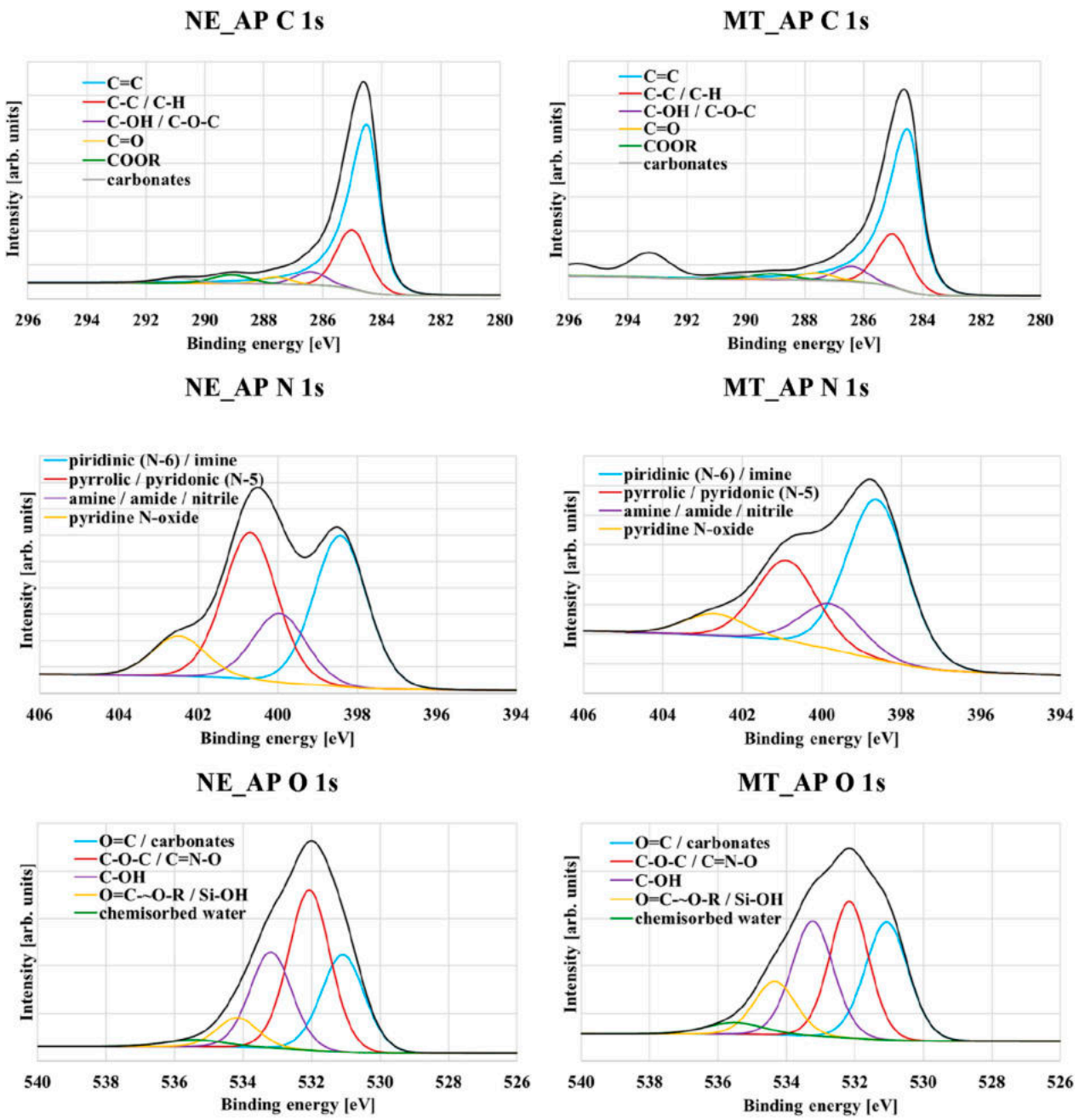

FIGURE 3
XPS spectra of C 1s, N 1s and O 1s regions for NE_AP and MT_AP activated biocarbons.

TABLE 4 Ash content and elemental composition of the activated biocarbons (wt%).

Sample	Ash	C^{daf}	N^{daf}	H^{daf}	S^{daf}	O^{diff}
NE_AP	17.5	77.9	3.9	1.3	0.0	17.0
MT_AP	23.5	74.7	3.1	1.7	0.0	20.5

^{daf}–dry-ash-free basis.
^{diff}–calculated by difference.

of 0.1 mol/dm^3) were used as desorbing agents, and the process lasted 24 h. After that time activated biocarbon was again separated and the concentrations of PAA or PEI in the supernatants were determined. The NE_AP activated biocarbon was dried after the desorption process and performed to the adsorption-desorption cycle studies. All adsorption and desorption tests were carried out at 25 °C. Each sample was measured 3 times and the differences between the obtained result values do not exceed 5%.

10.3389/fchem.2025.1621297

TABLE 5 Chemical composition of activated biocarbons based on XRF results.

Element	Content [mg/g]	
	NE_AP	MT_AP
P	0.075	0.119
S	0.012	0.024
Cl	0.003	0.124
K	0.005	0.333
Ca	0.320	0.399
Mn	-	0.003
Fe	0.002	0.005
Cu	-	0.005
Ga	0.001	-

Colloidal properties of activated biocarbons suspensions without and with adsorbates

The determinations of surface charge density (σ_0), zeta potential (ζ) and aggregates size were carried out at 25 °C for the following systems: NE_AP, NE_AP + PEI, NE_AP + PAA, NE_AP + PAA + PEI, NE_AP + Cd(II), NE_AP + Cd(II)+PEI, NE_AP + Cd(II)+PAA, NE_AP + As(V), NE_AP + As(V)+PEI, NE_AP + As(V)+PAA, MT_AP, MT_AP + PEI, MT_AP + PAA, MT_AP + PAA + PEI, MT_AP + Cd(II), MT_AP + Cd(II)+PEI, MT_AP + Cd(II)+PAA, MT_AP + As(V), MT_AP + As(V)+PEI and MT_AP + As(V)+PAA.

To determine the surface charge density (σ_0), 50 cm^3 of suspensions were prepared, each containing the given adsorbate at an initial concentration of 100 ppm, supporting electrolyte NaCl at a concentration of 0.001 mol/dm^3 and 0.054 g of NE_AP or 0.03 g of MT_AP. The prepared suspension was placed in a thermostated Teflon vessel (RE 204 thermostat, Lauda Scientific, Lauda-Königshofen, Germany). The glass and calomel electrodes (Beckman Instruments, Brea, United States) were introduced into the vessel to monitor pH changes using a pH-meter (pHM 240, Radiometer, Warsaw, Poland). The pH was adjusted by gradually adding 0.1 mol/dm^3 NaOH (titrant), using an automatic microburette (Dosimat 765, Metrohm, Herisau, Switzerland). The dependence of the σ_0 value on the pH of the suspension was determined using the Titr_v3 computer program, which also controlled the titration process. These calculations were based on the difference in the volume of NaOH added to the suspension and to the supporting electrolyte solution to achieve the same pH value (Janusz, 1994), using the following equation (Equation 7):

$$\sigma_0 = \frac{\Delta V c F}{m S} \tag{7}$$

where: ΔV–the difference in the volume of NaOH added to the suspension and to the supporting electrolyte solution to achieve the appropriate pH value [dm^3]; c–NaOH concentration [mol/dm^3], F–Faraday constant [C/mol], m–solid mass [g], S–solid surface area [m^2/g].

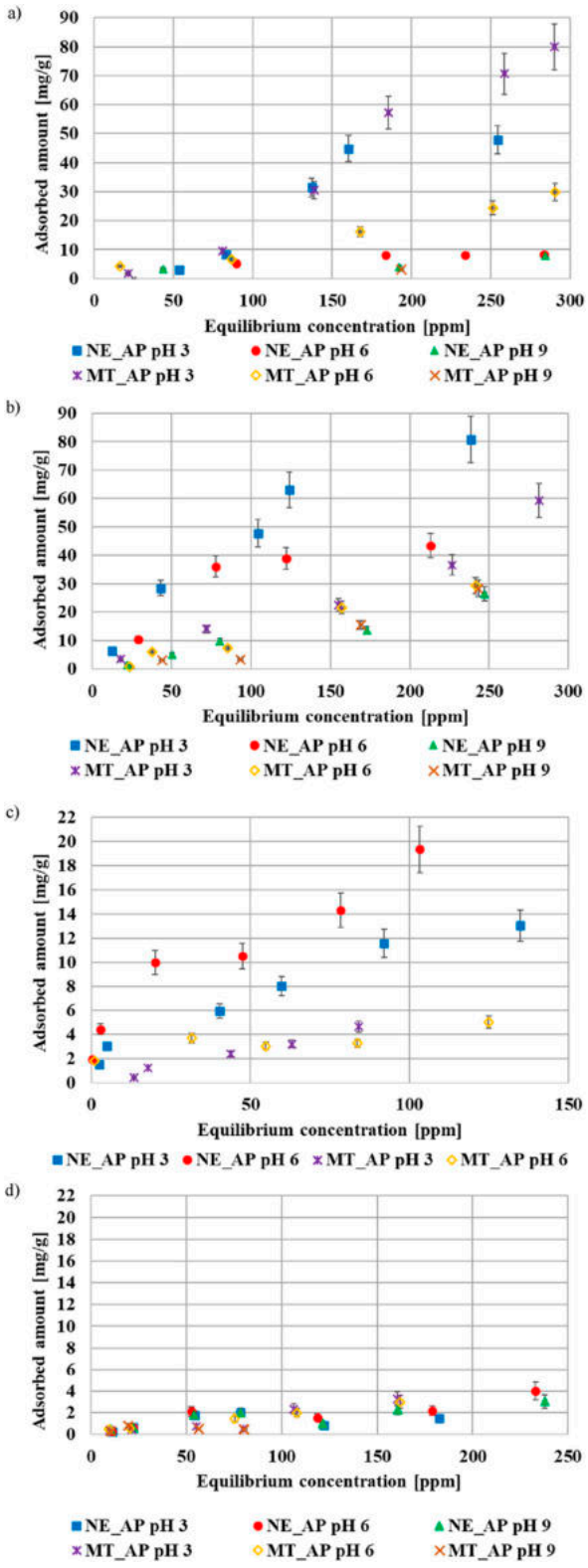

FIGURE 4
Adsorption isotherms of PEI **(a)**, PAA **(b)**, Cd(II) **(c)** and As(V) **(d)** on the activated biocarbons surface obtained at pH 3, 6, and 9.

TABLE 6 Calculated isotherms parameters of Cd(II) and As(V) ions adsorption on NE_AP activated biocarbon surface at pH 6.

Isotherm parameters		NE_AP	
		Cd(II)	As(V)
Experimental	q_{exp} [mg/g]	19.36	4.00
Langmuir	q_m [mg/g]	18.68	5.05
	K_L [dm^3/mg]	0.0698	0.0064
	R^2	0.8899	0.5424
Freundlich	n_F	2.7480	1.4278
	K_F [mg/g·(mg/dm^3)$^{1/n}$]	0.0607	0.5333
	R^2	0.9820	0.8665
Temkin	b_T [J/mol]	979	2673
	A_T [dm^3/g]	4.0195	0.1118
	R^2	0.8422	0.7374
Dubinin-Radushkevich	β	−3.0*10^{-9}	−8.1*10^{-9}
	ε [kJ/mol]	12.99	7.88
	q_m [mg/g]	37.96	18.03
	R^2	0.9720	0.8810

The zeta potential (ζ) and aggregate size of activated biocarbon particles, both in the presence and absence of adsorbates, were evaluated using the procedure described below. Initially, a suspension of 200 cm^3 volume was prepared, containing 200 ppm of tested polymer/s and/or metal ions, 0.001 mol/dm^3 NaCl as a supporting electrolyte, and 0.03 g of the carbonaceous material. The suspension was subjected to ultrasonic treatment using an ultrasonic head (XL 2020; Misonix, Farmingdale, United States) for 3 min. Appropriate adsorbates were then introduced into the suspension. The obtained suspension was divided into smaller portions, and the pH of each portion was adjusted to a value ranging from 3.0 to 10.0 (±0.1), using 0.1 mol/dm^3 HCl and NaOH solutions. pH adjustment was performed using a Φ360 pH meter (Beckman, Brea, United States). The zeta potential was determined using the laser Doppler electrophoresis technique with a Zetasizer Nano ZS (Malvern Instruments, Malvern, United Kingdom). This instrument measured the electrophoretic mobility of solid particles, both covered with adsorption layers and without them. The zeta potential (ζ) was then calculated from the electrophoretic mobility data using Henry's equation (Equation 8): (Ohshima, 1994):

$$U_e = \frac{2\varepsilon_0 \varepsilon \zeta}{3\eta} f(\kappa a) \quad (8)$$

where: U_e–solids electrophoretic mobility [cm^2/(V·s)], ε_0 – the electric permittivity of a vacuum [F/m], ε–dielectric constant, η–viscosity of dispersive phase [Pa·s], $f(\kappa a)$ – Henry's function.

The measurement was carried out 9 times and the error did not exceed 5%.

Additionally, the stability of the suspension was investigated by determining the average size of solid particles aggregates at pH 3, 6, and 9. In this case, the measurements were based on the static light scattering phenomenon. Each sample was measured three times and the error was less than 5%.

Results and discussion

Physicochemical characteristics of carbonaceous materials

Both obtained activated biocarbons have a mesoporous structure and well-developed specific surface area (Table 1). The material obtained from the mint herb residue shows significantly better textural parameters (surface area 666 m^2/g), while the adsorbent derived from the nettle herb remains is characterized by a greater concentration of the functional groups on its surface (Table 2). Both of these parameters have a strong impact on the activated biocarbons adsorption capacity. The average pore size of both adsorbents is approximately 2 nm, which allows to classify these materials as mesoporous. The surface of examined solids is dominated by basic functional groups, the concentration of which for NE_AP material is about 14 times higher than acid groups. The points of zero charge (pzc) occur at pH 8.5 and 9.7 for nettle- and mint-based samples, respectively, which confirmed the alkaline properties of both adsorbents. On the other hand, the isoelectric points (iep) of activated biocarbons (iep) are located at pH below 3 for NE-AP activated biocarbon and at pH 3.5 for MT_AP one, which are significantly lower than the pzc values. It may be the result of partial overlapping of the electrical double layers (edl) formed on the walls of the pores, which is a phenomenon often observed for mesoporous materials (Skwarek et al., 2014; Szewczuk-Karpisz et al., 2021).

Figure 2 presents the SEM images of the activated biocarbons. Despite the elongated shapes present in the structure of both materials, their surface layers differ significantly. The structure of NE_AP biocarbon is characterized by the presence of round holes and small pieces/particles on the surface. In the case of MT_AP material, the accumulation of smaller pieces on the surface is greater, beneath which a ribbed structure can be observed. These varied textural structures correspond to the activated biocarbons surface area, which is much greater in the case of the MT_AP sample.

According to the data presented in Table 3 and in Figure 3, both materials are characterized by a high carbon content exceeding 75 at %. The structure of both activated biocarbons is clearly dominated by C=C groups. Furthermore, the contents of C-C, C-H, C-OH, C-O-C, C=O and carbonate species are similar in both solids. The second most abundant element is oxygen, with a concentration of about 13 at%. In the case of NE_AP activated biocarbon the contribution of carbonyl groups is the highest, while for the material obtained from mint herb residue, the contents of hydroxyl, carbonyl, and ether groups are at a similar level. In turn, the share of carboxyl groups is the lowest in both solids. The content of nitrogen does not exceed 2 at%, although the XPS tests confirm the presence of pyridinic, pyrrolic and amine groups. XPS analysis also revealed the presence of mineral admixtures in the structure of the obtained activated biocarbons, which is a fairly typical phenomenon for carbonaceous materials produced from plant-derived waste biomass.

The results of elemental analysis (summarized in Table 4) confirmed that carbon is the main component of the obtained

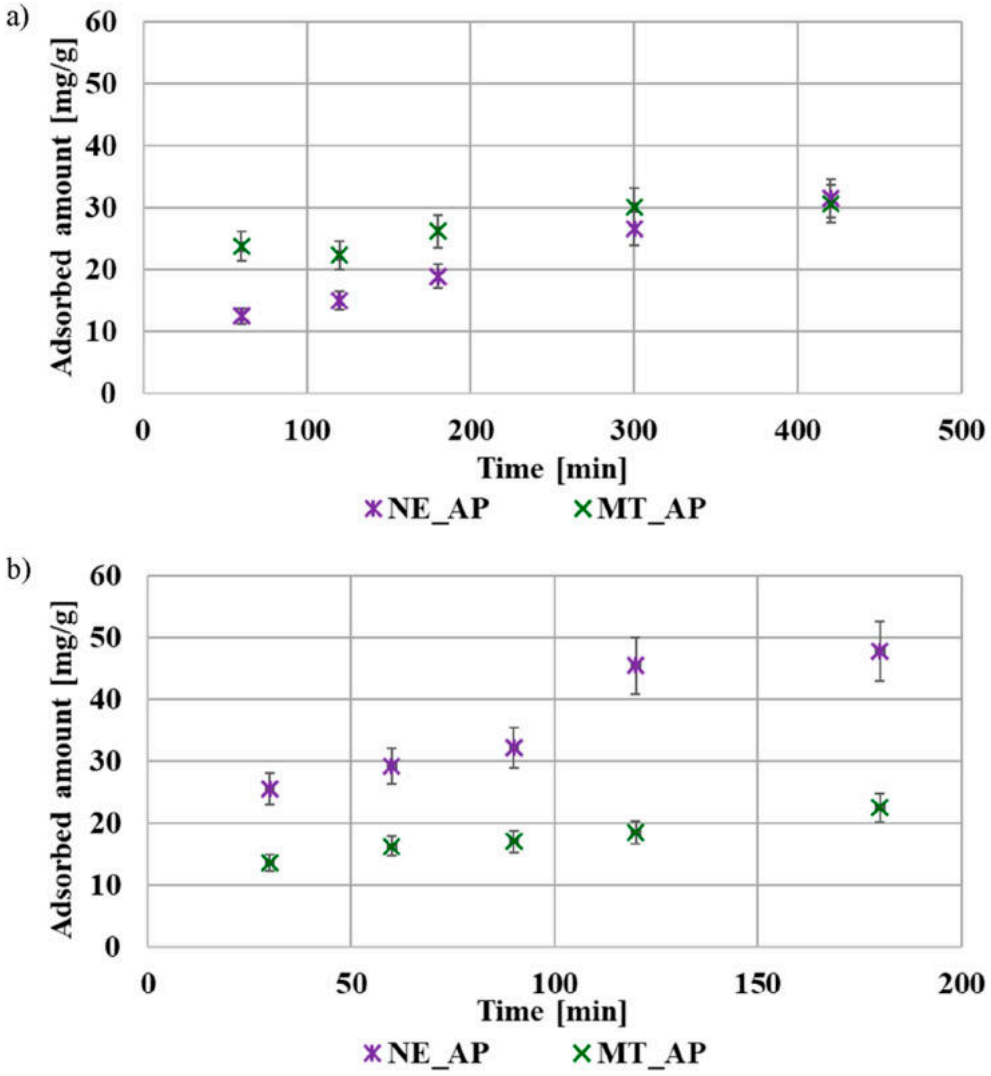

FIGURE 5
The adsorption kinetics of PEI **(a)** and PAA **(b)** on the surface of activated biocarbons at pH 3.

TABLE 7 Calculated kinetic parameters for the adsorption of PEI and PAA on the activated biocarbons surface at pH 3.

Kinetic parameters		NE_AP		MT_AP	
		PEI	PAA	PEI	PAA
Experimental	q_{exp} [mg/g]	31.45	47.79	30.54	22.45
Pseudo-first-order model	q_e [mg/g]	1.0140	1.0377	1.0130	1.0293
	k_1 [1/min]	10.4164	1.6189	7.6639	8.5941
	R^2	0.8240	0.8917	0.9468	0.7916
Pseudo-second-order model	q_e [mg/g]	46.0829	76.3359	33.6700	25.6410
	k_2 [g/(mg*min)]	0.00009	0.00013	0.00069	0.0011
	R^2	0.9300	0.8944	0.9909	0.9699

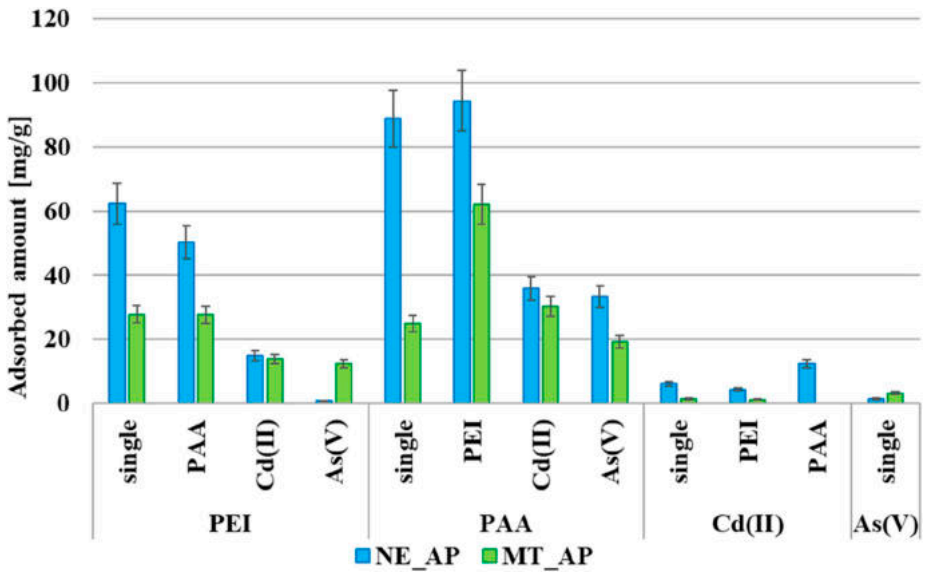

FIGURE 6
The adsorbed amounts of PAA, PEI, Cd(II) and As(V) on the surface of the activated biocarbons from single and binary solutions (C_0 200 ppm, pH 3).

materials. The high oxygen content is related to the large number of functional groups introduced as a result of partial gasification of the carbon matrix during heat treatment in the CO_2 atmosphere. The obtained data also indicate a high ash content in the obtained activated biocarbons. This is a consequence of the presence of numerous mineral admixtures in the structure of the starting materials, which do not decompose during the activation process.

Table 5 presents the results of the XRF analysis. No heavy metals were found in the composition of activated biocarbons, which proves that the obtained materials will not have a negative impact on the environment and their disposal should not pose any problems. The data show that, in addition to elements such as C, H, N, S, and O, both biocarbons also contain considerable amounts of phosphorus, calcium (particularly the sample derived from nettle) and potassium (especially the MT_AP material).

Adsorption capacity and regeneration efficiency of carbonaceous materials

The greatest adsorption of polyethyleneimine occurs at pH 3 (Figure 4a). Under these conditions, positively charged polymer chains are repulsed electrostatically by the positively charged adsorbent surface, forming an adsorption layer with perpendicular-orientated macromolecules. In turn, the increasing pH value causes the surface charge of the activated biocarbon to become negative, which results in the attractive interaction between the cationic polymer and adsorbent. The number of macromolecules adsorbed in parallel orientation increases, while the packing density of the adsorption layer decreases. Poly(acrylic acid) is also adsorbed in the greatest amount at pH 3 and its adsorption efficiency decreases with increasing pH. In this case, similarly to PEI, it is related to changes in the polymeric chain conformation (Figure 4b). At low pH values, most of the carboxyl groups is fully protonated and poly(acrylic acid) chains occur in a coiled conformation. The higher the pH is, the more PAA functional groups dissociate. This causes significant development of polymer chains, which create loosely packed adsorption layers and consequently lead to a reduction in the amount of adsorbed substance (Gęca et al., 2024a). The maximum adsorbed amounts of polymers observed in this study are higher than most values reported in the literature. The adsorption capacity of inorganic materials (such as metal oxides) towards ionic polymers does not exceed 30 mg/g (Alemdar et al., 2005; Chibowski et al., 2009; Liufu et al., 2005; Santhiya et a. 1999). In the case of activated carbons, the obtained results are comparable to our previous findings for carbonaceous materials derived from sage and lemon balm stalks via physical activation (Groszek et al., 2025).

The removal of cadmium(II) ions from an aqueous solution is less influenced by pH value compared to the polymers, but it is slightly more efficient at pH 6 (Figure 4c). In the case of As(V) ions, their adsorbed amounts are very low and similar in all systems (Figure 4d). The obtained isotherms data were fitted to theoretical models (Table 6). Both heavy metal ions' adsorption is best described by Freundlich and Dubinin-Radushkevich models, which indicates that the adsorption process takes place inside the pores and leads to the formation of multilayer adsorbate films (Foo and Hameed, 2010). The maximum adsorbed amounts of cadmium ions reported in the literature often exceed 100 mg/g, but the adsorbents used in these studies were mainly synthesized using aggressive chemical reagents (Meng et al., 2024; Tan et al., 2022; Yin et al., 2023). The amounts of Cd(II) ions adsorbed on the surface of environmentally friendly adsorbents are comparable to the values obtained in the presented studies (Anwar et al., 2010; Farasati et al., 2016). The adsorption of As(V) ions has been studied primarily using novel, chemically

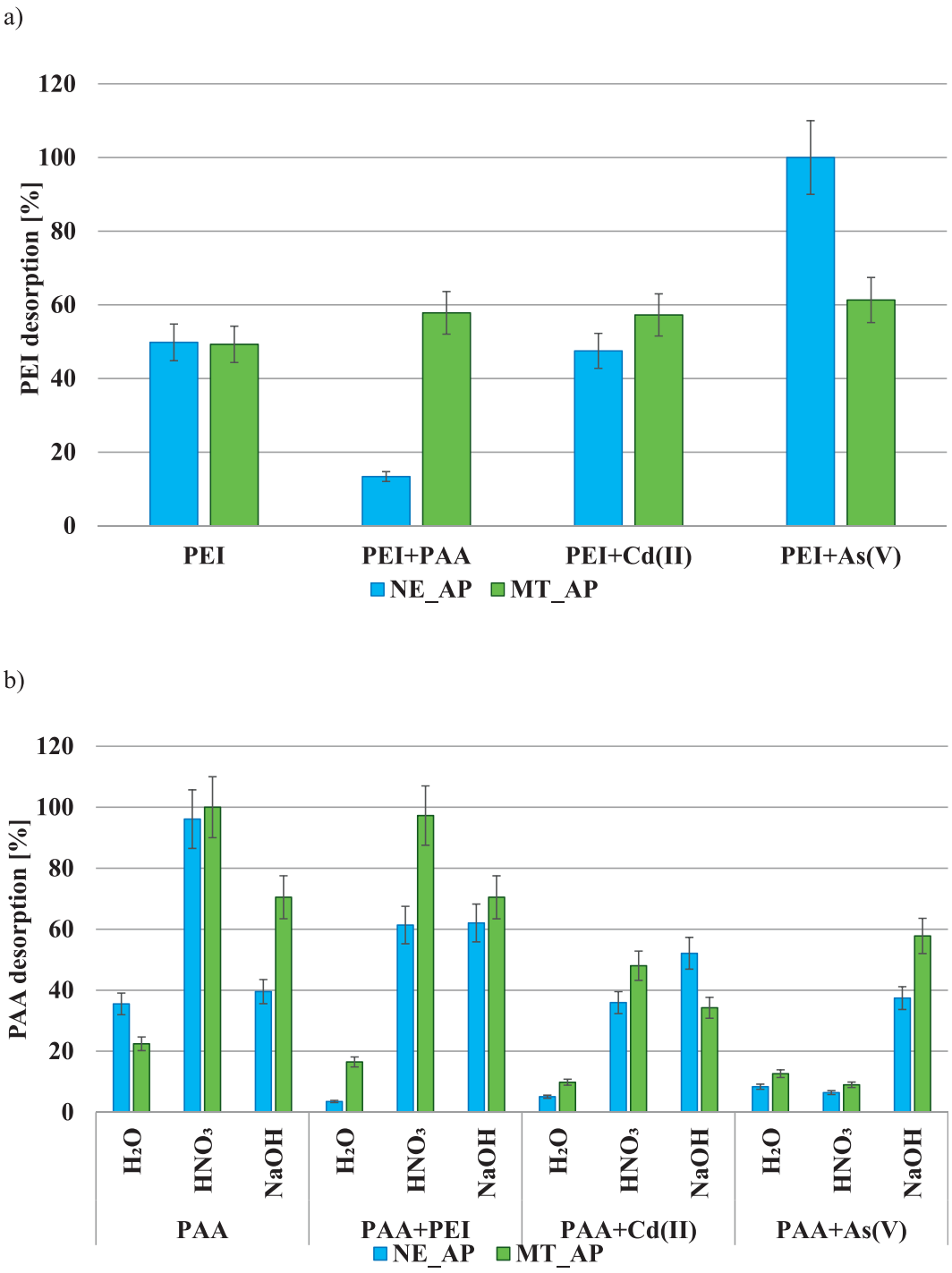

FIGURE 7
PEI **(a)** and PAA **(b)** desorption efficiency from the activated biocarbons surface with the usage of various desorption agents.

modified inorganic materials, whose adsorption capacity ranges from 30 to 200 mg/g (Đolić et al., 2021; He et al., 2023; Wu et al., 2022). In contrast, the application of eco-friendly carbonaceous materials for As(V) ions removal has been investigated to a very limited extent.

The adsorption kinetics results of the examined polymers are shown in Figure 5. The equilibrium state was reached after 6 h in the case of PEI and after 2 h in the case of PAA. This difference can be related to the size of both macromolecules at pH 3. The coiled poly(acrylic acid) molecules migrate faster through the bulk solution towards the adsorbent surface layer than the developed polyethyleneimine chains. The calculated theoretical parameters are listed in Table 7. Both polymers adsorption kinetics are better described by pseudo second-order model. This indicates that the polymer's adsorption on the activated biocarbons surface involved mainly electron exchange between adsorbent and adsorbate (chemical

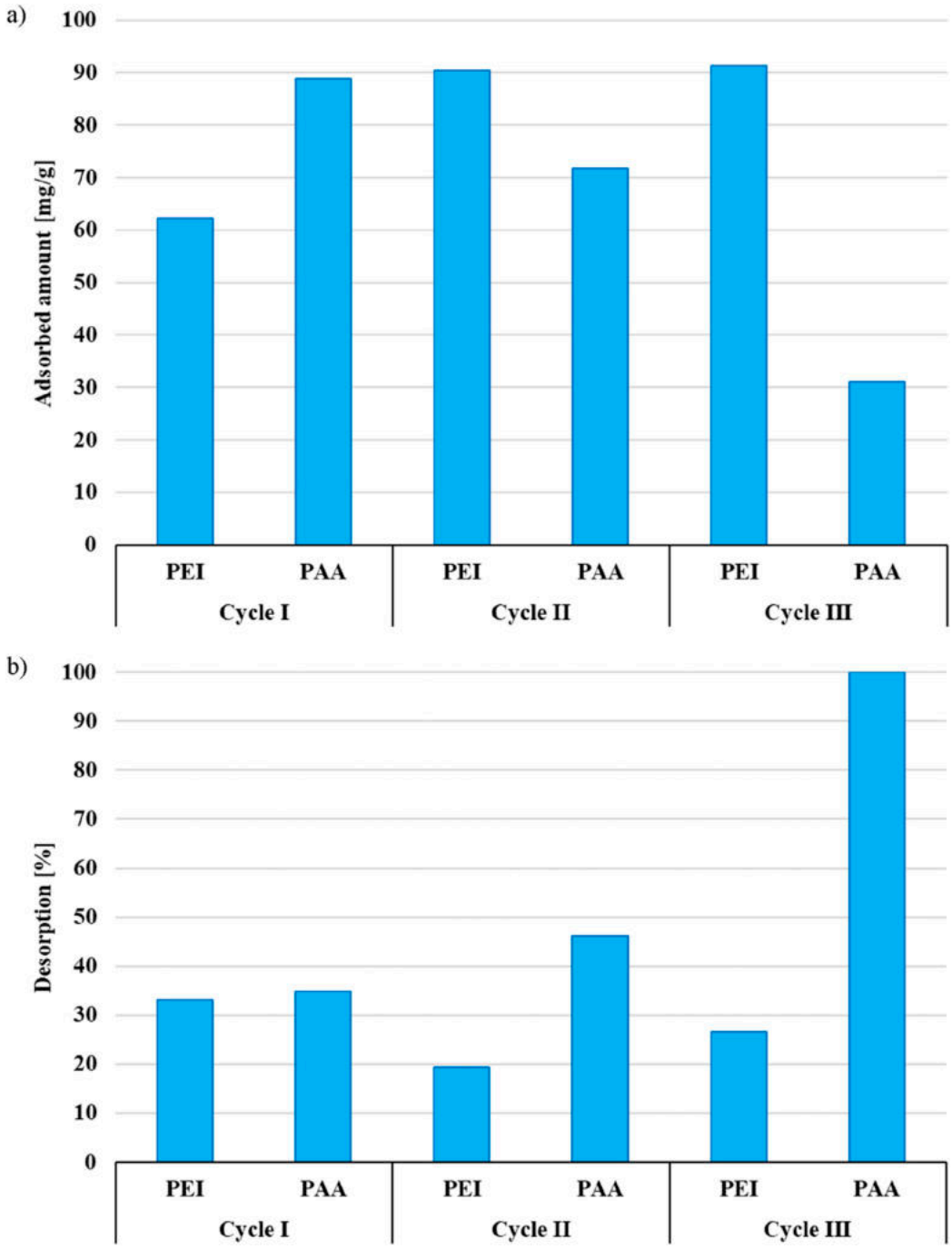

FIGURE 8
The adsorbed amount **(a)** and desorption efficiency **(b)** of polymers on/from the surface of NE_AP activated biocarbon in the adsorption-desorption cycles.

adsorption mechanism). Due to the presence of functional groups–carboxyl in the case of PAA, and amine in the case of PEI, hydrogen bonds can be formed between the polymeric chains and the functional groups present on the activated biocarbons surface (Wiśniewska et al., 2021).

According to the analysis of data presented in Figure 6, for most of the tested systems, activated biocarbon obtained from the nettle herb is a more effective adsorbent from both single and mixed adsorbate solutions. This confirms that the concentration of surface functional groups is of great importance for the adsorption capacity of carbonaceous material.

Poly(acrylic acid) and polyethyleneimine have a positive influence on their mutual adsorption (Santhiya et al., 1999). The adsorbed polymer chains can bind other macromolecules from the solution, forming multilayer adsorption structures (Gęca et al., 2024b). This effect is more noticeable in the case of PAA adsorption in the presence of PEI. Cationic polymer macromolecules are characterized by the larger linear dimensions at pH 3, which results in a greater number of

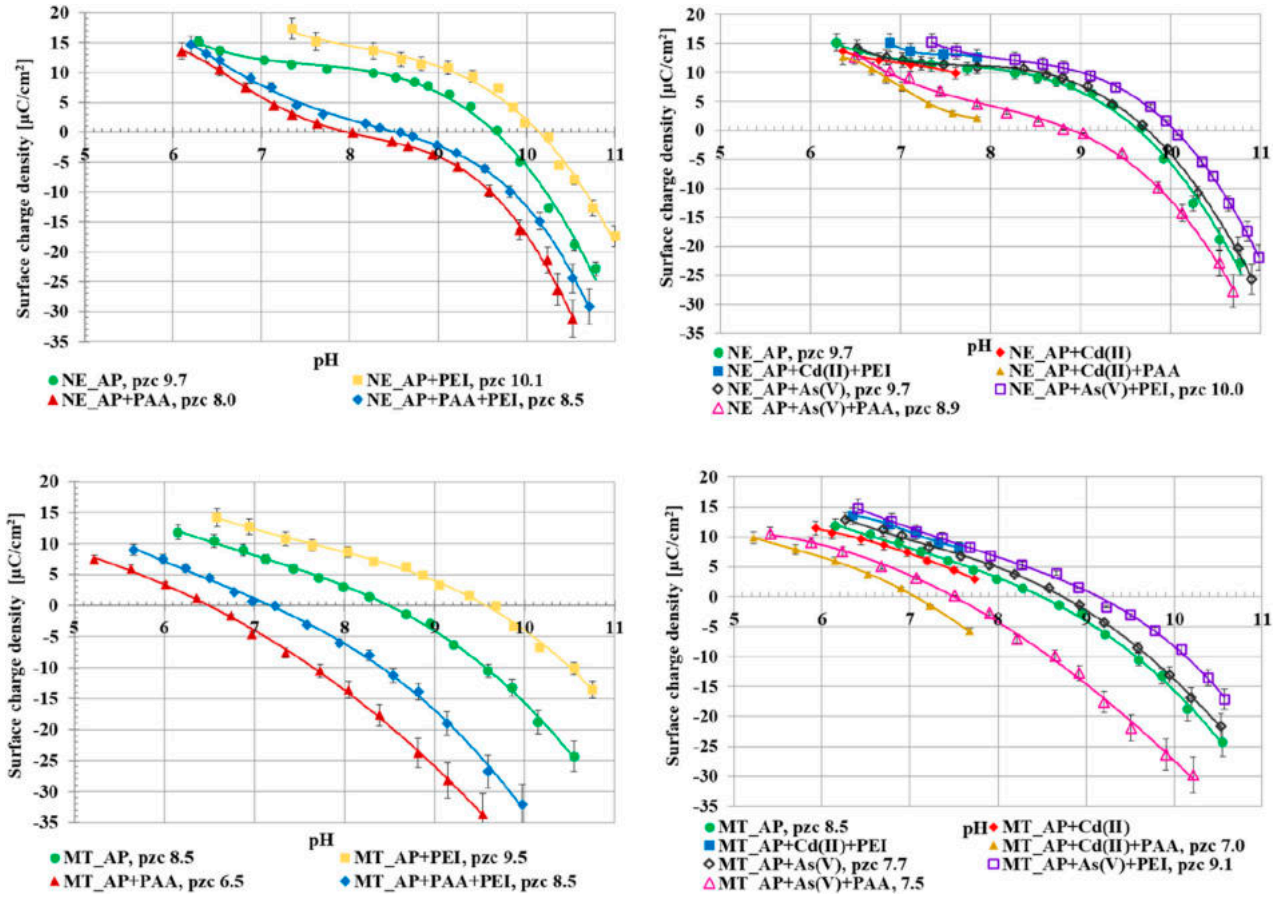

FIGURE 9
Surface charge density as a function of solution pH for NE_AP and MT_AP activated biocarbons particles dispersed in suspensions without as well as with single and binary adsorbates.

amine functional groups that can interact with carboxyl groups of PAA. In the opposite situation, the coiled chains of the anionic polymer have fewer available functional groups, resulting in a smaller increase in PEI adsorption.

In solutions containing both the cationic polymer PEI and Cd(II) ions, the adsorbed amounts of each component from the binary mixture are lower than in the corresponding single-component systems. This behaviour is characteristic of cadmium cations in multicomponent systems. In solutions containing Cd(II) together with Pb(II)/Zn(II), the amount of adsorbed cadmium ions is reduced by 40%–80% compared to a single-component Cd(II) systems (Lee and Shin, 2021; Wang et al., 2022; Li et al., 2023). Both substances with the same ionic character compete for active sites, which negatively impacts their simultaneous removal from the aqueous phase. In a binary solution of poly(acrylic acid) and cadmium(II) ions, polymer-metal complexes are created, which depending on the type of adsorbent can be adsorbed on the activated biocarbons surface or remain in the solution. However, PAA is generally adsorbed in greater amounts from the binary solution than the Cd(II) cations. The presence of As(V) anions causes a decrease in the amounts of both polymers adsorbed. Moreover, the presence of the macromolecular compounds completely inhibits the adsorption of inorganic anions. This phenomenon can be attributed to the formation of complexes between arsenic(V) ions and organic substances, which rather tend to remain in the solution than adsorb on the surface (Gęca et al., 2024c). Conversely, it has been shown that the presence of small amounts of inorganic compounds can increase the amount of As(V) adsorbed on the surface of chemically modified adsorbents. These findings emphasize the need for more detailed studies on the removal mechanisms operating in multicomponent systems (Wei et al., 2021; Zeng et al., 2024).

The desorption efficiency of the polymers is presented in Figure 7. Due to the impossibility of determining the concentration of polyethyleneimine in a solution with high ionic strength, in the case of this polymer only water was used for desorption tests. The most efficient desorption was observed in systems with As(V) ions, which can be related both to the small amount of adsorbed PEI and the weak binding of the polymer-metal complex to the adsorbent surface. The lowest desorption obtained in the NE_AP + PEI + PAA system indicates the strongest polyethyleneimine affinity to the surface of activated biocarbon derived from the nettle herb in the presence of poly(acrylic acid). In other systems the PEI desorption efficiency was about 50%.

In the case of PAA, H_2O was the least effective desorption agent. HNO_3 turned out the most effective substance in the single and PAA + PEI systems. In the presence of metal ions, NaOH allowed achieving the highest level of desorption. In general, the anionic

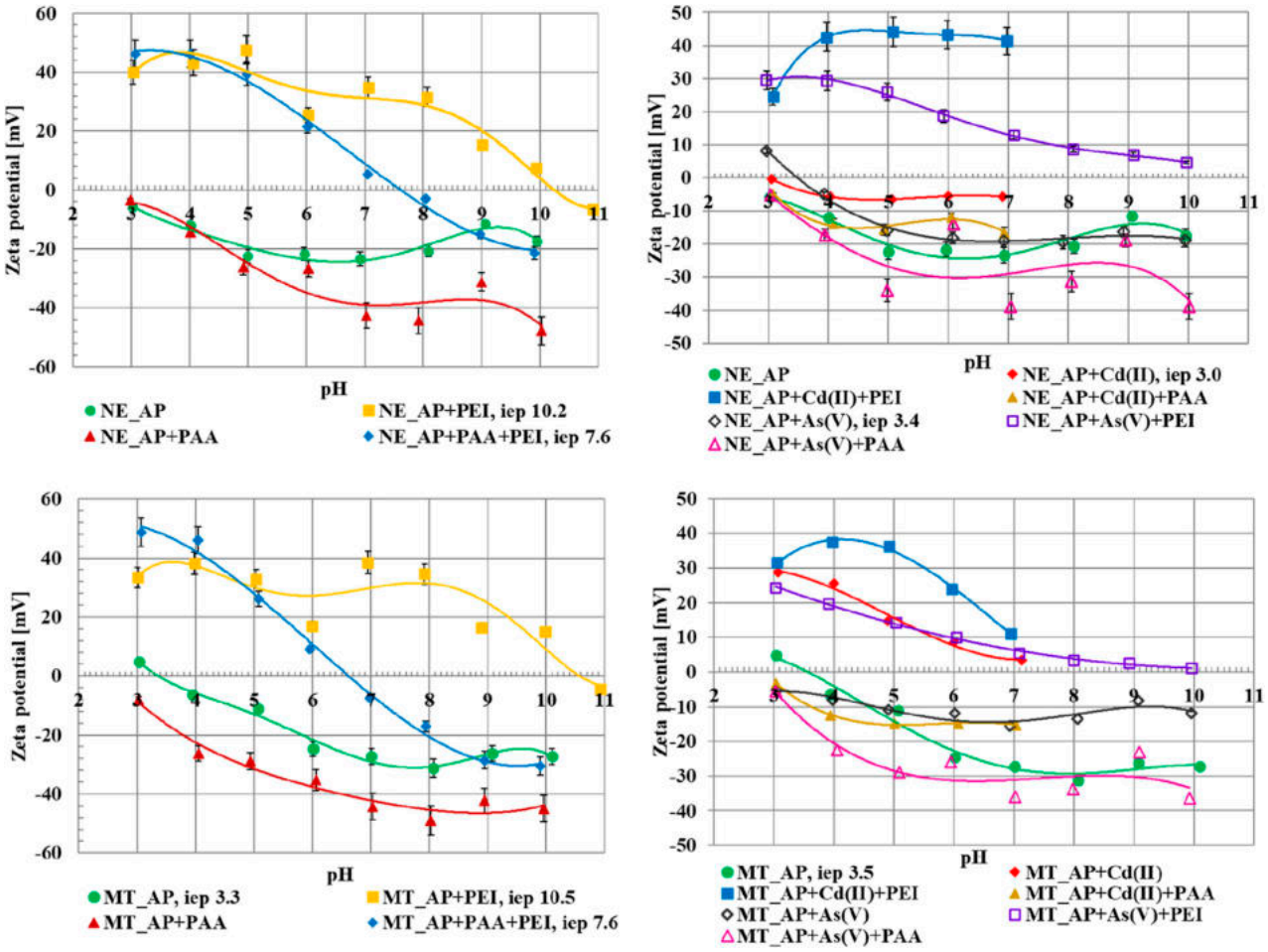

FIGURE 10
Zeta potential as a function of solution pH for NE_AP and MT_AP activated biocarbons particles dispersed in suspensions without as well as with single and binary adsorbates.

polymer is better desorbed from the surface of MT_AP activated biocarbon, which proved that more than twice lower concentration of the adsorbent functional groups is crucial for the PAA removal from the aqueous solution.

According to the data presented in Figure 8 the adsorbed amount of PEI increases with the increasing number of cycles. Due to the incomplete desorption (Figure 8b) of the cationic macromolecule and its perpendicular adsorption, the number of solid active sites increases. The permanently bonded PEI chains modify activated biocarbons' surface, increasing their adsorption capacity. On the other hand, the PAA adsorbed amount decreases in the subsequent cycles. It is related to the adsorption of coiled polymeric chains in the solid pores, which remain not desorbing, blocking these sites for other PAA macromolecules.

Electrokinetic properties and aggregation tendencies of aqueous suspensions of the carbonaceous materials

The dependencies of the surface charge density (σ_0) of the activated biocarbons, for the systems without as well as with single and binary adsorbates, as the function of solution pH are presented in Figure 9. Polyethyleneimine causes an increase in activated biocarbons surface charge density value, whereas the presence of poly(acrylic acid) decreases this parameter value. In both cases, it is related to the fact that not all segments of the adsorbed macromolecules are directly bound to the adsorbent active sites. The functional groups are also present in the loop and tail structures, located in the by-surface area, which increase or decrease the σ_0 parameter, according to the adsorbate chain charge (Wiśniewska and Nowicki, 2020). In the binary solution of two polymers, the intermediate value of the σ_0 is observed. However, the predominant impact of PAA is noticeable, due to its greater adsorption in the studied system.

In the solution containing As(V) ions, a slight increase in the surface charge density is observed. The adsorbing arsenic anions induce the creation of an additional number of surface groups with a positive charge. On the other hand, the adsorption of Cd(II) cations favours formation of additional number of negatively charged sites on the activated biocarbons surface, resulting in a decrease of surface charge density. It is a typical behaviour observed for small inorganic ions (Fijałkowska et al., 2019). In the systems of ionic polymers and heavy metal ions, the

TABLE 8 The size of aggregates formed by activated biocarbons particles in suspensions without as well as with single and binary adsorbates.

System	Aggregates size [nm]					
	NE_AP			MT_AP		
	pH 3	pH 6	pH 9	pH 3	pH 6	pH 9
Without adsorbates	2945	2411	1918	2040	2215	2229
PEI	3218	2115	2191	3137	2848	3809
PAA	2905	2177	2007	4290	2399	3016
Cd(II)	3829	11239	-	2401	8957	-
As(V)	10280	2580	4043	2572	3767	4275
PEI + PAA	475	348	421	729	737	694
PEI + Cd(II)	5287	2667	-	1979	2045	-
PAA + Cd(II)	2630	1215	-	3143	2750	-
PEI + As(V)	3180	3487	6101	3020	3571	4793
PAA + As(V)	2491	3017	4161	5029	2469	3873

effects accompanying macromolecules adsorption have a predominant impact on the σ_0 value, due to their large sizes and significantly greater adsorbed amounts.

The changes of zeta potential (ζ) of the activated biocarbons particles dispersed in the systems without as well as with single and binary adsorbates as the function of solution pH are shown in Figure 10. Polyethyleneimine adsorption causes an increase in zeta in zeta potential value, which can be explained by the presence of polymeric chains with the positively charged amine groups in the slipping plane area. Anionic polymer binding leads to a decrease in the ζ value as a result of the analogous mechanism (Gęca et al., 2022). The zeta potential in the suspension containing both polymers increases at low pH values, at which the dissociation of the PEI chain is the greatest. The higher the pH value is, the greater the dissociation of carboxyl groups present in the PAA molecules is, and the resultant lowering of electrokinetic potential value is noted.

In the presence of Cd(II) ions the zeta potential value increases. The change of the ζ value to less negative after divalent cations (Cd^{2+}) adsorption in comparison to monovalent supporting electrolyte ones (Na^{+}) is a common effect, described in the literature before (Yalçınkaya and Güler, 2006; Yukselen-Aksoy and Kaya, 2011). Due to the small adsorbed amount of the As(V) ions, their influence on the zeta potential value is not very noticeable. In the system containing Cd(II) ions and polymers, an intermediate effect to their single solutions is observed, whereas the simultaneous presence of polymers and arsenic(V) ions results in obtaining dependencies similar to those observed for single PAA or PEI systems.

The aggregate sizes of activated biocarbons suspensions without as well as with single and binary adsorbates are included in Table 8. In single adsorbate systems, the adsorbent aggregate sizes increase in comparison to the suspensions without additives. The adsorption layers of organic/inorganic substances can cause the attraction between activated biocarbons particles resulting in suspension destabilization. The small metal ions neutralize the activated biocarbons' surface charge which results in the coagulation of solid particles, whereas the polymeric chains in addition to the charge neutralization can also cause the bridging flocculation. Similar effects are observed in the binary systems containing As(V) ions, whereas the influence of Cd(II) ions in the presence of ionic polymers depends on the adsorbent type. On the other hand, the simultaneous presence of PEI and PAA has a stabilizing influence on the suspension. It can be explained by the interchain complexes creation which prevents the attraction between adsorbent particles (oppositely charged polymers neutralize each other's charge).

Conclusion

The plant-derived materials have been successfully used for the production of environmentally friendly carbonaceous adsorbents. The obtained activated biocarbons are characterized by moderately-developed surface area (368–666 m^2/g) and high concentration of the functional groups on their surface (2.19–4.89 mmol/g). The occurrence of a point of zero charge at high pH values (8.5–9.7) and predomination of basic functional groups on their surface proved that both materials show basic properties. The activated biocarbon derived from nettle herb residue shows the highest adsorption capacity for both polyethyleneimine and poly(acrylic acid). The maximum adsorbed amounts of the tested substances were 79.98 mg/g for PEI, 80.81 mg/g for PAA, 19.36 mg/g for Cd(II), and 4.00 mg/g for As(V).

The examined polymers and heavy metal ions have a small influence on the determination of their concentration in the mixed solution, however, it is easy to deal with this impact by the application of calibration curves obtained from the solution containing interferent. It was proved that polymers have a positive influence on their mutual adsorption, in turn, the simultaneous removal of ionic macromolecules and heavy metal ions results in a decrease in their adsorbed amounts. The examined activated biocarbons can be successfully regenerated through desorption. The most efficient system for PEI desorption was NE_AP + PEI + As(V)+H_2O and for PAA - NE_AP + PAA + HNO_3, in which polymer desorption reached 100%. Reuse of regenerated carbonaceous materials is also possible, as indicated by adsorption cycle studies.

Data availability statement

The raw data supporting the conclusions of this article will be made available by the authors, without undue reservation.

Author contributions

MG: Data curation, Formal Analysis, Investigation, Resources, Visualization, Writing – original draft, Writing – review and editing. MW: Conceptualization, Methodology, Supervision, Writing – original draft, Writing – review and editing. PN: Conceptualization, Data curation, Formal Analysis, Investigation,

Methodology, Software, Visualization, Writing – original draft, Writing – review and editing, Validation.

Funding

The author(s) declare that no financial support was received for the research and/or publication of this article.

Conflict of interest

The authors declare that the research was conducted in the absence of any commercial or financial relationships that could be construed as a potential conflict of interest.

Generative AI statement

The author(s) declare that no Generative AI was used in the creation of this manuscript.

Publisher's note

References

Alemdar, A., Öztekin, N., Güngör, N., Ece, Ö. I., and Erim, F. B. (2005). Effects of polyethyleneimine adsorption on the rheological properties of purified bentonite suspensions. *Colloids Surf. A* 252, 95–98. doi:10.1016/j.colsurfa.2004.10.009

Ali, I. (2012). New generation adsorbents for water treatment. *Chem. Rev.* 112, 5073–5091. doi:10.1021/cr300133d

Ali, I., and Gupta, V. K. (2006). Advances in water treatment by adsorption technology. *Nat. Protoc.* 1, 2661–2667. doi:10.1038/nprot.2006.370

Anwar, J., Shafique, U., Salman, M., Dar, A., and Anwar, S. (2010). Removal of Pb (II) and Cd (II) from water by adsorption on peels of banana. *Biores. Tech.* 101, 1752–1755. doi:10.1016/j.biortech.2009.10.021

Awad, A. M., Shaikh, S. M., Jalab, R., Gulied, M. H., Nasser, M. S., Benamor, A., et al. (2019). Adsorption of organic pollutants by natural and modified clays: a comprehensive review. *Sep. Purif. Technol.* 228, 115719. doi:10.1016/j.seppur.2019.115719

Bhatnagar, A., Sillanpää, M., and Witek-Krowiak, A. (2015). Agricultural waste peels as versatile biomass for water purification–A review. *Chem. Eng. J.* 270, 244–271. doi:10.1016/j.cej.2015.01.135

Boehm, H.-P., Diehl, E., Heck, W., and Sappok, R. (1964). Surface oxides of carbon. *Angew. Chem. Int. Ed. Engl.* 3 (10), 699–677. doi:10.1002/anie.196406691

Chibowski, S., Patkowski, J., and Grządka, E. (2009). Adsorption of polyethyleneimine and polymethacrylic acid onto synthesized hematite. *J. Colloid Interf. Sci.* 329 (1), 1–10. doi:10.1016/j.jcis.2008.09.075

Chibowski, S., Wiśniewska, M., Marczewski, A. W., and Pikus, S. (2003). Application of the SAXS method and viscometry for determination of the thickness of adsorbed polymer layers at the ZrO2 –polymer solution interface. *J. Colloid Interface Sci.* 267, 1–8. doi:10.1016/S0021-9797(03)00698-2

Crini, G., and Lichtfouse, E. (2019). Advantages and disadvantages of techniques used for wastewater treatment. *Environ. Chem. Lett.* 17, 145–155. doi:10.1007/s10311-018-0785-9

Crummett, W. B., and Hummel, R. A. (1963). The determination of traces of polyacrylamides in water. *J. Am. Water Work. Assoc.* 1 (55), 209–219. doi:10.1002/j.1551-8833.1963.tb01016.x

Das, T. K., and Bezbaruah, A. N. (2020). Comparative study of arsenic removal by iron-based nanomaterials: potential candidates for field applications. *Sci. Total Environ.* 764, 142914. doi:10.1016/j.scitotenv.2020.142914

Dias, J. M., Alvim-Ferraz, M. C., Almeida, M. F., Rivera-Utrilla, J., and Sánchez-Polo, M. (2007). Waste materials for activated carbon preparation and its use in aqueous-phase treatment: a review. *J. Environ. Manage.* 85 (4), 833–846. doi:10.1016/j.jenvman.2007.07.031

Đolić, M., Karanac, M., Radovanović, D., Umićević, A., Kapidžić, A., Veličković, Z., et al. (2021). Closing the loop: as (V) adsorption onto goethite impregnated coal-combustion fly ash as integral building materials. *J. Clean. Prod.* 303, 126924. doi:10.1016/j.jclepro.2021.126924

Farasati, M., Haghighi, S., and Boroun, S. (2016). Cd removal from aqueous solution using agricultural wastes. *Desalination Water Treat.* 57 (24), 11162–11172. doi:10.1080/19443994.2015.1043588

Fijałkowska, G., Wiśniewska, M., and Szewczuk-Karpisz, K. (2019). The structure of electrical double layer formed on the kaolinite surface in the mixed system of cationic polyacrylamide and lead (II) ions. *Physicochem. Probl. Min. Process.* 55. doi:10.5277/ppmp19044

Foo, K. Y., and Hameed, B. H. (2010). Insights into the modeling of adsorption isotherm systems. *Chem. Eng. J.* 156 (1), 2–10. doi:10.1016/j.cej.2009.09.013

Ganesamoorthy, R., Vadivel, V. K., Kumar, R., Kushwaha, O. S., and Mamane, H. (2021). Aerogels for water treatment: a review. *J. Clean. Prod.* 329, 129713. doi:10.1016/j.jclepro.2021.129713

Gęca, M., Wiśniewska, M., and Nowicki, P. (2024a). Investigation of ionic polymers stabilizing and flocculating properties in dispersed activated carbons systems. *Materials* 17, 693. doi:10.3390/ma17030693

Gęca, M., Wiśniewska, M., and Nowicki, P. (2024b). Preparation of biochars by conventional pyrolysis of herbal waste and their potential application for adsorption and energy purposes. *ChemPhysChem* 25, e202300507. doi:10.1002/cphc.202300507

Gęca, M., Wiśniewska, M., Nowicki, P., and Wójcik, G. (2024c). Arsenate and cadmium ions removal from multicomponent solutions of ionic polymers using mesoporous activated biocarbons. *J. Molec. Liq.* 407, 125270. doi:10.1016/j.molliq.2024.125270

Gęca, M., Wiśniewska, M., and Nowicki, P. (2022). Simultaneous removal of polymers with different ionic character from their mixed solutions using herb-based biochars and activated carbons. *Molecules* 27, 7557. doi:10.3390/molecules27217557

Groszek, M., Wójcik, G., Wiśniewska, M., and Nowicki, P. (2025). Application of environmentally friendly activated carbons derived from herbal industry waste for water purification: a study on the removal of selected organic and inorganic pollutants. *J. Water Process Eng.* 75, 107952. doi:10.1016/j.jwpe.2025.107952

He, J., Zheng, H., Ni, F., Shen, F., Xu, M., Tian, D., et al. (2023). Design and optimization of a novel Y-Fe-GO magnetic adsorbent for simultaneous removal of tetracycline and arsenic and adsorption mechanisms. *Chem. Eng. J.* 457, 141195. doi:10.1016/j.cej.2022.141195

Ioannidou, O., and Zabaniotou, A. (2007). Agricultural residues as precursors for activated carbon production - a review. *Renew. Sustain. Energy Rev.* 11, 1966–2005. doi:10.1016/j.rser.2006.03.013

Janusz, W. (1994). Electrical double layer in the system TiO_2 (anathase)/aqueous solution of NaCl. *Pol. J. Chem.* 68, 1871.

Kyzas, G. Z., and Kostoglou, M. (2014). Green adsorbents for wastewaters: a critical review. *Materials* 7, 333–364. doi:10.3390/ma7010333

Lee, H. S., and Shin, H. S. (2021). Competitive adsorption of heavy metals onto modified biochars: comparison of biochar properties and modification methods. *J. Env. Manag.* 299, 113651. doi:10.1016/j.jenvman.2021.113651

Li, Y., Liu, J., Wang, Y., Tang, X., Xu, J., and Liu, X. (2023). Contribution of components in natural soil to Cd and Pb competitive adsorption: semi-quantitative to quantitative analysis. *J. Haz. Mat.* 441, 129883. doi:10.1016/j.jhazmat.2022.129883

Liufu, S., Xiao, H., and Li, Y. (2005). Adsorption of poly (acrylic acid) onto the surface of titanium dioxide and the colloidal stability of aqueous suspension. *J. Colloid Interf. Sci.* 281, 155–163. doi:10.1016/j.jcis.2004.08.075

Meng, Z., Wu, J., Huang, S., Xin, L., and Zhao, Q. (2024). Competitive adsorption behaviors and mechanisms of Cd, Ni, and Cu by biochar when coexisting with microplastics under single, binary, and ternary systems. *Sci. Total Environ.* 913, 169524. doi:10.1016/j.scitotenv.2023.169524

Ohshima, H. (1994). A simple expression for Henry's function for the retardation effect in electrophoresis of spherical colloidal particles. *J. Colloid Interf. Sci.* 168, 269–271. doi:10.1006/jcis.1994.1419

Patkowski, J., Myśliwiec, D., and Chibowski, S. (2016). Validation of a new method for spectrophotometric determination of polyethylenimine. *Int. J. Polym. Anal. Charact.* 21, 486–494. doi:10.1080/1023666X.2016.1168651

Ruthiraan, M., Mubarak, N. M., Thines, R. K., Abdullah, E. C., Sahu, J. N., Jayakumar, N. S., et al. (2015). Comparative kinetic study of functionalized carbon nanotubes and magnetic biochar for removal of Cd^{2+} ions from wastewater. *Korean J. Chem. Eng.* 32, 446–457. doi:10.1007/s11814-014-0260-7

Santhiya, D., Subramanian, S., Natarajan, K. A., and Malghan, S. G. (1999). Surface chemical studies on the competitive adsorption of poly (acrylic acid) and poly (vinyl alcohol) onto alumina. *J. Colloid Interf. Sci.* 216 (1), 143–153. doi:10.1006/jcis.1999.6289

Schwarzenbach, R. P., Escher, B. I., Fenner, K., Hofstetter, T. B., Johnson, C. A., Von Gunten, U., et al. (2006). The challenge of micropollutants in aquatic systems. *Science* 313, 1072–1077. doi:10.1126/science.1127291

Shannon, M. A., Bohn, P. W., Elimelech, M., Georgiadis, J. G., Mariñas, B. J., and Mayes, A. M. (2008). Science and technology for water purification in the coming decades. *Nat* 452, 301–310. doi:10.1038/nature06599

Singh, N. B., Nagpal, G., Agrawal, S., and Rachna, (2018). Water purification by using adsorbents: a review. *Environ. Technol. Innov.* 11, 187–240. doi:10.1016/j.eti.2018.05.006

Skwarek, E., Janusz, W., and Sternik, D. (2014). Adsorption of citrate ions on hydroxyapatite synthetized by various methods. *J. Radioanal. Nucl. Chem.* 299, 2027–2036. doi:10.1007/s10967-013-2825-z

Soonmin, H., and Kabbashi, N. A. (2021). Review on activated carbon: synthesis, properties and applications. *Int. J. Eng. Trends Tech.* 69, 124–139. doi:10.14445/22315381/IJETT-V69I9P216

Szewczuk-Karpisz, K., Wiśniewska, M., Medykowska, M., Galaburda, M. V., Bogatyrov, V. M., Oranska, O. I., et al. (2021). Simultaneous adsorption of Cu(II) ions and poly(acrylic acid) on the hybrid carbon-mineral nanocomposites with metallic elements. *J. Hazard. Mat.* 412, 125138. doi:10.1016/j.jhazmat.2021.125138

Tan, W. T., Zhou, H., Tang, S. F., Zeng, P., Gu, J. F., and Liao, B. H. (2022). Enhancing Cd (II) adsorption on rice straw biochar by modification of iron and manganese oxides. *Environ. Pollut.* 300, 118899. doi:10.1016/j.envpol.2022.118899

Von Harpe, A., Petersen, H., Li, Y., and Kissel, T. (2000). Characterization of commercially available and synthesized polyethylenimines for gene delivery. *J. Control. Release* 69, 309–322. doi:10.1016/S0168-3659(00)00317-5

Wang, J., and Guo, X. (2020). Adsorption kinetic models: physical meanings, applications, and solving methods. *J. Hazard. Mat.* 390, 122156. doi:10.1016/j.jhazmat.2020.122156

Wang, Z., Geng, C., Bian, Y., Zhang, G., Zheng, C., and An, C. (2022). Effect of oxidative aging of biochar on relative distribution of competitive adsorption mechanism of Cd^{2+} and Pb^{2+}. *Sci. Rep.* 12, 11308. doi:10.1038/s41598-022-15494-y

Wei, J., Shen, B., Ye, G., Wen, X., Song, Y., Wang, J., et al. (2021). Selenium and arsenic removal from water using amine sorbent, competitive adsorption and regeneration. *Environ. Pollut.* 274, 115866. doi:10.1016/j.envpol.2020.115866

Wiśniewska, M., and Nowicki, P. (2020). Peat-based activated carbons as adsorbents for simultaneous separation of organic molecules from mixed solution of poly(acrylic acid) polymer and sodium dodecyl sulfate surfactant. *Colloids Surf. A* 585, 124179. doi:10.1016/j.colsurfa.2019.124179

Wiśniewska, M., Nowicki, P., Szewczuk-Karpisz, K., Gęca, M., Jędruchniewicz, K., and Oleszczuk, P. (2021). Simultaneous removal of toxic Pb(II) ions, poly(acrylic acid) and Triton X-100 from their mixed solution using engineered biochars obtained from horsetail herb precursor – impact of post-activation treatment. *Sep. Purif. Technol.* 276, 119297. doi:10.1016/j.seppur.2021.119297

Wu, Q., Gao, L., Huang, M., Mersal, G. A., Ibrahim, M. M., El-Bahy, Z. M., et al. (2022). Aminated lignin by ultrasonic method with enhanced arsenic (V) adsorption from polluted water. *Adv. Comp. Hybrid. Mater.* 5, 1044–1053. doi:10.1007/s42114-022-00492-5

Yahya, M. A., Al-Qodah, Z., and Ngah, C. Z. (2015). Agricultural bio-waste materials as potential sustainable precursors used for activated carbon production: a review. *Renew. Sustain. Energy Rev.* 46, 218–235. doi:10.1016/j.rser.2015.02.051

Yalçınkaya, E. E., and Güler, C. (2006). The effects of electrolyte concentration, ion species and pH on the zeta potential and electrokinetic charge density of montmorillonite. *Clay Min.* 41, 853–861. doi:10.1180/0009855064140224

Yang, K., Peng, J., Srinivasakannan, C., Zhang, L., Xia, H., and Duan, X. (2010). Preparation of high surface area activated carbon from coconut shells using microwave heating. *Bioresour. Technol.* 101, 6163–6169. doi:10.1016/j.biortech.2010.03.001

Yin, G., Chen, X., Sarkar, B., Bolan, N. S., Wei, T., Zhou, H., et al. (2023). Co-adsorption mechanisms of Cd (II) and as (III) by an Fe-Mn binary oxide biochar in aqueous solution. *Chem. Eng. J.* 466, 143199. doi:10.1016/j.cej.2023.143199

Yukselen-Aksoy, Y. E. L. İ. Z., and Kaya, A. J. E. E. S. (2011). A study of factors affecting on the zeta potential of kaolinite and quartz powder. *Environ. Earth Sci.* 62, 697–705. doi:10.1007/s12665-010-0556-9

Zeng, G., Si, M., Dong, C., Liao, Q., He, F., Johnson, V. E., et al. (2024). Adsorption behavior of lead, cadmium, and arsenic on manganese-modified biochar: competition and promotion. *Environ. Geochem. Health* 46, 86. doi:10.1007/s10653-024-01865-z

Zhou, Y., Zhang, L., and Cheng, Z. (2015). Removal of organic pollutants from aqueous solution using agricultural wastes: a review. *J. Molec. Liq.* 212, 739–762. doi:10.1016/j.molliq.2015.10.023

Lublin, 10.09.2025

mgr Marlena Groszek
Uniwersytet Marii Curie-Skłodowskiej w Lublinie,
Wydział Chemii, Instytut Nauk Chemicznych,
Katedra Radiochemii i Chemii Środowiskowej,
Pl. Marii Curie-Skłodowskiej 3, 20-031 Lublin
marlena.groszek@mail.umcs.pl

Rada Naukowa Instytutu Nauk Chemicznych
Uniwersytetu Marii Cure-Skłodowskiej
w Lublinie

Oświadczenie o współautorstwie

Niniejszym oświadczam, że mój udział w pracy **M. Groszek**, M. Wiśniewska, P. Nowicki, *Simultaneous determination of ionic polymers and heavy metal ions concentrations in aqueous solution after their adsorptive removal using eco-friendly activated biocarbons*, Frontiers in Chemistry, 2025, 13, 1621297, DOI: 10.3389/fchem.2025.1621297 [D5], obejmował przeprowadzenie eksperymentów, zestawienie i analizę uzyskanych wyników, przygotowanie manuskryptu i jego korektę po procesie oceny w redakcji oraz sformułowanie odpowiedzi na uwagi recenzentów.

Marlena Groszek

Lublin, 10.09.2025

prof. dr hab. Małgorzata Wiśniewska
Uniwersytet Marii Curie-Skłodowskiej w Lublinie,
Wydział Chemii, Instytut Nauk Chemicznych,
Katedra Radiochemii i Chemii Środowiskowej,
Pl. Marii Curie-Skłodowskiej 3, 20-031 Lublin
malgorzata.wisniewska@mail.umcs.pl

Rada Naukowa Instytutu Nauk Chemicznych
Uniwersytetu Marii Cure-Skłodowskiej
w Lublinie

Oświadczenie o współautorstwie

Niniejszym oświadczam, że mój udział w pracy: M. Groszek, **M. Wiśniewska**, P. Nowicki, *Simultaneous determination of ionic polymers and heavy metal ions concentrations in aqueous solution after their adsorptive removal using eco-friendly activated biocarbons*, Frontiers in Chemistry, 2025, 13, 1621297, DOI: 10.3389/fchem.2025.1621297 [D5], obejmował stworzenie koncepcji pracy, opracowanie metodyki badań, korektę manuskryptu - przed i po procesie recenzji oraz nadzór merytoryczny w czasie całego cyklu wydawniczego.

Małgorzata Wiśniewska

Poznań, 10.09.2025

dr hab. Piotr Nowicki, prof. UAM
Uniwersytet im. Adama Mickiewicza w Poznaniu,
Wydział Chemii, Zakład Chemii Stosowanej,
Ul. Uniwersytetu Poznańskiego 8, 61-614 Poznań
piotr.nowicki@amu.edu.pl

Rada Naukowa Instytutu Nauk Chemicznych
Uniwersytetu Marii Cure-Skłodowskiej
w Lublinie

Oświadczenie o współautorstwie

Niniejszym oświadczam, że mój udział w pracy: M. Groszek, M. Wiśniewska, **P. Nowicki,** *Simultaneous determination of ionic polymers and heavy metal ions concentrations in aqueous solution after their adsorptive removal using eco-friendly activated biocarbons*, Frontiers in Chemistry, 2025, 13, 1621297, DOI: 10.3389/fchem.2025.1621297 [D5], obejmował tworzenie koncepcji pracy, przeprowadzenie eksperymentów, analizę uzyskanych wyników, korektę manuskryptu - przed i po procesie recenzji oraz sformułowanie odpowiedzi na uwagi recenzentów.

Piotr Nowicki

D6. M. Gęca, M. Wiśniewska, P. Nowicki, *Simultaneous removal of polymers with different ionic character from their mixed solutions using herb-based biochars and activated carbons,* Molecules, 27, 2022, 7557, DOI: 10.3390/molecules27217557

molecules

MDPI

Article

Simultaneous Removal of Polymers with Different Ionic Character from Their Mixed Solutions Using Herb-Based Biochars and Activated Carbons

Marlena Gęca [1], Małgorzata Wiśniewska [1,*] and Piotr Nowicki [2]

[1] Department of Radiochemistry and Environmental Chemistry, Faculty of Chemistry, Institute of Chemical Sciences, Maria Curie- Sklodowska University in Lublin, M. Curie-Sklodowska Sq. 3, 20-031 Lublin, Poland
[2] Department of Applied Chemistry, Faculty of Chemistry, Adam Mickiewicz University in Poznań, Uniwersytetu Poznańskiego 8, 61-614 Poznań, Poland
* Correspondence: malgorzata.wisniewska@mail.umcs.pl

Abstract: Nettle and the sage herbs were used to obtain carbonaceous adsorbents. For the biochar preparation the precursors were dried and subjected to conventional pyrolysis. Activated carbons were obtained during precursor impregnation with phosphoric(V) acid and multistep pyrolysis. The textural parameters and acidic-basic properties of the obtained adsorbents were studied. The activated carbons prepared from the above herbs were characterized by the largely developed specific surface area. The obtained carbonaceous adsorbents were used for polymer removal from aqueous solution. Poly(acrylic acid) (PAA) and polyethylenimine (PEI) were chosen, due to their frequent presence in wastewater resulting from their extensive usage in many industrial fields. The influence of polymers on the electrokinetic properties of activated carbon were considered. PAA adsorption caused a decrease in the zeta potential and the surface charge density, whereas PEI increased these values. The activated carbons and biochars were used as polymer adsorbents from their single and binary solutions. Both polymers showed the greatest adsorption at pH 3. Poly (acrylic acid) had no significant effect on the polyethylenimine adsorbed amount, whereas PEI presence decreased the amount of PAA adsorption. Both polymers could be successfully desorbed from the activated carbons and biochar surfaces. The presented studies are innovatory and greatly required for the development of new environment protection procedures.

Keywords: activated carbon; biochar; simultaneous polymers adsorption; poly(acrylic acid); polyethylenimine; organic substances removal

Citation: Gęca, M.; Wiśniewska, M.; Nowicki, P. Simultaneous Removal of Polymers with Different Ionic Character from Their Mixed Solutions Using Herb-Based Biochars and Activated Carbons. *Molecules* **2022**, *27*, 7557. https://doi.org/10.3390/molecules27217557

Academic Editor: Oualid Hamdaoui

Received: 13 October 2022
Accepted: 31 October 2022
Published: 4 November 2022

1. Introduction

Limited reserves of natural resources are one of the most important problems facing present and future generations. Therefore, it is necessary to find new, nontoxic and renewable resources. Various types of green plants, capable of rebuilding the harvested parts of shoots, could be the solution to this global problem. Annual plants, such as herbs, grow and decompose through the year so their harvesting has no negative influence on the natural environment. The judicious use of raw plant materials would enable them to be an inexhaustible resource for different fields of industry [1].

Biochar and activated carbons prepared from plant material are environmentally friendly solids with largely developed surface areas and extensive porous structures. They are relatively easy to obtain, low-cost and regenerable adsorbents. Biochar and activated carbons are often used as heavy metal adsorbents [2–4]. Organic compound adsorption on the surface of these solids has been extensively studied [5,6]. However, the most common research has been concerned with the removal of dyes and pharmaceuticals from the liquid phase [7].

The usage of different kinds of polymers in modern industry and everyday life is constantly expanding. Poly(acrylic acid) (PAA) is used as a suspension stabilizer or destabilizer, as well as a dispersant agent in cosmetics and drugs [8–10]. In turn, polyethylenimine (PEI) finds application as the additive for papermaking and cell line cultures [9,11]. Both of the above polymers find application as a complexing agent for the removal of heavy metal ions from water [12]. The increasing demand for polymers has increased their amounts in sewage. Despite their wide usage, these macromolecular compounds can be dangerous for the environment. Their presence can disturb the natural balance and have negative effects on all living organisms. One of the ways to prevent polymeric pollution is their adsorption on activated carbons and biochars. Polymers adsorption on the surface of carbonaceous adsorbents has rarely been described. However, recent scientific reports have proved that the application of activated carbons or biochar for the removal of polymeric substances is not only possible, but also effective [13,14].

In the present study biochar and activated carbons, obtained from nettle and sage herbs, were used as poly (acrylic acid) and polyethylenimine adsorbents from their single and binary solutions. The textural parameters and acidic–basic properties of the obtained materials were determined. The influence of the presence of poly (acrylic acid) and polyethylenimine in the system on surface and electrokinetic properties (connected with the structure of the electrical double layer) of carbon sorbents was also studied. The effect of solution pH on the adsorption process was evaluated and its mechanism proposed. Additionally, the regeneration possibilities of the applied materials were examined and the most effective desorbing agents were selected. As mentioned above, there has been little research on the usage of biochars or activated carbons as macromolecular substance adsorbents. The presented results are even more innovative because the simultaneous removal of two polymers with different ionic characters using biochar or activated carbons has not been described before. The description of the structure of the mixed polymeric layer enables understanding of the mechanisms governing the binding of macromolecules at the interface, and, thus, of the optimization of procedures for their removal from the liquid phase during wastewater treatment.

2. Results

2.1. Physicochemical Properties of the Prepared Adsorbents

Table 1 shows the elemental composition of the obtained adsorbents. All solids contain mainly carbon (78–90 wt. %); however, the products of chemical activation with H_3PO_4 contain significantly more of this element. The obtained materials also differed, quite significantly, with regard to nitrogen content. For pyrolysis products, the content of N^{daf} (^{daf}—dry-ash free basis) ranged from 2.77 to 1.78 wt. %, while in the analogous activated carbons it was clearly lower and reached 1.13 wt. % for the NE_AC sample obtained from the nettle herb and 0.24% for the SA_AC biochar obtained from the sage herb. Mg, Ca and K were present only in the biochar structure, and the activated carbons did not contain these elements, which were probably removed during the activation process. As indicated by the SEM pictures presented in Figure 1, the obtained carbonaceous materials also exhibited some differences in morphology.

Table 1. Elemental composition of the obtained adsorbents [wt. %].

Adsorbent	C	O	N	P	Ca	Mg	K	Others
NE_AC	90.62	7.66	1.13	0.59	-	-	-	-
SA_AC	89.61	8.81	0.24	0.63	-	-	-	0.71
NE_B	78.76	16.35	2.77	0.14	1.23	0.27	0.30	0.18
SA_B	81.31	15.50	1.78	0.20	0.47	0.38	0.15	0.21

However, much greater differentiation was observed in the case of textural parameters. As follows from the data collected in Table 2, both activated carbons had a largely

developed surface area of over 800 m^2/g; however, the product derived from the sage herb fared better in this regard. Both biochars surface areas were slightly over 2 m^2/g, which proved that the activation process had a much greater influence on the porous structure formation of the absorbents. Activated carbon pore volumes were also much greater than those obtained for the biochars. The mean pore size was about 4 nm for the activated carbons and about 10 nm for the biochar, which allowed classification of all adsorbents as mesoporous materials. Larger pore sizes are desirable for the adsorption of large polymer macromolecules. The yields of the pyrolysis and activation processes were below 50% and higher for the adsorbents obtained from the sage herb. The total amount of the surface functional group (Table 3) was greater for the biochars in comparison to the activated carbons. The NE_B biochar was characterized by a significantly greater amount of basic surface groups than the acidic ones, whereas the SA_B sample contained comparable contents of both types of functional groups. In turn, the activation products (especially the NE_AC sample) were characterized by a significant predominance of acidic groups on their surfaces. What is more, a larger total amount of surface functional groups was observed in the case of the solids obtained from the nettle herb.

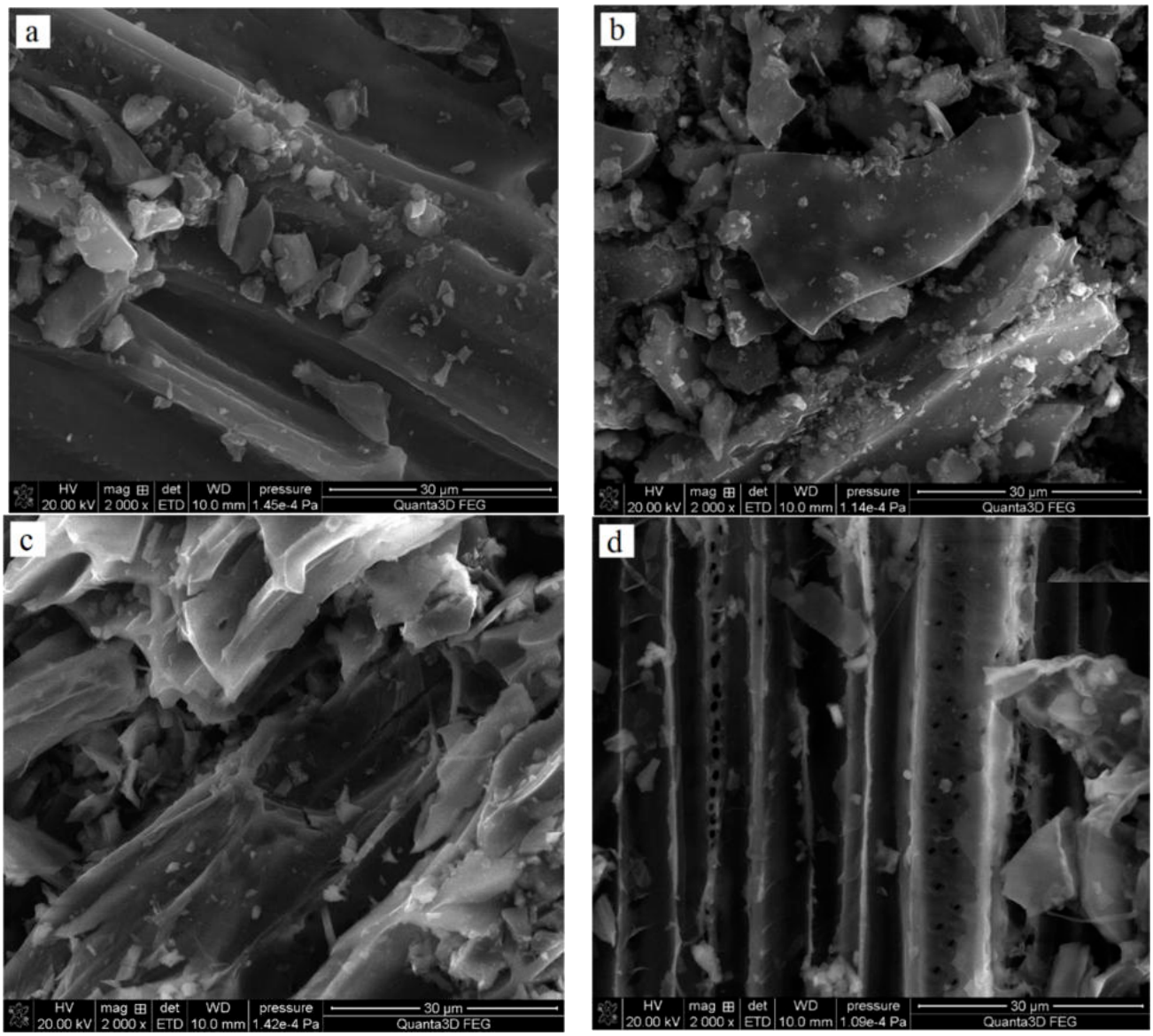

Figure 1. SEM images of NE_AC (**a**) and SA_AC (**b**) activated carbons and NE_B biochar (**c**) and SA_B (**d**) biochar.

Table 2. Textural parameters of the prepared activated carbons and biochars.

Adsorbent	Pyrolysis/ Activation Yield [wt. %]	Surface Area [m^2/g]		Pore Volume [cm^3/g]		Mean Pore Size [nm]	Micropore Contribution
		Total	Micropore	Total	Micropore		
NE_AC	37.7	801	157	0.847	0.074	4.231	0.087
SA_AC	40.3	842	155	0.826	0.074	3.926	0.090
NE_B	42.9	2.5	-	0.006	-	9.594	-
SA_B	45.8	2.1	-	0.006	-	10.555	-

Table 3. Acidic-basic properties of the prepared biochars and activated carbons.

Adsorbent	Acidic Groups [mmol/g]	Basic Groups [mmol/g]	Total Amount [mmol/g]
NE_AC	0.858	0.272	1.130
SA_AC	0.436	0.215	0.651
NE_B	1.041	1.753	2.794
SA_B	1.109	1.008	2.197

2.2. Adsorbents Electrokinetic Characteristic

The studies on the activated carbon surface charge densities confirmed the acidic properties of both adsorbents. The point of zero charge (pzc) is a pH value at which the concentration of positively charged surface groups is the same as the concentration of negatively charged ones, so the total surface charge is equal to zero. The pzc of the NE_AC activated carbon occurred at pH 3.1 and in the case of SA_AC at pH 4.0 (Figure 2). The poly (acrylic acid) addition caused a slight decrease of the σ_0 value in the whole range of studied pH in comparison to the system without the polymer. This was caused by the presence of negatively charged carboxyl groups of the adsorbed PAA macromolecules in the by-surface layer of the solution. This effect has been previously described [15,16]. On the other hand, the polyethylenimine presence in the solution caused increase in the surface charge density. This resulted from the presence of the cationic amino groups of adsorbed PEI macromolecules in the by-surface layer of the solution, which were not directly bound with the solid surface, similar to PAA interfacial behavior [17]. In the case of the positively charged PEI chains, its conformation on the negatively charged surface (above pH_{pzc}, namely 3-4) was flatter (in comparison to the negatively charged PAA chains), which assured a large accumulation of positive charges in the surface layer.

The pH_{pzc} value for the NE_AC activated carbon in the presence of both polymers was 4.0, and for the SA_AC, 4.1. This was an intermediate effect compared to the single polymer systems. Positively charged polyethyleneimine and negatively charged poly (acrylic acid) were both adsorbed onto the activated carbons at the same time, which caused the pH_{pzc} value in the binary solution to be between the pH_{pzc} value of the single PEI solution and the single PAA solution.

Both applied biochars were characterized by basic properties of the surface. The NE_B biochar pH_{pzc} occurred at 7.3 and for the SA_B sample at 8.6. The difference in the acid/base properties of the biochars and activated carbons was evidently associated with the use of H_3PO_4 as the activating agent.

The zeta potential studies showed that the isoelectric point (iep) occurred at pH 4.9 for the NE_AC activated carbon and at pH 6.2 for the SA_AC one. The pH_{iep} value for the NE_B biochar occurred at 6.1 and for the SA_B one at 5.2 (Figure 3). The isoelectric point is a pH value at which the number of adsorbate ions/functional groups with positive and negative charges, accumulated in the slipping plane area, are the same (the zeta potential has a zero value). For all materials there was a difference between the pH_{pzc} and pH_{iep} values. The activated carbons isoelectric point occurred at higher pH values than the point of zero charge of these adsorbents and for the biochar the pH_{pzc} value was higher than pH_{iep}. This was related to the partial overlapping of the electrical double layers (edl) that formed on the pore walls, the effects of which on mesoporous materials have been previously described in the literature [14,18]. The poly (acrylic acid) presence in the suspension caused a decrease

in the zeta potential value. The opposite tendency was observed after the addition of polyethyleneimine. This could be explained by the presence of the ionic polymer groups (negatively charged in the case of PAA and positively charged for PEI) in the slipping plane area [19]. The zeta potential value in the suspension containing both polymers increased in comparison to the suspension without any adsorbates, which could have been caused by a few different factors, e.g., the presence of molecules with the opposite charge as well as the shift of the slip plane [20]. The negatively charged PAA macromolecules were repulsed from the negatively charged activated carbon surfaces at higher pH values which caused shift of the slipping plane by the polymeric chains adsorbed perpendicularly to the solid surface and the pH_{iep} value decreased. In turn, the presence of the positively charged PEI molecule (which was adsorbed flatter) in the slipping plane area caused the pH_{iep} value to increase. Generally speaking, the simultaneous presence of both polymers on the adsorbent surface had an intermediate effect, in comparison to the single polymer systems.

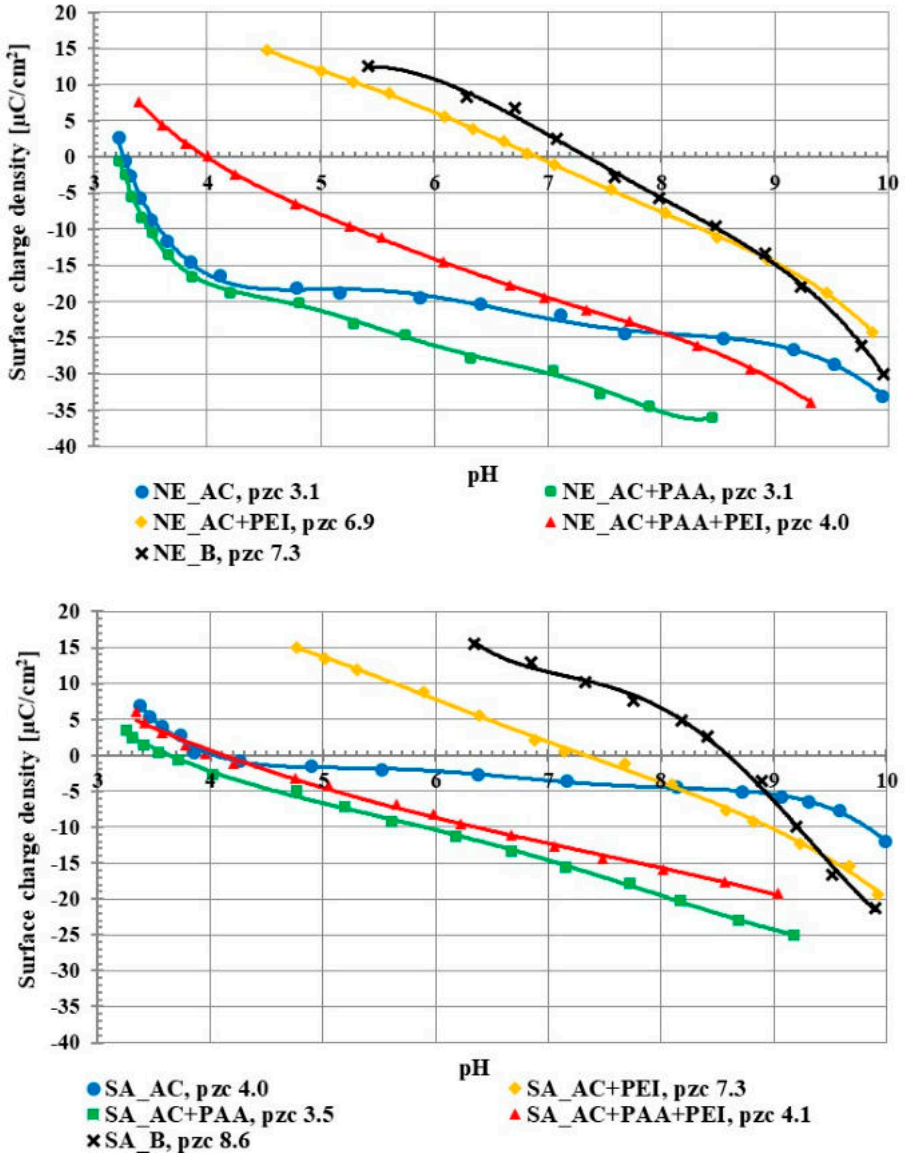

Figure 2. Surface charge density of NE_AC activated carbon and NE_B biochar (**a**), SA_AC activated carbon and SA_B biochar (**b**) in the systems without and with the single and binary adsorbates (C_0 100 ppm).

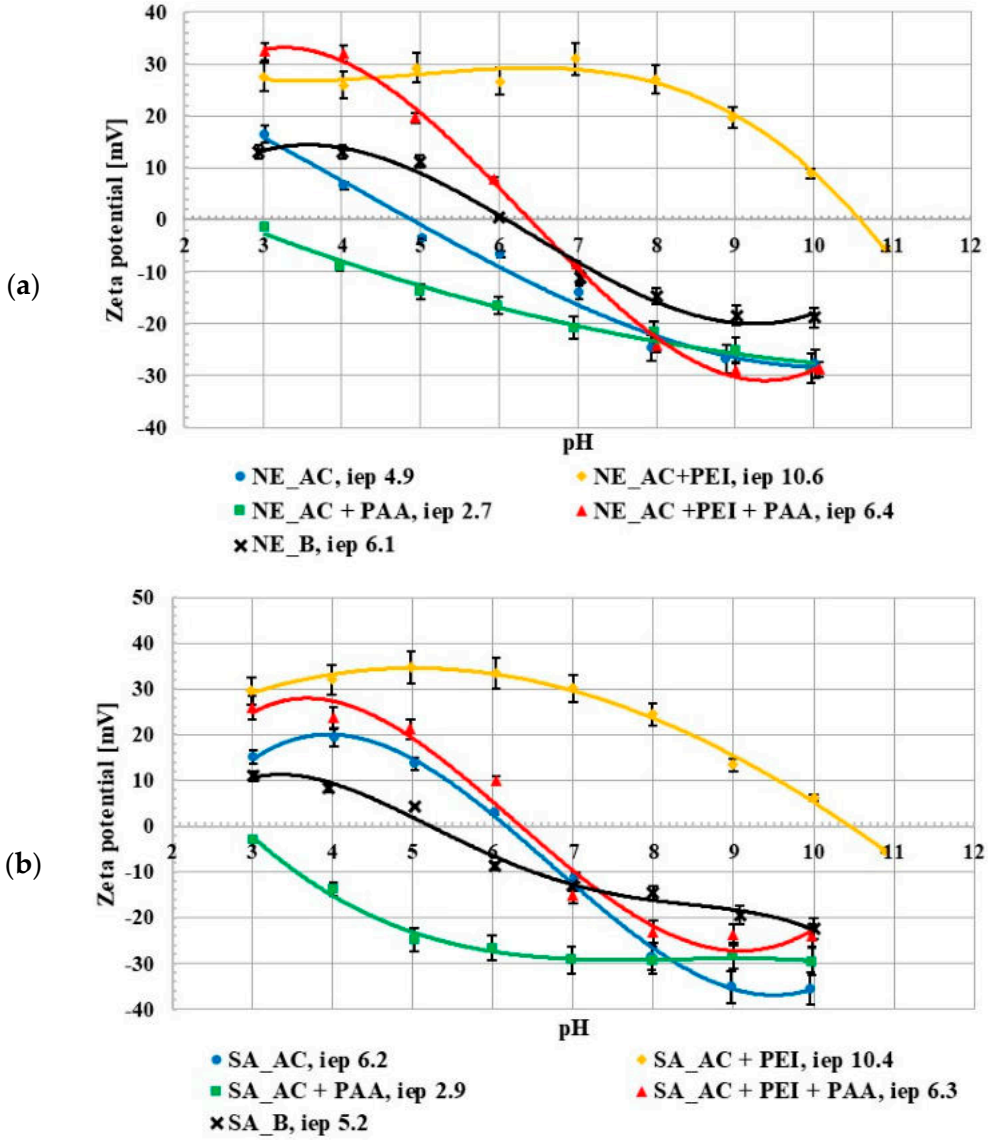

Figure 3. Zeta potential of NE_AC activated carbon and NE_B biochar (**a**), SA_AC activated carbon and SA_B biochar (**b**) particles in the system without and with the single and binary adsorbates (C_0 100 ppm).

Table 4 presents the activated carbons and biochar aggregates sizes. The obtained data proved that the presence of the polymers (in particular PAA) had a very small effect on the NE_AC activated carbon aggregate size at pH 3. The aggregate sizes in the single adsorbate systems were also similar to the system without any adsorbate at pH 6 and 9. However, both polymers being present in the solution could form polymer–polymer complexes at higher pH values, which resulted in the larger size of NE_AC activated carbon aggregates in the binary solution at pH 6 and 9. The presence of poly (acrylic acid) considerably affected the SA_AC activated carbon aggregate size at pH 3 and 9. On the other hand, at pH 6 the polyethylenimine caused increase in size of the aggregates formed by the activated carbon obtained from the sage herb. Both polymers present in the solution had the greatest effect on aggregate size at pH 6, due to the polymer–polymer complex formations. In general, sizes of aggregates formed by both biochar were considerably larger than those formed by the analogous activated carbons.

Table 4. Aggregates sizes of activated carbons and biochars in the system without the polymers as well as in the single and binary adsorbates.

System	Size of Aggregates [nm]		
	pH 3	**pH 6**	**pH 9**
NE_AC	509.5	478.2	448.5
NE_AC + PAA	499.2	405.4	433.7
NE_AC + PEI	459.1	516.4	519.3
NE_AC + PAA + PEI	599.9	1099.7	741.9
SA_AC	327.8	430.9	517.4
SA_AC + PAA	701.0	441.4	4002.0
SA_AC + PEI	475.0	842.1	370.9
SA_AC + PAA + PEI	204.0	874.6	289.2
NE_B	1257.0	731.2	1448.0
SA_B	688.2	1799	1494.0

2.3. Adsorption–Desorption Studies

Figure 4 shows the adsorption isotherms of poly (acrylic acid) and polyethylenimine at pH 3, 6 and 9. Both activated carbons were characterized by the acidic character of the surface so at low pH values they were negatively charged, which favored electrostatic adsorption of the cationic PEI, and, in a way, limited the anionic PAA adsorption. Nevertheless, in the examined system the adsorbed amounts of PAA were larger than those of PEI. The poly (acrylic acid) adsorption was mostly caused by the chemical interactions and hydrogen bond creation. The greater PAA adsorbed amounts were mostly caused by its coiled conformation at pH 3, in contrast to the developed PEI conformation.

The obtained results proved that the greatest PAA adsorbed amount occurred at pH 3. This was directly related to its conformation, at pH 3 pol y(acrylic acid) assumed the most coiled conformation due to minimal dissociation of its functional groups. For this reason, the adsorption of PAA coils in the pores was also possible under such pH conditions. As a result, the PAA adsorbed amount was the greatest at pH 3 (dense packing of adsorption layers).

At pH 6 and 9 PAA chains developed, which limited the polymer adsorption in the porous structure of the adsorbent. The PAA adsorption on the negatively charged activated carbon surfaces was possible due to hydrogen bond formations [21].

The pH value had a smaller effect on the polyethyleneimine adsorption. This was related to the high value of PEI pK_b, which was over 9, so at all studied pH values polyethyleneimine assumed the developed conformation. Similar to PAA, polyethyleneimine showed minimally greater affinity for the solid surface at pH 3. In such a case, its adsorption was mostly caused by favorable electrostatic interactions [22]. At pH 3 polyethyleneimine was completely dissociated (it had a positive charge) and the acidic activated carbons were negatively charged at this pH value. Thus, the adsorbent surface attracted the polymer molecules.

In general, polymers were adsorbed in greater amounts on the NE_AC activated carbon in relation to the SA_AC one. This could have been caused by a greater amount of functional group present on the NE_AC surface in comparison to SA_AC. The sample obtained from the nettle herb contained almost twice as many functional groups as the material prepared from the sage herb.

The maximum amount adsorbed on the NE_AC surface at pH 3 was 273 mg/g for PAA and 156 mg/g for PEI. The poly (acrylic acid) adsorbed amount on the NE_AC activated carbon was greater than on the activated carbon obtained from cherry stones, 25 mg/g, in [23], and on the biocarbon obtained from peanut shells, 50 mg/g, as well as on the carbon adsorbent prepared from corncobs, 80 mg/g, in [24].

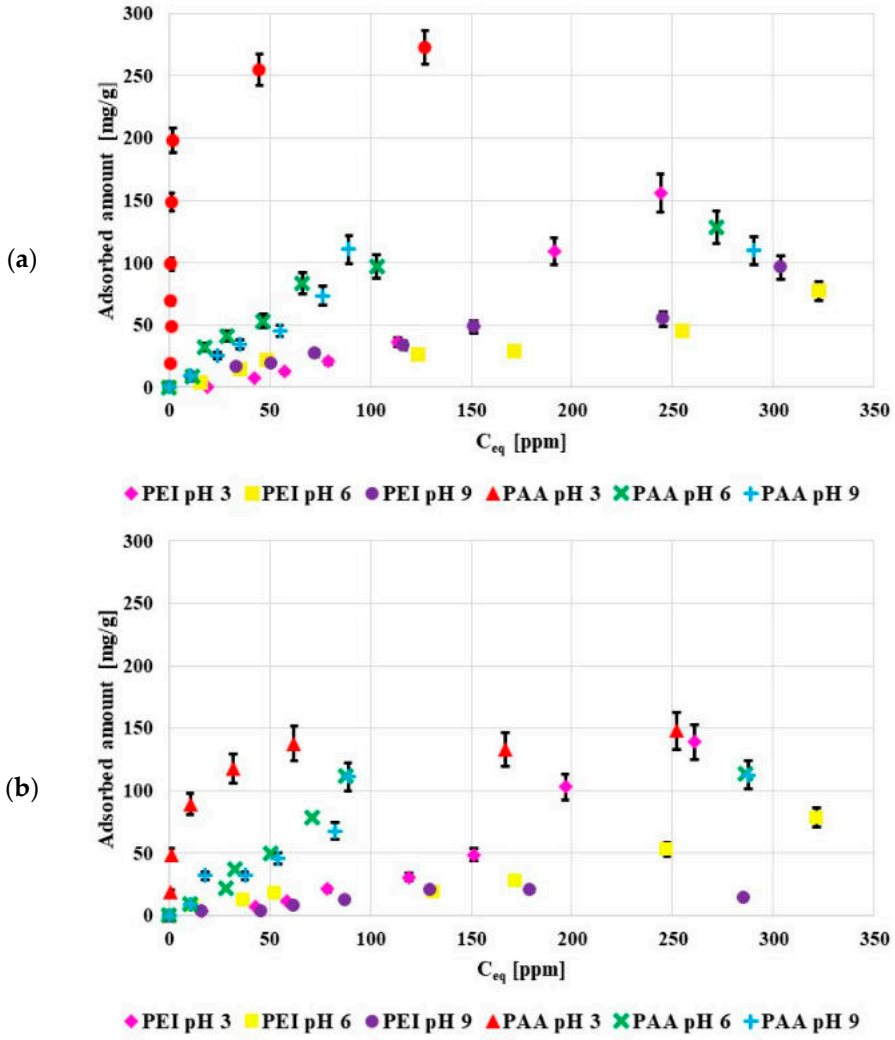

Figure 4. Poly(acrylic acid) and polyethyleneimine adsorption isotherms on the surface of NE_AC (**a**) and SA_AC (**b**) activated carbons (C_0 100 ppm).

The kinetic data showed that the equilibrium state was reached after 60 min in the solution containing poly (acrylic acid) and after 10min in the solution containing polyethylenimine (Figure 5). The shorter time in the solution containing PEI was probably caused by a smaller adsorption amount in comparison to the solution containing PAA. The obtained results of kinetic measurements were fitted to the pseudo first- and pseudo second-order equations (Table 5). The data obtained for both polymers were better described by the pseudo second-order model. This indicated that the adsorption of these compounds on the prepared activated carbons mainly involved chemical interactions.

The amounts of polymers adsorbed from the single and binary systems on the surface of activated carbons and biochars at pH 3 are presented in Figure 6. It is clearly visible that poly (acrylic acid) was adsorbed better on the activated carbons than polyethylenimine. Most probably the polymers' conformations (PAA being coiled and PEI developed) was responsible for this. Both activated carbons had similar textural properties so both types of macromolecules were adsorbed on their surfaces at a similar level. The polyethyleneimine adsorption was not affected by poly (acrylic acid). Small PAA molecules (with the coiled conformation) were probably adsorbed in the pores, so they did not impede the PEI adsorption on the solid surfaces. However, the developed PEI chains could block the porous structure of activated carbons for the poly (acrylic acid) adsorption, which resulted in decrease in the PAA adsorbed amount, in comparison to its adsorption from the single solution. The polymer–polymer complex formations could also affect macromolecule

adsorption from the binary solution. However, at pH 3 these complexes hardly formed due to the coiled conformation of undissociated PAA chains.

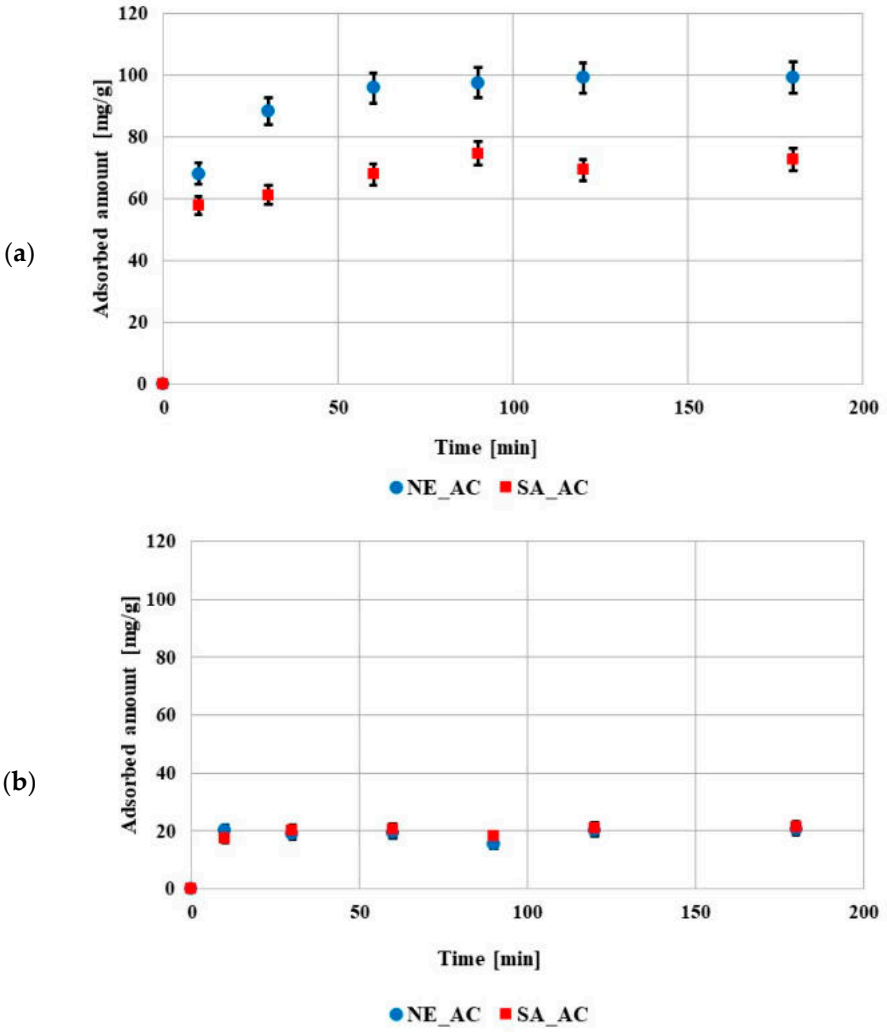

Figure 5. Adsorption kinetics of poly (acrylic acid) (**a**) and polyethyleneimine (**b**) on both activated carbons surfaces (pH 3, C_0 100 ppm).

Table 5. Kinetic parameters of the PAA/PEI adsorption on the activated carbons.

Calculated Parameters	Pseudo-First-Order Model			Pseudo-Second-Order Model		
	q_e [mg/g]	k_1 [1/min]	R^2	q_e [mg/g]	k_2 [g/(mg·min)]	R^2
	PAA					
NE_AC	1.03624	8.03309	0.9376	102.041	0.00237	0.9999
SA_AC	1.02768	6.86179	0.9556	71.9424	0.00476	0.9976
	PEI					
NE_AC	1.0329	1.22266	0.6614	20.5339	0.05842	0.9693
SA_AC	1.01837	1.6098	0.699	21.322	0.05418	0.9913

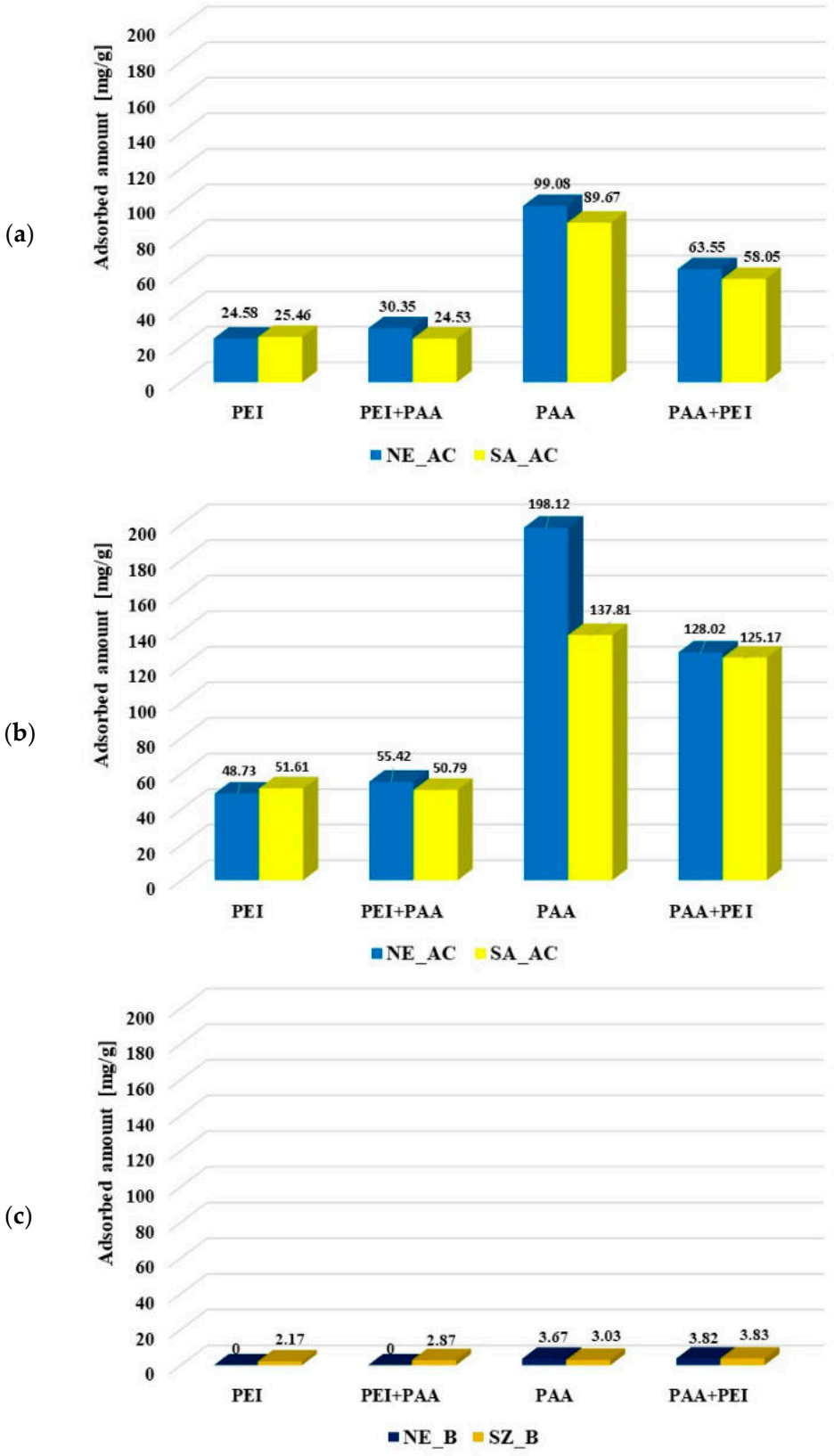

Figure 6. Poly (acrylic acid) and polyethyleneimine adsorbed amounts on the activated carbons surface at pH 3 from the single and binary solutions of the initial concentrations C_0 100 ppm (**a**) and C_0 200 ppm (**b**) as well as on the biochars' surfaces (C_0 100 ppm) (**c**).

The polyethylenimine adsorption on the NE_B biochar was difficult to determine due to rinsing out the adsorbent components resulting in increase of the solution's ionic strength, which made PEI–$CuCl_2$ complex formation impossible. In the case of polyethylenimine adsorption on the SA_B biochar, such a problem did not occur. The PEI adsorbed amount was significantly smaller on the biochar (2.17 mg/g) than on the corresponding activated carbon SA_AC (25.46 mg/g). The presence of poly (acrylic acid) had a slightly positive effect on its adsorption (2.87 mg/g). The PAA adsorbed amount (3.67 mg/g, 3.03 mg/g) on the biochar was considerably smaller than on the surface of activated carbons (99.08 mg/g, 89.67 mg/g). The cationic polymer presence in the solution had a positive effect on the poly (acrylic acid) adsorption on the SA_B biochar (3.83 mg/g), but did not practically affect the amount of PAA adsorbed on the NE_B biochar (3.82 mg/g). Smaller adsorption of polymers on the biochars was first of all caused by their unfavorable textural parameters. It should also be noted that poly (acrylic acid) and polyethylenimine could have a positive effect on mutual adsorption due to the polymer–polymer complex formation.

The analysis of the XPS data presented in Table 6 shows that the adsorption of polymer pollutants led to significant changes on the surface of the NA_AC activated carbon. As a result of PAA adsorption, the oxygen content almost doubled, which was most likely due to the formation of a polymeric layer rich in carboxyl groups on the adsorbent surface. On the other hand, adsorption of PEI on the surface of activated carbon was accompanied by an almost threefold increase in nitrogen content, indicating the formation of an adsorbate layer rich in -NH- or -NH_2 groups. Moreover, the adsorption of polyethyleneimine caused the appearance of small amounts of chlorine in the tested material (the source of which were Cl^- supporting electrolyte anions having high affinity to the PEI cationic groups). In the case of the system containing activated carbon and both polymers, there was a significant increase in the content of both nitrogen and oxygen, which indicated a permanent bond of both adsorbates to the adsorbent surface.

Table 6. Content of elements in the surface layer of NE_AC carbon without, and in the presence of, polymeric adsorbates.

Element	NE_AC	NE_AC + PAA	NE_AC + PEI	AC + PAA + PEI
Cl [at. %]	-	-	1.3	0.8
N [at. %]	1.1	0.6	2.9	5.4
O [at. %]	8.6	16.6	13.0	16.1
P [at. %]	0.8	0.6	0.6	0.8
C [at. %]	89.5	82.2	82.2	76.9

The data obtained from polymer desorption studies are presented in Table 7. Poly (acrylic acid) was desorbed using H_2O, HNO_3 and NaOH. The greatest desorption effectiveness was obtained for the system NE_AC+PAA using a sodium base (61.01%). Water, as well as nitric acid, were not effective desorption agents (efficacy below 3%). Desorption from the surface of biochars with NaOH was impossible. NaOH rinsed out biochar components which caused the black color of the solution and made spectrophotometric determination impossible. The H_2O and HNO_3 turned out to be better PAA desorbing agents from the surface of biochars than from the surface of activated carbons. The greatest poly (acrylic acid) desorption from the biochars structure was obtained for the NE_B + PAA + PEI system using water (34.19%). Due to the increasing ionic strength of the solution, only water was used for the polyethylenimine desorption. The greatest desorption efficiencies were obtained from the systems of NE_AC+PEI (44.15%) and SA_B+PEI (44.08%).

Table 7. Percentage desorption of poly(acrylic acid) and polyethyleneimine from the activated carbons and biochar surfaces from the single and binary systems using H_2O, HNO_3 and NaOH.

Desorption Agent	Desorption [%]		
	H_2O	HNO_3	NaOH
System	**PAA**		
NE_AC + PAA	1.36	2.76	61.01
NE_AC + PAA + PEI	1.23	1.81	47.68
SA_AC + PAA	2.53	2.00	46.45
SA_AC + PAA + PEI	1.36	2.42	48.59
NE_B + PAA	6.57	8.95	-
NE_B + PAA + PEI	34.19	7.08	-
SA_B + PAA	18.01	6.40	-
SA_B + PAA + PEI	2.19	7.81	-
System	**PEI**		
NE_AC + PEI	44.15	-	-
NE_AC + PEI + PAA	4.52	-	-
SA_AC + PEI	24.73	-	-
SA_AC + PEI + PAA	9.69	-	-
NE_B + PEI	-	-	-
NE_B + PEI + PAA	-	-	-
SA_B + PEI	44.08	-	-
SA_B + PEI + PAA	34.80	-	-

3. Materials and Methods

3.1. Adsorbates

Poly (acrylic acid), PAA, and polyethylenimine, PEI were applied in this study as macromolecular adsorbates. Poly (acrylic acid) (Fluka, Saint Louis, MO, USA), with an average molecular weight equal to 2000 Da, is a weak polyelectrolyte with anionic character, due to the presence of carboxyl groups in its macromolecules. The PAA pK_a value is about 4.5. At this pH value 50% of its carboxyl groups are dissociated [25]. Increase in the dissociation degree of carboxyl groups causes more and more expanded conformation of polymeric chains in the solution. At pH 3 the polymer has the most coiled conformation as the result of minimal PAA ionization.

Polyethylenimine (Sigma Aldrich, Saint Louis, MO, USA), with an average molecular weight equal to 2000 Da, is a cationic polymer. It assumes the highest positive charge density in aqueous solution when it is fully protonated. PEI pK_b is about 9 (at this pH value the polyethylenimine dissociation degree is 0.5) and at this pH value, polyethylenimine is in a more coiled form, caused by the partial dissociation of amine groups (the PEI dissociation degree value at pH 6 is about 0.999, whereas at pH 3 it is equal to 1) [26,27]. PEI occurs in the form of branched chains, due to the presence of the amine groups [9].

3.2. Biochars and Activated Carbons Preparation

The nettle herb (NE) and the sage herb (SA) were used as precursors of carbonaceous adsorbents. In the first step of biochar preparation, the stalks were cut into 1.5–2.0 cm pieces and dried at 110 °C. The fragmented and dried materials were next subjected to conventional pyrolysis using a horizontal resistance furnace equipped with a quartz tube reactor (one-zone model PRW75/LM, Czylok, Jastrzębie-Zdrój, Poland). About 15 g of the precursors was placed in the nickel boats, heated to 400 °C (with a rate 5 °C/min) and thermostated at the final pyrolysis temperature for 60 min. After pyrolysis, the samples were cooled down in a nitrogen atmosphere (Linde Gaz, Kościan, Poland) with a flow rate of 170 cm^3/min. The obtained biochars were denoted as NE_B and SA_B.

In order to obtain the activated carbons, both precursors were impregnated with 50% phosphoric(V) acid solution (STANLAB, Lublin, Poland), at the precursor: activating factor

weight ratio equal to 1:2. After 24 h of impregnation process at room temperature, the samples were dried at 110 °C to complete the evaporation of water. Then, the impregnated samples were placed into the quartz boats and heated in a nitrogen atmosphere (flow rate 200 cm^3/min). In the first stage, the samples were heated to the temperature of 200 °C at a rate of 5 °C/min. Then, the materials were annealed at that temperature for 30 min. In the next step, the samples were heated to the final activation temperature of 500 °C (at the rate of 5 °C/min) and again annealed for 30 min. After that time, the samples were cooled down to room temperature in a nitrogen atmosphere. The solids were washed with 10 dm^3 of hot distilled water in a vacuum filtration funnel with a glass sintered disc and dried to a constant mass at 110 °C. The obtained activated carbons were denoted as NE_AC and SA_AC.

3.3. Characterization of the Biochars and Activated Carbons

The SEM technique (Quanta 250 FEG by FEI, Waltham, MA, USA) was applied for determination of surface morphology and elemental composition (detector Octane Elect Plus by EDAX, Berwyn, IL, USA) of the examined solids.

The total micropore surface area, total pore/micropore volume and average pore diameter were determined by nitrogen adsorption—desorption measured at −196 °C using ASAP 2420 (Accelerated Surface Area and Porosimetry System) provided by Micromeritics (Norcross, GA, USA).

The surface functional group content was determined according to the Boehm method (back titration method), described in detail in our earlier paper [28]. The volumetric standards of 0.1 mol/dm^3 sodium hydroxide and 0.1 mol/dm^3 hydrochloric acid (Avantor Performance Materials, Gliwice, Poland) were used as the titrants. The value of pH was determined by the following procedure: samples of 0.25 g were placed in vials, to each of them 25 cm^3 of distilled water was added and the content was stirred by a magnetic stirrer for 12 h. The pH of the obtained suspensions was measured by means of a CP –401 pH-meter (ELMETRON, Zabrze, Poland), equipped with a combined glass electrode EPS-1.

The XPS (X-ray photoelectron spectroscopy) apparatus (Gammadata Scienta, Uppsala, Sweden) was used to determine the elemental composition of the surface layer of the NE_AC activated carbon without, and in the presence of, polymeric adsorbates.

3.4. Electrokinetic Parameters Determination

The determination of surface charge density (σ_0) of the biochars and activated carbon particles with or without the selected adsorbates was performed applying the potentiometric titration method. A quantity of 50 cm^3 of suspension containing 100 ppm of adsorbates, 0.001 mol/dm^3 of NaCl supporting electrolyte and 0.025 g of NE_AC, 0.025 g of SA_AC or 0.5 g of biochars was used for the purpose. The examined solution was placed in a thermostated Teflon vessel (RE 204 thermostat, Lauda Scientific, Lauda-Königshofen, Germany), in which glass and calomel electrodes (Beckman Instruments, Brea, CA, USA) were introduced to monitor pH changes (pHM 240 pH meter, Radiometer, Warsaw, Poland) after each portion of base—NaOH, with a concentration of 0.1 mol/dm^3 (automatic Dosimat 765 microburette, Metrohm, Opacz-Kolonia, Poland) was added. The measurements were made at 25 °C. The changes in the σ_0 value, as a function of solution pH, were calculated with the computer program "Titr_v3", which also controlled the course of the titration process. These calculations were based on the difference in the base volume added to the suspension and the supporting electrolyte solution providing the specified pH value [29].

The zeta potential (ζ) of the biochars and activated carbon particles with and without selected adsorbates was determined. A quantity of 200 cm^3 of the suspension containing the polymeric adsorbate with a concentration of 100 ppm, NaCl as the supporting electrolyte (0.001 mol/dm^3) and 0.03 g of the solid was prepared. These systems were subjected to the action of ultrasounds (XL 2020 ultrasonic head, Misonix, Farmingdale, NY, USA) for 3 min and divided into several parts. In each of the obtained samples a different pH value (changing in the range from 3 to 11) was adjusted. For this purpose, the solutions

of HCl and NaOH, with concentrations of 0.1 mol/dm^3, as well as a Φ360 Ph—meter (Beckman, Brea, CA, USA) were used. The measurements were performed at 25 °C in the suspensions with and without the single and binary adsorbates applying the Doppler laser electrophoresis method and Zetasizer Nano ZS (Malvern Instruments, Malvern, UK): NE_B + NaCl, SA_B + NaCl, NE_AC + NaCl, SA_AC + NaCl, NE_AC + NaCl + PAA, NE_AC + NaCl + PEI, SA_AC + NaCl + PAA, SA_AC + NaCl + PEI, NE_AC + NaCl + PAA + PEI, SA_AC + NaCl + PAA + PEI. The apparatus allowed measurement of the electrophoretic mobility of the solid particles without, and covered with, the adsorbate layers. Based on the obtained results, the zeta potential (ζ) was calculated using Henry's equation [30]. Additionally, the aggregate sizes of the examined solids formed at pH 3, 6 and 9 in the analogous suspensions were determined using the above-mentioned apparatus (based on the static light scattering phenomenon).

3.5. Adsorption–Desorption Studies

The adsorbed/desorbed amounts of PAA and PEI were determined using the static method based on the change of the adsorbate concentration in the solution before and after the process. The polymer concentrations were measured using the UV–Vis spectrophotometer Carry 100 (Varian, Palo Alto, Santa Clara, CA, USA). The PAA concentration was determined based on its reaction with hyamine 1622 resulting in formation of a white-colored complex, absorbing light at the wavelength 500 nm [31]. In turn, the PEI concentration was determined based on its reaction with $CuCl_2$, which gives a blue-colored complex, absorbing light at the wavelength of 285 nm [32]. The adsorption isotherms of single adsorbates were obtained using the solutions with initial concentration changing in the range of 20–400 ppm. The suspensions were prepared by the addition of 0.01 g of activated carbon to the 10 cm^3 of solution containing 0.001 mol/dm^3 of the supporting electrolyte and the appropriate adsorbate. The adsorption process was carried out for 24 h at pH 3, 6 and 9. The adsorption kinetics were studied at pH 3 at specific time intervals, after 10, 30, 60, 90, 120, 180 min, using the analogous procedure of concentration determination as well as the adsorbates with the initial concentration of 100 ppm. The obtained data were fitted to the pseudo first-order (Equation (1)) and the pseudo second-order models of adsorption (Equation (2)) [33]:

$$\frac{dq_t}{dt} = k_1(q_e - q_t) \quad (1)$$

$$\frac{dq_t}{dt} = k_2(q_e - q_t)^2 \quad (2)$$

where q_e isthe adsorbed amount at the equilibrium state [mg/g], q_t isthe adsorbed amount after time t [mg/g], k_1 is the equilibrium rate constant [1/min], and k_2 is the equilibrium rate constant [g/(mg·min)].

The adsorption from the binary solutions was performed at the adsorbate initial concentration of 100 ppm, for 24 h. The adsorption on the biochars and the activated carbons was examined using a suspension containing 0.25 g of the biochar and 0.01g of activated carbon, 100 ppm of the appropriate adsorbate and 10 ppm of NaCl (at pH 3, 24 h). After the adsorption was complete the solids were separated from the solutions using a microcentrifuge (Centrifuge MPW 233e MPW Med. Instruments, Warsaw, Poland) and the concentration of adsorbates in the supernatants determined. The separated solids with the adsorbed polymers were, next, subjected to the desorption process (for 24 h) using the H_2O, HNO_3 and NaOH solutions (the acid and base with concentrations of 0.1 mol/dm^3). All desorption tests were carried out at 25 °C.

4. Conclusions

The activated carbons obtained from nettle and sage herbs had largely developed surface areas. The biochars obtained from the same precursors possessed a significantly smaller surface area, which confirmed that the activation process had a huge impact on the surface area, as well as on development of the porous structure. The obtained adsorbents

were characterized by a mesoporous structure which favored the adsorption of pollutants with large molecular sizes. The activation process also affected the acidic/basic properties of solids (biochars are basic in nature, while activated carbons exhibit acidic character at the surface).

It was proved that carbonaceous materials obtained from nettle and sage herbs can be used as effective polymer adsorbents from aqueous solutions. Poly(acrylic acid) was better adsorbed on the surface of all examined solids than polyethylenimine. In turn, the greatest adsorption of both polymers was observed at pH 3 on the NE_AC surface (the maximum value of the PAA adsorption was 273 mg/g, whereas for PEI it was156 mg/g). The PEI adsorption at pH 3 was not affected by poly(acrylic acid) with the coiled conformation. In turn, PEI molecules with highly developed conformation could block the porous structure of activated carbons for PAA adsorption (PAA adsorbed amount decrease from mixed system of adsorbates). It was also proved that the regeneration of the examined solids was possible; however, at a level not exceeding 50%.

Author Contributions: Conceptualization, M.W., M.G. and P.N.; methodology, M.W., M.G. and P.N.; investigation, M.G. and P.N.; resources, M.G. and P.N.; data curation, M.W. and M.G.; writing—original draft preparation, M.G.; writing—review and editing, M.W. and P.N.; visualization, M.G.; supervision, M.W. and P.N. All authors have read and agreed to the published version of the manuscript.

Funding: This research received no external funding.

Institutional Review Board Statement: Not applicable.

Informed Consent Statement: Not applicable.

Data Availability Statement: Data are contained within the article.

Conflicts of Interest: The authors declare no conflict of interest.

Sample Availability: Samples of the biochars are available from the authors upon reasonable request.

References

1. Peters, C.M. *Sustainable Harvest of Non-Timber Plant Resources in Tropical Moist Forests: An Ecological Primer*; Biodiversity Support Program: Washington, DC, USA, 1994.
2. Cobbina, S.J.; Duwiejuah, A.B.; Quainoo, A.K. Single and simultaneous adsorption of heavy metals onto groundnut shell biochar produced under fast and slow pyrolysis. *Int. J. Environ. Sci. Technol.* **2019**, *16*, 3081–3090. [CrossRef]
3. Zheng, L.; Gao, Y.; Du, J.; Zhang, W.; Huang, Y.; Zhao, Q.; Duan, L.; Liu, Y.; Naidu, R.; Pan, X. Single and binary adsorption behaviour and mechanisms of Cd^{2+}, Cu^{2+} and Ni^{2+} onto modified biochar in aqueous solutions. *Processes* **2021**, *9*, 1829. [CrossRef]
4. Jiang, T.-Y.; Jiang, J.; Xu, R.-K.; Li, Z. Adsorption of Pb(II) on variable charge soils amended with rice-straw derived biochar. *Chemosphere* **2012**, *89*, 249–256. [CrossRef] [PubMed]
5. Hu, B.; Tang, Y.; Wang, X.; Wu, L.; Nong, J.; Yang, X.; Guo, J. Cobalt-gadolinium modified biochar as an adsorbent for antibiotics in single and binary systems. *Microchem. J.* **2021**, *166*, 106235. [CrossRef]
6. Su, L.; Zhang, H.; Oh, K.; Liu, N.; Luo, Y.; Cheng, H.; Zhang, G.; He, X. Activated biochar derived from spent *Auricularia auricula* substrate for the efficient adsorption of cationic azo dyes from single and binary adsorptive systems. *Water Sci. Technol.* **2021**, *84*, 101–121. [CrossRef]
7. Gęca, M.; Wiśniewska, M.; Nowicki, P. Biochars and activated carbons as adsorbents of inorganic and organic compounds from multicomponent systems–A review. *Adv. Colloid Interface Sci.* **2022**, *305*, 102687. [CrossRef]
8. Yang, S.; Fu, Y.; Jeong, S.H.; Park, K. Application of poly(acrylic acid) superporous hydrogel microparticles as a super-disintegrant in fast-disintegrating tablets. *J. Pharm. Pharmacol.* **2004**, *56*, 429–436. [CrossRef]
9. Müller, M.; Keßler, B.; Fröhlich, J.; Poeschla, S.; Torger, B. Polyelectrolyte complex nanoparticles of poly(ethyleneimine) and poly(acrylic acid): Preparation and applications. *Polymers* **2011**, *3*, 762–778. [CrossRef]
10. Szewczuk-Karpisz, K.; Wiśniewska, M.; Medykowska, M.; Galaburda, M.V.; Bogatyrov, V.M.; Oranska, O.I.; Błachnio, M.; Oleszczuk, P. Simultaneous adsorption of Cu(II) ions and poly(acrylic acid) on the hybrid carbon-mineral nanocomposites with metallic elements. *J. Hazard. Mater.* **2021**, *412*, 125138. [CrossRef]
11. Vancha, A.R.; Govindaraju, S.; Parsa, K.V.; Jasti, M.; González-García, M.; Ballestero, R.P. Use of polyethyleneimine polymer in cell culture as attachment factor and lipofection enhance. *BMC Biotechnol.* **2004**, *4*, 23. [CrossRef]
12. Mbareck, C.; Nguyen, Q.T.; Alaoui, O.T.; Barillier, D. Elaboration, characterization and application of polysulfone and polyacrylic acid blends as ultrafiltration membranes for removal of some heavy metals from water. *J. Hazard. Mater.* **2009**, *171*, 93–101. [CrossRef] [PubMed]

13. Navarathna, C.; Keel, M.G.; Rodrigo, P.M.; Carrasco, C.; Ramirez, A.; Jamison, H.; Mohan, D.; Mlsna, T.E. 16-Biochar and biochar composites for poly- and perfluoroalkyl substances (PFAS) sorption. In *Sustainable Biochar for Water and Wastewater Treatment*; Elsevier: Amsterdam, The Netherlands, 2022; pp. 555–595. [CrossRef]
14. Wiśniewska, M.; Nowicki, P.; Szewczuk-Karpisz, K.; Gęca, M.; Jędruchniewicz, K.; Oleszczuk, P. Simultaneous removal of toxic Pb(II) ions, poly(acrylic acid) and Triton X-100 from their mixed solution using engineered biochars obtained from horsetail herb precursor–Impact of post-activation treatment. *Sep. Purif. Technol.* **2021**, *276*, 119297. [CrossRef]
15. Wiśniewska, M.; Nowicki, P. Peat-based activated carbons as adsorbents for simultaneous separation of organic molecules from mixed solution of poly(acrylic acid) polymer and sodium dodecyl sulfate surfactant. *Colloids Surf. A Physicochem. Eng. Asp.* **2020**, *585*, 124179. [CrossRef]
16. Wiśniewska, M.; Szewczuk-Karpisz, K. Removal possibilities of colloidal chromium (III) oxide from water using polyacrylic acid. *Environ. Sci. Pollut. Res.* **2013**, *20*, 3657–3669. [CrossRef]
17. Szewczuk-Karpisz, K.; Fijałkowska, G.; Wiśniewska, M.; Wójcik, G. Chromium(VI) reduction and accumulation on the kaolinite surface in the presence of cationic soil flocculant. *J. Soils Sediments* **2020**, *20*, 3688–3697. [CrossRef]
18. Skwarek, E.; Janusz, W.; Sternik, D. Adsorption of citrate ions on hydroxyapatite synthetized by various methods. *J. Radioanal. Nucl. Chem.* **2014**, *299*, 2027–2036. [CrossRef]
19. Wiśniewska, M.; Chibowski, S.; Wawrzkiewicz, M.; Onyszko, M.; Bogatyrov, V.C.I. Basic Red 46 Removal from Sewage by Carbon and Silica Based Composite: Equilibrium, Kinetic and Electrokinetic Studies. *Molecules* **2022**, *27*, 1043. [CrossRef]
20. Vincent, B. The effect of adsorbed polymers on dispersion stability. *Adv. Colloid Interface Sci.* **1974**, *4*, 193–277. [CrossRef]
21. Kasprzyk-Hordern, B. Chemistry of alumina, reactions in aqueous solution and its application in water treatment. *Adv. Colloid Interface Sci.* **2004**, *110*, 19–48. [CrossRef]
22. Summers, R.S.; Roberts, P.V. Activated carbon adsorption of humic substances. *J. Colloid Interface Sci.* **1998**, *122*, 382–397. [CrossRef]
23. Wiśniewska, M.; Nowicki, P.; Nosal-Wiercińska, A.; Pietrzak, R.; Szewczuk-Karpisz, K.; Ostolska, I.; Sternik, D. Adsorption of poly(acrylic acid) on the surface of microporous activated carbon obtained from cherry stones. *Colloids Surf. A Physicochem. Eng. Asp.* **2017**, *514*, 137–145. [CrossRef]
24. Wiśniewska, M.; Nowicki, P. Simultaneous removal of lead(II) ions and poly(acrylic acid) macromolecules from liquid phase using of biocarbons obtained from corncob and peanut shell precursors. *J. Mol. Liq.* **2019**, *296*, 111806. [CrossRef]
25. Chibowski, S.; Wiśniewska, M.; Marczewski, A.W.; Pikus, S. Application of the SAXS method and viscometry for determination of the thickness of adsorbed polymer layers at the ZrO_2 –polymer solution interface. J. *Colloid Interface Sci.* **2003**, *267*, 1–8. [CrossRef]
26. Von Harpe, A.; Petersen, H.; Li, Y.; Kissel, T. Characterization of commercially available and synthesized polyethylenimines for gene delivery. *J. Control. Release* **2000**, *69*, 309–322. [CrossRef]
27. Ochiai, H.; Anabuki, Y.; Kojima, O.; Tominaga, K.; Murakami, I. Dissociation of poly(allylammonium) cations in salt solutions. *J. Polym. Sci. Part B Polym. Phys.* **1990**, *28*, 233–240. [CrossRef]
28. Bazan-Wozniak, A.; Nowicki, P.; Pietrzak, R. The effect of demineralization on the physicochemical and sorption properties of activated bio-carbons. *Adsorption* **2019**, *25*, 337–343. [CrossRef]
29. Janusz, W. Electrical double layer in the system TiO2 (anathase)/aqueous solution of NaCl. *Polish J. Chem.* **1994**, *68*, 1871–1880.
30. Ohshima, H. A Simple Expression for Henry's Function for the Retardation Effect in Electrophoresis of Spherical Colloidal Particles. J. *Colloid Interface Sci.* **1994**, *168*, 269–271. [CrossRef]
31. Crummett, W.B.; Hummel, R.A. The determination of traces of polyacrylamides in water. *J. Am. Water Work. Assoc. 1* **1963**, *55*, 209–219. [CrossRef]
32. Patkowski, J.; Myśliwiec, D.; Chibowski, S. Validation of a new method for spectrophotometric determination of polyethylenimine. *Int. J. Polym. Anal. Charact.* **2016**, *21*, 486–494. [CrossRef]
33. Ho, Y.S.; McKay, G. Sorption of dye from aqueous solution by peat. *Chem. Eng. J.* **1998**, *70*, 115–124. [CrossRef]

Lublin, 10.09.2025

mgr Marlena Groszek
Uniwersytet Marii Curie-Skłodowskiej w Lublinie,
Wydział Chemii, Instytut Nauk Chemicznych,
Katedra Radiochemii i Chemii Środowiskowej,
Pl. Marii Curie-Skłodowskiej 3, 20-031 Lublin
marlena.groszek@mail.umcs.pl

Rada Naukowa Instytutu Nauk Chemicznych
Uniwersytetu Marii Cure-Skłodowskiej
w Lublinie

Oświadczenie o współautorstwie

Niniejszym oświadczam, że mój udział w pracy: **M. Gęca**, M. Wiśniewska, P. Nowicki, *Simultaneous Removal of Polymers with Different Ionic Character from Their Mixed Solutions Using Herb-Based Biochars and Activated Carbons,* Molecules, 27, 2022, 7557. DOI: 10.3390/molecules27217557 [D6], obejmował stworzenie koncepcji artykułu, przeprowadzenie eksperymentów, analizę uzyskanych wyników, przygotowanie pierwszej wersji manuskryptu oraz odpowiedzi na uwagi recenzentów.

Marlena Groszek

Lublin, 10.09.2025

prof. dr hab. Małgorzata Wiśniewska
Uniwersytet Marii Curie-Skłodowskiej w Lublinie,
Wydział Chemii, Instytut Nauk Chemicznych,
Katedra Radiochemii i Chemii Środowiskowej,
Pl. Marii Curie-Skłodowskiej 3, 20-031 Lublin
malgorzata.wisniewska@mail.umcs.pl

Rada Naukowa Instytutu Nauk Chemicznych
Uniwersytetu Marii Cure-Skłodowskiej
w Lublinie

Oświadczenie o współautorstwie

Niniejszym oświadczam, że mój udział w pracy: M. Gęca, **M. Wiśniewska**, P. Nowicki, *Simultaneous Removal of Polymers with Different Ionic Character from Their Mixed Solutions Using Herb-Based Biochars and Activated Carbons,* Molecules, 27, 2022, 7557. DOI: 10.3390/molecules27217557 [D6], obejmował stworzenie koncepcji artykułu, interpretację uzyskanych wyników, korektę manuskryptu – przed i po procesie recenzji oraz nadzór merytoryczny w czasie całego cyklu wydawniczego.

Małgorzata Wiśniewska

Poznań, 10.09.2025

dr hab. Piotr Nowicki, prof. UAM
Uniwersytet im. Adama Mickiewicza w Poznaniu,
Wydział Chemii, Zakład Chemii Stosowanej,
Ul. Uniwersytetu Poznańskiego 8, 61-614 Poznań
piotr.nowicki@amu.edu.pl

Rada Naukowa Instytutu Nauk Chemicznych
Uniwersytetu Marii Cure-Skłodowskiej
w Lublinie

Oświadczenie o współautorstwie

Niniejszym oświadczam, że mój udział w pracy: M. Gęca, M. Wiśniewska, **P. Nowicki**, *Simultaneous Removal of Polymers with Different Ionic Character from Their Mixed Solutions Using Herb-Based Biochars and Activated Carbons,* Molecules, 27, 2022, 7557. DOI: 10.3390/molecules27217557 [D6], obejmował opracowanie metodyki badań, przeprowadzenie eksperymentów, analizę uzyskanych wyników, korektę manuskryptu – przed i po procesie recenzji oraz nadzór merytoryczny w czasie całego cyklu wydawniczego.

Piotr Nowicki

D7. M. Gęca, M. Wiśniewska, T. Urban, P. Nowicki, *Temperature effect on ionic polymers removal from aqueous solutions using activated carbons obtained from biomass,* Materials, 16, 2022, 350, DOI: 10.3390/ma16010350

materials

MDPI

Article

Temperature Effect on Ionic Polymers Removal from Aqueous Solutions Using Activated Carbons Obtained from Biomass

Marlena Gęca [1,*], Małgorzata Wiśniewska [1,*], Teresa Urban [1] and Piotr Nowicki [2]

[1] Department of Radiochemistry and Environmental Chemistry, Institute of Chemical Sciences, Faculty of Chemistry, Maria Curie-Sklodowska University in Lublin, M. Curie-Sklodowska Sq. 3, 20-031 Lublin, Poland
[2] Department of Applied Chemistry, Faculty of Chemistry, Adam Mickiewicz University in Poznań, Uniwersytetu Poznańskiego 8, 61-614 Poznań, Poland
* Correspondence: marlena.geca@wp.pl (M.G.); malgorzata.wisniewska@mail.umcs.pl (M.W.)

Abstract: The main aim of this study was the determination of temperature influence on adsorption mechanisms of anionic poly(acrylic acid) (PAA) and cationic polyethylenimine (PEI) on the surface of activated carbons (AC) obtained via chemical activation of nettle (NE) and sage (SA) herbs. All measurements were performed at pH 3 at three temperature values, i.e., 15, 25 and 35 °C. The adsorption/desorption of these polymers from single and mixed solution of adsorbates was also investigated. The viscosity studies were additionally performed to obtain hydrodynamic radius values characterizing polymeric macromolecules conformation in the solution. These data are very important for the explanation of changes of linear dimensions of polymer chains with the rise of temperature caused by the modification of polymer–solvent interactions. Moreover, the XPS studies for the systems showing the highest adsorbed amounts in the specific temperature conditions were carried out. These were the systems containing PEI, PAA and NE–AC activated carbon at 25 °C. In such a case, the maximum adsorption capacity towards PAA macromolecules from a single solution of adsorbate reaches the value of 198.12 mg/g. Additionally, the thermodynamic parameters including the free energies of adsorption, as well as changes in free enthalpy and entropy were calculated.

Keywords: activated biocarbons; temperature effect; poly(acrylic acid); polyethyleneimine; polymers simultaneous removal; hydrodynamic radius of polymeric coil

Citation: Gęca, M.; Wiśniewska, M.; Urban, T.; Nowicki, P. Temperature Effect on Ionic Polymers Removal from Aqueous Solutions Using Activated Carbons Obtained from Biomass. *Materials* **2023**, *16*, 350. https://doi.org/10.3390/ma16010350

Academic Editor: Zebin Yu

Received: 30 November 2022
Revised: 22 December 2022
Accepted: 27 December 2022
Published: 30 December 2022

1. Introduction

Carbonaceous materials are widely used in industry and water treatment technologies [1,2]. However, the most popular is their application for heavy metals removal. Therefore, it should not be surprising that heavy metals adsorption on the surface of different types of adsorbents is reported extensively [3–5]. On the other hand, many other substances are currently present in wastewater. Thus, the simultaneous removal of molecules of various chemical characteristics is a very important issue, which requires explanation and extensive studies. Adsorption on the surface of carbonaceous adsorbents could also be successfully used for water remediation from all types of pollutants [6,7].

Polymers are present in the wastewaters in great amounts due to their wide application in various branches of industry, agriculture and ecology [8–17]. They are often synthetic substances, whose effect on organisms have not been completely explained and they can be potentially dangerous. For this reason, new and more effective methods of polymers removal from aquatic environments are constantly sought and aimed at innovative materials of this type that accompany the development of modern technologies. One of the techniques which meets this criterion is adsorption with activated carbons usage [18–20]. It should be noted that polymeric chain conformation in the aqueous solution, determining the maximum amounts of adsorbed macromolecules and structure of their surface layer, depends, among others, on the polymer type and its molecular weight, solution pH and ionic

strength, as well as temperature [21,22]. All these parameters affect adsorption efficiency and as a consequence of the stability of such systems.

Polymers dilution in the solution proceeds in two stages. In the first one, the polymer swells due to solvent molecule penetration inside the polymer macromolecules, which causes an increase of the polymeric sample volume, maintaining its original shape. In the second stage, the solvent diffuses between polymer macromolecules, separates them from each other and the homogeneous solution is formed [23]. The final polymers conformation in the solution are the result of two component contributions: solvent–segment interactions and segment–segment interactions with van der Walls forces. The solvent whose action on the polymer significantly exceeds the segment–segment interactions is regarded to be the good one. When the polymer–solvent interaction is not able to overcome the van der Waals forces, the polymer precipitates from the solution [24]. The temperature at which the macromolecule size is equal to the undisturbed one is called θ temperature (theta temperature). A solvent at the temperature θ becomes an ideal one. At the temperature lower than θ, polymer–polymer interactions are favorable. The polymer conformation is more coiled in order to minimize polymers–solvent contacts and maximize the polymer–polymer contacts. When the solution temperature is higher than θ temperature, the opposite effect occurs [25]. Polymeric coils develop due to favourable solvent–polymer interactions.

The main aim of the presented manuscript was to determine influence of temperature on an anionic poly(acrylic acid) (PAA) and cationic polyethylenimine (PEI) adsorption mechanism on the surface of activated carbons (AC) obtained from nettle (NE) and the sage (SA) herbs. The simultaneous adsorption/desorption of both polymers with different ionic characteristics was also investigated. The viscosity, adsorption and desorption measurements were performed at three temperature values, i.e., 15, 25 and 35 °C. The viscosity study enabled determination of linear dimensions of polymeric chains in an aqueous solution with the increasing temperature, which can be very helpful in describing the structure of the polymeric layers formed at the activated carbon–solution interface [26]. Understanding the mechanisms controlling the process of adsorption removal of polymers at different temperatures is crucial for the effective control of many technological operations involving them, often carried out in a wide range of temperatures.

2. Materials and Methods

2.1. Adsorbents and Adsorbates

Activated carbons (AC) used as the adsorbents were obtained from nettle (NE) and sage (SA) herbs. The preparation procedure and physicochemical characteristics were described in detail in the previous manuscript [27]. Both precursors were impregnated with the 50% phosphoric(V) acid solution (STANLAB, Lublin, Poland) and heated in the nitrogen atmosphere (flow rate 200 cm^3/min) with first step at 200 °C (temperature build-up 5 °C/min) for 30 min and the second one at 500 °C (temperature build-up 5 °C/min) for 30 min. The obtained activated carbons were denoted as NE–AC and SA–AC, respectively. Their textural parameters and acidic/basic properties are presented in Table 1. The textural characterization of the activated carbons was based on the nitrogen adsorption-desorption isotherms measured at –196 °C on a sorptometer ASAP 2020 manufactured by Micrometrics Instrument Corporation (Norcross, GA, USA). The content of the surface functional groups of acidic and basic nature was evaluated according to the Boehm method [28], using volumetric standards of 0.1 mol/dm^3 NaOH (POCh, Gliwice, Poland) and 0.1 mol/dm^3 HCl (Chempur, Piekary Śląskie, Poland) as the titrants.

Table 1. Textural parameters and acidic/basic properties of the prepared activated carbons.

Adsorbent	Surface Area [m^2/g]		Pore Volume [cm^3/g]		Mean Pore Size [nm]	Acidic Groups [mmol/g]	Basic Groups [mmol/g]	Total Amount [mmol/g]
	Total	Micropore	Total	Micropore				
NE–AC	801	157	0.847	0.074	4.231	0.858	0.272	1.130
SA–AC	842	155	0.826	0.074	3.926	0.436	0.215	0.651

Poly(acrylic acid) (PAA) and polyethylenimine (PEI) were used as adsorbates. Both PAA and PEI were characterized by the weight average molecular weights equal to 2000 Da. Poly(acrylic acid) (Fluka, Saint Louis, USA) is a weak polyelectrolyte with an anionic character (carboxyl groups are present in its macromolecules) with a pK_a value of about 4.5. Thus, at pH 3, at which all measurements were carried out (due to maximal adsorption of both polymers under such conditions), its ionization is minimal [29]. Polyethylenimine (Sigma Aldrich, Saint Louis, MO, USA) is a cationic polymer (amine groups are present in its chains) with a pK_b value of about 9 [30]. At pH 3, PEI molecules occur in a completely dissociated form. The single (only PAA or only PEI) and mixed (PAA and PEG simultaneously) systems of adsorbates were investigated.

The NaCl solution (POCh, Gliwice, Poland) with a concentration of 0.001 mol/dm^3 was used as the basic electrolyte. The HCl (Chempur, Piekary Śląskie, Poland) and NaOH (POCh, Gliwice, Poland) solutions with concentrations ranging from 0.01 to 1 mol/dm^3 were used for the adjustment of the solution pH. All reagents were of analytical grade.

2.2. Viscosity Measurements

Viscosity measurements were applied to determine the linear dimensions of the polymer chain in aqueous solution. Based on the Flory–Fox theory, the root-mean-square chain end-to-end distance—$\left(\overline{r^2}\right)^{1/2}$ and the hydrodynamic radius of the polymer coil—R_h were calculated [24,31]. These experiments were performed using the rotational CVO 50 rheometer with the "double gap" measuring system (Bohlin Instruments, Malvern, UK). For this purpose, the following equations were applied:

$$R_h = f\frac{\left(\overline{r^2}\right)^{1/2}}{6^{1/2}} \quad (1)$$

$$\left(\overline{r^2}\right)^{1/2} = \sqrt[3]{\left(\frac{[\eta]M}{F}\right)} \quad (2)$$

$$[\eta] = \lim_{c\to 0}\eta_r \quad (3)$$

$$\eta_r = \frac{\frac{\eta_p}{\eta_0} - 1}{c} \quad (4)$$

where: $[\eta]$—the intrinsic viscosity (determined from dependence of reduced viscosity (η_r) versus the polymer concentration (c) by extrapolating the straight line to c = 0); η_p—the polymer solution viscosity; η_0—the water viscosity; F—the universal Flory–Fox constant approximately equal to $2.1\cdot10^{21}$ (for the polymers in good solvents) [24,31]; M—the polymer molecular weight; f—the constant value, irrespective of the polymer molecular weight (f = 0.66 [32,33]).

Viscosity studies were performed in the supporting electrolyte solution—NaCl with a concentration of 0.001 mol/dm^3 at pH 3, at which the highest adsorptions of both polymers were observed [27] and at three values of temperatures, namely 15, 25 and 35 °C. The examined concentrations of aqueous polymeric samples were as follows: 10, 50, 100, 150, 200, 300 and 400 ppm.

2.3. Adsorption–Desorption Measurements

For adsorption–desorption studies, 10 cm^3 of suspensions containing 0.001 mol/dm^3 of NaCl (supporting electrolyte), 200 ppm of appropriate polymer and 0.01 g of activated carbon were used. The adsorption process was carried out for 24 h at pH 3 at 15, 25 and 35 °C. After the adsorption completion, the solids were separated from solutions using microcentrifuge (Centrifuge MPW 233e MPW Med. Instruments, Warsaw, Poland) and the concentrations of adsorbates in the supernatants were determined. The separated solids with adsorbed macromolecular substances were next subjected to the desorption

using H_2O, HNO_3 (POCh, Gliwice, Poland) and NaOH solutions (the acid and base with concentrations of 0.1 mol/dm^3). After 24 h, the adsorbates concentrations were determined. All adsorbed/desorbed amounts were examined using a static method based on a decrease/increase in the polymers concentration in the solution before and after the adsorption/desorption process. The following formula was used for this purpose:

$$q_e = \frac{(C_0 - C_e)V}{m} \tag{5}$$

where: q_e—the polymer adsorbed/desorbed amount at the equilibrium state, C_0 and C_e—the polymer concentrations in the solution before adsorption and at the equilibrium state, respectively, V—the volume of the solution, m—the mass of the solid.

PEI and PAA concentrations in the solution were determined using UV-VIS spectrophotometry (Carry 100, Varian, Palo Alto, CA, USA). The poly(acrylic acid) concentration was determine using its reaction with hyamine 1622 (Sigma Aldrich, Saint Louis, MO, USA), which gives a white-coloured complex [34]. In turn, the polyethylenimine concentration was obtained based on its reaction with $CuCl_2$ (POCh, Gliwice, Poland), resulting in the formation of a blue-coloured complex [35].

The PAA and PEI adsorption kinetics were studied at pH 3 at 15, 25 and 35 °C for the NE–AC sample (the time intervals were: 10, 30, 60, 90, 120, 180 min). The procedures of concentration determination described above, as well as the adsorbates with the initial concentration of 100 ppm, were examined. The obtained data were fitted to the pseudo-first order and the pseudo-second order models of adsorption [36]:

$$\frac{dq_t}{dt} = k_1(q_e - q_t) \tag{6}$$

$$\frac{dq_t}{dt} = k_2(q_e - q_t)^2 \tag{7}$$

where: q_e—the adsorbed amount at the equilibrium state, q_t—the adsorbed amount after time t, k_1—the equilibrium rate constant, k_2—the equilibrium rate constant.

Two different commercially available activated carbon materials were used—purolite (PRT) (Lenntech, Delfgauw, The Netherlands), with a specific surface area of 900–1000 m^2/g, and lewatite (LWT) (Lanxess, Dortmund, Germany), characterized by a specific surface area of 550–650 m^2/g. The adsorption studies with their usage were performed at the same conditions as for the applied herbs-based activated carbons.

The XPS (X-ray photoelectron spectroscopy) apparatus (Gammadata Scienta, Uppsala, Sweden) was used to determine elemental composition of NE–AC activated carbon and adsorbed forms in the surface layers of both polymers at pH 3 and at 25 °C. For such a system and under such conditions, the greatest adsorption of polymeric substances was obtained.

2.4. Thermodynamic Studies

The thermodynamic parameters of PAA and PEI adsorption on activated carbons were calculated at three different temperatures using the formulas [37–39]:

$$\Delta G^\circ = -RTlnK_cC_0 \tag{8}$$

$$K_c = \frac{q_e}{C_e} \tag{9}$$

$$lnK_cc^0 = \frac{\Delta S^\circ}{R} - \frac{\Delta H^\circ}{RT} \tag{10}$$

where: ΔG°—the change of free energy of the system, ΔH°—the change of free enthalpy of the system, ΔS°—the change of free entropy of the system, R—gaseous constant (8.314 J/mol K), T—temperature, K_c—distribution constant at equilibrium, C_0—the initial

concentration of adsorbate (200 mg/dm^3) [38–40], q_e—the adsorbed amount of the polymer at equilibrium, C_e—the equilibrium concentration of solution.

3. Results

3.1. Linear Dimensions of Poly(Acrylic Acid) and Polyethyleneimine Chains in Aqueous Solutions at Different Temperatures

The dependencies of intrinsic viscosities of polymer solutions as a function of their concentrations leading to [η] determination are presented in Figure 1, whereas the calculated parameters characterizing linear dimensions of polymeric chains are listed in Table 2 [40,41].

Analysis of the data above suggests that a temperature increase causes increase of both the root-mean-square chain end-to-end distance and the hydrodynamic radius of the polymer coil values in the case of the two examined polymers. Such behavior is a result of the changes in solvent quality and polymer–solvent interactions [23].

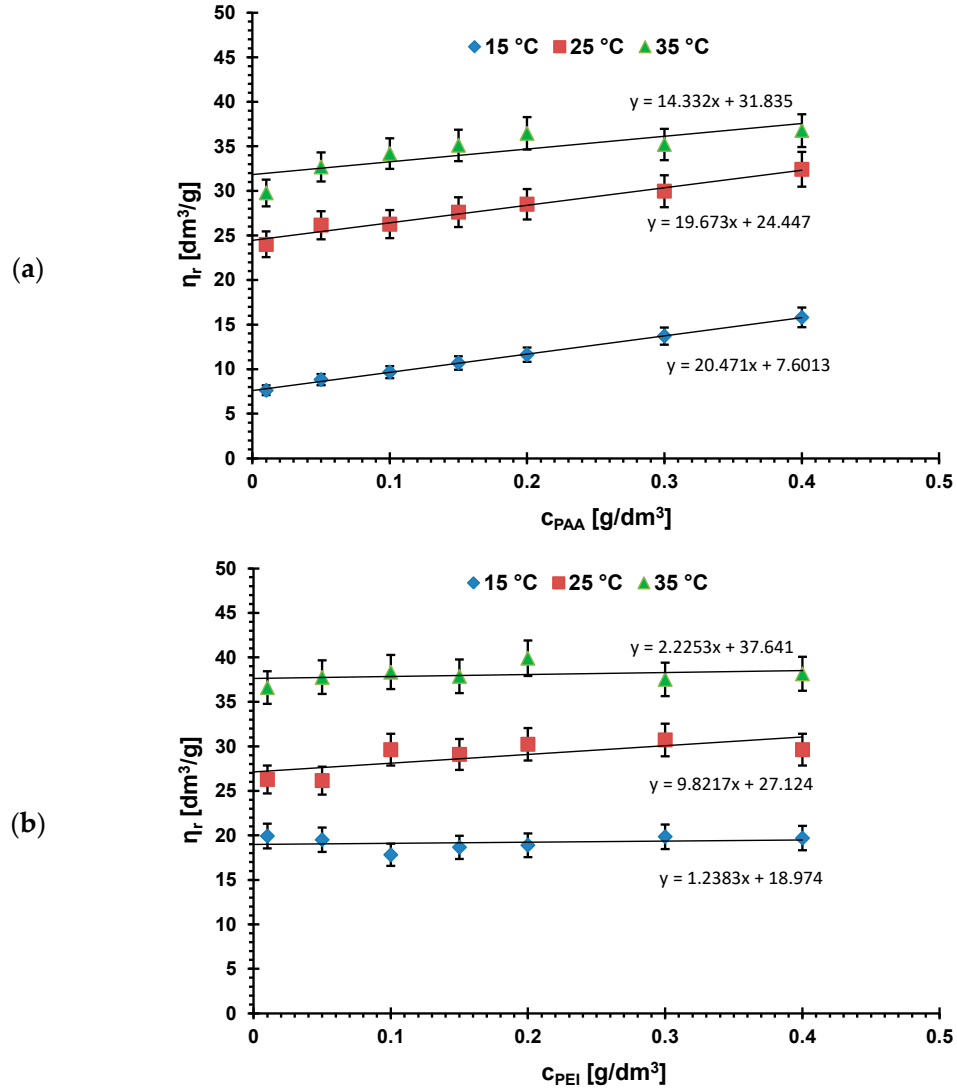

Figure 1. Intrinsic viscosities of (**a**) PAA and (**b**) PEI solutions as a function of their concentrations at different temperatures, pH 3.

Table 2. Characteristics of linear dimensions of poly(acrylic acid) and polyethyleneimine macromolecules in the aqueous solutions at pH 3 under different temperature conditions.

Temperature	$[\eta]$ [dm^3/g]	$(\overline{r^2})^{1/2}$ [nm]	R_h [nm]
	PAA		
15 °C	7.601	1.96	0.53
25 °C	24.447	2.85	0.77
35 °C	31.835	3.16	0.85
	PEI		
15 °C	18.974	2.66	0.72
25 °C	27.124	3.00	0.81
35 °C	37.641	3.35	0.90

The theta temperature of poly(acrylic acid) in aqueous solution is 14 °C [42]. The dimensions of polymer chains in this state satisfy the statistical requirements of the Gauss theory, which is why they are sometimes termed as the Gauss coils. Under temperature conditions lower than theta temperature, polymer coil conformation changes to a globular shape to minimize the polymer–solvent contacts and maximize the contacts between the segments (coil-globule transition and phases separation occur). PAA aqueous solution shows the UCST type phase diagram (with upper critical solution temperature), below which the solution separates into two uniform phases with different compositions (cloud point is reached) [43]. At 15 °C (very close to the theta temperature), the polymer coils (additionally practically undissociated at pH 3) have the smallest dimensions (0.53 nm). Further increase of temperature causes improvement of solvent quality and polymer segments interactions with solvent molecules more and more preferred. This is why the $(\overline{r^2})^{1/2}$ and R_h values increase at temperatures of 25 and 35 °C.

A similar trend is observed for the cationic polyethyleneimine. Nevertheless, due to the total dissociation of its functional groups at pH 3, the linear dimensions of PEI macromolecules are greater than in the case of PAA. The aqueous solution of PEI shows LCST (lower critical solution temperature) behavior and the reported cloud point is about 97 °C [44,45]. Due to the fact that the examined temperature range (15–35 °C) remains distant from this PEI critical conditions, the differences of the $(\overline{r^2})^{1/2}$ and R_h values with temperature increase are slightly smaller than that observed for poly(acrylic acid) samples.

3.2. Adsorption–Desorption Properties of the Activated Carbons in Single and Mixed Solutions of Poly(Acrylic Acid) and Polethyleneimine at Different Temperatures

Both polymers adsorbed amounts (expressed in mg/g and as percentage of polymer removal) on the activated carbons surface from single and mixed systems of adsorbates at pH 3 at three examined temperatures, as presented in Figures 2 and 3.

Previous studies on activated carbons surface charge density confirm the acidic properties of both adsorbents. The point of zero charge (pzc) of NE–AC activated carbon occurs at pH 3.1 and, in case of SA–AC one, at pH 4.0 [27]. It means that at pH 3, at which the polymers adsorption were carried out, NE–AC activated carbon surface is practically neutral, whereas SA–AC one slightly positively charged. Thus, the electrostatic conditions have small influence on the polymer adsorption at pH 3, only for minimally dissociated PAA macromolecules the weak electrostatic attraction with SA–AC surface takes place. Due to the considerably higher content of functional groups and noticeably greater mean pore size in the case of the NE–AC activated carbon (Table 1), PAA adsorption is higher on this carbonaceous material surface than on the SA–AC one, both from single and mixed adsorbate systems, at all examined temperatures. The PEI adsorption is considerably lower as a result of total dissociation of its functional groups and more stretched conformation causing solid pore entry blockade.

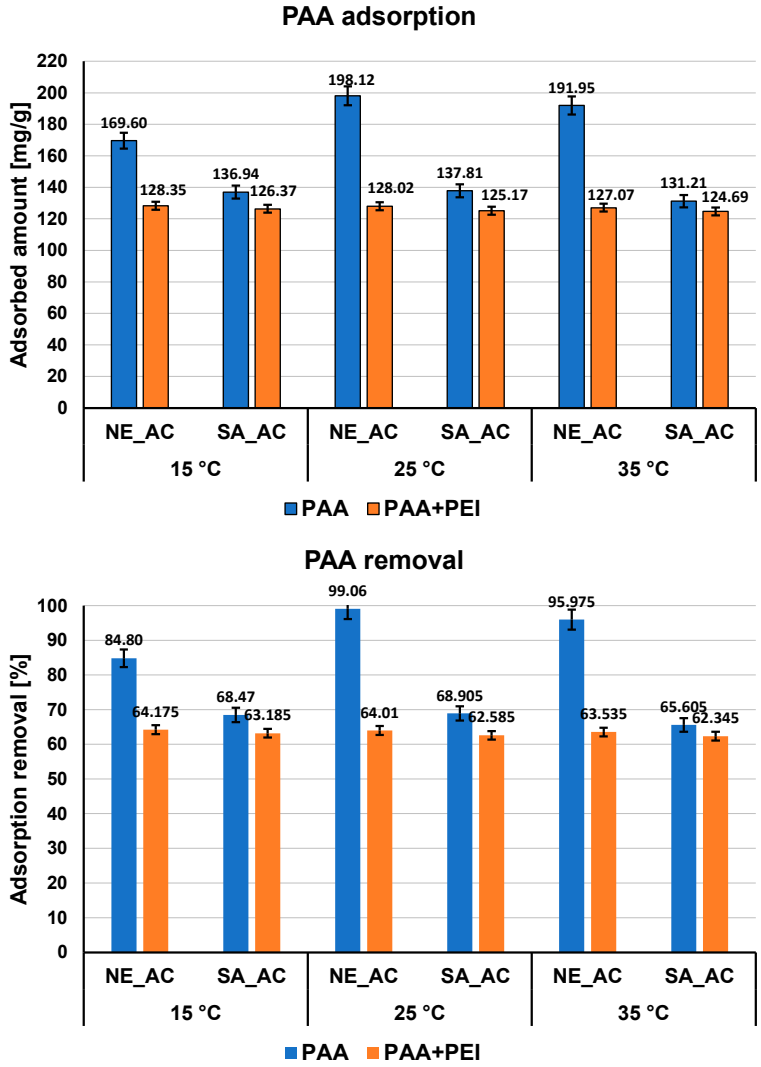

Figure 2. PAA adsorbed amounts (**a**) and its percentage removal (**b**) from the activated carbons surface in single and mixed systems of adsorbates at three examined temperatures, pH 3.

The temperature influence on the adsorbed amount of the examined polymers is significantly greater for poly(acrylic acid) (Figure 2) than polyethyleneimine (Figure 3). The largest differences occur for NE–AC activated carbon, for which the adsorption at 15 °C is lower than at 25 and 35 °C, noting that adsorption reaches its maximum at 25 °C (about 198 mg/g). At 15 °C, PAA macromolecules possess nearly ideal conformation (the hydrodynamic radius is the smallest—0.53 nm). Such coiled conformation limited exposition of polymeric functional groups towards the solid surface (which interact each other forming mainly hydrogen bonds [40]) and the smallest PAA adsorption level is observed. Moreover, the temperature conditions close to theta and critical ones make polymer coils less soluble in water, which affects their tendency to accumulate at the interface. The greatest adsorption of PAA on the NE–AC surface at 25 °C is probably a result of the smaller packing of polymeric segments in adsorbed coils with larger size (R_h assumes value 0.77 nm) and the increasing affinity of the polymer to the solvent molecules, the quality of which improves. These factors enable effective interaction of polymer carboxylic groups with the surface of the NE–AC adsorbent and effective penetration of macromolecules into this solid pores. On the other hand, at 35 °C, the PAA adsorption is smaller by about 6 mg/g than at 25 °C, due to further increase of the hydrodynamic radius of the polymeric chains, which results in a more flat conformation of adsorbed PAA chains on the positively charged NE–AC surface. This results in partial blockade of the entrance

to the solid pores for adsorbing macromolecules. The temperature influence in the case of PEI and mixed adsorbate systems is rather minimal and, in most cases, it remains within the measurement error.

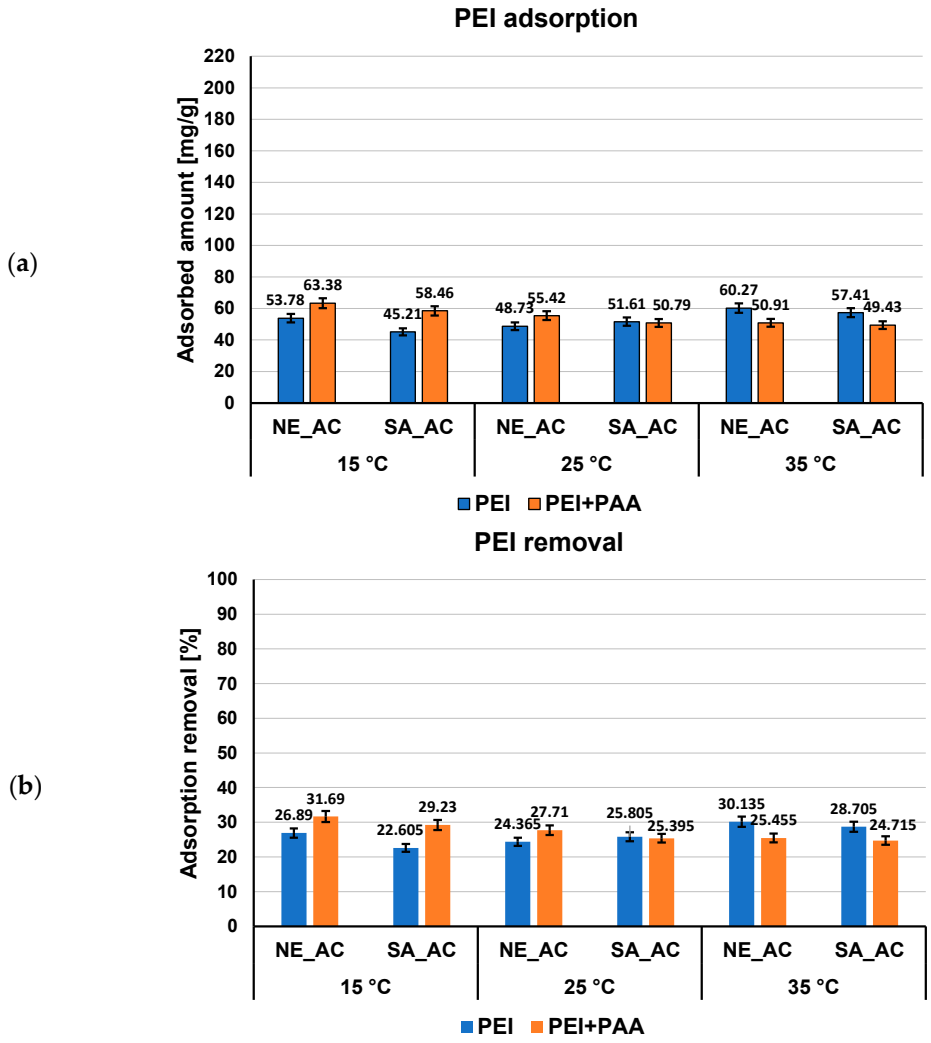

Figure 3. PEI adsorbed amounts (**a**) and its percentage removal (**b**) from the activated carbons surface in single and mixed systems of adsorbates at three examined temperatures, pH 3.

Both examined polymers show a higher affinity to the surface of activated carbons obtained from plant material than to the surface of the commercially available activated carbons (Figures 4 and 5). Moreover, the effects on mutual adsorption on the surface of LWT and PRT are opposite to that taking place during the adsorption onto NE–AC and SA–AC activated carbons. Poly(acrylic acid) is better adsorbed from the binary solutions on the surface of commercial adsorbents, whereas polyethylenimine adsorbed amounts decrease in the presence of PAA.

The kinetic studies (Figure 6) performed in the NE–AC system as a function of temperature show that the equilibrium state was reached after 60 min in the solution containing poly(acrylic acid) and after 10 min in the solution containing polyethylenimine. The obtained results of kinetic measurements were fitted to the pseudo-first order and pseudo-second order equations (Table 3). The analysis of kinetic parameters indicated that for both polymers, the pseudo-second order model described better their adsorption behavior at the activated carbon–solution interface.

Table 3. Kinetic parameters of the PAA/PEI adsorption on the NE–AC activated carbon.

Calculated Parameters	Pseudo-First Order Model			Pseudo-Second Order Model		
	q_e [mg/g]	k_1 [1/min]	R^2	q_e [mg/g]	k_2 [g/(mg·min)]	R^2
			PAA			
15 °C	1.02881	8.65444	0.8313	94.3396	0.00185	0.9982
25 °C	1.03624	7.91933	0.9420	102.041	0.00221	0.9999
35 °C	1.03241	7.22797	0.9190	71.9424	0.00472	0.9854
			PEI			
15 °C	1.02316	5.31486	0.9339	30.1205	0.00587	0.9989
25 °C	1.01329	1.22266	0.6614	20.5339	0.02061	0.9995
35 °C	1.02439	6.2257	0.8792	24.2718	0.00362	0.9949

(**a**)

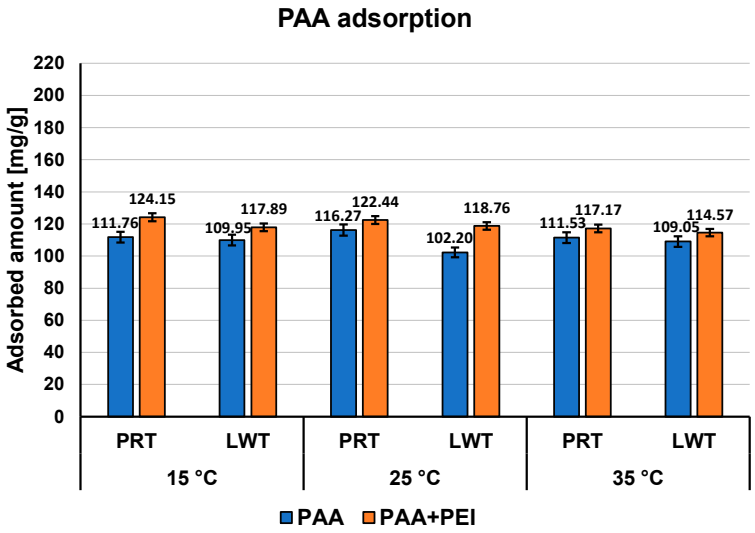

(**b**)

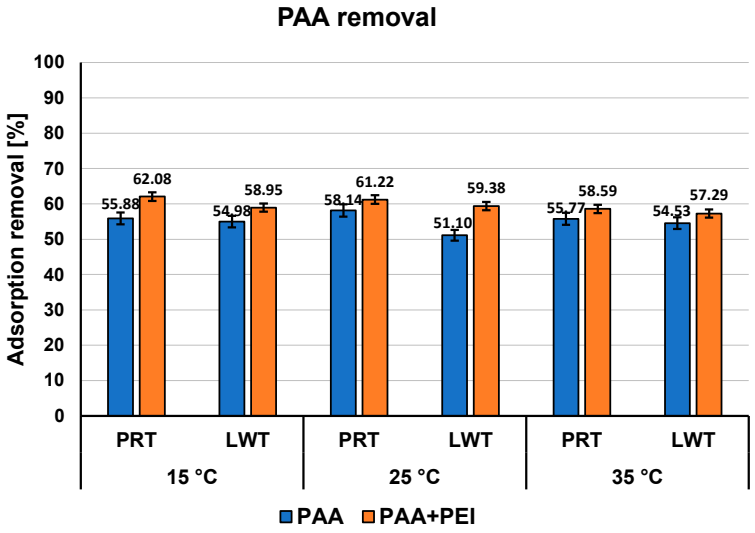

Figure 4. PAA adsorbed amounts (**a**) and its percentage removal (**b**) from the commercial materials surface in single and mixed systems of adsorbates at three examined temperatures, pH 3.

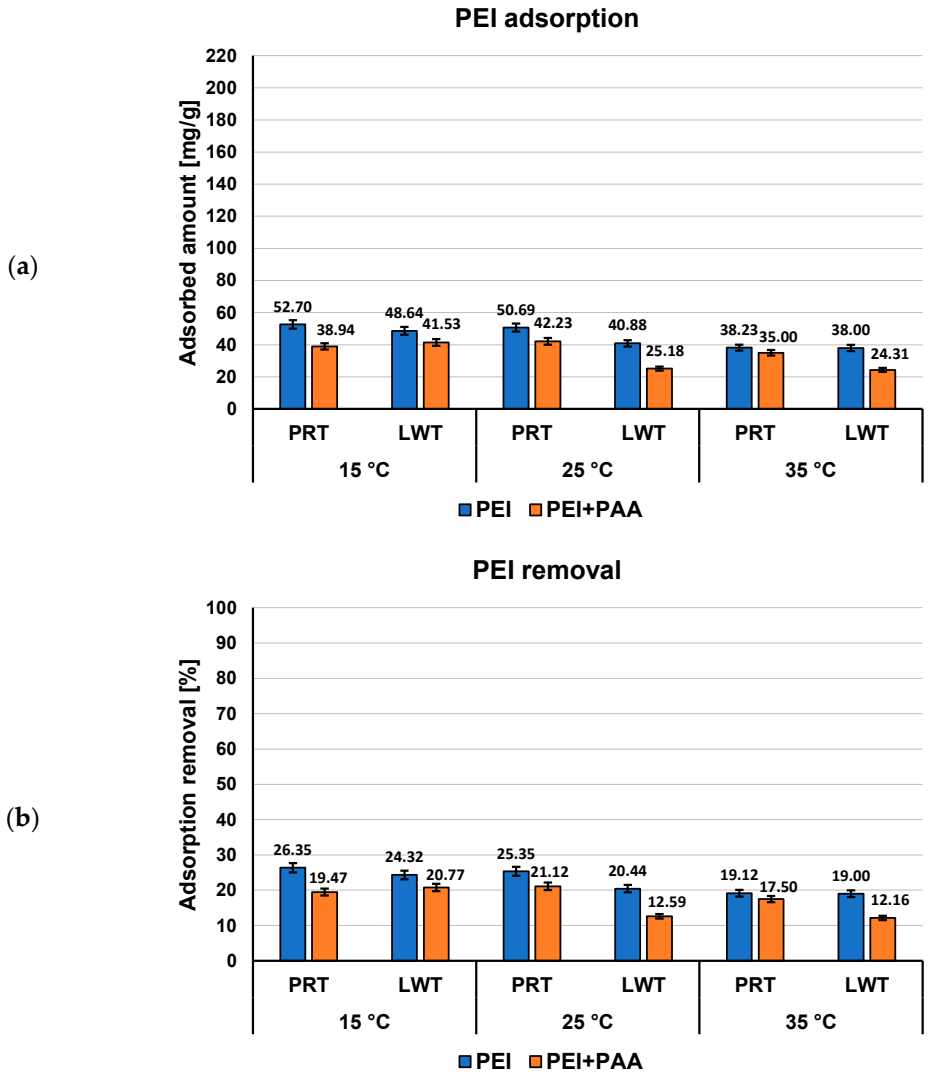

Figure 5. PEI adsorbed amounts (**a**) and its percentage removal (**b**) from the commercial materials surface in single and mixed systems of adsorbates at three examined temperatures, pH 3.

The results of the desorption studies from single and mixed systems of the examined polymers are presented in Table 4. In the case of PAA containing systems, the greatest percentages of desorption were obtained after usage of NaOH (45.5–61.23%). The HNO_3 turned out to be not very effective in the regeneration of activated carbons, similarly to H_2O. The desorption of PEI was only realized by the use of water. In this case, desorption percentages of polyethyleneimine from single systems reaches an even value of 44.15%. In the case of mixed systems of adsorbates, the PEI desorption is considerably limited due to the formation of PAA + PEI complexes [27]. This indicates that PEI bonding to the surface of examined carbon materials is much weaker than PAA macromolecules. The influence of temperature on the adsorbed polymers desorption is rather minimal.

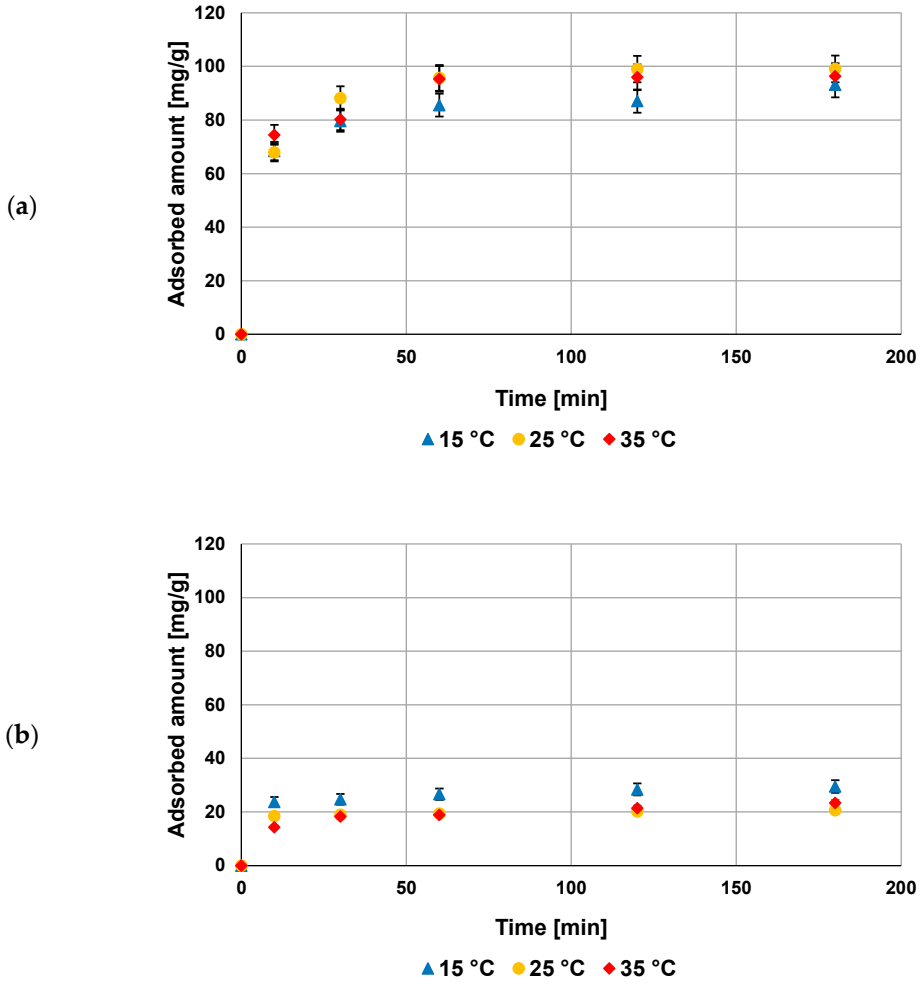

Figure 6. Adsorption kinetics of PAA (**a**) and PEI (**b**) on NE–AC activated carbon surface at three examined temperatures, pH 3.

The free energy of adsorption (ΔG^0) was calculated using Equations (8) and (9), whereas entropy and enthalpy were evaluated from the van't Hoff plots presented in Figure 7. All thermodynamic parameters are collected in Table 5.

The negative values of ΔG° at all examined temperatures show that the adsorption process of polymeric substances was spontaneous. The greatest values of ΔG° were observed in the case of the NE–AC + PAA system at 25 °C, for which the largest adsorption was obtained. The free energy of adsorption changes in the range 9.7–24.7 kJ/mol, which corresponds with the energy of hydrogen bonds formation and electrostatic interactions. The positive values of ΔH° confirmed the endothermic nature of the process. Moreover, the positive ΔS° values indicate an irregular increase of randomness at the activated carbon–polymer interface during the adsorption process.

Table 4. Percentage desorption of polymers from activated carbons surface from the single and mixed adsorbate systems under different temperature conditions.

Desorption Agent	Desorption [%]		
	H_2O	HNO_3	NaOH
	PAA, 15 °C		
NE_AC + PAA	2.44	2.93	61.23
NE_AC + PAA + PEI	3.35	4.70	50.60
SA_AC + PAA	3.86	3.84	57.58
SA_AC + PAA + PEI	4.53	5.56	55.55
	PEI, 15 °C		
NE_AC + PEI	13.97	-	-
NE_AC + PEI + PAA	2.79	-	-
SA_AC + PEI	14.81	-	-
SA_AC + PEI + PAA	0.56	-	-
	PAA, 25 °C		
NE_AC + PAA	1.36	2.76	61.01
NE_AC + PAA + PEI	1.23	1.81	47.68
SA_AC + PAA	2.53	2.00	46.45
SA_AC + PAA + PEI	1.36	2.42	48.59
	PEI, 25 °C		
NE_AC + PEI	44.15	-	-
NE_AC + PEI + PAA	4.52	-	-
SA_AC + PEI	24.73	-	-
SA_AC + PEI + PAA	9.69	-	-
	PAA, 35 °C		
NE_AC + PAA	1.55	2.90	56.65
NE_AC + PAA + PEI	2.93	8.85	45.50
SA_AC + PAA	3.91	5.34	54.10
SA_AC + PAA + PEI	5.86	8.32	53.35
	PEI, 35 °C		
NE_AC + PEI	36.28	-	-
NE_AC + PEI + PAA	5.40	-	-
SA_AC + PEI	39.29	-	-
SA_AC + PEI + PAA	4.61	-	-

Table 5. Thermodynamic parameters of PAA and PEI adsorption on activated carbons surface.

Adsorbent	T (°C)	K_c (dm^3/g)	ΔH° (kJ/mol)	ΔS° (kJ/(mol·K))	ΔG° (kJ/mol)
			PAA		
NE_AC	15	5.58	55.4	212.4	−16.8
	25	105.38			−24.7
	35	23.84			−21.7
SA_AC	15	2.17	1.1	10.3	−14.5
	25	2.22			−15.1
	35	2.24			−15.6
			PEI		
NE_AC	15	0.37	5.7		10.9
	25	0.32			
	35	0.43			
SA_AC	15	0.29	11.8		30.9
	25	0.35			
	35	0.40			

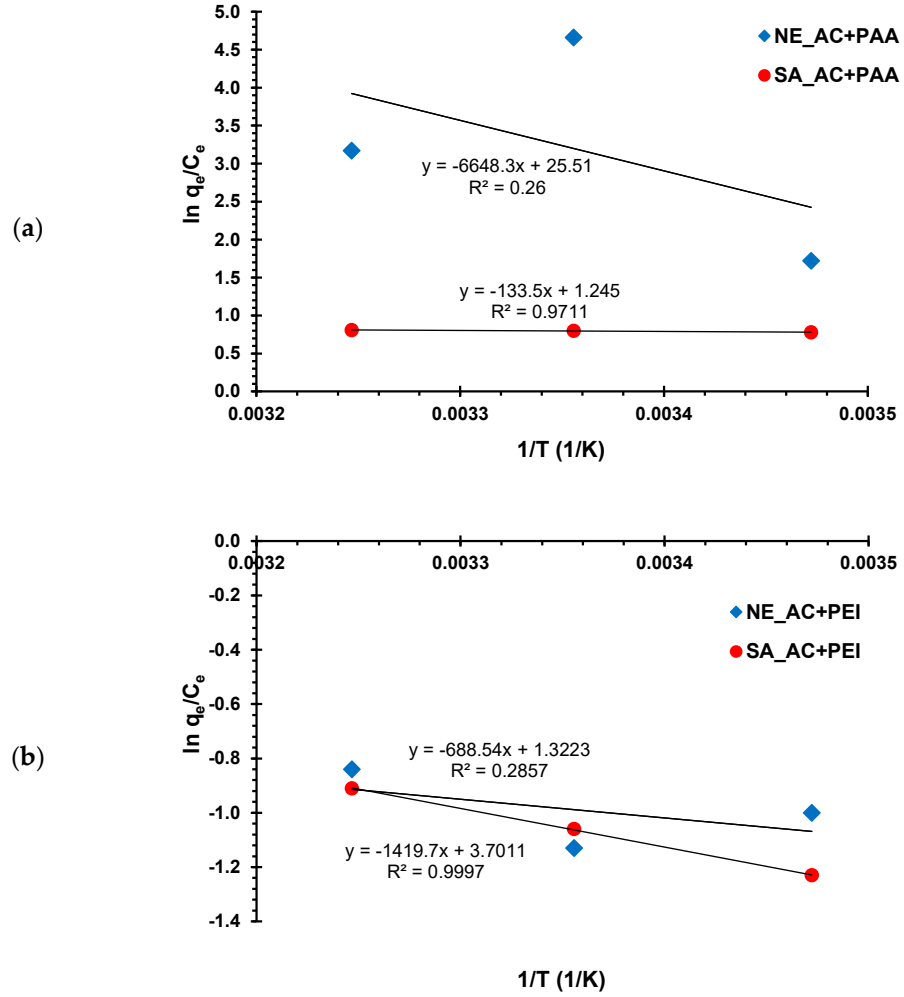

Figure 7. The van't Hoff plots for calculation of enthalpy and entropy in (**a**) PAA and (**b**) PEI—activated carbon systems.

3.3. XPS Study of Polymeric Adsorption Layers Formed on the NA–AC Activated Carbons Surface at 25 °C

The XPS spectra of the NE–AC sample obtained before and after PAA and PEI adsorption (Figures 8–10 and Table 6) confirm the formation of a polymer film on the surface of the tested activated carbon. As a result of poly(acrylic acid) adsorption, a significant decrease in carbon content is observed, accompanied by an increase in the contribution of oxygen. This proves that the polymer (rich in carboxyl groups) is permanently bonded to the adsorbent surface. In the case of the system containing NE–AC activated carbon and polyethyleneimine, a slightly different situation is observed. As a consequence of adsorption of the polymer rich in nitrogen functional species, the contribution of the nitrogen and oxygen increases simultaneously; however, the nitrogen content is almost three times higher than in the system without the polymer. This clearly indicates the permanent bonding of the polymer with the activated carbon surface. We have quite a similar relationship in case of the system containing carbonaceous adsorbent and both polymers at the same time. The increase in the content of both heteroatoms is even greater than for the previously discussed system. This may indicate mutual interactions between the molecules of individual polymers.

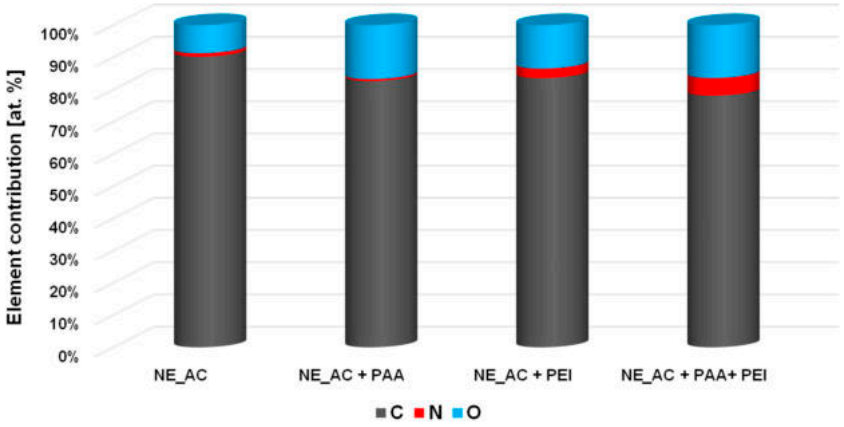

Figure 8. Elemental composition of the activated carbon's surface before and after adsorption of polymers at 25 °C [at. %].

(**a**)

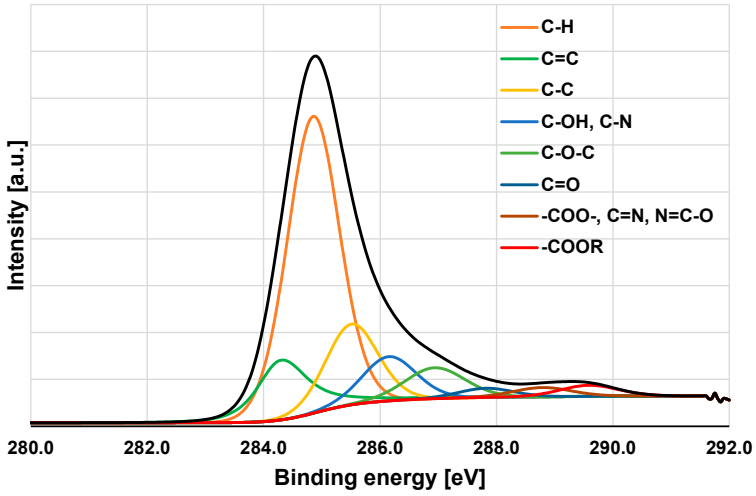

(**b**)

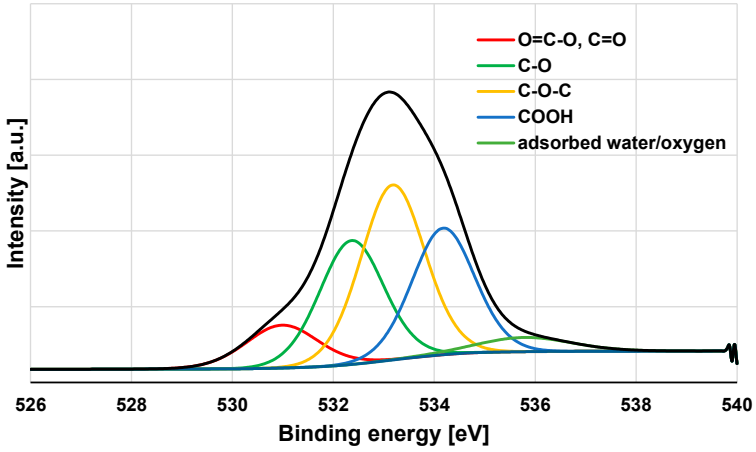

Figure 9. C 1s (**a**) and O 1s (**b**) spectra of NE–AC activated carbon before polymers adsorption.

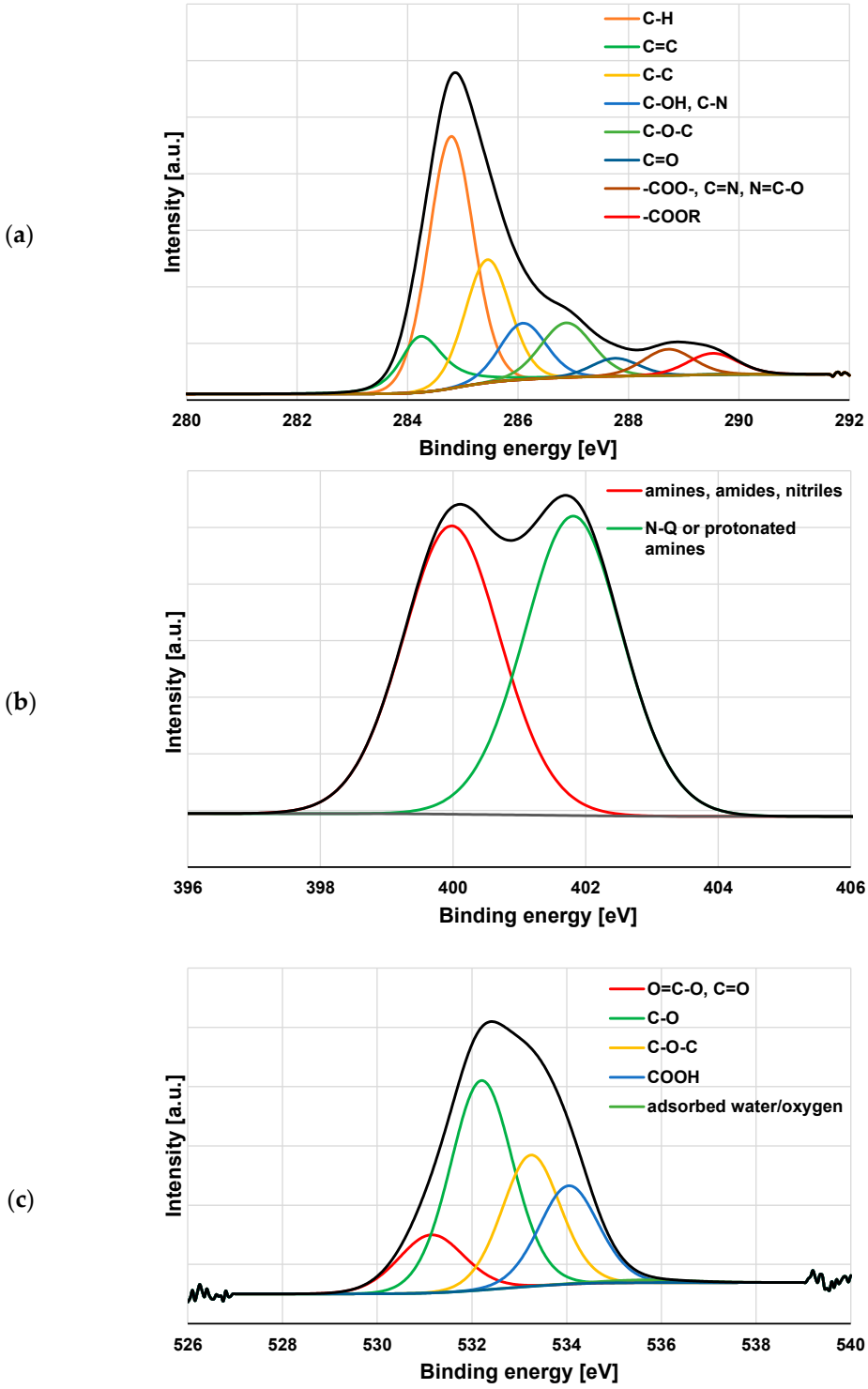

Figure 10. C 1s (**a**), N 1s (**b**) and O 1s (**c**) spectra of NE–AC activated carbon after PAA and PEI simultaneous adsorption.

According to the data presented in Table 6, as the result of both polymers adsorption, there are not only quantitative changes in the elemental carbon content at the surface, but also qualitative ones. This is especially well seen in the case of the simultaneous removal of PAA and PEI from an aqueous solution. The NE–AC sample contains carbon mainly in the form of such groups as: C-H, C=C, C-C, C-OH and C-O-C, as well as small amounts of C=O, -C=N, N=C-O and COOR. After both polymers adsorption, the contribution of C=C (284.3 eV) and, in particular, C-H (284.8 eV) [46–49] significantly decreases, while the

share of the other forms increases to different degrees. In case of the systems NE–AC + PEI and NE–AC + PEI +PAA, particularly noteworthy is the two-fold increase in the content of C=N, N=C-O (288.8 eV) [50–52] and COOR type groups (289.6 eV) [53]. In order to better illustrate the changes taking place on the activated carbon surface as a result of both polymers adsorption, the selected spectra of C 1s, N 1s and O 1s are presented in Figures 9 and 10.

Table 6. The main C 1s photopeaks of the investigated samples [47–53].

Species	Binding Energy [eV]	NE_AC	NE_AC + PAA	NE_AC + PEI	NE_AC + PAA + PEI
C-H	284.85	53.2	50.5	47.2	39.9
C=C sp^2	284.29	12.0	13.5	14.4	9.9
C-C sp^3	285.51	14.5	15.0	14.0	19.6
C-OH, C-N	286.15	8.2	6.9	5.8	9.2
C-O-C	286.94	6.4	8.3	8.4	10.0
C=O	287.82	1.7	2.1	1.8	3.0
COO-, C=N, N=C-O	288.79	1.9	2.0	4.3	4.6
COOR	289.59	2.2	1.7	4.2	3.8

4. Conclusions

The examined carbonaceous materials obtained by chemical activation of nettle and sage herbs can be used as the effective adsorbents of poly(acrylic acid) and polyethyleneimine from the aqueous solutions at different temperatures (changing in the range 15–35 °C). The temperature increase causes an increase in the linear dimensions of polymeric chains (expressed as root-mean-square chain end-to-end distance and the hydrodynamic radius) for both examined polymers. At 15 °C (very close to the PAA theta temperature), the poly(acrylic acid) coils (additionally minimally dissociated at pH 3) have the smallest dimensions (hydrodynamic radius is 0.53 nm).

Due to the total dissociation of polyethylene functional groups at pH 3, the linear dimensions of PEI macromolecules are greater than in the case of PAA. The temperature influence on the adsorbed amounts of the examined polymers is significantly greater for poly(acrylic acid) than polyethyleneimine. The largest differences occur for NE–AC activated carbon, for which the adsorption reaches its maximum at 25 °C (about 198 mg/g). This can be result of the smaller packing of polymeric segments in adsorbed coils and the increasing affinity of the polymer to the solvent molecules (facilitated penetration of macromolecules into solid pores). The thermodynamic studies indicate that the adsorption process of polymeric substances was spontaneous, has endothermic nature, and takes place mainly through hydrogen bonds formation.

It was also proved that poly(acrylic acid) is most efficiently desorbed by the use of a NaOH solution (maximal desorption about 61%). Weakly bonded polyethyleneimine undergo desorption even by water (maximal desorption about 44%). XPS studies confirmed that both polymers form stable films on the surface of the tested activated carbon, leading to significant changes in the content of carbon, oxygen and nitrogen on the border of the adsorbent–adsorbate phases.

Author Contributions: Conceptualization, M.W. and P.N.; methodology, M.W., M.G, T.U. and P.N.; validation, M.W. and M.G.; formal analysis, M.W., M.G., T.U. and P.N.; investigation, T.U., M.G. and P.N.; resources, M.W. and P.N.; data curation, M.G. and P.N; writing—original draft preparation, M.W., M.G. and P.N.; writing—review and editing, M.W., M.G. and P.N.; visualization, M.G., supervision, M.W. and P.N. All authors have read and agreed to the published version of the manuscript.

Funding: This research received no external funding.

Institutional Review Board Statement: Not applicable.

Informed Consent Statement: Not applicable.

Data Availability Statement: Data are contained within the article.

Conflicts of Interest: The authors declare no conflict of interest.

References

1. Yan, B.; Feng, L.; Zheng, J.; Zhang, Q.; Jiang, S.; Zhang, C.; Ding, Y.; Han, J.; Chen, W.; He, S. High performance supercapacitors based on wood-derived thick carbon electrodes synthesized via green activation process. *Inorg. Chem. Front.* **2022**, *9*, 6108–6123. [CrossRef]
2. Lewoyehu, M. Comprehensive review on synthesis and application of activated carbon from agricultural residues for the remediation of venomous pollutants in wastewater. *J. Anal. Appl. Pyrol.* **2021**, *159*, 105279. [CrossRef]
3. Zhang, Z.; Wang, T.; Zhang, H.; Liu, Y.; Xing, B. Adsorption of Pb(II) and Cd(II) by magnetic activated carbon and its mechanism. *Sci. Total Environ.* **2021**, *757*, 143910. [CrossRef] [PubMed]
4. Zhu, S.; Khan, M.A.; Kameda, T.; Xu, H.; Wang, F.; Xia, M.; Yoshioka, T. New insights into the capture performance and mechanism of hazardous metals Cr^{3+} and Cd^{2+} onto an effective layered double hydroxide based material. *J. Hazard. Mat.* **2022**, *426*, 128062. [CrossRef] [PubMed]
5. Guan, X.; Yuan, X.; Zhao, Y.; Bai, J.; Li, Y.; Cao, Y.; Chen, Y.; Xiong, T. Adsorption behaviors and mechanisms of Fe/Mg layered double hydroxide loaded on bentonite on Cd (II) and Pb (II) removal. *J. Colloid Interf. Sci.* **2022**, *612*, 572–583. [CrossRef] [PubMed]
6. Jjagwe, J.; Olupot, P.W.; Menya, E.; Kalibbala, H.M. Synthesis and application of Granular activated carbon from biomass waste materials for water treatment: A review. *J. Biores. Bioprod.* **2021**, *6*, 292–322. [CrossRef]
7. Obey, G.; Adelaide, M.; Ramaraj, R. Biochar derived from non-customized matamba fruit shell as an adsorbent for wastewater treatment. *J. Biores. Bioprod.* **2022**, *7*, 109–115. [CrossRef]
8. Sojka, R.E.; Bjorneberg, D.L.; Entry, J.A.; Lentz, R.D.; Orts, W.J. Polyacrylamide in agriculture and environmental land management. *Adv. Agron.* **2007**, *92*, 75–162. [CrossRef]
9. Abidin, A.Z.; Puspasari, T.; Nugroho, W.A. Polymers for enhanced oil recovery technology. *Proc. Chem.* **2012**, *4*, 11–16. [CrossRef]
10. Huang, D.L.; Wang, R.Z.; Liu, Y.G.; Zeng, G.M.; Lai, C.; Xu, P.; Lu, B.A.; Xu, J.J.; Wang, C.; Huang, C. Application of molecularly imprinted polymers in wastewater treatment: A review. *Environ. Sci. Pollut. Res.* **2015**, *22*, 963–977. [CrossRef]
11. Sung, Y.K.; Kim, S.W. Recent advances in polymeric drug delivery systems. *Biomat. Res.* **2020**, *24*, 12. [CrossRef] [PubMed]
12. Mitura, S.; Sionkowska, A.; Jaiswal, A. Biopolymers for hydrogels in cosmetics: Review. *J. Mat. Sci. Mat. Med.* **2020**, *31*, 50. [CrossRef] [PubMed]
13. Jarpa-Parra, M.; Chen, L. Applications of Plant Polymer-Based Solid Foams: Current Trends in the Food Industry. *Appl. Sci.* **2021**, *11*, 9605. [CrossRef]
14. Shen, Z.; Rajabi-Abhari, A.; Oh, K.; Lee, S.; Chen, J.; He, M.; Lee, H.L. The Effect of a Polymer-Stabilized Latex Cobinder on the Optical and Strength Properties of Pigment Coating Layers. *Polymers* **2021**, *13*, 568. [CrossRef]
15. Bolto, B.; Xie, Z. The Use of Polymers in the Flotation Treatment of Wastewater. *Processes* **2019**, *7*, 374. [CrossRef]
16. Li, Z.; Zhong, S.; Lei, H.; Chen, R.; Yu, Q.; Li, H.L. Production of novel bioflocculant by Bacillus licheniformis X14 and its application to low temperature drinking water treatment. *Biores. Tech.* **2009**, *100*, 3650–3656. [CrossRef] [PubMed]
17. Ang, T.; Kiatkittipong, K.; Kiatkittipong, W.; Chua, S.; Lim, J.W.; Show, P.; Bashir, M.J.K.; Ho, Y. Insight on extraction and characterisation of biopolymers as the green coagulants for microalgae harvesting. *Water* **2020**, *12*, 1388. [CrossRef]
18. Wu, Q.; Dong, S.; Wang, L.; Li, X. Single and competitive adsorption behaviors of Cu^{2+}, Pb^{2+} and Zn^{2+} on the biochar and magnetic biochar of pomelo peel in aqueous solution. *Water* **2021**, *13*, 868. [CrossRef]
19. Maged, A.; Dissanayake, P.D.; Yang, X.; Pathirannahalage, C.; Bhatnagar, A.; Ok, Y.S. New mechanistic insight into rapid adsorption of pharmaceuticals from water utilizing activated biochar. *Environ. Res.* **2021**, *202*, 111693. [CrossRef]
20. Wiśniewska, M.; Nowicki, P. Simultaneous removal of lead(II) ions and poly(acrylic acid) macromolecules from liquid phase using of biocarbons obtained from corncob and peanut shell precursors. *J. Molec. Liq.* **2019**, *296*, 111806. [CrossRef]
21. Zhu, S.; Ye, Z.; Liu, Z.; Chen, Z.; Li, J.; Xiang, Z. Adsorption Characteristics of Polymer Solutions on Media Surfaces and Their Main Influencing Factors. *Polymers* **2021**, *13*, 1774. [CrossRef] [PubMed]
22. Chornaya, V.; Lipatov, Y.; Todosijchuk, T.; Menzheres, G. Effect of Temperature on the Structure of Adsorption Layers Formed by Adsorption of Polymers in the Transition Region from Dilute to Semidilute Solutions. *J. Colloid Interf. Sci.* **2002**, *255*, 36–43. [CrossRef]
23. Wiśniewska, M. A Review of Temperature Influence on Adsorption Mechanism and Conformation of Water Soluble Polymers on the Solid Surface. *J. Disp. Sci. Tech.* **2011**, *32*, 1605–1623. [CrossRef]
24. Flory, P.J. *Principles of Polymer Chemistry*; Cornell University Press: Ithaca, NY, USA, 1953.
25. Brochard, F.; De Gennes, P.G. Dynamical scaling for polymers in theta solvents. *Macromolecules* **1997**, *10*, 1157–1161. [CrossRef]
26. Zhao, D.; Schneider, D.; Fytas, G.; Kumar, S.K. Controlling the thermomechanical behavior of nanoparticle/polymer films. *ACS Nano* **2014**, *8*, 8163–8173. [CrossRef] [PubMed]
27. Gęca, M.; Wiśniewska, M.; Nowicki, P. Simultaneous Removal of Polymers with Different Ionic Character from Their Mixed Solutions Using Herb-Based Biochars and Activated Carbons. *Molecules* **2022**, *27*, 7557. [CrossRef] [PubMed]
28. Boehm, H.P.; Diehl, E.; Heck, W.; Sappok, R. Surface oxides of carbon. *Angew. Chem. Int. Ed.* **1964**, *3*, 669–677. (In English) [CrossRef]

29. Wiśniewska, M. Study of the influence of temperature and the ionic strength of the solution on the adsorption and conformation of poly(acrylic acid) macromolecules on the ZrO_2 surface. *Ads. Sci. Tech.* **2006**, *24*, 673–686. [CrossRef]
30. Von Harpe, A.; Petersen, H.; Li, Y.; Kissel, T. Characterization of commercially available and synthesized polyethylenimines for gene delivery. *J. Control. Release* **2000**, *69*, 309–322. [CrossRef] [PubMed]
31. Mohanty, J.N.; Nayak, P.L.; Lenka, S. Determination of unperturbated dimensions of polymers in binary solvent mixtures from viscosity measurements. *Colloid Polym. Sci.* **1987**, *265*, 982–985. [CrossRef]
32. Garvey, M.J.; Tadros, T.F.; Vincent, B. A comparison of the volume occupied by macromolecules in the adsorbed state and in bulk solution: Adsorption of narrow molecular weight fractions of poly (vinyl alcohol) at the polystyrene/water interface. *J. Colloid Interf. Sci.* **1974**, *49*, 57–68. [CrossRef]
33. Fox, T.G., Jr.; Fox, J.C.; Flory, P.J. The Effect of Rate of Shear on the Viscosity of Dilute Solutions of Polyisobutylene. *J. Am. Chem. Soci.* **1951**, *73*, 1901–1904. [CrossRef]
34. Crummett, W.B.; Hummel, R.A. The determination of traces of polyacrylamides in water. *J. Am. Water Works Assoc.* **1963**, *1*, 55, 209–219. [CrossRef]
35. Patkowski, J.; Myśliwiec, D.; Chibowski, S. Validation of a new method for spectrophotometric determination of polyethylenimine. *Int. J. Polym. Anal. Charact.* **2016**, *21*, 486–494. [CrossRef]
36. Ho, Y.S.; McKay, G. Sorption of dye from aqueous solution by peat. *Chem. Eng. J.* **1998**, *70*, 115–124. [CrossRef]
37. Liu, Y. Is the free energy change of adsorption correctly calculated? *J. Chem. Eng. Data* **2009**, *54*, 1981–1982. [CrossRef]
38. Muhammad, A.; Shah, A.H.A.; Bilal, S.; Rahman, G. Basic blue dye adsorption from water using polyaniline/magnetite (Fe_3O_4) composites: Kinetic and thermodynamic aspects. *Materials* **2019**, *12*, 1764. [CrossRef] [PubMed]
39. Wiśniewska, M.; Wawrzkiewicz, M.; Onyszko, M.; Medykowska, M.; Nosal-Wiercińska, A.; Bogatyrov, V. Carbon-Silica Composite as Adsorbent for Removal of Hazardous, C.I. Basic Yellow 2 and C.I. Basic Blue 3 Dyes. *Materials* **2021**, *14*, 3245. [CrossRef]
40. Wiśniewska, M.; Nowicki, P. Peat-based activated carbons as adsorbents for simultaneous separation of organic molecules from mixed solution of poly(acrylic acid) polymer and sodium dodecyl sulfate surfactant. *Colloids Surf. A* **2020**, *585*, 124179. [CrossRef]
41. Chibowski, S.; Wiśniewska, M.; Opala Mazur, E. The effect of temperature on the adsorption and conformation of polyacrylic acid macromolecules at the ZrO_2–polymer solution interface. *Powder Tech.* **2004**, *141*, 12–19. [CrossRef]
42. Silberberg, A.; Eliassaf, J.; Katchalsky, A. Temperature-dependence of light scattering and intrinsic viscosity of hydrogen bonding polymers. *J. Polym. Sci.* **1957**, *23*, 259–284. [CrossRef]
43. Flemming, P.; Münch, A.S.; Fery, A.; Uhlmann, P. Constrained thermoresponsive polymers–new insights into fundamentals and applications. *Beilstein J. Org. Chem.* **2021**, *17*, 2123–2163. [CrossRef]
44. Gibson, F.W. Stabilization of Submicron Metal Oxide Particles in Aqueous Media. Ph.D. Thesis, Virginia Tech, Blacksburg, Virginia, 1998.
45. Fukuda, Y.; Abe, D.; Tanaka, Y.; Uchida, J.; Suzuki, N.; Miyai, T.; Sasanuma, Y. Solution properties of poly(N-methylethylene imine), a highly hydrophilic polycation. *Polym. J.* **2016**, *48*, 1065–1072. [CrossRef]
46. Yan, B.; Zheng, J.; Feng, L.; Du, C.; Jian, S.; Yang, W.; Wu, Y.A.; Jiang, S.; He, S.; Chen, W. Wood-derived biochar as thick electrodes for high-rate performance supercapacitors. *Biochar* **2022**, *4*, 50. [CrossRef]
47. Kim, C.; Zhu, C.; Aoki, Y.; Habazaki, H. Heteroatom-doped porous carbon with tunable pore structure and high specific surface area for high performance supercapacitors. *Electrochim. Acta* **2019**, *314*, 173–187. [CrossRef]
48. Zheng, S.; Zhang, J.; Deng, H.; Du, Y.; Shi, X. Chitin derived nitrogen-doped porous carbons with ultrahigh specific surface area and tailored hierarchical porosity for high performance supercapacitors. *J. Bioresour. Bioprod.* **2021**, *6*, 142–151. [CrossRef]
49. Koinuma, M.; Tateishi, H.; Hatakeyama, K.; Miyamoto, S.; Ogata, C.; Funatsu, A.; Taniguchi, T.; Matsumoto, Y. Analysis of reduced graphene oxides by X-ray Photoelectron spectroscopy and electrochemical capacitance. *Chem. Lett.* **2013**, *42*, 924–926. [CrossRef]
50. Teng, W.; Zhou, Q.; Wang, X.; Che, H.; Du, Y.; Hu, P.; Li, H.; Wang, J. Biotemplating preparation of N,O-codoped hierarchically porous carbon for high-performance supercapacitors. *Appl. Surf. Sci.* **2021**, *566*, 150613. [CrossRef]
51. Rabchinskii, M.K.; Ryzhkov, S.A.; Kirilenko, D.A.; Ulin, N.V.; Baidakova, M.V.; Shnitov, V.V.; Pavlov, S.I.; Chumakov, R.G.; Stolyarova, D.Y.; Besedina, N.A.; et al. From graphene oxide towards aminated graphene: Facile synthesis, its structure and electronic properties. *Sci. Rep.* **2020**, *10*, 6902. [CrossRef]
52. Nowicki, P.; Pietrzak, R.; Wachowska, H. X-ray Photoelectron spectroscopy study of nitrogen-enriched active carbons obtained by ammoxidation and chemical activation of brown and bituminous coals. *Energy Fuels* **2010**, *24*, 1197–1206. [CrossRef]
53. Radaelli, G.; Heredia-Guerrero, J.A.; Masood, M.T.; Ceseracciu, L.; Davis, A.; Carzino, R.; Prato, M.; Bayer, I.S.; Athanassiou, A. Highly Effective antiadhesive coatings from ph-modified water-dispersed perfluorinated acrylic copolymers: The case of vulcanizing rubber. *Adv. Mater. Interf.* **2016**, *3*, 1600069. [CrossRef]

Lublin, 10.09.2025

mgr Marlena Groszek
Uniwersytet Marii Curie-Skłodowskiej w Lublinie,
Wydział Chemii, Instytut Nauk Chemicznych,
Katedra Radiochemii i Chemii Środowiskowej,
Pl. Marii Curie-Skłodowskiej 3, 20-031 Lublin
marlena.groszek@mail.umcs.pl

Rada Naukowa Instytutu Nauk Chemicznych
Uniwersytetu Marii Cure-Skłodowskiej
w Lublinie

Oświadczenie o współautorstwie

Niniejszym oświadczam, że mój udział w pracy: **M. Gęca**, M. Wiśniewska, T. Urban, P. Nowicki, *Temperature Effect on Ionic Polymers Removal from Aqueous Solutions Using Activated Carbons Obtained from Biomass,* Materials, 16, 2022, 350. DOI: 10.3390/ma16010350 [D7], obejmował opracowanie metodyki badań, przeprowadzenie eksperymentów, analizę uzyskanych wyników, przygotowanie manuskryptu i jego korektę po procesie oceny w redakcji oraz sformułowanie odpowiedzi na uwagi recenzentów.

Marlena Groszek

Lublin, 10.09.2025

prof. dr hab. Małgorzata Wiśniewska
Uniwersytet Marii Curie-Skłodowskiej w Lublinie,
Wydział Chemii, Instytut Nauk Chemicznych,
Katedra Radiochemii i Chemii Środowiskowej,
Pl. Marii Curie-Skłodowskiej 3, 20-031 Lublin
malgorzata.wisniewska@mail.umcs.pl

Rada Naukowa Instytutu Nauk Chemicznych
Uniwersytetu Marii Cure-Skłodowskiej
w Lublinie

Oświadczenie o współautorstwie

Niniejszym oświadczam, że mój udział w pracy: M. Gęca, **M. Wiśniewska**, T. Urban, P. Nowicki, *Temperature Effect on Ionic Polymers Removal from Aqueous Solutions Using Activated Carbons Obtained from Biomass,* Materials, 16, 2022, 350. DOI: 10.3390/ma16010350 [D7], obejmował stworzenie koncepcji artykułu, opracowanie metodyki badań, interpretację uzyskanych wyników, korektę manuskryptu – przed i po procesie recenzji oraz nadzór merytoryczny w czasie całego cyklu wydawniczego.

Małgorzata Wiśniewska

Lublin, 10.09.2025

dr Teresa Urban
Uniwersytet Marii Curie-Skłodowskiej w Lublinie,
Wydział Chemii, Instytut Nauk Chemicznych,
Katedra Radiochemii i Chemii Środowiskowej,
Pl. Marii Curie-Skłodowskiej 3, 20-031 Lublin
teresa.urban@mail.umcs.pl

Rada Naukowa Instytutu Nauk Chemicznych
Uniwersytetu Marii Cure-Skłodowskiej
w Lublinie

Oświadczenie o współautorstwie

Niniejszym oświadczam, że mój udział w pracy: M. Gęca, M. Wiśniewska, **T. Urban**, P. Nowicki, *Temperature Effect on Ionic Polymers Removal from Aqueous Solutions Using Activated Carbons Obtained from Biomass,* Materials, 16, 2022, 350. DOI: 10.3390/ma16010350 [D7], obejmował opracowanie metodyki badań, przeprowadzenie eksperymentów i analizę uzyskanych wyników.

Urban Teresa

Poznań, 10.09.2025

dr hab. Piotr Nowicki, prof. UAM
Uniwersytet im. Adama Mickiewicza w Poznaniu,
Wydział Chemii, Zakład Chemii Stosowanej,
Ul. Uniwersytetu Poznańskiego 8, 61-614 Poznań
piotr.nowicki@amu.edu.pl

Rada Naukowa Instytutu Nauk Chemicznych
Uniwersytetu Marii Cure-Skłodowskiej
w Lublinie

Oświadczenie o współautorstwie

Niniejszym oświadczam, że mój udział w pracy M. Gęca, M. Wiśniewska, T. Urban, **P. Nowicki**, *Temperature Effect on Ionic Polymers Removal from Aqueous Solutions Using Activated Carbons Obtained from Biomass,* Materials, 16, 2022, 350. DOI: 10.3390/ma16010350 [D7], obejmował stworzenie koncepcji artykułu, opracowanie metodyki badań, przeprowadzenie eksperymentów, analizę uzyskanych wyników, korektę manuskryptu – przed i po procesie recenzji oraz nadzór merytoryczny w czasie całego cyklu wydawniczego.

Piotr Nowicki

D8. M. Gęca, M. Wiśniewska, P. Nowicki, K. Jędruchniewicz, *Cd(II) and As(V) removal from the multicomponent solutions in the presence of ionic polymers using carbonaceous adsorbents obtained from herbs,* Pure and Applied Chemistry, 2023, 95, 5, 563-578, DOI: 10.1515/pac-2023-020

Conference paper

Marlena Gęca*, Małgorzata Wiśniewska, Piotr Nowicki and Katarzyna Jędruchniewicz

Cd(II) and As(V) removal from the multicomponent solutions in the presence of ionic polymers using carbonaceous adsorbents obtained from herbs

https://doi.org/10.1515/pac-2023-0201

Abstract: Biochars and activated carbons obtained from the nettle and the sage herbs were used for Cd(II), As(V), poly(acrylic acid) and polyethylenimine simultaneous adsorption from the multicomponent aqueous solutions. Electrokinetic studies proved that both activated carbons show acidic character of the surface. The point of zero charge of the sample obtained from the nettle herb occurs at pH 3.1, whereas that of the adsorbent obtained from the sage herb at pH 4.0. Cd(II) adsorption causes the decrease in the surface charge density and the zeta potential of both activated carbons, whereas As(V) addition results in the increase of solid surface charge density and its impact on the zeta potential value depends on adsorbent type. In case of the simultaneous presence of metals and polymers, the adsorbed macromolecules have greater influence on the surface charge density and the zeta potential values than the metal ions. Cd(II) and As(V) are well adsorbed on the examined activated carbons irrespective of the solution pH (changing in the range 3–9). Maximum adsorption were 218.27 mg/g for Cd(II) and 205.53 mg/g for As(V). The polymers presence causes a decrease (80–90 %) of both metal ions adsorbed amounts, whereas the poly(acrylic acid) and polyethylenimine adsorption mechanism in the presence of cadmium and arsenic ions depends on the adsorbent type and polymer-metal interactions.

Keywords: Activated carbons; biochars; heavy metals adsorption; ICGC-9; plant precursors; polymers and metals simultaneous removal.

Introduction

Heavy metals are one of the most dangerous environment pollution. They are considered as the most lethal, inorganic, anthropogenic contaminants [1]. They are one of the most common water and soil pollutants due to their great solubility. For the all above mentioned reasons heavy metal ions should be effectively removed from water. The current wastewater treatment methods are strongly related to their economic aspects [2]. Thus, new, cheap methods of sewage treatment should be constantly developed and elaborated.

Cadmium is a heavy metal which is delivered to the environment from the agricultural and industrial sources. This is a very dangerous element due to its accumulation in plants and animals with the long-life time

Article note: A collection of invited papers based on presentations at the 9th International Conference on Green Chemistry (ICGC-9) held in Athens, Greece, 5–9 September 2022.

***Corresponding author: Marlena Gęca**, Department of Radiochemistry and Environmental Chemistry, Institute of Chemical Sciences, Faculty of Chemistry, Maria Curie-Skłodowska University in Lublin, M. Curie-Skłodowska Sq. 3, 20-031 Lublin, Poland, e-mail: marlena.geca@wp.pl

Małgorzata Wiśniewska and Katarzyna Jędruchniewicz, Department of Radiochemistry and Environmental Chemistry, Institute of Chemical Sciences, Faculty of Chemistry, Maria Curie-Skłodowska University in Lublin, M. Curie-Skłodowska Sq. 3, 20-031 Lublin, Poland

Piotr Nowicki, Department of Applied Chemistry, Faculty of Chemistry, Adam Mickiewicz University in Poznań, Uniwersytetu Poznańskiego 8, 61-614 Poznań, Poland

equal 25–30 years [3]. Cd(II) present in plants affects the nitrate absorption and transport. It also inhibits the photosynthesis which can slow down growth and reduce the efficiency of the process [4]. In the human body cadmium changes the DNA expression, inhibits the heme synthesis and impairs the mitochondrial function potentially inducing apoptosis [5]. According to the World Health Organization the cadmium concentration in the drinking water should not exceed 0.003 mg/dm^3 [6].

The Cd(II) and As(V) can be successfully adsorbed on the surface of nanoparticles [7–9]. However their removal from aqueous solution is difficult due to the low particles size. The carbonaceous materials don't have this disadvantages because they have highly developed specific surface area and their modification is rather simple. The surface complexation and precipitation are the prevailing mechanisms of Cd(II) adsorption on the surface of carbonaceous adsorbents [10, 11]. The cadmium adsorbed amounts are greater at pH below 7, above this value Cd(II) precipitates from solution which make the adsorption studies impossible. The studies on the cadmium adsorption in the presence of other heavy metals showed that Cd(II) is more effectively adsorbed from the single solution [12–14]. The obtained maximum Cd(II) adsorbed amount on the surface of biochar derived from cannabis was 175.43 mg/g [15].

In nature arsenic is commonly associated with gold, copper and lead ores. This is a highly toxic element, however, it is essential for some organisms life [16]. Arsenic toxicity depends on its form, the inorganic arsenicals are more toxic than the organic ones. The most common toxic mode of this element is the inactivation of enzyme systems [17]. Arsenic is a carcinogen element exerting a negative effect on almost all human organs [18]. Despite the risks described above, arsenic is still present in some drinking water reservoirs [19]. The WHO guideline for the arsenic concentration in the drinking water is 10 mg/dm^3 [20].

Adsorption is one of the main methods of As(V) removal from water. Metal oxides, zero-valent iron and iron composites are used for this purpose. However, arsenic removal from aqueous solution using the adsorbent of natural origin are the most effective method [21]. The iron-modified activated carbons and biochars are most widely used of all carbonaceous materials. The iron modification increases the arsenic adsorbed amount in comparison to the analogues commercial non-modified adsorbents. The chemical adsorption proved to be the main mechanism. In general As(V) is better adsorbed from the acidic solution [22, 23]. The mixture of apricot, peach stones and almond shells biochars was the most effective for As(V) removal (42.92 mg/g) [24–29].

In the present studies the biochars and activated carbons obtained from the nettle and the sage herbs were used as Cd(II), As(V), anionic poly(acrylic acid) and cationic polyethylenimine adsorbents. To determine the adsorption mechanisms the electrokinetic properties of carbonaceous materials in the metals and polymers presence were studied. The assessment of the pH effect on the Cd(II) and As(V) adsorbed amount was also done. Moreover, the adsorption kinetics was examined and the most probable adsorption mechanisms were proposed. The heavy metal ions and ionic polymers effect on the simultaneous adsorption on the biochars and activated carbons surface was also studied. Additionally, the regeneration possibilities of exhausted materials were examined and the most effective desorbing agents were selected. The presented studies have innovatory character, because the usage of biochars and activated carbons for the simultaneous metals and polymers removal from the aqueous solutions is extremely rarely described in the literature [29–32]. What is more, the ionic polymers adsorption from their single systems is also poorly discussed. The increasing usage of polymers in the various branches of industry resulted in an increase in their concentration detected in the wastewaters. For this reason, it is necessary to found new, effective, simple and cheap methods of macromolecules removal from aqueous solution. Moreover, the possibility of desorption of these substances (enabling adsorbent regeneration) is extremely important, which allow them to be used multiple times and significant reduce the reagent costs.

Experimental

Materials

Biochars (B) and activated carbons (AC) obtained from the nettle (NE) and the sage (SA) herbs were used as adsorbents. The preparation and characterization of the obtained materials were described in our previous paper [33]. The solids textural parameters and acidic-basic properties are summarised in Table 1.

Table 1: Textural parameters and acidic-basic properties of the activated carbons and biochars.

Adsorbent	Surface area [m^2/g]	Pore volume [cm^3/g]	Mean pore size [nm]	Acidic groups concentration [mmol/g]	Basic groups concentration [mmol/g]	Total surface groups concentration [mmol/g]
NE_B	2.527	0.006	9.594	1.041	1.753	2.794
SA_B	2.182	0.006	10.555	1.109	1.008	2.197
NE_AC	800.760	0.847	4.231	0.858	0.272	1.130
SA_AC	841.955	0.826	3.926	0.436	0.215	0.651

The applied poly(acrylic acid) (PAA) (Fluka, Saint Louis, USA) is a weak polyelectrolyte with the anionic character (originating from the carboxyl groups present in its molecules) with the average molecular weight equal 2000 Da. The PAA pK_a value is about 4.5, so at pH 3 its ionization is minimal [34]. On the other hand, polyethylenimine (PEI) (Sigma Aldrich, Saint Louis, USA) is a cationic polymer (amine groups present in the polymeric chains) characterized by the average molecular weight equal 2000 Da. The PEI pK_b is about 9, at pH 3 it is almost completely dissociated [35].

The sources of metal ions were $CdN_2O_6{\cdot}4H_2O$ and KH_2AsO_4 (Sigma Aldrich, Saint Louis, USA). Cadmium nitrate tetrahydrate is well soluble in water but only at pH below 8. Cd(II) precipitates at pH above 8, and due to this limitation all analyses with the cadmium usage were conducted at pH below 8. Potassium arsenate is well soluble at all examined pH values, however, the hydration of AsO_4^{3-} ions changes. At low pH the arsenate ions are fully hydrated and with the increasing pH value the hydration level decreases – the following forms occur in the aqueous solution: H_3AsO_4, H_2AsO^{4-}, $HAsO_4^{2-}$, AsO_4^{3-}.

Surface and electrokinetic parameters determination

All measurements were performed at 25 °C in the suspensions without as well as with single or binary adsorbates. The examined systems were as follows: NE_B + NaCl, NE_AC + NaCl, NE_AC + NaCl + Cd, NE_AC + NaCl + Cd + PAA, NE_AC + NaCl + Cd + PEI, NE_AC + NaCl + As, NE_AC + NaCl + As + PAA, NE_AC + NaCl + As + PEI, SA_B + NaCl, SA_AC + NaCl, SA_AC + NaCl + Cd, SA_AC + NaCl + Cd + PAA, SA_AC + NaCl + Cd + PEI, SA_AC + NaCl + As, SA_AC + NaCl + As + PAA and SA_AC + NaCl + As + PEI.

The determination of the surface charge density (σ_0) of the biochars and activated carbons particles without or with the selected adsorbates was made applying the potentiometric titration method. 50 cm^3 of the suspension containing the examined adsorbates (with the initial concentration (C_0) 100 ppm), the NaCl supporting electrolyte (with the concentration 0.001 mol/dm^3) and 0.025 g of NE_AC, 0.024 g of SA_AC or 0.5 g of biochars was used for that purpose. The examined solution was placed in the thermostated Teflon vessel (RE 204 thermostat, Lauda Scientific, Lauda-Königshofen, Germany), in which the glass and calomel electrodes (Beckman Instruments, Brea, USA) were introduced to monitor the pH changes (pHM 240 pH meter, Radiometer, Warsaw, Poland) after each portion of the added titrant – NaOH with the concentration of 0.1 mol/dm^3 (automatic Dosimat 765 microburette, Metrohm, Herisau, Switzerland) The measurements were performed at 25 °C. The changes in the σ_0 value as a function of solution pH were calculated with the computer program "Titr_v3", which controlled also the course of the titration process. These calculations were based on the difference in the titrant volume added to the suspension and the supporting electrolyte solution providing the specified pH value [36].

The zeta potential (ζ) of the activated carbon and the biochar particles without and with the selected adsorbates was determined using the following procedure. The 200 cm^3 suspensions containing the examined metals and polymers with the concentration 100 ppm, NaCl supporting electrolyte (0.001 mol/dm^3) and 0.03 g of the solid were prepared. The system was subjected to the action of ultrasounds (XL 2020 ultrasonic head, Misonix, Farmingdale, USA) for 3 min and divided into several parts. In each of the obtained samples a different pH value (changing in the range from 3 to 11 for As(V), and from 3 to 7 for Cd(II)) was adjusted. For this purpose the solutions of HCl and NaOH with the concentrations 0.1 mol/dm^3 as well as Φ360 pH – meter (Beckman, Brea, USA) were used.

The measurements were made applying the Doppler laser electrophoresis method and Zetasizer Nano ZS (Malvern Instruments, Malvern, United Kingdom). This apparatus allowed to measure the electrophoretic mobility of the solid particles without and covered with the adsorption layers. Based on the obtained results, the zeta potential (ζ) was calculated using the Henry's equation [37]. Moreover, the average aggregate sizes of the examined solids formed at pH 3, 6 and 9 (only for the As(V) containing systems) in the analogous suspensions were determined using the above mentioned apparatus (based on the static light scattering phenomenon).

Adsorption-desorption studies

The adsorbed amounts of all substances were determined at 25 °C using the static method based on the decrease in the Cd(II), As(V), PAA or PEI concentrations in the solutions before and after the adsorption process. The Cd(II) and As(V) concentrations were established by the Inductively Coupled Plasma-Optical Emission Spectrometry (iCAP™ 7200 ICP-OES analyzer, Thermo Fisher Scientific, Waltham, USA). In turn, the polymers concentrations were determined using the UV–VIS spectrophotometry (Carry 100, Varian, Palo Alto, USA). Due to the fact that neither PAA nor PEI absorbs light, the poly(acrylic acid) concentration was obtained based on its reaction with hyamine 1622, which gives a white-coloured complex absorbing light at the wavelength 500 nm [38]. On the other hand, the polyethylenimine concentrations were determined based on its reaction with $CuCl_2$, which gives a blue-coloured complex absorbing light at the wavelength 285 nm [39].

The adsorbent dosage influence on metal ions adsorbed amount was tested using 15 cm^3 of solution containing of supporting electrolyte (with concentration of 0.001 mol/dm^3) and appropriate adsorbate (with initial concentration of 100 ppm). The 0.0015 g, 0.015 g or 0.03 g of activated carbon was added to the system and the adsorption test was performed at pH 3 during 24 h. The adsorption isotherms were obtained at pH 3, 6, 9 for As(V) and at pH 3, 6 for Cd(II). The initial metal ions concentrations were changed in the range 20–500 ppm. The suspensions were prepared by the addition of 0.015 g of the activated carbon to 15 cm^3 of the solution containing the supporting electrolyte (with the final concentration 0.001 mol/dm^3) and the appropriate adsorbate. The adsorption tests were conducted for 24 h. The metal ions adsorption isotherm data were modelled using the Langmuir (eq. 1), Freundlich (eq. 2), Temkin (eq. 3), Dubinin-Radushkievich (eq. 4) and Redlich-Peterson (eq. 5) equations [40]:

$$q_e = \frac{q_m K_L C_e}{1 + K_L C_e} \tag{1}$$

$$q_e = K_F C_e^{1/n_F} \tag{2}$$

$$q_e = \frac{RT}{b_T} \ln A_T + \frac{RT}{b_T} \ln\ C_e \tag{3}$$

$$q_e = q_m \exp\ \left(-\beta \varepsilon^2\right) \tag{4}$$

$$q_e = \frac{K_{RP} C_e}{1 + a C_e^{\ n_{RP}}} \tag{5}$$

where: q_e – the adsorbed amount at the equilibrium [mg/g], q_m – the maximum adsorption capacity in the Langmuir model [mg/g], K_L – the Langmuir parameter [dm^3/mg], C_e – the equilibrium aqueous phase concentration [mg/dm^3], K_F – the Freundlich parameter [mg/g (mg/dm^3)$^{1/n}$], n_F – the Freundlich constant, R – gas constant 8.314 J/(mol K), T – temperature [K], b_T – Temkin constant [J/mol], A_T – Temkin constant [L/g], β – Dubinin-Radushkievich constant, ε – adsorption potential [kJ/mol], K_{RP} – Redlich-Peterson constant [L/g], a – Redlich-Peterson parameter [(L/mg)^n], n_{RP} – exponential factor.

The adsorption kinetics was examined at pH 3 after the time periods: 10, 30, 60, 90, 120 and 180 min using the analogous procedures of the concentration determination and the adsorbates with the initial concentration of 100 ppm. The results of metal ions adsorption kinetics were fitted to the pseudo first-order (eq. 6) and pseudo second-order (eq. 7) models [41]:

$$\frac{dq_t}{dt} = k_1(q_e - q_t) \tag{6}$$

$$\frac{dq_t}{dt} = k_2(q_e - q_t)^2 \tag{7}$$

where: q_e – the adsorbed amount in the equilibrium state [mg/g], q_t – the adsorbed amount after time "t" [mg/g], k_1 – the equilibrium rate constant [1/min], k_2 – the equilibrium rate constant [g/(mg·min)].

The temperature effect on the metal ions adsorbed amount was tested at 15, 25 and 35 °C. The adsorption tests were performed for 24 h, at pH 3, with the adsorbate initial concentration 100 ppm.

The adsorption from the binary solutions was conducted for 24 h (the adsorbates initial concentrations were 200 ppm). The adsorption on the biochars surface was examined at pH 3 using the suspension containing 0.1 g of the solid, appropriate adsorbate (with the concentration 200 ppm) and the NaCl supporting electrolyte (with the concentration 0.001 mol/dm^3).

After the adsorption completion the solids were separated from the solutions using the microcentrifuge (Centrifuge MPW 233e MPW Med. Instruments, Warsaw, Poland) and the concentrations of adsorbates in the supernatants were determined.

The separated solids with the adsorbed substances were next subjected to the desorption using the H_2O, HNO_3 and NaOH solutions (the acid and base with the concentrations 0.1 mol/dm^3). After 24 h the adsorbates concentration was determined. All desorption tests were carried out at 25 °C.

Results and discussion

Electrokinetic characterization of carbonaceous materials suspensions without and with heavy metal ions and polymers

The dependencies of surface charge density as a function of solution pH of adsorbents in the presence of metal ions and polymers are shown in Fig. 1. The NE_AC activated carbon point of zero charge ($_{pzc}$) occurs at pH 3.3 and the SA_AC one at pH 4.0. The cadmium ions presence causes a decrease of the surface charge density of both adsorbents, whereas the arsenic presence results in the increase of this parameter values. Such behaviour is typically noted for simple inorganic ions, whose binding results in creation of the additional number of surface groups with the opposite charge [42]. The positively charged Cd(II) ions undergo adsorption on the solids surface and induce formation of additional negatively charged surface groups. On the other hand, the adsorption of negatively charged As(V) ions results in positively charged surface sites formation. In the case of the polymers present in the mixed systems, simultaneously with heavy metal ions, a different tendency is observed. For the positively charged polyethylenimine macromolecules the increase in the surface charge density takes place, whereas for the negatively charged poly(acrylic acid) chains the decrease in this parameter is visible [43]. This is related to large sizes of polymeric molecules (considerable length of their chains) and thus not all polymer segments can be directly adsorbed on the solid surface. Depending on the macromolecules conformation, only a limited number of their segments form the "train" structures of adsorbed chains, most of them occur in the "loop" and "tail" structures in the by-surface layer. The functional groups associated with the latter ones are of decisive importance for the sign and total value of the surface charge. Due to the H_3PO_4 activation both obtained activated carbons are characterized by surface acidic properties whereas non-modified biochars possess basic character of the surface. The NE_B pH_{pzc} occurs at 7.3 and for SA_B material at 8.6.

Figure 2 presents the adsorbents zeta potential without and with the presence of applied adsorbates. As one can see, the Cd(II) cations adsorption results in the decrease of both adsorbents zeta potential value in the whole examined pH range. In the case of the NE_AC activated carbon it causes shift of the pH_{iep} ($_{iep}$-isoelectric point) value from 4.9 to 3.9 and for the SA_AC one from 6.2 to 5.3. The observed difference in the location of the point of zero charge and the isoelectric point can be related to partial overlapping of the electrical double layers (*edl*) formed on the pore walls and that effect occurring in the case of mesoporous materials was described in the

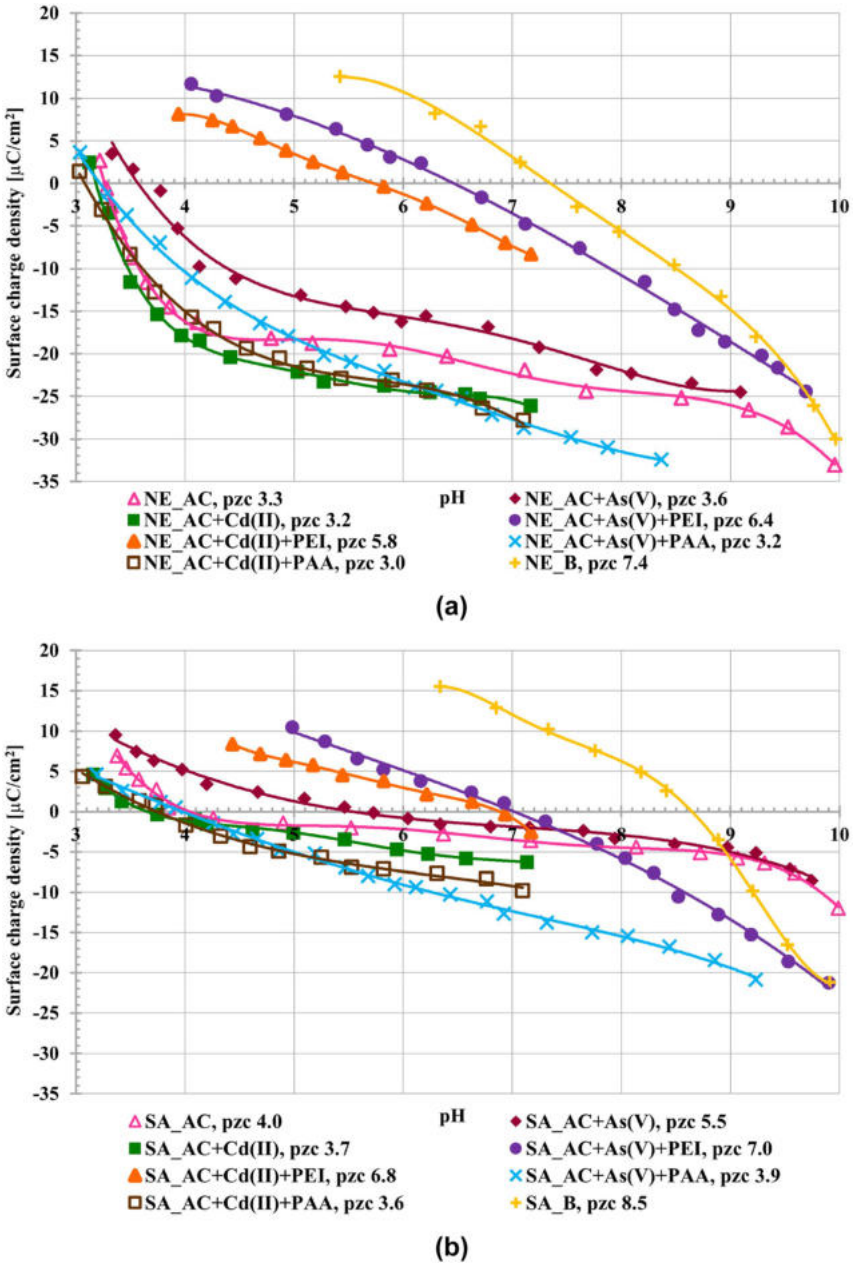

Fig. 1: Surface charge density of NE_AC activated carbon and NE_B biochar (a), SA_AC activated carbon and SA_B biochar (b) particles in the systems without as well as with single and binary adsorbates.

literature [44]. The Cd(II) adsorption is mostly governed by the electrostatic attraction with the solid surface and these unhydrated cations are located in the inner Helmholtz plane of *edl*. It affects accumulation of positive charge on the activated carbons surface, which is neutralized by negative moieties and supporting electrolyte ions located in the slipping plane area [45]. The As(V) anions also cause the decrease in the zeta potential value, which can be a result of their partial or total hydration. The arsenic anions with the hydration layers locate in the outer Helmholtz plane of the stiff part of *edl*. The ionic polymers presence in the suspensions has a considerably greater impact on the zeta potential than small metal ions. In the PEI containing systems the increase in the zeta potential was observed, whereas in the PAA presence the zeta potential values decrease. Both tendencies are related to the presence of ionic functional groups of the adsorbed polymer (positively charged amine ones in the PEI molecules and negatively charged carboxyl ones in the PAA chains) in the slipping plane area. Additionally, their large size and thus significant thickness of the polymeric adsorption layer can cause the shift of the slipping

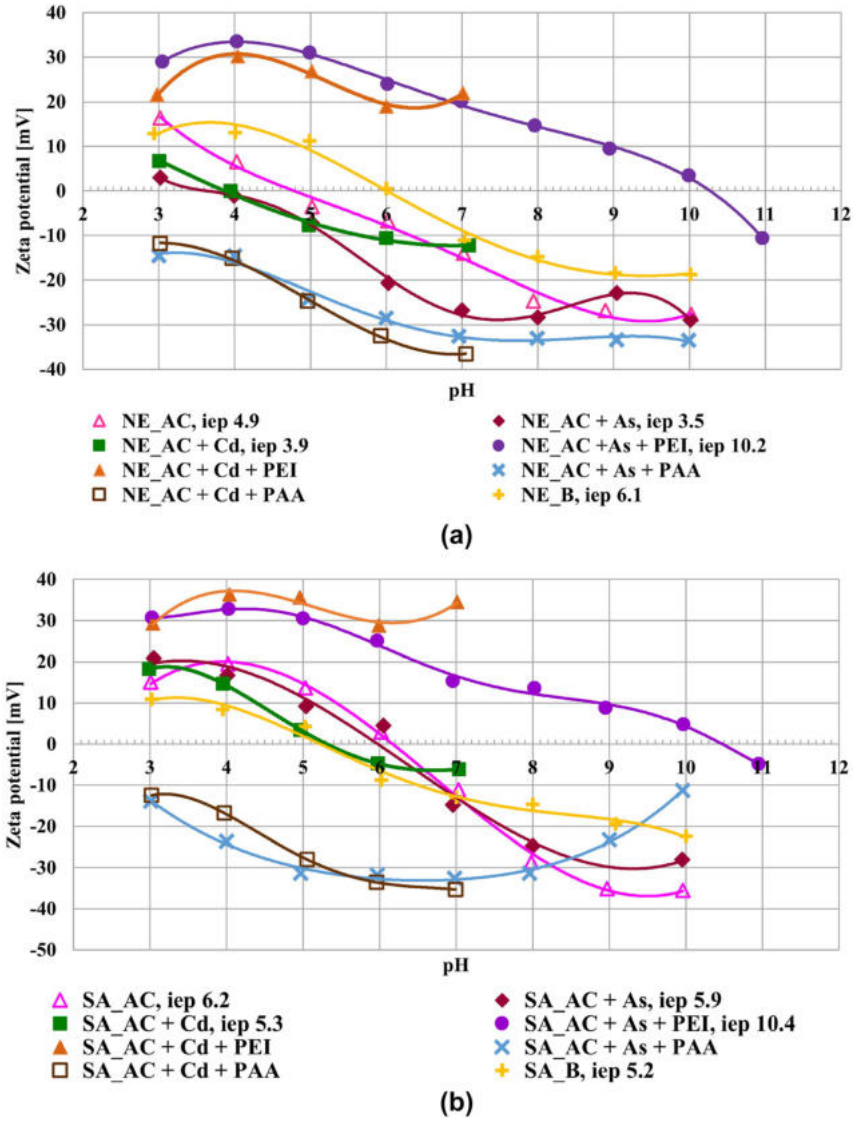

Fig. 2: Zeta potential of NE_AC activated carbon and NE_B biochar (a), SA_AC activated carbon and SA_B biochar (b) particles in the systems without as well as with single and binary adsorbates.

plane resulting in reduction of zeta potential values [46]. The pH_{iep} value for the NE_B biochar occurs at 6.1 and for the SA_B one at 5.2.

The metal-polymer complexes formation also influences the surface charge density and zeta potential values [47]. The cadmium cation can interact electrostatically with the negatively charged poly(acrylic acid) chains whereas the arsenic anion has affinity for the positively charged amine groups present in the polyethylenimine structure. On the other hand oxygen present in the As(V) ion can form hydrogen bonds with the carboxyl or amine group present in the polymers chains. All the mechanisms can lead to the formation of intra- and intermolecular complexes.

The aggregate sizes formed without as well as with single and binary adsorbates are listed in Table 2. The obtained results proved that the Cd(II) presence leads to the increase in both solid aggregate sizes at pH 3 and 6, but at higher pH this effect is more noticeable. The polyethylenimine addition to the systems with cadmium reduces this impact. Both activated carbons aggregate sizes increase in the presence of Cd(II) and PEI at pH 3 and 6. The cadmium ions and poly(acrylic acid) molecules present in the suspensions caused the SA_AC aggregate sizes increase and the decrease in the NE_AC aggregates size. The As(V) presence in the solution results in the increase of both adsorbents aggregate sizes. The polyethylenimine addition has no significant impact on the aggregate

Table 2: Aggregate sizes of activated carbons and biochars in the system without as well as with the single and binary adsorbates (C_0 100 ppm).

System	Size of aggregates [nm]		
	pH 3	pH 6	pH 9
NE_AC	509.5	478.2	448.5
NE_AC + Cd	722.4	823.6	–
NE_AC + Cd + PEI	587.6	653.8	–
NE_AC + Cd + PAA	408.2	358.5	–
NE_AC + As	496.5	832.1	484.5
NE_AC + As + PEI	433.4	488.2	557.6
NE_AC + As + PAA	532.8	415.7	483.9
SA_AC	327.8	430.9	517.4
SA_AC + Cd	683.1	1257	–
SA_AC + Cd + PEI	490.2	484.8	–
SA_AC + Cd + PAA	422.1	441.9	–
SA_AC + As	562.4	678.3	762.1
SA_AC + As + PEI	520.5	620.4	783.8
SA_AC + As + PAA	446.8	880.0	575.2
NE_B	1257	731.2	1448
SA_B	688.2	1799	1494

sizes in comparison to the single arsenic systems. The As(V) and PAA presence in the system has slight influence on both activated carbons aggregate sizes in comparison to the system without adsorbates. The biochars form aggregates with greater size compared to activated carbons in the systems without adsorbates.

Adsorption/desorption properties of carbonaceous materials in relation to heavy metal ions and polymers

Figure 3 presents the effect of adsorbent dosage on Cd(II) and As(V) adsorbed amount on the surface of NE_AC and SA_AC activated carbons. The obtained results proved that the metal ions adsorbed amounts decrease with the increasing adsorbent dosage. This is attributed to the decrease of adsorbed amount expressed in the mg of adsorbate per g of adsorbent as the adsorbent mass increased, even though the adsorption of metal ions increased due to availability of larger surface area and thus more numerous adsorption sites [48].

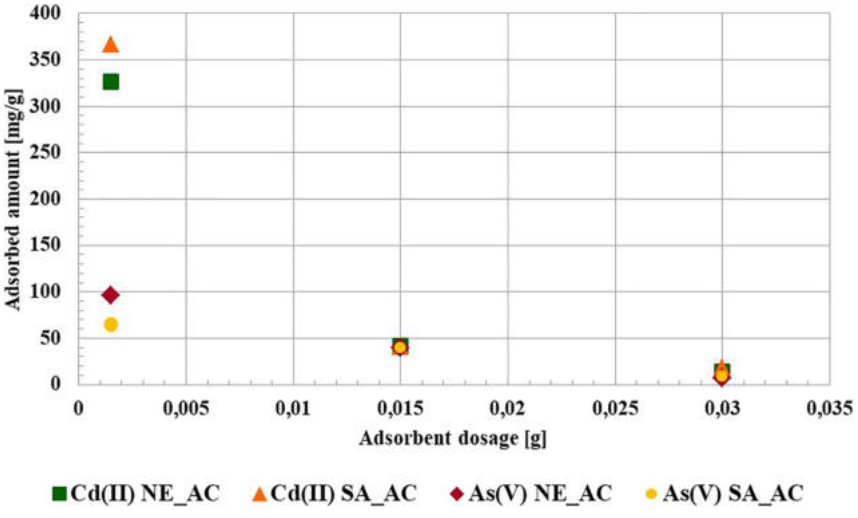

Fig. 3: Effect of adsorbent dosage on Cd(II) and As(V) adsorbed amounts on the surface of NE_AC and SA_AC activated carbons (C_0 100 ppm, pH 3).

The metals ions adsorption isotherms at different pH values are shown in Fig. 4. Both examined activated carbons adsorb cadmium and arsenic on similar levels, though Cd(II) is inconsiderably better adsorbed. The difference in the adsorbed amounts of Cd(II) and As(V) can be attributed to the different radius of their hydrated ions [49]. The Cd^{2+} crystal radius is 0.97 Å and the hydrated radius is 4.26 Å. On the other hand, the As-O distance in the arsenate ion is over 1.6 Å, which gives a much larger ion radius [50, 51]. The adsorption isotherms do not reach plateau so the carbonaceous adsorbents are able to bind larger amounts of metal ions. However, their determination is impossible due to the applied method limitations. Nevertheless, the obtained Cd(II) and As(V) maximum adsorbed amounts were greater than these presented in the literature (Table 3). Changes in the pH values have a slight effect on the Cd(II) and As(V) adsorbed amounts, however, both metals are better adsorbed at higher pH. Increasing pH favours cadmium and arsenic surface precipitation through the formation of chemical bonds with the solid functional groups. In the case of As(V) anions containing oxygen atoms, the hydrogen bonds can be also created. The adsorption isotherms were fitted to the Langmuir, Freundlich, Temkin, Dubinin-Radushkievich, Redlich-Peterson and Hill models (Table 4). Analysis of these data leads to the conclusion that the Redlich-Peterson and Freundlich models describe the best the obtained adsorption isotherms, which proved that adsorption occurs with the non-uniform distribution of energy and the monolayer is not formed [52].

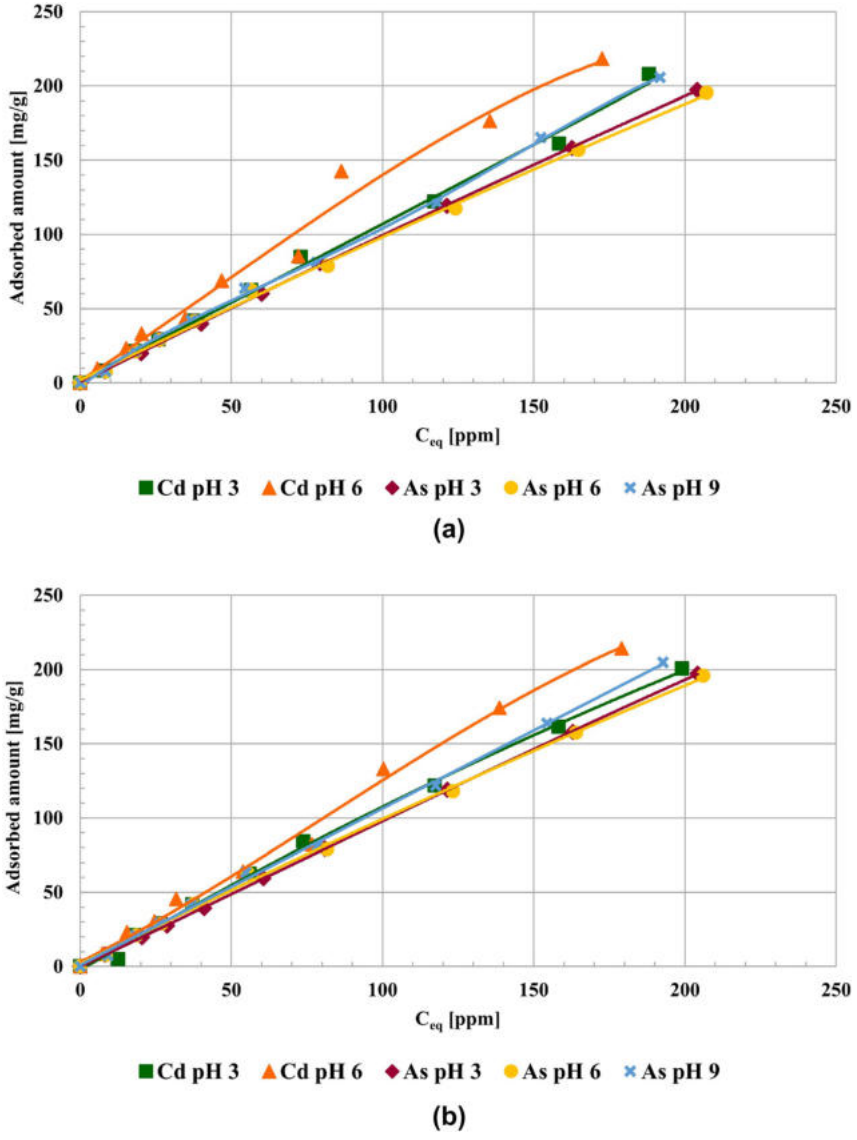

Fig. 4: Cd(II) and As(V) adsorption isotherms on the surface of NE_AC (a) and SA_AC (b) (C_0 100 ppm).

Table 3: Cd(II) and As(V) adsorbed amounts on the surfaces of different carbonaceous materials.

Metal	Adsorbed amount [mg/g]	Adsorbent	Reference
Cd(II)	175.43	Biochar obtained from the cannabis	[15]
	6.66	Rice straw derived biochar	[11]
	13.50	Aged biochar obtained from the corn stalk	[13]
	61.08	Peanut shells based biochar	[14]
	218.27	Activated carbon obtained from the nettle herb	Present study
	214.00	Activated carbon obtained from the sage herb	Present study
As(V)	3.385	Iron impregnated activated carbon	[24]
	42.92	Iron-incorporated activated carbon	[27]
	5.00	Iron-modified activated carbons	[30]
	34.00	Fe–Mn modified granular activated carbon	[26]
	205.53	Activated carbon obtained from the nettle herb	Present study
	204.87	Activated carbon obtained from the sage herb	Present study

Table 4: Adsorption and kinetic parameters of Cd(II) and As(V) binding on the activated carbons surface.

Model		Calculated parameters			
Isotherm parameters		Cd(II)		As(V)	
		NE_AC	SA_AC	NE_AC	SA_AC
Langmuir	q_m [mg/g]	2602	1534	4874	18418
	K_L [dm^3/mg]	0.000438	0.00751	0.000212	0.000053
	R^2	0.3282	0.8153	0.2489	0.5017
Freundlich	n_F	1.022077	1.026594	1.010203	0.998702
	K_F [mg/g(mg/dm^3)$^{1/n}$]	0.009194	0.009421	0.010069	0.010283
	R^2	0.9984	0.9982	0.9984	0.9999
Temkin	b_T [J/mol]	178.2028	125.535	180.253	179.688
	A_T [dm^3/g]	0.103798	1.235083	0.111268	0.110699
	R^2	0.9915	0.9493	0.9909	0.9917
Dubinin-Radushkevich	β	0.000023	0.000058	0.000022	0.000021
	ε [kJ/mol]	0.146783	0.093093	0.151851	0.152744
	q_m [mg/g]	44.7611	44.8060	47.6750	44.9823
	R^2	0.6968	0.6999	0.7475	0.7051
Redlich-Peterson	K_{RP} [dm^3/g]	1.6124	1.0304	0.9759	0.9710
	a [(dm^3/mg)^n]	83.0136	123.0439	52.6990	56.5958
	R^2	0.9931	0.9955	0.9995	0.9999
Kinetics parameters					
Pseudo first-order model linear	q_e [mg/g]	1.00501	0.99671	0.98345	1.0023
	k_1 [1/min]	1.39239	0.1239	0.2911	0.33854
	R^2	0.3558	0.0314	0.6322	0.5352
Pseudo second-order model	q_e [mg/g]	41.3223	42.735	39.8406	39.3701
	k_2 [g/(mg × min)]	0.01442	0.02515	0.01921	0.03729
	R^2	0.9947	0.9965	0.9992	0.9999

The obtained results of adsorption kinetic measurements are presented in Fig. 5. They indicate that the equilibrium state was reached after 10 min (for both metals and onto both adsorbents). Such a short time is caused by small ions sizes and great development of adsorbent surface area. The adsorption kinetics was fitted to the pseudo first-order and pseudo second-order equations (Table 3). The respective data concerning both metals are better described by the pseudo second-order model. This indicates that the adsorption of these compounds involves mainly chemical interactions.

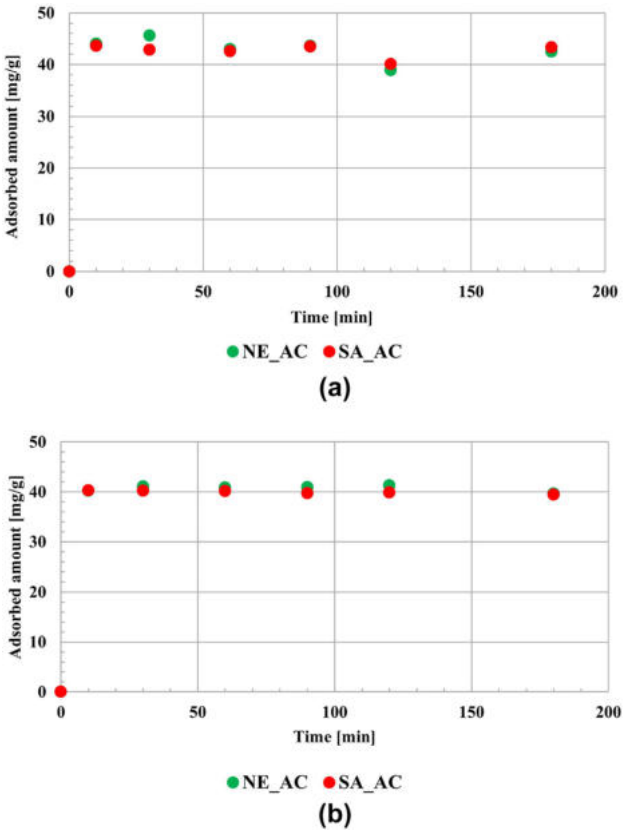

Fig. 5: Adsorption kinetics of Cd(II) (a) and As(V) (b) on both activated carbons (pH 3, C_0 100 ppm).

The temperature effect on the Cd(II) and As(V) adsorption is presented in Fig. 6. Both examined metal ions demonstrate the greatest adsorption at 25 °C. At 15 °C cadmium and arsenic ions have higher affinity to the SA_AC activated carbon surface, whereas at 35 °C to the NE_AC one. The temperature have higher impact on the As(V) adsorbed amount, which can be related to greater size of arsenic ion compared to the Cd(II) one.

Figure 7 presents the Cd(II), As(V), PEI and PAA adsorbed amounts on the activated carbons and biochars surface from the single and binary solutions at pH 3. Arsenic ions (~80 mg/g) and polyethylenimine (~50 mg/g) are adsorbed on the similar level on the NE_AC and SA_AC materials. Poly(acrylic acid) and cadmium ions are adsorbed better on the activated carbon obtained from the nettle herb (~198 mg/g, ~105 mg/g) than on that

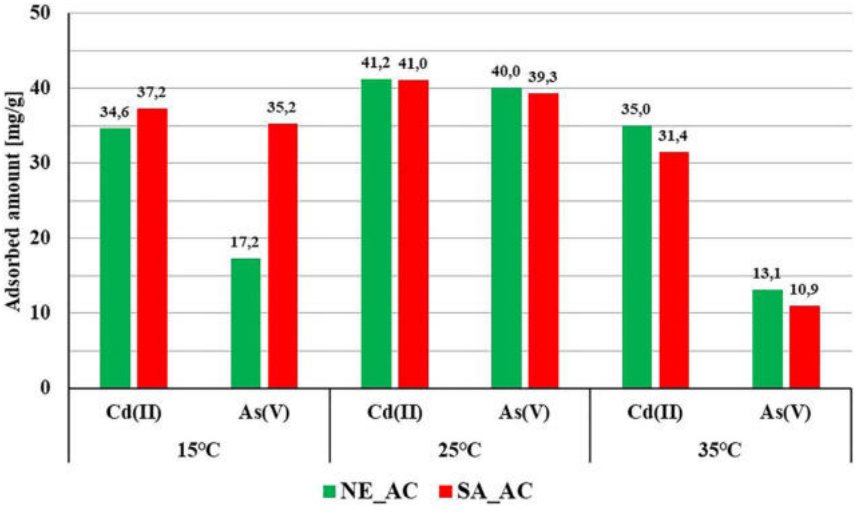

Fig. 6: The temperature influence on the Cd(II) and As(V) adsorbed amounts on the surface of activated carbons (pH 3, C_0 100 ppm).

obtained from the sage one (~138 mg/g, ~87 mg/g, respectively). A higher concentration of the functional groups is observed on the NE_AC activated carbon surface which can explain this effect. The polymers presence decreases As(V) and Cd(II) affinity for the surface of examined adsorbents significantly. This can be related to the PAA and PEI molecules considerable size, which can block the adsorption sites. In the case of polymers adsorbed amount, the As(V) presence has also negative influence on the PEI adsorption. The Cd(II) effect on the polyethylenimine adsorbed amount depends on the adsorbent type, on the surface of adsorbent with a higher content of surface functional groups the PEI adsorbed amount increases. The metal ions influence on the PAA adsorbed amount on the surface of NE_AC activated carbons is difficult to estimate, due to the total PAA removal from the solution. On the surface of SA_AC the poly(acrylic acid) adsorbed amount increases in the presence of Cd(II) and As(V), however the cadmium ions impact is more noticeable. This can be related to the polymer-metal complex creation through the hydrogen and chemical bonds. These complexes can have an inter- and intra-molecular structure, thus they can be formed within one polymeric chain and between two macromolecules. Moreover, the molecules with the same charge can be adsorbed on the same active sites. The activated carbon surfaces are positively charged at pH 3. That indicates the polyethylenimine and cadmium ions repulsion, whereas poly(acrylic acid) and arsenic ions are attracted by the solid surface. The competition between PEI and Cd(II) and between PAA and As(V) takes place [53].

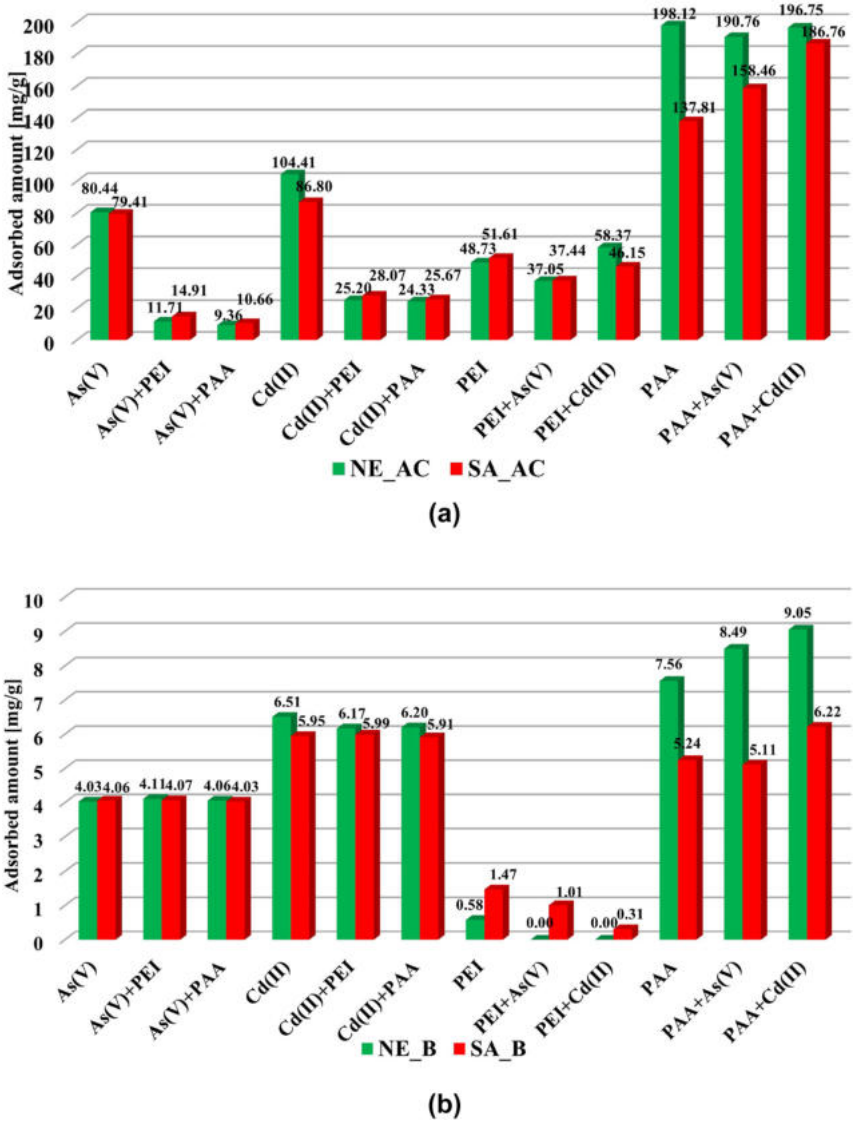

Fig. 7: Cd(II), As(V), poly(acrylic acid) and polyethyleneimine adsorbed amount from single and binary solutions onto activated carbons (a) and biochars (b) (C_0 100 ppm, pH 3).

Biochars are definitely worse adsorbents than the activated carbons. Due to their considerably smaller surface area the adsorbed amounts of all substances are smaller than 10 mg/g. As(V) and Cd(II) are adsorbed on the similar level on both biochars and the polymer does not affect their adsorption. However, the cadmium ions adsorbed amounts are greater than the As(V) on both biochars surfaces. Metal ions have negative influence on the PEI adsorption on SA_B surface. The polyethylenimine adsorbed amount on NE_B in the presence of metal ions was impossible to be determined. As a result of high ionic strength of the solution solid components rinsed out. From the single solution it is better adsorbed on the SA_B material than on the NE_B one. Both metals ions affect PAA adsorption favourably. Poly(acrylic acid) is the best adsorbed substance on the NE_B biochar. This can be related to the higher content of surface functional groups (Table 1).

Cadmium and arsenic are strongly bound to the activated carbons surface. The desorbed amounts of both metal ions from the single and binary systems do not exceed 10 % (Table 5). Cadmium desorption was not studied using NaOH due to the metal precipitation at high pH values. In the case of the surface of biochars only Cd(II) can be effectively desorbed using HNO_3 (~25 %). Polyethylenimine is desorbed the most effectively from the single system NE_AC + PEI (44.2 %) and from the binary one SA_AC + PEI + Cd (43.5 %). It was desorbed only with the usage of H_2O, because HNO_3 and NaOH increase the solution ionic strength and make PEI determination impossible. Poly(acrylic acid) is the most effectively removed from the activated carbons surface with the usage of NaOH and from the biochars surface with H_2O. NaOH was not used for the desorption from the surface of biochars due to rinsing out the solid components and making determination impossible.

Table 5: Percentage desorption of Cd(II), As(V), poly(acrylic acid) and polyethyleneimine from the activated carbons and biochars surface from the single and binary systems using the H_2O, HNO_3 and NaOH desorbing agents (*with concentration of* 0.1 mol/dm^3, *desorption time* 24 h).

Desorption agent	**Desorption [%]**		
System	**H_2O**	**HNO_3 Cd(II)**	**NaOH**
NE_AC + Cd	6.8	6.9	–
NE_AC + Cd + PEI	7.5	5.3	–
NE_AC + Cd + PAA	4.8	7.4	–
SA_AC + Cd	4.6	6.5	–
SA_AC + Cd + PEI	5.2	5.2	–
SA_AC + Cd + PAA	3.6	5.7	–
NE_B + Cd	0.1	28.3	–
NE_B + Cd + PEI	0.3	24.9	–
NE_B + Cd + PAA	1.0	27.0	–
SA_B + Cd	0.3	28.2	–
SA_B + Cd + PEI	0.3	27.1	–
SA_B + Cd + PAA	1.0	23.0	–
System	As(V)		
NE_AC + As	7.8	5.9	9.2
NE_AC + As + PEI	6.1	8.0	9.8
NE_AC + As + PAA	6.9	7.4	6.8
SA_AC + As	6.6	6.9	5.0
SA_AC + As + PEI	5.8	9.1	6.8
SA_AC + As + PAA	4.4	6.8	5.4
NE_B + As	4.1	7.2	–
NE_B + As + PEI	8.3	8.4	–
NE_B + As + PAA	6.5	6.2	–
SA_B + As	8.0	5.9	–
SA_B + As + PEI	6.7	5.0	–
SA_B + As + PAA	5.4	7.5	–
System	PEI		
NE_AC + PEI	44.2	–	–
NE_AC + PEI + Cd	28.3	–	–

Table 5: (continued)

Desorption agent	Desorption [%]		
	H_2O	HNO_3	NaOH
System		Cd(II)	
NE_AC + PEI + As	20.8	–	–
SA_AC + PEI	24.7	–	–
SA_AC + PEI + Cd	43.5	–	–
SA_AC + PEI + As	24.2	–	–
System	PAA		
NE_AC + PAA	1.4	2.8	61.0
NE_AC + PAA + Cd	0.6	1.3	56.8
NE_AC + PAA + As	1.3	2.5	56.9
SA_AC + PAA	2.5	2.0	46.5
SA_AC + PAA + Cd	2.6	1.5	49.5
SA_AC + PAA + As	1.9	1.9	51.0
NE_B + PAA	6.6	9.0	–
NE_B + PAA + Cd	12.6	5.9	–
NE_B + PAA + As	13.7	4.2	–
SA_B + PAA	18.0	6.4	–
SA_B + PAA + Cd	31.1	6.8	–
SA_B + PAA + As	44.4	9.2	–

Conclusions

Activated carbons and biochars obtained from the nettle and the sage herbs can be used for simultaneous heavy metal ions and polymers removal from the aqueous solutions. The electrokinetic studies showed that the adsorption of negatively charged As(V) ions on the activated carbons causes an increase in the surface charge density due to positively charged sites creation on the surface, whereas the Cd(II) adsorption has the opposite effect.

The hydrated arsenic ions locate in the outer Helmholtz plane of stiff part of *edl* and cause a decrease in the zeta potential. On the other hand, the cadmium cations location in the inner Helmholtz plane of the stiff part of *edl* results in the zeta potential increase. Both Cd(II) and PAA decrease the zeta potential and surface density charge values. The PEI presence in the solution causes the zeta potential and surface charge density increase. In the binary solution containing the metal ions and the polymers, the macromolecular compounds have decisive influence on the adsorbent electrokinetic properties.

Due to the well-developed specific surface area, a high content of surface functional groups and a large size of pores the activated carbons prepared from the nettle and the sage herbs are effective adsorbents of heavy metal ions and polymers. The poly(acrylic acid) adsorbed amounts become the greatest levels both in the single and binary solution (198.12 mg/g and 196.75 mg/g). As(V), Cd(II) and PEI can be successfully removed from the single component solution, however, the presence of another adsorbate usually reduces the efficiency of this process. Electrostatic interactions as well as hydrogen and chemical bonds creation between the metals ions and the polymers chains cause metal-polymer complex formation and influence all substances adsorbed amounts. On the other hand, competition between the individual adsorbates with the same sign of charge takes place. Cd(II) and As(V) isotherms do not reach plateau, due to the limitation in the concentration determination methods. The maximum adsorbed amount of metal ions were 218.27 mg/g for Cd(II) and 205.53 mg/g for As(V), however the maximal adsorption capacities of activated carbons are probably greater. The metal ions are strongly bound to the adsorbents surface and they are desorbed to a small extent, whereas polymers can be effectively removed from the solids surfaces (the maximal desorption reaches the level of 61 %). The desorbed amounts of all substances are similar from the single and binary solutions.

References

[1] V. S. Kanwar, A. Sharma, A. L. Srivastav, L. Rani. *Environ. Sci. Pollut. Res.* **27**, 44835 (2020), https://doi.org/10.1007/s11356-020-10713-3.
[2] P. Goyal, S. Srivastava. *J. Hazard. Mater.* **172**, 1206 (2009), https://doi.org/10.1016/j.jhazmat.2009.07.125.
[3] G. Genchi, M. S. Sinicropi, G. Lauria, A. Carocci, A. Catalano. *Int. J. Environ. Res. Publ. Health* **17**, 3782 (2020), https://doi.org/10.3390/ijerph17113782.
[4] M. P. Benavides, S. M. Gallego, M. L. Tomaro. *Braz. J. Plant Physiol.* **17**, 21 (2005), https://doi.org/10.1590/S1677-04202005000100003.
[5] R. A. Bernhoft. *Sci. World J.* **2013**, 1 (2013), https://doi.org/10.1155/2013/394652.
[6] World Health Organization. *Cadmium in drinking-water: background document for development of WHO guidelines for drinking-water quality (No. WHO/SDE/WSH/03.04/80)*, World Health Organization (2004).
[7] S. Sobhanardakani, R. Zandipak. *Environ. Monit. Assess.* **187**, 1 (2015), https://doi.org/10.1007/s10661-015-4635-y.
[8] S. Sobhanardakani, R. Zandipak. *Clean Technol. Environ. Policy* **19**, 1913 (2017), https://doi.org/10.1007/s10098-017-1374-5.
[9] F. Talebzadeh, S. Sobhanardakani, R. Zandipak. *Sep. Sci. Technol.* **52**, 622 (2017), https://doi.org/10.1080/01496395.2016.1262873.
[10] M. Kavand, P. Eslami, L. Razeh. *J. Water Process Eng.* **34**, 101151 (2020), https://doi.org/10.1016/j.jwpe.2020.101151.
[11] L. Qian, M. Chen, B. Chen. *J. Soils Sediments* **15**, 1130 (2015), https://doi.org/10.1007/s11368-015-1073-y.
[12] S. J. Cobbina, A. B. Duwiejuah, A. K. Quainoo. *Int. J. Environ. Sci. Technol.* **16**, 3081 (2019), https://doi.org/10.1007/s13762-018-1910-9.
[13] Y. Liu, L. Wang, X. Wang, F. Jing, R. Chang, J. Chen. *Sci. Total Environ.* **725**, 138419 (2020), https://doi.org/10.1016/j.scitotenv.2020.138419.
[14] L. Zheng, Y. Gao, J. Du, W. Zhang, Y. Huang, Q. Zhao, L. Duan, Y. Liu, R. Naidu, X. Pan. *Processes* **9**, 1829 (2021), https://doi.org/10.3390/pr9101829.
[15] A. H. Omidi, M. Cheraghi, B. Lorestani, S. Sobhanardakani, A. Jafari. *SN Appl. Sci.* **2**, 1 (2020), https://doi.org/10.1007/s42452-020-2954-2.
[16] R. S. Oremland, J. F. Stolz. *Science* **300**, 939 (2003), https://doi.org/10.1126/science.108190.
[17] B. K. Mandal, K. T. Suzuki. *Talanta* **58**, 201 (2002), https://doi.org/10.1016/S0039-9140(02)00268-0.
[18] K. S. M. Abdul, S. S. Jayasinghe, E. P. Chandana, C. Jayasumana, P. M. C. De Silva. *Environ. Toxicol. Pharmacol.* **40**, 828 (2015), https://doi.org/10.1016/j.etap.2015.09.016.
[19] U. Rehman, S. Khan, S. Muhammad. *Expo Health* **12**, 243 (2020), https://doi.org/10.1007/s12403-019-00308-w.
[20] World Health Organization. *Guidelines for drinking-water quality: first addendum to the fourth edition* (2017).
[21] S. Alka, S. Shahir, N. Ibrahim, M. J. Ndejiko, D. V. N. Vo, F. Abd Manan. *J. Clean. Prod.* **278**, 123805 (2021), https://doi.org/10.1016/j.jclepro.2020.123805.
[22] D. Borah, S. Satokawa, S. Kato, T. Kojima. *J. Colloid Interface Sci.* **319**, 53 (2008), https://doi.org/10.1016/j.jcis.2007.11.019.
[23] E. Diamadopoulos, S. Ioannidis, G. P. Sakellaropoulos. *Water Res.* **27**, 1773 (1993), https://doi.org/10.1016/0043-1354(93)90116-Y.
[24] X. J. Gong, Y. S. Li, Y. Q. Dong, W. G. Li. *Chemosphere* **250**, 126275 (2020), https://doi.org/10.1016/j.chemosphere.2020.126275.
[25] M. Kalaruban, P. Loganathan, T. V. Nguyen, T. Nur, M. A. H. Johir, T. H. Nguyen, M. V. Trinh, S. Vigneswaran. *J. Environ. Manag.* **239**, 235 (2019), https://doi.org/10.1016/j.jenvman.2019.03.053.
[26] J. Nikić, J. Agbaba, M. A. Watson, A. Tubić, M. Šolić, S. Maletić, B. Dalmacija. *J. Environ. Sci. Health, Part A* **54**, 168 (2019), https://doi.org/10.1080/10934529.2018.1541375.
[27] H. L. Rahman, H. Erdem, M. Sahin, M. Erdem. *Water, Air, Soil Pollut.* **231**, 1 (2020), https://doi.org/10.1007/s11270-019-4378-4.
[28] N. Sahu, J. Singh, J. R. Koduru. *Environ. Res.* **200**, 111431 (2021), https://doi.org/10.1016/j.envres.2021.111431.
[29] M. Medykowska, M. Wiśniewska, K. Szewczuk-Karpisz. *International Conference on Nanotechnology and Nanomaterials*, pp. 55–67, Springer, Cham (2020).
[30] C. Nieto-Delgado, J. Gutiérrez-Martínez, J. R. Rangel-Méndez. *J. Environ. Sci.* **76**, 403 (2019), https://doi.org/10.1016/j.jes.2018.06.002.
[31] K. Szewczuk-Karpisz, M. Wiśniewska, M. Medykowska, M. V. Galaburda, V. M. Bogatyrov, O. I. Oranska, M. Błachnio, P. Oleszczuk. *J. Hazard. Mater.* **412**, 125138 (2021), https://doi.org/10.1016/j.jhazmat.2021.125138.
[32] M. Wiśniewska, P. Nowicki. *J. Mol. Liq.* **296**, 111806 (2019), https://doi.org/10.1016/j.molliq.2019.111806.
[33] M. Gęca, M. Wiśniewska, P. Nowicki. *Molecules* **27**, 7557 (2022), https://doi.org/10.3390/molecules27217557.
[34] S. Chibowski, M. Wiśniewska, A. W. Marczewski, S. Pikus. *J. Colloid Interface Sci.* **267**, 1 (2003), https://doi.org/10.1016/S0021-9797(03)00698-2.
[35] A. Von Harpe, H. Petersen, Y. Li, T. Kissel. *J. Controlled Release* **69**, 309 (2000), https://doi.org/10.1016/s0168-3659(00)00317.
[36] W. Janusz. *Polish J. Chem.* **68**, 1871 (1994).
[37] H. Ohshima. *J. Colloid Interface Sci.* **168**, 269 (1994), https://doi.org/10.1006/jcis.1994.1419.
[38] W. B. Crummett, R. A. Hummel. *J. Am. Water Works Assoc.* **55**, 209 (1963), https://doi.org/10.1002/j.1551-8833.1963.tb01016.x.
[39] J. Patkowski, D. Myśliwiec, S. Chibowski. *Int. J. Polym. Anal. Charact.* **21**, 486 (2016), https://doi.org/10.1080/1023666X.2016.1168651.
[40] K. Y. Foo, B. H. Hameed. *Chem. Eng. J.* **156**, 2 (2010), https://doi.org/10.1016/j.cej.2009.09.013.
[41] J. Wang, X. Guo. *J. Hazard. Mater.* **390**, 122156 (2020), https://doi.org/10.1016/j.jhazmat.2020.122156.
[42] M. Medykowska, M. Wiśniewska, K. Szewczuk-Karpisz, R. Panek. *J. Mol. Liq.* **357**, 119144 (2022), https://doi.org/10.1016/j.molliq.2022.119144.
[43] M. Wiśniewska, I. Ostolska, K. Szewczuk-Karpisz, S. Chibowski, K. Terpiłowski, V. M. Gun'ko, V. I. Zarko. *J. Nanoparticle Res.* **17**, 1 (2015), https://doi.org/10.1007/s11051-014-2831-2.

[44] M. Wiśniewska, P. Nowicki, K. Szewczuk-Karpisz, M. Gęca, K. Jędruchniewicz, P. Oleszczuk. *Sep. Purif. Technol.* **276**, 119297 (2021), https://doi.org/10.1016/j.seppur.2021.119297.
[45] G. Fijałkowska, M. Wiśniewska, K. Szewczuk-Karpisz. *Physicochem. Probl. Miner. Process.* **55**, 1339 (2019), https://doi.org/10.5277/ppmp19044.
[46] S. Chibowski, E. Grządka, J. Patkowski. *Colloids Surf. A Physicochem. Eng. Asp.* **326**, 191 (2008), https://doi.org/10.1016/j.colsurfa.2008.05.038.
[47] M. Wiśniewska, G. Fijałkowska, K. Szewczuk-Karpisz, T. Urban, A. Nosal-Wiercińska, G. Wójcik. *Adsorption* **25**, 41 (2019), https://doi.org/10.1007/s10450-018-9990-x.
[48] M. Kavand, T. Kaghazchi, M. Soleimani. *Kor. J. Chem. Eng.* **31**, 692 (2014), https://doi.org/10.1007/s11814-013-0280-8.
[49] J. S. Kwon, S. T. Yun, J. H. Lee, S. O. Kim, H. Y. Jo. *J. Hazard. Mater.* **174**, 307 (2010), https://doi.org/10.1016/j.jhazmat.2009.09.052.
[50] J. Mähler, I. Persson, R. B. Herbert. *Dalton Trans.* **42**, 1364 (2013), https://doi.org/10.1039/C2DT31906C.
[51] E. R Nightingale, Jr. *J. Phys. Chem.* **63**, 1381 (1959), https://doi.org/10.1021/j150579a011.
[52] M. Achak, A. Hafidi, N. Ouazzani, S. Sayadi, L. Mandi. *J. Hazard. Mater.* **166**, 117 (2009), https://doi.org/10.1016/j.jhazmat.2008.11.036.
[53] H. Cheng, Y. Liu, X. Li. *J. Hazard. Mater.* **415**, 125749 (2021), https://doi.org/10.1016/j.jhazmat.2021.125749.

Lublin, 10.09.2025

mgr Marlena Groszek
Uniwersytet Marii Curie-Skłodowskiej w Lublinie,
Wydział Chemii, Instytut Nauk Chemicznych,
Katedra Radiochemii i Chemii Środowiskowej,
Pl. Marii Curie-Skłodowskiej 3, 20-031 Lublin
marlena.groszek@mail.umcs.pl

Rada Naukowa Instytutu Nauk Chemicznych
Uniwersytetu Marii Cure-Skłodowskiej
w Lublinie

Oświadczenie o współautorstwie

Niniejszym oświadczam, że mój udział w pracy: **M. Gęca**, M. Wiśniewska, P. Nowicki, K. Jędruchniewicz, *Cd(II) and As(V) removal from the multicomponent solutions in the presence of ionic polymers using carbonaceous adsorbents obtained from herbs,* Pure and Applied Chemistry, 2023, 95, 5, 563-578. DOI: 10.1515/pac-2023-0201 [D8], obejmował opracowanie koncepcji badań, przeprowadzenie eksperymentów, analizę uzyskanych wyników, przygotowanie manuskryptu i jego korektę po procesie oceny w redakcji oraz sformułowanie odpowiedzi na uwagi recenzentów.

Marlena Groszek

Lublin, 10.09.2025

prof. dr hab. Małgorzata Wiśniewska
Uniwersytet Marii Curie-Skłodowskiej w Lublinie,
Wydział Chemii, Instytut Nauk Chemicznych,
Katedra Radiochemii i Chemii Środowiskowej,
Pl. Marii Curie-Skłodowskiej 3, 20-031 Lublin
malgorzata.wisniewska@mail.umcs.pl

Rada Naukowa Instytutu Nauk Chemicznych
Uniwersytetu Marii Cure-Skłodowskiej
w Lublinie

Oświadczenie o współautorstwie

Niniejszym oświadczam, że mój udział w pracy: M. Gęca, **M. Wiśniewska**, P. Nowicki, K. Jędruchniewicz, *Cd(II) and As(V) removal from the multicomponent solutions in the presence of ionic polymers using carbonaceous adsorbents obtained from herbs,* Pure and Applied Chemistry, 2023, 95, 5, 563-578. DOI: 10.1515/pac-2023-0201 [D8], obejmował korektę manuskryptu – przed i po procesie recenzji oraz nadzór merytoryczny w czasie całego cyklu wydawniczego.

Małgorzata Wiśniewska

Poznań, 10.09.2025

dr hab. Piotr Nowicki, prof. UAM
Uniwersytet im. Adama Mickiewicza w Poznaniu,
Wydział Chemii, Zakład Chemii Stosowanej
Ul. Uniwersytetu Poznańskiego 8, 61-614 Poznań
piotr.nowicki@amu.edu.pl

Rada Naukowa Instytutu Nauk Chemicznych
Uniwersytetu Marii Cure-Skłodowskiej
w Lublinie

Oświadczenie o współautorstwie

Niniejszym oświadczam, że mój udział w pracy: M. Gęca, M. Wiśniewska, **P. Nowicki**, K. Jędruchniewicz, *Cd(II) and As(V) removal from the multicomponent solutions in the presence of ionic polymers using carbonaceous adsorbents obtained from herbs,* Pure and Applied Chemistry, 2023, 95, 5, 563-578. DOI: 10.1515/pac-2023-0201 [D8], obejmował stworzenie koncepcji pracy, przeprowadzenie eksperymentów, analizę uzyskanych wyników, korektę pierwszej wersji manuskryptu oraz przygotowanie odpowiedzi na uwagi recenzentów.

Piotr Nowicki

Lublin, 10.09.2025

dr Katarzyna Jędruchniewicz
ARKONA Laboratorium Farmakologii
Stomatologicznej Grzegorz Kalbarczyk
Uniwersytet Marii Curie-Skłodowskiej w Lublinie,
Wydział Chemii, Instytut Nauk Chemicznych,
Katedra Radiochemii i Chemii Środowiskowej
Jedruchniewicz.katarzyna@gmail.com

Rada Naukowa Instytutu Nauk Chemicznych
Uniwersytetu Marii Cure-Skłodowskiej
w Lublinie

Oświadczenie o współautorstwie

Niniejszym oświadczam, że mój udział w pracy: M. Gęca, M. Wiśniewska, P. Nowicki, **K. Jędruchniewicz**, *Cd(II) and As(V) removal from the multicomponent solutions in the presence of ionic polymers using carbonaceous adsorbents obtained from herbs,* Pure and Applied Chemistry, 2023, 95, 5, 563-578. DOI: 10.1515/pac-2023-0201 [D8], obejmował oznaczenie stężenia jonów metali w roztworach przed i po adsorpcji.

Katarzyna Jędruchniewicz

D9. M. Gęca, M. Wiśniewska, P. Nowicki, *Investigation of ionic polymers stabilizing and flocculating properties in dispersed activated carbons systems,* Materials, 2024, 17, 693, DOI: 10.3390/ma17030693

materials

MDPI

Article

Investigation of Ionic Polymers' Stabilizing and Flocculating Properties in Dispersed Activated Carbons Systems

Marlena Gęca [1,*], Małgorzata Wiśniewska [1,*] and Piotr Nowicki [2]

[1] Department of Radiochemistry and Environmental Chemistry, Institute of Chemical Sciences, Faculty of Chemistry, Maria Curie-Sklodowska University in Lublin, M. Curie-Sklodowska Sq. 3, 20-031 Lublin, Poland
[2] Department of Applied Chemistry, Faculty of Chemistry, Adam Mickiewicz University in Poznań, Uniwersytetu Poznańskiego 8, 61-614 Poznań, Poland; piotrnow@amu.edu.pl
* Correspondence: marlena.geca@mail.umcs.pl (M.G.); malgorzata.wisniewska@mail.umcs.pl (M.W.)

Abstract: Activated carbons obtained via the thermochemical treatment of lemon balm and mint herbs were applied for ionic polymers adsorption, which directly affects the stability of these types of aqueous suspensions. The examined carbonaceous materials were characterized by well-developed specific surface area (approximately 1000 m^2/g) and mesoporous structure. The adsorbed amounts of anionic poly(acrylic acid) and cationic polyethyleneimine from one-component solutions reached significant levels, but the efficiency of adsorption of these compounds from binary solutions slightly decreased. Moreover, the ionic polymers showed stabilizing properties towards the activated carbons suspensions. For both adsorbents, the most stable suspensions were systems containing both types of polymeric macromolecules with different ionic characters. This was due to the occurrence of electrosteric and depletion stabilization mechanisms. Furthermore, the zeta potential and size of particle aggregates were also influenced by the presence of polymers in the aqueous suspensions of activated carbons.

Keywords: activated carbons; stabilization–flocculation properties; poly(acrylic acid); polyethyleneimine; binary polymer solution

Citation: Gęca, M.; Wiśniewska, M.; Nowicki, P. Investigation of Ionic Polymers' Stabilizing and Flocculating Properties in Dispersed Activated Carbons Systems. *Materials* **2024**, *17*, 693. https://doi.org/10.3390/ma17030693

Academic Editor: Magdalena Sobiesiak

Received: 9 January 2024
Revised: 25 January 2024
Accepted: 29 January 2024
Published: 1 February 2024

1. Introduction

In the field of environmental remediation and water treatment, the effective removal of pollutants from aqueous media remains a critical challenge. Activated carbons, thanks to their large surface area and polydisperse porous structure, have emerged as versatile adsorbents for a diverse range of contaminants [1,2]. The flocculation process involving polymeric bridges formation between dispersed particles is important in water treatment technologies. Understanding the various mechanisms of highly-dispersed suspensions destabilization is essential for the efficient purification of aqueous solutions [3–5].

Ionic polymers, with their unique physicochemical properties, can affect the stability of activated carbons suspensions. These polymers, characterized by the presence of charged functional groups along their chains, have demonstrated the ability to interact with dispersed particles and influence their stability and aggregation [6]. These macromolecules' influence on suspension stability is based on a few mechanisms: steric, electrosteric and depletion stabilization [7,8]. Steric stabilization results from polymer adsorption on the solid surface, which reduces the Van der Waals attraction between particles [9]. The electrosteric mechanism is a combination of electrostatic and steric stabilization. Polymeric adsorption layers lead to a decrease in the electrostatic and Van der Waals flocculation forces [10]. On the other hand, unadsorbed polymers chains remaining in the solution cause suppression of the depletion attraction, or depletion stabilization [11].

Poly(acrylic acid) (PAA) finds applications in many sectors, including, but not limited to, drug delivery, adhesives, textiles and biomedical engineering. It is commonly used to

produce hydrogel drug-releasing systems [12,13]. The presence of carboxyl groups in PAA macromolecules enables the direct functionalisation of hydrogels via chemical and physical cross-linking [14]. In turn, polyethyleneimine (PEI) is a cationic polymer characterized by a high density of amine functional groups. This imparts PEI molecules' unique properties, which have attracted significant attention in the fields of materials science, biotechnology and beyond. Additionally, this structure of PEI chains enables the formation of cross-links [15,16]. The possibility of adopting many different conformations on the surface of solid particles by adsorbed chains of ionic polymers has a strong impact on the stability of dispersed systems in which they occur.

In the present study, the poly(acrylic acid) and polyethyleneimine solutions, as well as activated carbons obtained from lemon balm and mint herbs, were used as components of aqueous suspensions. The zeta potential and size of aggregates of carbonaceous materials in solutions without and in the presence of single and binary polymer adsorbates were determined. The influence of polymers in one- and two-component systems on the stability of activated carbon suspensions was checked. Moreover, the impact of PAA and PEI on their mutual adsorption and the structure of mixed adsorption layers were also studied. The adsorption of ionic polymers on an activated carbon surface is rarely studied, while the mechanisms of processes that occur at the solid–solution interface are almost never investigated. However, with industrial development, the amounts of various types of macromolecular compounds in the natural environment are constantly increasing. They can disturb the natural balance and interfere with the wastewater treatment process. For this reason, there is a constant need to investigate the behaviour of such colloidal systems in order to develop more efficient techniques to separate these substances from aqueous solutions.

2. Materials and Methods

2.1. Materials

Activated carbons (AC) obtained from lemon balm (LB) and mint (MT) herbs were used in this study. The plant material was impregnated in a H_3PO_4 solution for 24 h and then subjected to a two-stage heating program (200 °C and 500 °C) for adsorbent preparation. The detailed procedure for adsorbents preparation was described in our previous paper [17]. The textural characterization of the activated carbons was based on nitrogen adsorption–desorption isotherms using the Brunauer–Emmett–Teller (BET) equation at a relative pressure range of 0.03–0.25. The content of acidic and basic functional groups was determined applying the Boehm titration method [18–20].

The specific surface area of examined materials was 950 m^2/g for LB_AC and 1145 m^2/g for MT_AC. Both activated carbons were mesoporous materials with an average pore diameter of approximately 5 nm. The total pore volume of LB_AC activated carbons was 1.10 cm^3/g, and that of MT_AC activated carbons was 1.47 cm^3/g. The total content of surface groups of material obtained from the lemon balm herb was 0.987 mmol/g, and the content of surface groups of material derived from the mint herb was 0.794 mmol/g. The tested activated carbons were characterized by a highly developed surface area and a high total pore volume in comparison to other materials described in the literature (Table 1).

Adsorption, stability, electrokinetic and aggregation measurements were performed at pH 3, at which the ionic polymers used demonstrated the highest affinity to both activated carbons' surfaces—their adsorbed amounts were the largest. All of these measurements were performed at 25 °C in the following systems: LB_AC, LB_AC+PAA, LB_AC+PEI, LB_AC+PAA+PEI, MT_AC, MT_AC+PAA, MT_AC+PEI and MT_AC+PAA+PEI.

Table 1. Comparison of the preparation procedure and textural parameters of activated carbons obtained as a result of chemical activation of biomass.

Precursor	Preparation Conditions	Surface Area [m^2/g]	Total Pore Volume [cm^3/g]	Reference
Lemon balm herb	Impregnation with H_3PO_4, two stage heating program (200 °C, 500 °C)	950	1.10	Present study
Mint herb	Impregnation with H_3PO_4, two stage heating program (200 °C, 500 °C)	1145	1.47	Present study
Peanut hulls	Chemical activation with $ZnCl_2$, heating for 6 h at temp. range 300–750 °C	420	0.17	[21]
Chestnut wood	Impregnation with H_3PO_4, heating at 500 °C for 4 h	783	0.44	[22]
Pineapple peels	Carbonized at 700 °C, activation with KOH in microwave oven	1006	0.59	[23]
Pineapple peels	Carbonized at 700 °C, activation with K_2CO_3 in microwave oven	680	0.45	[23]
Tomato processing solid waste	Impregnation with $ZnCl_2$, carbonization at 600 °C, for 1 h	1093	1.57	[24]
Cotton cake	Impregnation with H_3PO_4, heating at 450 °C for 2 h	584	0.30	[25]
Shea cake	Impregnation with H_3PO_4, heating at 450 °C for 2 h	1148	0.61	[25]

Anionic poly(acrylic acid) (PAA) (Fluka, Saint Louis, MO, USA) with an average molecular weight equal to 2000 Da is an anionic polymer containing carboxyl functional groups. At pH 3, it occurs in a coiled form due to minimal ionization; the dissociation degree of PAA functional groups is approximately 0.03 [26].

Polyethyleneimine (PEI) (Sigma Aldrich, Saint Louis, MO, USA) with an average molecular weight of 2000 Da is a cationic macromolecular substance (with amine functional groups). At pH 3, its polymer chain is completely dissociated and assumes the conformation characterized by significant expansion in the aqueous solution [27].

The surface morphologies of activated carbons without and with adsorbed poly(acrylic acid) or polyethyleneimine were determined by applying the SEM technique (Quanta 250 FEG by FEI, Waltham, MA, USA; detector Octane Elect Plus by EDAX, Berwyn, IL, USA). SEM images of both activated carbons are presented in Figure 1, whereas Figure 2 shows the morphology of the MT_AC sample in the presence of polymers.

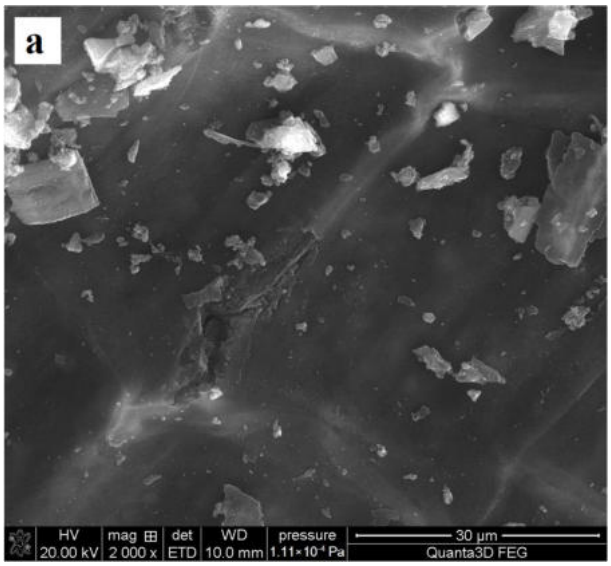

Figure 1. *Cont.*

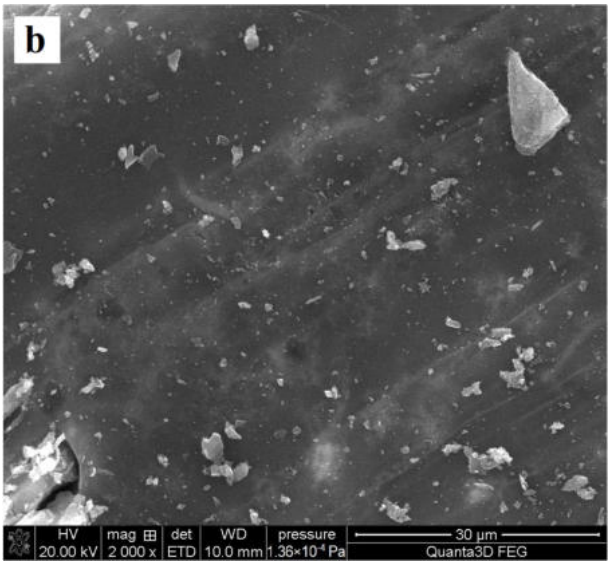

Figure 1. SEM images of MT_AC (**a**) and LB_AC (**b**) activated carbons.

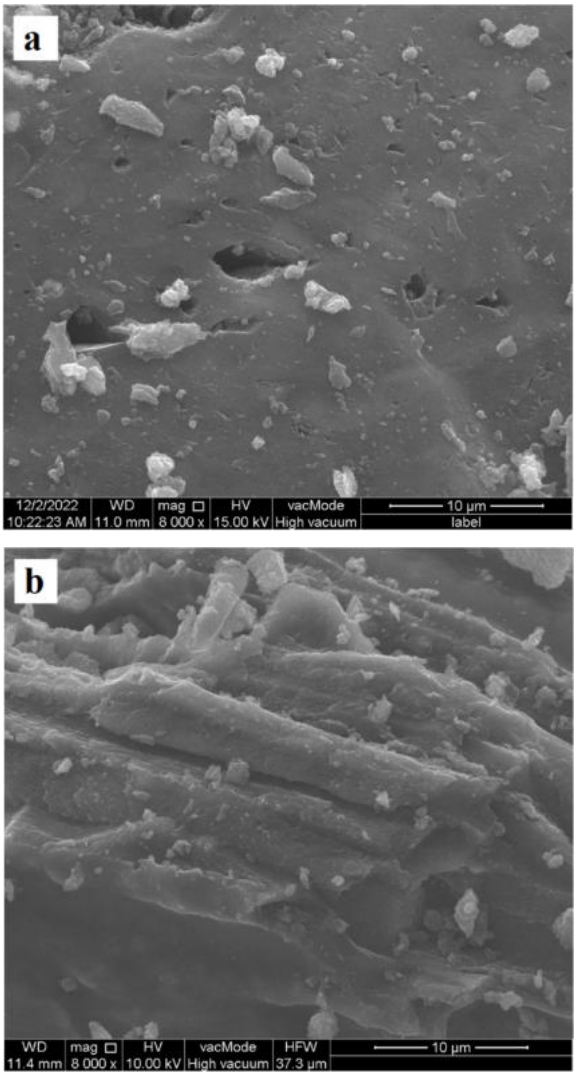

Figure 2. *Cont*.

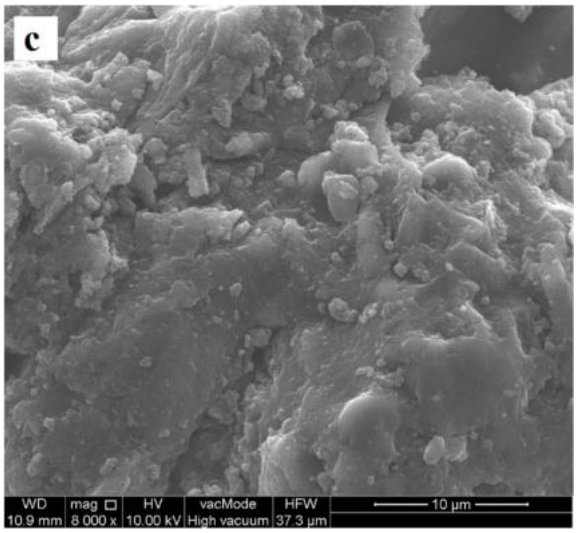

Figure 2. SEM images of MT_AC activated carbon without (**a**) as well as with PAA (**b**) and PEI (**c**) adsorbates.

2.2. Surface Charge Density, Zeta Potential and Aggregate Sizes Determination

Determination of the surface charge density (σ_0) of activated carbons particles without or with the selected adsorbates was performed by applying the potentiometric titration method. For this purpose, 50 cm^3 of a suspension containing 0.025 g of activated carbon, 100 ppm of adsorbates and 0.001 mol/dm^3 of NaCl supporting electrolyte was used. These measurements were performed in a thermostated Teflon vessel (RE 204 thermostat, Lauda Scientific, Lauda-Königshofen, Germany) in which glass and calomel electrodes (Beckman Instruments, Brea, CA, USA) were placed. Changes in the σ_0 value as a function of solution pH were calculated with the computer program "Titr_v3" [28].

The zeta potential (ζ) and size of activated carbons particles aggregates (without and with the polymer/s) were determined using the following procedure. First, 200 cm^3 of suspension containing the tested polymers with a concentration of 100 ppm, NaCl supporting electrolyte (0.001 mol/dm^3) and 0.03 g of the solid was prepared. The system was subjected to the action of ultrasounds (XL 2020 ultrasonic head, Misonix, Farmingdale, NY, USA) for 3 min, and then the pH of the obtained sample was adjusted to 3. For this purpose, solutions of HCl and NaOH with concentrations of 0.1 mol/dm^3 as well as a Φ360 pH meter (Beckman, Brea, CA, USA) were used. Zeta potential measurements were performed by applying the Doppler laser electrophoresis method and a Zetasizer Nano ZS (Malvern Instruments, Malvern, UK). This device facilitated measurement of the electrophoretic mobility of solid particles without, and covered with, polymeric adsorption layers. Based on obtained results, the zeta potential (ζ) was calculated using the Henry's equation [29]. In turn, the average size of aggregates of tested solids was determined based on the static light scattering phenomenon. In the case of suspensions containing polymer/s, the macromolecular compound was added directly after the sonication process, and such samples were immediately subjected to appropriate measurement.

2.3. Adsorption Studies

Adsorption tests were performed at 25 °C for 24 h; 10 cm^3 of suspension containing 0.1 g of activated carbon, 200 ppm of the appropriate polymer and 0.001 mol/dm^3 of NaCl as the supporting electrolyte was used. Adsorption was carried out in single and binary systems of polymeric adsorbates. After the process was completed, solids were separated from solutions using the MPW 233e microcentrifuge (MPW Med. Instruments, Warsaw, Poland). The amounts of adsorbed polymers were determined using the static method based on the change in the adsorbate concentration in the solution before and after the process. The concentration of poly(acrylic acid) was determined based on its reaction with

hyamine 1622, which resulted in the formation of a white-colored complex. The obtained compound absorbed light at a wavelength of 500 nm [30]. In the case of polyethyleneimine, a reaction with $CuCl_2$ was used. This formed a blue-colored complex that absorbed light at a wavelength of 285 nm [31]. The UV–Vis spectrophotometer Carry 100 (Varian, Palo Alto, CA, USA) was used for absorbance measurements.

2.4. Stability Tests

The spectrophotometric method was applied for stability studies (spectrophotometer Carry 100, Varian, Palo Alto, CA, USA). For this purpose, 10 cm^3 of suspension containing 0.01 g of activated carbon, 0.001 mol/dm^3 of NaCl (supporting electrolyte) and 200 ppm of appropriate adsorbate was prepared. The pH of the sample was adjusted to 3 using HCl and NaOH solutions with concentrations of 0.1 mol/dm^3 as well as a Φ360 pH meter (Beckman, Brea, CA, USA). The exemplary absorbance dependencies obtained for LB_AC and MT_AC activated carbons suspensions at different wavelengths are presented in Figure 3. The wavelength of 500 nm was chosen for further study, due to the lack of interferences and small changes in the recorded signal. The absorbance of tested suspensions was measured for 5 h at 15 min intervals.

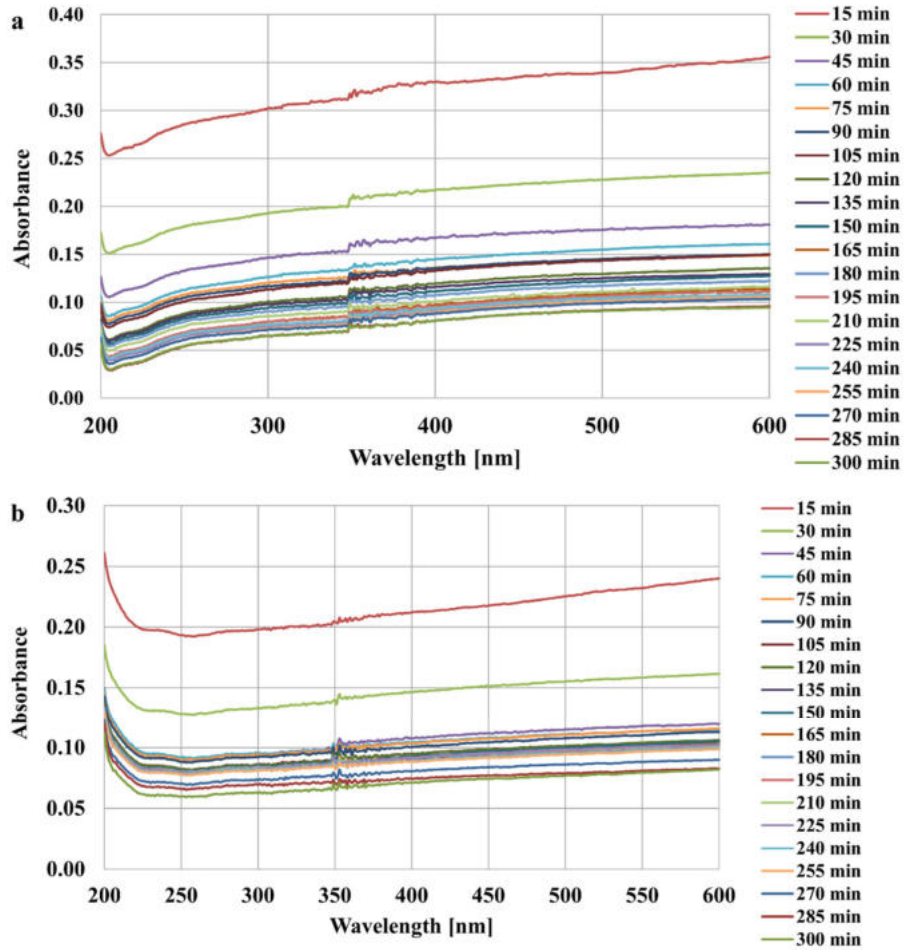

Figure 3. The absorbance of LB_AC (**a**) and MT_AC (**b**) activated carbons suspensions at different wavelengths.

3. Results and Discussion

3.1. Electrical Double-Layer Structure and Aggregation Properties of Activated Carbons in the Presence of Ionic Polymers

The surface charge density and zeta potential values of examined activated carbons at pH 3 are presented in Table 2. The surface charge density of the material obtained from the

lemon balm was 4.52 μC/cm^2, whereas the surface charge density of the material obtained from the mint herb was 2.54 μC/cm^2. The presence of poly(acrylic acid) slightly decreased the surface charge density at pH 3. The attraction between positively charged adsorbents surfaces and the anionic polymer is favorable for PAA adsorption under such pH conditions. The presence of polyethyleneimine increased the surface charge density. The impact of PEI on the examined value was more noticeable due to the repulsion between positively charged polymeric macromolecules and the adsorbent surface. The polymeric chains were not fully adsorbed on the activated carbons surface in the form of train structures (by all their segments). Some amino groups present in the loop and tail structures of adsorbed chains were located in the by-surface area, which affected the surface charge density value. In the binary solution, an intermediate effect, in comparison to the single solution, was observed. The zeta potential of LB_AC activated carbon was 3.90 mV, whereas that of MT_AC activated carbon was −4.72 mV. These values are close to zero, which proved that the isoelectric points of both materials occured at a pH of approximately 3. Poly(acrylic acid) present in the solution caused decreases in zeta potential values, whereas in the system containing polyethyleneimine the zeta potential increased. This was caused by the charged polymeric functional groups of adsorbed macromolecules located on the border of the compact and diffusive parts of the electrical double layer (edl) formed at the activated carbon–solution interface [32]. In the binary solution, the greatest increase in the zeta potential was observed. At pH 3, PAA occurs in a coiled form, and can be adsorbed on the surface of activated carbon as well as inside its solid pores (due to PAA macromolecules small hydrodynamic radius of 0.77 nm), whereas the mean pore size of both adsorbents is approximately 5 nm [33]. PEI chains under these conditions assume considerably developed conformation and their adsorption is mostly limited to the outer surface of carbonaceous adsorbents. Due to the poly(acrylic acid) occupation of active sites on the solid surface, a greater amount of polyethyleneimine molecules remained in the slipping plane area, which resulted in an additional increase in the zeta potential value. The binary system was presumably the most stable among all tested suspensions because the higher the absolute value of the zeta potential, the greater the probability that the studied suspension will be stable [34].

Table 2. The surface charge density and zeta potential of LB_AC and MT_AC activated carbons at pH 3 without adsorbates as well as in single and binary adsorbates systems.

System	Surface Charge Density [μC/cm^2]		Zeta Potential [mV]	
	LB_AC	MT_AC	LB_AC	MT_AC
Without adsorbates	4.52	2.54	3.90	−4.72
PAA	2.52	1.47	−3.00	−4.19
PEI	14.33	14.59	26.02	19.77
PAA + PEI	11.23	3.40	32.08	33.42

The presence of poly(acrylic acid) caused an increase in the size of the aggregates of both activated carbons (Figure 4). The adsorption of coiled PAA molecules induced changes in the surface charge density leading to the strongest attraction between adsorbent particles. The adsorption of negatively charged polymeric chains causes the neutralization of the positive surface charge of activated carbons. MT_AC activated carbon contains a smaller number of surface functional groups, which results in lower adsorption of poly(acrylic acid). In this case, the polymeric coils create a less compact adsorption layer and there is a possibility of bridging interactions occurrence. As a result, larger aggregates can be created, which, due to their loose structure, remain in the solution (the stabilization effect is observed). In suspensions containing PEI or both polymer adsorbates, no significant changes in the size of LB_AC and MT_AC aggregates were observed. Large aggregates usually flocculate faster; however, stable macroaggregates also exist [35]. Aggregates with a well-developed surface area can undergo sedimentation more slowly, due to the buoyancy forces of the solvent, and thus remain in the bulk solution for a long time.

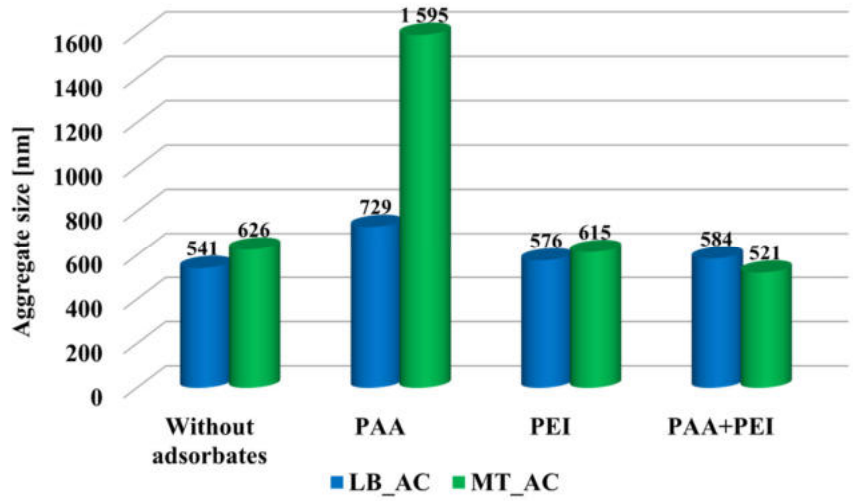

Figure 4. Sizes of LB_AC and MT_AC activated carbons aggregates at pH 3 (without adsorbates, as well as in single and binary adsorbate systems).

3.2. Adsorption Layer Structure of Ionic Polymers on the Activated Carbons Surface

The anionic polymer showed greater affinity to the surface of LB_AC activated carbon (Figure 5). The higher content of functional surfaces groups for this material guaranteed the possibility of binding a larger number of macromolecule segments to the active sites of the solid. Polyethyleneimine was adsorbed in similar amounts on the surfaces of both adsorbents, as a result of its considerably developed conformation, which is less sensitive to the number of available active sites on the solid surface. The anionic polymer was adsorbed in a greater amount in comparison to the cationic one. It was related to a completely different polymers conformation at pH 3. PAA occurs in a coiled form and can be adsorbed both on the surface and in the pores of adsorbents, whereas developed PEI chains are mainly adsorbed only on the outer surface of activated carbons [17]. Moreover, the surface charge of the adsorbents at pH 3 was positive, which resulted in attraction between the anionic polymeric coils and the activated carbon particles. Such favorable electrostatic interactions resulted in the formation of a densely packed polymeric layer. In the case of PEI, the adsorption layer consisted of developed chains located perpendicularly to the solid surface. In the binary solutions, the adsorbed amounts of both polymers decreased due to competition between macromolecules with opposite ionic natures [36].

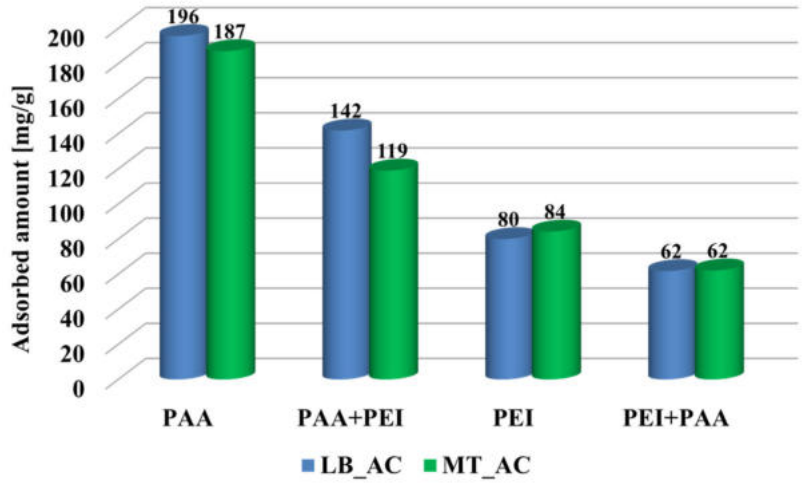

Figure 5. Adsorbed amounts of poly(acrylic acid) (PAA, PAA + PEI) and polyethyleneimine (PEI, PEI + PAA) on the surface of LB_AC and MT_AC activated carbons at pH 3 in single and binary adsorbates systems.

3.3. Stability Mechanisms of Activated Carbons Suspensions in the Presence of Ionic Polymers

Results of stability tests are presented in Figures 6 and 7. The higher the absorbance value, the more stable the suspension (due to the presence of solid particles in the entire volume of the solution). The presence of poly(acrylic acid) had no significant effect on the stability of the LB_AC activated carbon suspension. The polymer was probably adsorbed most in the pores of the adsorbent, which did not significantly affect the interactions of solid particles. On the other hand, polyethyleneimine adsorption caused a noticeable deterioration in the stability of the system. The positively charged surface of the material obtained from the lemon balm caused the perpendicular adsorption of PEI cationic chains. Molecules were extended at considerable distances from the solid surface, which resulted in bridging flocculation by forming polymeric connections between neighboring particles (Figure 8a) [37]. In a different way, poly(acrylic acid) caused the stabilization of the MT_AC system due to electrosteric mechanisms occurrence (Figure 8b). Both activated carbons systems were the most stable in the simultaneous presence of PAA and PEI. All above-mentioned stabilization mechanisms occurred in binary systems. Additionally, depletion stabilization forces might appear (Figure 8c). Free chains that remained in the solution due to the lower adsorbed amount in the binary systems prevented colloidal particles from forming large aggregates and suspension destabilization [38].

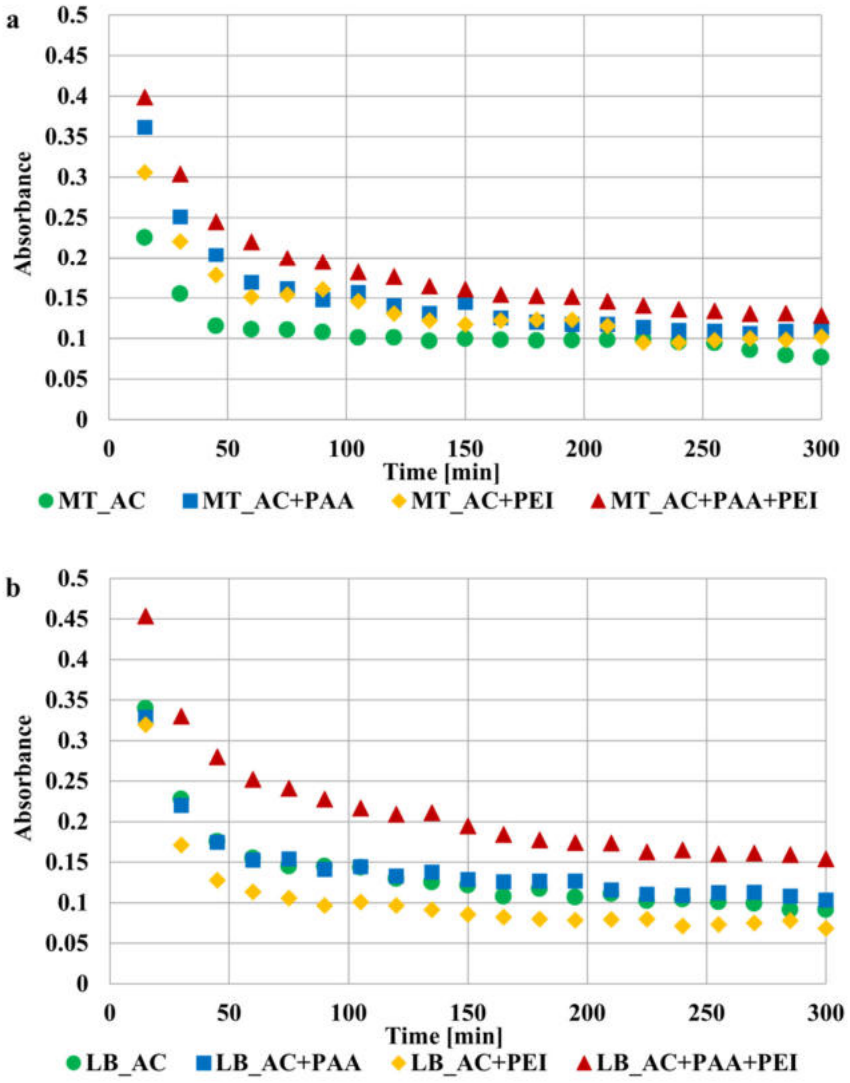

Figure 6. The stability of LB_AC (**a**) and MT_AC (**b**) activated carbons suspensions at pH 3 in single and binary adsorbate systems.

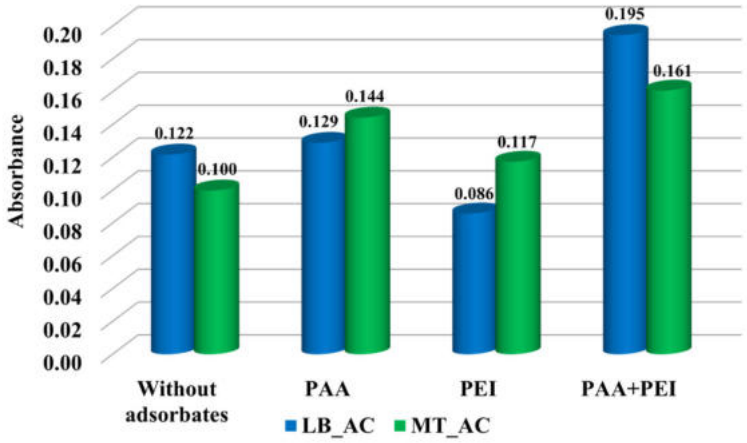

Figure 7. The absorbance of LB_AC and MT_AC activated carbons suspensions at pH 3 in single and binary adsorbate systems after 150 min.

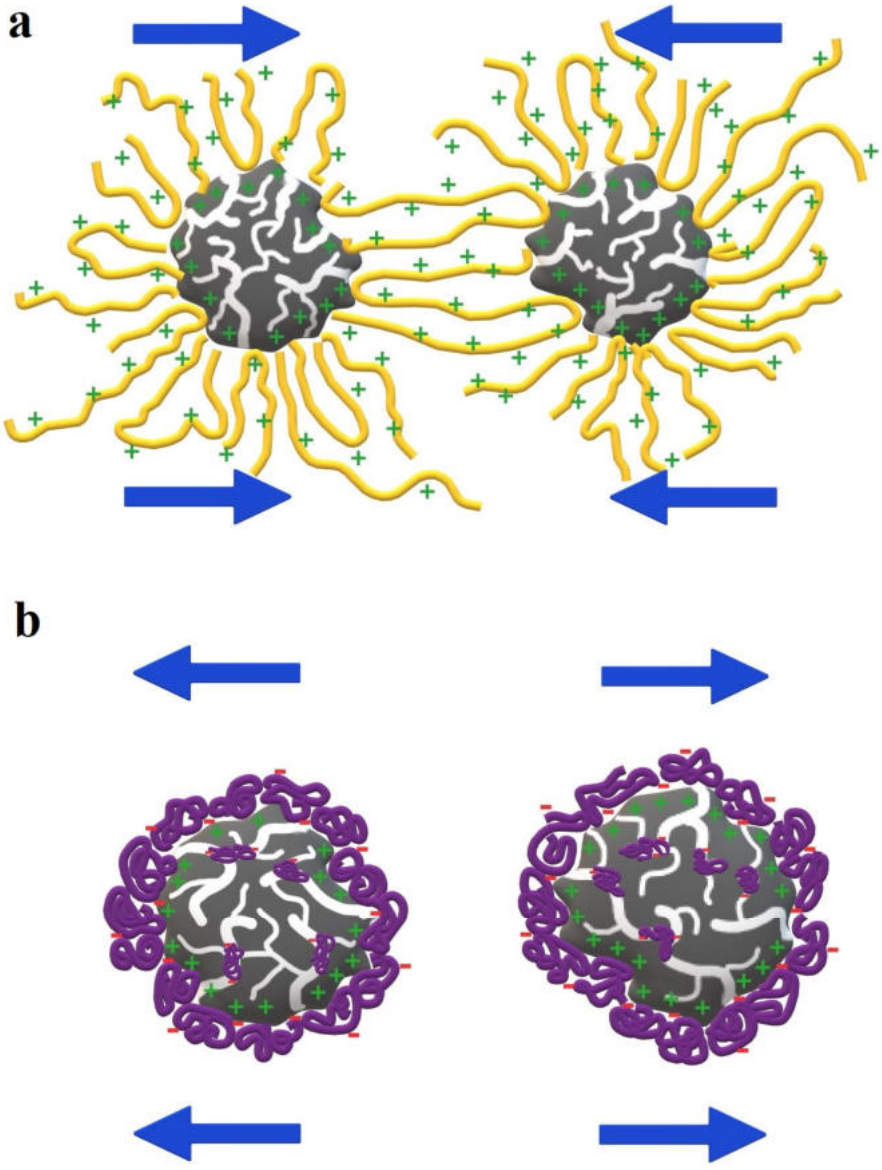

Figure 8. *Cont*.

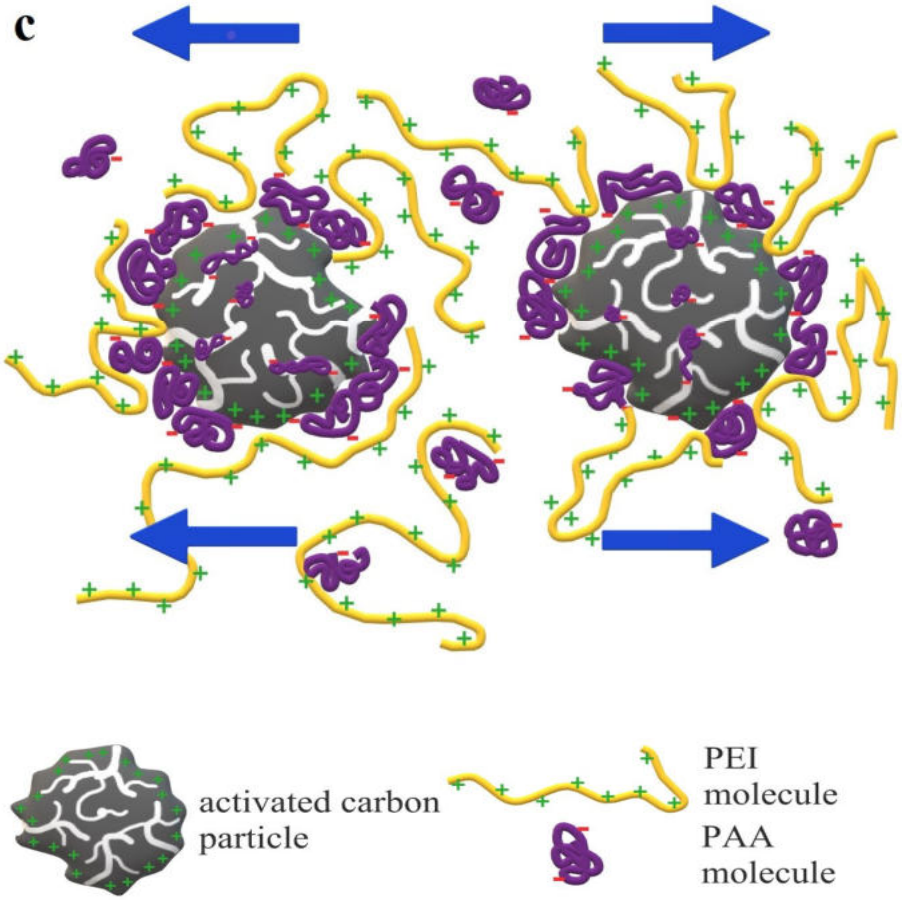

Figure 8. The major stabilization/destabilization mechanisms of PEI—the bridging flocculation (**a**), PAA—the electrosteric stabilization (**b**), and the binary system—the combined electrosteric and depletion stabilization (**c**).

4. Conclusions

The tested activated carbons were characterized by high adsorption capacities towards ionic polymers. The adsorbed amounts reached levels of approximately 190 mg/g for poly(acrylic acid) and approximately 80 mg/g for polyethyleneimine. The adsorption of polymers from their binary solutions decreased noticeably due to the competition of polymeric chains assuming completely different conformations in tested systems at pH 3. Ionic polymers had a strong impact on the activated carbons suspensions' stability. Their presence also affected the surface charge density, zeta potential and aggregates sizes formed by solid particles. The most perpendicular adsorption of significantly developed PEI chains on the LB_AC activated carbon surface caused the destabilization of suspension via bridging flocculation. On the other hand, steric and electrosteric stabilization occurred in systems containing MT_AC material and ionic polymers. Binary systems were the most stable due to the occurrence of an additional stabilization mechanism coming from depletion forces. The competition between polyethyleneimine and poly(acrylic acid) macromolecules resulted in some polymeric chains remaining in the solution, which noticeably reduced the flocculation tendency.

Author Contributions: Conceptualization, M.W. and P.N.; methodology, M.W., M.G. and P.N.; validation, M.W. and M.G.; formal analysis, M.W., M.G. and P.N.; investigation, M.G. and P.N.; re-sources, M.W. and P.N.; data curation, M.G. and P.N.; writing—original draft preparation, M.W., M.G. and P.N.; writing—review and editing, M.W., M.G. and P.N.; visualization, M.G.; supervision, M.W. and P.N. All authors have read and agreed to the published version of the manuscript.

Funding: This research received no external funding.

Institutional Review Board Statement: Not applicable.

Informed Consent Statement: Not applicable.

Data Availability Statement: Data are contained within the article.

Conflicts of Interest: The authors declare no conflicts of interest.

References

1. Gęca, M.; Wiśniewska, M.; Nowicki, P. Biochars and activated carbons as adsorbents of inorganic and organic compounds from multicomponent systems—A review. *Adv. Colloid Interface Sci.* **2022**, *305*, 102687. [CrossRef]
2. Sultana, M.; Rownok, M.H.; Sabrin, M.; Rahaman, M.H.; Alam, S.N. A review on experimental chemically modified activated carbon to enhance dye and heavy metals adsorption. *Clean. Eng. Technol.* **2022**, *6*, 100382. [CrossRef]
3. Krahnstöver, T.; Wintgens, T. Optimizing the flocculation of powdered activated carbon in wastewater treatment by dosing iron salt in single-and two-stage processes. *J. Water Proc. Eng.* **2017**, *20*, 130–137. [CrossRef]
4. Wiśniewska, M.; Chibowski, S.; Urban, T. Effect of the presence of cationic polyacrylamide on the surface properties of aqueous alumina suspension-stability mechanism. *Appl. Surf. Sci.* **2014**, *320*, 843–851. [CrossRef]
5. Ueno, K.; Watanabe, M. From colloidal stability in ionic liquids to advanced soft materials using unique media. *Langmuir* **2011**, *27*, 9105–9115. [CrossRef] [PubMed]
6. Wiśniewska, M.; Nowicki, P. Peat-based activated carbons as adsorbents for simultaneous separation of organic molecules from mixed solution of poly (acrylic acid) polymer and sodium dodecyl sulfate surfactant. *Colloids Surf. A* **2020**, *585*, 124179. [CrossRef]
7. Kong, H.J.; Bike, S.G.; Li, V.C. Electrosteric stabilization of concentrated cement suspensions imparted by a strong anionic polyelectrolyte and a non-ionic polymer. *Cem. Concr. Res.* **2006**, *36*, 842–850. [CrossRef]
8. Kim, S.; Hyun, K.; Moon, J.Y.; Clasen, C.; Ahn, K.H. Depletion stabilization in nanoparticle–polymer suspensions: Multi-length-scale analysis of microstructure. *Langmuir* **2015**, *31*, 1892–1900. [CrossRef] [PubMed]
9. Fritz, G.; Schädler, V.; Willenbacher, N.; Wagner, N.J. Electrosteric stabilization of colloidal dispersions. *Langmuir* **2002**, *18*, 6381–6390. [CrossRef]
10. Kong, H.J.; Bike, S.G.; Li, V.C. Development of a self-consolidating engineered cementitious composite employing electrosteric dispersion/stabilization. *Cem. Concr. Compos.* **2003**, *25*, 301–309. [CrossRef]
11. Semenov, A.N.; Shvets, A.A. Theory of colloid depletion stabilization by unattached and adsorbed polymers. *Soft Matter* **2015**, *11*, 8863–8878. [CrossRef]
12. Pourmadadi, M.; Farokh, A.; Rahmani, E.; Eshaghi, M.M.; Aslani, A.; Rahdar, A.; Ferreira, L.F.R. Polyacrylic acid mediated targeted drug delivery nano-systems: A review. *J. Drug Deliv. Sci. Technol.* **2023**, *80*, 104169. [CrossRef]
13. Wang, Y.; Wang, J.; Yuan, Z.; Han, H.; Li, T.; Li, L.; Guo, X. Chitosan cross-linked poly (acrylic acid) hydrogels: Drug release control and mechanism. *Colloids Surf. B* **2017**, *152*, 252–259. [CrossRef]
14. Cozens, E.J.; Roohpour, N.; Gautrot, J.E. Comparative adhesion of chemically and physically crosslinked poly (acrylic acid)-based hydrogels to soft tissues. *Eur. Polym. J.* **2021**, *146*, 110250. [CrossRef]
15. Jung, H.; Jeon, S.; Jo, D.H.; Huh, J.; Kim, S.H. Effect of crosslinking on the CO_2 adsorption of polyethyleneimine-impregnated sorbents. *Chem. Eng. J.* **2017**, *307*, 836–844. [CrossRef]
16. Wang, Z.; Park, H.N.; Won, S.W. Adsorption and Desorption Properties of Polyethylenimine/Polyvinyl Chloride Cross-Linked Fiber for the Treatment of Azo Dye Reactive Yellow 2. *Molecules* **2021**, *26*, 1519. [CrossRef] [PubMed]
17. Gęca, M.; Wiśniewska, M.; Nowicki, P. Simultaneous Removal of Polymers with Different Ionic Character from Their Mixed Solutions Using Herb-Based Biochars and Activated Carbons. *Molecules* **2022**, *27*, 7557. [CrossRef] [PubMed]
18. Boehm, H.P.; Diehl, E.; Heck, W.; Sappok, R. Surface oxides of carbon. *Angew. Chem. Int. Ed. Engl.* **1964**, *3*, 669–677. [CrossRef]
19. Singh, S.B.; De, M. Scope of doped mesoporous (<10 nm) surfactant-modified alumina templated carbons for hydrogen storage applications. *Int. J. Energy Res.* **2019**, *43*, 4264–4280. [CrossRef]
20. Singh, S.B.; Dastgheib, S.A. Physicochemical transformation of graphene oxide during heat treatment at 110–200 °C. *Carbon Trends* **2023**, *10*, 100251. [CrossRef]
21. Girgis, B.S.; Yunis, S.S.; Soliman, A.M. Characteristics of activated carbon from peanut hulls in relation to conditions of preparation. *Mater. Lett.* **2002**, *57*, 164–172. [CrossRef]
22. Gómez-Serrano, V.; Cuerda-Correa, E.M.; Fernandez-Gonzalez, M.C.; Alexandre-Franco, M.F.; Macias-Garcia, A. Preparation of activated carbons from chestnut wood by phosphoric acid-chemical activation. Study of microporosity and fractal dimension. *Mater. Lett.* **2005**, *59*, 846–853. [CrossRef]
23. Foo, K.Y.; Hameed, B.H. Porous structure and adsorptive properties of pineapple peel based activated carbons prepared via microwave assisted KOH and K_2CO_3 activation. *Microporous Mesoporous Mater.* **2012**, *148*, 191–195. [CrossRef]
24. Sayğılı, H.; Güzel, F. High surface area mesoporous activated carbon from tomato processing solid waste by zinc chloride activation: Process optimization, characterization and dyes adsorption. *J. Clean. Prod.* **2016**, *113*, 995–1004. [CrossRef]
25. Ibrahim, T.; Moctar, B.L.; Tomkouani, K.; Gbandi, D.B.; Victor, D.K.; Phinthè, N. Kinetics of the adsorption of anionic and cationic dyes in aqueous solution by low-cost activated carbons prepared from sea cake and cotton cake. *Am. Chem. Sci. J.* **2013**, *4*, 38–57. [CrossRef]

26. Chibowski, S.; Wiśniewska, M.; Marczewski, A.W.; Pikus, S. Application of the SAXS method and viscometry for determination of the thickness of adsorbed polymer layers at the ZrO_2 –polymer solution interface. *J. Colloid Interface Sci.* **2003**, *267*, 1–8. [CrossRef] [PubMed]
27. Von Harpe, A.; Petersen, H.; Li, Y.; Kissel, T. Characterization of commercially available and synthesized polyethylenimines for gene delivery. *J. Control. Release* **2000**, *69*, 309–322. [CrossRef] [PubMed]
28. Janusz, W. Electrical double layer in the system TiO_2 (anathase)/aqueous solution of NaCl. *Pol. J. Chem.* **1994**, *68*, 1871–1880.
29. Ohshima, H. A Simple Expression for Henry's Function for the Retardation Effect in Electrophoresis of Spherical Colloidal Particles. *J. Colloid Interface Sci.* **1994**, *168*, 269–271. [CrossRef]
30. Crummett, W.B.; Hummel, R.A. The determination of traces of polyacrylamides in water. *J. Am. Water Works Assoc.* **1963**, *55*, 209–219. [CrossRef]
31. Patkowski, J.; Myśliwiec, D.; Chibowski, S. Validation of a new method for spectrophotometric determination of polyethylenimine. *Int. J. Polym. Anal.* **2016**, *21*, 486–494. [CrossRef]
32. Gęca, M.; Wiśniewska, M.; Nowicki, P.; Jędruchniewicz, K. Cd(II) and As(V) removal from the multicomponent solutions in the presence of ionic polymers using carbonaceous adsorbents obtained from herbs. *Pure Appl. Chem.* **2023**, *95*, 563–578. [CrossRef]
33. Gęca, M.; Wiśniewska, M.; Urban, T.; Nowicki, P. Temperature Effect on Ionic Polymers Removal from Aqueous Solutions Using Activated Carbons Obtained from Biomass. *Materials* **2023**, *16*, 350. [CrossRef]
34. Ostolska, I.; Wiśniewska, M. Application of the zeta potential measurements to explanation of colloidal Cr_2O_3 stability mechanism in the presence of the ionic polyamino acids. *Colloid Polym. Sci.* **2014**, *292*, 2453–2464. [CrossRef] [PubMed]
35. Márquez, C.O.; Garcia, V.J.; Cambardella, C.A.; Schultz, R.C.; Isenhart, T.M. Aggregate-Size Stability Distribution and Soil Stability. *Soil Sci. Soc. Am. J.* **2004**, *68*, 725.
36. Bey, H.B.; Hot, J.; Baumann, R.; Roussel, N. Consequences of competitive adsorption between polymers on the rheological behaviour of cement pastes. *Cem. Concr. Compos.* **2014**, *54*, 17–20. [CrossRef]
37. Pelssers EG, M.; Stuart MA, C.; Fleer, G.J. Kinetics of bridging flocculation. Role of relaxations in the polymer layer. *J. Chem. Soc. Faraday Trans.* **1990**, *86*, 1355. [CrossRef]
38. Wiśniewska, M. A review of temperature influence on adsorption mechanism and conformation of water soluble polymers on the solid surface. *J. Dispers. Sci. Technol.* **2011**, *32*, 1605–1623. [CrossRef]

Lublin, 10.09.2025

mgr Marlena Groszek
Uniwersytet Marii Curie-Skłodowskiej w Lublinie,
Wydział Chemii, Instytut Nauk Chemicznych,
Katedra Radiochemii i Chemii Środowiskowej,
Pl. Marii Curie-Skłodowskiej 3, 20-031 Lublin
marlena.groszek@mail.umcs.pl

Rada Naukowa Instytutu Nauk Chemicznych
Uniwersytetu Marii Cure-Skłodowskiej
w Lublinie

Oświadczenie o współautorstwie

Niniejszym oświadczam, że mój udział w pracy: **M. Gęca,** M. Wiśniewska, P. Nowicki, *Investigation of Ionic Polymers' Stabilizing and Flocculating Properties in Dispersed Activated Carbons Systems,* Materials, 2024, 17, 693, DOI: 10.3390/ma17030693 [D9], obejmował opracowanie metodyki badań, przeprowadzenie eksperymentów, analizę uzyskanych wyników, przygotowanie manuskryptu i jego korektę po procesie recenzji.

Marlena Groszek

Lublin, 10.09.2025

prof. dr hab. Małgorzata Wiśniewska
Uniwersytet Marii Curie-Skłodowskiej w Lublinie,
Wydział Chemii, Instytut Nauk Chemicznych,
Katedra Radiochemii i Chemii Środowiskowej,
Pl. Marii Curie-Skłodowskiej 3, 20-031 Lublin
malgorzata.wisniewska@mail.umcs.pl

Rada Naukowa Instytutu Nauk Chemicznych
Uniwersytetu Marii Cure-Skłodowskiej
w Lublinie

Oświadczenie o współautorstwie

Niniejszym oświadczam, że mój udział w pracy M. Gęca, **M. Wiśniewska**, P. Nowicki, *Investigation of Ionic Polymers' Stabilizing and Flocculating Properties in Dispersed Activated Carbons Systems,* Materials, 2024, 17, 693, DOI: 10.3390/ma17030693 [D9], obejmował stworzenie koncepcji pracy, interpretację uzyskanych wyników, korektę manuskryptu - przed i po procesie recenzji oraz nadzór merytoryczny w czasie całego cyklu wydawniczego.

Małgorzata Wiśniewska

Poznań, 10.09.2025

dr hab. Piotr Nowicki, prof. UAM
Uniwersytet im. Adama Mickiewicza w Poznaniu,
Wydział Chemii, Zakład Chemii Stosowanej,
Ul. Uniwersytetu Poznańskiego 8, 61-614 Poznań
piotr.nowicki@amu.edu.pl

Rada Naukowa Instytutu Nauk Chemicznych
Uniwersytetu Marii Cure-Skłodowskiej
w Lublinie

Oświadczenie o współautorstwie

Niniejszym oświadczam, że mój udział w pracy: M. Gęca, M. Wiśniewska, **P. Nowicki**, *Investigation of Ionic Polymers' Stabilizing and Flocculating Properties in Dispersed Activated Carbons Systems,* Materials, 2024, 17, 693, DOI: 10.3390/ma17030693 [D9], obejmował stworzenie koncepcji pracy, opracowanie metodyki badań, interpretację uzyskanych wyników, korektę manuskryptu pierwszej wersji manuskryptu, przygotowanie odpowiedzi na uwagi recenzentów oraz nadzór merytoryczny w czasie całego cyklu wydawniczego.

Piotr Nowicki

D10. M. Gęca, M. Wiśniewska, P. Nowicki, G. Wójcik *Arsenate and cadmium ions removal from multicomponent solutions of ionic polymers using mesoporous activated biocarbons*, Journal of Molecular Liquids, 2024, 407, 125270, DOI: 10.1016/j.molliq.2024.125270

Journal of Molecular Liquids 407 (2024) 125270

Contents lists available at ScienceDirect

Journal of Molecular Liquids

journal homepage: www.elsevier.com/locate/molliq

Arsenate and cadmium ions removal from multicomponent solutions of ionic polymers using mesoporous activated biocarbons

Marlena Gęca [a], Małgorzata Wiśniewska [a,*], Piotr Nowicki [b], Grzegorz Wójcik [c]

[a] Department of Radiochemistry and Environmental Chemistry, Faculty of Chemistry, Institute of Chemical Sciences, Maria Curie-Sklodowska University in Lublin, M. Curie-Sklodowska Sq. 3, 20-031 Lublin, Poland
[b] Department of Applied Chemistry, Faculty of Chemistry, Adam Mickiewicz University in Poznań, Uniwersytetu Poznańskiego 8, 61-614 Poznań, Poland
[c] Department of Inorganic Chemistry, Faculty of Chemistry, Institute of Chemical Sciences, Maria Curie-Sklodowska University in Lublin, M. Curie-Sklodowska Sq. 3, 20-031 Lublin, Poland

ARTICLE INFO

Keywords:
Heavy metal ions
Simultaneous removal
Multicomponent solution
Water purification
Activated biocarbon
Plant biomass utilization

ABSTRACT

Activated biocarbons (AC) obtained in the process of simultaneous pyrolysis and activation of lemon balm (LB) and mint (MT) herbs with H_3PO_4 were used to purify aqueous solutions of cadmium, arsenate, polyethylenimine (PEI) and poly(acrylic acid) (PAA). The metals show high toxicity in the whole range of their concentrations, whereas the polymers are cytotoxic at high concentrations.

The efficiency of As(V) removal from an aqueous solution depends on the pH value, while the Cd(II) adsorption on the activated biocarbons surface is independent on this parameter. The maximum adsorbed amounts are 135.8 mg/g for Cd(II) and 109.6 mg/g for As(V), respectively. The removal of metals ions and polymers from binary systems is lower in comparison to the one-component solutions. This is a consequence of the formation of polymer-metal complexes, that tend to remain in the solution. Additionally, the surface charge density, zeta potential, the size of activated biocarbons aggregates in the aqueous suspensions and the influence of toxic metal ions on the determination of the concentration of polymers in water samples was investigated. The obtained results proved that the PEI concentration can be effectively determined in the presence of metal ions, whereas the procedure of PAA determination requires additional validation.

1. Introduction

The global demand for drinking water increases every year. Unfortunately, the amount of pollutants entering water reservoirs is also increasing. The coexistence of polymers and heavy metals in aqueous solutions represents a unique challenge in terms of environmental remediation and industrial processes [1,2]. Polymers, encompassing a diverse class of organic compounds, and heavy metal ions, known for their high toxicity and persistence, often co-occur in the industrial effluents and wastewater [3]. Their combined presence poses a serious threat to the environmental and human health, necessitating effective removal strategies [4,5]. Polyethylenimine have strong chelating properties and can easily bond with have metal ions [6]. Moreover this polymer is used in the gene-delivery system and it can penetrate cell membranes [7]. The simultaneous presence of polyethylenimine and heavy metal ions in water can be very dangerous for human and animal health and life. For example: the consumption of arsenic can cause the lung, kidney or liver cancer, whereas the cadmium affects the respiratory system, reproduction, kidneys and bones [8,9]. Wastewater treatment is essential for recovering freshwater for human activities and farming [10].

Adsorption is one of the most common wastewater treatment methods due to its simplicity, efficiency and relatively low cost. There are many materials that are used as adsorbents, such as zeolites, oxides, carbonaceous materials and functionalized metal nanoparticles [11]. Activated biocarbons due to their large surface area, well-developed pore structure and presence of various types of surface functional groups are the most widely applied carbonaceous materials [12,13]. Moreover they are environmental friendly, obtained from renewable resources and their utilization does not cause problems.

Determination of polymers concentration in an aqueous solution is a complicated and often multi-stage process. However due to the possible ionic polymers toxicity in high conventions it is necessary to effectively determine them in the aqueous solution [14,15]. The complexation of

* Corresponding author.
E-mail address: malgorzata.wisniewska@mail.umcs.pl (M. Wiśniewska).

https://doi.org/10.1016/j.molliq.2024.125270
Received 19 April 2024; Received in revised form 4 June 2024; Accepted 11 June 2024
Available online 13 June 2024

Table 1
The textural and acidic-basic properties of the tested activated biocarbons.

Adsorbent	LB_AC	MT_AC
Textural parameters		
Surface area [m^2/g]	950	1145
Pore volume [cm^3/g]	1.100	1.465
Mean pore size [nm]	4.630	5.115
Acidic-basic properties		
Acidic groups content [mmol/g]	0.682	0.494
Basic groups content [mmol/g]	0.305	0.300

polymeric macromolecules with another substance is the most commonly applied reaction type. On the other hand, macromolecules can often create complexes with the different types of substances, not only with the one which is used in the procedure. This may interfere with their determination [16]. To avoid errors in the determination procedure, it is necessary to investigate the impact of the possible interferences on the polymer complexation process. A common mistake is the application of the procedure for a specific polymer without checking the possible influence of other substances present in the tested solution.

The aim of the presented research was to determine the concentration of ionic polymers in the presence of metals ions in the multicomponent solutions. Calibration curves were obtained using single and binary systems. Anionic poly(acrylic acid), cationic polyethylenimine, Cd(II) cations and As(V) anions were used as components of the mixed solutions. The activated biocarbons obtained from waste plant material were applied for the water purification process. The selection of plant materials as feedstock for carbonaceous adsorbents production was motivated by their sustainability and cost-effectiveness [17,18]. The influence of metals ions and polymers on their simultaneous adsorption was checked. The cadmium and arsenate adsorption isotherms were obtained at different pH values. The kinetics of the process were also investigated. Additionally, the surface charge density, zeta potential as well as the size of activated biocarbons aggregates in the aqueous suspensions (without and in the presence of inorganic and/or organic adsorbates) were examined. Such systems are common in water purification technologies, but the removal of heavy metals using activated carbons (without and in the presence of ionic polymers) has not been examined by other research groups.

2. Experimental

2.1. Materials

Activated biocarbons (AC) were obtained using two types of waste biomass – lemon balm (LB) and mint (MT) herb. The plant material was impregnated in the H_3PO_4 for 24 h, dried overnight at 110 °C and subjected to heat treatment at 500 °C for 0.5 h. The detailed procedure for adsorbents preparing was presented in the previous article [19]. The textural and acidic-basic properties of the activation products are presented in Table 1. The SEM images of examined adsorbents are shown in Fig. 1.

As can be seen, both activated biocarbons are characterized by a quite similar structure, which consists of pores, crevices and cracks of various sizes and elongated shapes, which is quite typical for materials obtained from plant biomass. In addition, small, bright particles are visible on the surface and in the cavities of the structure. These are most likely fragments of a mineral substance (ash), which from the adsorption point of view is an unnecessary ballast.

Cd(II) ions used in the study were introduced into the solution in the form of $CdN_2O_6{\cdot}4H_2O$ (Sigma Aldrich, Saint Louis, USA). This salt is well soluble in water at pH below 8. Above this pH value, cadmium ions form hardly soluble precipitate. Due to that limitation all Cd(II) involving studies were performed at the pH range 3–7.

KH_2AsO_4 (Sigma Aldrich, Saint Louis, USA) was used as As(V) source. Potassium arsenate is highly soluble over the entire pH range, however, the hydration of arsenate ions changes. At high pH values, the ion is completely dehydrated and occurs in the AsO_4^{3-} form. As the pH value increases, the level of hydration decrease and takes the following forms: H_3AsO_4, $H_2AsO_4^-$ and $HAsO_4^{2-}$.

Anionic poly(acrylic acid) (PAA) (Fluka, Saint Louis, USA) containing carboxyl functional groups was also used in the studies. Its average molecular weight is 2000 Da and at pH 3 ionization of this polymer is minimal (macromolecule occurs in the coiled form).

Polyethylenimine (PEI) (Sigma Aldrich, Saint Louis, USA) is a cationic substance (containing amine groups) with average molecular weight of 2000 Da. At pH 3 polymer chain is fully dissociated and assumes the conformation of significantly expanded molecule in the aqueous solution.

2.2. Determination of adsorbates concentration

Cd(II) ions concentration was determined using Inductively Coupled Plasma-Optical Emission Spectrometry (iCAP™ 7200 ICP-OES analyzer, Thermo Fisher Scientific, Waltham, USA) at a wavelength of 228,8 nm. An ICP Optical Emission Spectrometer Varian 720-ES (Palo Alto, USA) was used to determine the As(V) concentration determination (at λ = 189 nm). For both metal ions, the power of 1 kW, the plasma flow of 15 L/min and the nebulizer flow of 0.75 L/min were used. The polymers concentrations were established by UV–VIS spectrophotometry (Carry 100, Varian, Palo Alto, USA).

For PAA determination purposes 1 cm^3 of 20 % NaOH was added to 5 cm^3 of the solution containing polymer. The system was heated at 90 °C for 40 min, and then the solution was cooled down. Next the pH value of the sample was adjusted to 10 and the system was transferred to the flasks of 25 cm^3 volume. 1 cm^3 of hyamine 1622 was added and filled up with the double distilled water to a mark. After 15 min the absorbance of formed white-coloured complex was measured at a wavelength of 500 nm [20]. Poly(acrylic acid) calibration curves were obtained in the concentration range of 25–300 ppm. In binary solutions, the concentration of As(V) and Cd(II) ions was 200 ppm each.

Polyethylenimine concentration was tested based on its reaction with cupric chloride, resulting in the formation of blue-coloured complex, absorbing light at a wavelength of 285 nm. For this purpose 0.005 cm^3 of 0.5 mol/dm^3 $CuCl_2$ was added to 5 cm^3 of the polymer solution. The absorbance was measured after 10 min [21]. Calibration curves were obtained with a PEI concentration of 25–200 ppm. The concentration of As(V) and Cd(II) ions in the binary solutions was 200 ppm.

2.3. Surface and electrokinetic studies

The potentiometric titration method was applied for the surface charge density (σ_0) of the activated biocarbons particles without or with the selected adsorbates determination. 50 cm^3 of the suspension containing 0.02 g of activated biocarbon, the tested metals ions or/and polymers (with the initial concentration (C_0) of 100 ppm) and the NaCl supporting electrolyte (with the concentration of 0.001 mol/dm^3) were used for this purpose. The suspension was placed in the thermostated Teflon vessel (RE 204 thermostat, Lauda Scientific, Lauda-Königshofen, Germany). Glass and calomel electrodes (Beckman Instruments, Brea, USA) were used to monitor the pH changes of the system after each portion of the added titrant – NaOH with the concentration of 0.1 mol/dm^3 (automatic Dosimat 765 microburette, Metrohm, Herisau, Switzerland). Changes in the σ_0 value as a function of solution pH were determined using the computer program "Titr_v3", which also controlled the course of the titration process. These calculations were based on the difference in the volume of the titrant added to the suspension and the supporting electrolyte solution providing a specific pH value [22].

Zetasizer Nano ZS (Malvern Instruments, Malvern, United Kingdom)

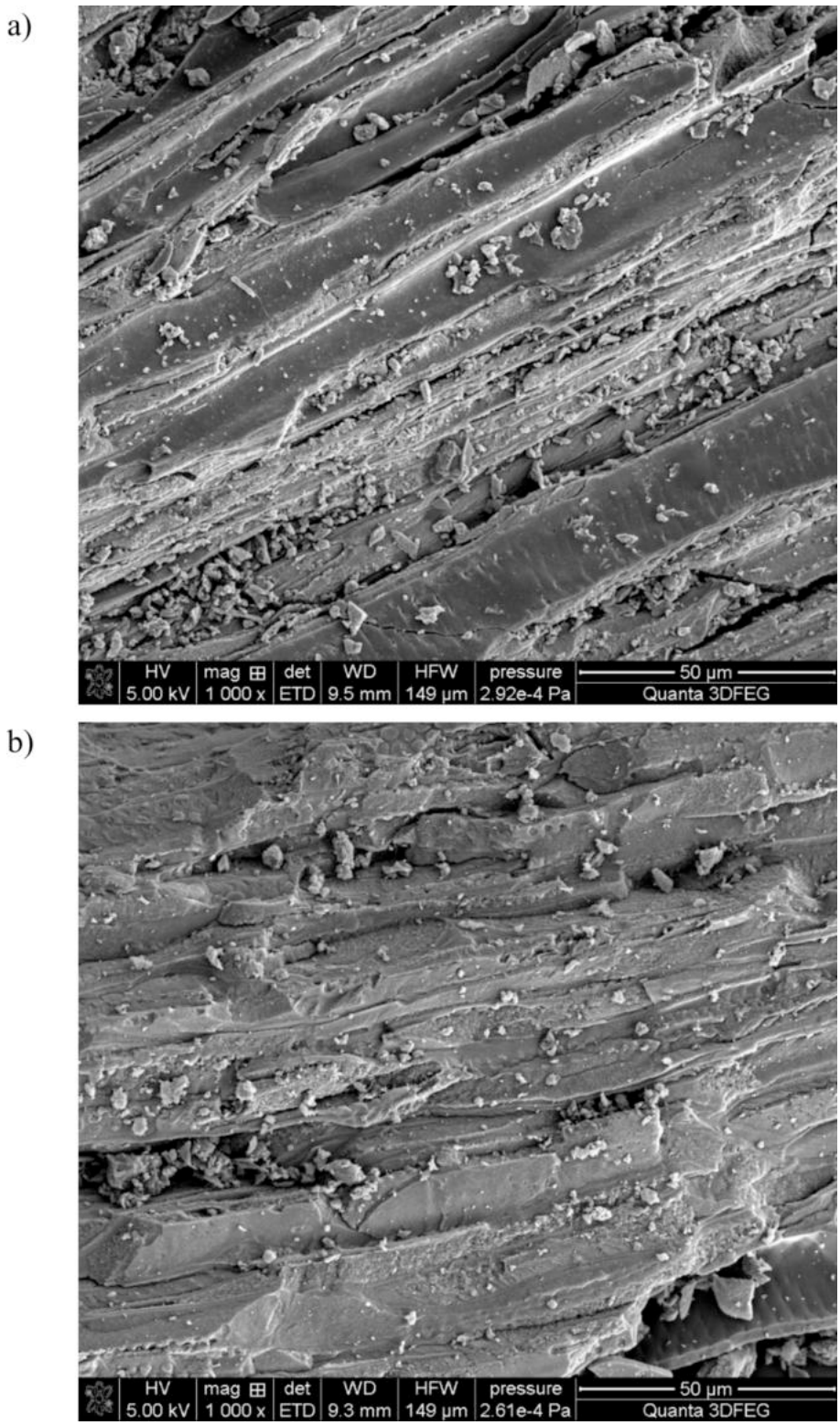

Fig. 1. SEM images of MT_AC (a) and LB_AC activated biocarbons (b).

was used to determine the zeta potential (ζ) and the average size of activated biocarbons aggregates, according to the following procedure: 200 cm^3 of suspension containing 0.03 g of the solid, the tested adsorbates with the concentration of 100 ppm as well as NaCl supporting electrolyte (0.001 mol/dm^3) was prepared. The system was subjected to the action of ultrasounds (XL 2020 ultrasonic head, Misonix, Farmingdale, USA) for 3 min and divided into several parts. A different pH value was set in each of the obtained samples (varying from 3 to 7 for Cd (II) and from 3 to 11 for As(V) ions, respectively). For this purpose the solutions of HCl and NaOH with the concentrations of 0.1 mol/dm^3 as well as Φ360 pH– meter (Beckman, Brea, USA) were used. The Doppler laser electrophoresis method was used to determine the zeta potential. The equipment used enables measurement of the electrophoretic mobility of the activated biocarbon particles without as well as covered

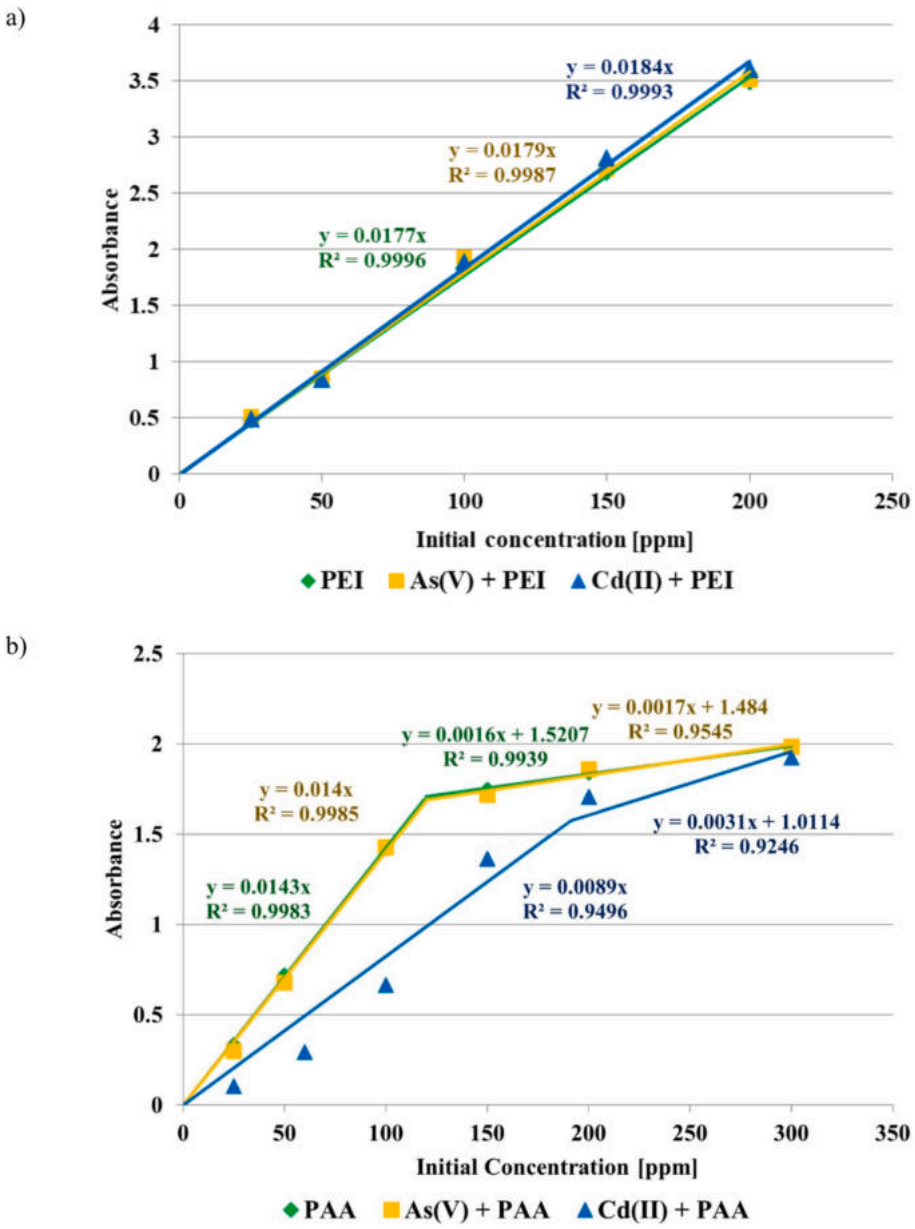

Fig. 2. Calibration curves of polyethylenimine (a) and poly(acrylic acid) (b) obtained in the systems without and with metal ions.

with the adsorption layers. Based on the obtained results, the zeta potential (ζ) was calculated using the Henry's equation [23]. The average size of aggregates formed in the tested suspensions was determined based on the static light scattering phenomenon, using Zetasizer Nano ZS apparatus. The measurement error did not exceed 5 %.

All measurements were carried out at a temperature of 25 °C in the following systems: LB_AC + NaCl, LB_AC + NaCl + Cd(II), LB_AC + NaCl + Cd(II) + PAA, LB_AC + NaCl + Cd(II) + PEI, LB_AC + NaCl + As(V), LB_AC + NaCl + As(V) + PAA, LB_AC + NaCl + As(V) + PEI, MT_AC + NaCl, MT_AC + NaCl + Cd(II), MT_AC + NaCl + Cd(II) + PAA, MT_AC + NaCl + Cd(II) + PEI, MT_AC + NaCl + As(V), MT_AC + NaCl + As(V) + PAA and MT_AC + NaCl + As(V) + PEI.

2.4. Adsorption studies

Adsorption isotherms of heavy metals ions were acquired in the following conditions: 0.01 g of activated biocarbon was added to 10 cm^3 of solution containing 0.001 mol/dm^3 of NaCl (supporting electrolyte) and the appropriate adsorbate with the initial concentration changing in the range 50–800 ppm. These studies were performed at pH 3, 6 and 9 for As(V) ions as well as at pH 3 and 6 for Cd(II) ions. Adsorption tests were conducted for 24 h at a temperature of 25 °C. Data on metal ion adsorption isotherms were modelled using the Langmuir (Eq. (1).), Freundlich (Eq. (2).) and Dubinin-Radushkievich (Eq. (3).) equations:

$$q_e = \frac{q_m K_L C_e}{1 + K_L C_e} \quad (1)$$

$$q_e = K_F C_e^{1/n} \quad (2)$$

$$q_e = q_m \exp(-\beta\varepsilon^2) \quad (3)$$

where q_e – the adsorbed amount at the equilibrium [mg/g], q_m – the maximum adsorption capacity in a particular model [mg/g], K_L – the Langmuir parameter [L/mg], C_e – the equilibrium adsorbate concentration [mg/L], K_F – the Freundlich parameter [mg/g·(mg/L) $^{-1/nF}$], β – Dubinin-Radushkievich constant, ε – adsorption potential [kJ/mol].

Kinetic tests were performed using 10 cm^3 of solution containing

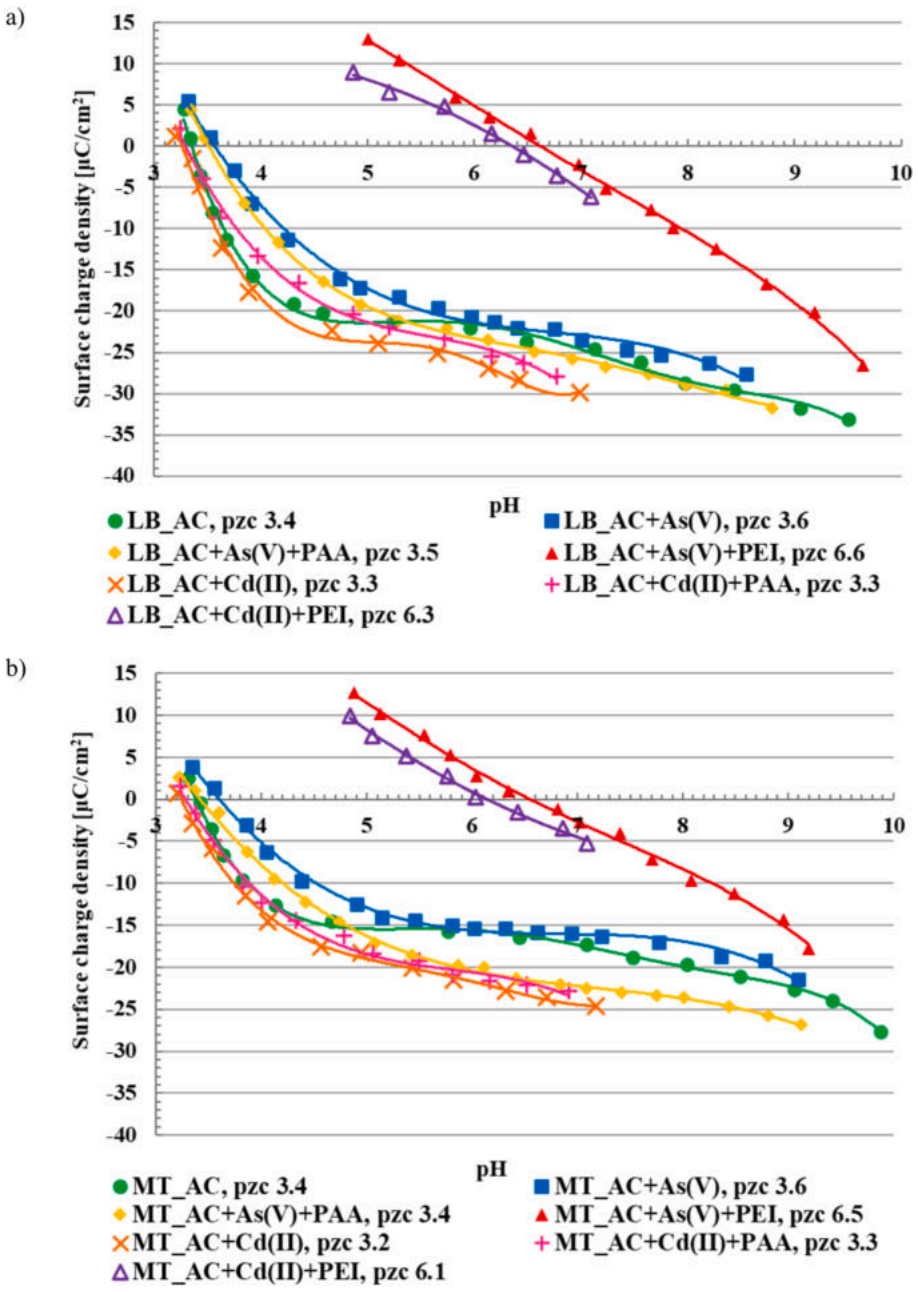

Fig. 3. Surface charge density of LB_AC (a) and MT_AC (b) activated biocarbons in the systems without adsorbates as well as with single and binary adsorbates.

metal ions with the concentration 200 ppm, supporting electrolyte (NaCl) with the concentration of 0.001 mol/dm^3 and 0.01 g of the adsorbent. Adsorption was carried out within 0.5–8 h time intervals, at a temperature of 25 °C and at pH 3. The obtained data were fitted to the pseudo-first-order (PFO, Eq. (4).) and the pseudo-second-order kinetic models (PSO, Eq. (5).) [24]:

$$\frac{dq_t}{dt} = k_1(q_e - q_t) \quad (4)$$

$$\frac{dq_t}{dt} = k_2(q_e - q_t)^2 \quad (5)$$

where q_e – the adsorbed amount at the equilibrium [mg/g], q_t – the adsorbed amount after time "t" [mg/g], k_1 – the equilibrium rate constant of the PFO model [1/min], k_2 – the equilibrium rate constant of the PSO model [g/(mg·min)].

10 cm^3 of suspension containing 200 ppm of appropriate adsorbate (polymer and/or metal), 0.001 mol/dm^3 of NaCl as supporting electrolyte and 0.01 g of activated biocarbon were used for the adsorption studies from single and binary systems (24 h, pH 3, 25 °C). Adsorption studies were realized in one- and two-component systems

The sorption capacity of activated biocarbons in relation to individual adsorbates was determined using the static method, based on the difference in concentrations of substances in the solutions before and after the processes. The measurement error of all studies did not exceed 5 %.

3. Results and discussion

3.1. Determination of polymer concentration in the heavy metal ions presence

The calibration curves of PAA and PEI obtained in the single and binary solutions are presented in Fig. 2. Presence of As(V) and Cd(II)

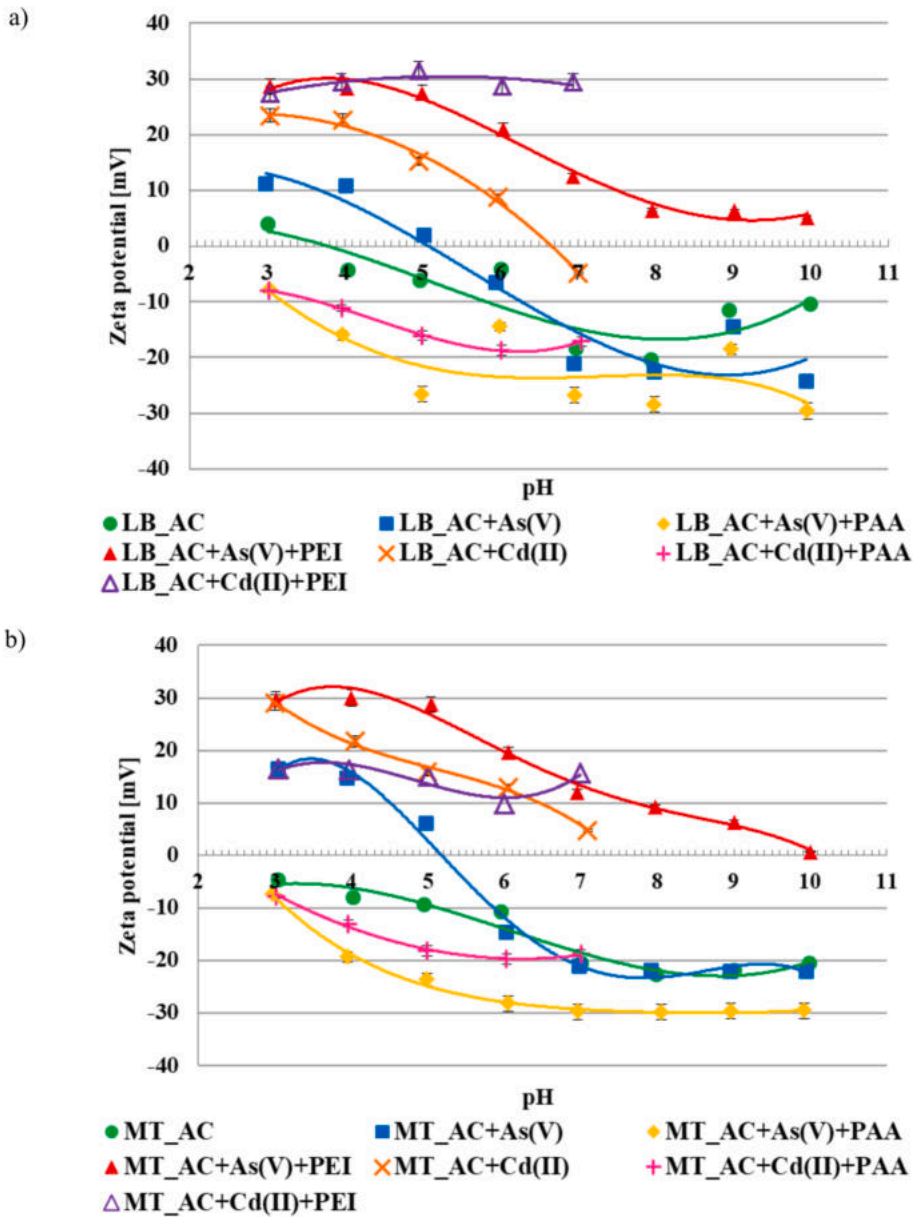

Fig. 4. Zeta potential of LB_AC (a) and MT_AC (b) activated biocarbons in the systems without as well as with single and binary adsorbates.

ions have no significant influence on the polyethylenimine determination. The complexation reaction between PEI and metals strongly depends on the substrates concentration ratio [25]. Cu(II) applied in the PAA concentration determination procedure as $CuCl_2$, occurs in solution in a higher concentration (0.5 mol/dm^3) than the other metals, which is preferable for complex formation. Despite the fact that As(V) and Cd(II) ion can react with the polymer macromolecule they don't disturb the complexation reaction [26,27]. In the case of poly(acrylic acid), the calibration curve obtained in the presence of As(V) ions overlaps with that one obtained in the absence of that metal anions. However, in the case of the system containing Cd(II) ions, the experimental points on calibration curve are noticeably shifted to the lower concentration of the polymer. This is probably related to the heating step of the PAA concentration determination procedure. At this stage the 20 % NaOH is added to the system, which causes a significant increase in the pH value of the solution (above 12). In such conditions cadmium precipitate is formed (this process begins at pH above 8), which may interfere with the reaction of PAA with hyamine.

3.2. Structure of electrical double layer formed on the activated biocarbon particles surface and its influence on the suspension stability

The obtained surface charge density results confirmed the acidic properties of activated biocarbons. The point of zero charge (pzc) of both materials occurs at pH 3.4 (Fig. 3). In the system containing As(V) ions, the surface charge density values slightly increase. Arsenate occurs in the solution in an anionic form. The adsorption of negatively charged molecules caused the formation of an additional number of positively charged surface groups, resulting in the increase in the surface charge density [28]. In the presence of Cd(II) ions the opposite effect takes place. The positively charged cadmium cations cause the formation of additional number of negatively charged surface groups [29]. In the binary systems of metal ions and polymer chains, the influence of the macromolecular compound on the surface charge density is prevailing. The polymers impact on the adsorbent surface properties is related to the large sizes of polymeric chains, which cannot be adsorbed directly by all their segments on the solid surface. Some parts of the chains form "loop" and "tail" structures and the functional groups present in these

Table 2
The size of activated biocarbons aggregates in the system without adsorbates as well with single and binary adsorbates.

System	Size of aggregates [nm]		
	pH 3	pH 6	pH 9
LB_AC	541	614	521
LB_AC + As(V)	621	747	751
LB_AC + As(V) + PAA	465	485	402
LB_AC + As(V) + PEI	515	544	582
LB_AC + Cd(II)	587	859	–
LB_AC + Cd(II) + PAA	477	284	–
LB_AC + Cd(II) + PEI	483	560	–
MT_AC	626	818	769
MT_AC + As(V)	752	878	925
MT_AC + As(V) + PAA	245	423	511
MT_AC + As(V) + PEI	495	539	703
MT_AC + Cd(II)	558	903	–
MT_AC + Cd(II) + PAA	494	314	–
MT_AC + Cd(II) + PEI	556	524	–

structures (located in the by-surface layer of the solution) affect the surface density charge. According to this theory, cationic polyethylenimine causes an increase in the value of this parameter, whereas in the case of anionic poly(acrylic acid) a decrease in the surface charge density is observed [30].

Fig. 4 shows the zeta potential of tested activated biocarbons in the systems without adsorbates as well as with the single and binary adsorbates. Positively charged cadmium ions, adsorbed mainly electrostatically due to favorable attractive forces, are located mostly in the outer Hemholtz layer, which causes the increase in the zeta potential value [31]. The influence of As(V) ions on the activated biocarbons zeta potential depends on the pH value and is related to the hydration of arsenate anions, which are located in the slipping plane area. At lower pH values, the As(V) species is fully hydrated and occurs in the H_3AsO_4 and $H_2AsO_4^-$ forms, but as the pH value increases the $HAsO_4^{2-}$ and AsO_4^{3-} forms begin to dominate in the solutions. The greater the number of completely dehydrated ions in the solution, the lower the zeta potential. In the binary systems, polymers have the dominant influence on the zeta potential values. Due to the considerable length of polymeric molecules and their ability to undergo conformational changes, some of the functional groups present in the chains are located in the slipping plane area. The presence of cationic amino groups results in the increase in the value of the electrokinetic potential, whereas the presence of anionic carboxyl groups causes the decrease in the zeta potential [19].

The size of the aggregates of both activated biocarbons depends

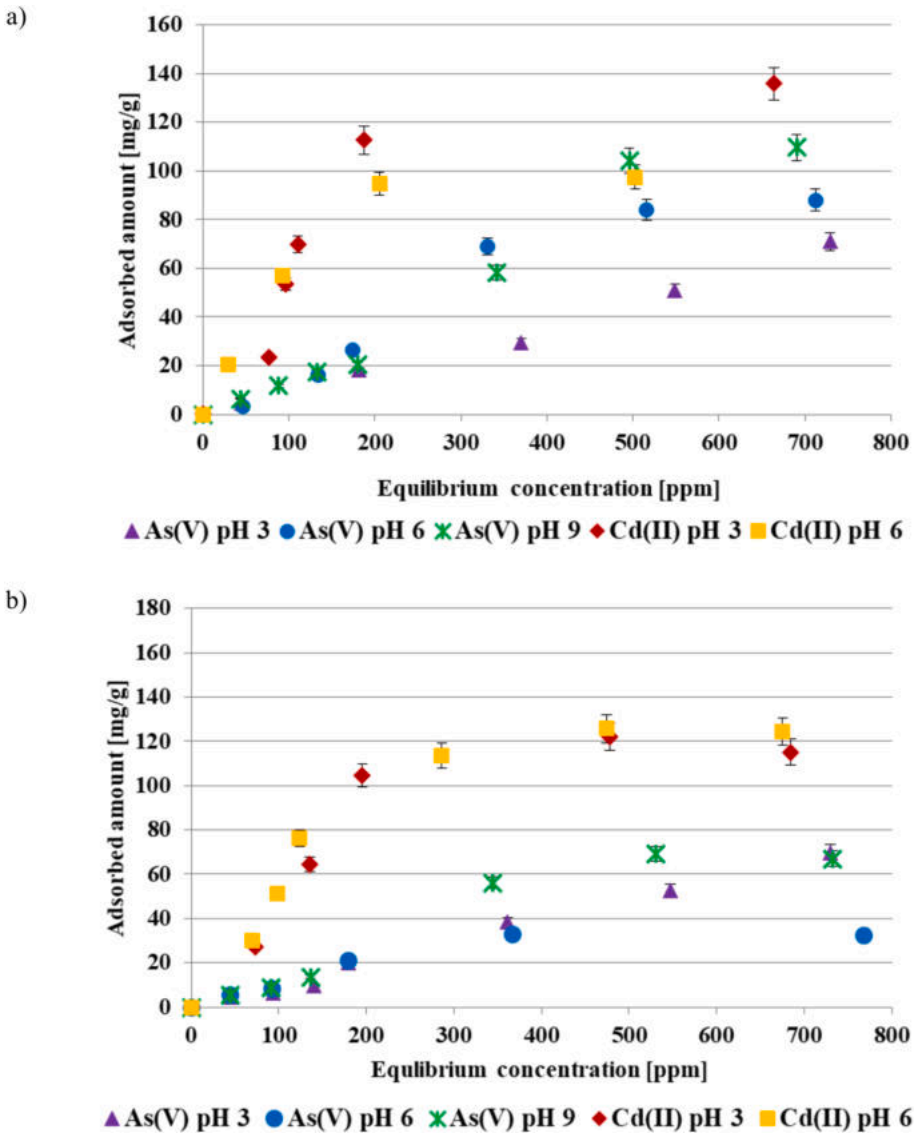

Fig. 5. Amounts of Cd(II) and As(V) ions adsorbed at pH 3, 6 and 9 on the surface of LB_AC (a) and MT_AC (b) activated biocarbon.

Table 3
The metals adsorbed amount on the surface of different carbonaceous materials.

Adsorbent	Maximum adsorbed amount [mg/g]	Reference
Cd(II)		
Activated carbon obtained from the lemon balm	135.8	Present study
Magnetized activated carbon prepared from the rape straw	73.7	[33]
Activated carbon derived from the datestone seeds	166.7	[34]
Commercial activated charcoal	129.4	[35]
Magnetic biochar composites	46.9	[36]
Biochar derived from poplar saw dust	49.3	[37]
As(V)		
Activated carbon obtained from the lemon balm	109.6	Present study
δ-MnO_2 modified activated carbon	13.3	[38]
Iron-Incorporated activated carbon	42.9	[39]
Modified peanut shell biochar	1.9	[40]
Activated Carbon supported by nano zero-valent iron	12.0	[41]

slightly on the pH value (Table 2). In the case of single metal systems, the higher the pH value, the larger the aggregates are observed. Cadmium adsorption resulted in a decrease in the repulsion between the carbonaceous adsorbent particles. As the amount of adsorbed metal ions increases, the repulsion decreases, which destabilizes the suspension. Negatively charged arsenic ions form hydrogen and chemical bonds with the surface groups of activated biocarbons, which exposes neutral sites on the adsorbent surface. Neutral solids particles are characterized by a lower tendency to repel, which results in larger aggregate sizes. This effect is more noticeable for systems containing cadmium. Its positively charged molecules neutralize the negatively charged surface of the adsorbent, which results in greater formation of aggregates. The system is more stable in the presence of polymers due to steric and electrosteric stabilization [32].

3.3. Structure of the adsorption layer formed on the activated biocarbons surface

As shown by the data presented in Fig. 5, for both tested activated biocarbons the adsorption of Cd(II) ions is more effective than for As(V). In the case of the MT_AC sample cadmium removal is independent of the solution pH, whereas for LB_AC sample it is better adsorbed at pH 3. In turn, As(V) ions show the greatest affinity to the surface of tested carbonaceous materials at pH 9. Under these conditions, the arsenate anion is fully hydrated and have the smallest negative charge, which results in the least repulsion between the ions and the adsorbent surface. The maximum adsorption capacities are 135.8 mg/g for Cd(II) (LB_AC, pH 3) and 109.6 mg/g for As(V) (LB_AC, pH 9), respectively. The greater adsorption of both metal ions observed in the case of LB_AC activated biocarbon is most likely the result of a higher content of surface functional groups. The comparison of cadmium and arsenate adsorbed amount on different carbonaceous materials are presented in Table 3. The maximum adsorbed amount of cadmium is on the similar level to some dates found in the literature. On the other hand, As(V) adsorption on the surface of activated biocarbons is not common studied and the obtained maximum adsorption capacities are much greater than the ones present in the literature.

The calculated parameters of the Langmuir, Freundlich and Dubinin-Radushkevich models are presented in Table 4. The As(V) ions adsorption is the best described by Freundlich and Dubinin-Radushkevich models, which indicates that the adsorption process takes place inside the pores and the multilayer of adsorbate is formed. Analysis of the cadmium isotherm calculated data leads to the conclusion that there is no dominant adsorption mechanism. For each of the models used, the R^2 values are similar. Cd(II) ions can form both mono- and multilayer structures on the adsorbents surface. In addition, the adsorption in the pores of activated biocarbons is also possible [42].

The removal of ionic polymers is affected by the pH of the solution, so the multicomponent systems containing macromolecules can exhibit many different behaviors. To ensure effective industrial water treatment all possible conditions should be tested. Due to the common studies on As(V) ions adsorption at high pH values, the pH 3 was selected for further research, despite the lower adsorption of arsenate ions [43–45]. Furthermore, both polymers achieve the highest adsorption level at pH 3 [46].

Fig. 6 presents the adsorption kinetics of As(V) and Cd(II) ions on the tested carbonaceous materials surface. The maximum equilibrium amount of adsorbed arsenate is reached after 4 h, which is quite a long time for small metal ions. However, a similar trend was previously observed in the case of As(V) adsorption on the surface of granular activated biocarbon [47]. Unfortunately, cadmium adsorption equilibrium state is only reached after 6–8 h. Such long periods of time needed to reach the equilibrium state for both metal ions can be associated with the slow process of the activated biocarbons structure penetration and reaction with internal active sites [36].

The calculated kinetic parameters are presented in Table 5. The adsorption of Cd(II) ions is better fitted to the pseudo first-order model, which proved that the physical adsorption is predominant. In the case of As(V) ions the chemical interaction are main adsorption mechanism. The difference in the adsorption mechanisms of the tested metals is most likely due to their different ionic forms and hydration abilities.

The percentage of As(V), Cd(II), PAA and PEI removal from the single

Table 4
Calculated parameters of Cd(II) and As(V) adsorption isotherms.

Isotherm parameters		Cd(II)		As(V)	
		LB_AC	MT_AC	LB_AC	MT_AC
Experimental	q_{exp} [mg/g]	135.8	115.2	70.95	66.45
Langmuir	q_m [mg/g]	212.77	166.67	555.56	357.14
	K_L [dm^3/mg]	0.0030	0.0042	0.0002	0.0002
	R^2	0.6737	0.8646	0.1428	0.0884
Freundlich	n_F	1.5272	1.6636	1.0612	0.9477
	K_F [mg/g·(mg/dm^3)$^{1/n}$]	0.4127	0.3438	7.8886	14.8799
	R^2	0.6715	0.7665	0.9912	0.9665
Dubinin-Radushkevich	β	$-8.9*10^{-9}$	$-8.1*10^{-9}$	$-1.3*10^{-8}$	$-1.4*10^{-8}$
	ε [kJ/mol]	7.4942	7.8447	6.2891	5.9057
	q_m [mol/g]	1	1	1	1
	R^2	0.7099	0.8070	0.9845	0.9573

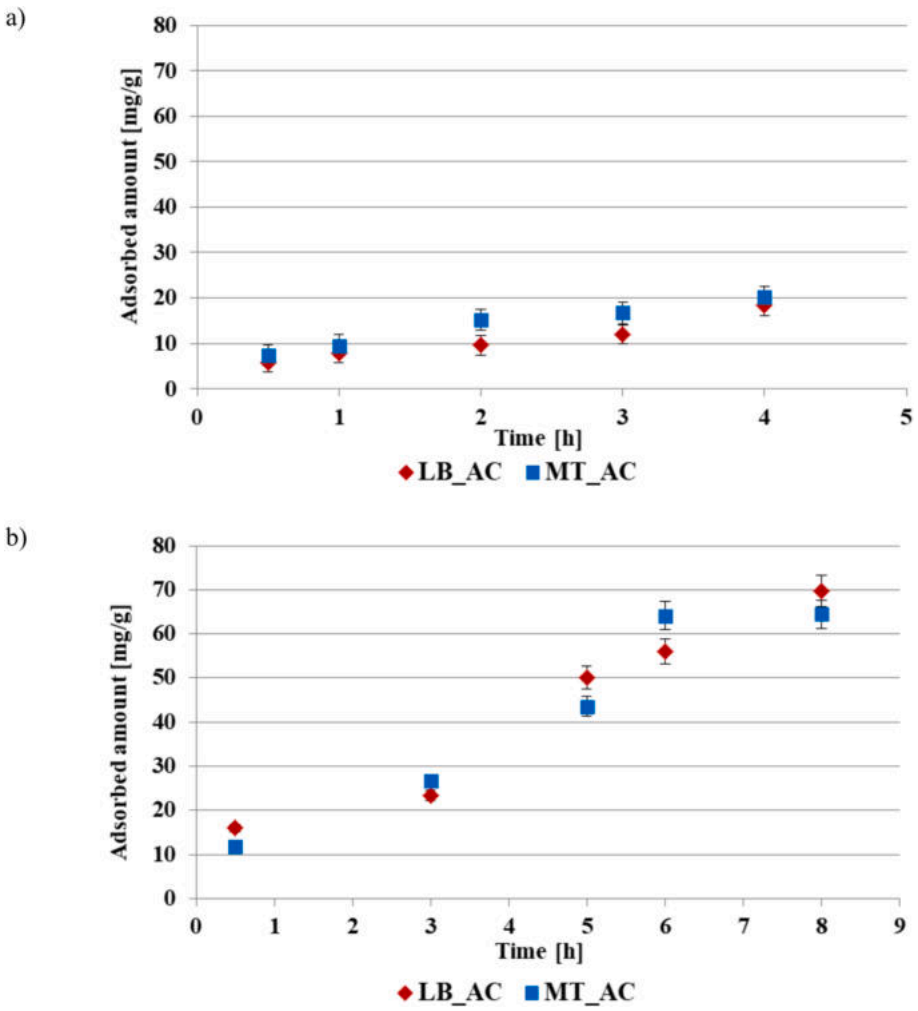

Fig. 6. Adsorption kinetics of As(V) (a) and Cd(II) (b) on the surface of LB_AC and MT_AC activated biocarbons (C_0 200 ppm, pH 3).

Table 5
Calculated parameters of Cd(II) and As(V) adsorption kinetic.

Kinetics parameters		Cd(II)		As(V)	
		LB_AC	MT_AC	LB_AC	MT_AC
Experimental	q_{exp} [mg/g]	69.70	64.50	18.38	20.23
Pseudo first-order model linear	q_e [mg/g]	0.9878	0.9854	0.9808	0.9797
	k_1 [1/min]	12.7646	12.5999	8.7056	8.5107
	R^2	0.6661	0.7808	0.6671	0.7927
Pseudo second-order model	q_e [mg/g]	104.17	112.36	24.04	27.17
	k_2 [g/(mg·min)]	0.00002	0.00002	0.00032	0.00038
	R^2	0.3968	0.6157	0.7534	0.9687

and binary systems are presented in Fig. 7. These data clearly indicate that the adsorption efficiency of both metal ions decrease in the presence of polymers, which may be the result of blocking surface-active sites by large polymeric chains. At pH 3 poly(acrylic acid) and polyethylenimine are removed in greater amounts than As(V) and Cd(II) ions. In the case of PAA this is mainly related to its coiled conformation under this conditions, which allows the macromolecules to penetrate the pores of activated biocarbons. In turn, polyethylenimine chain at pH 3 is completely developed which results in perpendicular adsorption enhancing the polymer packing on the surface of carbonaceous material. The efficiency of PEI removal decreases in the binary systems. The formed polymer-metal complexes probably tend to remain in the solution. The As(V) and Cd(II) ions influence on the poly(acrylic acid) adsorption is hard to define due to its almost completely removal from all systems.

4. Conclusions

The concentration of poliethylenimine in aqueous solutions could be determined in the presence of heavy metal ions without any interferences, whereas the poly(acrylic acid) concentration determination is disturbed by the cadmium(II) ions, because of long and multistep analytical procedure of PAA concentration determination. This indicates that the ionic polymers concentration determination procedure need to be validated before its usage for PAA quantitative analysis in the multicomponent systems.

All tested adsorbates affect the surface charge density and zeta potential of activated biocarbons as well as the size of their aggregates in aqueous suspensions. As(V) anions cause the increase in the σ_0 and ζ values, whereas the Cd(II) cations cause the decrease in the surface charge density and, at the same time, the increase in the zeta potential. Both ionic polymers present in the solution reduce the impact of metals ions and have a dominant influence on the values of the tested parameters. Single-metallic systems are characterized by larger aggregate size than analogous suspensions without adsorbates. In turn, the presence of ionic polymers reduces the size of the aggregates.

The effectiveness of As(V) ions adsorption depends significantly on the pH of the solution (due to the changes in arsenate ions hydration).

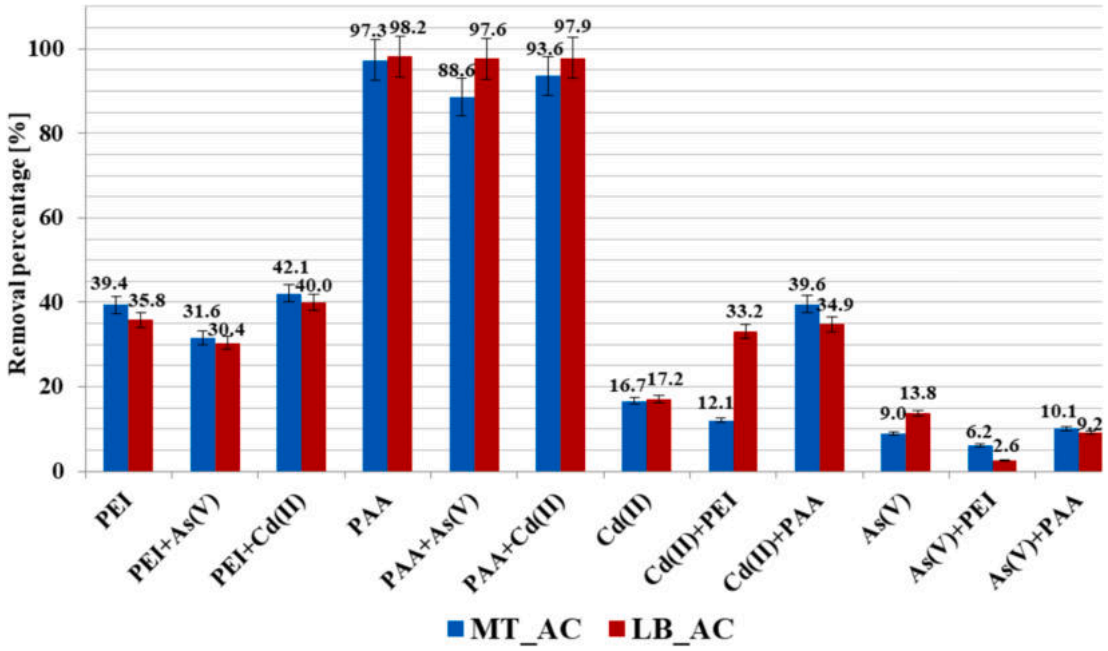

Fig. 7. Removal percentage of As(V), Cd(II), PAA and PEI from single and binary systems using LB_AC and MT_AC activated biocarbons (C_0 200 ppm, pH 3).

The maximum adsorbed amount is observed at pH 9, when these ions are completely dehydrated. In turn, the removal of Cd(II) ions from an aqueous solution depends only to a small extent on the pH value. The maximum adsorption capacities are 135.8 mg/g for Cd(II) (LB_AC, pH 3) and 109.6 mg/g for As(V) (LB_AC, pH 9), respectively. Kinetic studies have shown that it takes a few hours to reach the equilibrium state. What is more, the presence of ionic polymers has a negative effect on the As(V) and Cd(II) ions removal from aqueous solutions. It was shown, that applied mesoporous carbons (obtained via the waste plant biomass management) can be successfully used in the adsorptive removal of arsenate and cadmium ions (in the amounts comparable or higher than that obtained for other carbonaceous materials) from multi-component aqueous solution containing ionic polymers.

CRediT authorship contribution statement

Marlena Gęca: Writing – original draft, Visualization, Resources, Methodology, Investigation, Formal analysis. **Małgorzata Wiśniewska:** Writing – review & editing, Writing – original draft, Supervision, Data curation, Conceptualization. **Piotr Nowicki:** Writing – original draft, Visualization, Methodology, Investigation. **Grzegorz Wójcik:** Resources, Methodology, Investigation.

Declaration of competing interest

The authors declare that they have no known competing financial interests or personal relationships that could have appeared to influence the work reported in this paper.

Data availability

Data will be made available on request.

References

[1] S. Sarkar, E. Guibal, F. Quignard, A.K. SenGupta, Polymer-supported metals and metal oxide nanoparticles: synthesis, characterization, and applications, J. Nanopart. Res. 14 (2012) 1–24, https://doi.org/10.1007/s11051-011-0715-2.
[2] J. Virkutyte, R.S. Varma, Green synthesis of metal nanoparticles: biodegradable polymers and enzymes in stabilization and surface functionalization, Chem. Sci. 2 (2011) 837–846, https://doi.org/10.1039/C0SC00338G.
[3] W. Lin, F. Su, M. Lin, M. Jin, Y. Li, K. Ding, Q. Chen, Q. Qian, X. Sun, Effect of microplastics PAN polymer and/or Cu^{2+} pollution on the growth of Chlorella pyrenoidosa, Environ. Pollut. 265 (2020) 114985, https://doi.org/10.1016/j.envpol.2020.114985.
[4] M. Tunali, E.N. Uzoefuna, M.M. Tunali, O. Yenigun, Effect of microplastics and microplastic-metal combinations on growth and chlorophyll a concentration of Chlorella vulgaris, Sci. Total Environ. 743 (2020) 140479, https://doi.org/10.1016/j.scitotenv.2020.140479.
[5] N. Naqash, S. Prakash, D. Kapoor, R. Singh, Interaction of freshwater microplastics with biota and heavy metals: a review, Environ. Chem. Lett. 18 (2020) 1813–1824, https://doi.org/10.1007/s10311-020-01044-3.
[6] Z.M. Ayalew, X. Guo, X. Zhang, Synthesis and application of polyethyleneimine (PEI)-based composite/nanocomposite material for heavy metals removal from wastewater: a critical review, J. Hazard. Mater. Adv. 8 (2022) 100158, https://doi.org/10.1016/j.hazadv.2022.100158.
[7] C. Zhang, F.G. Wu, P. Hu, Z. Chen, Interaction of polyethylenimine with model cell membranes studied by linear and nonlinear spectroscopic techniques, J. Phys. Chem. C 118 (2014) 12195–12205, https://doi.org/10.1021/jp502383u.
[8] B.S. Rathi, P.S. Kumar, A review on sources, identification and treatment strategies for the removal of toxic Arsenic from water system, J. Hazard. Mater. 418 (2021) 126299, https://doi.org/10.1016/j.jhazmat.2021.126299.
[9] M.T. Hayat, M. Nauman, N. Nazir, S. Ali, N. Bangash, Environmental hazards of cadmium: past, present, and future. Cadmium Toxicity and Tolerance in Plants, Academic Press, 2019.
[10] T.A. Saleh, M. Mustaqeem, M. Khaled, Developing water treatment technologies in removing heavy metal ions from wastewater: a review, Environ. Nanotech. Monit. Manag. 17 (2022) 100617, https://doi.org/10.1016/j.enmm.2021.100617.
[11] W. Xiao, X. Jiang, X. Liu, W. Zhou, Z.N. Garba, I. Lawan, L. Wang, Z. Yuan, Adsorption of organic dyes from wastewater by metal-doped porous carbon materials, J. Cleaner Prod. 284 (2021) 124773, https://doi.org/10.1016/j.jclepro.2020.124773.
[12] J. Ouyang, L. Zhou, Z. Liu, J.Y. Heng, W. Chen, Biomass-derived activated carbons for the removal of pharmaceutical mircopollutants from wastewater: a review, Sep. Purif. Tech. 253 (2020) 117536, https://doi.org/10.1016/j.seppur.2020.117536.
[13] K.Y. Foo, B.H. Hameed, Utilization of rice husks for the production of activated carbons: preparation and characterization, Biores. Tech. 175 (2010) 1236–1240, https://doi.org/10.1016/j.biortech.2011.07.102.
[14] C. Brunot, L. Ponsonnet, C. Lagneau, P. Farge, C. Picart, BGrosgogeat, Cytotoxicity of polyethyleneimine (PEI), precursor base layer of polyelectrolyte multilayer films, Biomat. 28 (2007) 632–640, https://doi.org/10.1016/j.biomaterials.2006.09.026.
[15] Y.B. Kilinc, Z.M. Akdeste, R.C. Koc, M. Bagirova, A. Allahverdiyev, Synthesis and characterization of antigenic influenza A M2e protein peptide-poly (acrylic) acid bioconjugate and determination of toxicity in vitro, Bioeng. 5 (2014) 357–362, https://doi.org/10.4161/21655979.2014.969131.
[16] R.A. Beauvais, S.D. Alexandratos, Polymer-supported reagents for the selective complexation of metal ions: an overview, Reac. Funct. Polym. 36 (1998) 113–123, https://doi.org/10.1016/S1381-5148(98)00016-9.
[17] D. Adinata, W.M.A.W. Daud, M.K. Aroua, Preparation and characterization of activated carbon from palm shell by chemical activation with K_2CO_3, Biores. Tech. 98 (2007) 145–149, https://doi.org/10.1016/j.biortech.2005.11.006.

[18] A. Bazan-Wozniak, R. Pietrzak, Adsorption of organic and inorganic pollutants on activated bio-carbons prepared by chemical activation of residues of supercritical extraction of raw plants, Chem. Eng. J. 393 (2020) 124785, https://doi.org/10.1016/j.cej.2020.124785.
[19] M. Gęca, M. Wiśniewska, P. Nowicki, Simultaneous removal of polymers with different ionic character from their mixed solutions using herb-based biochars and activated carbons, Molecules 27 (2022) 7557, https://doi.org/10.3390/molecules27217557.
[20] W.B. Crummett, R.A. Hummel, The determination of traces of polyacrylamides in water, J. Am. Water Works Assoc. 1 (1963) 209–219, https://doi.org/10.1002/J.1551-8833.1963.TB01016.X.
[21] J. Patkowski, D. Myśliwiec, S. Chibowski, Validation of a new method for spectrophotometric determination of polyethylenimine, Int. J. Polym. Anal. Charact. 21 (2016) 486–494, https://doi.org/10.1080/1023666X.2016.1168651.
[22] W. Janusz, Electrical double layer in the system TiO_2 (anathase)/aqueous solution of NaCl, Polish J. Chem. 68 (1994) 1871–1880.
[23] H. Ohshima, A simple expression for Henry's function for the retardation effect in electrophoresis of spherical colloidal particles, J. Colloid Interf. Sci. 168 (1994) 269–271, https://doi.org/10.1006/jcis.1994.1419.
[24] J. Wang, X. Guo, Adsorption kinetic models: physical meanings, applications, and solving methods, J. Hazard. Mat. 390 (2020) 122156, https://doi.org/10.1016/j.jhazmat.2020.122156.
[25] V.N. Kislenko, L.P. Oliynyk, Complex formation of polyethyleneimine with copper (II), nickel (II), and cobalt (II) ions, J. Polym. Sci. Part A 40 (2002) 914–922, https://doi.org/10.1002/pola.10157.
[26] N.S. Alsaiari, F.M. Alzahrani, K.M. Katubi, A. Amari, F.B. Rebah, M.A. Tahoon, Polyethylenimine-modified magnetic chitosan for the uptake of arsenic from water, Appl. Sci. 11 (2021) 5630, https://doi.org/10.3390/app11125630.
[27] Y. Snoussi, M. Abderrabba, A. Sayari, Removal of cadmium from aqueous solutions by adsorption onto polyethylenimine-functionalized mesocellular silica foam: Equilibrium properties, J. Taiwan Inst. Chem. Eng. 66 (2016) 372–378, https://doi.org/10.1016/j.jtice.2016.06.015.
[28] C.H. Liu, Y.H. Chuang, T.Y. Chen, Y. Tian, H. Li, M.K. Wang, W. Zhang, Mechanism of arsenic adsorption on magnetite nanoparticles from water: thermodynamic and spectroscopic studies, Environ. Sci. Tech. 49 (2015) 7726–7734, https://doi.org/10.1021/acs.est.5b00381.
[29] M. Wiśniewska, M. Marciniak, M. Gęca, K. Herda, R. Pietrzak, P. Nowicki, Activated biocarbons obtained from plant biomass as adsorbents of heavy metal ions, Materials 15 (2022) 5856, https://doi.org/10.3390/ma15175856.
[30] M. Wiśniewska, P. Nowicki, K. Szewczuk-Karpisz, M. Gęca, K. Jędruchniewicz, P. Oleszczuk, Simultaneous removal of toxic Pb(II) ions, poly(acrylic acid) and Triton X-100 from their mixed solution using engineered biochars obtained from horsetail herb precursor – impact of post-activation treatment, Sep. Purif. Tech. 276 (2021) 119279, https://doi.org/10.1016/j.seppur.2021.119297.
[31] K. Szewczuk-Karpisz, M. Wiśniewska, M. Medykowska, V.M. Bogatyrov, Z. Sokołowska, Adsorption layer structure on the surface of carbon-silica composite in the presence of proteins of different internal stability and Cu (II) ions–the effect on solid aggregation, J. Molec. Liq. 309 (2020) 113072, https://doi.org/10.1016/j.molliq.2020.113072.
[32] M. Wiśniewska, K. Terpiłowski, S. Chibowski, T. Urban, V.I. Zarko, V.M. Gun'ko, Investigation of stabilization and destabilization possibilities of water alumina suspension in polyelectrolyte presence, Int. J. Mineral Process. 132 (2014) 34–42, https://doi.org/10.1016/j.minpro.2014.08.007.
[33] Z. Zhang, T. Wang, H. Zhang, Y. Liu, B. Xing, Adsorption of Pb (II) and Cd (II) by magnetic activated carbon and its mechanism, Sci. Total Environ. 757 (2021) 143910, https://doi.org/10.1016/j.scitotenv.2020.143910.
[34] G. Sharma, M. Naushad, Adsorptive removal of noxious cadmium ions from aqueous medium using activated carbon/zirconium oxide composite: isotherm and kinetic modelling, J. Molec. Liq. 310 (2020) 113025, https://doi.org/10.1016/j.molliq.2020.113025.
[35] C.O. Aniagor, M. Elshkankery, A.J. Fletcher, O.M. Morsy, E.S. Abdel-Halim, A. Hashem, Equilibrium and kinetic modelling of aqueous cadmium ion and activated carbon adsorption system, Water Conserv. Sci. Eng. 6 (2021) 95–104, https://doi.org/10.1007/s41101-021-00107-y.
[36] Z.H. Khan, M. Gao, W. Qiu, M.S. Islam, Z. Song, Mechanisms for cadmium adsorption by magnetic biochar composites in an aqueous solution, Chemosphere 246 (2020) 125701, https://doi.org/10.1016/j.chemosphere.2019.125701.
[37] D. Chen, X. Wang, X. Wang, K. Feng, J. Su, J. Dong, The mechanism of cadmium sorption by sulphur-modified wheat straw biochar and its application cadmium-contaminated soil, Sci. Total Environ. 714 (2020) 136550, https://doi.org/10.1016/j.scitotenv.2020.136550.
[38] Y. Wang, H. Liu, S. Wang, X. Li, X. Wang, Y. Jia, Simultaneous removal and oxidation of arsenic from water by δ-MnO_2 modified activated carbon, J. Environ. Sci. 94 (2020) 147–160, https://doi.org/10.1016/j.jes.2020.03.006.
[39] H.L. Rahman, H. Erdem, M. Sahin, M. Erdem, Iron-incorporated activated carbon synthesis from biomass mixture for enhanced arsenic adsorption, Water Air Soil Pollut. 231 (2020) 1–17, https://doi.org/10.1007/s11270-019-4378-4.
[40] R. Kushwaha, R.S. Singh, D. Mohan, Comparative study for sorption of arsenic on peanut shell biochar and modified peanut shell biochar, Biores. Tech. 375 (2023) 128831, https://doi.org/10.1016/j.biortech.2023.128831.
[41] H. Zhu, Y. Jia, X. Wu, H. Wang, Removal of arsenic from water by supported nano zero-valent iron on activated carbon, J. Hazard. Mater. 172 (2009) 1591–1596, https://doi.org/10.1016/j.jhazmat.2009.08.031.
[42] K.Y. Foo, B.H. Hameed, Insights into the modeling of adsorption isotherm systems, Chem. Eng. J. 156 (2010) 2–10, https://doi.org/10.1016/j.cej.2009.09.013.
[43] C.L. Chuang, M. Fan, M. Xu, R.C. Brown, S. Sung, B. Saha, C.P. Huang, Adsorption of arsenic (V) by activated carbon prepared from oat hulls, Chemosphere 61 (2005) 478–483, https://doi.org/10.1016/j.chemosphere.2005.03.012.
[44] M.E. Sigrist, L. Brusa, H.R. Beldomenico, L. Dosso, O.M. Tsendra, M.B. González, C. L. Pieck, C.R. Vera, Influence of the iron content on the arsenic adsorption capacity of Fe/GAC adsorbents, J. Environ. Chem. Eng. 2 (2014) 927–934, https://doi.org/10.1016/j.jece.2014.02.013.
[45] E. Deliyanni, T.J. Bandosz, K.A. Matis, Impregnation of activated carbon by iron oxyhydroxide and its effect on arsenate removal, J. Chem. Tech. Biotech. 88 (2013) 1058–1066, https://doi.org/10.1002/jctb.3938.
[46] M. Gęca, M. Wiśniewska, T. Urban, P. Nowicki, Temperature effect on ionic polymers removal from aqueous solutions using activated carbons obtained from biomass, Materials 16 (2023) 350, https://doi.org/10.3390/ma16010350.
[47] M. Kalaruban, P. Loganathan, T.V. Nguyen, T. Nur, M.A.H. Johir, T.H. Nguyen, M. V. Trinh, S. Vigneswaran, Iron-impregnated granular activated carbon for arsenic removal: application to practical column filters, J. Environ. Manag. 239 (2019) 235–243, https://doi.org/10.1016/j.jenvman.2019.03.053.

Lublin, 10.09.2025

mgr Marlena Groszek
Uniwersytet Marii Curie-Skłodowskiej w Lublinie,
Wydział Chemii, Instytut Nauk Chemicznych,
Katedra Radiochemii i Chemii Środowiskowej,
Pl. Marii Curie-Skłodowskiej 3, 20-031 Lublin
marlena.groszek@mail.umcs.pl

Rada Naukowa Instytutu Nauk Chemicznych
Uniwersytetu Marii Cure-Skłodowskiej
w Lublinie

Oświadczenie o współautorstwie

Niniejszym oświadczam, że mój udział w pracy: **M. Gęca**, M. Wiśniewska, P. Nowicki, G. Wójcik *Arsenate and cadmium ions removal from multicomponent solutions of ionic polymers using mesoporous activated biocarbons*, Journal of Molecular Liquids, 2024, 407, 125270, DOI: 10.1016/j.molliq.2024.125270 [D10], obejmował opracowanie metodyki badań, przeprowadzenie eksperymentów, analizę i interpretację uzyskanych wyników, przygotowanie manuskryptu i sformułowanie odpowiedzi na uwagi recenzentów.

Lublin, 10.09.2025

prof. dr hab. Małgorzata Wiśniewska
Uniwersytet Marii Curie-Skłodowskiej w Lublinie,
Wydział Chemii, Instytut Nauk Chemicznych,
Katedra Radiochemii i Chemii Środowiskowej,
Pl. Marii Curie-Skłodowskiej 3, 20-031 Lublin
malgorzata.wisniewska@mail.umcs.pl

Rada Naukowa Instytutu Nauk Chemicznych
Uniwersytetu Marii Cure-Skłodowskiej
w Lublinie

Oświadczenie o współautorstwie

Niniejszym oświadczam, że mój udział w pracy: M. Gęca, **M. Wiśniewska**, P. Nowicki, G. Wójcik *Arsenate and cadmium ions removal from multicomponent solutions of ionic polymers using mesoporous activated biocarbons*, Journal of Molecular Liquids, 2024, 407, 125270, DOI: 10.1016/j.molliq.2024.125270 [D10], obejmował stworzenie koncepcji pracy, korektę manuskryptu - przed i po procesie recenzji oraz nadzór merytoryczny w czasie całego cyklu wydawniczego.

Małgorzata Wiśniewska

Poznań, 10.09.2025

dr hab. Piotr Nowicki, prof. UAM
Uniwersytet im. Adama Mickiewicza w Poznaniu,
Wydział Chemii, Zakład Chemii Stosowanej,
Ul. Uniwersytetu Poznańskiego 8, 61-614 Poznań
piotr.nowicki@amu.edu.pl

Rada Naukowa Instytutu Nauk Chemicznych
Uniwersytetu Marii Cure-Skłodowskiej
w Lublinie

Oświadczenie o współautorstwie

Niniejszym oświadczam, że mój udział w pracy: M. Gęca, M. Wiśniewska, **P. Nowicki**, G. Wójcik *Arsenate and cadmium ions removal from multicomponent solutions of ionic polymers using mesoporous activated biocarbons*, Journal of Molecular Liquids, 2024, 407, 125270, DOI: 10.1016/j.molliq.2024.125270 [D10], obejmował opracowanie metodyki pomiarów, przeprowadzenie eksperymentów, interpretację uzyskanych wyników oraz przygotowanie pierwszej wersji pracy.

Piotr Nowicki

Lublin, 10.09.2025

dr hab. Grzegorz Wójcik, prof. UMCS
Uniwersytet Marii Curie-Skłodowskiej w Lublinie,
Wydział Chemii, Instytut Nauk Chemicznych,
Katedra Chemii Nieorganicznej,
Pl. Marii Curie-Skłodowskiej 2, 20-031 Lublin
grzegorz.wojcik2@mail.umcs.pl

Rada Naukowa Instytutu Nauk Chemicznych
Uniwersytetu Marii Cure-Skłodowskiej
w Lublinie

Oświadczenie o współautorstwie

Niniejszym oświadczam, że mój udział w pracy: M. Gęca, M. Wiśniewska, P. Nowicki, **G. Wójcik** *Arsenate and cadmium ions removal from multicomponent solutions of ionic polymers using mesoporous activated biocarbons*, Journal of Molecular Liquids, 2024, 407, 125270, DOI: 10.1016/j.molliq.2024.125270 [D10], obejmował przeprowadzenie oznaczeń stężenia jonów metali przed i po adsorpcji.

Grzegorz Wójcik